SDC - 91 - 114

CALORIMETER REVIEW AND TECHNICAL BOARD MEETING

SEPTEMBER 12 - 14, 1991

SSCL

Enclosed are presentations by:

Jimmy Proudfoot	Argonne National Laboratory
Larry Price	Argonne National Laboratory
Dan Green	Fermilab
Jim Freeman	Fermilab
Gerry Abrams	Lawrence Berkeley Laboratory
Yoshinobu Unno	KEK
Christopher Heartly	Fermilab
Kenneth Einsweiler	Lawrence Berkeley Laboratory
Taka Kondo	KEK
Bill Edwards	Lawrence Berkeley Laboratory
David Bintinger	SSCL
W.T. Ford	University Of Colorado
Gary Feldman	Harvard University
Michael Barnett	Lawrence Berkeley Laboratory
W. R. Frisken	York University
R. Kephart	Fermilab

CALORIMETER REVIEW AND TECHNICAL BOARD MEETING
SEPTEMBER 12 -14, 1991
SSCL

Presentation by:

Jimmy Proudfoot

Argonne National Laboratory

AND7746

SCINTILLATOR TILE-FIBER CALORIMETER DESIGN PARAMETERS and COST

J. Proudfoot, *Argonne National Laboratory*

September 12, 1991

- Overall Performance
- Physics Issues
- Mechanical Conceptual Design
- Optical System Conceptual Design
- Cost

Parameter	Requirement	Model A	Model B
EM allowed cracks	$< 5 - 10\%$	~ 0	1.5%
holes $/\eta/ < \eta max$		1.5%	1.5%
Total electron acceptance	$> .9$	$> 98\%$	$> 97\%$
Energy Resolution			
EM stochastic term	14-20%/$\sqrt{E_T}$	12	13.5
EM constant term	$< 1 - 2\%$	ok	ok
HAD stochastic term	50-75%/$\sqrt{E_T}$	65	60
HAD constant term	$< 4\%$	< 4	2
Time stability	$< 1\%$ after correction	ok	ok
e/h response	< 1.3	< 1.2	1.0-1.05
Spatial uniformity			
EM	$< 5\%$ loss	$< 2\%$	$< 2\%$
HAD		$< 5\%$	$< 5\%$
Dynamic range			
EM	20 MeV-2 TeV	30 MeV	30 MeV
HAD	50 MeV-5 TeV	60 MeV	60 MeV
Time resolution			
EM	$\sigma \sim 5nsec, E_T > 15$	$< 2nsec$	< 2 nsec
HAD	$\sigma \sim 5nsec, E_T > 100$	$< 2nsec$	< 2 nsec
Signal peaking time	< 200 nsec	$\sim 10nsec$	~ 10 nsec
Baseline rest.	100 nsec $< \tau < 6\mu$ sec	$\sim 30nsec$	~ 30 nsec
Noise	< 5 GeV, Δ R=.3	0	0
Pileup	< 5 GeV, Δ R=.3	ok	ok

Table 1: Critical Performance Requirements

PHYSICS ISSUES

- Di-Jet Mass & Calorimeter Depth
- Z–> JJ & Hadron Transverse Segmentation
- b–> e ν Tagging and Hadron Transverse Segmentation
- b–> e ν Tagging & SM Strip Length
- Hermiticity & Solenoid Support Integration

HAC1 PHILOSPHY OPTIONS

- Use Fe and Calibrate at Asymptotic Energies
- Use Lead and Design Compensating Calorimeter

Calorimeter Depth.

Di-Jet Mass Resolution.

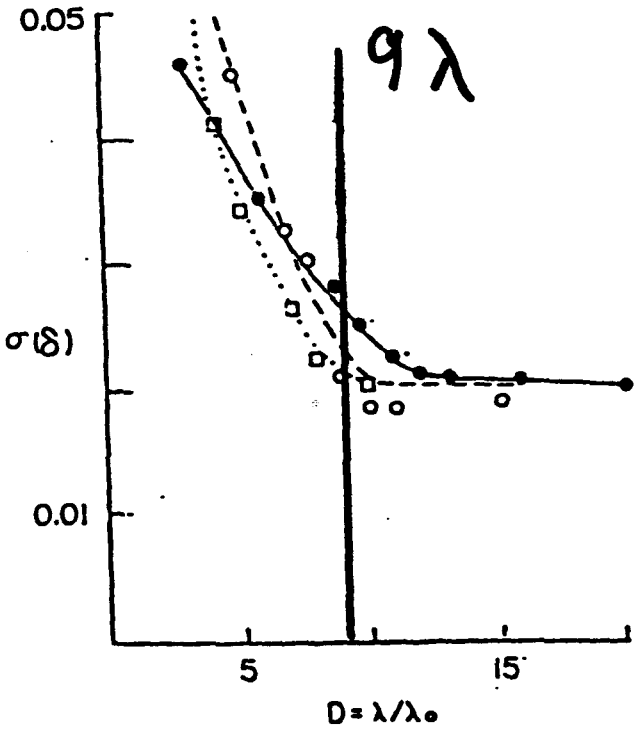

Figure 2.1 dM/M, fraction dijet mass resolution for the highest accessible mass (10 TeV), as a function of depth (D) in interaction lengths. The points correspond to different parameterizations of data, CCFR data solid, WA3 data open, Lab E data boxes.

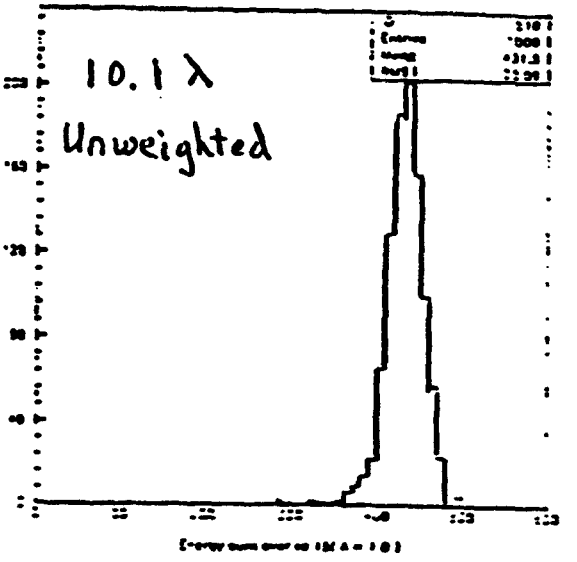

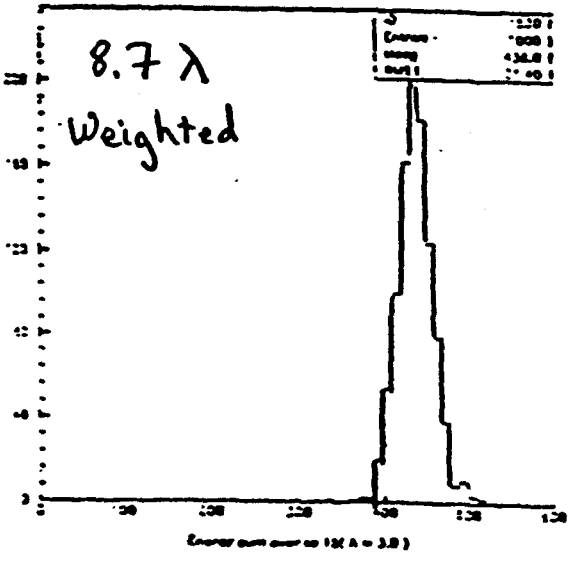

Calorimeter (HAC) Transverse Granularity

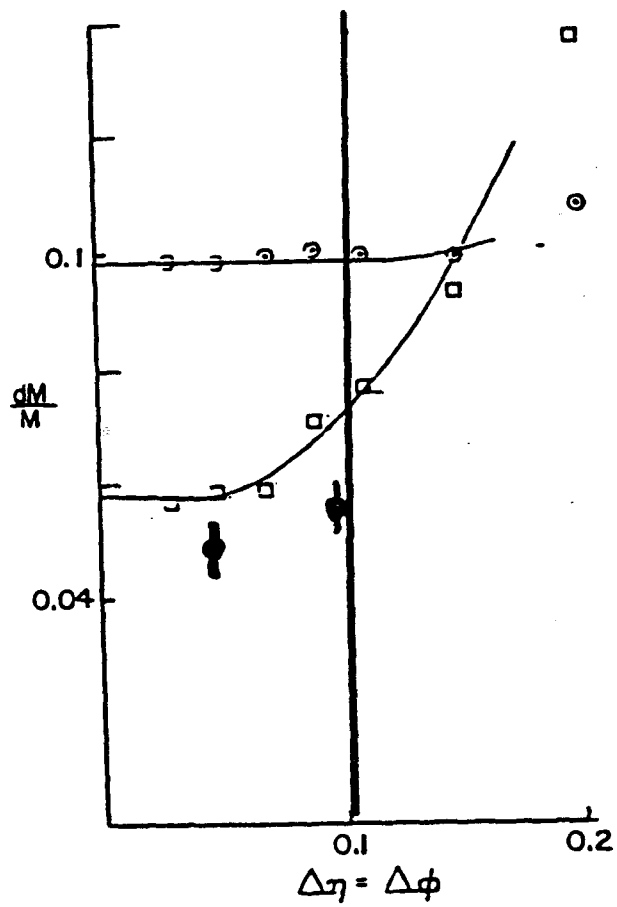

$Z^0 \to JJ$.

$(P_t^Z = 0.55\ \text{TeV})$

ϕ ABW Analys

$(\Delta\eta + \Delta\phi = 0.05$:

Em.

Figure 2.5 Fractional mass resolution for $Z \to jj$ for low P_T Z's, . , and boosted Z with $P_T = 0.55$ TeV similar to those from a 1.1 TeV Higgs, o ,as a function of tower transverse segmentation.

HAC1 Transverse Granularity

$Z^0 \rightarrow JJ$. [SDC-91-00081]

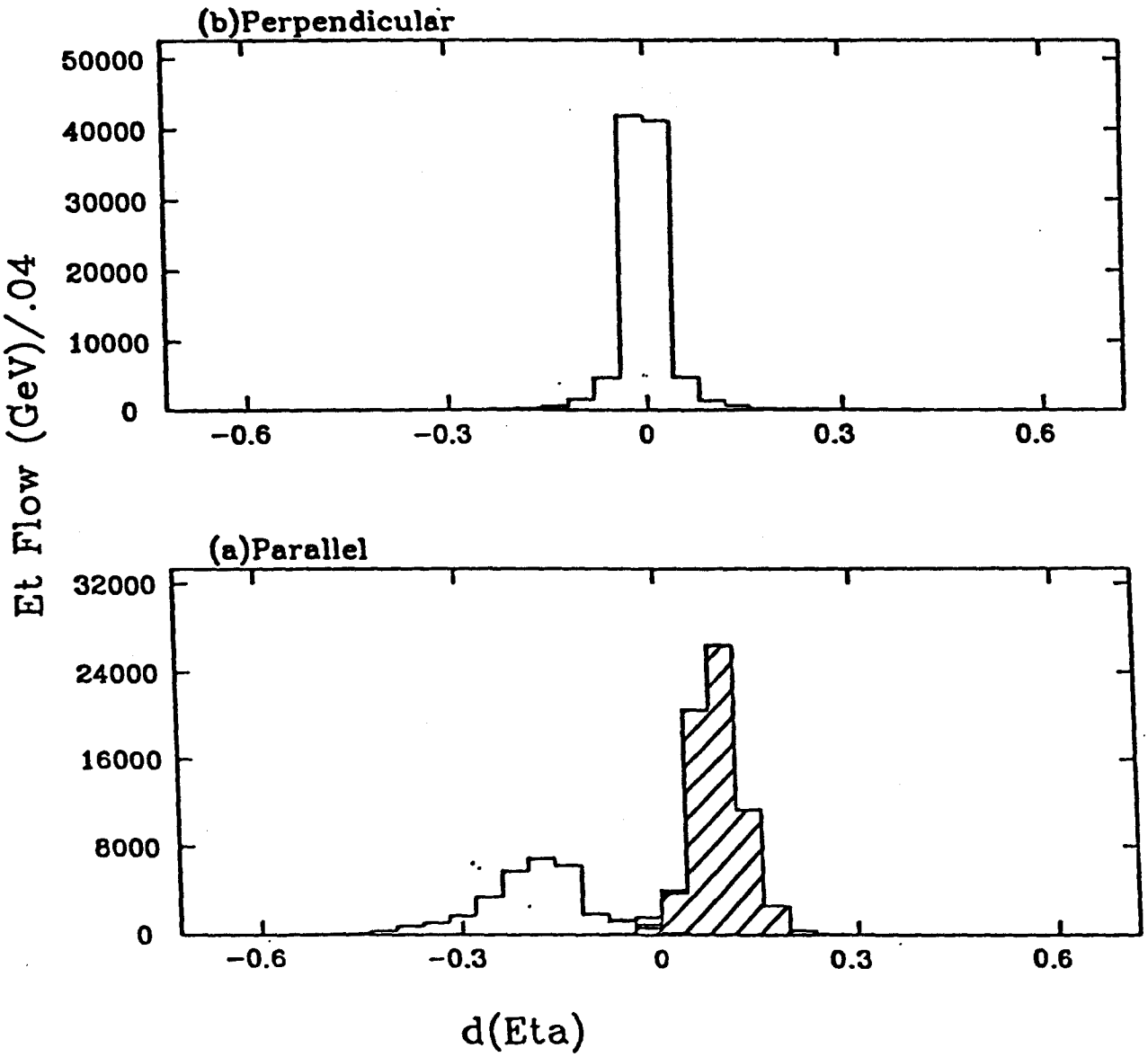

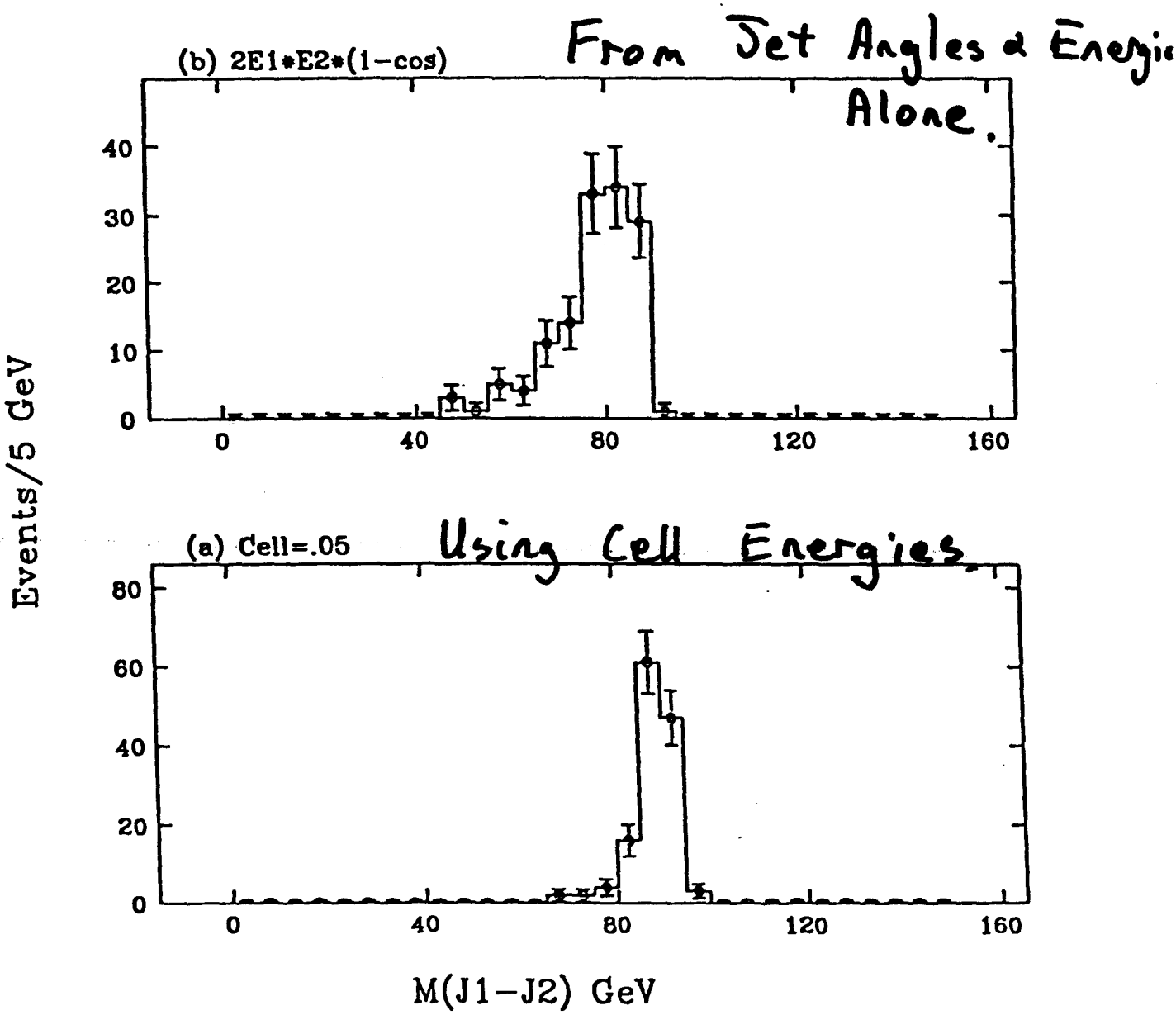
(b) 2E1*E2*(1-cos)
From Jet Angles & Energie
Alone.
(a) Cell=.05
Using Cell Energies.
Events/5 GeV
M(J1-J2) GeV
0
10
20
30
40
0
20
40
60
80
0
40
80
120
160

Figure (4)

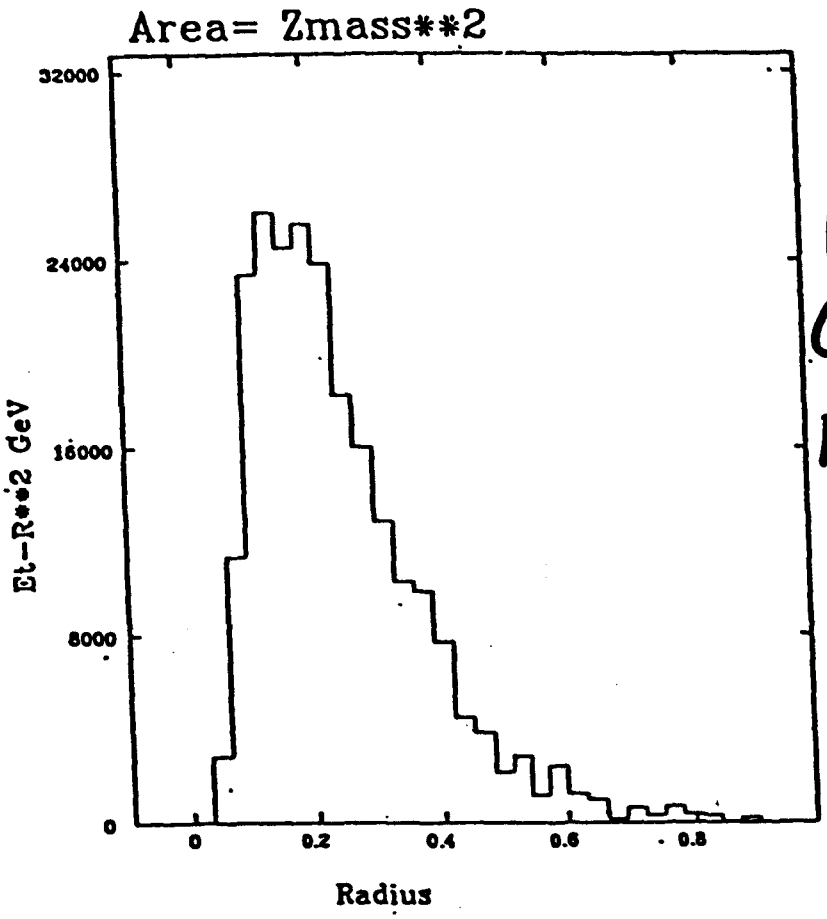

∴ Require Large Cone (≳ 0.6) To Fully Measure Z Mass.

Include Effect of Shower Spreading in Calorimeter. [SDC-91-00083]

Table 1.

B	Res.	Sim.	HAD=.05X.05	HAD=.1X.1
off	off	off	-2.04/2.67	-1.29/3.68
on	off	off	+4.54/4.03	+5.20/4.92
on	on	off	+4.60/4.86	+5.26/5.53
on	off	on	+7.93/3.94	+8.85/4.21
on	on	on	+8.02/4.68	+8.97/4.95

6% Diff.

b → eν Tagging in Top Decays

SDC-91-0005

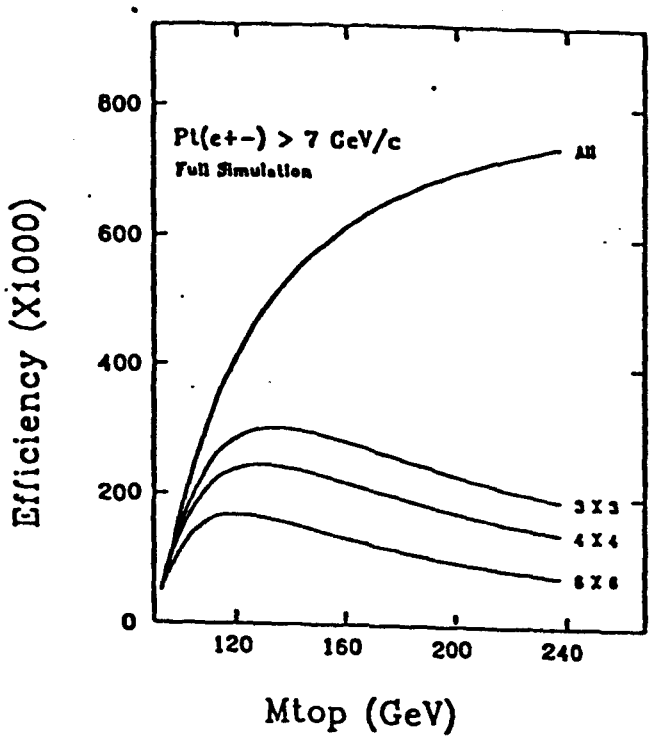

Figure 18

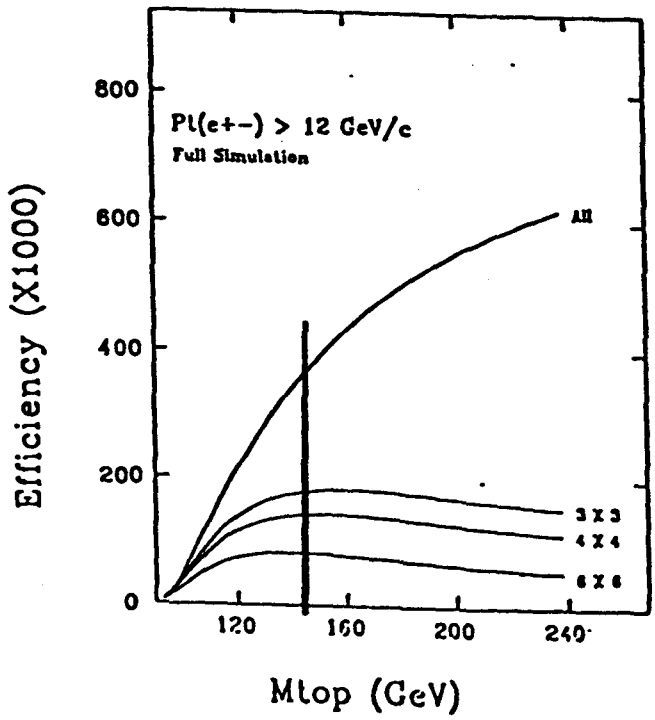

Figure 19

20% Loss of Efficiency going from 3 x 3 to 4 x HACI Isolat Cone.

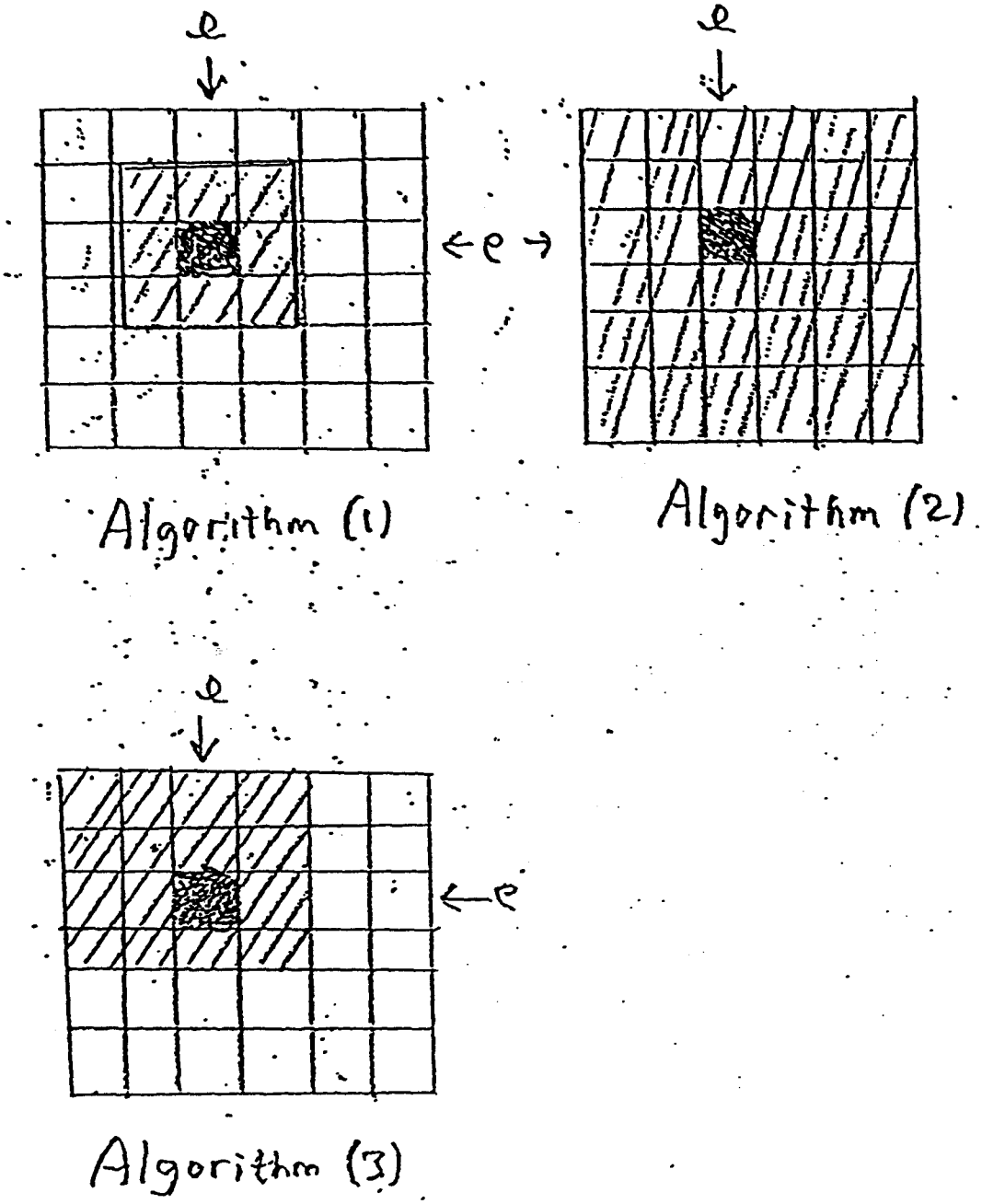

Figure 5

Solid Square = Electron Cell (.05 × .05)
Shaded Region = Definition of Hadron Energy

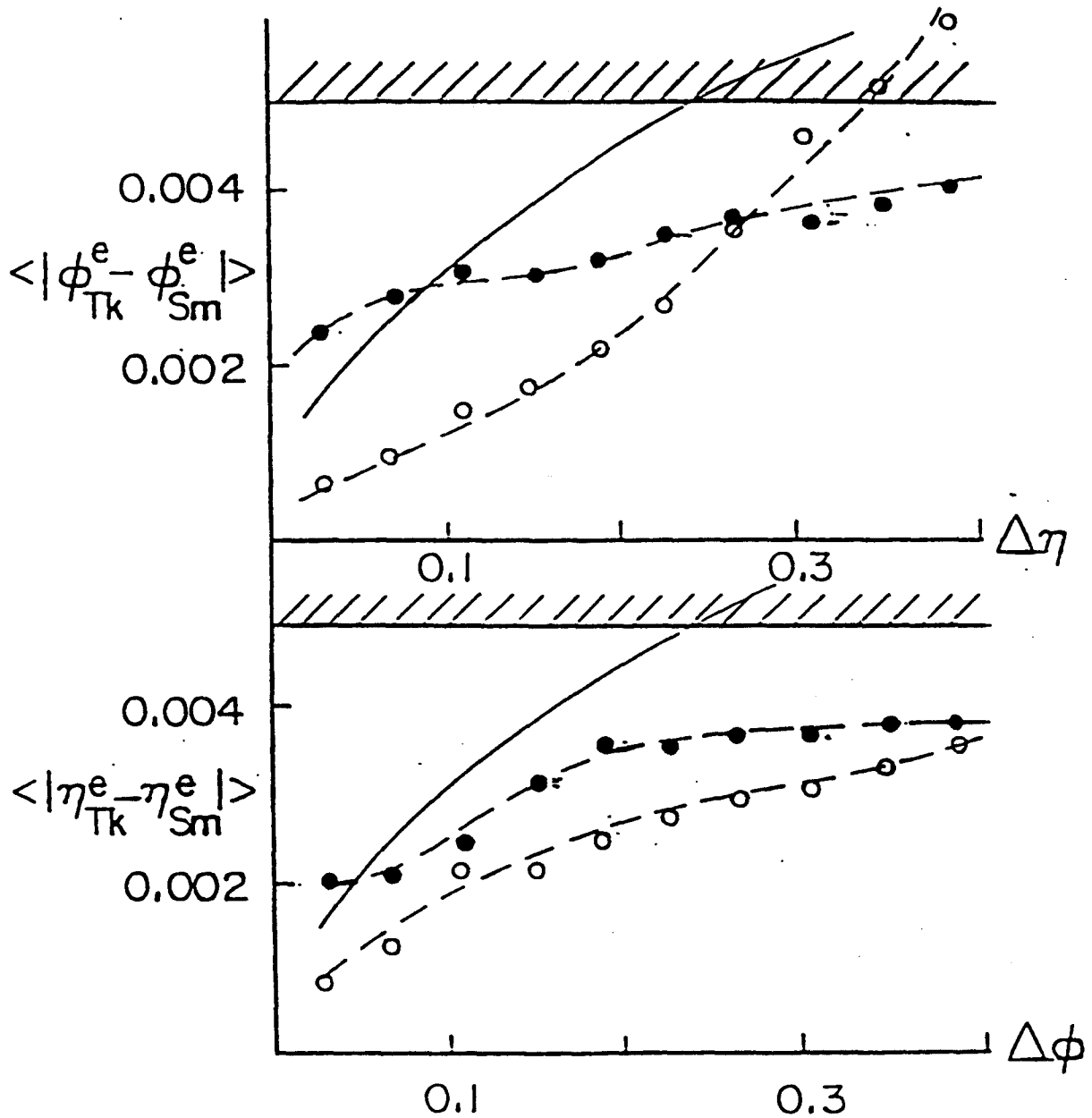

Figure 2.9 The mean deviation between the SM centroid and the exact tracking position as a function of strip length for t → Wb → ceν events. Strip width is 0.01. Points are , , field on, o , field off x 1/10. The solid curve is $\sqrt{length}$. The dashed curve is to guide the eye through the data. The shaded portion corresponds to the region where the matching error is > 1/2 the strip width. a) azimuthal strips, b) rapidity.

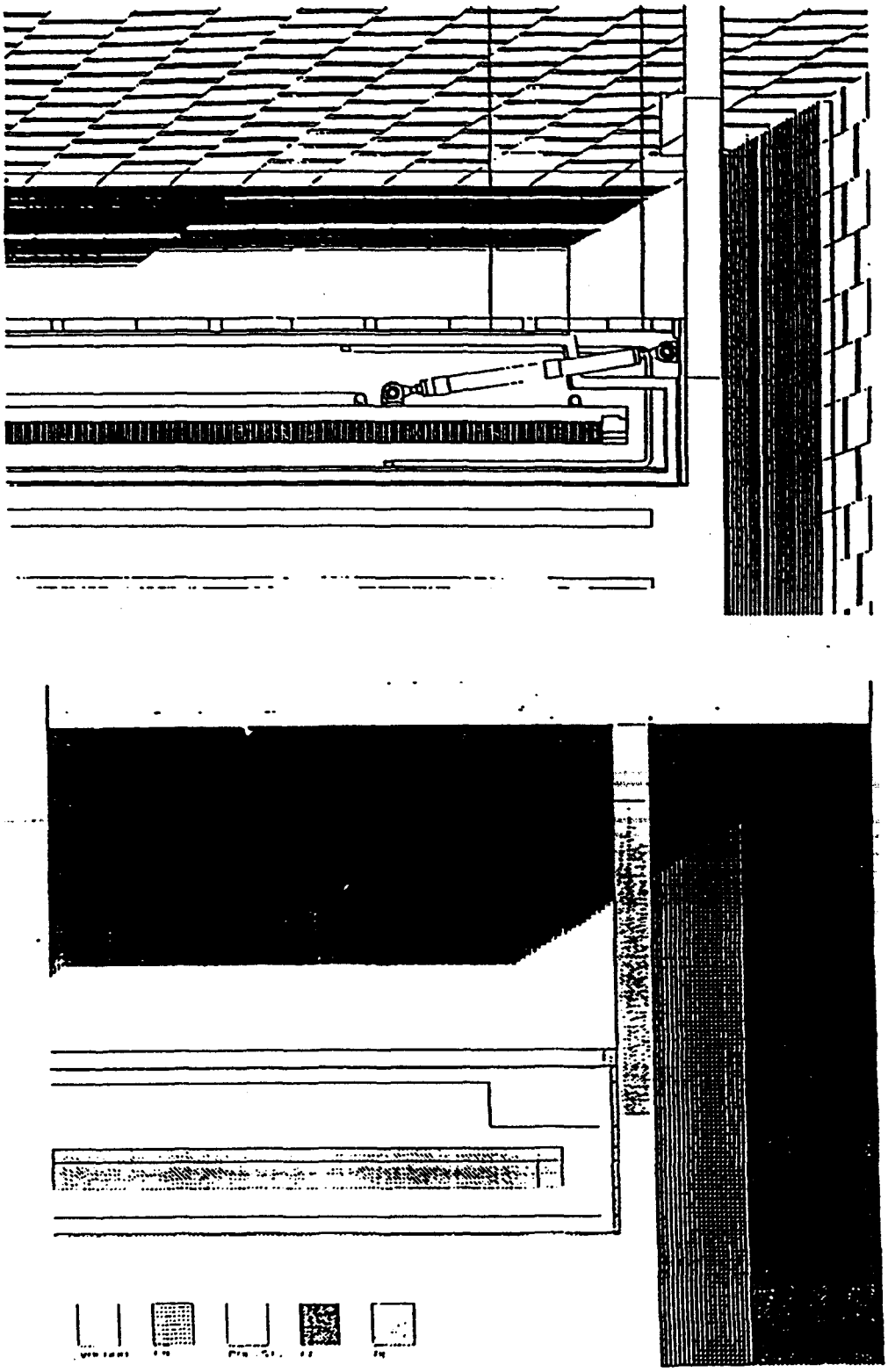

Figure 2.10 a)Solenoid drawing b) EGS model

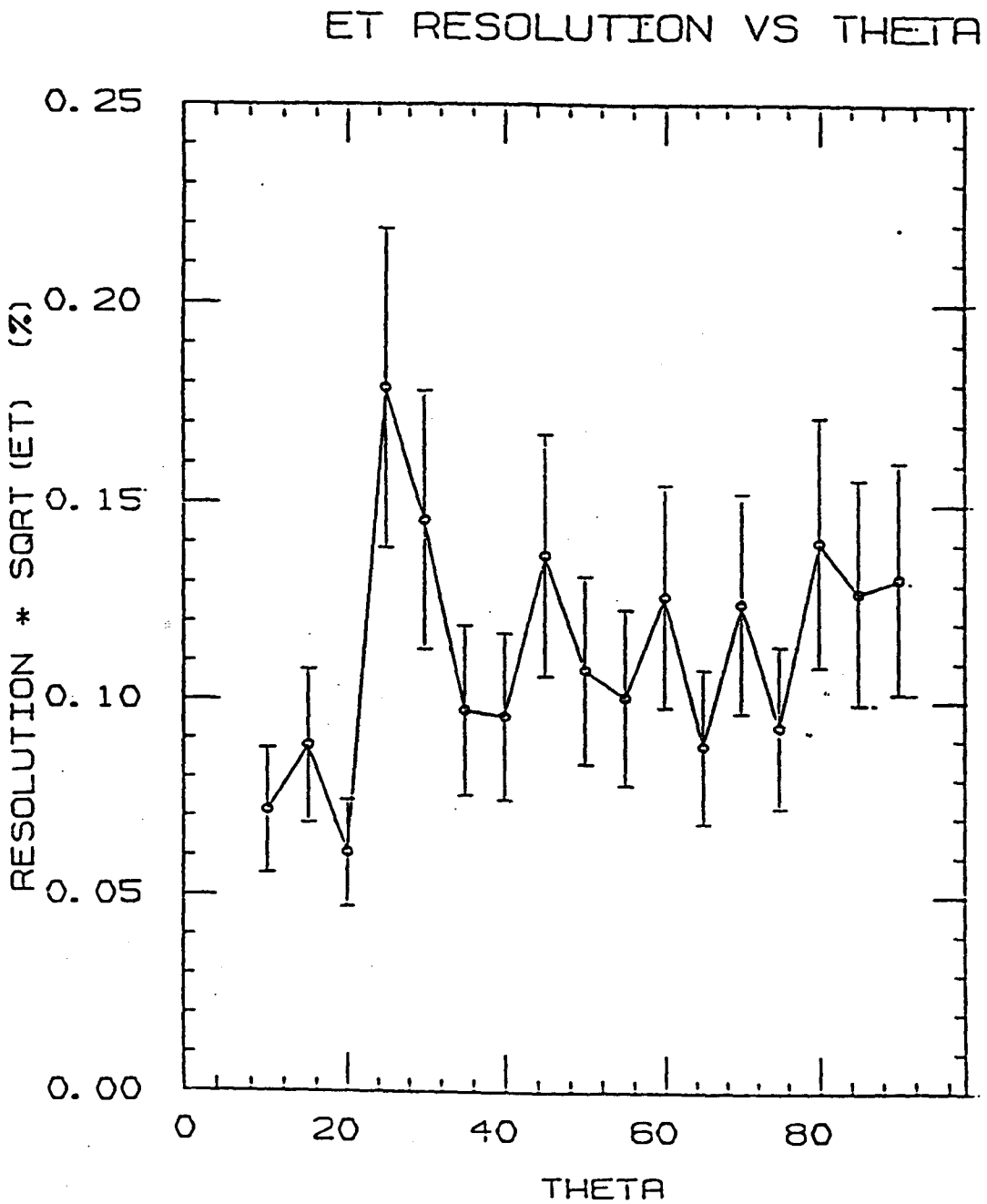

Figure 2.11 Coarse eta scan

Design Goals of the "Iron" Calorimeter

("Lead")

- Optimize EM Calorimetry
  - maximum sampling density subject to cost constraints
  - maximum hermeticity (no cracks or missing towers)
  - no support bulkheads or other projective structural elements.

- Adequate Hadronic Performance for lowest cost
  - minimum sampling consistent with adequate resolution
  - simplest absorber structure
  - provide strong structural base for EM calorimeter support

- Minimize Coil Forces and Magnetic Nonuniformity
  - iron absorber as close as possible to end of current sheet
  - lower internal stresses at same value of central field, or
  - higher value of central field for same internal stresses.

- Least Obtrusive Barrel/Endcap Transition
  - Lowest Xo Solenoid Support Structures
  - non-projective (vertical) crack through EM calorimeter
  - support arms not in ϕ-coincidence with cable plant.

- Simple Replacement of Endcap Scintillator
  - Endcap EM scintillator replaceable during few week shutdov
  - Endcap Hadron scintillator replaceable during few month sh

(Pb)

Detector	EM	HAC1	HAC2
BARREL	1/8" Pb	1" Fe	2" Fe
ENDCAP	1/4" Pb	2" Fe	4" Fe

Table 1: Absorber Sampling thicknesses in the "Iron" calorimeter design. Scintillator tile thickness is 2.5mm in all cases.

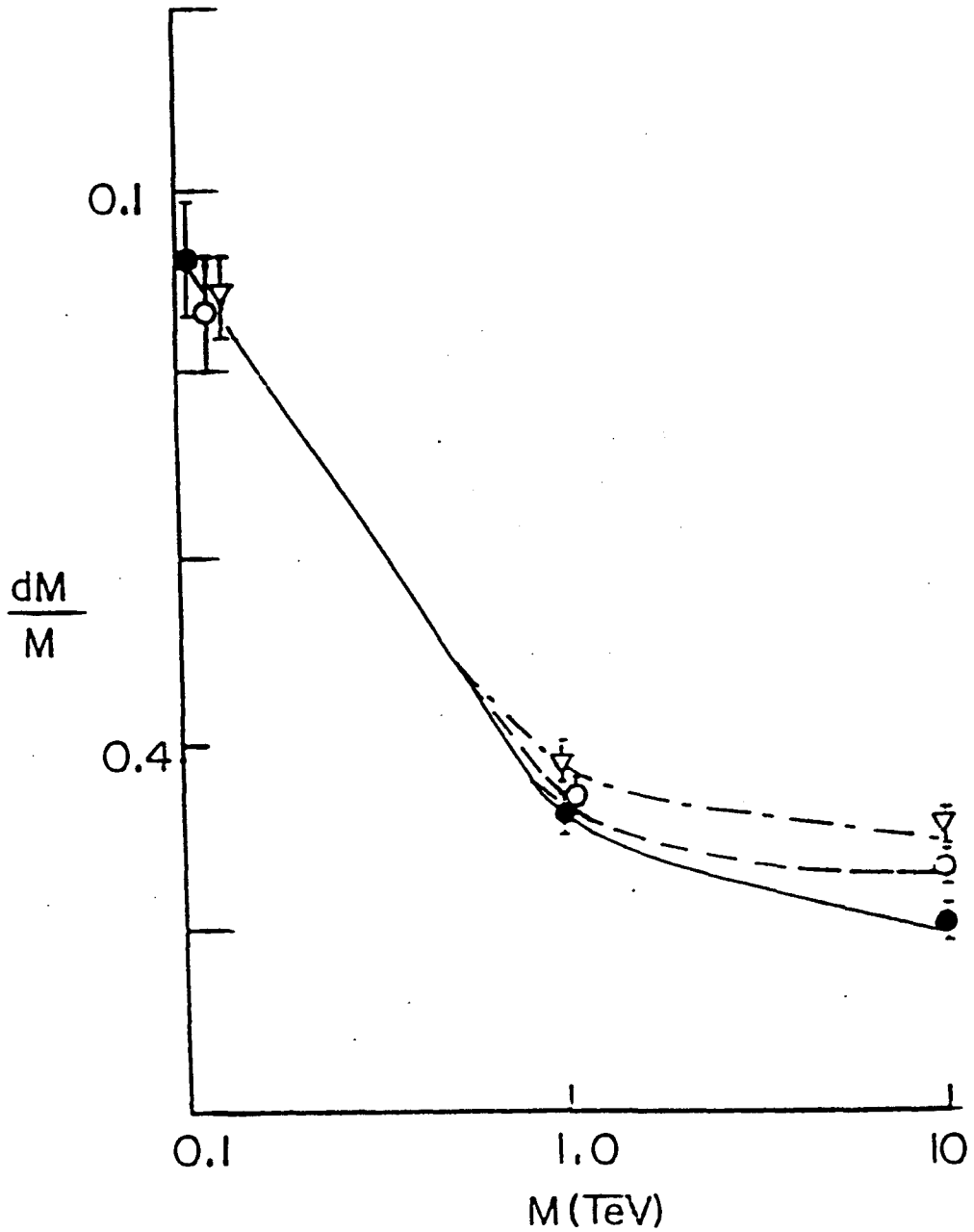

Figure 2.17 Dijet mass resolution as a function of mass. The points are for the "default" SDC calorimeter, . ,a calibrated calorimeter with e/h = 1.3, o , and a calorimeter with e/h = 1.3 which is only calibrated at asymptotic energies, V.

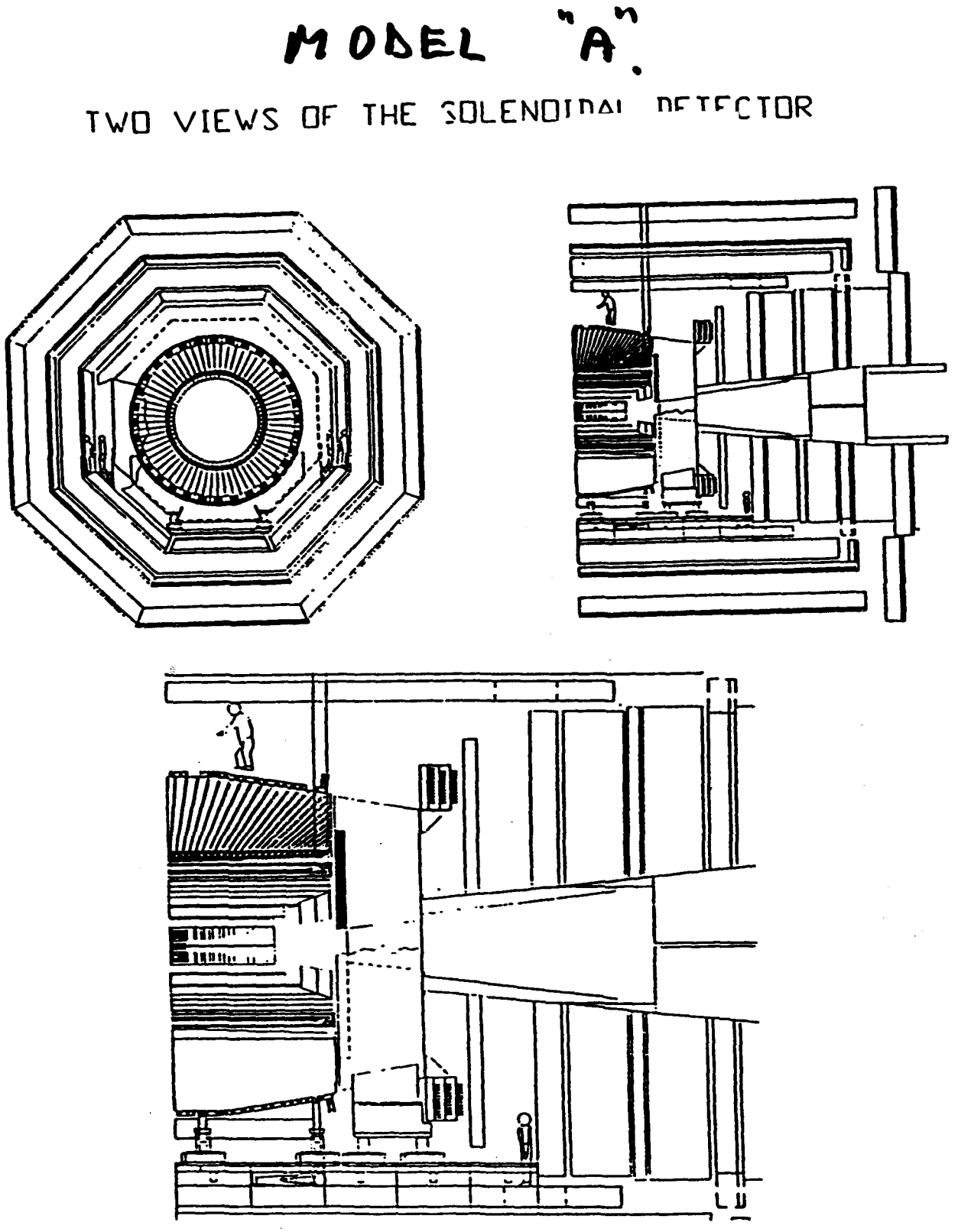

Figure 3.1(a) - $R - \phi$ view and $R - Z$ half-view of the "Iron" calorimeter engineering design.

Figure 3.1(b) - $R - Z$ half-view of the "Iron" calorimeter engineering design.

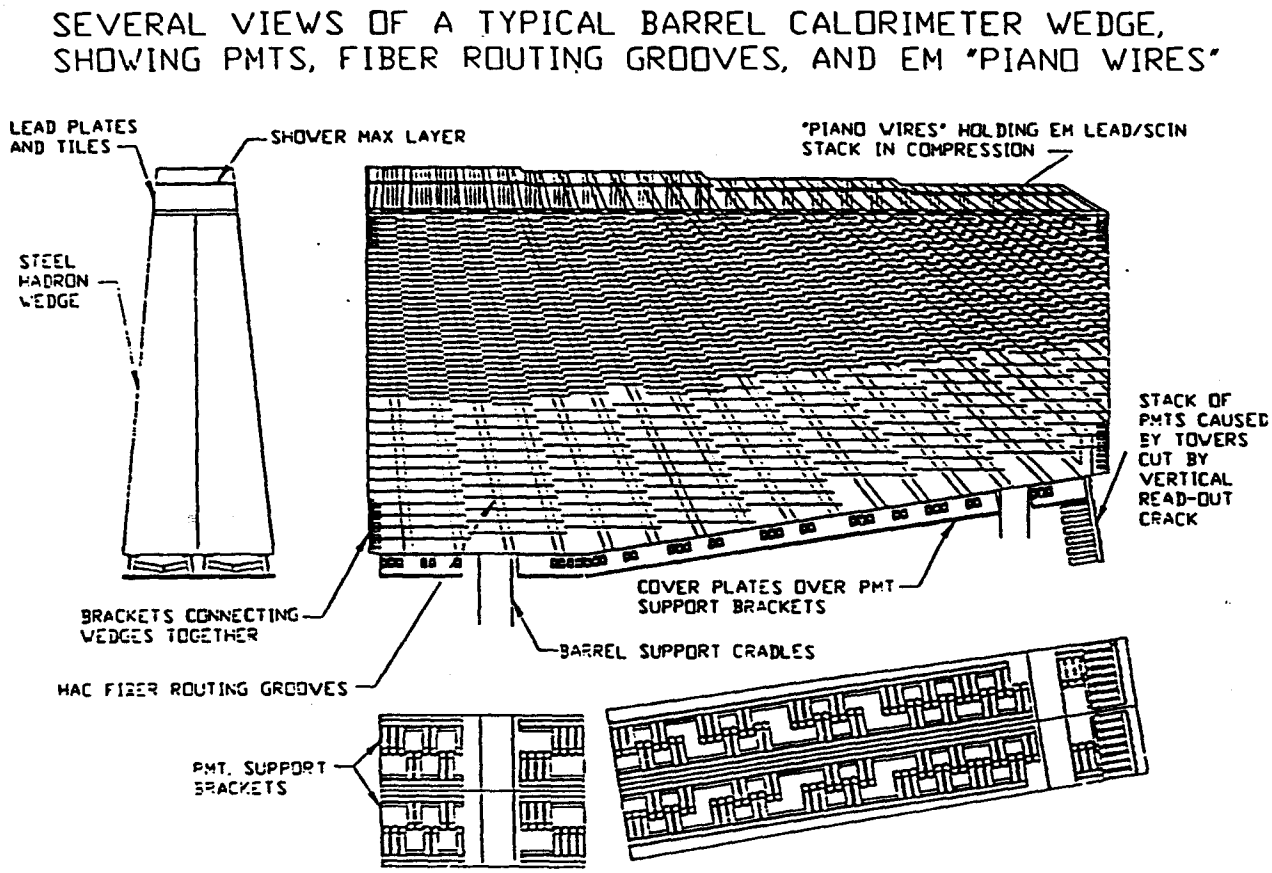

Figure 3.1(c) - Several views of a typical barrel calorimeter wedge, showing PMTs, fiber routing grooves, and EM "Piano Wires".

CROSS SECTIONS THROUGH THE END CAP SHOWING TILE SHAPES

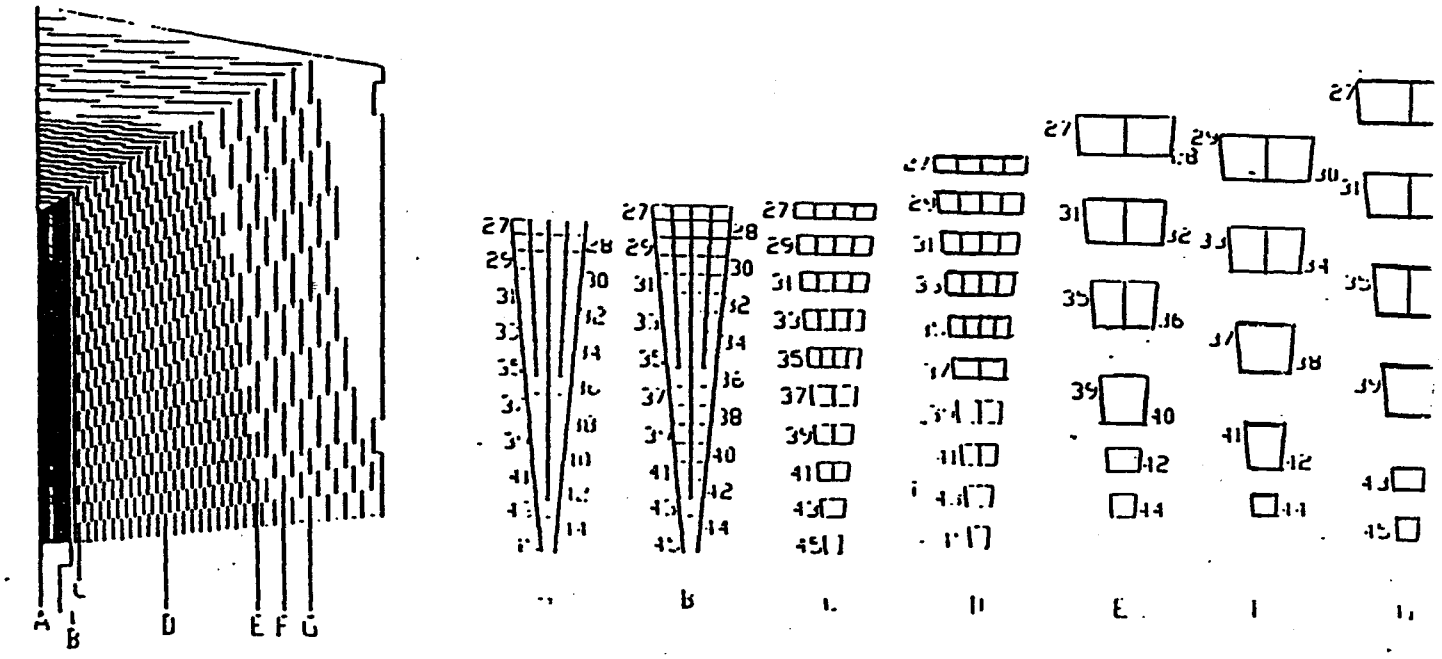

Figure 2.7 End Cap Segmentation

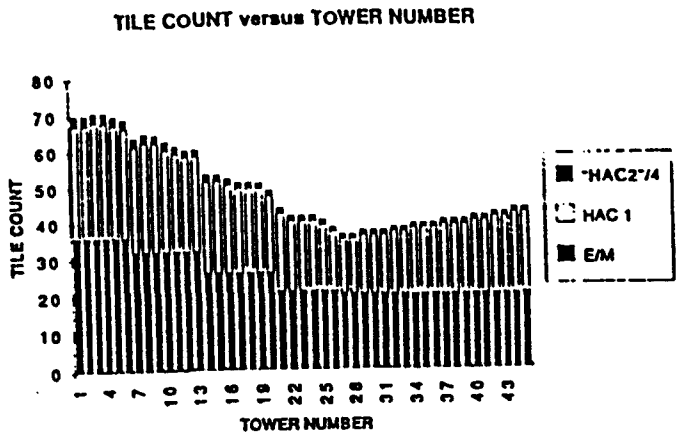

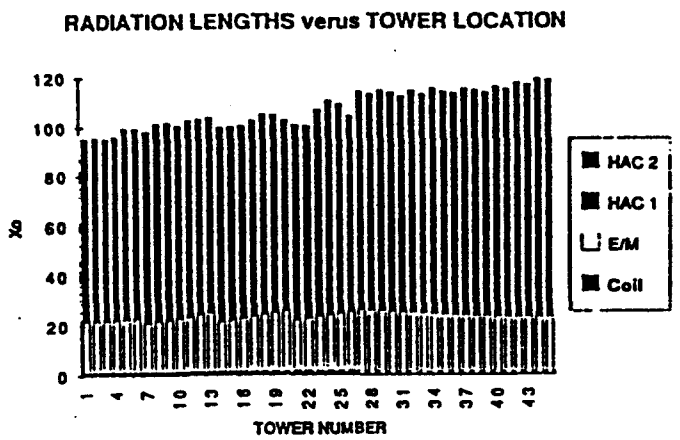

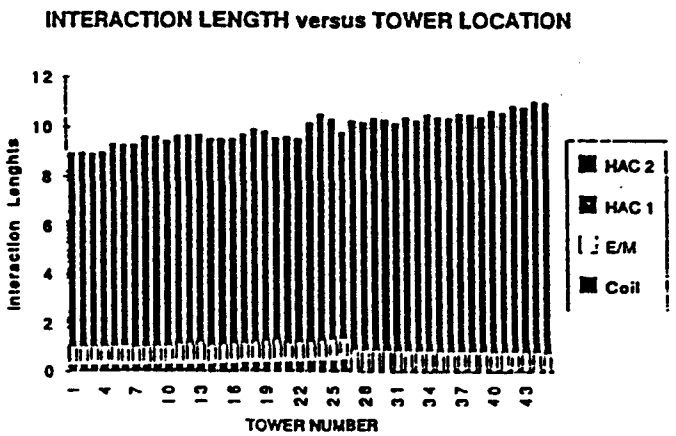

Figure 3.2 - Scintillator tile counts as a function of tower number in the iron calorimeter design. The HAC2 tile counts have been averaged over 4 towers to reflect the decreased segmentation in HAC2. Note that the majority of tiles are in the EM section.

Figure 3.3 - Calorimeter depth in radiation lengths X_0 as a function of tower number. The target for the depth for the EM calorimeter was to stay between between 22 and 25 X_0.

Figure 3.4 - Calorimeter depth in interaction lengths λ_P as a function of tower number. The target for the depth for the full calorimeter was 9λ at 90 degrees and 11λ at 5.7 degrees.

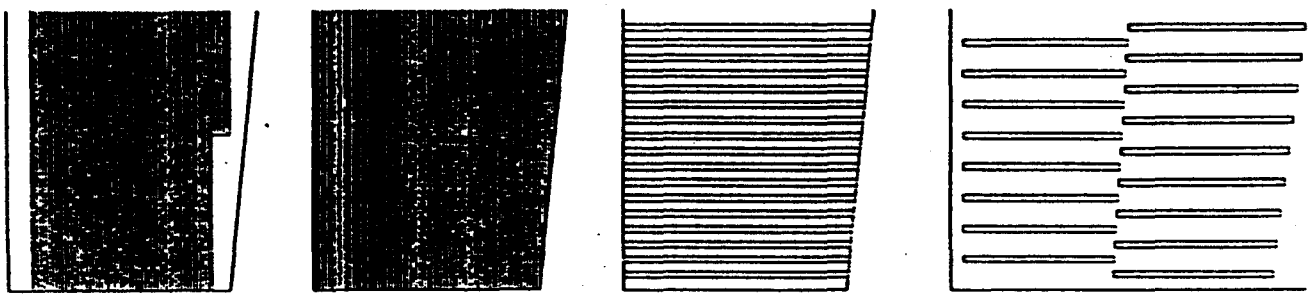

END VIEWS OF THREE DIFFERENT STYLES OF WEDGE STEEL

SIDE VIEW OF SLOTS FOR TILES

1/8" THICK PUNCHED LAMINATIONS BETWEEN SIDE PLATES. SIDE PLATES HELD TOGETHER BY THREADED RODS. THIS METHOD IS A FALL-BACK SOLUTION IF THE FUSION BONDING TECHNIQUE FAILS IN DEVELOPMENT.

1/8" THICK LAMINATIONS FUSED TOGETHER IN OVEN WITH A REDUCING ATMOSPHERE. MAY BE THE CHEAPEST ONCE FABRICATION VARIABLES ARE UNDERSTOOD AND RELIABILITY OF BOND ATTAINED.

"THICK" PLATE METHOD USING MILLED PLATES AND SPACERS PLUG WELDED TOGETHER. LOWER PIECE COUNTS BUT MORE LABOR INTENSIVE TO DO PLUG WELDING.

SKETCH SHOWING THREE DIFFERENT FABRICATION TECHNIQUES FOR THE BARREL 1/64 STEEL HADRON WEDGES

Figure 3.9 - Three fabrication techniques for fabricating the iron block of the Barrel Hadron calorimeter.

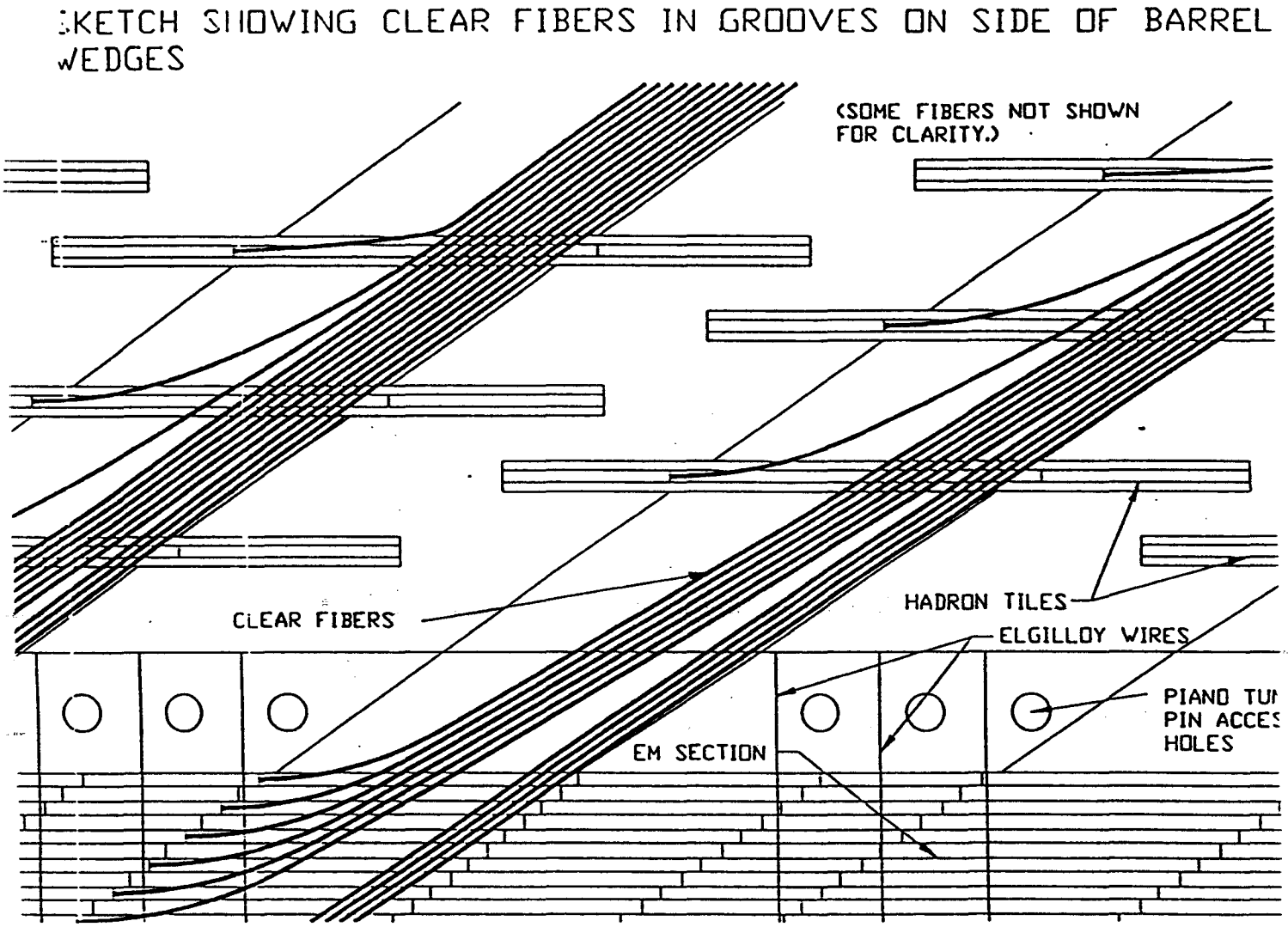

Figure 3.7 - Side view of the Barrel EM calorimeter, showing fiber routing pattern and "piano wires" for stack compression.

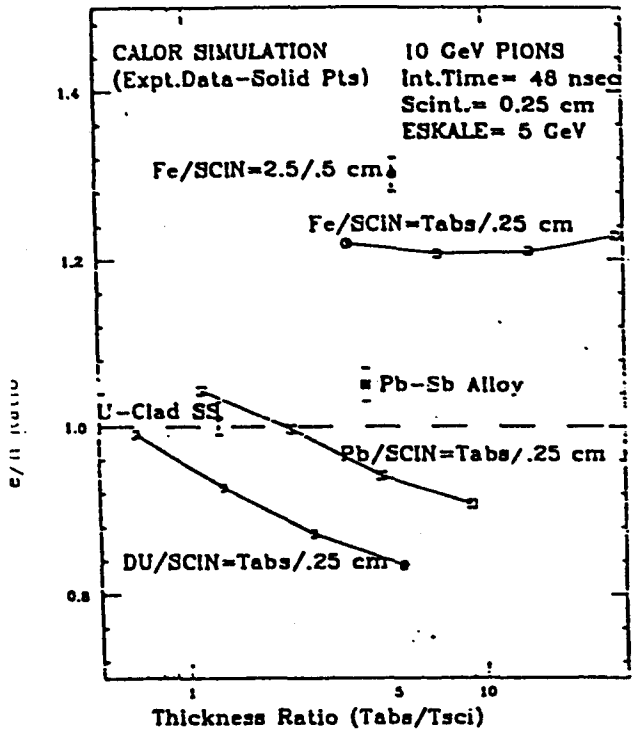

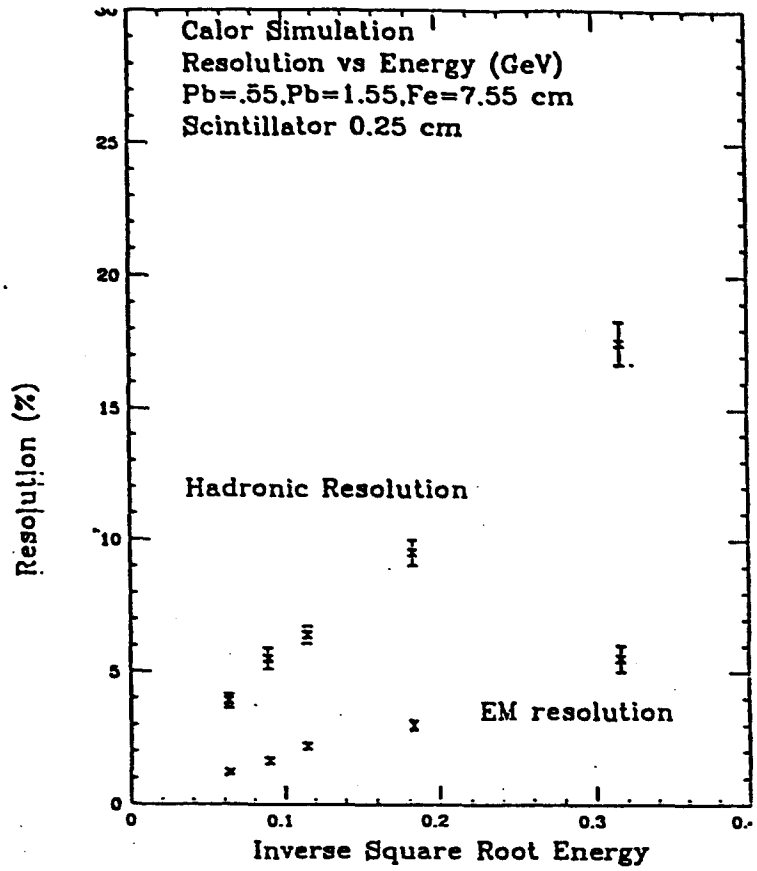

Pb/SCIN= 0.56/0.25 cm, Fe/SCIN= 1.75/0.25 cm, ESKALE=5GeV

Configuration		Simple Sum	(dE/dX)ΔX Weighting	EMC Cali. Correction wrt. (dE/dX) weightg =0.715	e/h =1.00 Correction wrt. (dE/dX) weightg =0.846
Pb 8λ	e/h	0.99±.02			
	Reso.	9.7±.75			
Pb 6λ,Fe 2λ	e/h	0.99±.02	1.00±.0	1.01±.02	1.00
	Reso.	11.2±.75	11.1±.78	11.0±.77	10.5±.75
Pb 4λ,Fe 4λ	e/h	1.03±.02	0.98±.02	1.00±.02	1.00
	Reso.	13.6±.75	11.2±.78	10.6±.77	10.5±.75
Pb 2λ,Fe 6λ	e/h	1.26±.02	0.94±.02	1.06±.02	1.00
	Reso.	23.3±.75	14.1±.75	12.0±.75	12.0±.75
Pb 1λ,Fe 7λ	e/h	1.65±.02	0.90±.02	1.12±.02	1.00
	Reso.	27.3±.75	14.5±.80	13.0±.77	12.9±.75
Fe 8λ	e/h	1.19±.02			
	Reso	17.5±.75			

Table 3: HADRONIC RESOLUTION AND e/h RATIO FOR LEAD-IRON CONFIGURATIONS (10 GeV π^-)

MODEL "B"

Tile/Fiber Descope 4 Calorimeter

(Quadrant Cross Section)

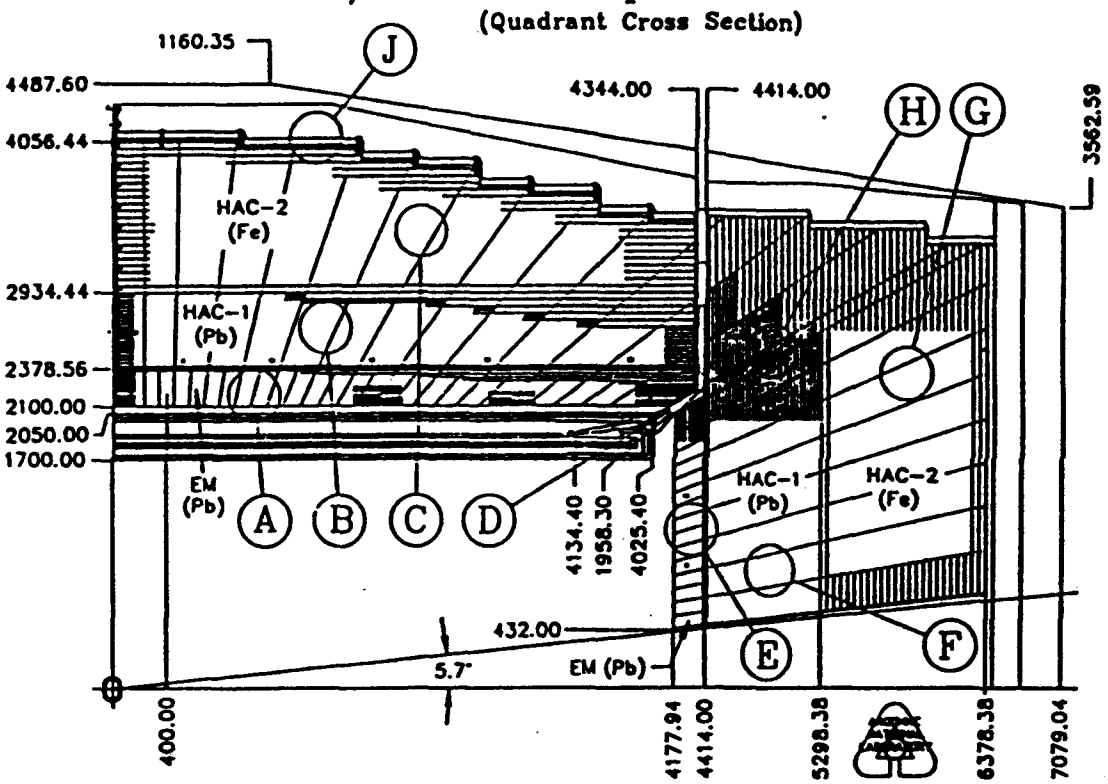

Tile/Fiber Descope 2 Calorimeter

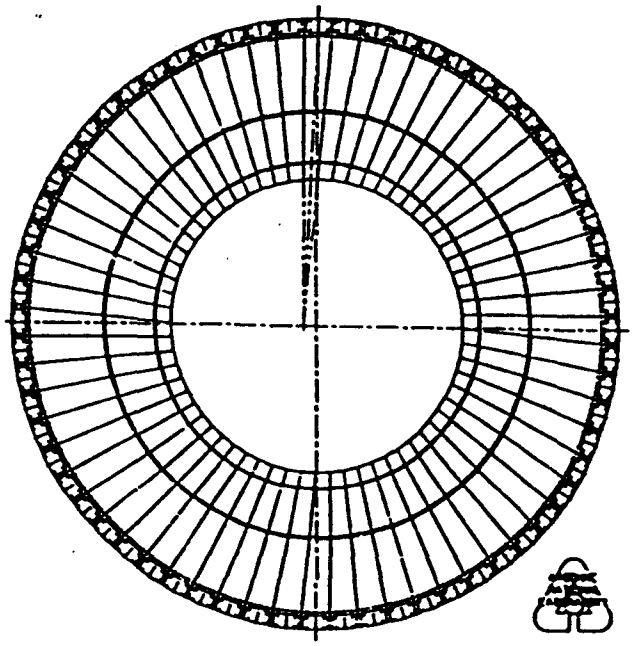

Figure 4.1 a)MODEL B Quadrant Cross section, b) End Section

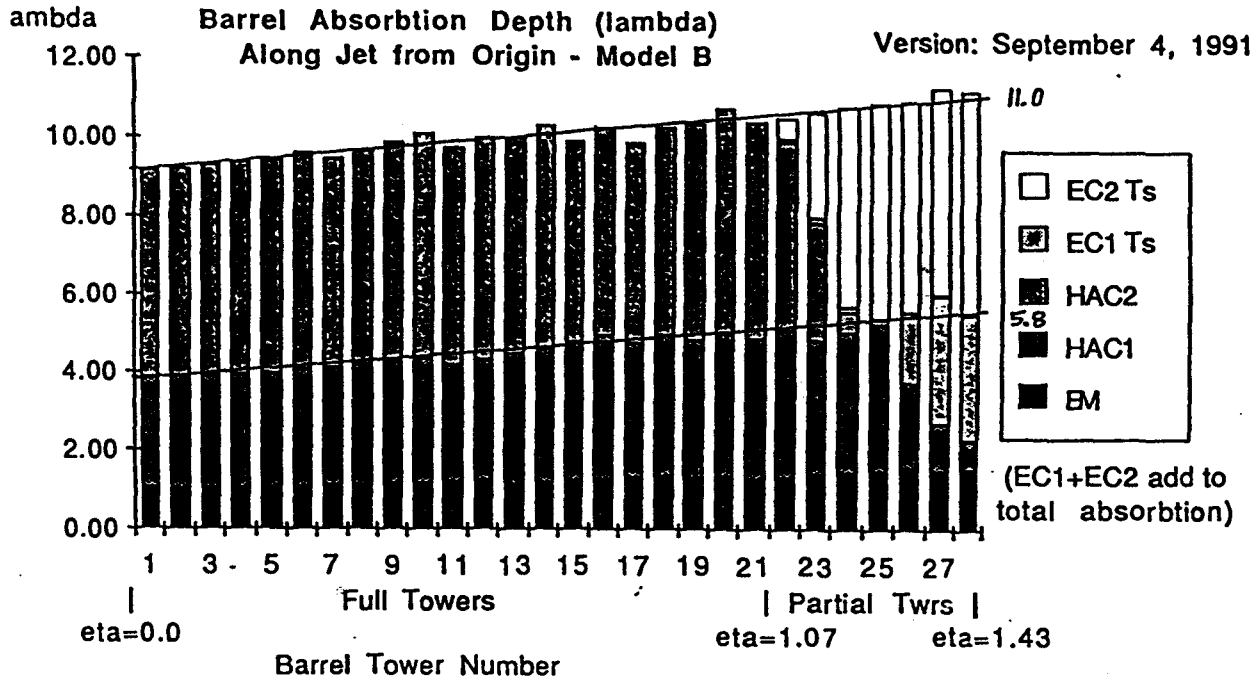
ambda
Barrel Absorbtion Depth (lambda)
Along Jet from Origin - Model B
Version: September 4, 1991
12.00
10.00
8.00
6.00
4.00
2.00
0.00
11.0
5.8
EC2 Ts
EC1 Ts
HAC2
HAC1
EM
(EC1+EC2 add to total absorbtion)
1 3 5 7 9 11 13 15 17 19 21 23 25 27
Full Towers
Partial Twrs
eta=0.0
eta=1.07
eta=1.43
Barrel Tower Number

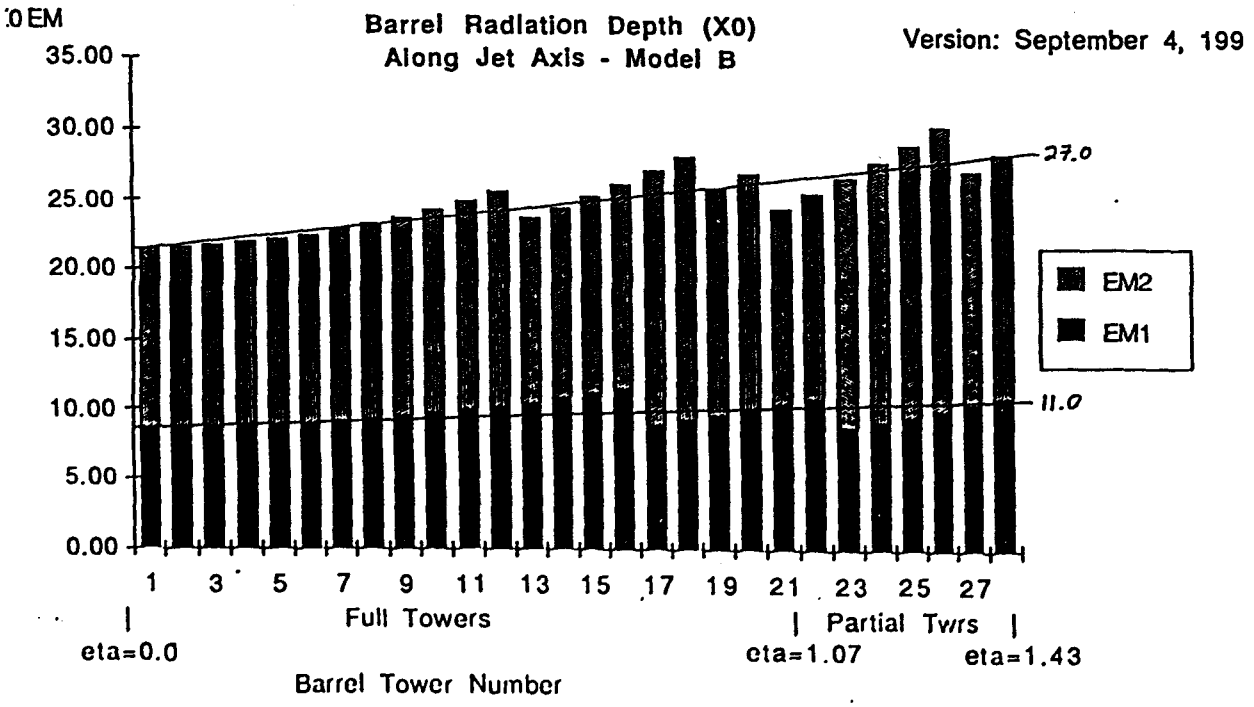
0 EM
Barrel Radiation Depth (X0)
Along Jet Axis - Model B
Version: September 4, 199
35.00
30.00
25.00
20.00
15.00
10.00
5.00
0.00
27.0
11.0
EM2
EM1
1 3 5 7 9 11 13 15 17 19 21 23 25 27
Full Towers
Partial Twrs
eta=0.0
eta=1.07
eta=1.43
Barrel Tower Number

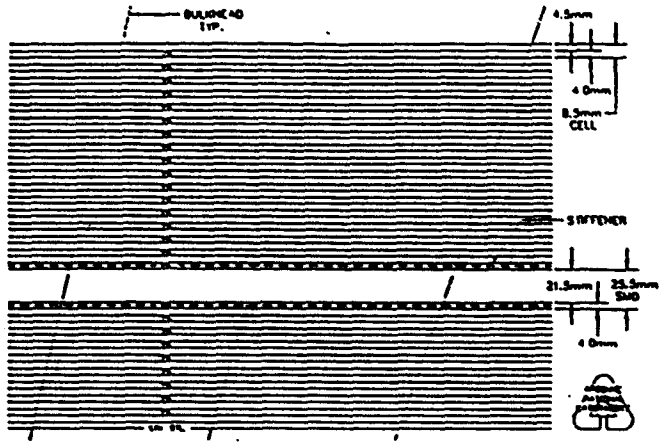

(A) Barrel EM Structure

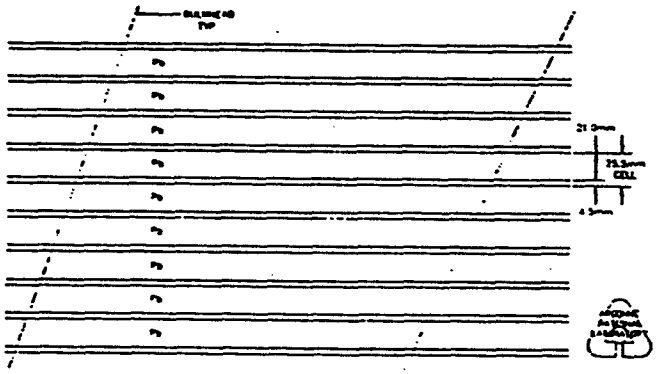

(B) Barrel HAC-1 Structure

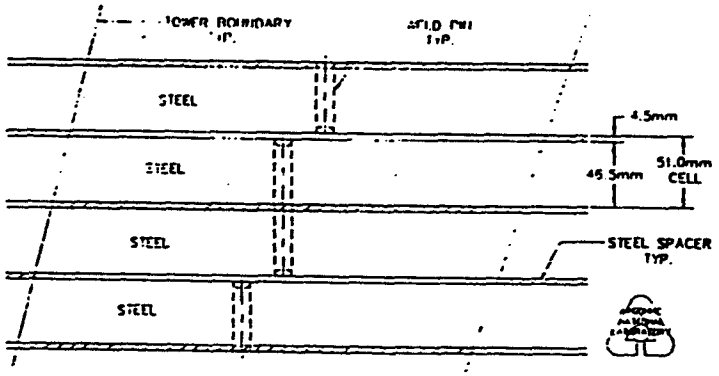

(C) Barrel HAC-2 Structure (Welded Plate Design)

Figure 4.2 Barrel EM Structure

Figure 4.3 Barrel HAC1 Structure

Figure 4.4 Barrel HAC2 Structure

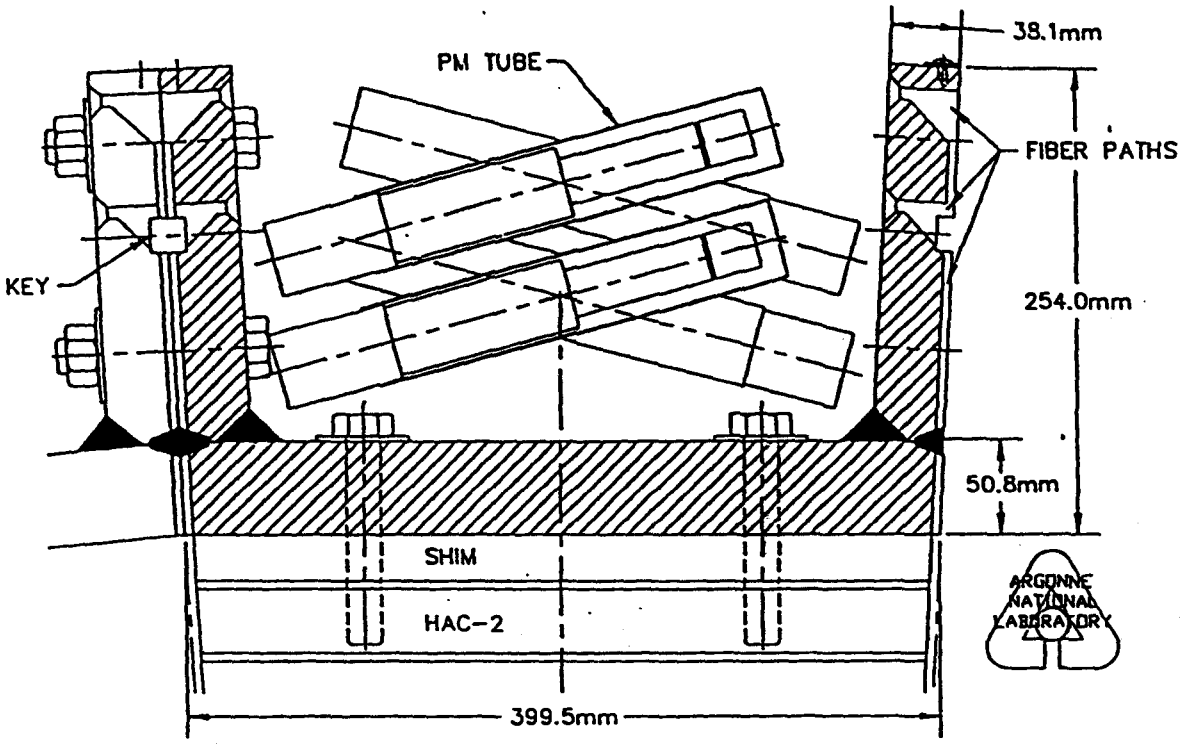

Ⓙ Support Channel-Module

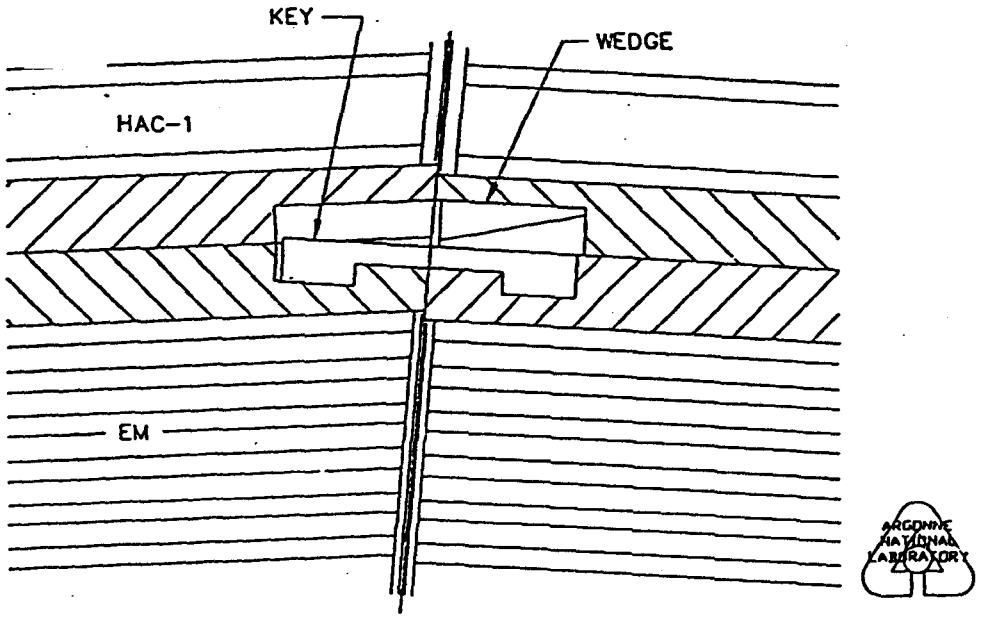

Inner Module Connection

Figure 4.10 a) Support Channel-Module, b)Inner Module Connection

"EGG-CRATE"
STAINLESS STEEL
SHELL.

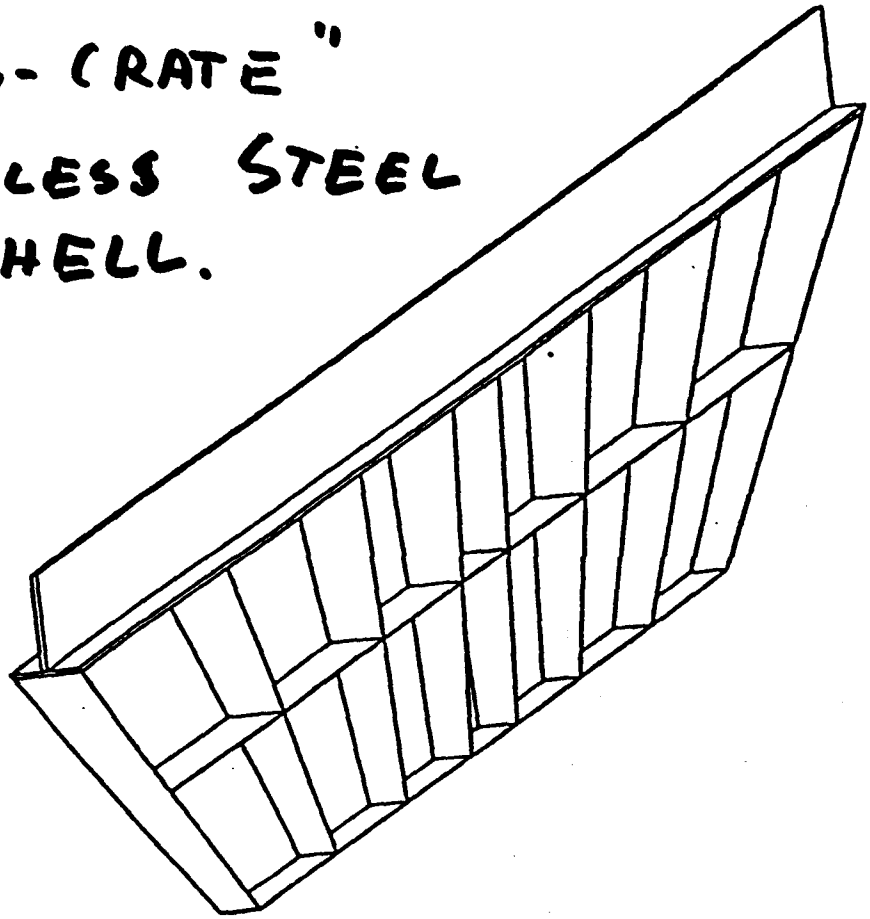

FABRICATION FACILITY

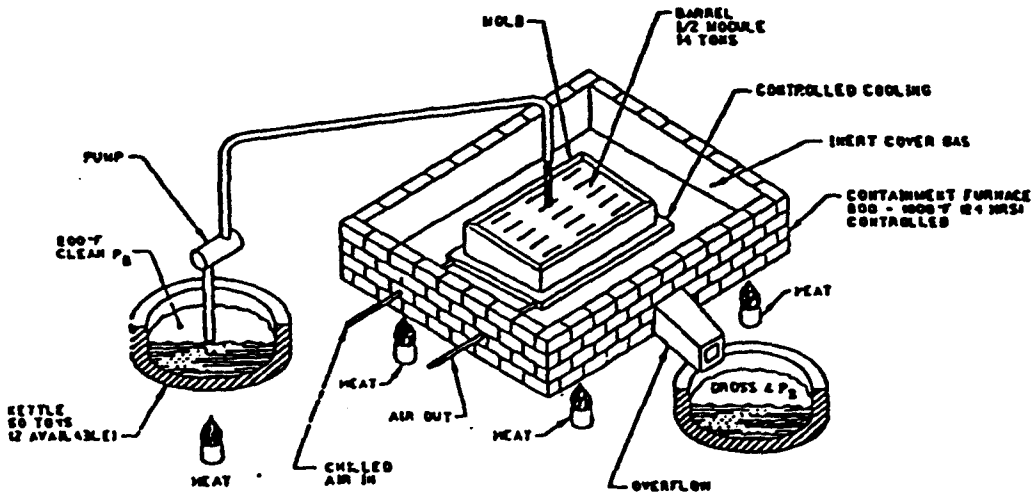

ESTIMATED COST APPROX. $200,000

ADVANTAGES

1.) GOOD THERMAL CONTROL
2.) ELIMINATE DROSS BY CONTINUOUS FLOW
3.) CONTROLLED COOLING
4.) ABILITY TO TOP OFF (SHRINKAGE)
5.) ABILITY TO CONTROL COOLING
6.) ABILITY TO CONTROL ATMOSPHERE

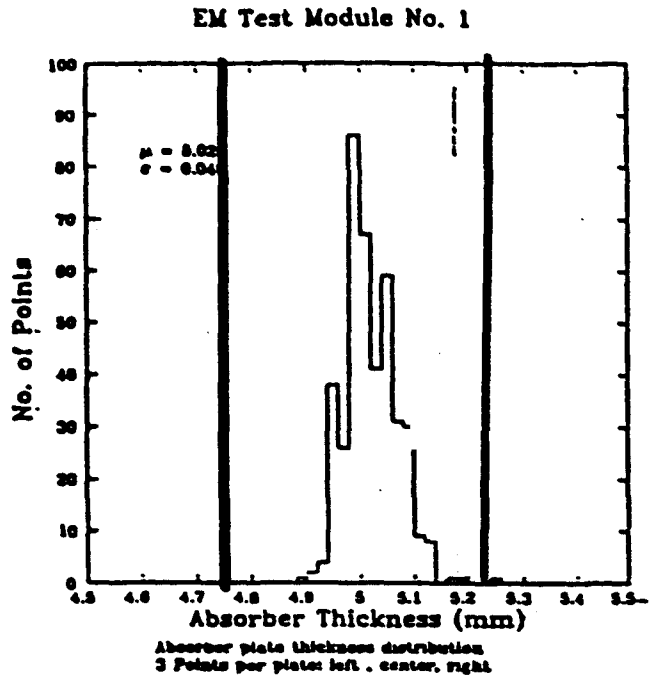

$\mu = 5.03$
$\sigma = 0.05.$

Figure 11.2 Absorber plate thickness and flatness uniformity for plates cast in EM Test Module 1.

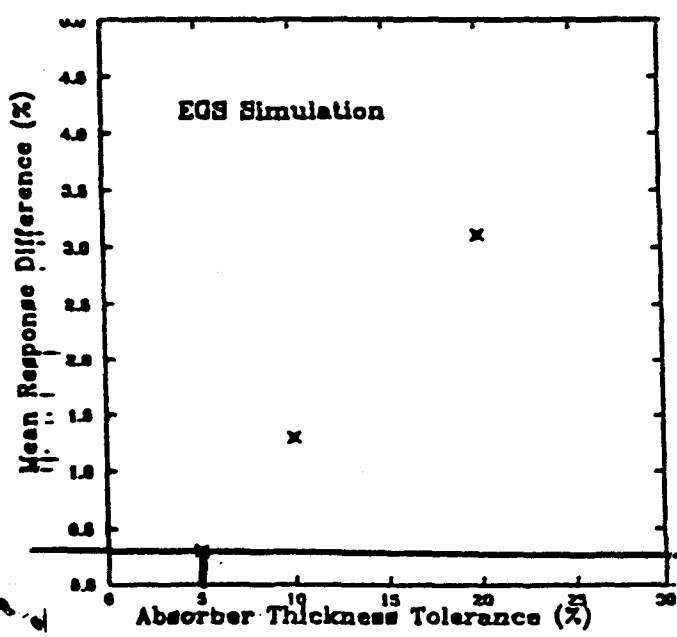

~0.3% Const. Term

5% Abs. Tol.

Figure 11.3 EGS prediction of expected non-uniformity as a function of absorber thickness specification[2]

STRESS IN LEAD
3 O'CLOCK POSITION

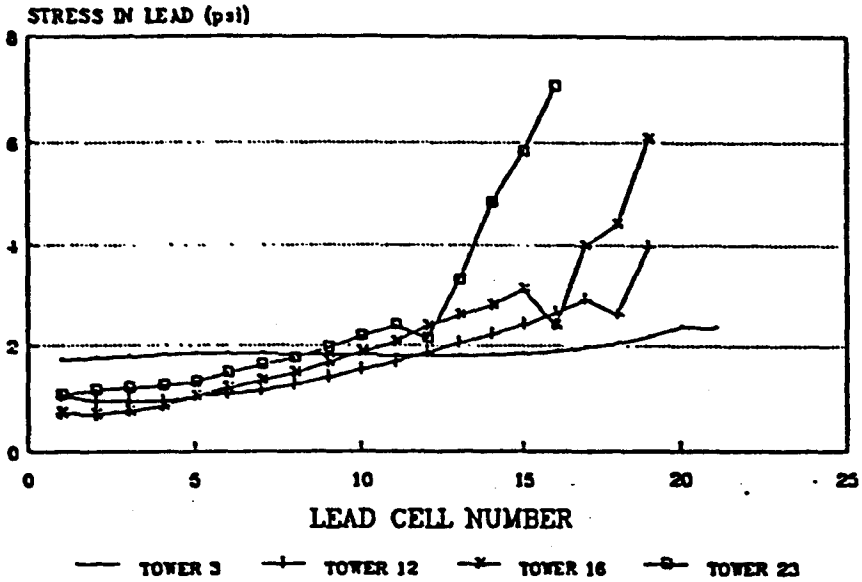

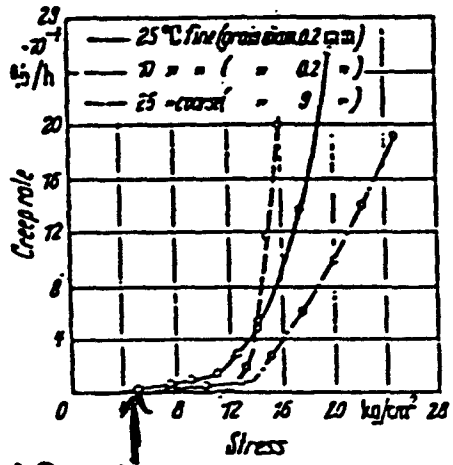

60 psi.

Fig. 222.
Creep rate of commercial lead in relation to load. (According to v. HANFFSTENGEL and HANEMANN).

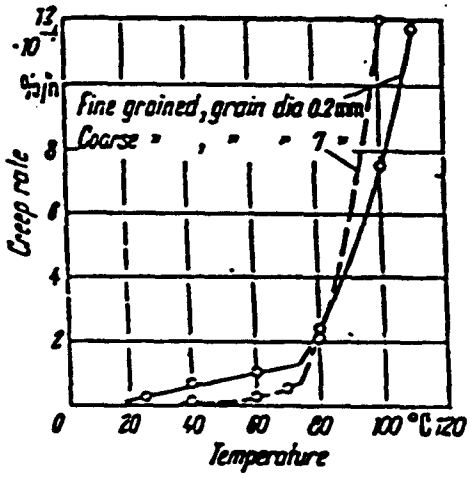

Fig. 223.
Creep rate of commercial lead in relation to temperature. Stress 5 kg/cm². (According to v. HANFFSTENGEL and HANEMANN).

NONDENOMINATIONAL DESIGN ELEMENTS

- Support Concept
- Assembly Concept
- Magnetic Model Analysis
- Endcap EM Replacement Concept
- Shower Maximum Detector Concept
- Photomultiplier Integration Concept
- Optical System Conceptual Design
- Calibration Concept

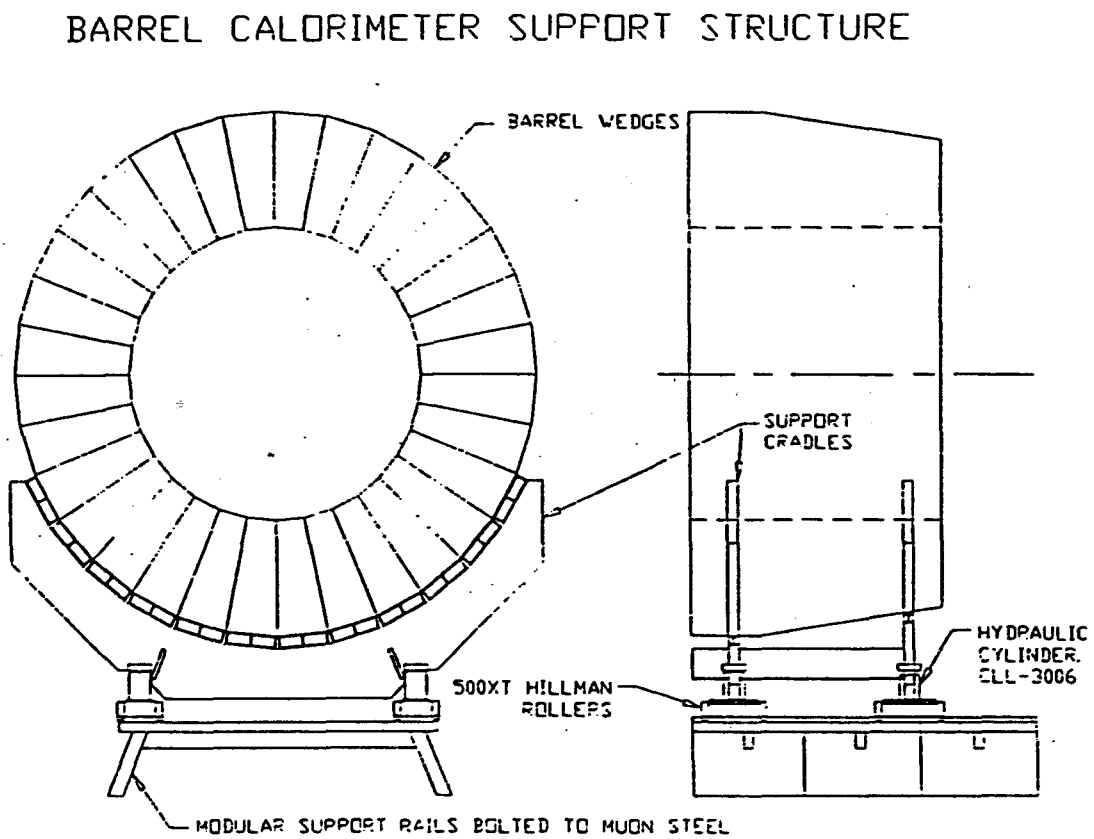

Figure 3.15(a) - Barrel calorimeter support structure. In the iron design, only two cradles and Hillman rollers are required.

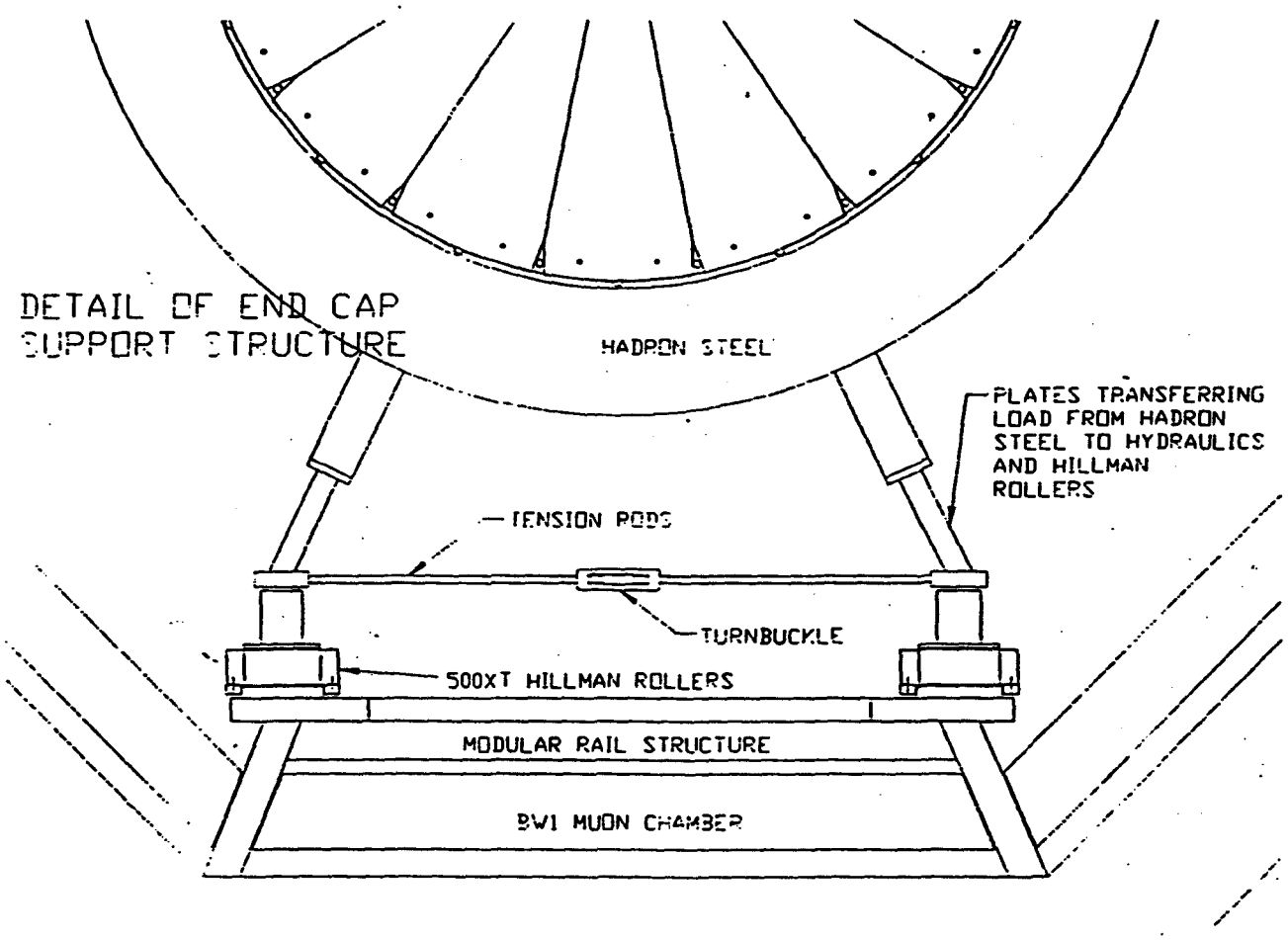

Figure 3.27 - End view of the Endcap support structure.

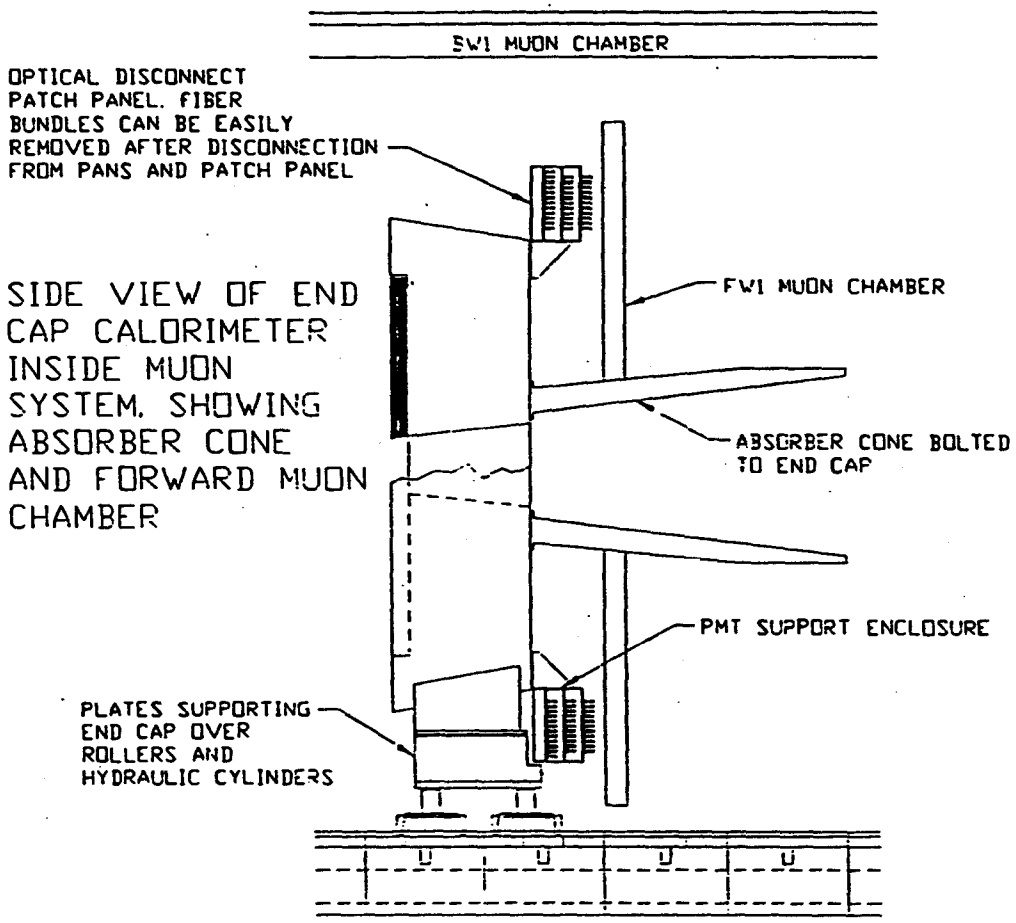

Figure 3.22 - Side view of Endcap calorimeter including possible positions of the PMT array.

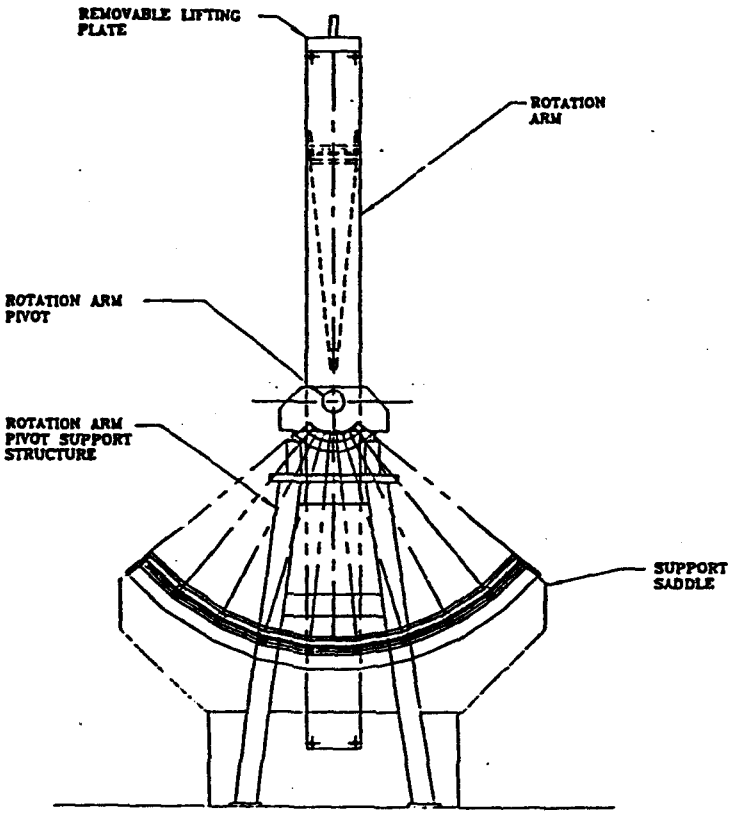

Figure 4.33 Endcap HAC assembly support pivot and installation sequence.

Magnetic Field Uniformity.

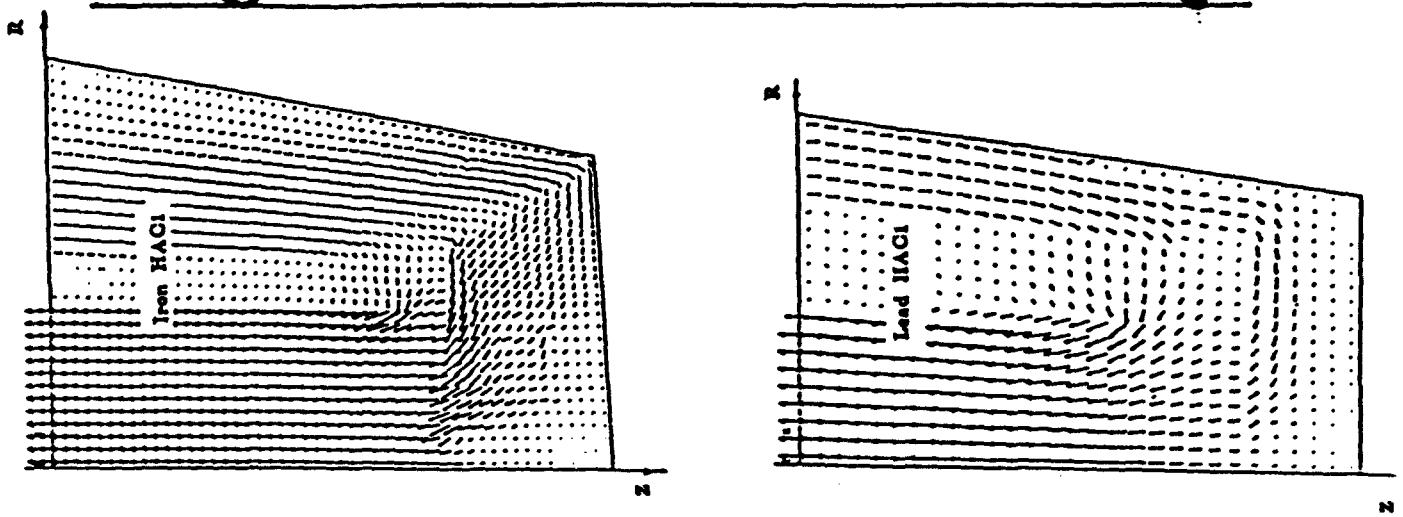

Figure 5.3 Magnetic Model magnetic flux for the Model A and Model B geometries.

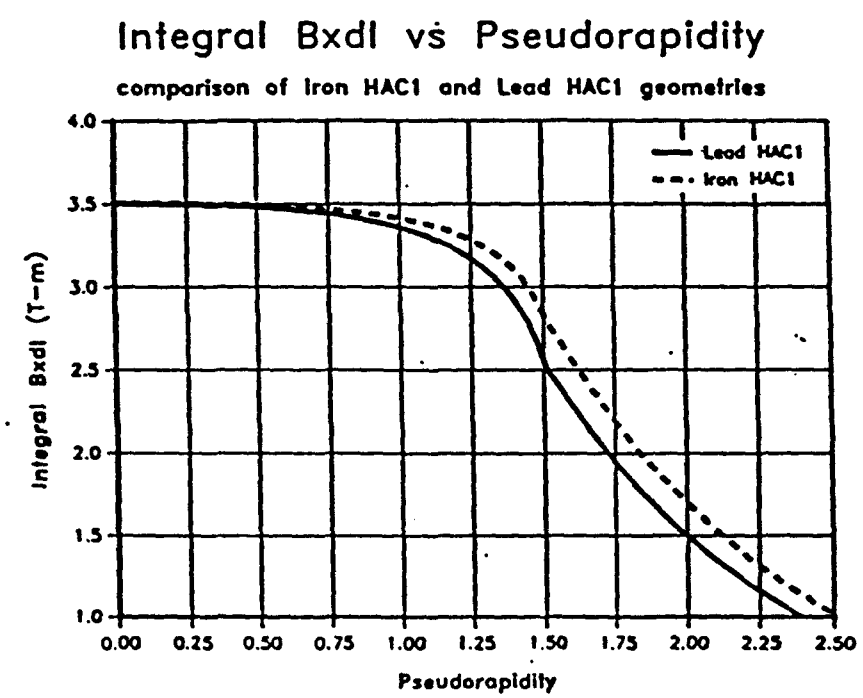

3.19 EM CALORIMETER REPLACEMENT PROCEDURE

3.19.1 Asumptions

- All Layers of EM Need Replacement
- Readout Fiber "Extension Cords" Outside of Radiation Field are OK
- Spare "Pizza Pan Assemblies" of Scintillator Tested and Ready
- 2-6 Person Shift Crew Depending on Task
- No Competition for Tracker Access
- No Undue Overhead for Radiation Safety
- Local Facility Exists for Printing Phototube Masks
  from PMT Measurements

3.20 Task Sequence for for EM Scintillator Replacement

- Retract Endwall Minimum of 1.5m
- Uncable Optical Harnesses & Secure Ends
- Disconnect Source Tube Assemblies
- Attach Extender Bars, Open Up Stack
- Remove & Replace Scint. Octants
  160 Octants @20 Mins Ea.
- Recompress Stack and Remove Extender Bars
- Reconnect Optical Harnesses & Source Tubes
- Source Measurement
  (80 Channels/wedge) * (4 mins/scan)
- Problem Fixup & Source Check
- Install PMT Masks
  (2000 PMTs) * (1 min/mask) * (2 two-man crews)
- Final Source Scan Verify Masks
- Attach & Verify Nitrogen Purge
- Close Endwall

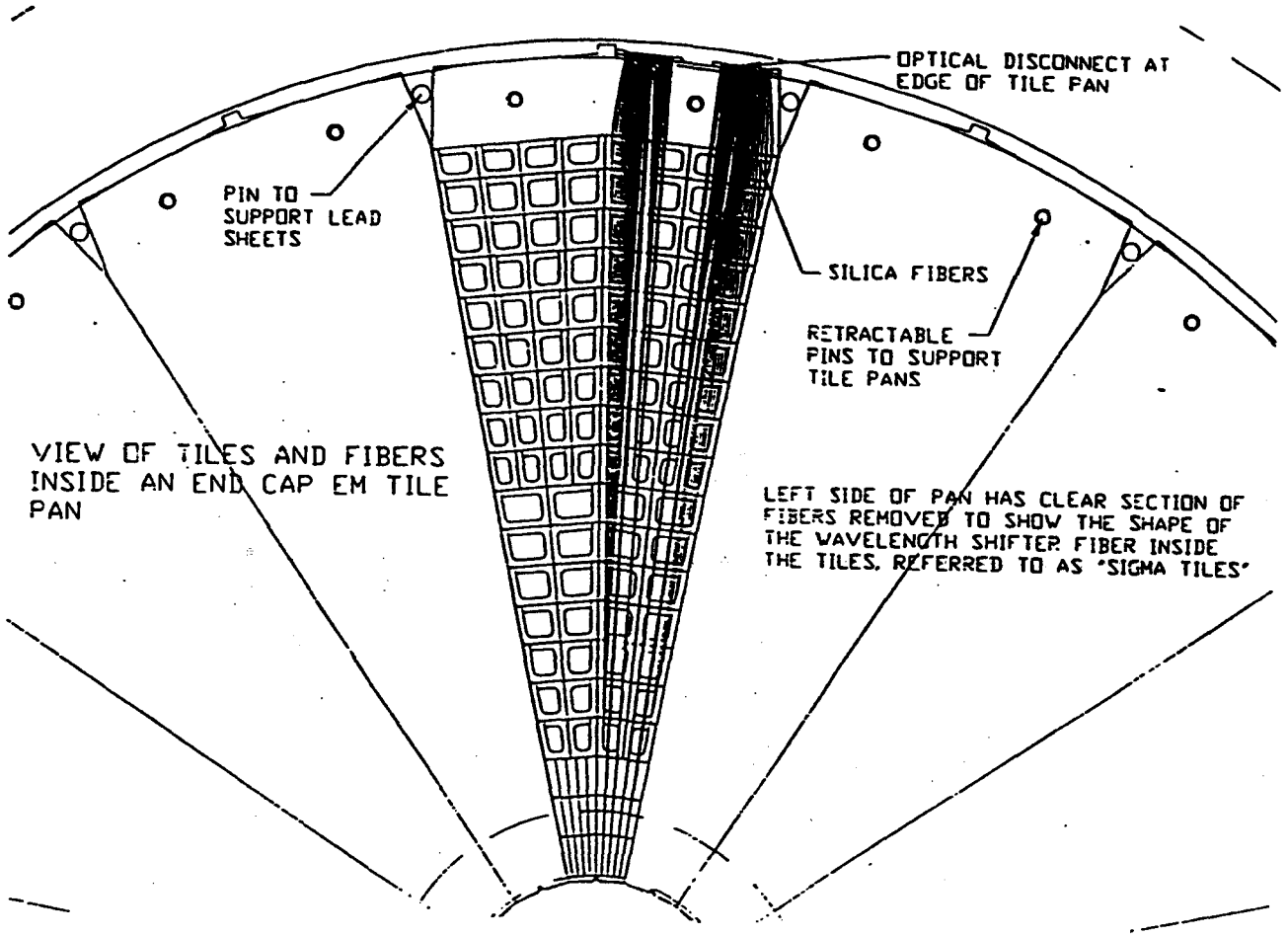

Figure 3.17 - View of tiles and fibers inside a "pizza pan" sector of the Endcap EM calorimeter. Each pan features an optical disconnect to aid in assembly. Note the "sigma tile" pattern in the outer tiles, and the high density of readout fiber in the inner tiles.

The EM absorber is a series of stainless-clad lead disks supported by posts at the outer circumference.

Shower Maximum Detector Concept.

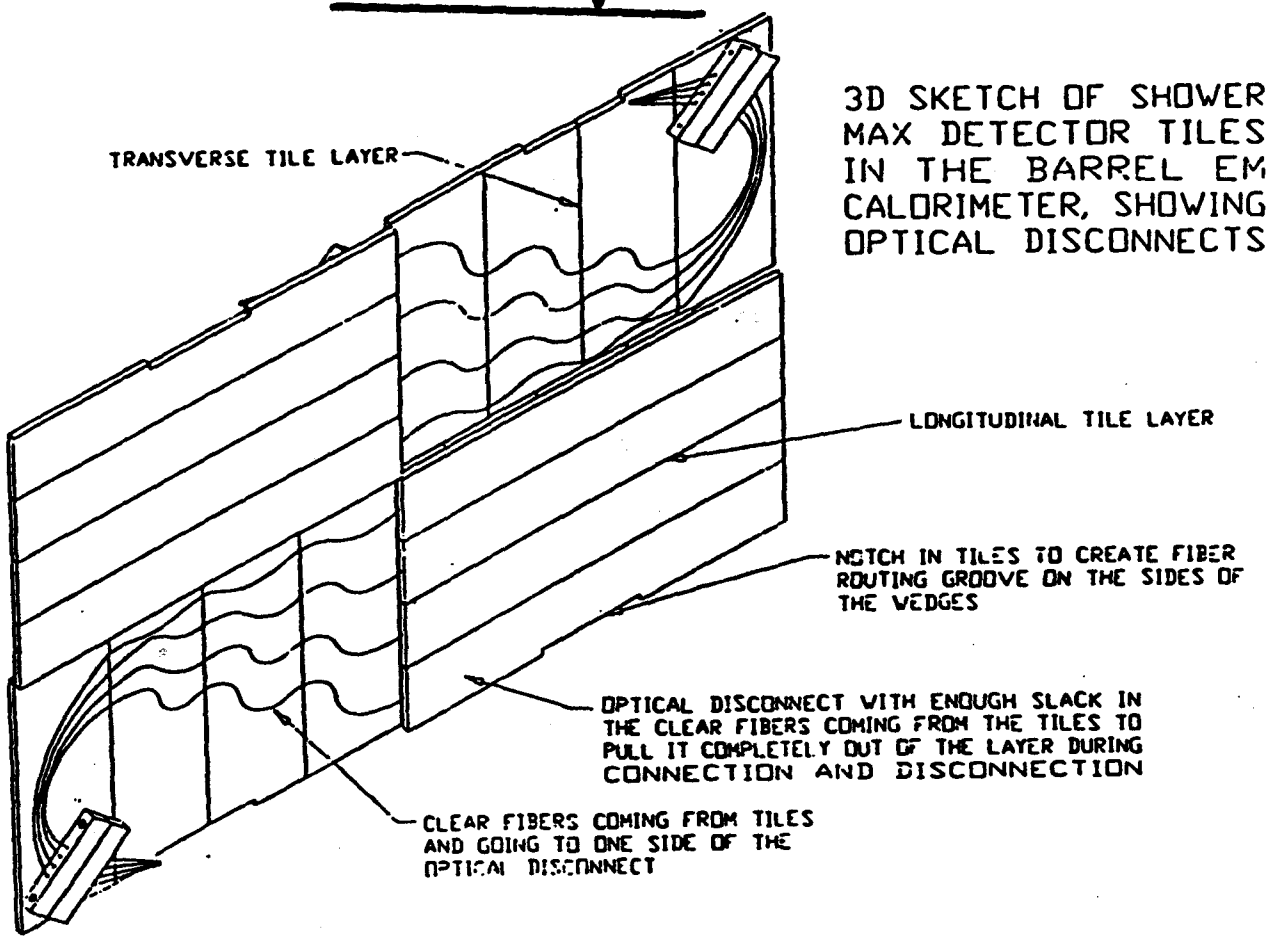

Figure 3.12 - Fiber routing in the EM shower-max assembly. The assembly contains two planes of scintillator strips for the X and Y views. The fiber routing is done between the planes. The clear readout fibers have an optical disconnect which is mounted between the planes, and canted slightly to allow the shower-max readout fibers to join the bundles for the EM calorimeter tiles.

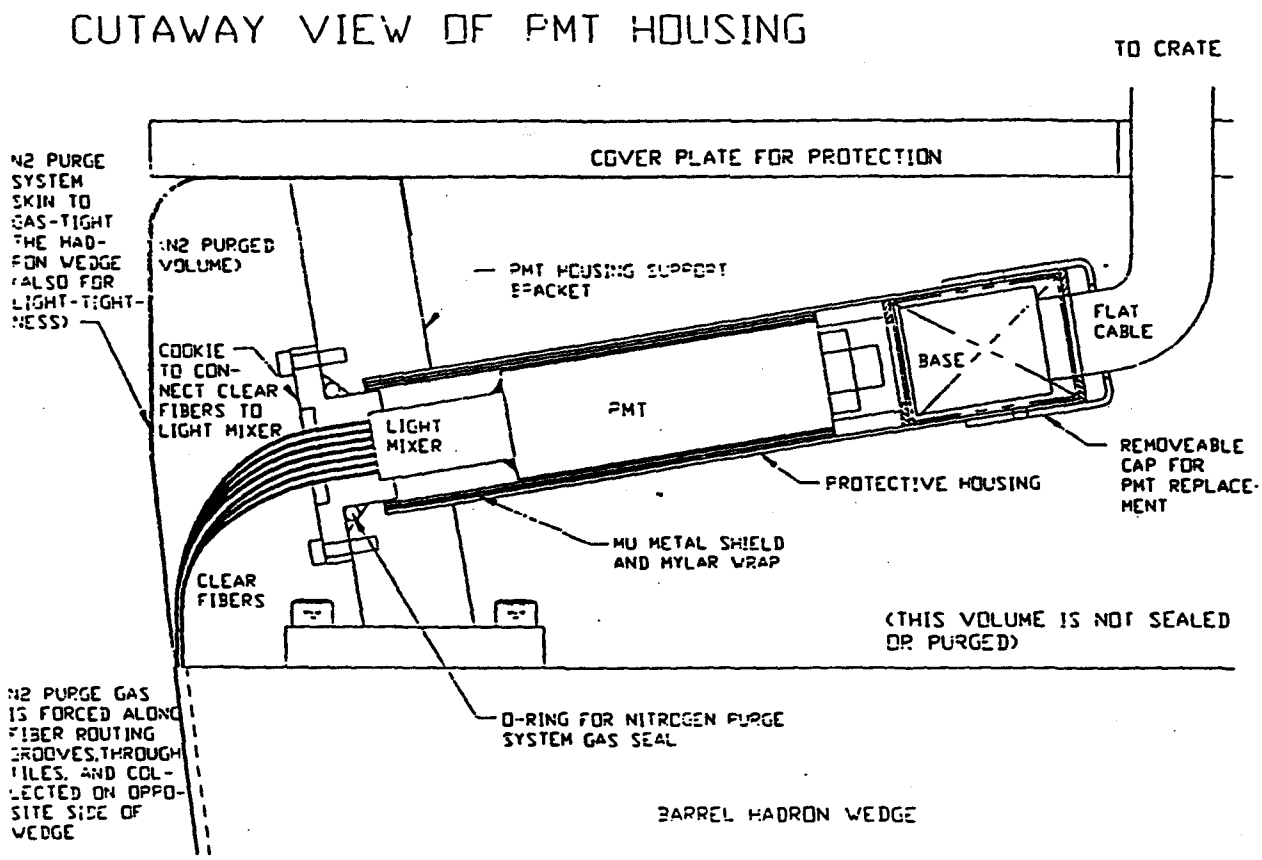

Figure 3.10 - Phototube housing and support bracket at the corner of a wedge, including fiber routing, N_2 purge and light-tightness seals.

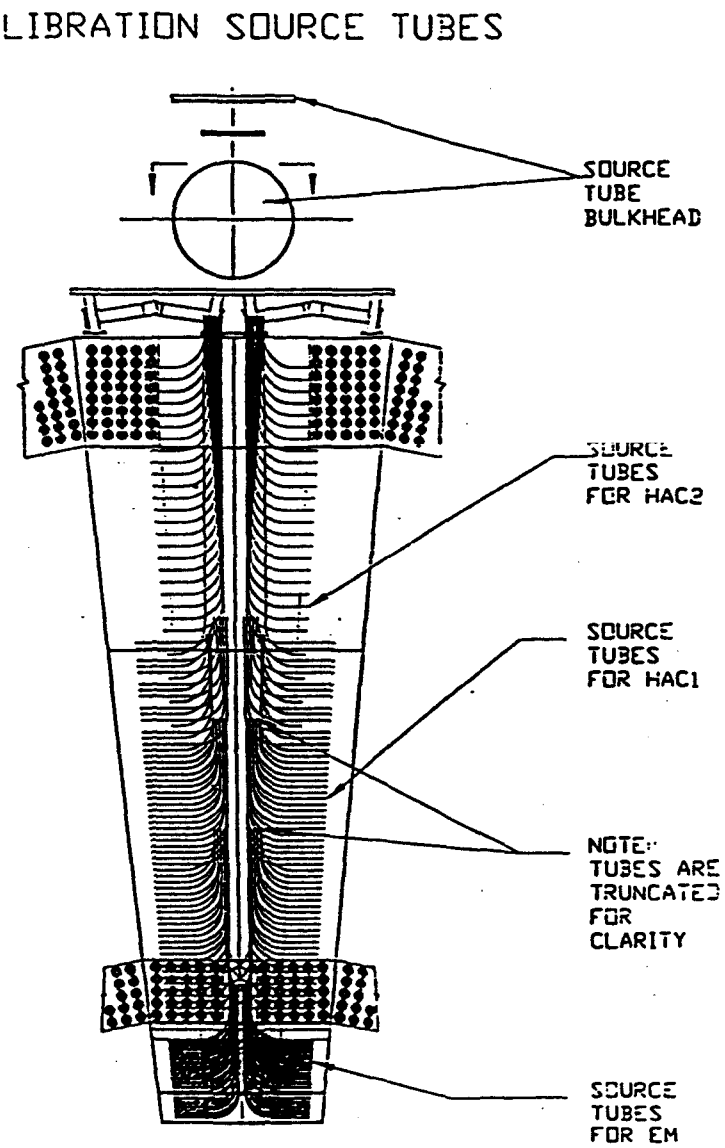

Figure 3.14 - Calibration source tube routing in the barrel, as viewed from the 90-degree crack.

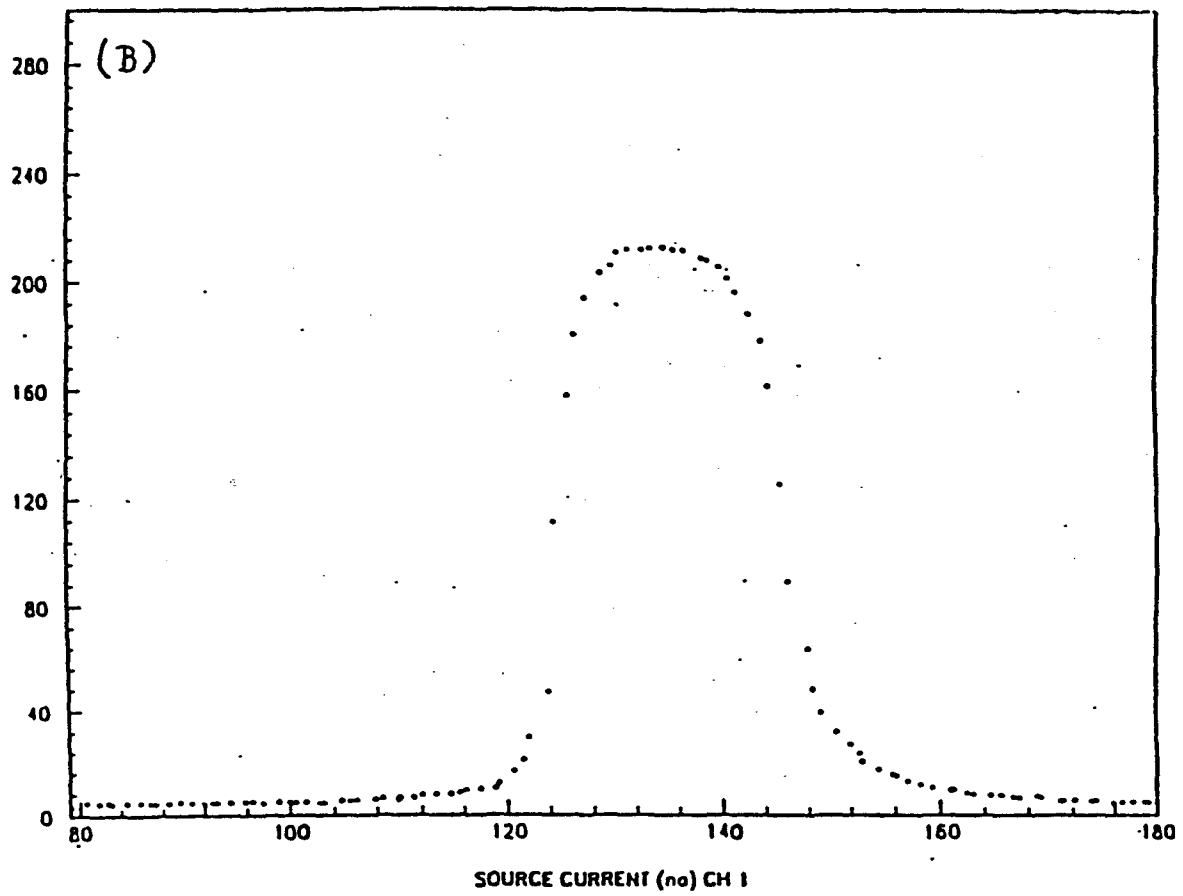

Figure 6.14b Current induced by the radioactive source vs position for a tile. The peak is well measured.

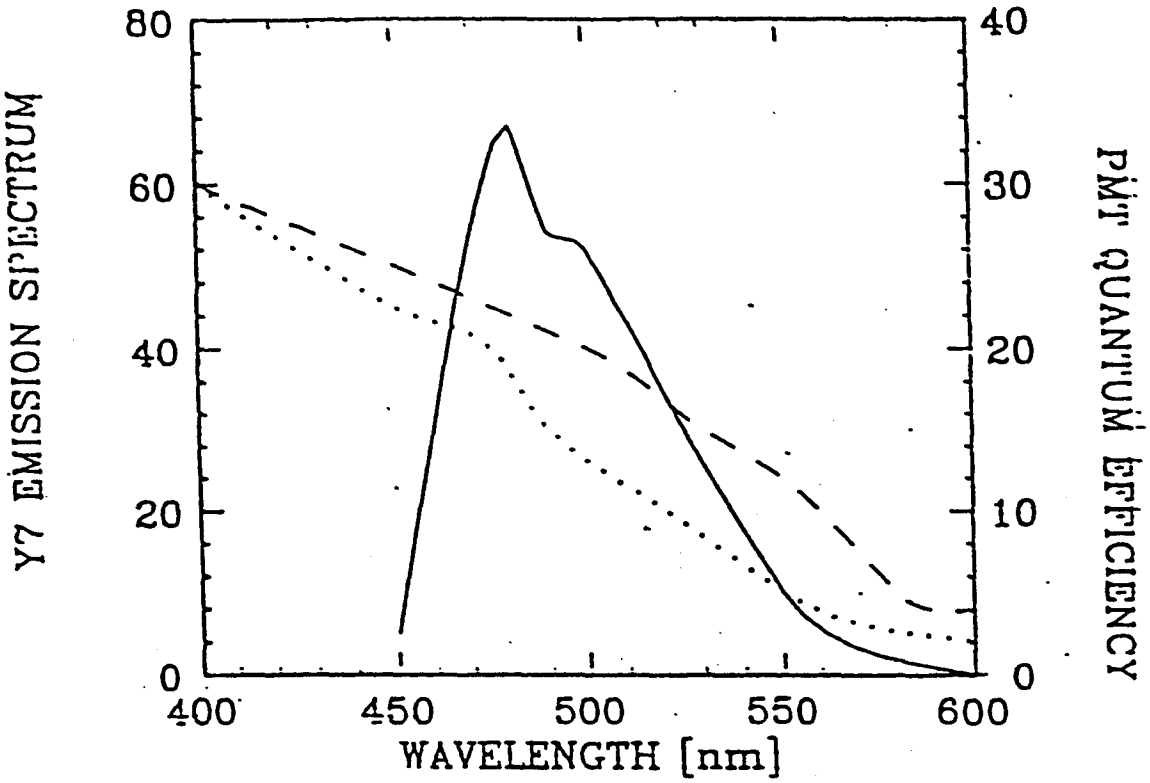

Figure 6.9 Emission spectrum for Y7 (solid curve). Quantum efficiency spectrum for bialkali photocathode (dots) and Phillips 2081 extended green photocathode (dashes) are also shown.

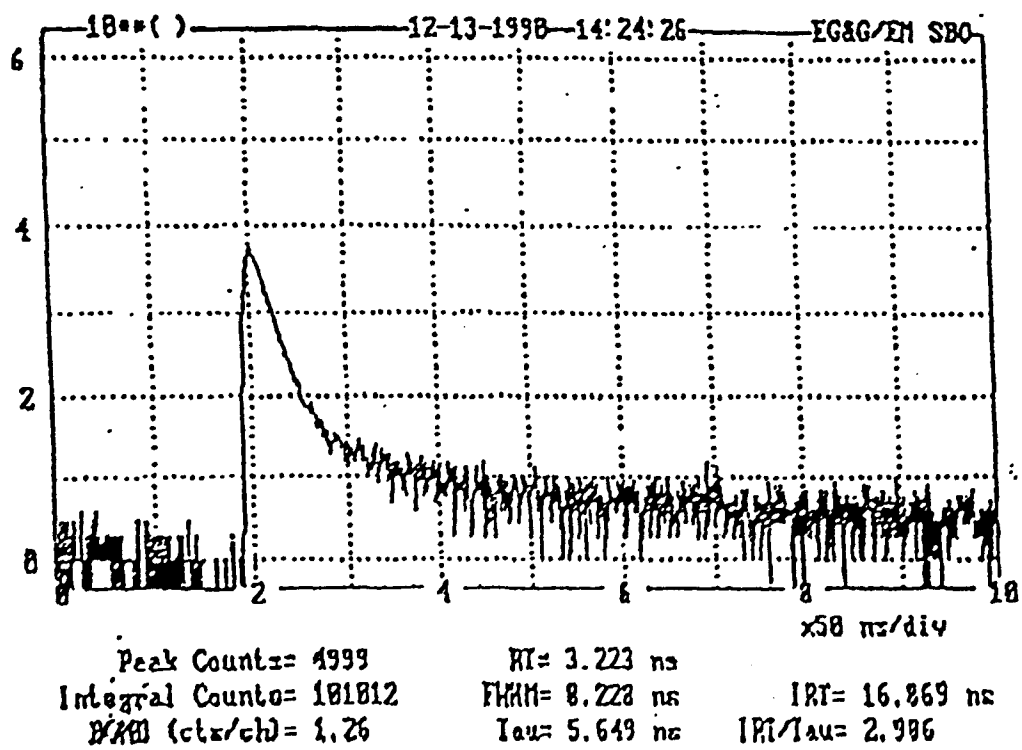

Figure 8.11 The time response of a green shifter (emitting at 520 nm).

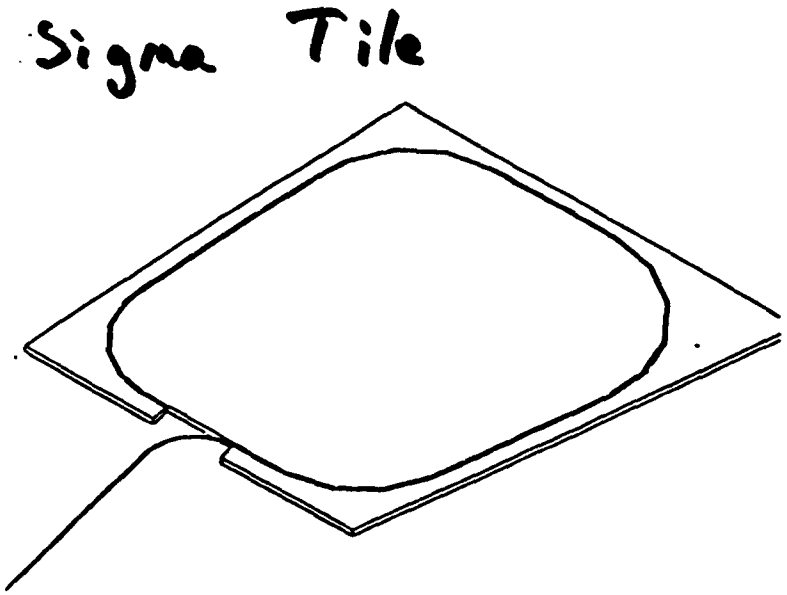

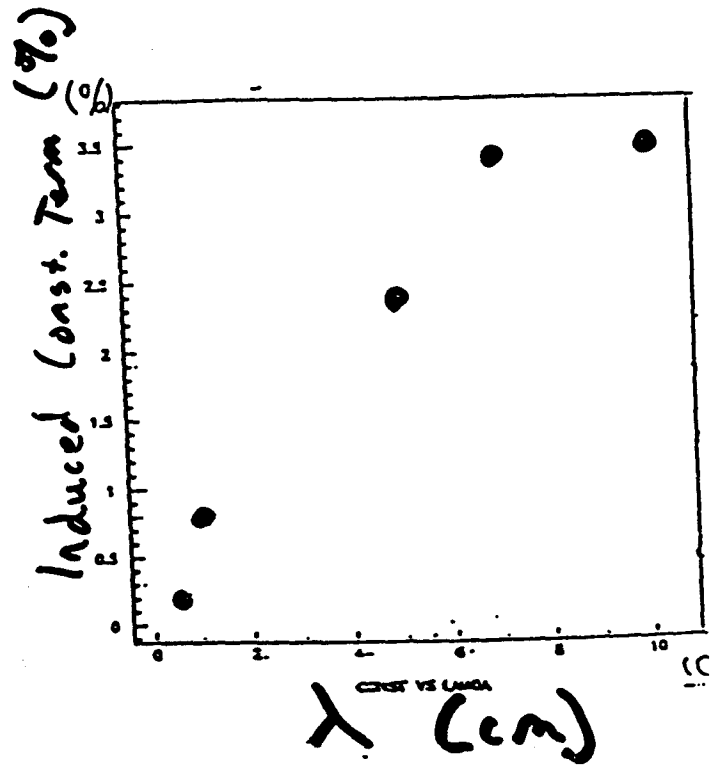

Figure 6.4 Constant term in energy resolution vs wavelength for a sinusoidally va ing transverse response. Note that short wavelength variations do not generate degrad resolution.

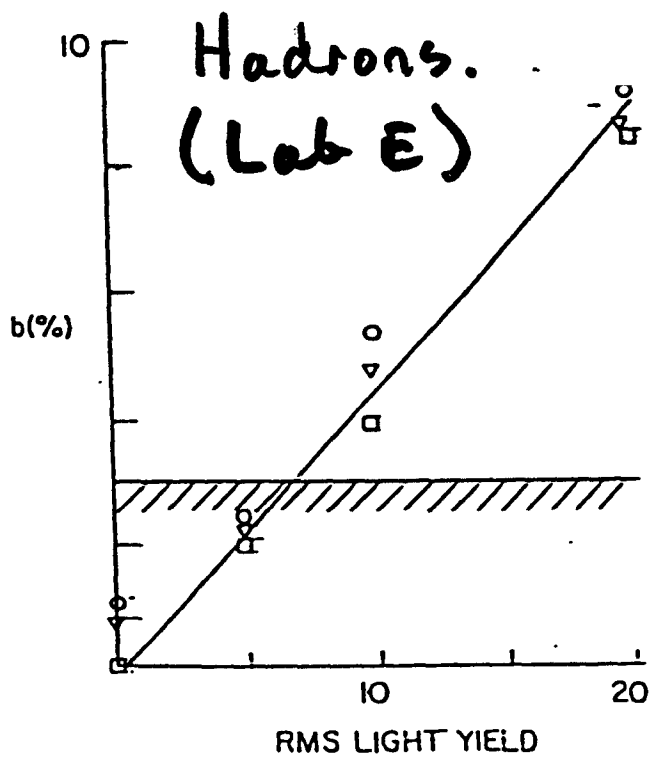

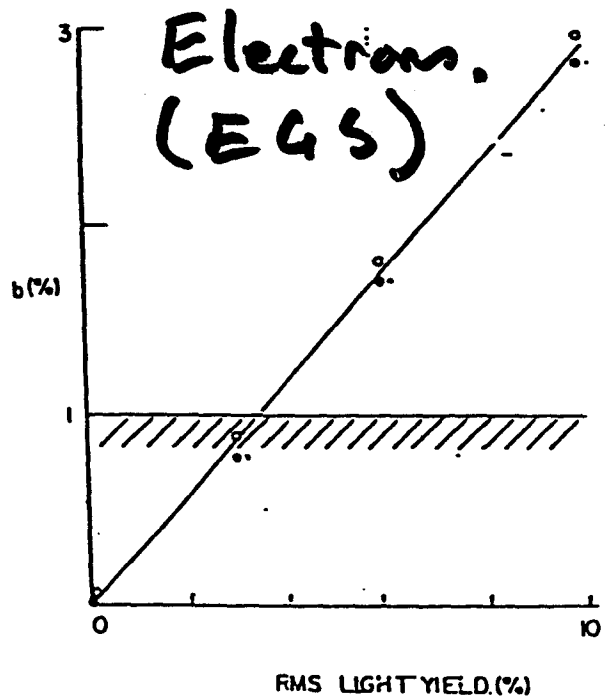

Figure 6.3 Constant term in resolution (b) vs tile-to-tile light yield variation for EGS simulated electromagnetic showers for 10 and 30 GeV electrons

Figure 6.2 Constant term in resolution (b) vs tile-to-tile light yield variation for hadron showers. Test beam data from the "Lab E" spectrometer were used at beam energies of 0.1, 0.2, and 0.45 TeV.

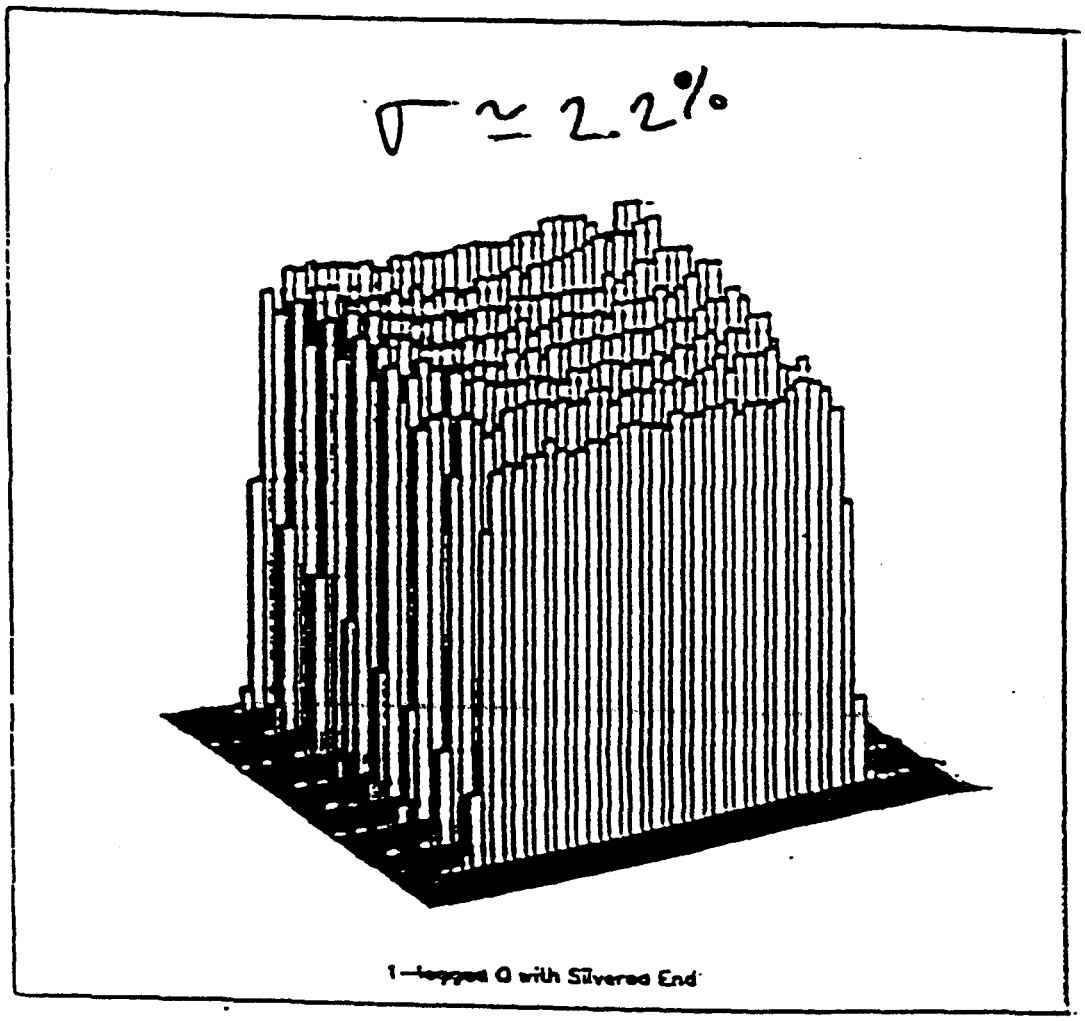

Figure 6.11 Transverse response map for a "Sigma" tile.

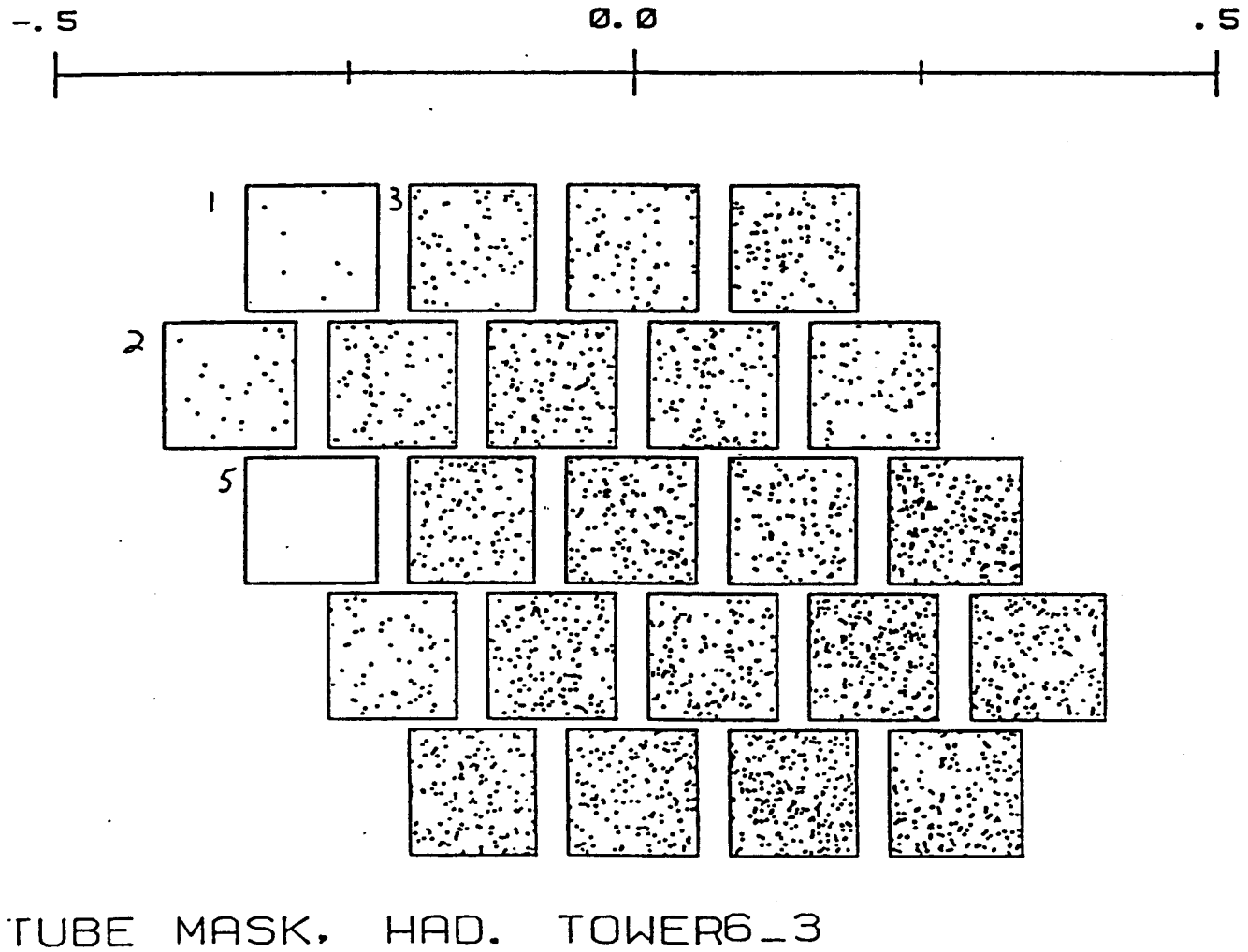

Figure 6.16 Computer output tused to form a neutral density filter for longitudinal masking.

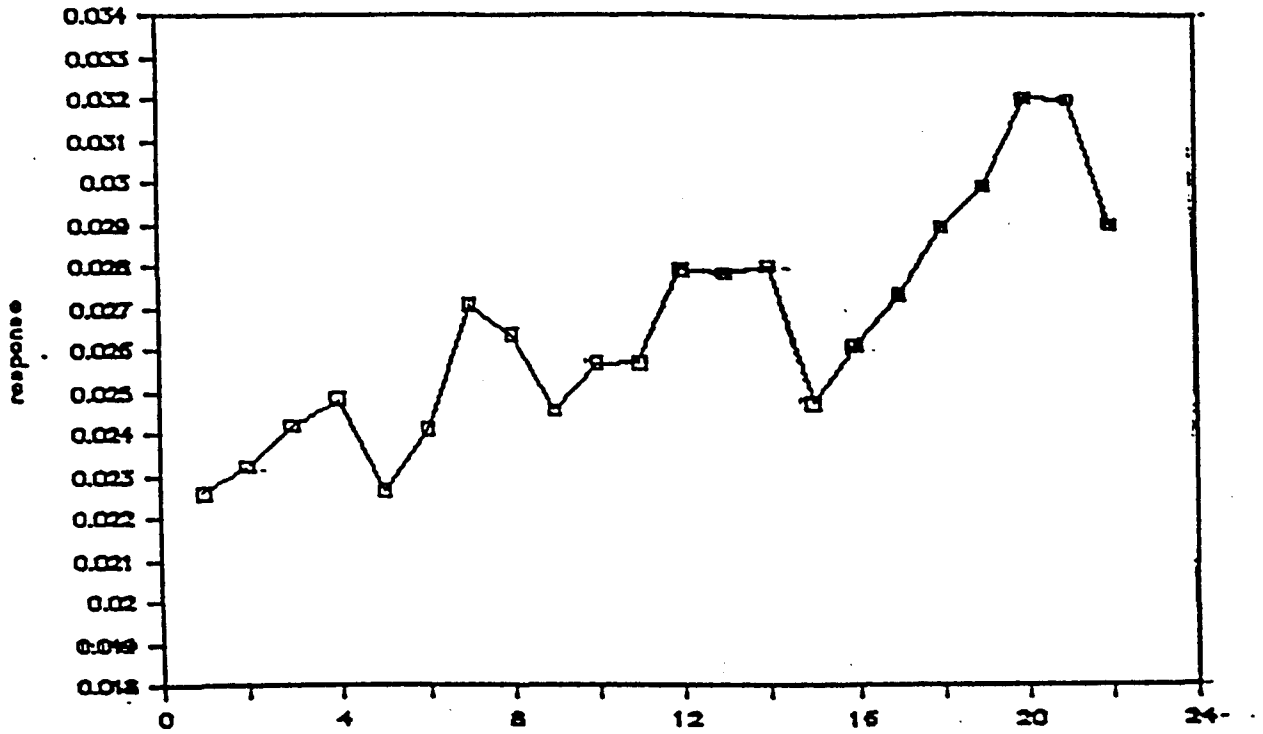

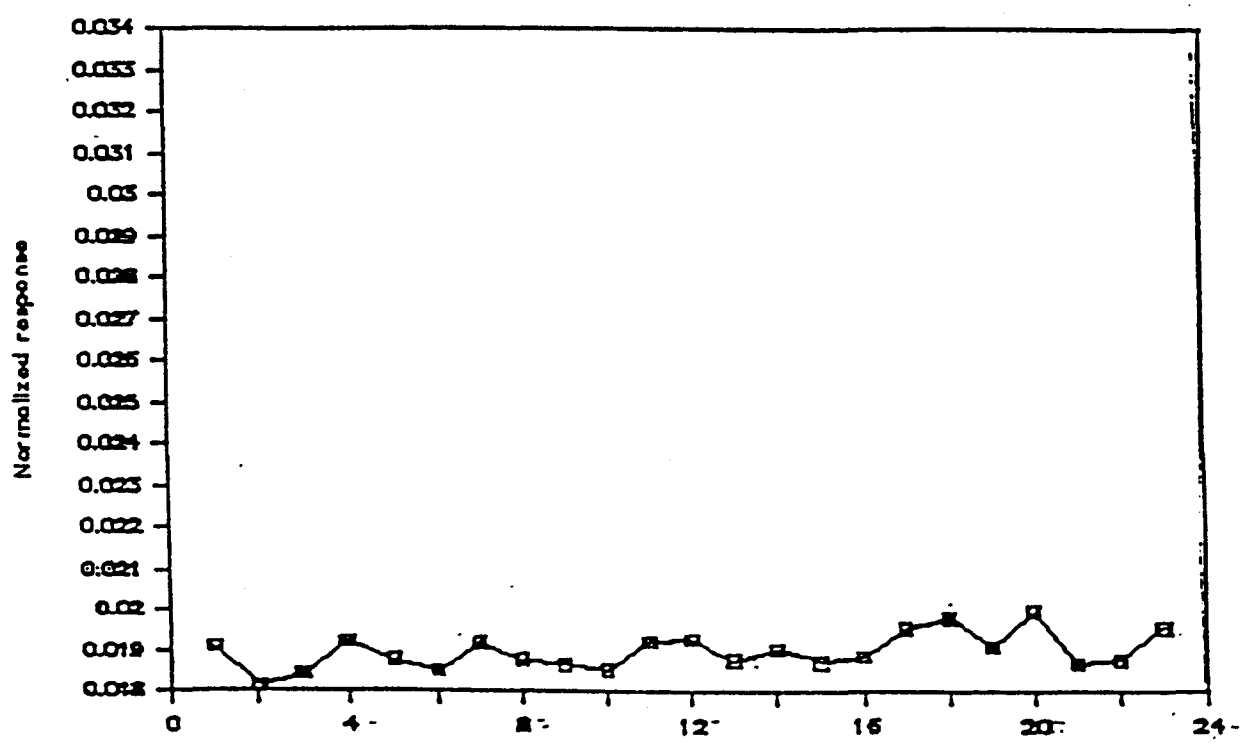

Figure 6.17 a) The longitudinal response of tiles in a tower. The hortizontal scale is tile number ranging from 1 (front) to 23 (back). The vertical scale is relative light yield. The RMS variation is 11.5%.

b) The same tower as in (a), after longitudinal masking. The RMS variation is now 2.6%.

COMMON CRITICAL ISSUE

Radiation Damage to Scintillator and Shifter Fiber

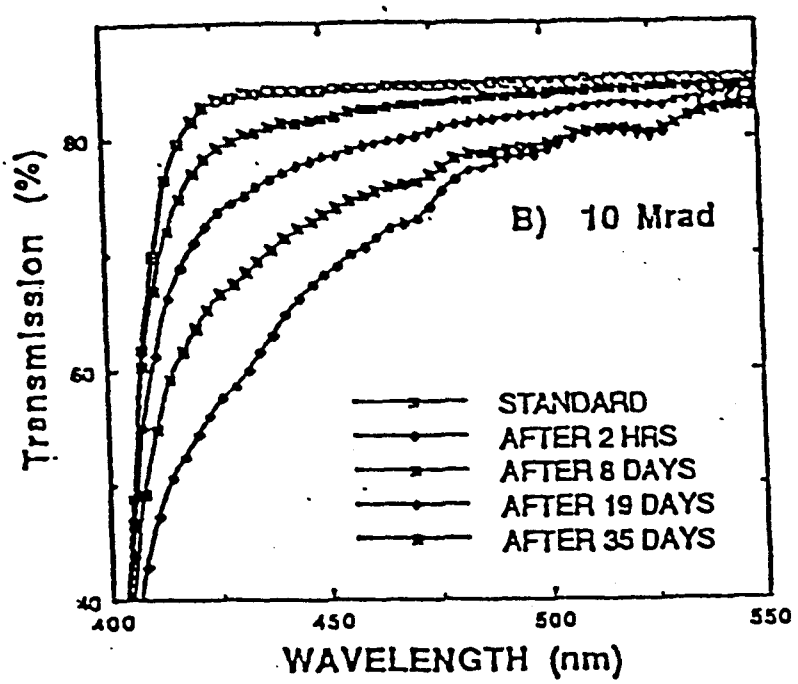

Figure 8.8 Transimission across 5 mm RH-1 scintillator plate before and after radiation as a function of wavelength.

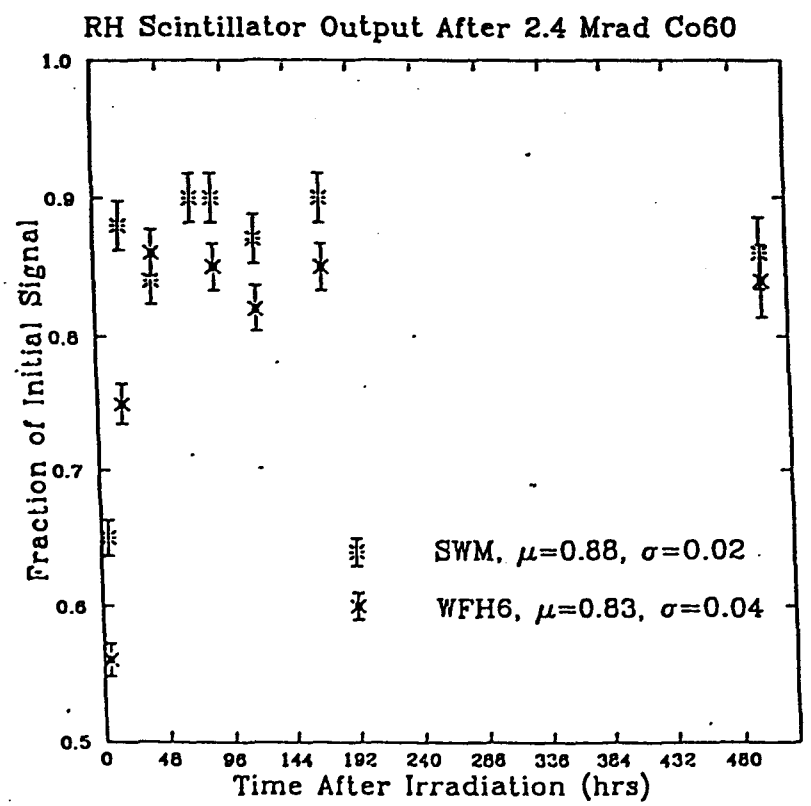

Figure 8.12 Average light output from 3 disks of 2 inches diameter read out using 2 wraps of 1 mm BCF91A.

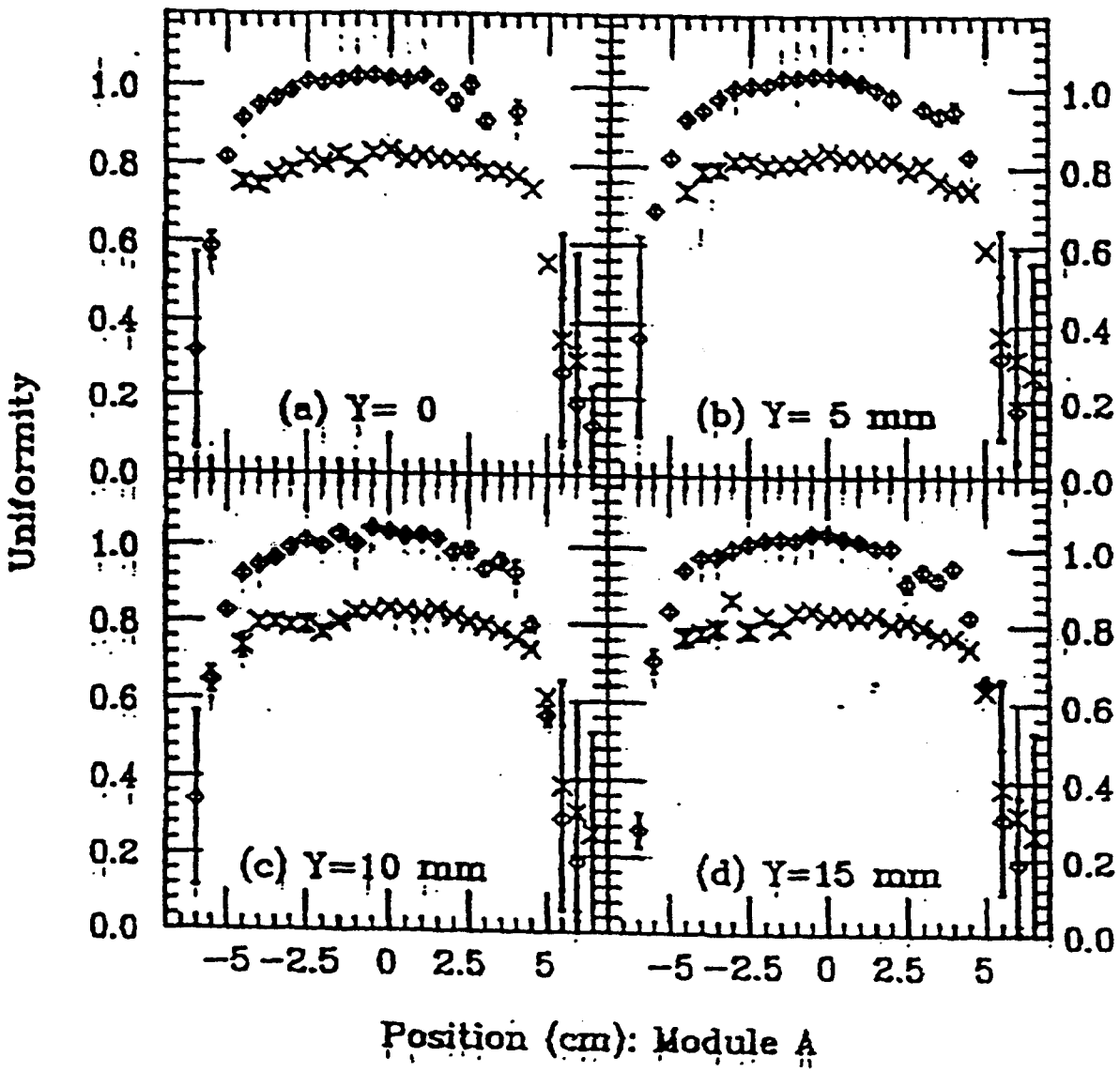

Figure 8.5 Transverse scan using an electron beam for the KEK tests. Data are shown for various strips traversing the tile both before and after 1 Mrad. applied dose.

Tile/Fiber Calorimeter Cost Estimates
'Baseline' and 'Model B' Descope Versions

Version: 8/4/1991 (FY 1991 $M)

WBS - Item	'Baseline'			'Model B'		
	Base	Cont.	Total	Base	Cont.	Total
2.1 - Barrel Calorimeter	92.33	22.13	114.46	68.31	16.74	85.05
2.1.1 Module Components	50.15	11.65	61.79	33.45	8.04	41.49
2.1.2 Module Assembly	3.64	0.98	4.62	2.62	0.71	3.33
2.1.3 Module Support Structure	4.72	0.78	5.50	4.14	0.69	4.83
2.1.4 Eqp., Tooling & Fixtures	10.74	3.49	14.23	8.22	2.73	10.94
2.1.5 (not used here)	0.00	0.00	0.00	0.00	0.00	0.00
2.1.6 Facilities	3.10	1.17	4.27	3.10	1.17	4.27
2.1.7 Surface Assembly	2.50	0.62	3.12	1.86	0.46	2.33
2.1.8 Project/Facility Mgmt.	15.87	2.86	18.72	13.53	2.43	15.96
2.1.9 R&D, Prototypes	1.08	0.41	1.48	1.05	0.40	1.44
8.2.1,2 Install & Test in Cavern	0.55	0.19	0.73	0.34	0.12	0.46
2.2 - Endcap Calorimeters	46.96	14.05	61.00	30.94	9.13	40.08
2.2.1 Module Components	29.43	9.43	38.87	17.41	5.53	22.94
2.2.2 Module Assembly	2.36	0.79	3.16	1.52	0.49	2.01
2.2.3 Module Support Structure	3.77	0.66	4.43	3.31	0.58	3.89
2.2.4 Eqp., Tooling & Fixtures	2.64	1.15	3.79	2.42	1.07	3.49
2.2.5 (not used here)	0.00	0.00	0.00	0.00	0.00	0.00
2.2.6 Facilities	0.46	0.15	0.61	0.46	0.15	0.61
2.2.7 Surface Assembly	1.59	0.45	2.03	1.18	0.34	1.52
2.2.8 Project/Facility Mgmt.	5.53	0.99	6.52	3.86	0.70	4.56
2.2.9 R&D, Prototypes	0.30	0.11	0.41	0.26	0.10	0.36
8.2.1,2 Install & Test in Cavern	0.89	0.30	1.19	0.52	0.18	0.69
Total Central Calorimeter	139.29	36.18	175.47	99.25	25.88	125.13
Rollup by Component Type:						
Mech. Structures & Fixtures	46.32	12.61	58.93	33.48	9.56	43.04
Scin. Components & Facilities	31.14	10.22	41.36	18.57	6.10	24.66
PMT Components & Facilities	21.88	5.13	27.01	14.11	3.42	17.53
Support Structures & Facilities	13.34	2.64	15.98	11.27	2.20	13.47
Erection/Lowering/Hall Costs	3.84	1.21	5.05	3.12	0.97	4.10
Management	21.39	3.85	25.24	17.39	3.13	20.52
R&D/Prototype	1.37	0.52	1.89	1.31	0.50	1.81
Rollup by Function Type:						
EM System	47.59	12.14	59.74	34.26	8.76	43.02
SPD System	23.33	5.91	29.24	16.85	4.28	21.13
HAC1 System	25.62	6.79	32.41	18.05	4.81	22.86
HAC2 System	30.63	8.21	38.84	21.41	5.79	27.20
Support System	12.12	3.12	15.24	8.67	2.24	10.91

Table I

Tile/Fiber Central Calorimeter
'Model B' Cost Variations

VERSION: September 6, 1991

Prepared by D. Scherbarth, WSTC

Meets All SDC Physics Goals.

Item	Descope No. 10	11	12	13	14
Longitudinal Barrel EM Channels	1	2	1	2	1
Longitudinal Endcap EM Channels	2	2	2	2	2
Shower Max Tiles/Tower	12	12	12	12	12
Shower Max Tiles/MAPMT	64	64	64	64	64
HAC1 Transverse Granularity	.1x.1	.1x.1	.05x.05	.05x.05	.05x.05
HAC2 Transverse Granularity	.1x.1	.1x.1	.05x.05	.05x.05	.1x.1
Total standard PMTs	18,464	25,632	35,072	42,240	26,768
Total 64-anode MAPMTs	1,884	1,884	1,884	1,884	1,884
Total Tiles	442K	442K	729K	729K	609K
Cost (FY91 $M)*	125.1	129.0	143.1	147.0	135.1

*Costs include Installation in the detector and Prototype costs. R&D costs are not included. Dominant cost derivatives are: $540/PMT; $30/tile.

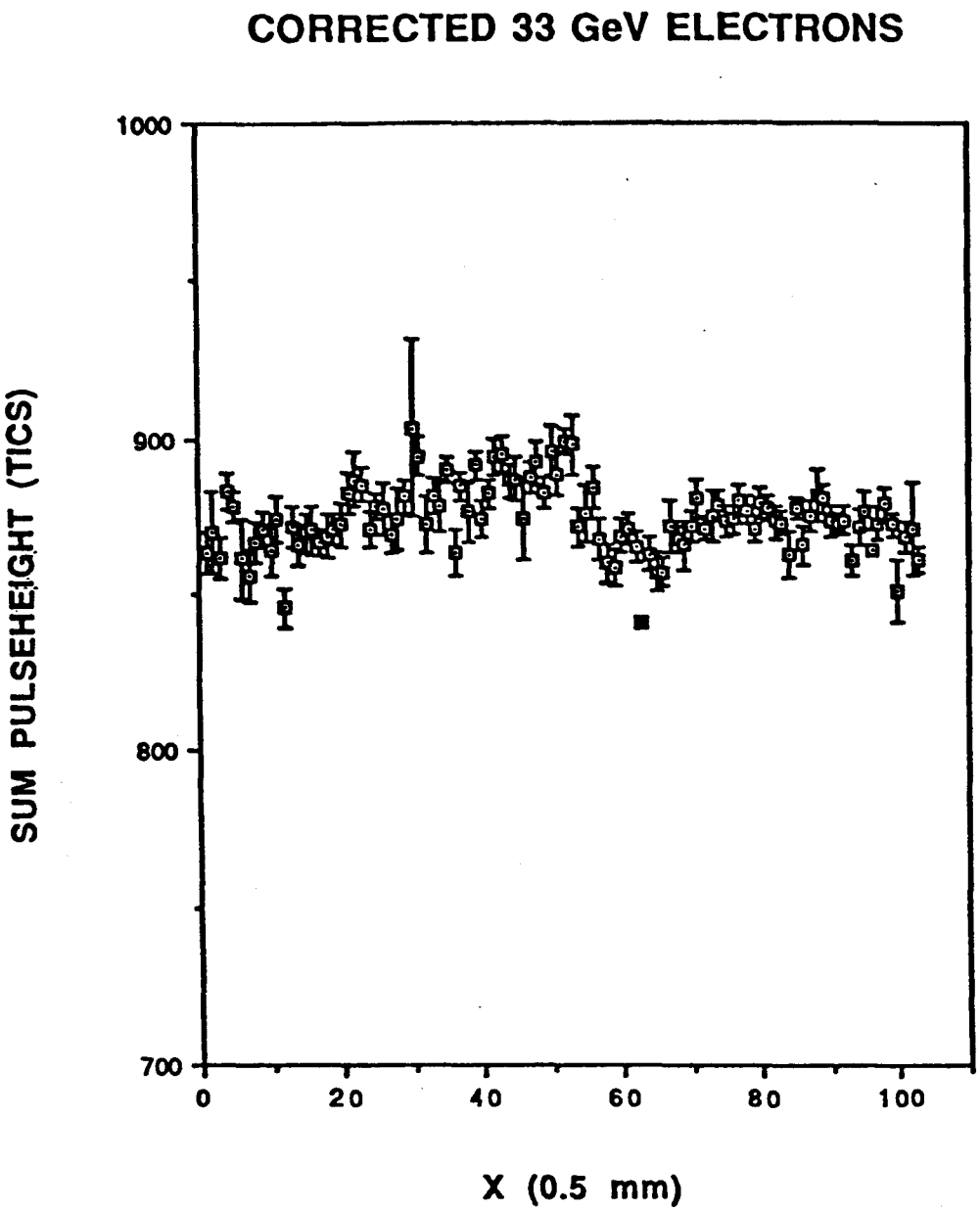
CORRECTED 33 GeV ELECTRONS
SUM PULSEHEIGHT (TICS)
1000
900
800
700
0
20
40
60
80
100
X (0.5 mm)

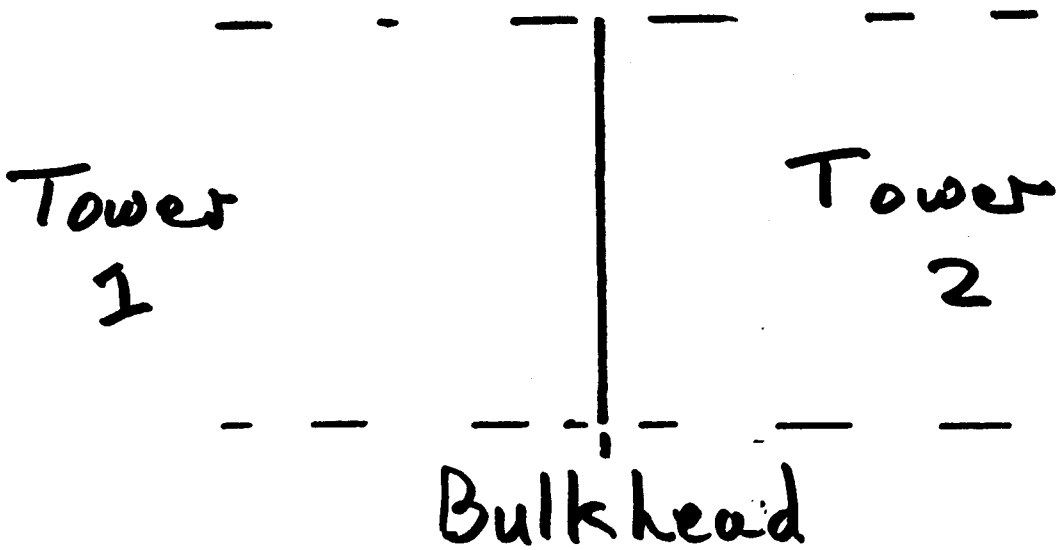
Tower 1
Tower 2
Bulkhead

CALORIMETER REVIEW AND TECHNICAL BOARD MEETING
SEPTEMBER 12 -14, 1991
SSCL

Presentation by:

Larry Bartozek

Fermilab

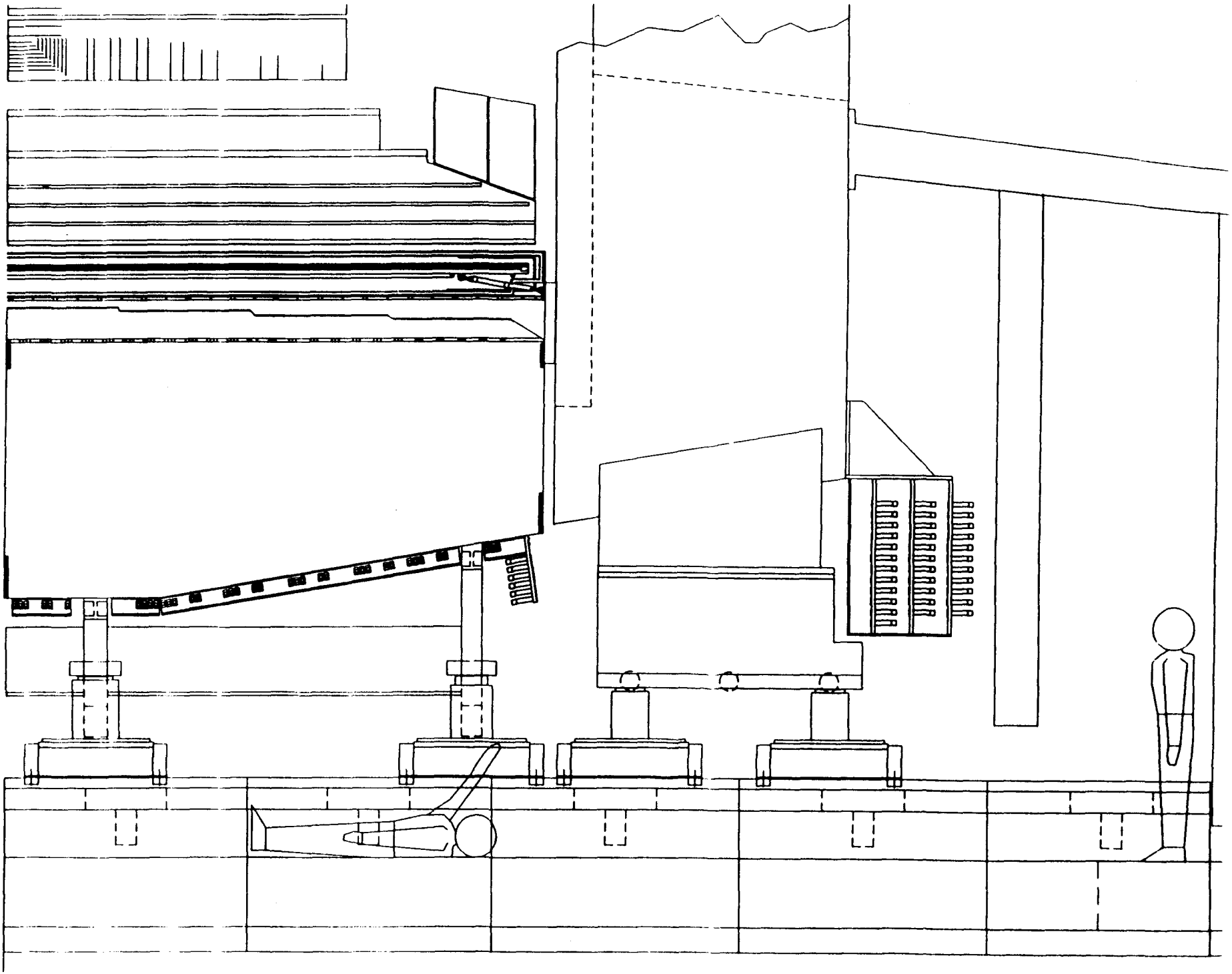

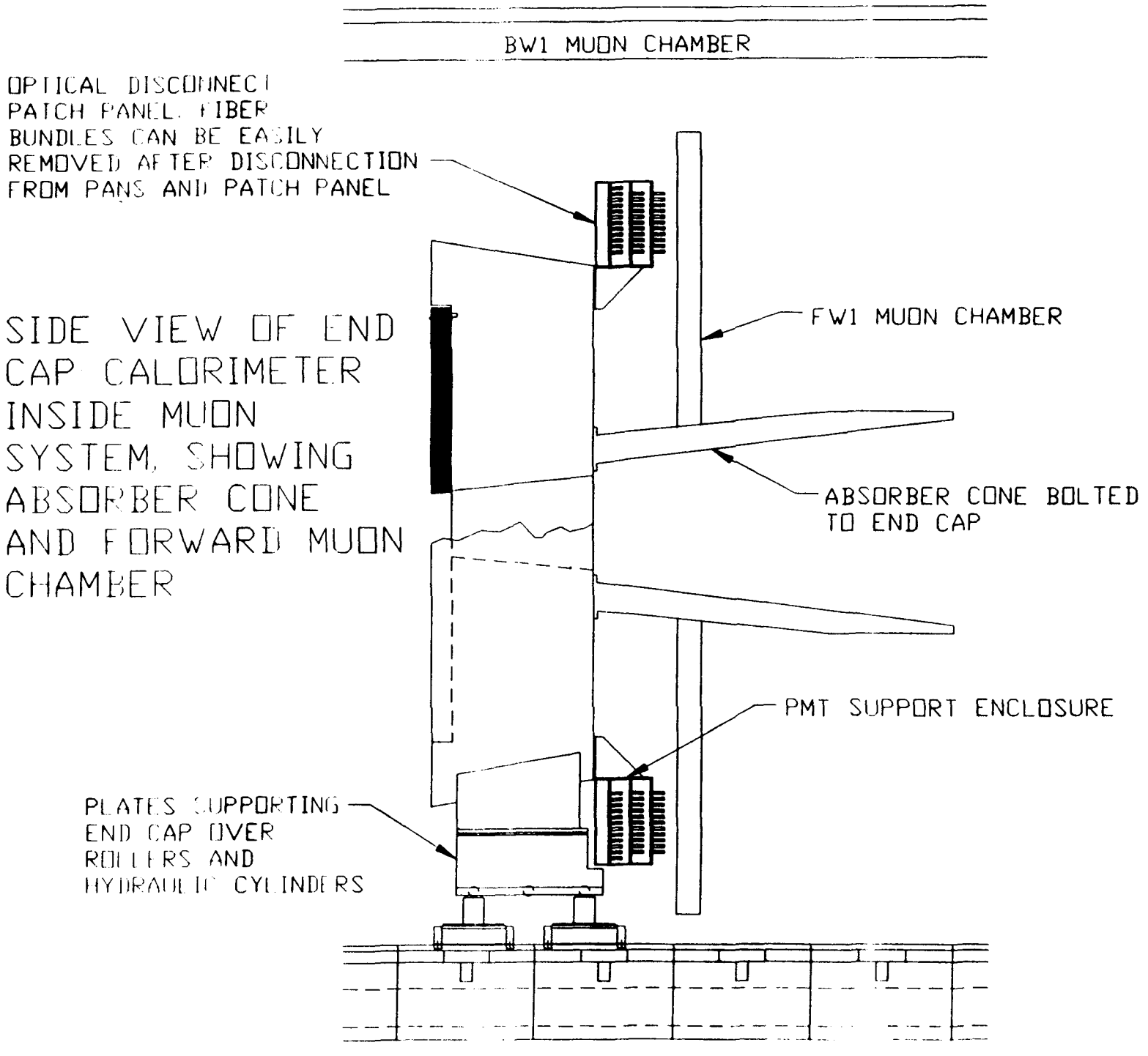
BW1 MUON CHAMBER
OPTICAL DISCONNECT PATCH PANEL. FIBER BUNDLES CAN BE EASILY REMOVED AFTER DISCONNECTION FROM PANS AND PATCH PANEL
SIDE VIEW OF END CAP CALORIMETER INSIDE MUON SYSTEM, SHOWING ABSORBER CONE AND FORWARD MUON CHAMBER
FW1 MUON CHAMBER
ABSORBER CONE BOLTED TO END CAP
PMT SUPPORT ENCLOSURE
PLATES SUPPORTING END CAP OVER ROLLERS AND HYDRAULIC CYLINDERS

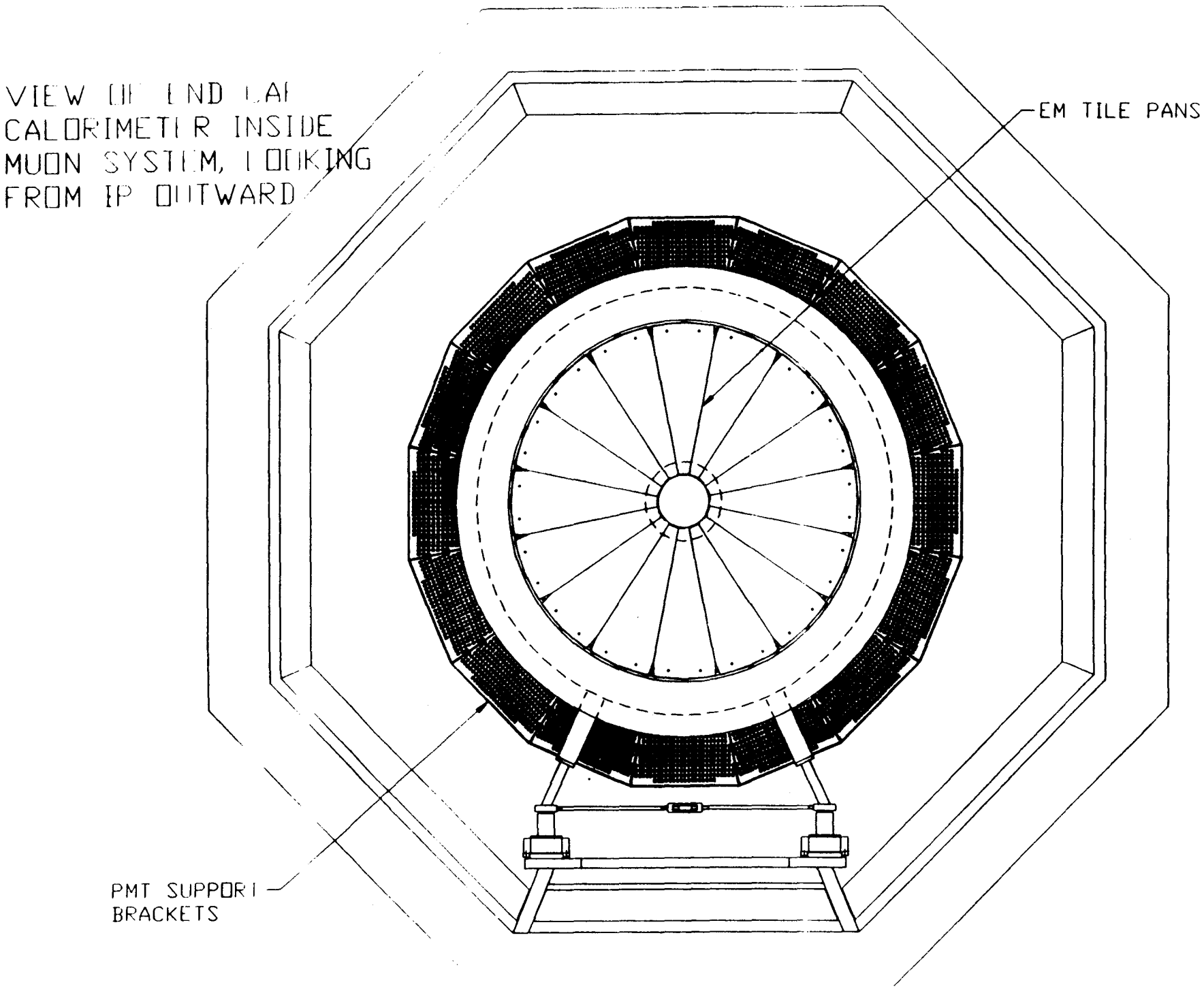
VIEW OF END CAP
CALORIMETER INSIDE
MUON SYSTEM, LOOKING
FROM IP OUTWARD
EM TILE PANS
PMT SUPPORT
BRACKETS

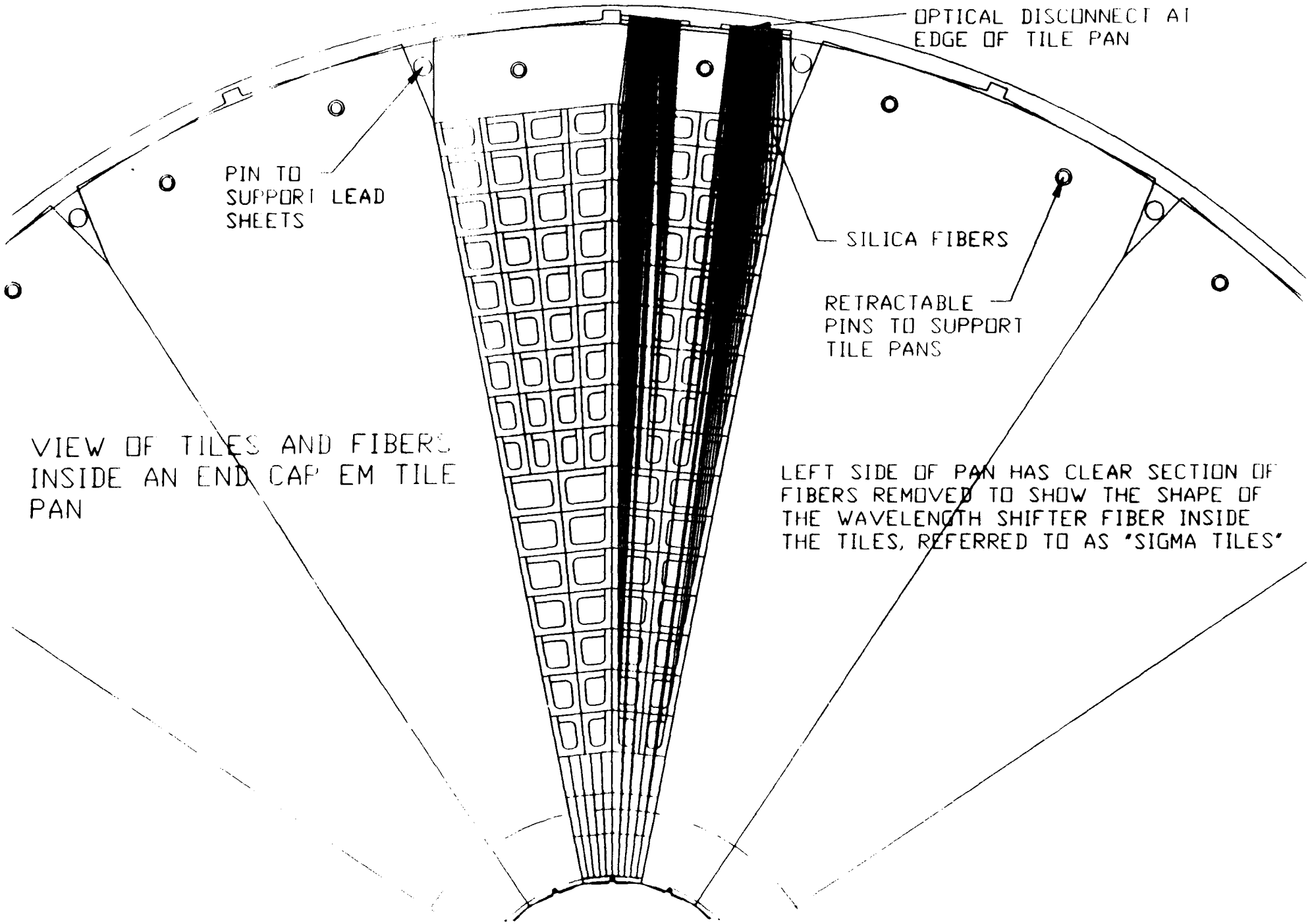
OPTICAL DISCONNECT AT
EDGE OF TILE PAN
PIN TO
SUPPORT LEAD
SHEETS
SILICA FIBERS
RETRACTABLE
PINS TO SUPPORT
TILE PANS
VIEW OF TILES AND FIBERS
INSIDE AN END CAP EM TILE
PAN
LEFT SIDE OF PAN HAS CLEAR SECTION OF
FIBERS REMOVED TO SHOW THE SHAPE OF
THE WAVELENGTH SHIFTER FIBER INSIDE
THE TILES, REFERRED TO AS "SIGMA TILES"

SKETCH OF STEEL FABRICATION TECHNIQUE FOR THE HADRON SECTION OF THE END CAP CALORIMETER, SHOWING C SHAPED PLATES AND WEDGE SPACERS

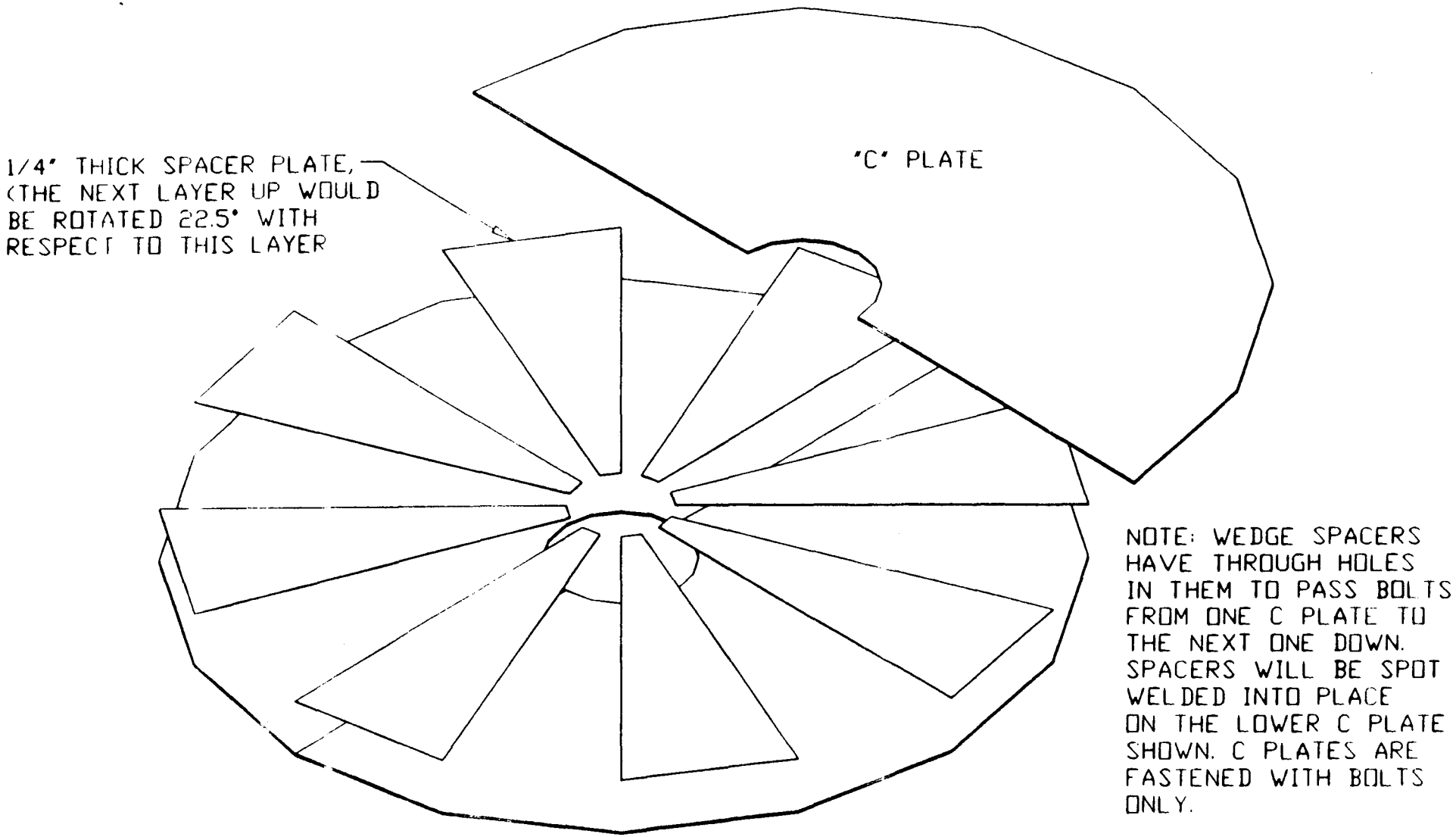

DETAIL OF RETRACTING PIN MECHANISM WHICH SUPPORTS EM TILE PANS AND ALLOWS THEM TO BE REMOVED INDIVIDUALLY AFTER THE LEAD HAS BEEN PULLED FORWARD

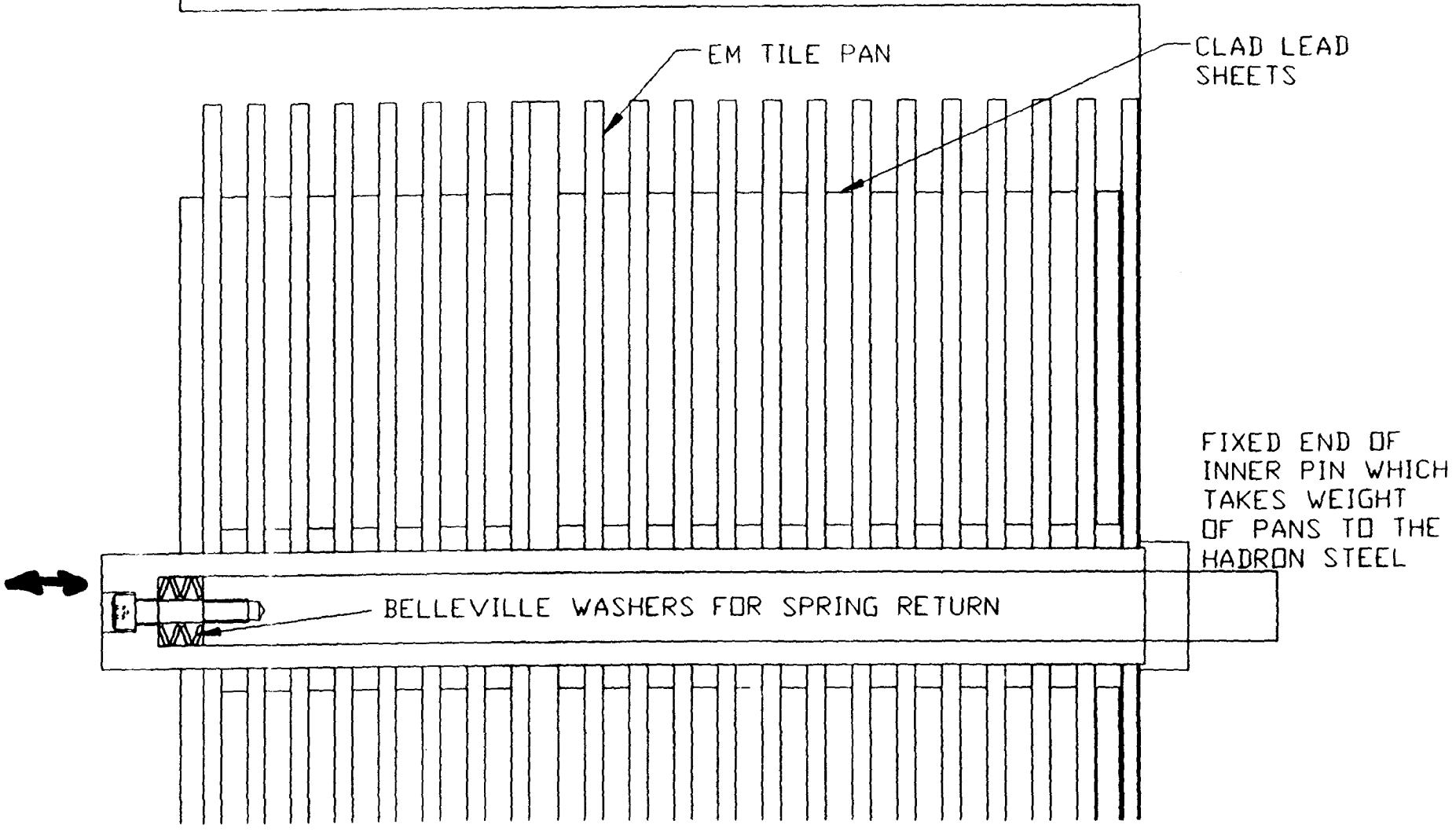

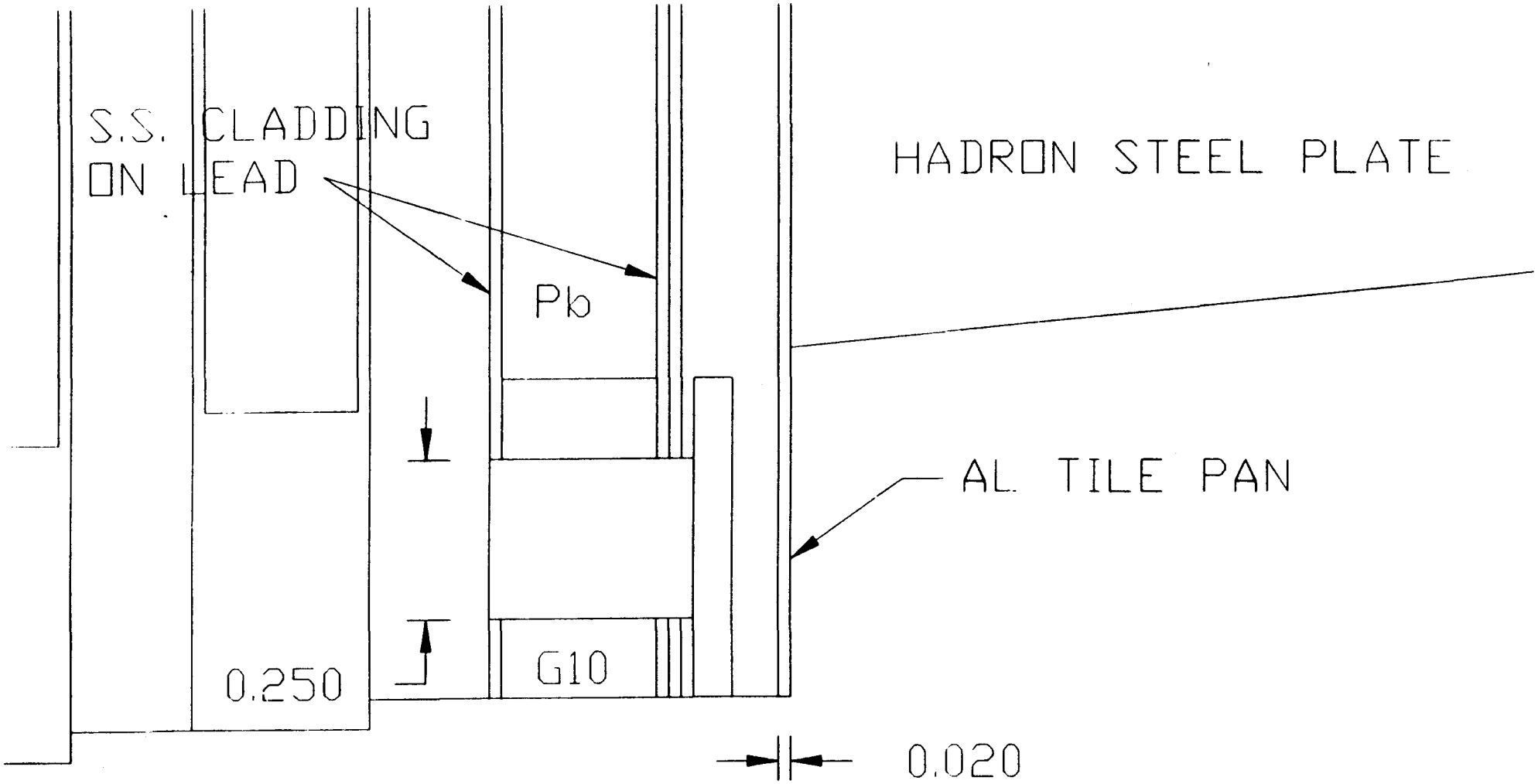

CUTAWAY SIDE VIEW OF TYPICAL FASTENER USED TO ATTACH TILE PANS TO CLAD LEAD SHEETS FOR EASE OF REMOVAL

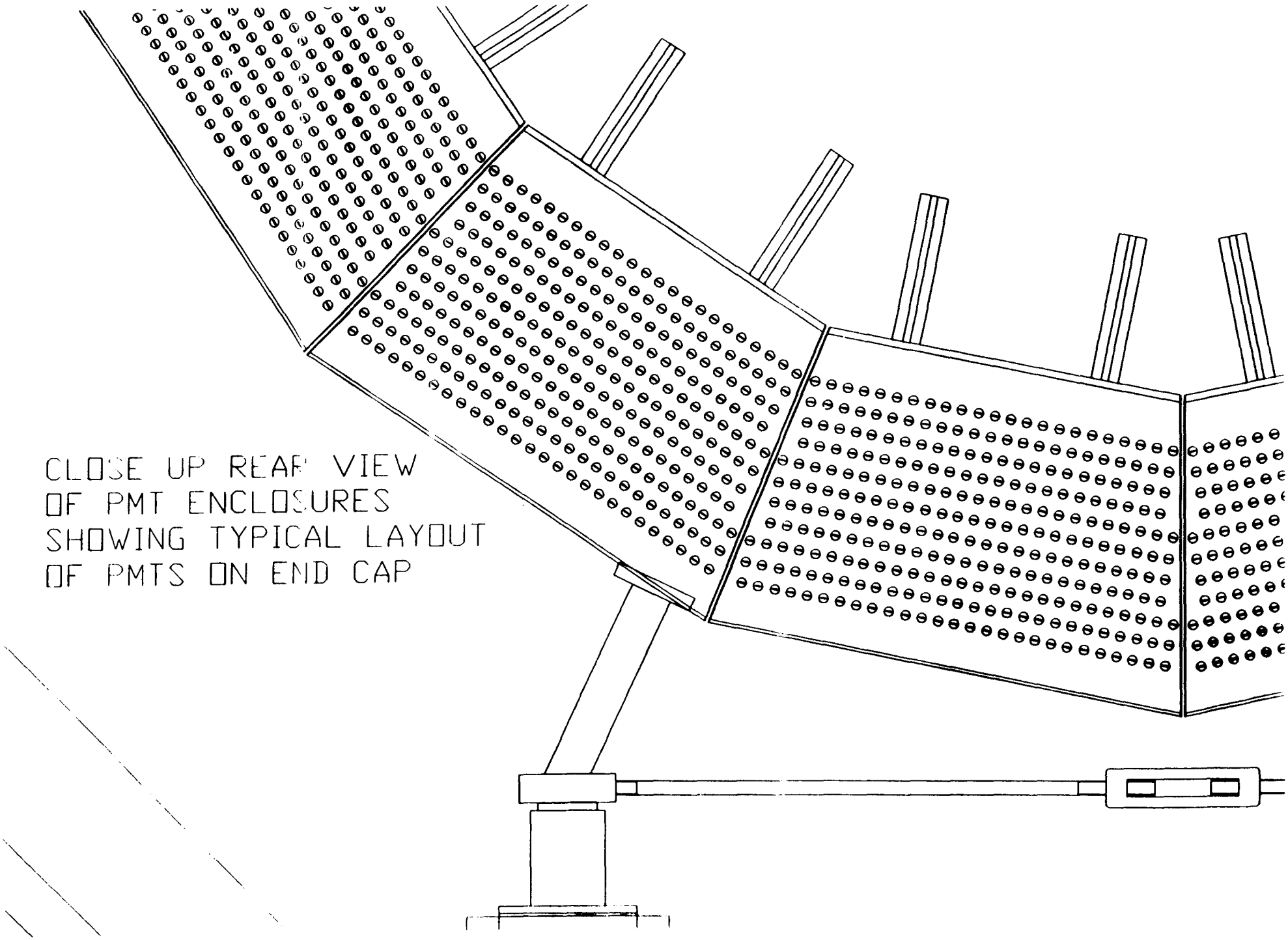
CLOSE UP REAR VIEW
OF PMT ENCLOSURES
SHOWING TYPICAL LAYOUT
OF PMTS ON END CAP

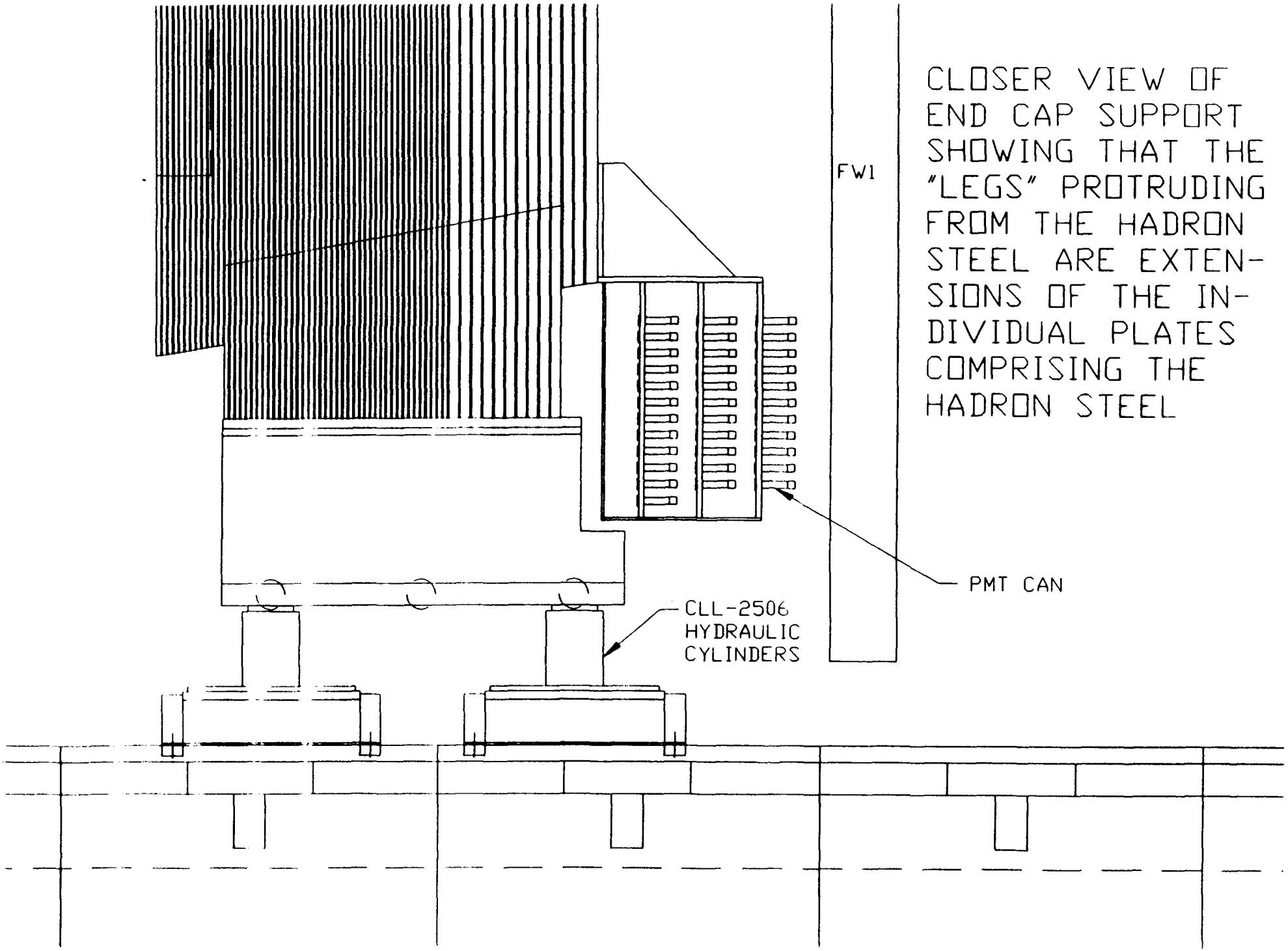

CLOSER VIEW OF END CAP SUPPORT SHOWING THAT THE "LEGS" PROTRUDING FROM THE HADRON STEEL ARE EXTENSIONS OF THE INDIVIDUAL PLATES COMPRISING THE HADRON STEEL

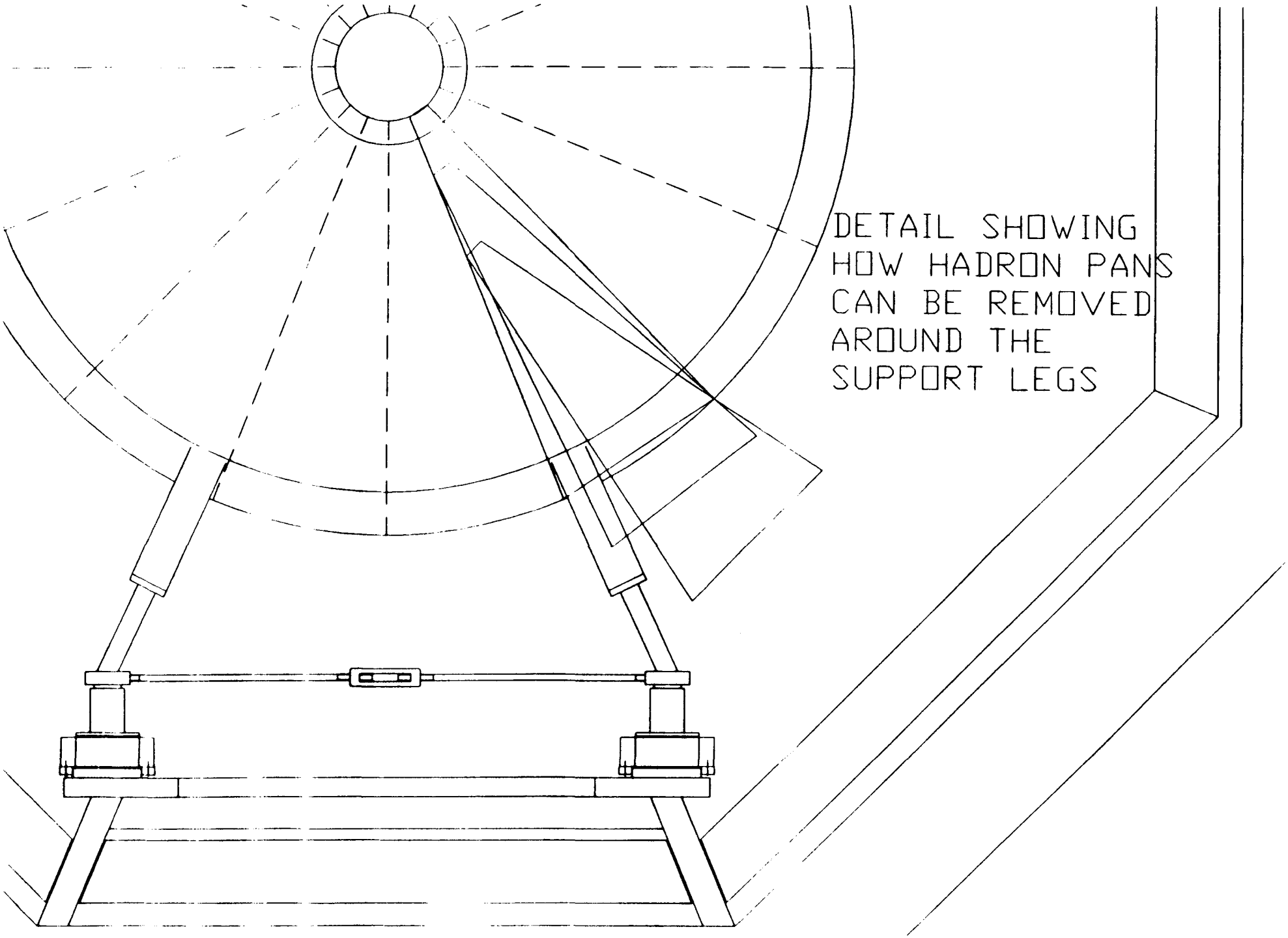
DETAIL SHOWING
HOW HADRON PANS
CAN BE REMOVED
AROUND THE
SUPPORT LEGS

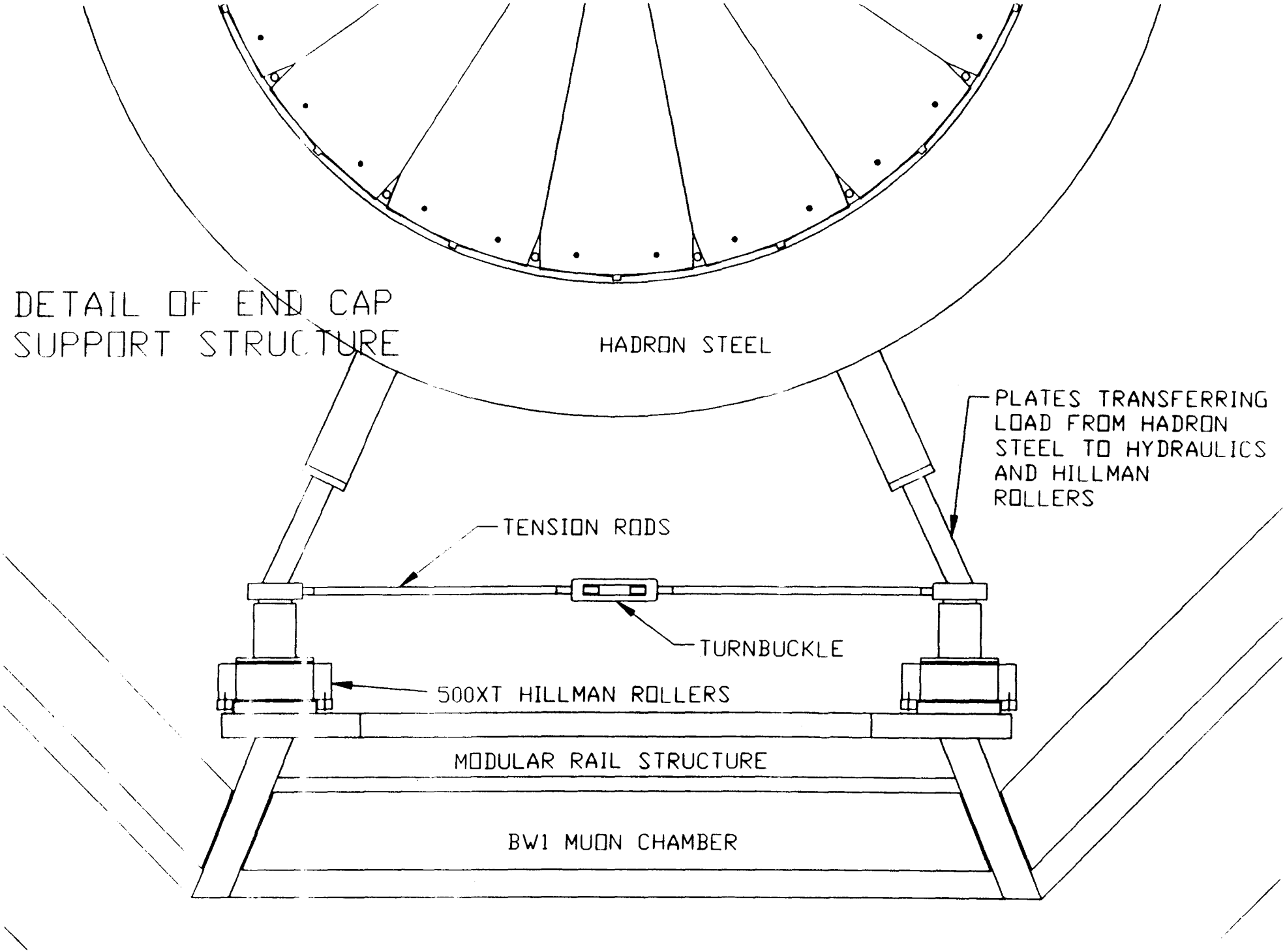
DETAIL OF END CAP
SUPPORT STRUCTURE
HADRON STEEL
PLATES TRANSFERRING
LOAD FROM HADRON
STEEL TO HYDRAULICS
AND HILLMAN
ROLLERS
TENSION RODS
TURNBUCKLE
500XT HILLMAN ROLLERS
MODULAR RAIL STRUCTURE
BW1 MUON CHAMBER

CUTAWAY VIEW OF SEGMENTED ABSORBER CONE BOLTED TO THE DOWNSTREAM END OF THE END CAP CALORIMETER

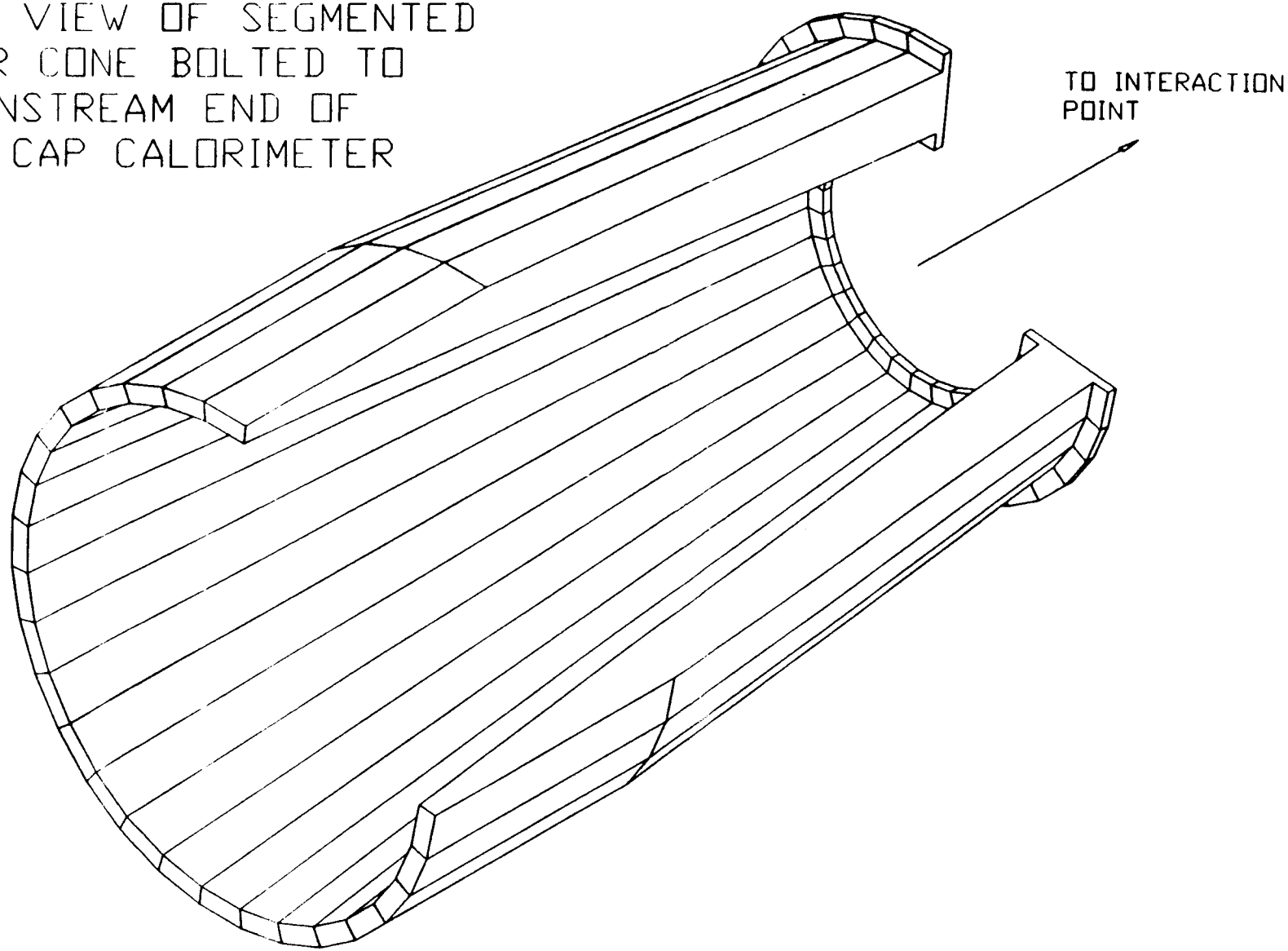

3.19 EM CALORIMETER REPLACEMENT PROCEDURE

3.19.1 Asumptions

- All Layers of EM Need Replacement
- Readout Fiber "Extension Cords" Outside of Radiation Field are OK
- Spare "Pizza Pan Assemblies" of Scintillator Tested and Ready
- 2-6 Person Shift Crew Depending on Task
- No Competition for Tracker Access
- No Undue Overhead for Radiation Safety
- Local Facility Exists for Printing Phototube Masks from PMT Measurements

- DO IT INSIDE MUON STEEL

3.20 Task Sequence for for EM Scintillator Replacement

- Retract Endwall Minimum of 1.5m
- Uncable Optical Harnesses & Secure Ends
- Disconnect Source Tube Assemblies
- Attach Extender Bars, Open Up Stack
- Remove & Replace Scint. Octants
  160 Octants @20 Mins Ea.
- Recompress Stack and Remove Extender Bars
- Reconnect Optical Harnesses & Source Tubes
- Source Measurement
  (80 Channels/wedge) * (4 mins/scan)
- Problem Fixup & Source Check
- Install PMT Masks
  (2000 PMTs) * (1 min/mask) * (2 two-man crews)
- Final Source Scan Verify Masks
- Attach & Verify Nitrogen Purge
- Close Endwall

Total time ≈ 1-1½ months SINGLE SHIFT
(Could halve the time by multiple shifts)

END CAP EM SECTION
INITIAL COSTS

WBS	TASK TITLE	BASE ($)	CONT.	BASE + CONT. ($)
2.2.1.1.1	EM Absorber Structure	1,881,075	1.36	2,558,262
2.2.1.2.1	EM Scintillator Assy.	920,579	1.40	1,288,811
2.2.1.2.2	SMD Scintillator Assy.	569,491	1.44	820,067
2.2.2.1.1	EM Scint. Insertion into Absorber	412,043	1.35	556,258
2.2.2.1.2	SMD Scint. Insertion into Absorber	219,537	1.39	305,151
TOTAL	WITHOUT ABSORBER STRUCTURE			2,470,24[illegible]
TOTAL	WITH ABSORBER STRUCTURE			5,528,555

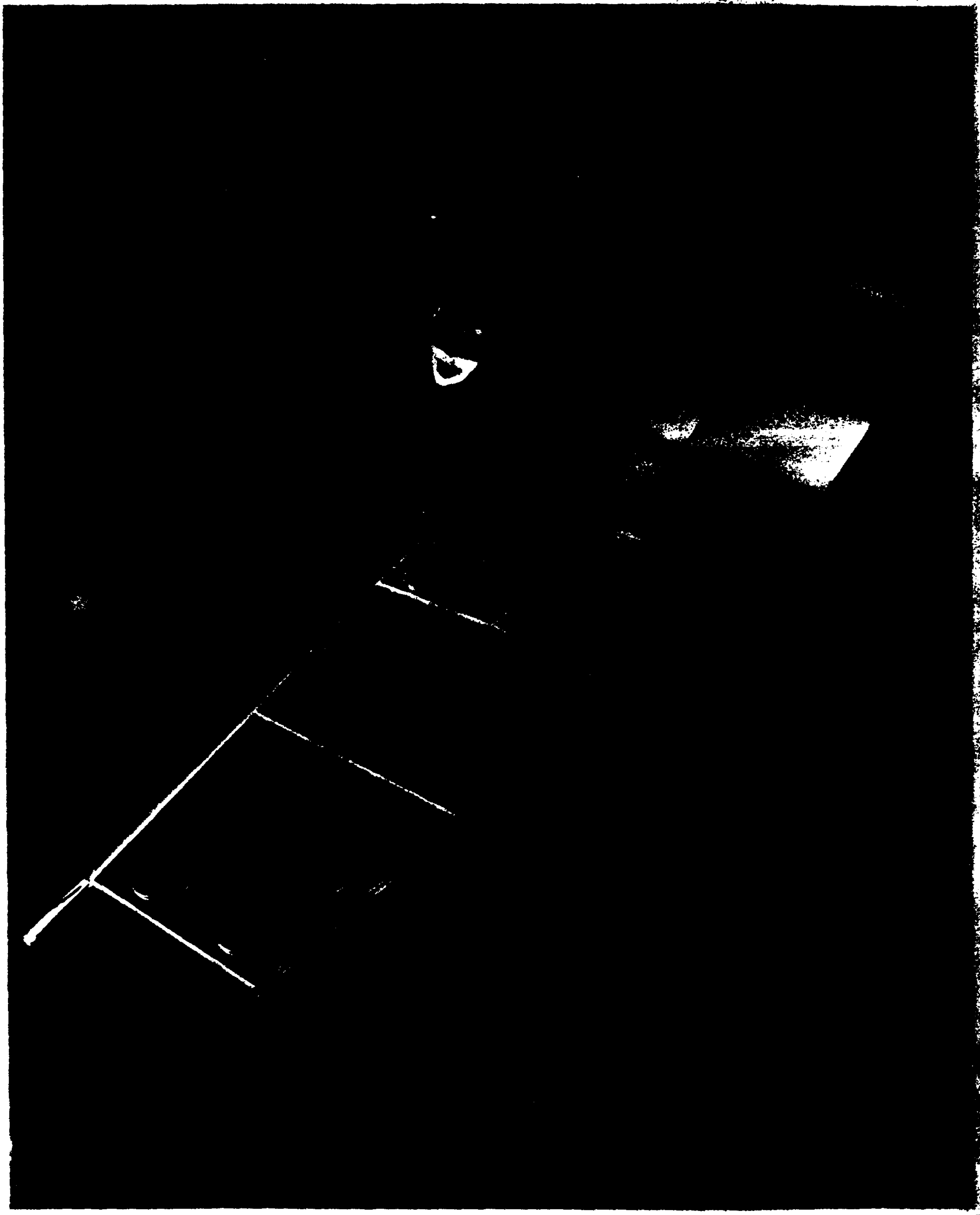

M-387-8

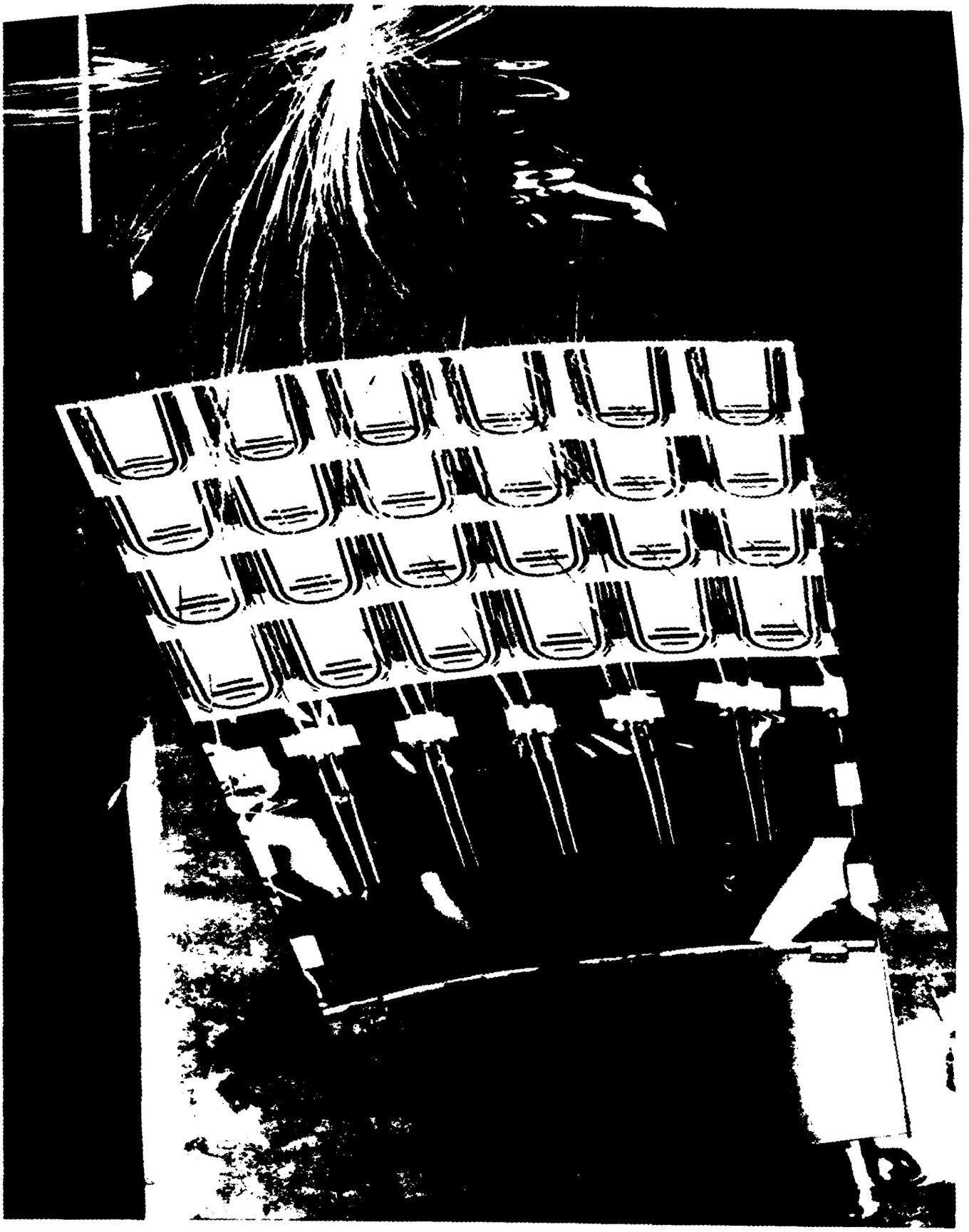

P-2JP-14

CALORIMETER REVIEW AND TECHNICAL BOARD MEETING
SEPTEMBER 12 -14, 1991
SSCL

Presentation by:

Larry Price

Argonne National Laboratory

TILE FIBER TEST EMC PERFORMANCE

SDC Technical Board

L. E. Price

September 12, 1991

How good are the pieces?

- Absorber Thickness

  $\sigma = 1\%$

- Optical System

  Testing system

  Light Yield 3 p.e./mip-layer

  Transverse uniformity $\sigma \sim 1\%$

  Longitudinal uniformity $\sigma = 8\%$

  Scintillator thickness $\sigma = 3.6\%$

  Fibers + splices $\sigma = 3.8\%$

  May want to mask

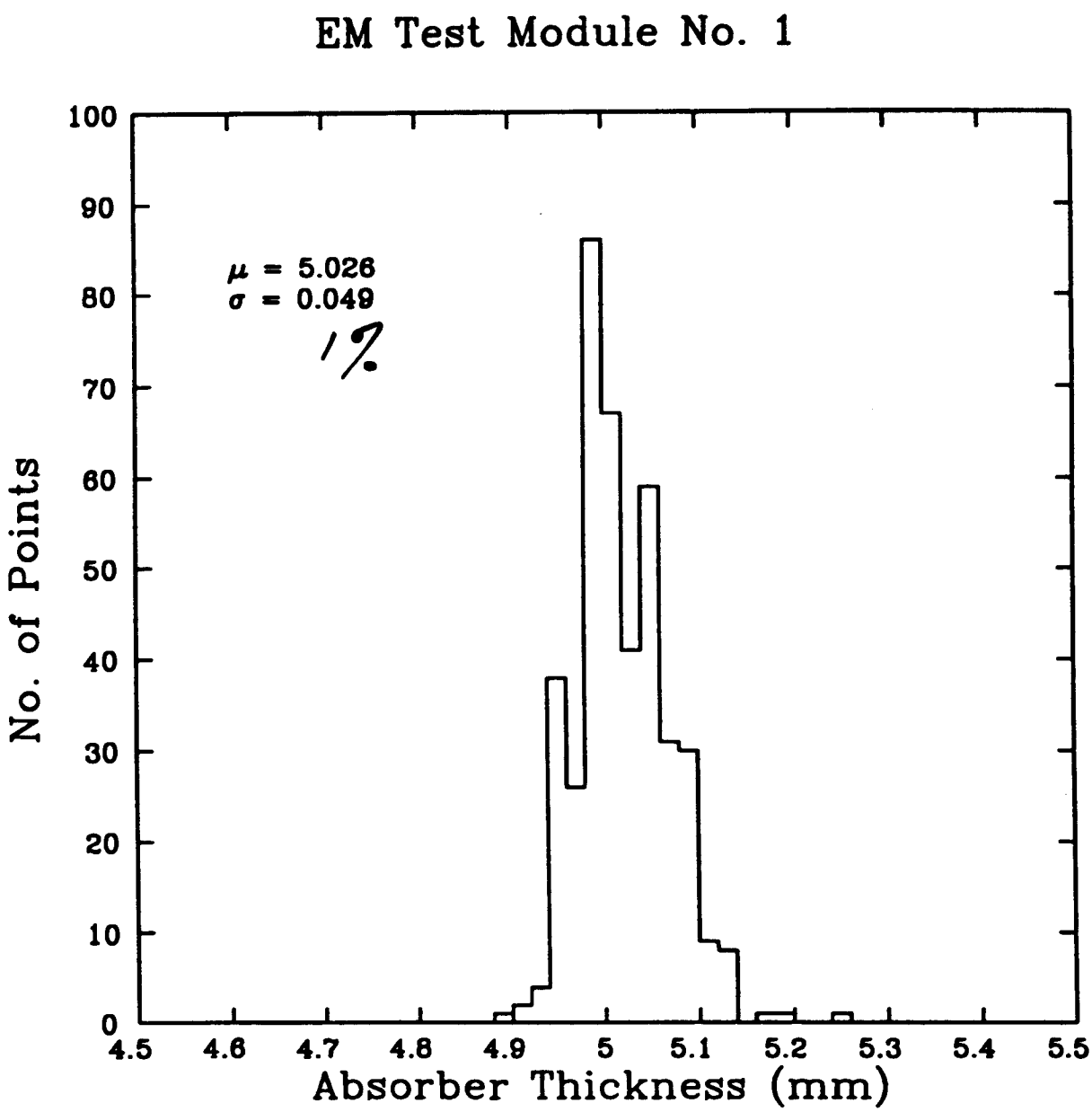

Absorber plate thickness distribution
3 Points per plate: left , center, right

TILE-FIBER TEST SYSTEM

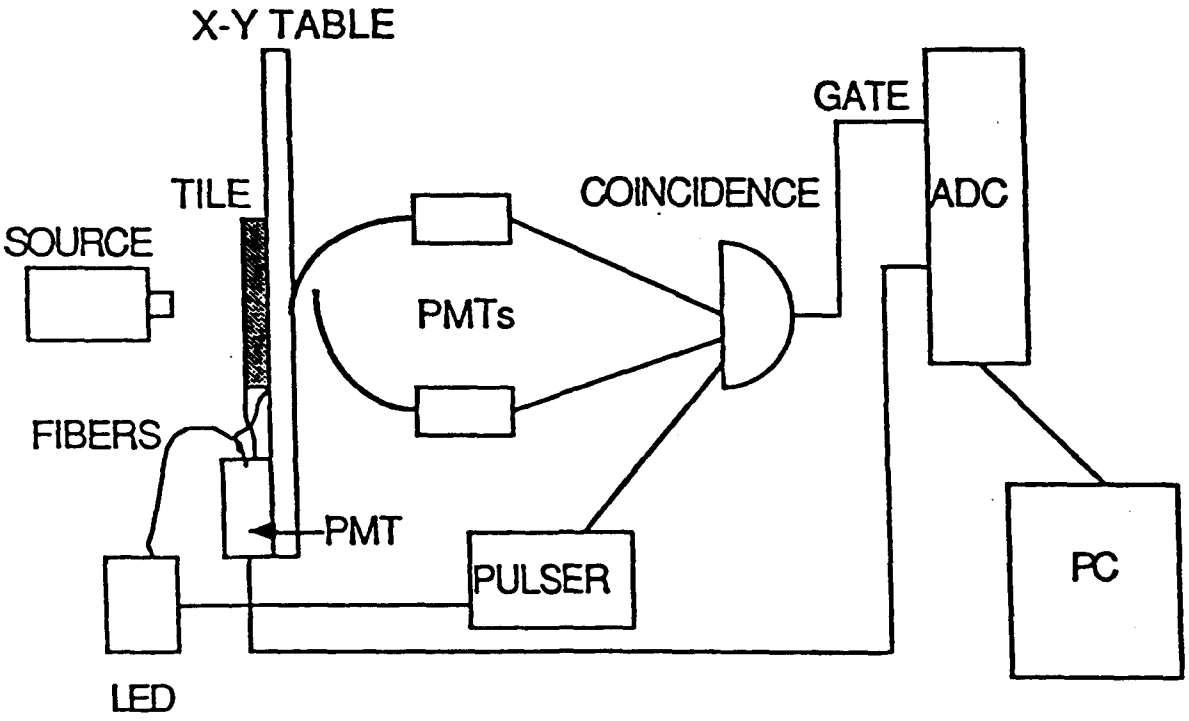

Figure 1

Ru^{106} Beam Transport

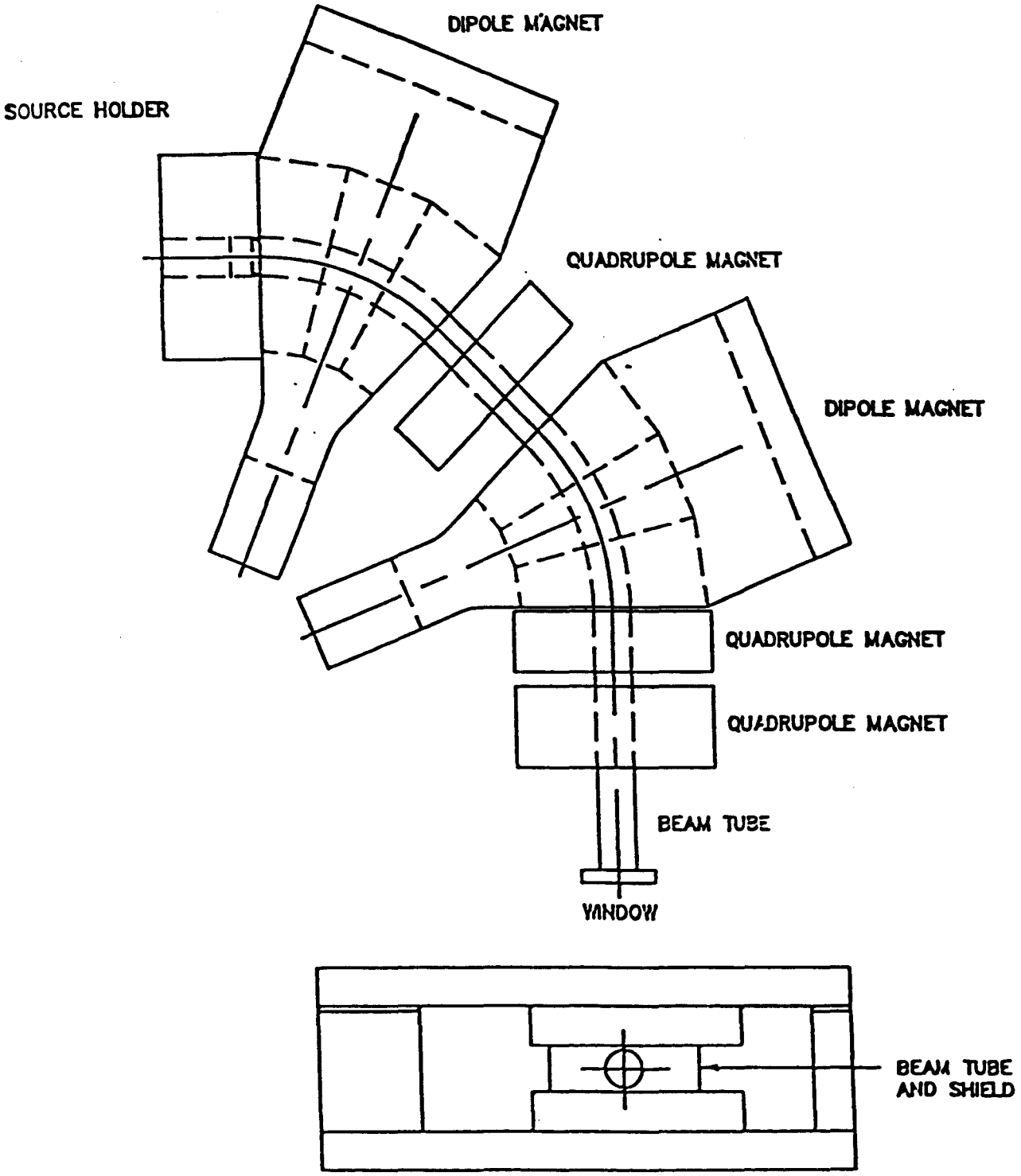

Figure 2

LIGHT YIELD AT CENTER NO MASKING

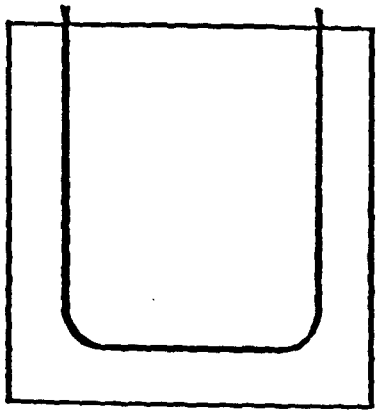

RECTANGULAR EDGE

WRAP:	pe/mip
BLACK TEDLAR	0.9
WHITE PAPER	1.66
AL. MYLAR	2.47

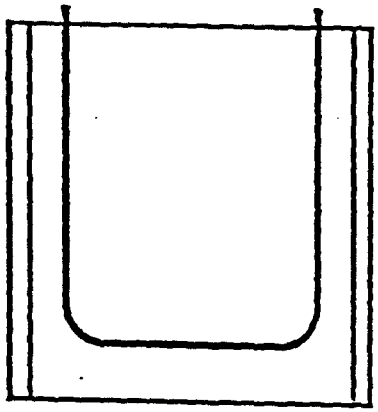

ANGLE CUT EDGE

AL. MYLAR 1.75

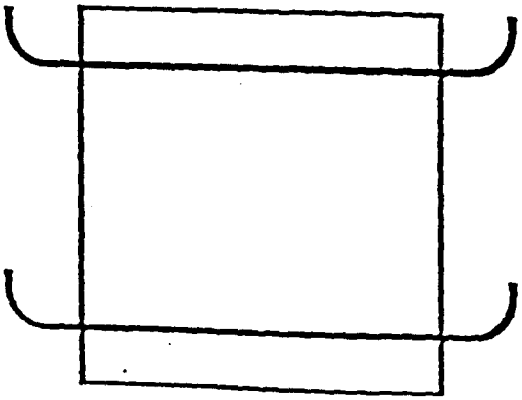

AL. MYLAR 2.0

ALL DATA FOR
2.8 M OF CLEAR
FIBER

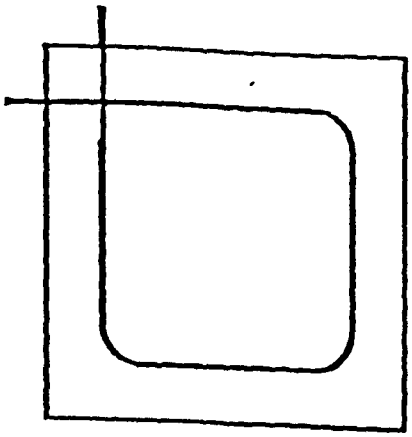

AL. MYLAR 3.0 pe/mip

Figure 5

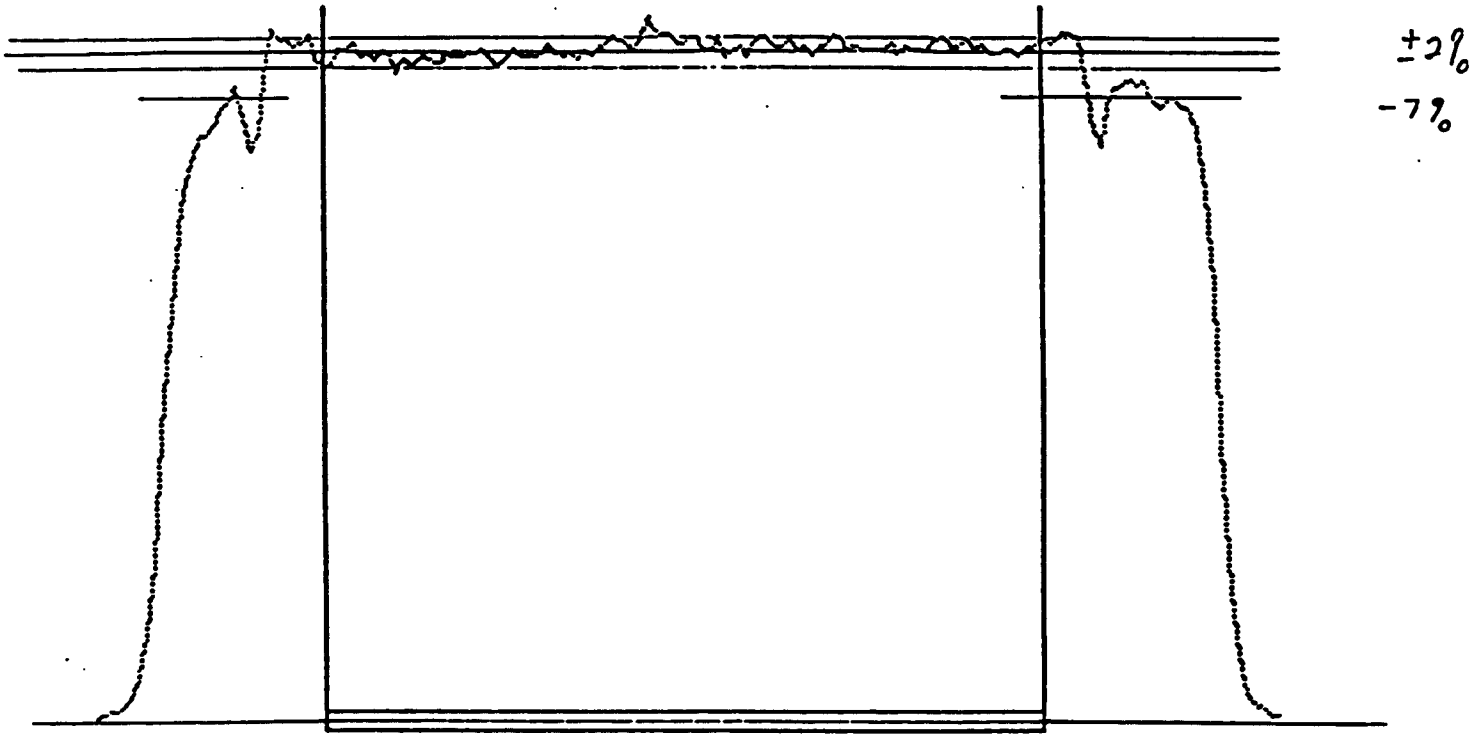

CORNER - TO CORNER SCAN OF TILE

LASER CUT
T229 BD1

Figure 14

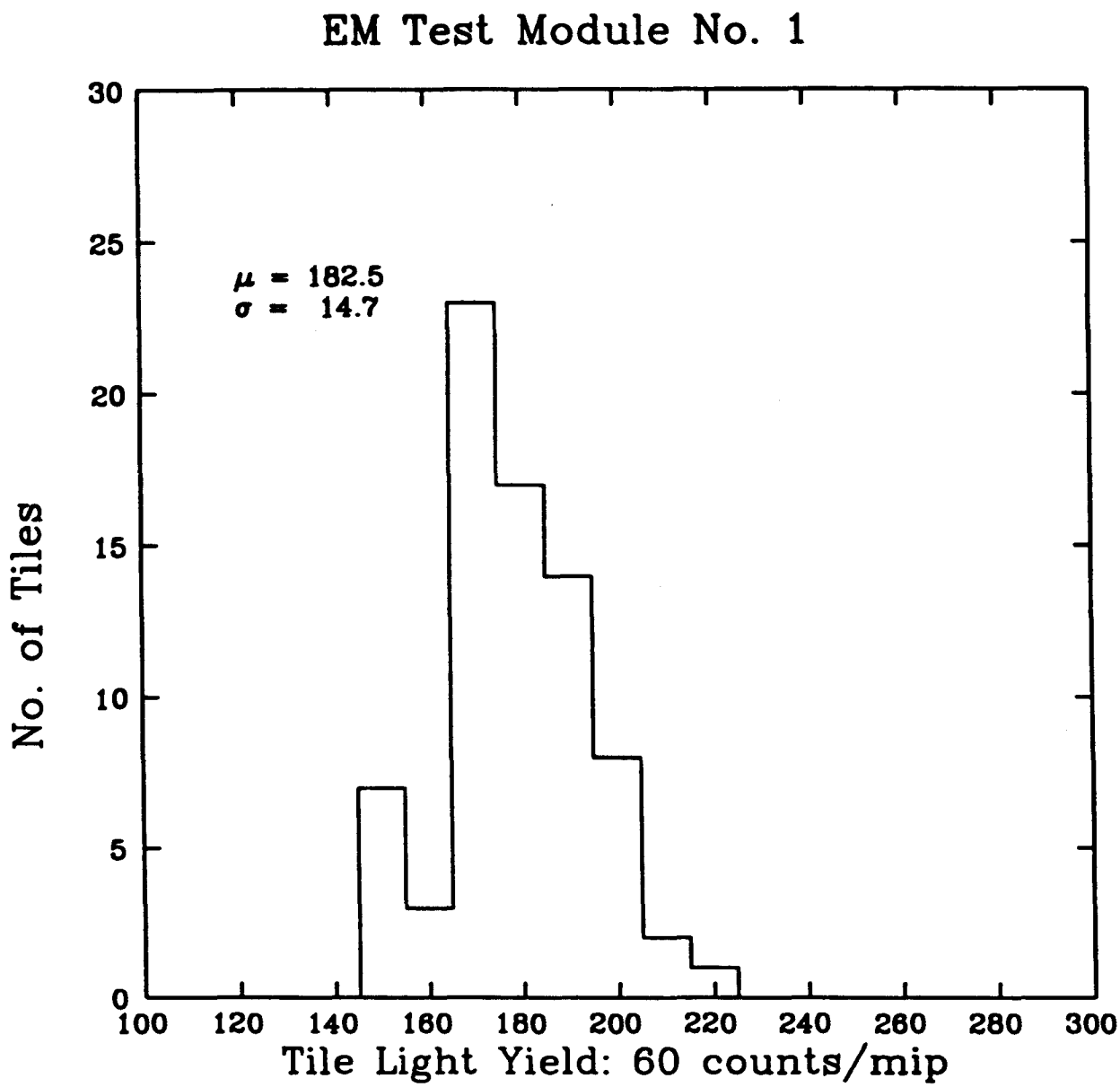

Scintillator tile light yield at center as measured by collimated Ruthinium source

del/M-TIME S cut

$\sigma = 3.8\%$

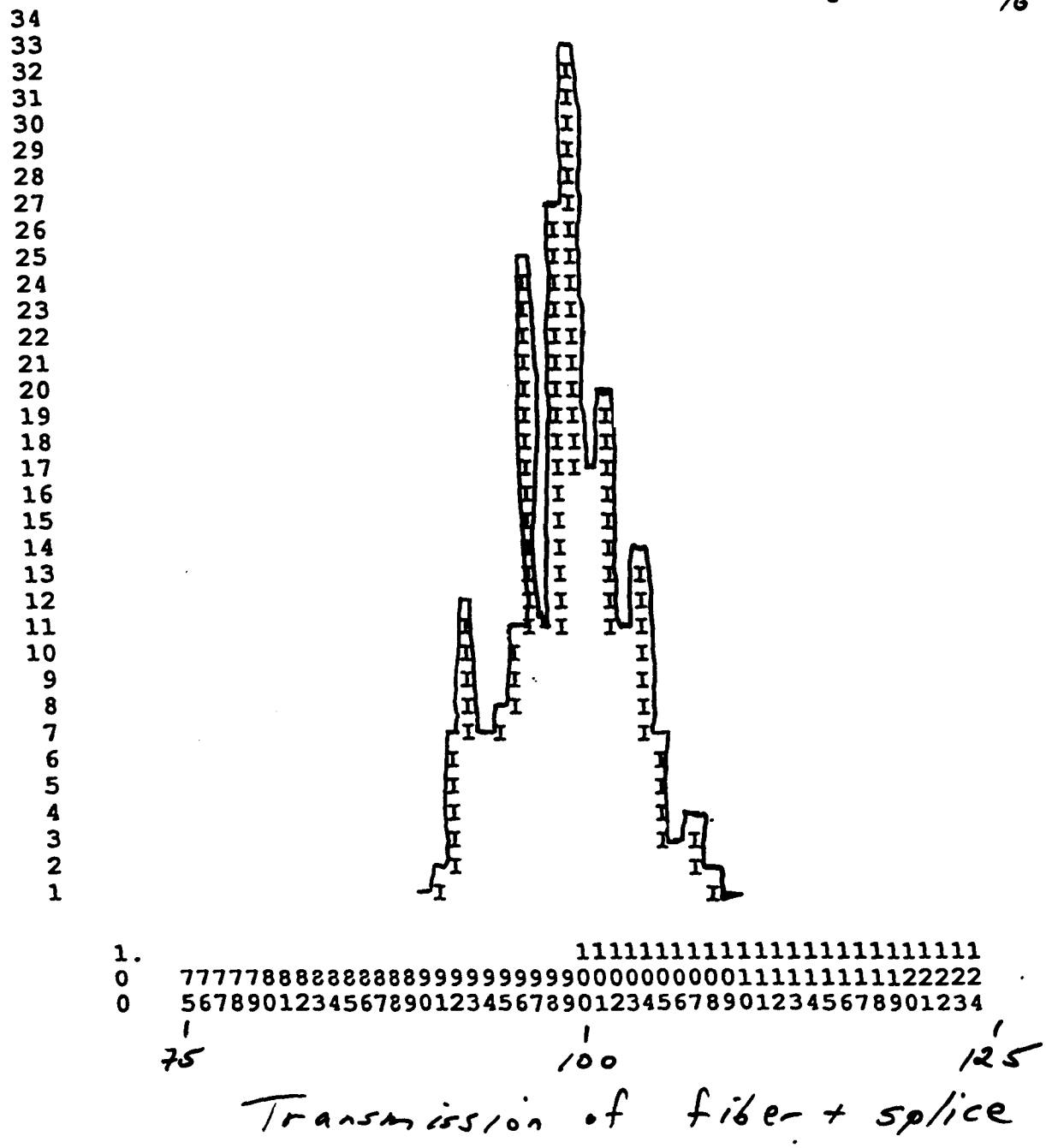

Transmission of fiber + splice

Figure 18

How good is the whole calorimeter?

- Testbeam measurements

  September 1-6, 1991

  3 towers instrumented

- Beamline setup

  Momentum tagging to $\sigma = 1.5\%$

  2 gas Cerenkov counters to tag electrons

  Beam 30-50% electrons

  Tunable 15-35 GeV. Can go to 100-150 GeV but rarely
  Data at (14), 19, 25, 33 GeV

  PWC's

- Resolution

  Matches calculation of $18\%\sqrt{E}$

  No evidence of constant term

- Uniformity

  Undersize scintillator emphasizes dip at bulkhead

  ...Which is mostly correctable

- Light yield

  Light to Tower 1 attenuated by neutral density filter

FNAL MP BEAMLINE

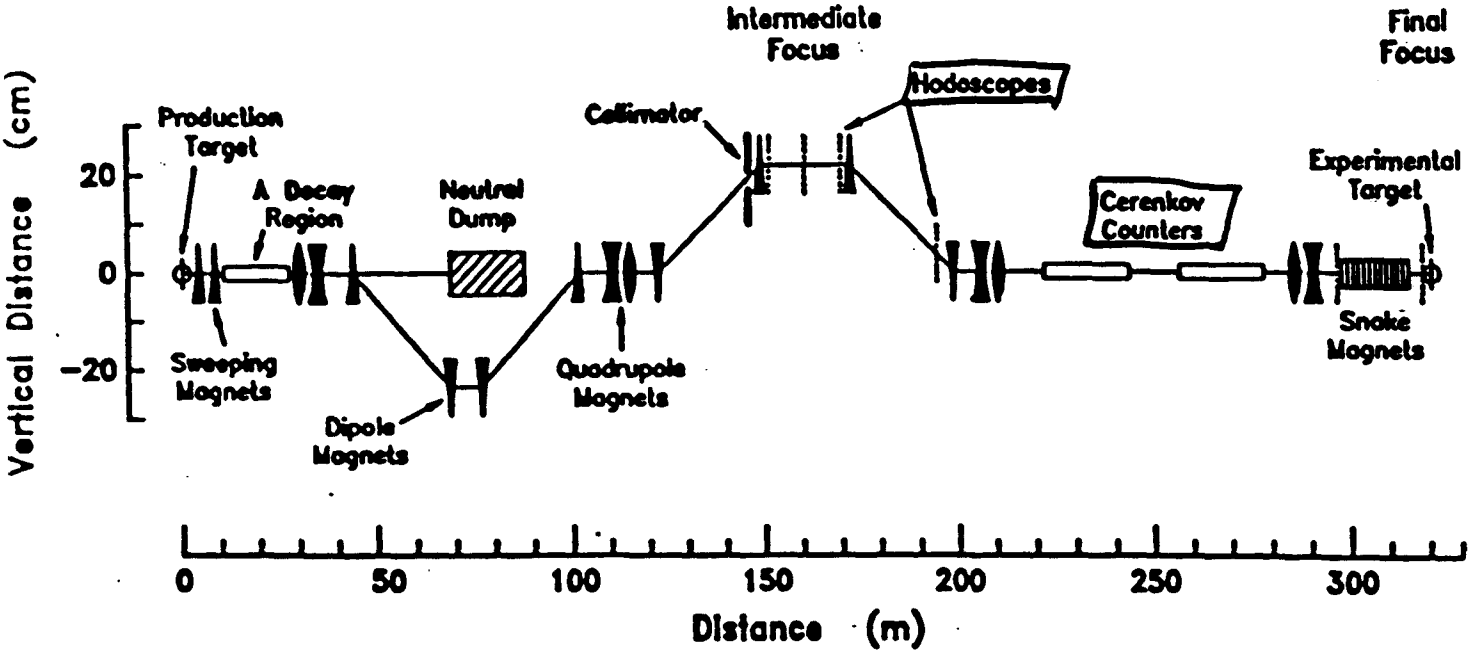

Figure 5

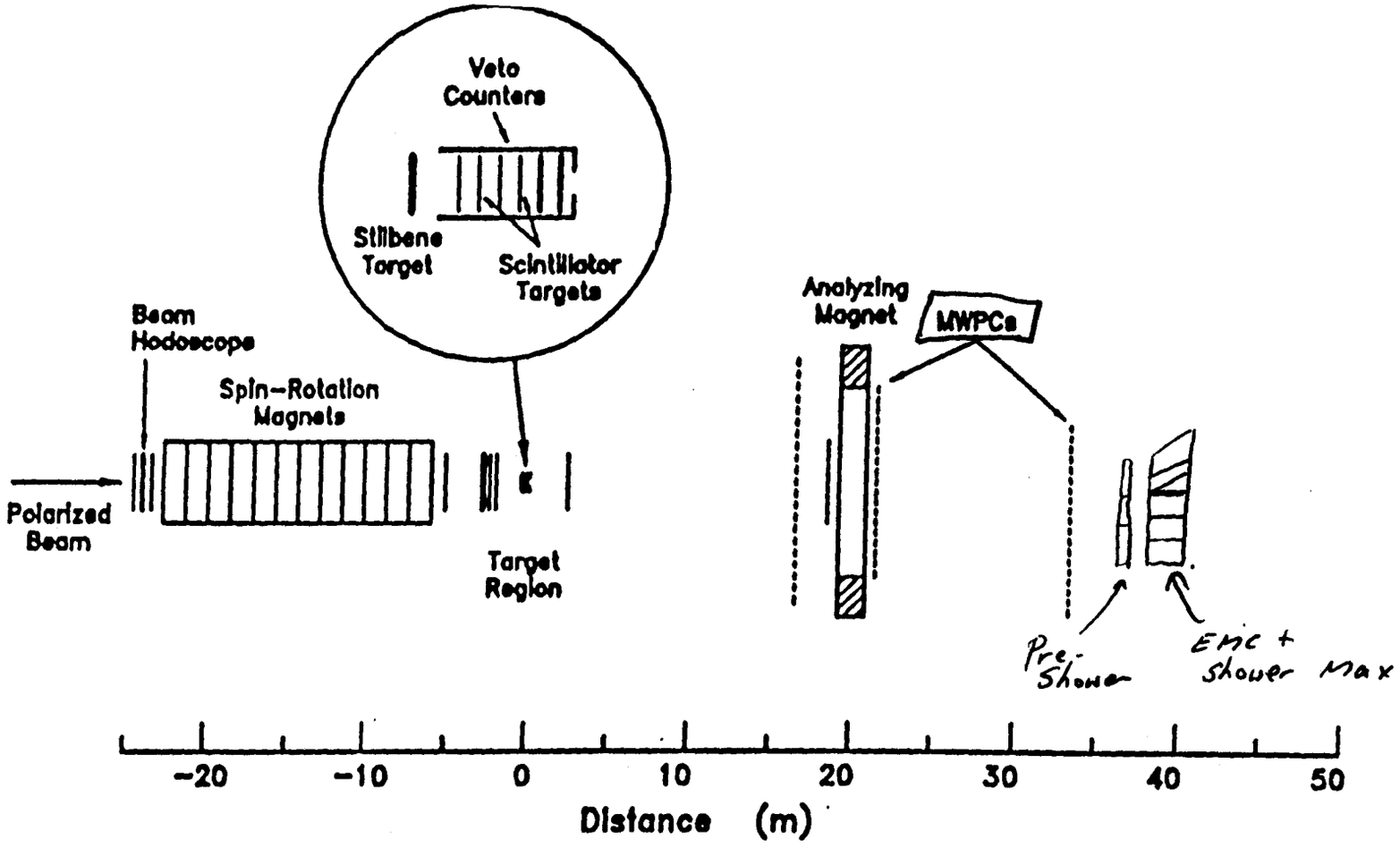
Veto Counters
Stilbene Target
Scintillator Targets
Beam Hodoscope
Spin-Rotation Magnets
Polarized Beam
Target Region
Analyzing Magnet
MWPCs
Pre-Shower
EMC + Shower Max
-20
-10
0
10
20
30
40
50
Distance (m)

Figure 25

EMC RESPONSE TO ELECTRONS

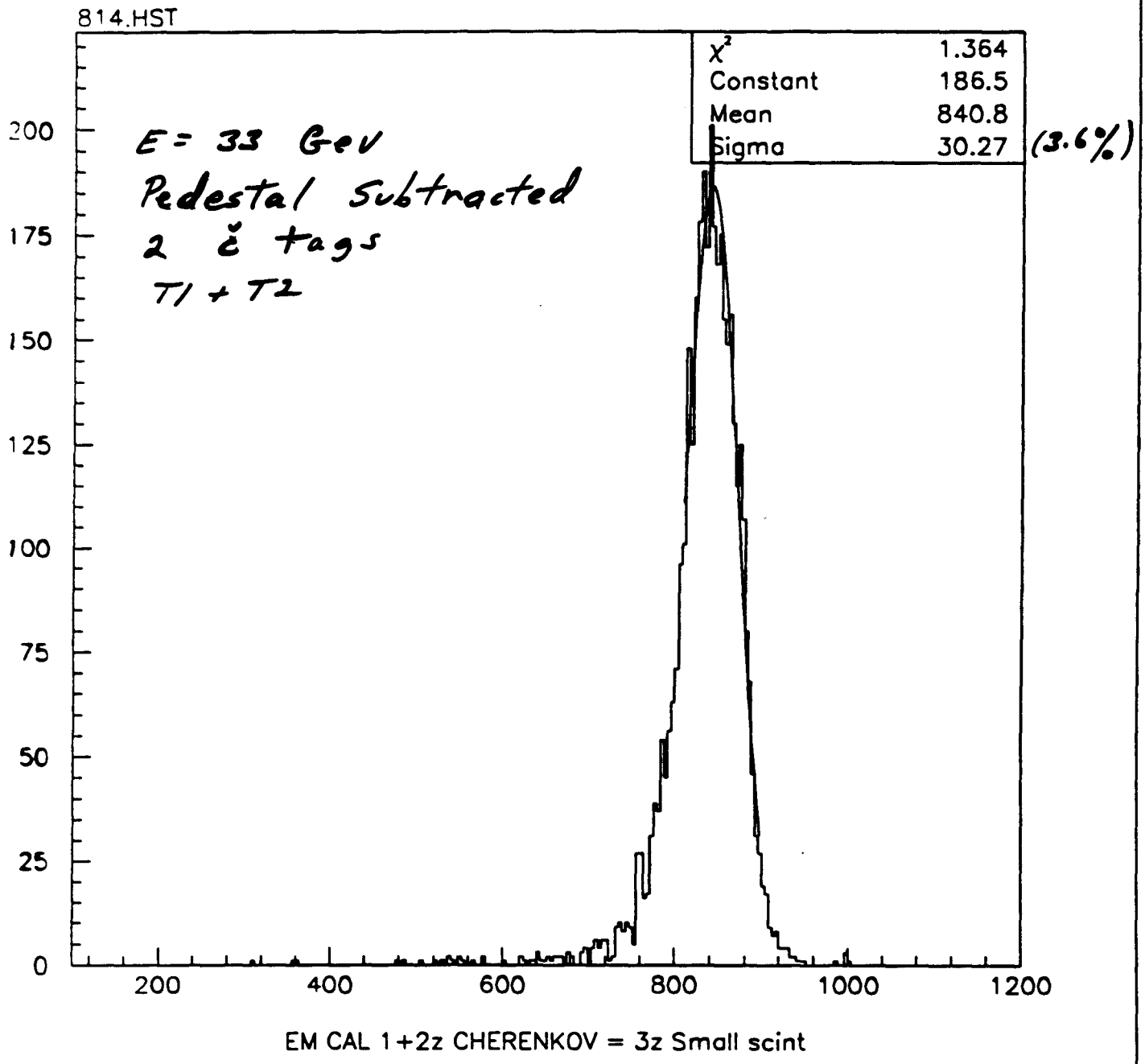

T1 + T2 Pulse height (Counts)

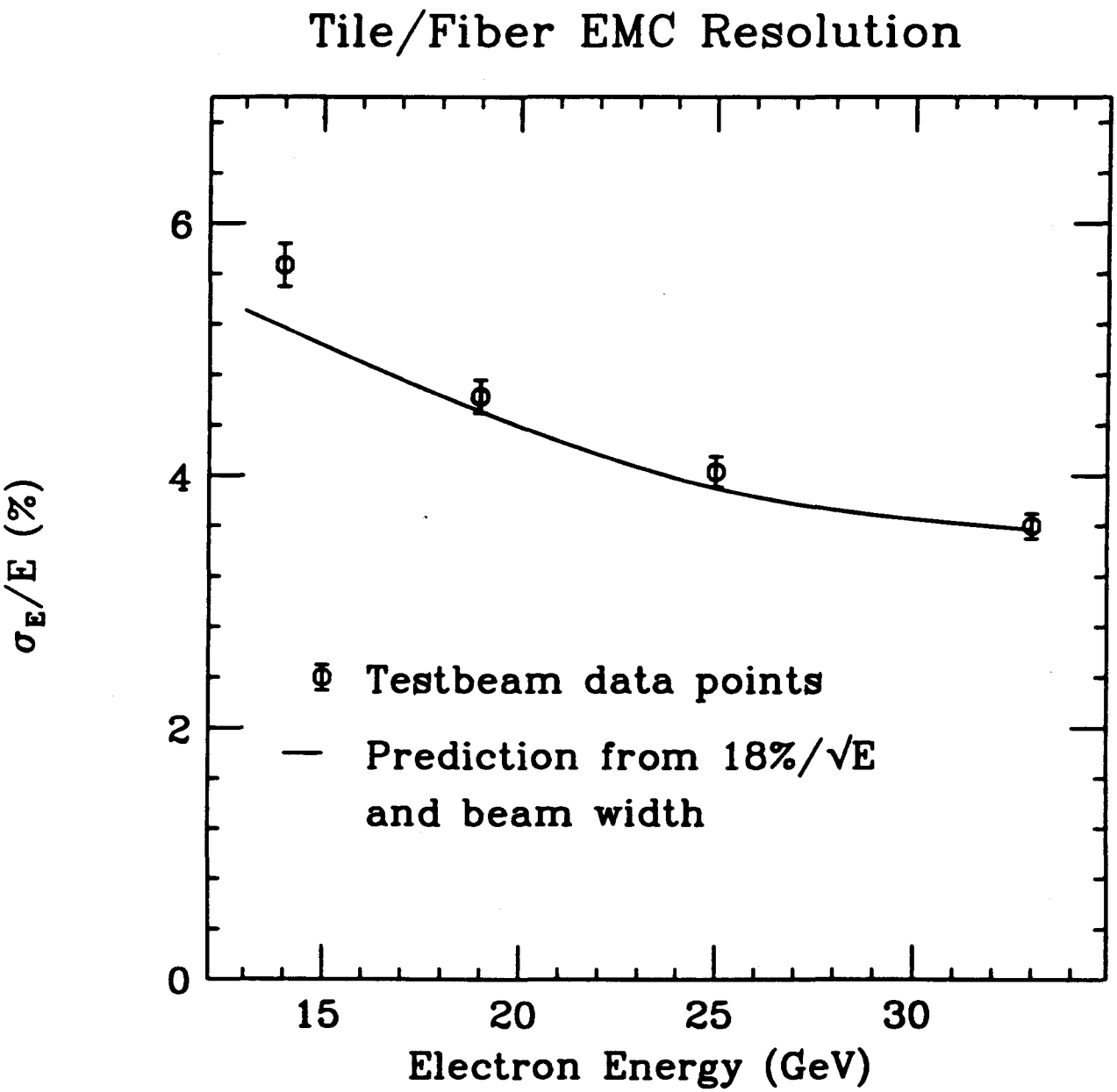
Tile/Fiber EMC Resolution
6
4
2
0
15
20
25
30
Electron Energy (GeV)
σE/E (%)
Φ Testbeam data points
— Prediction from 18%/√E
and beam width

TRANSVERSE SCAN

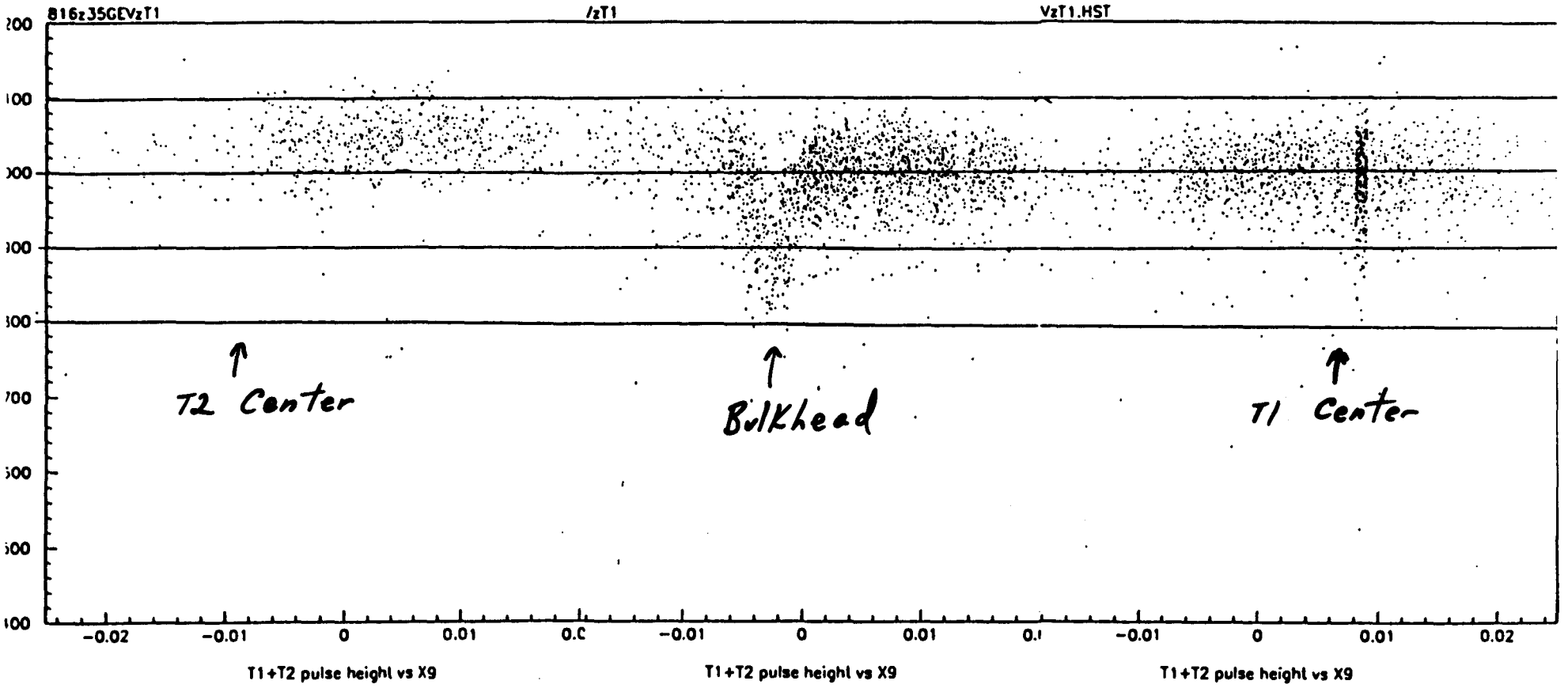

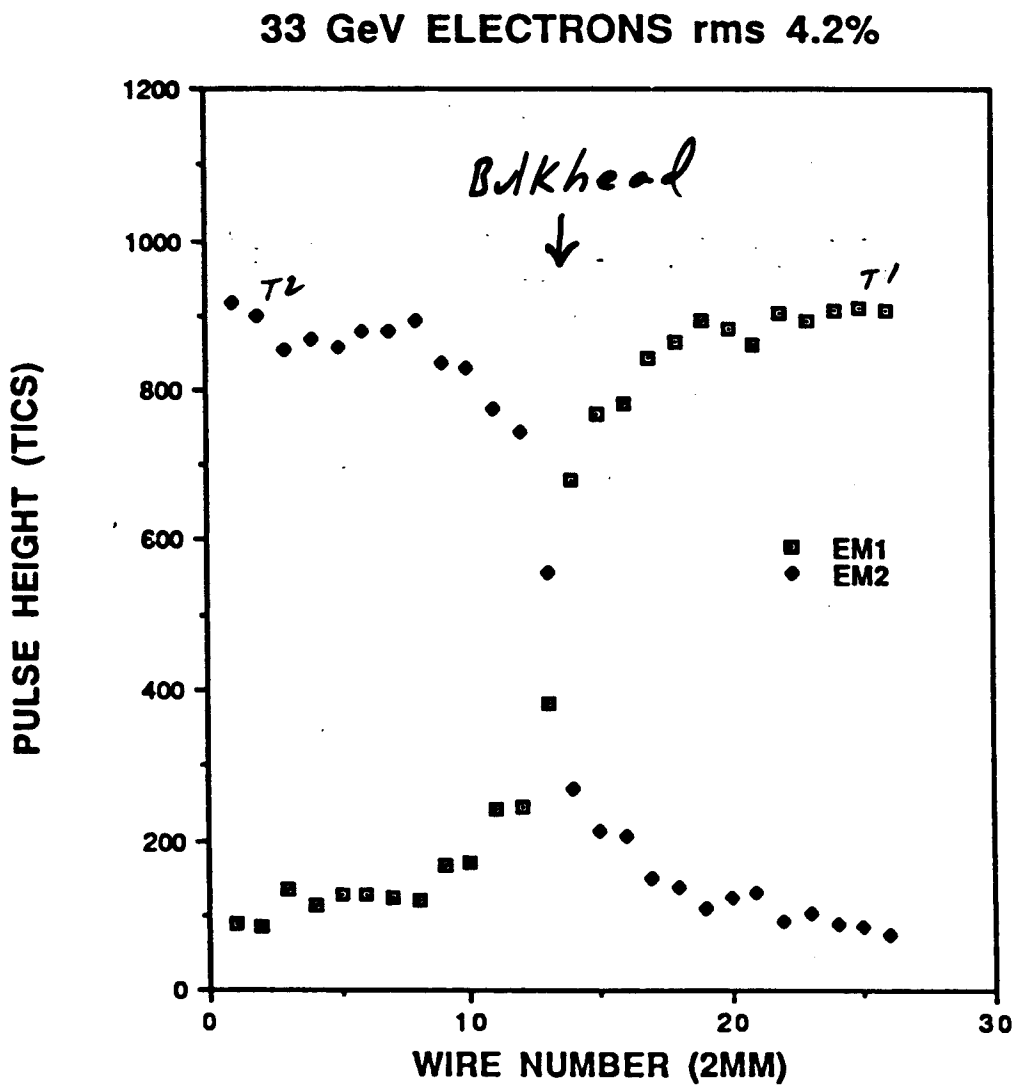

Figure 11.10 Uncorrected transverse uniformity of response across Tower 1 - Tower 2 region.

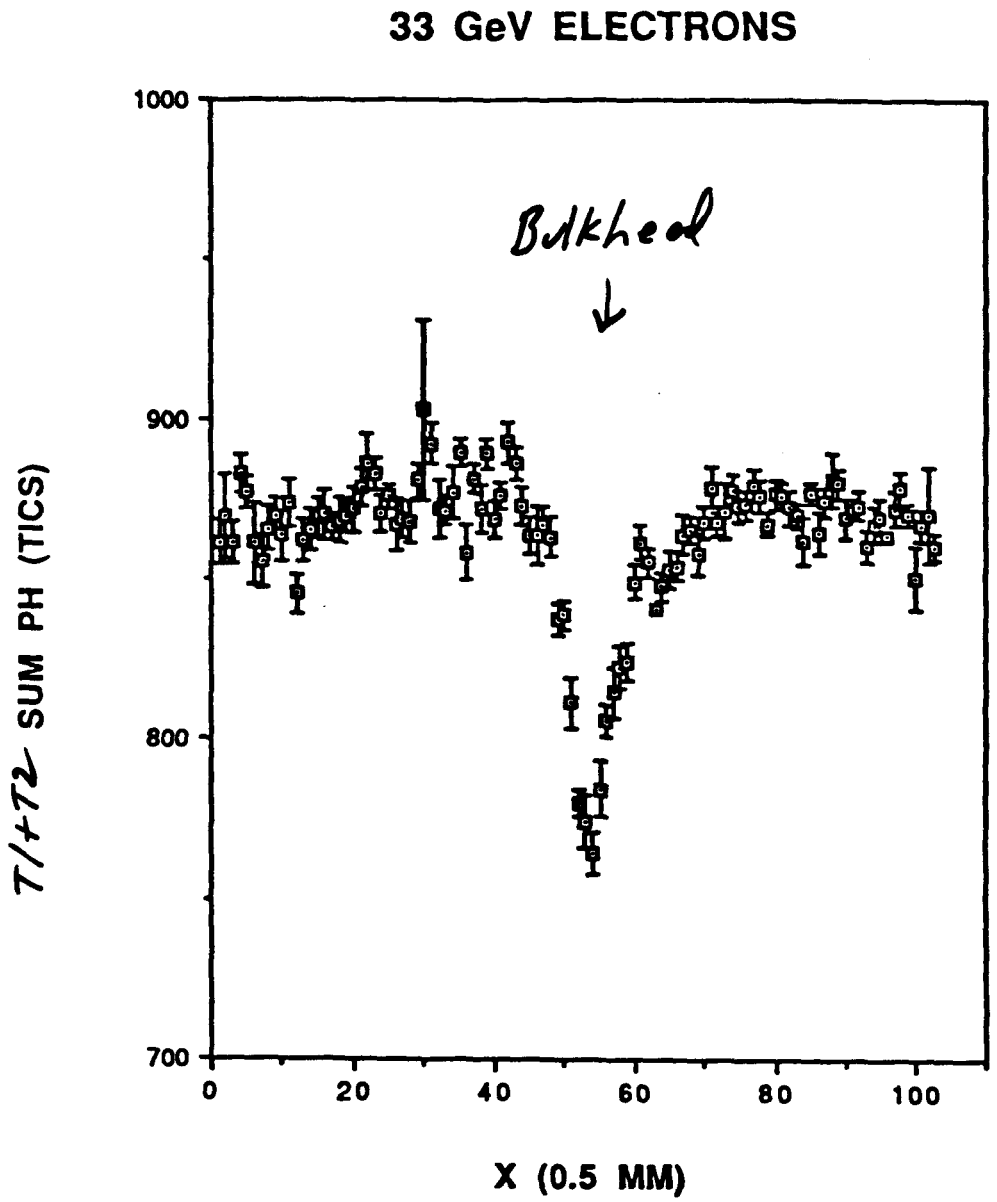
33 GeV ELECTRONS
Bulkhead
1000
900
800
700
0
20
40
60
80
100
T/+72 SUM PH (TICS)
X (0.5 MM)

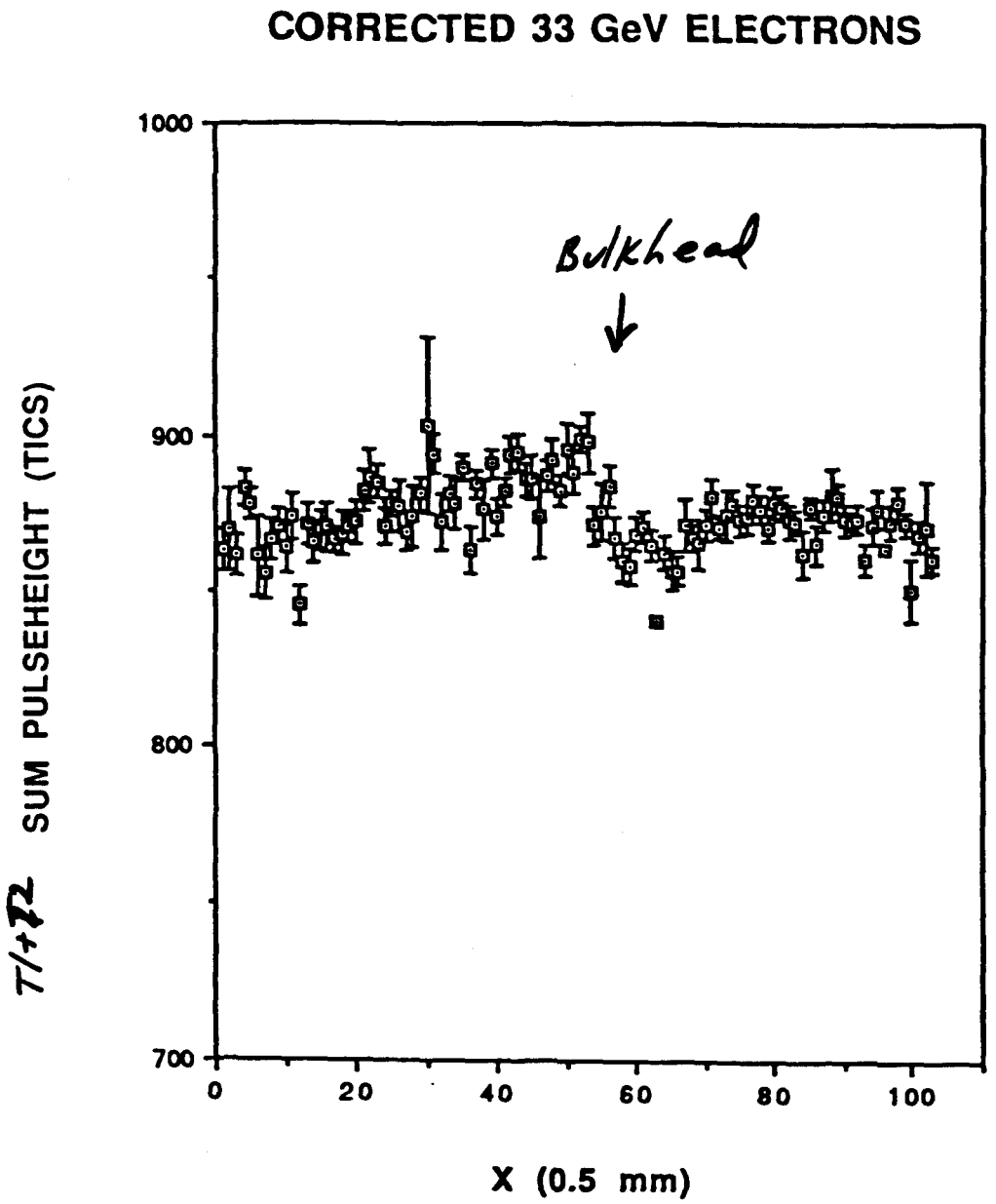
CORRECTED 33 GeV ELECTRONS
Bulkhead
1000
900
800
700
0
20
40
60
80
100
X (0.5 mm)
T1+T2 SUM PULSEHEIGHT (TICS)

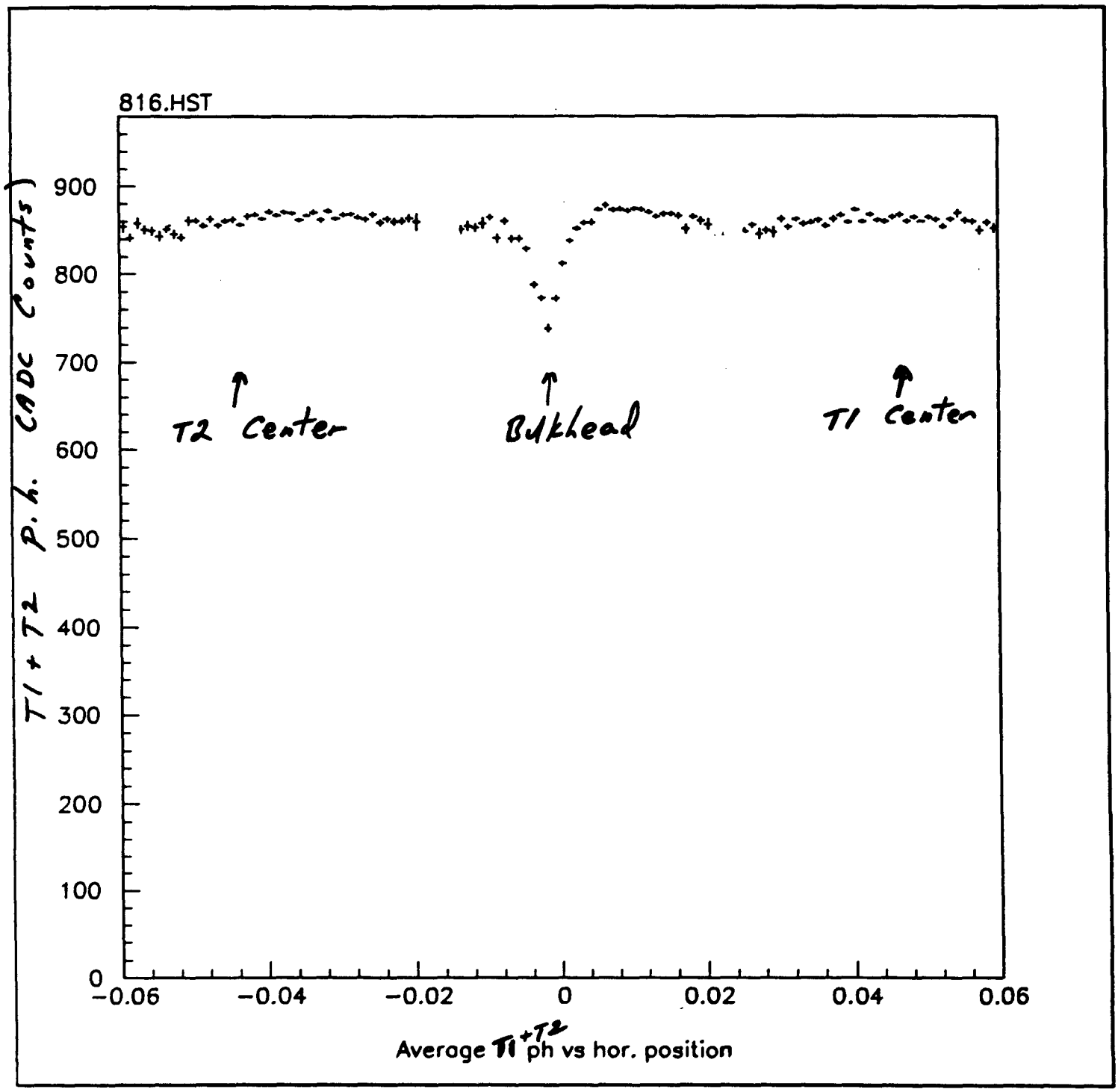
816.HST
T1 + T2 p.h. (ADC Counts)
900
800
700
600
500
400
300
200
100
0
−0.06
−0.04
−0.02
0
0.02
0.04
0.06
T2 Center
Bulkhead
T1 Center
Average T1+T2 ph vs hor. position

TEST OF PHOTOELECTRON STATISTICS

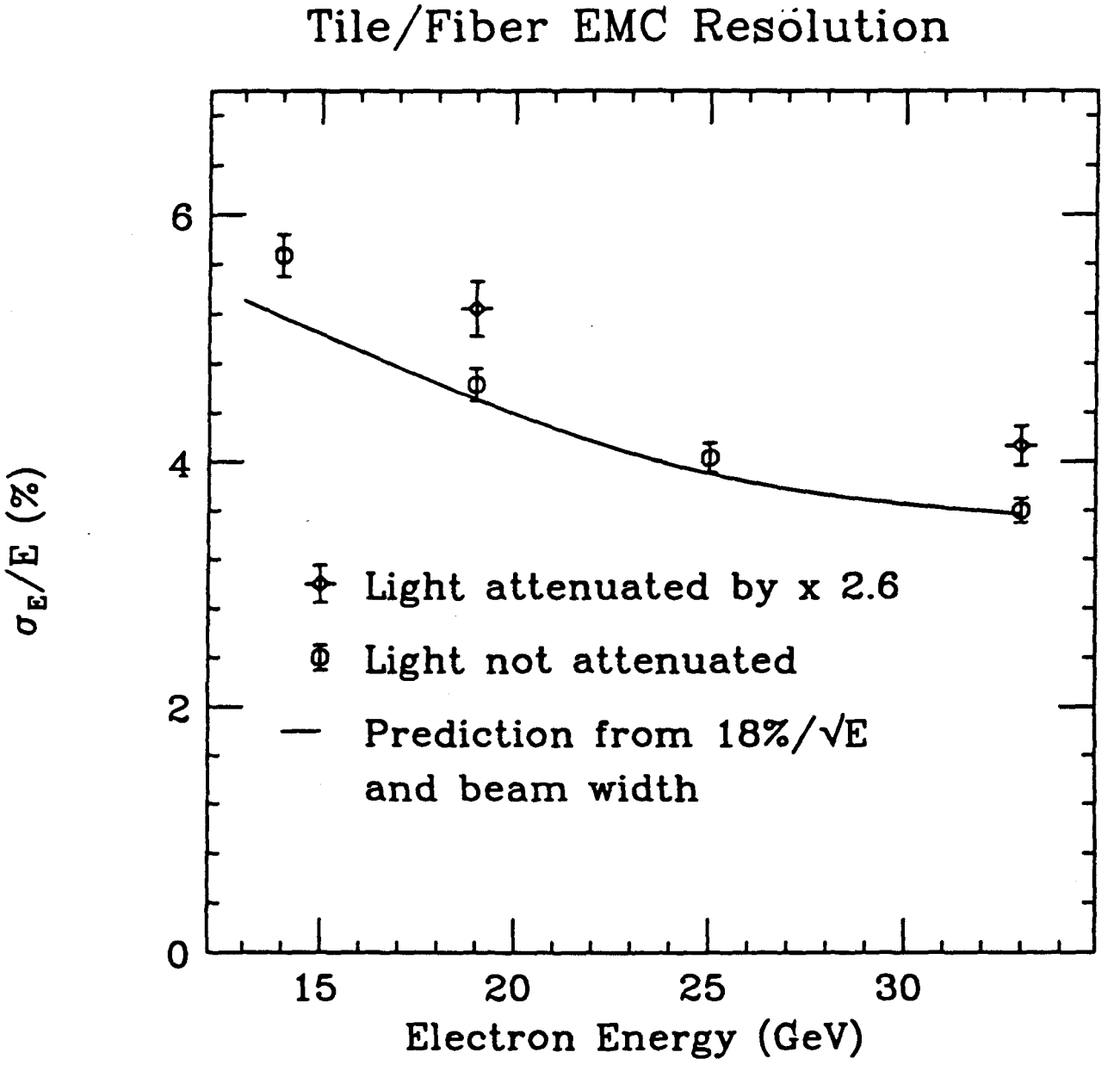

E	σ_E/E Unatten.	Atten.	$\frac{\sigma_N}{\sigma_0}$	Unattenuated photoelectrons	P.E./E
33 ~~19~~ GeV	3.6%	4.1	0.4	3905	118 ± 24 /GeV
19 ~~35~~	4.6	5.2	0.4	2657	139 ± 35 /GeV

Conclusions

- Test EMC performs as designed

  Light yield

  Resolution

  Uniformity

- FNAL is a good place to do tests...when there is beam

CALORIMETER REVIEW AND TECHNICAL BOARD MEETING
SEPTEMBER 12 -14, 1991
SSCL

Presentation by:

Dan Green

Fermilab

ORG
9/91

CRITICAL ISSUES FOR TILE / FIBER

1) OPTICS ✓

2) CALIBRATION ✓

3) RADDAM ✓ BARREL

4) REFURBISH (REMASK) ✓ ENDCAP
OR REPLACE

1) SEE CDR
+ TEST BEAM
DATA

} PROOF OF PRINCIPLE

OPTICS AND CALIBRATION ARE

CLOSELY CONNECTED:

USE Cs "SOURCE TUBES" TO

MEASURE LONGITUDINAL NONUNIFORMITIES

E.G. RADDAM TEST MODULE

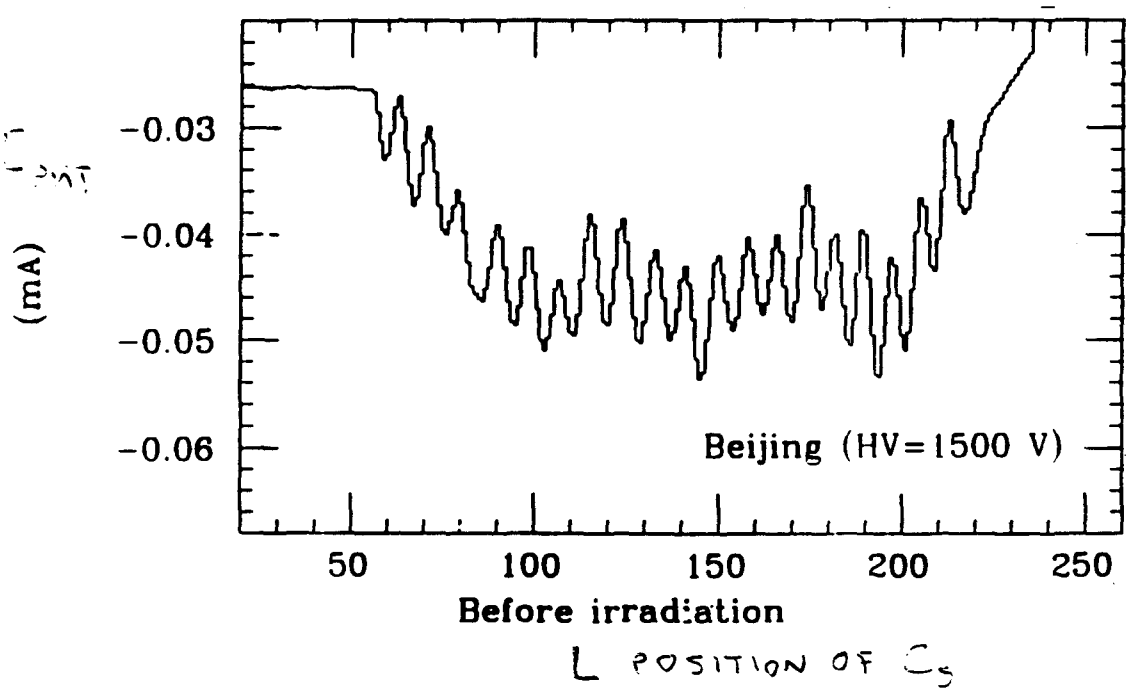

Figure 8.3 longitudinal source scan of a Beijing module.

NE SOURCE ⟹ MANY "SPIGOTS"
GET RELATIVE CALIBRATION TO

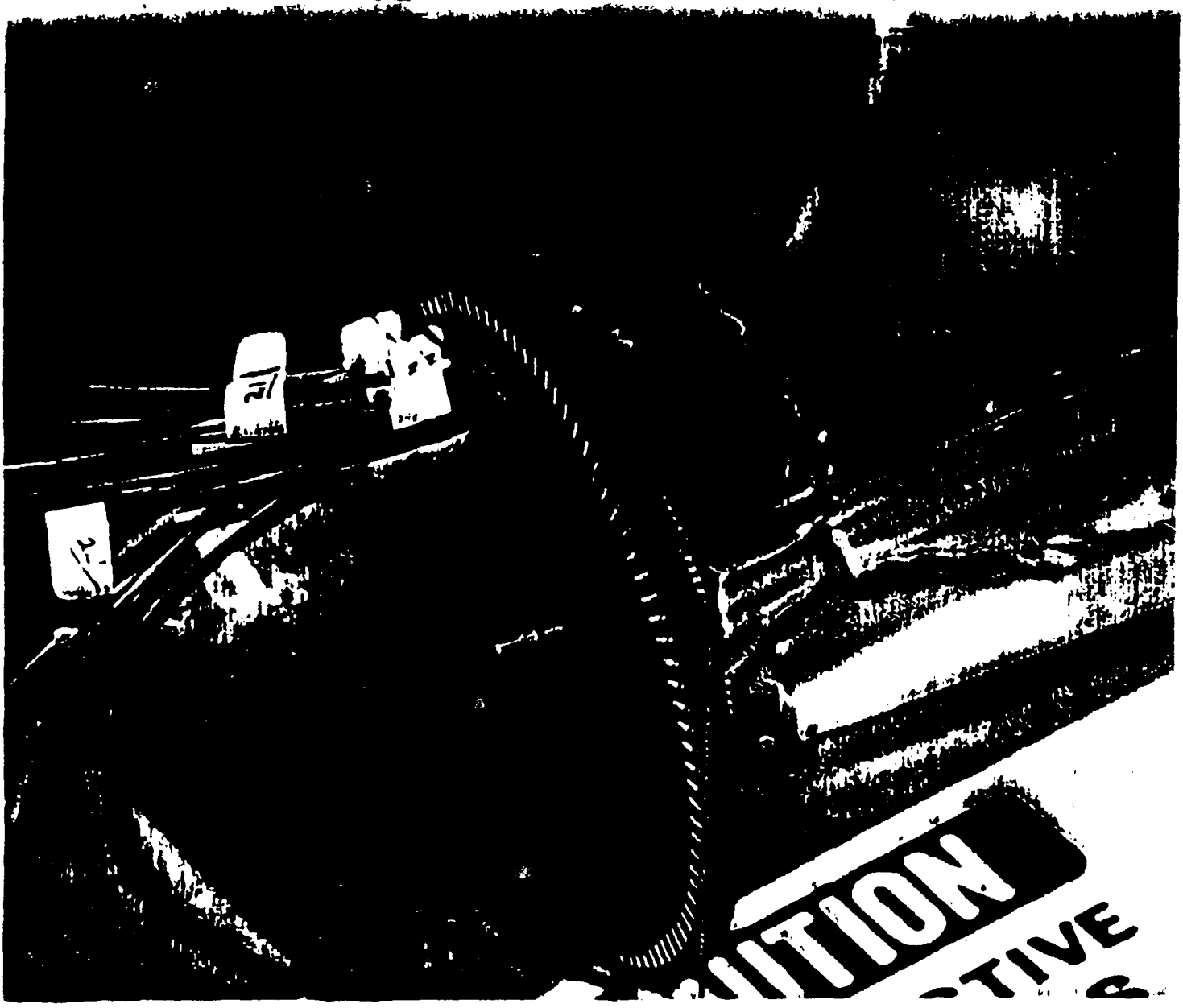

Figure 6.14 The source wire "Gatling Gun" driver developed by V. Barnes, Purdue.

DO NOT TRY TO MAKE TILES TOO UNIFORM;
MEASURE (USING SOURCES) AND CORRECT

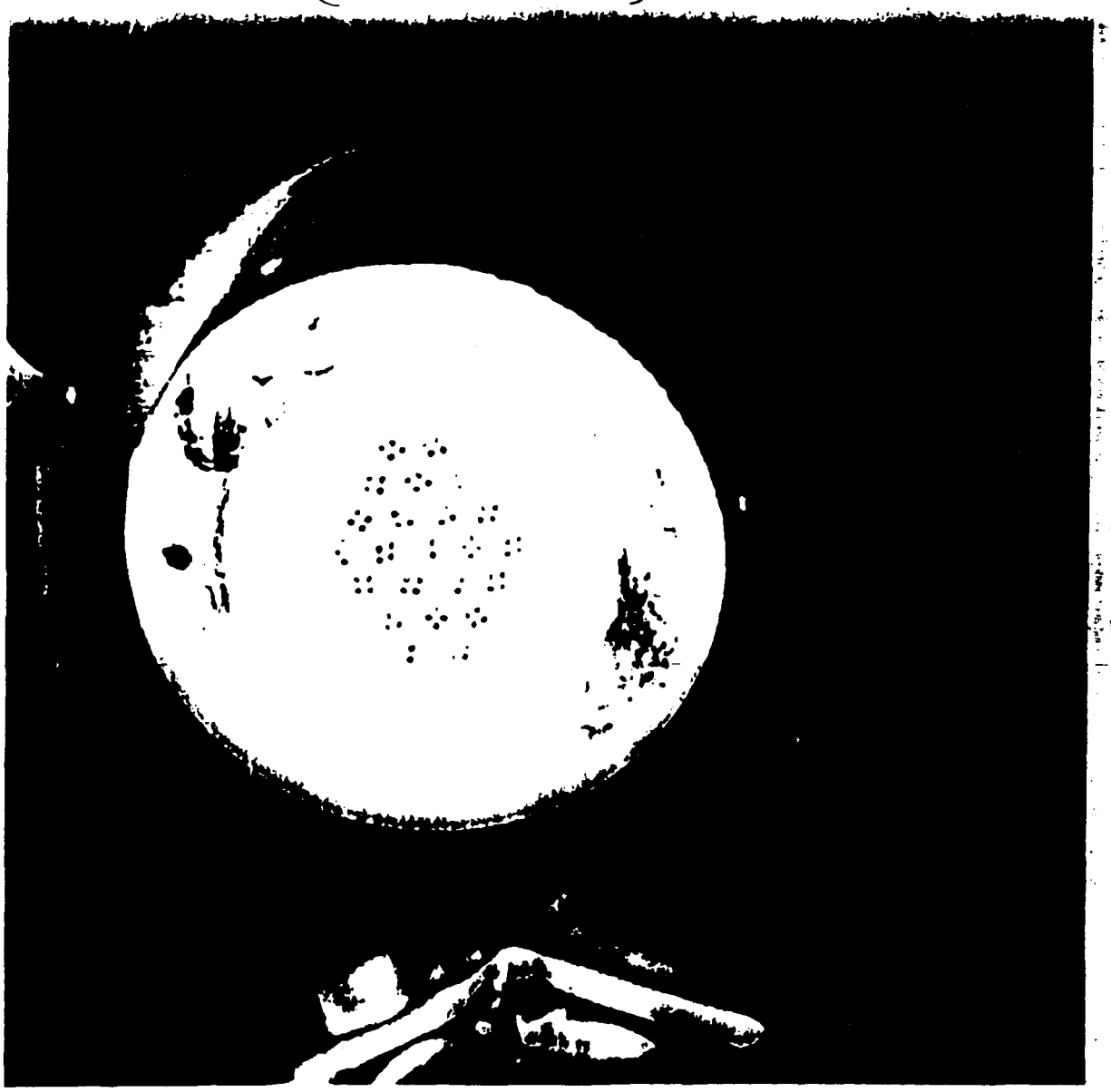

TILE,
WLS FIBER
SPLICE
CLEAR FIBE
ALL
"NULLED
OUT"
IN
SITU

N.B. WITH ENOUGH LIGHT
YOU CAN ITERATE TO
REFLATTEN RESPONSE
AFTER RADIATION
DAMAGE

"REMASK"

Figure 6.15 Phototube cookie. The fibers from each tile of a tower go into a separate hole in the cookie.

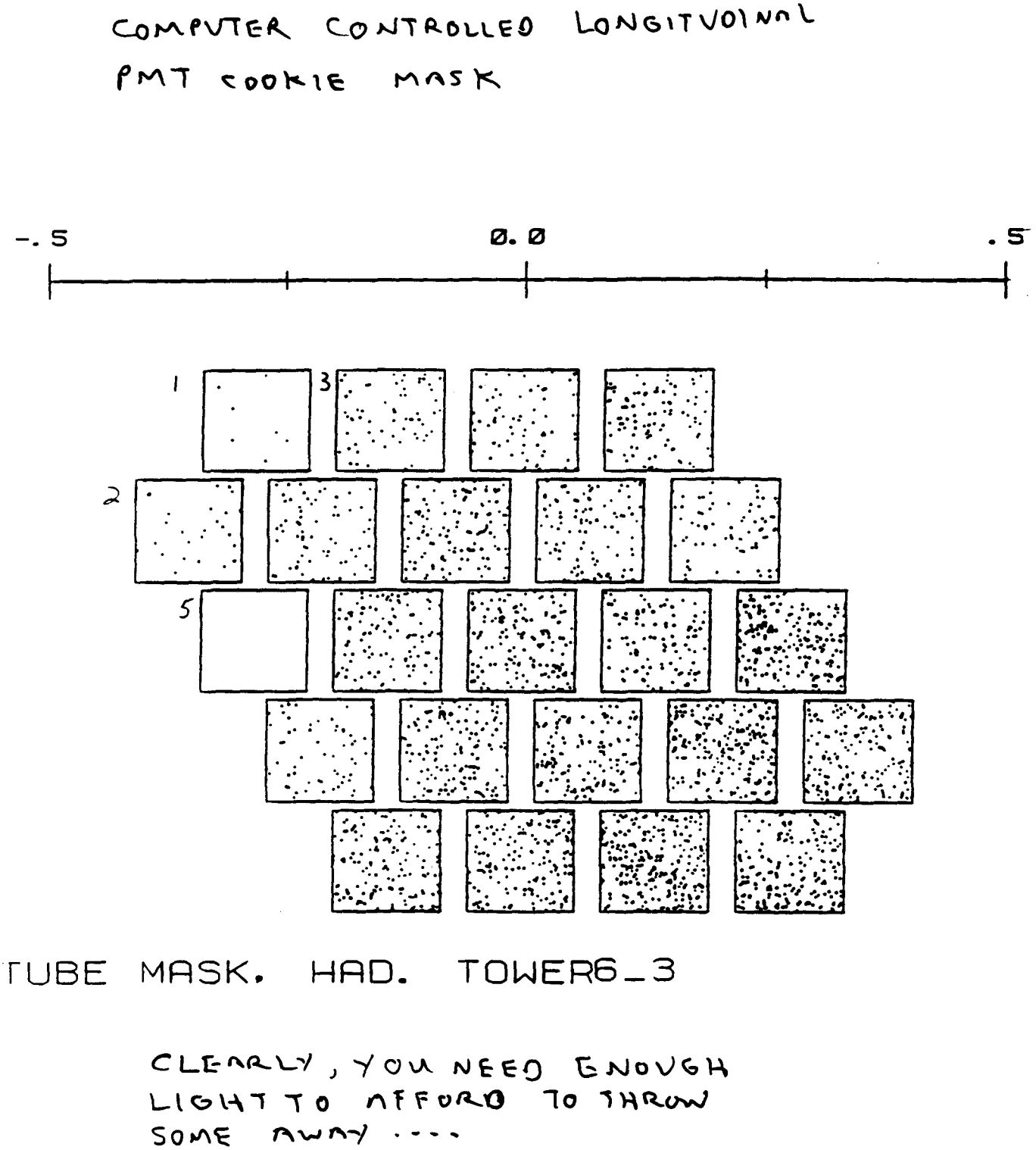

Figure 6.16 Computer output tused to form a neutral density filter for longitudinal masking.

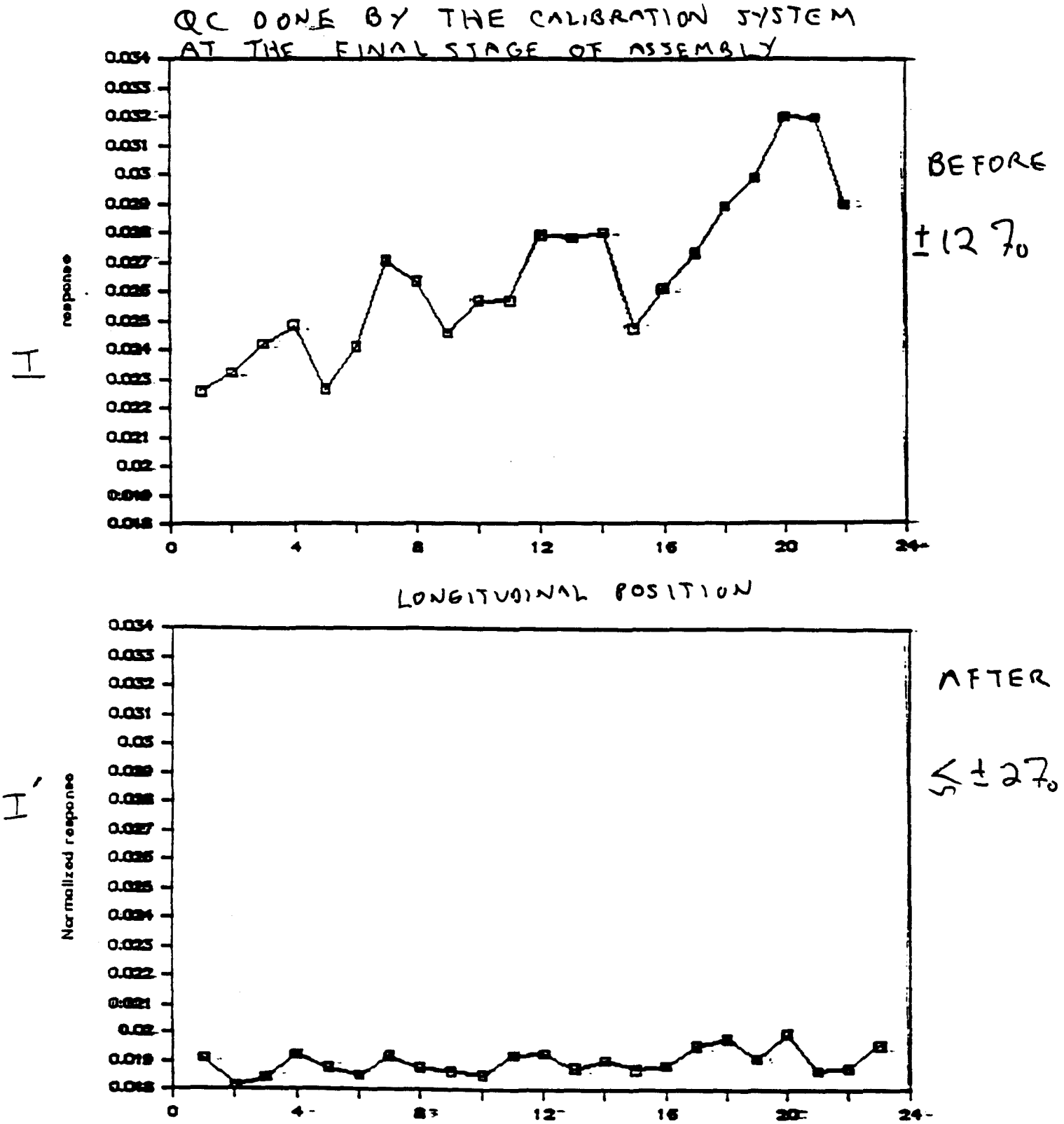

Figure 6.17 a) The longitudinal response of tiles in a tower. The hortizontal scale is tile number ranging from 1 (front) to 23 (back). The vertical scale is relative light yield. The RMS variation is 11.5%.

b) The same tower as in (a), after longitudinal masking. The RMS variation is now 2.6%.

DOES IT WORK? ⇒ J. FREEMAN CDF TEST
HANGING FILE TE

ANL/WSTC EM TEST DATA

$\sigma/\langle\rangle = 1.6\%$

CDF TESTBEAM, THICKER Pb

AGREES WITH THICKNESS $\sqrt{t}$ SCALING

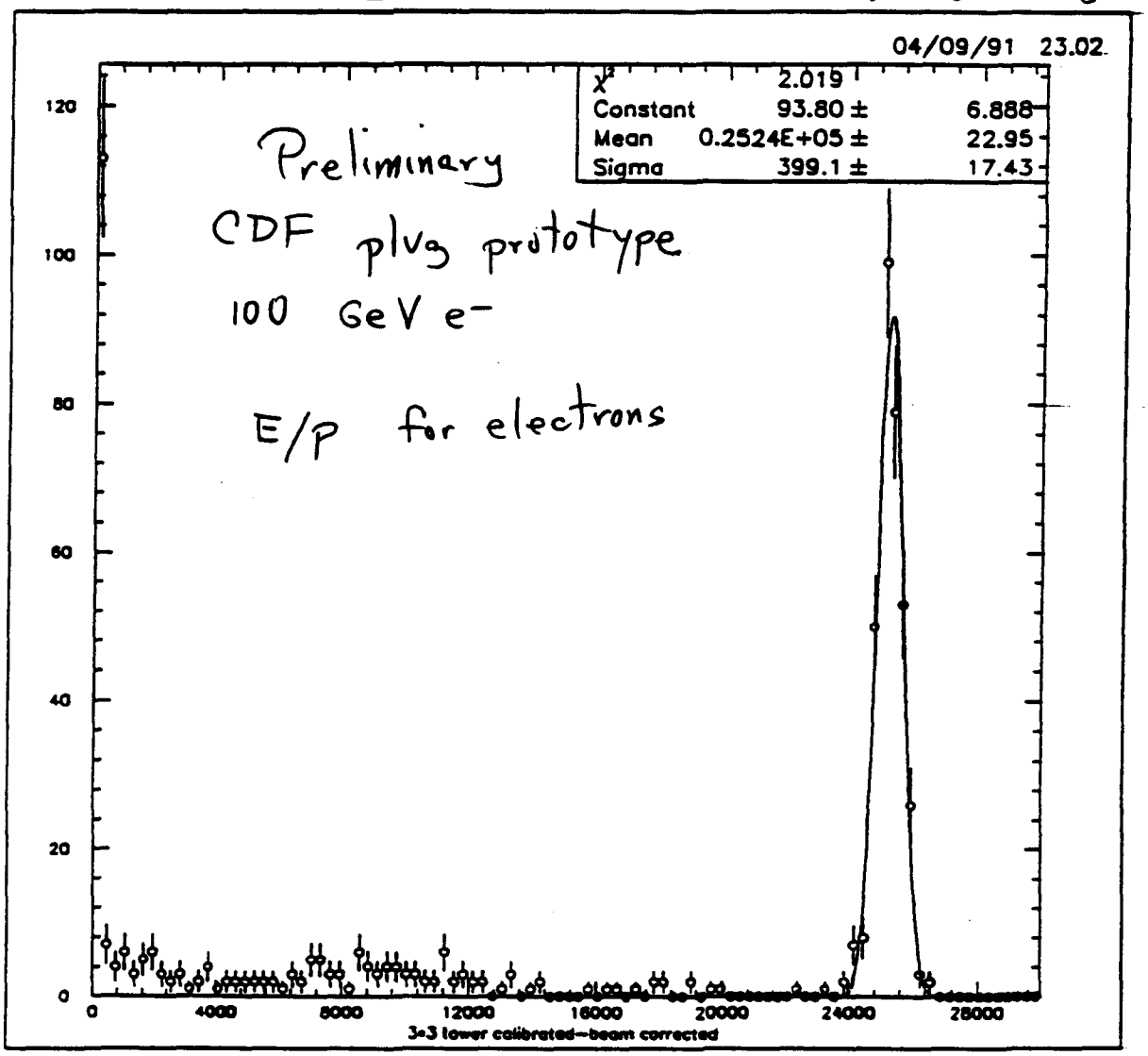

CALIBRATION SOURCE TUBES

CALIBRATION IN PLACE; GOOD TO ±2%
(REPEATED MEASUREMENT)

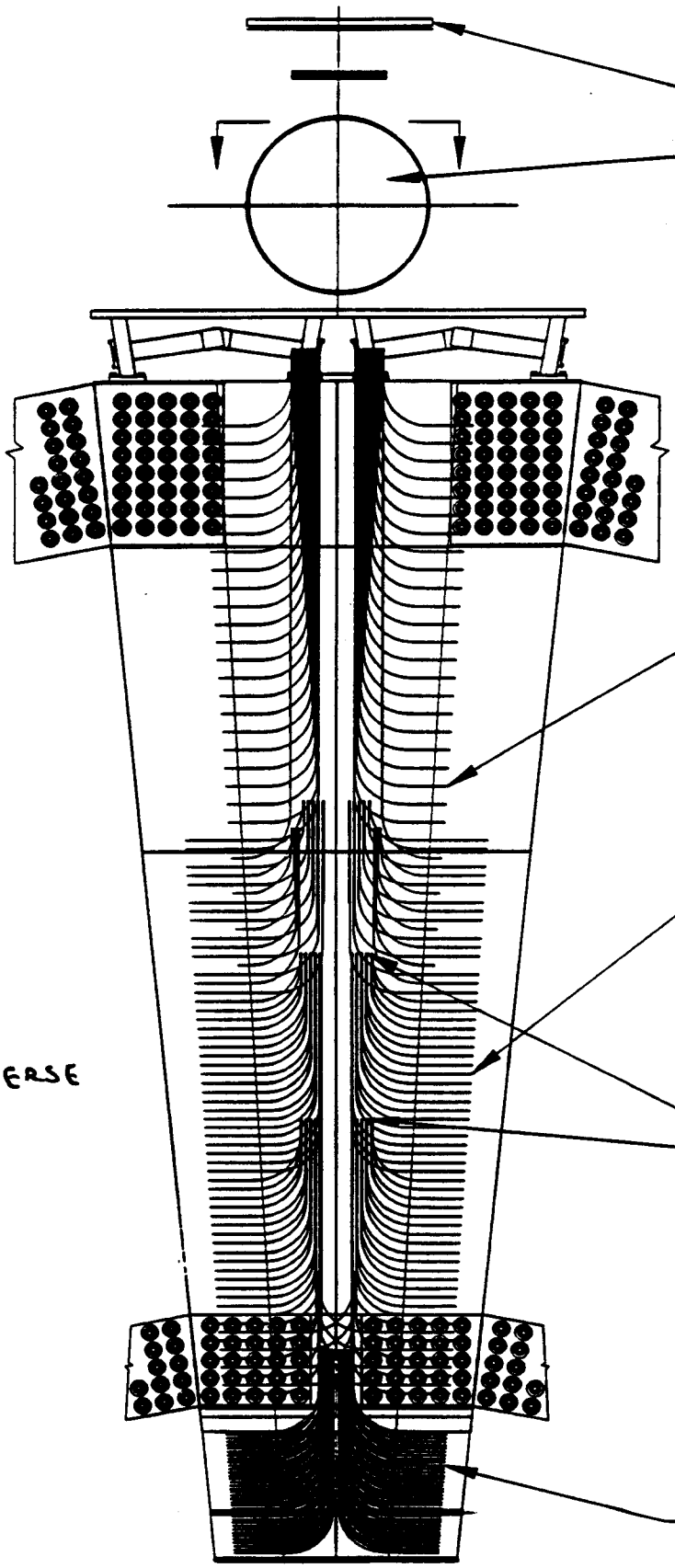

EACH TILE HAS A TRANSVERSE SCAN

IN SITU: 10^4 $Z \to ee$/MRAD!, ~10 $Z \to ee$/TOWER/DAY

ORG
8/91

RADIATION DAMAGE FOR SDC TILE/FIBER CALORIMETRY

(RELATED TO OPTICS MASKING
AIR GAP QUICK DISCONNECTS

Ⓐ THEORY:

1) WHAT / WHERE IS THE DOSE?

2) GIVEN DAMAGE, WHAT IS THE CONSEQUENCE?

EGS $d \Rightarrow dE/E$

Ⓑ EXPERIMENT:

1) WHAT IS THE RELATION OF DOSE TO DAMAGE? $D \Rightarrow d$

2) FEB-JUNE 1991: QUICK "COOK" WITH EXISTING PLASTICS ⇒ PROOF OF PRINCIPLE FOR BARREL FOR 100 YEARS AT DESIGN LUMINOSITY?

REPORT @ LBL
OPTIMISM
- ANNEAL -
PESSIMISM
- LOW DOSE RATE

YOU ARE HERE

3) DEVELOP MODELS
OCT 91 - JUNE 92: SECOND ROUND, SLOW "COOK", END CAP REGION ....

THERE IS A MODEL TO RELATE DAMAGE TO PHYSICS

WHAT HAPPENS TO THE DAMAGED AREA?
NONLINEARITY INDUCED BY NONUNIFORMITY

RADDAM - EGS

$dE/E \Leftarrow d$

$\sigma = \frac{0.12}{\sqrt{E}} \oplus 0.01$

- UNCORRECTED INDUCED ERROR (BARREL)

dE/E

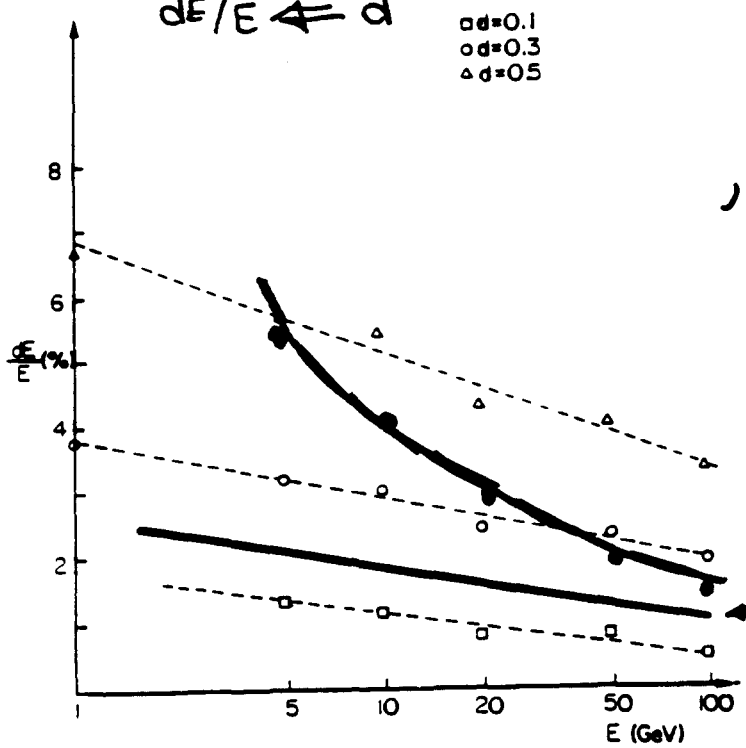

$d = 0.2$ is safe.

- CORRECTED INDUCED ERROR

(USE 2 EM COMPARTMENTS ENDCAP)

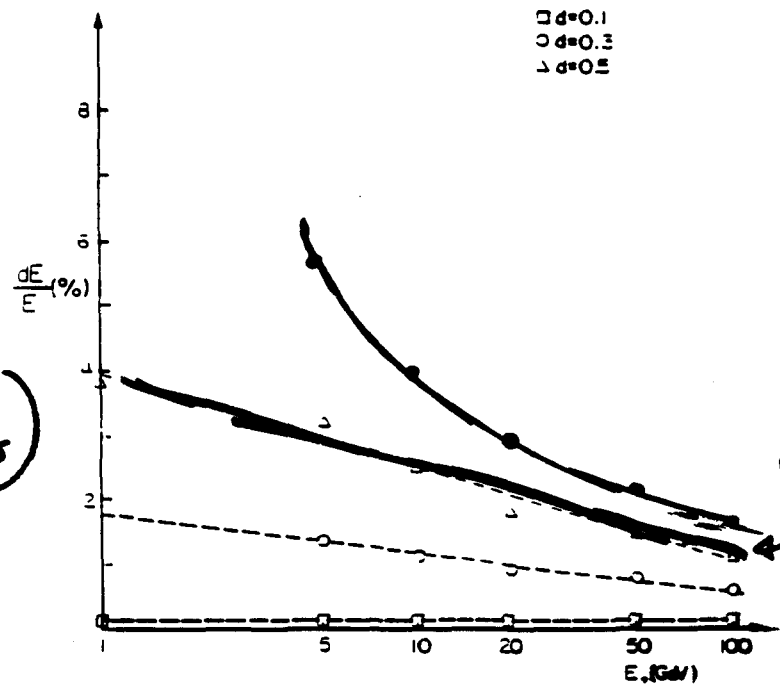

$d = 0.5$ is safe.

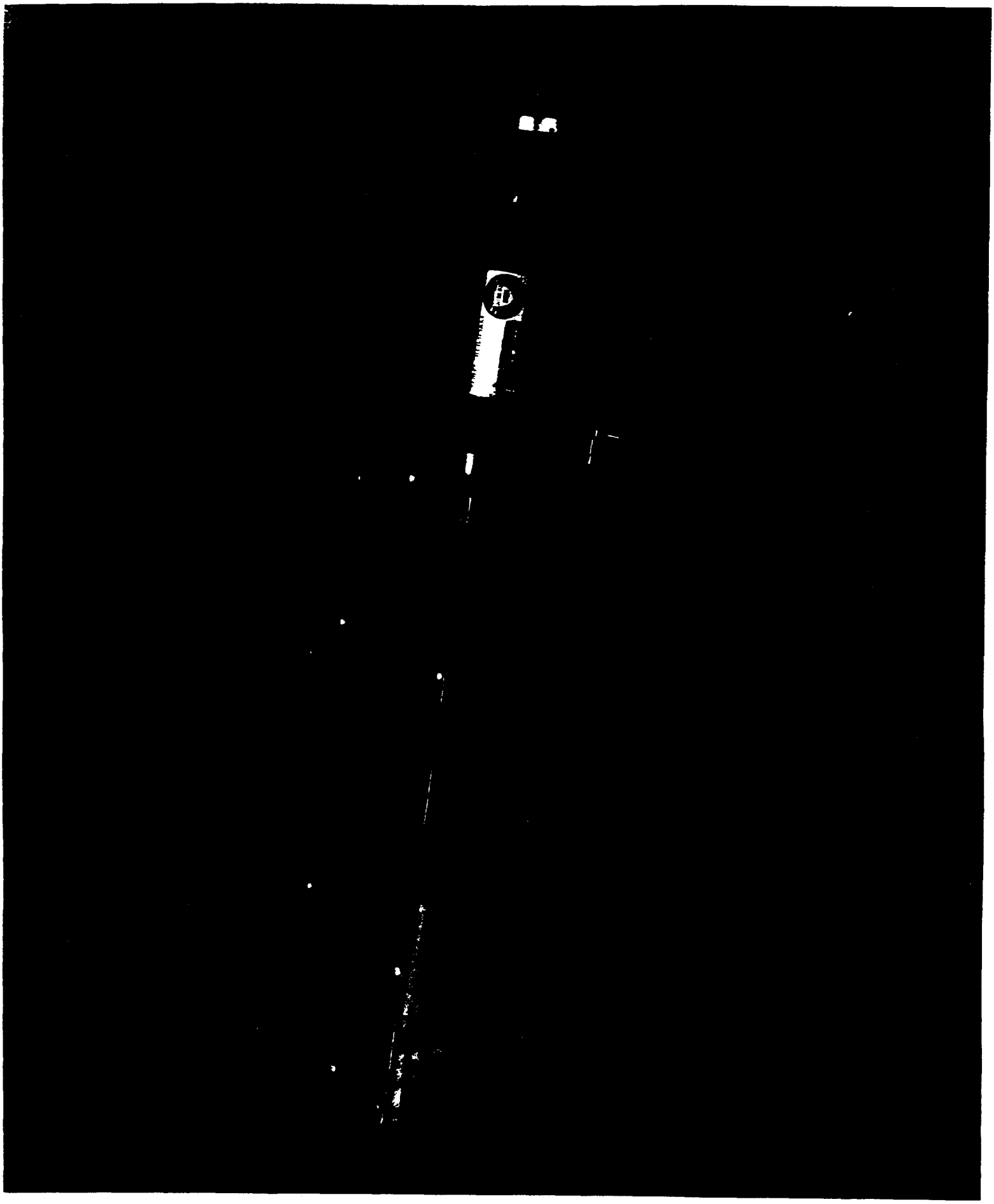

PURDUE SOURCE TUBES (V. BARNES)

Cs SOURCES –

USE IN IHEP BEIJING TEST

SINCLAY ALSO

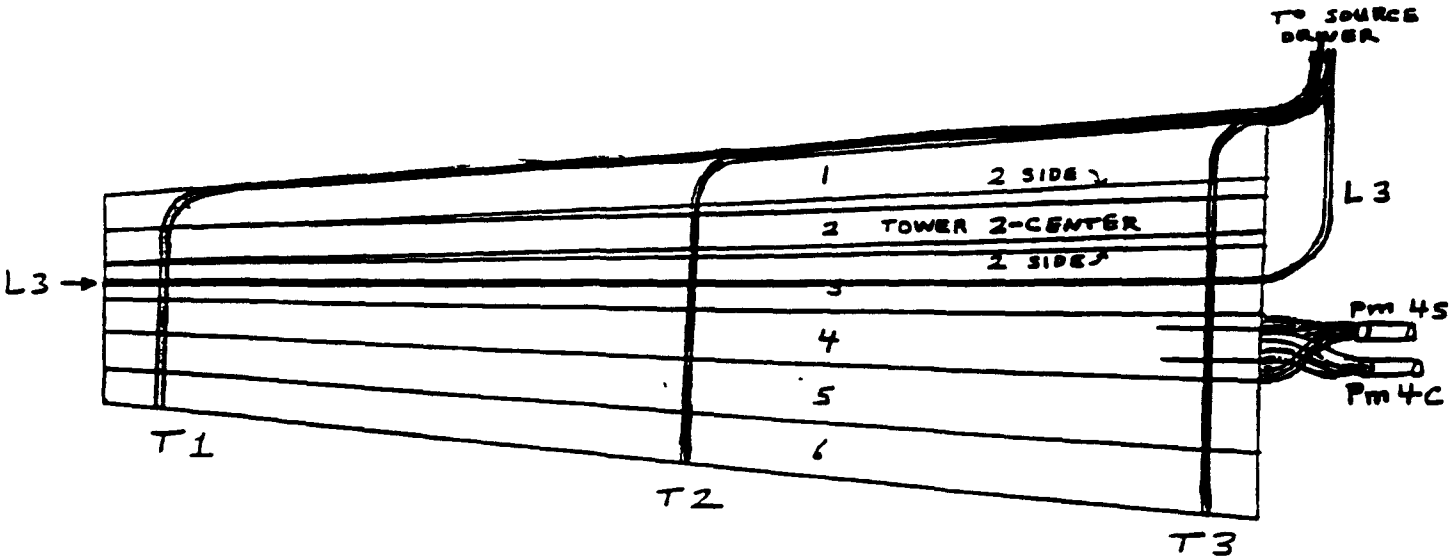

Fig. 3 Layout showing one typical longitudinal tube and all three transverse tubes.

L TUBES: MEASURE THE DAMAGE PROFILE

$$F(t)$$

$$f(t) = 1 - d\left[e^{-(t-t_0)^2/2\sigma^2}\right]$$

T TUBES: LOOK AT NON-UNIFORMITY CAUSED BY DAMAGE IN LIGHT "CONVERSION"

MEASURED WITH SOURCE SCAN

RELATIVE
T TUBE SCAN
0.MRAD TO 4.0 MRAD

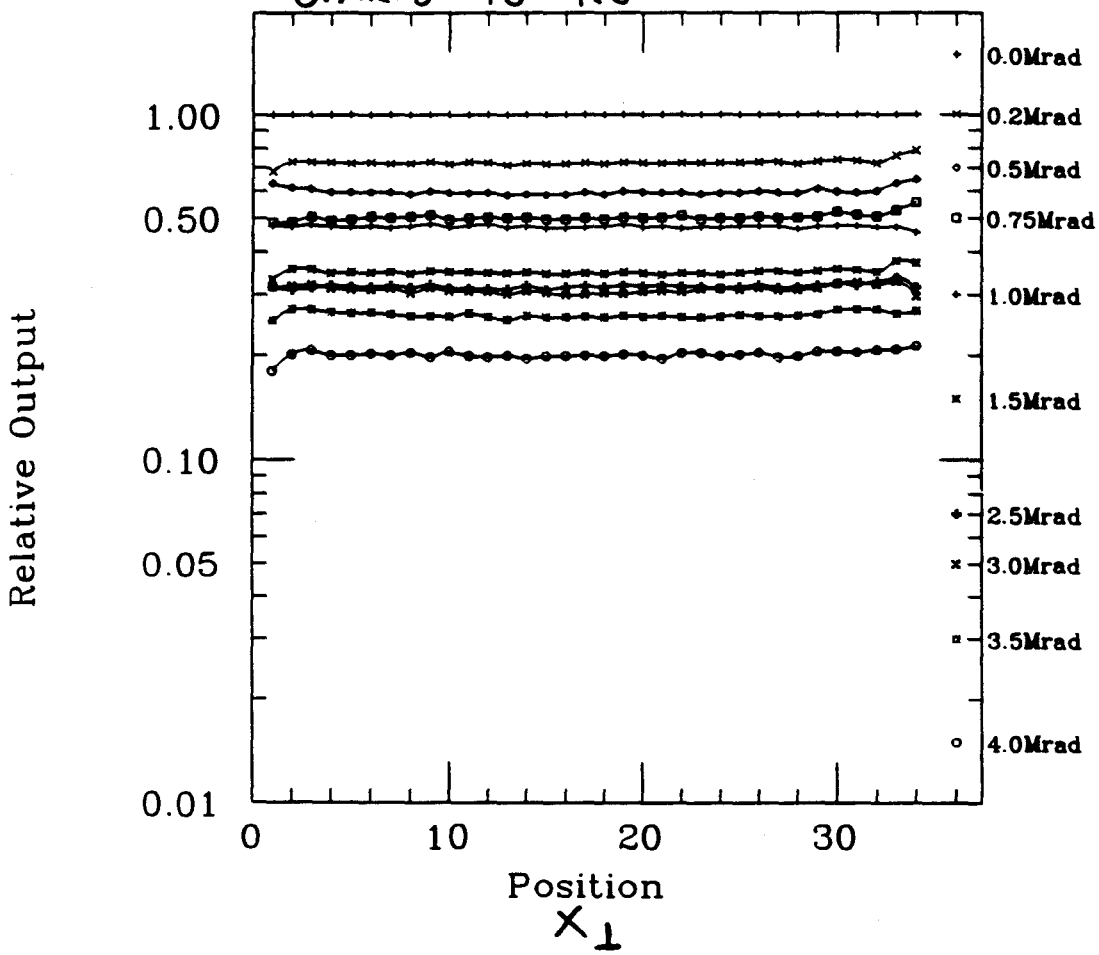

⇒ NO MAJOR NONLINEARITIES UP TO 4 MRAD

IT IS IMPORTANT THAT NO ⊥ NON-UNIFORMITIES BE INDUCED SO THAT ADDITIONAL CONSTANT TERMS NOT BE INDUCED

BEIJING IHEP DATA, 0.0 TO 4.0 MRAD

NO ANNEAL

TILE MODULE #5 L2 AIR

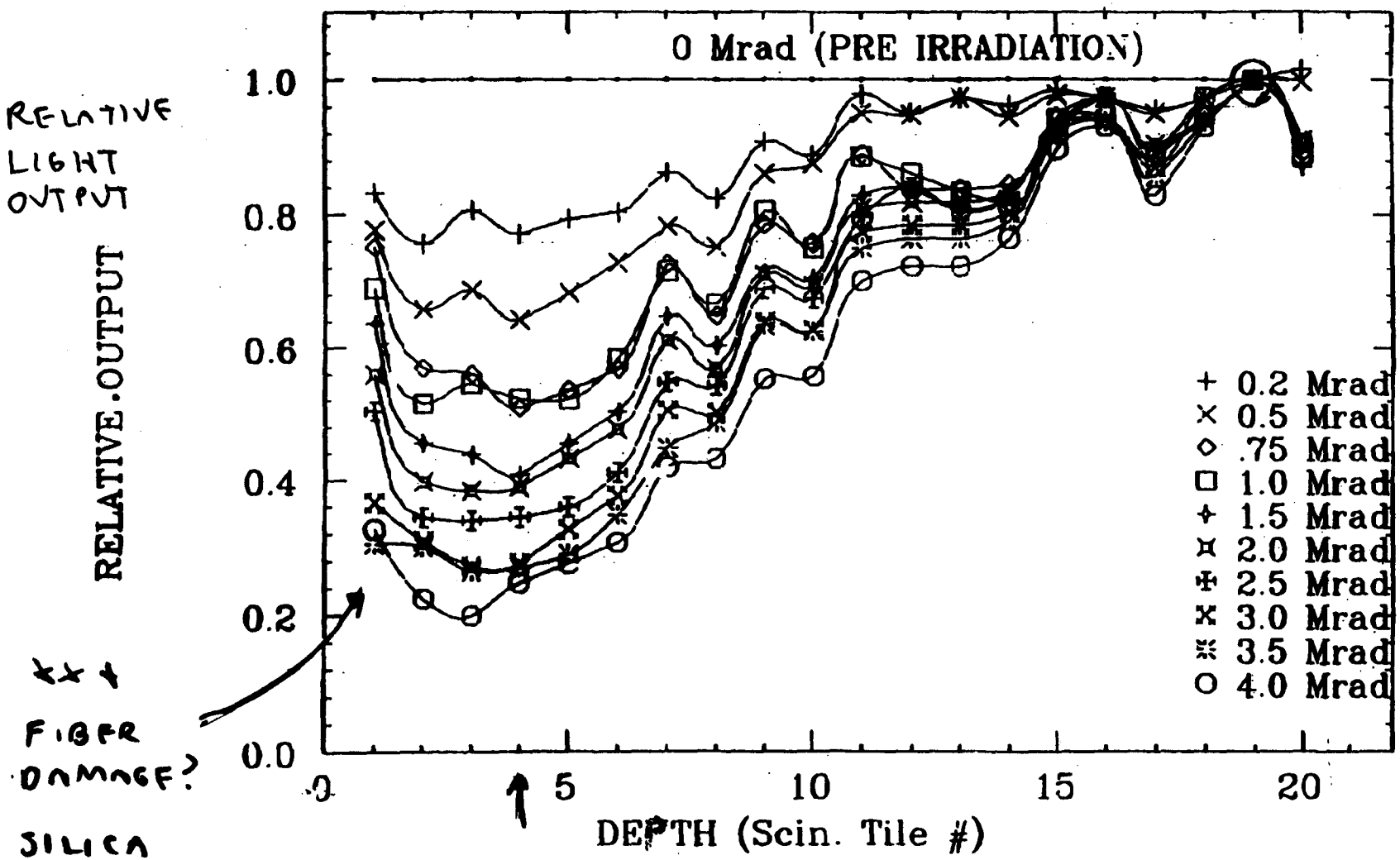

xx + FIBER DAMAGE?

SILICA FIBER TEST

1-d

SACLAY DATA

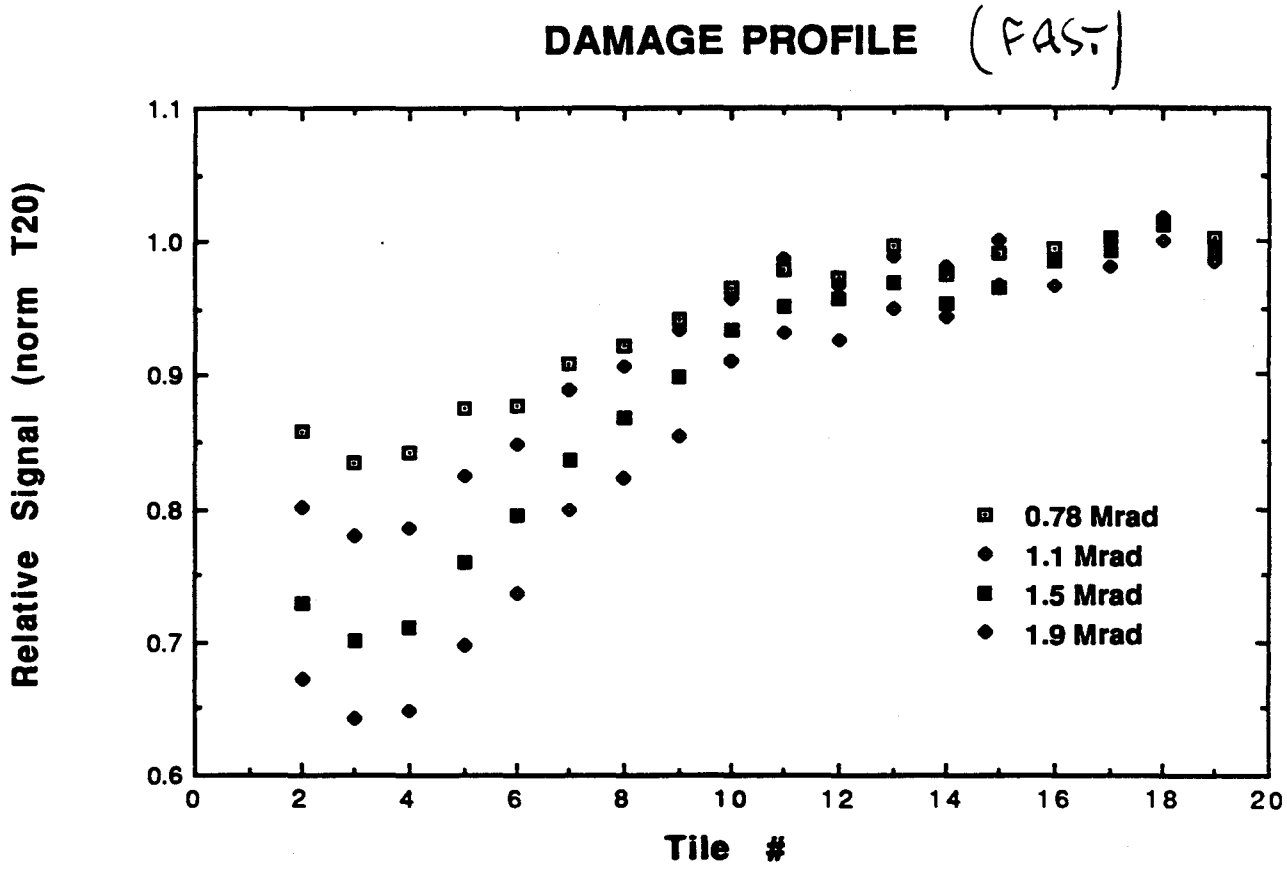

DEPTH

ZEUS TEST

SCSN 38 , 1 MRAD

ANNEALING OF RADIATION INDUCED ABSORPTION

$$\begin{cases} 1/\lambda = 1/\lambda_0 + 1/\lambda^* \\ 1/\lambda^* = [a\,f(\tau) + b]\,D \;, \quad f(\tau) = e^{-\tau/T} \end{cases}$$

1 MRAD FAST EXPOSURE ANNEALING

$$x_{DIFF} \sim \sqrt{\tau}$$

THERE ARE LONG DIFFUSION TIMES

YIELD

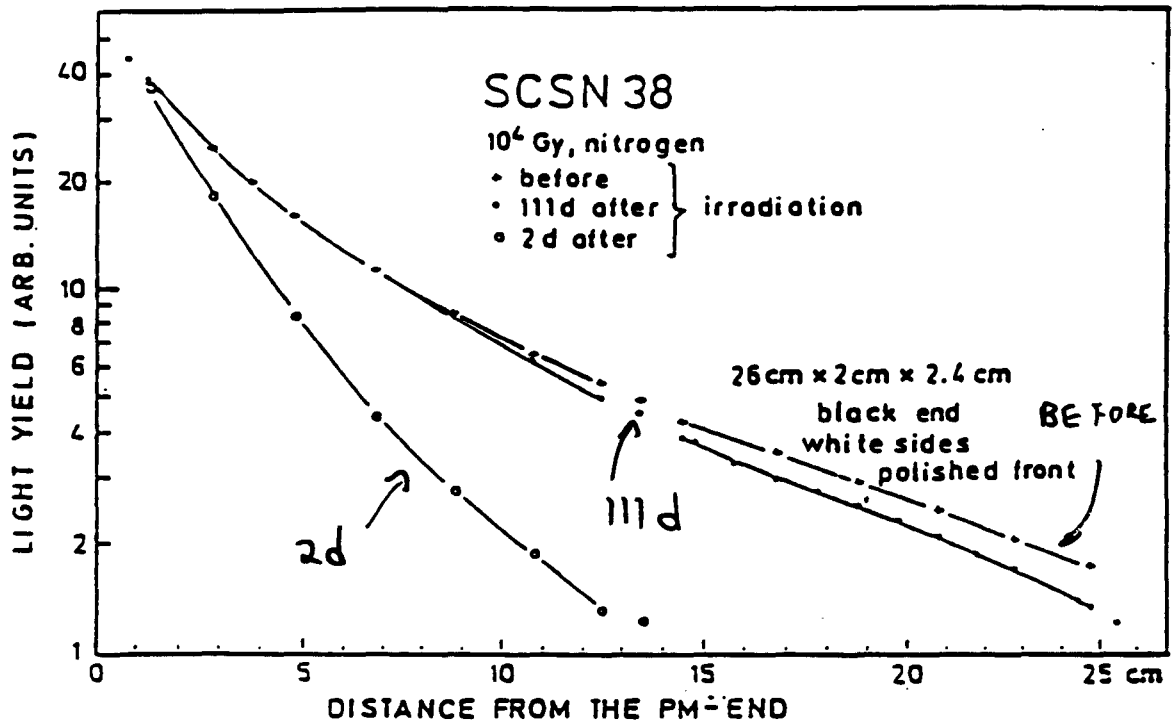

x_{11}

SACLAY DATA

Preliminary

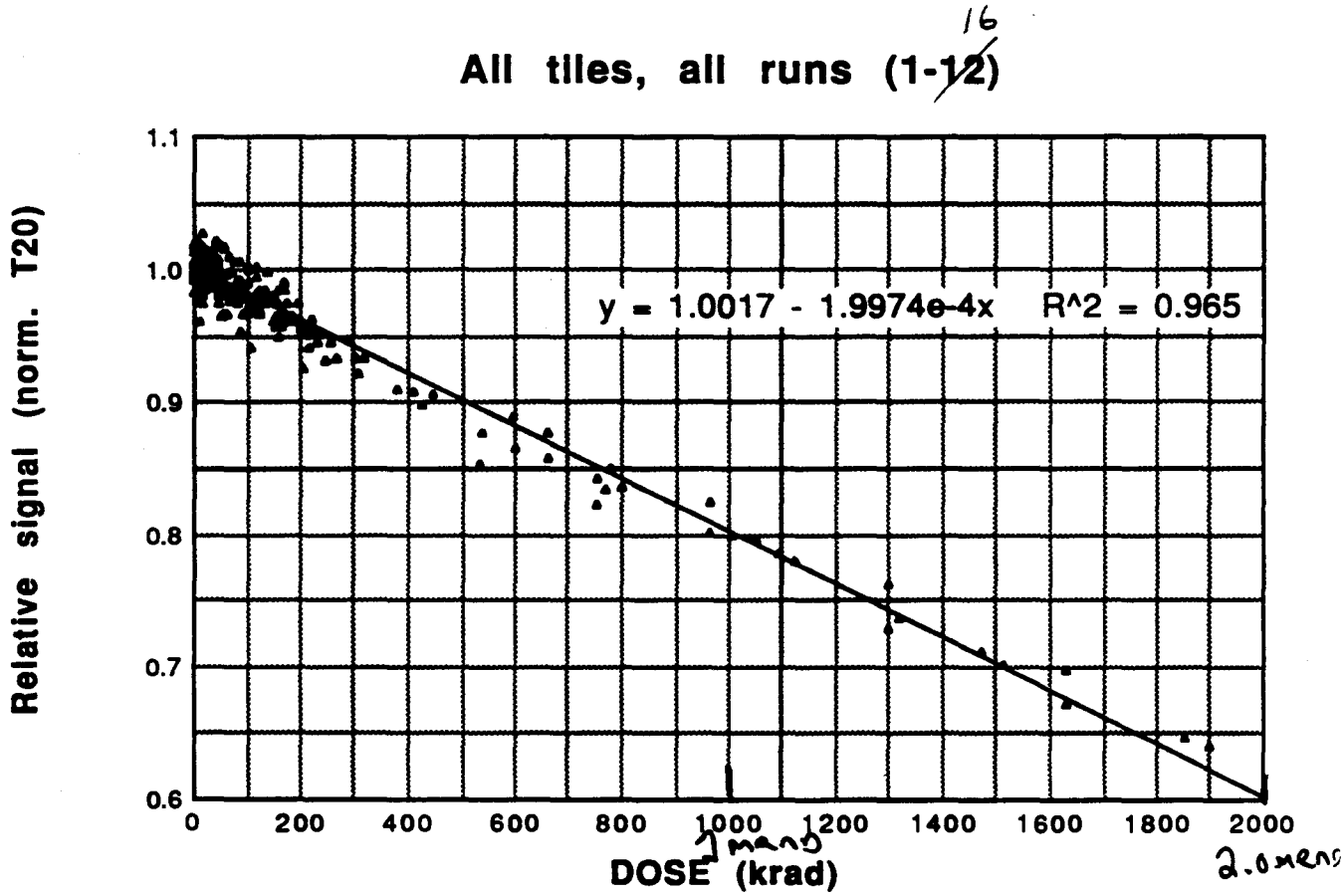

1-d

D

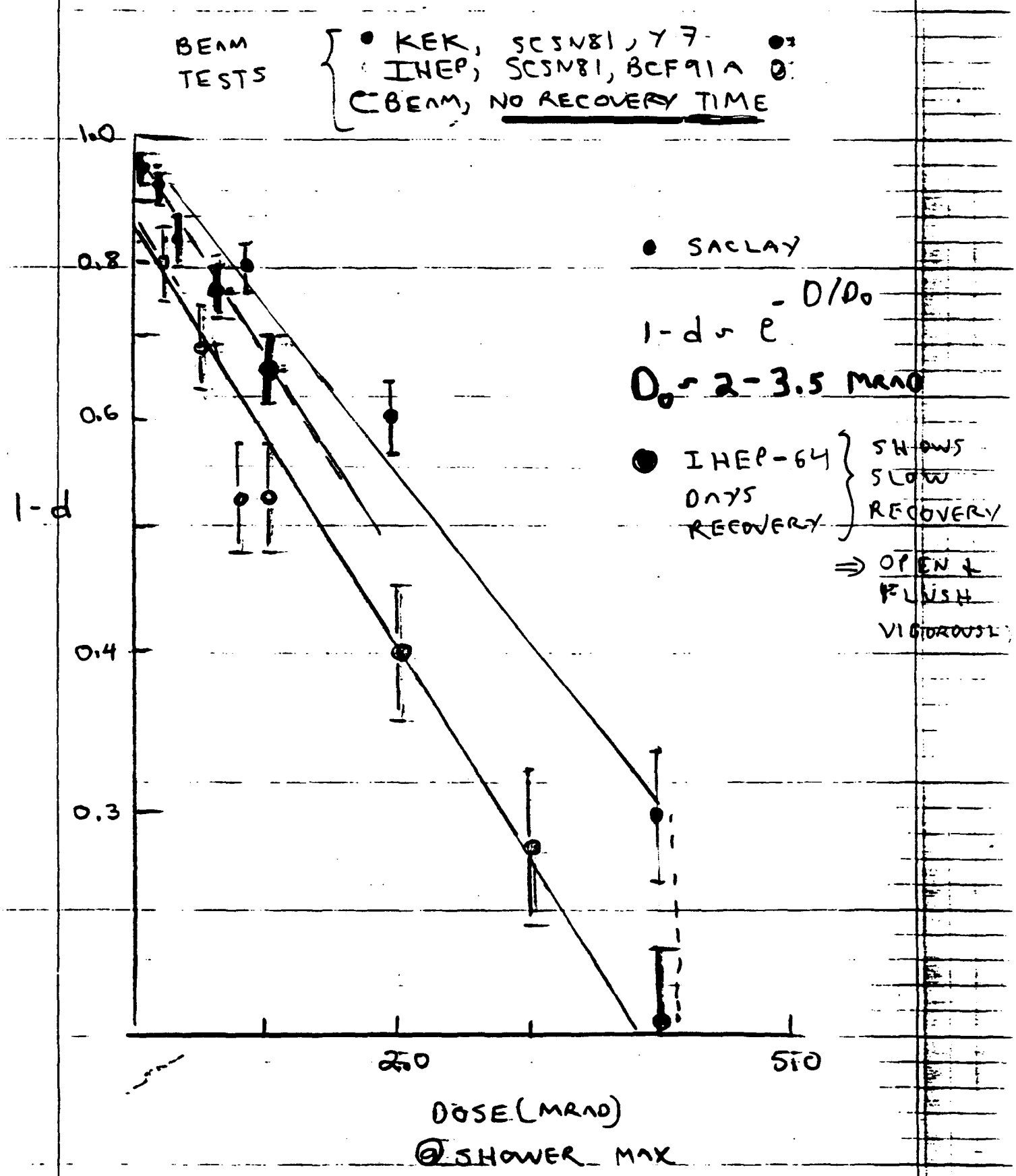
BEAM TESTS
KEK, SCSN81, Y7
IHEP, SCSN81, BCF91A
BEAM, NO RECOVERY TIME
1.0
0.8
0.6
0.4
0.3
1-d
SACLAY
$1-d \sim e^{-D/D_0}$
$D_0 \sim 2-3.5$ MRAD
IHEP-64 DAYS RECOVERY
SHOWS SLOW RECOVERY
⇒ OPEN & FLUSH VIGOROUSLY
250
500
DOSE (MRAD)
@ SHOWER MAX

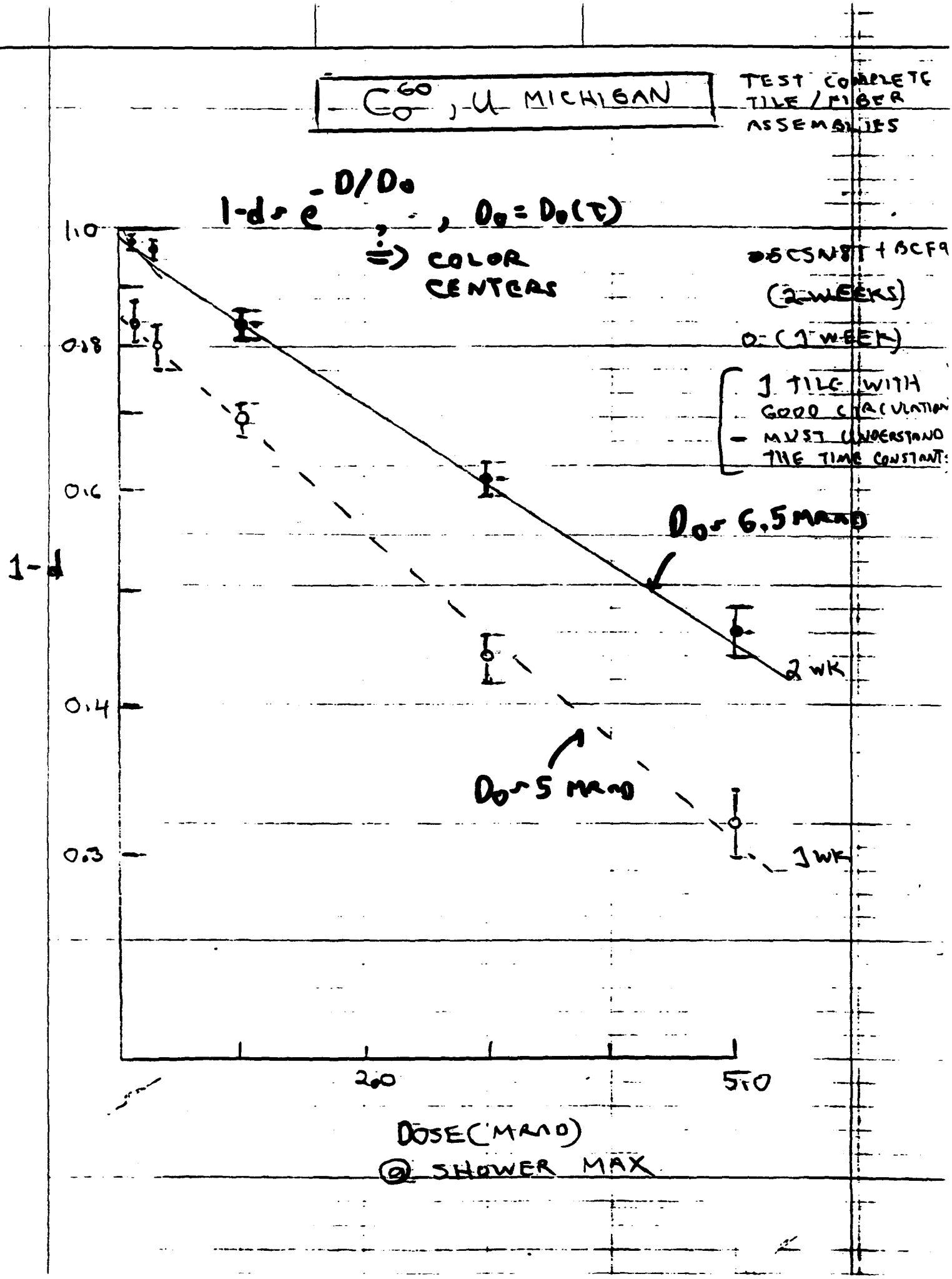
Co^{60}, U MICHIGAN
TEST COMPLETE TILE / FIBER ASSEMBLIES
$1-d \sim e^{-D/D_0}$, $D_0 = D_0(\tau)$
⇒ COLOR CENTERS
BCSN38 + BCF9
(2 WEEKS)
(1 WEEK)
1 TILE WITH GOOD CALIBRATION
MUST UNDERSTAND THE TIME CONSTANTS
$D_0 \sim 6.5$ MRAD
$D_0 \sim 5$ MRAD
2 WK
1 WK
1-d
1.0
0.8
0.6
0.4
0.3
200
500
DOSE (MRAD)
@ SHOWER MAX

WHAT ABOUT LOW DOSE RATES?

(OPTIMIST — ANNEAL
PESSIMIST — LOW DOSE RATES)

E.G.

A FNAL FIXED TARGET BEAM COUNTER

(TEST SETUP WITH GOOD DOSIMETRY FOR "LONG TERM")

DO WE HAVE EXPERIENCE WITH LONG TERM DOSES?

BEAM = 5 MHZ, DUTY FACTOR 1/3

1 YR = 10^7 SEC

BEAM SPOT 1CM × 1CM

$\therefore 5 \times 10^{13}/cm^2$

1 MIP = 1.5 MeV/(gm/cm²)

$\Rightarrow 7.5 \times 10^{19}$ eV/(gm/cm²)

$\rho \sim 1.0$ gm/cm³

$\Rightarrow 7.5 \times 10^{19}$ eV/gm

7.5×10^{22} eV/kg

12,000 JOULE/kg

1.2 MRAD

FNAL FT TYPICALLY USES NE110 (RAD SOFT)

GLASS (RAD SOFT)

DOES LIGHT OUTPUT FALL 2X?

IN A 2 YEAR "EXPOSURE"?

LOW DOSE RATE

(N. GIOKARIS
9/9/91)

$\dot{D}$ = 150 RAD/HR } IN AIR

D = 385 KRAD

Co^{60} EXPOSURE

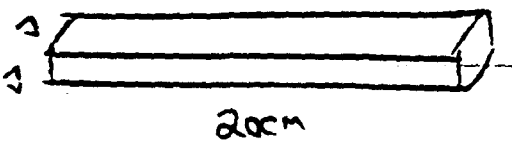

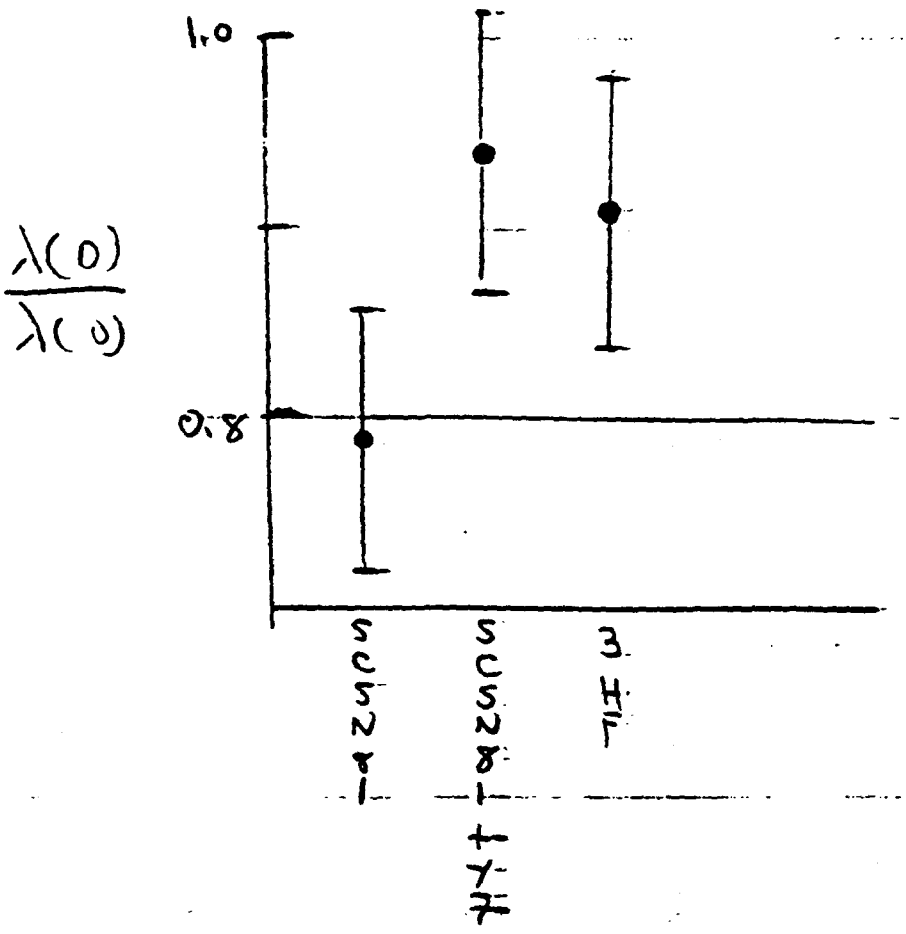

AGREES WITH HIGH DOSE RATE WITHIN ERRORS ?

⇒ ANNEALS WHILE TAKING DOSE ?

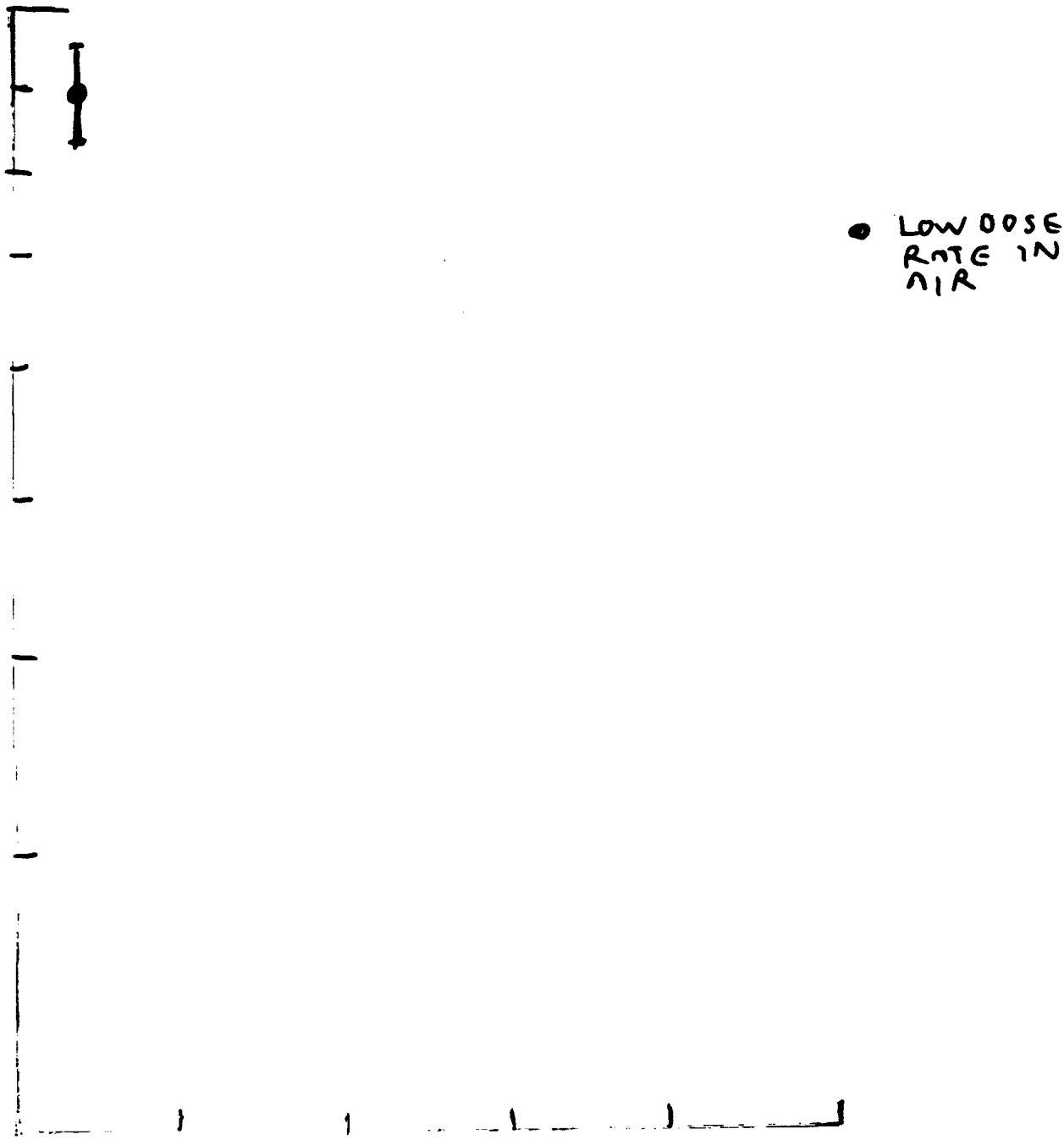
LOW DOSE
RATE IN
AIR

RADDAM PROGRAM

* 1. LOW DOSE RATE: FEW MONTHS
@ U. MICHIGAN
SCSN81 + BCF91 (BARREL)
WITH/WITHOUT N_2 PURGE
O_2 ?

2. Co^{60} (e) "SCREENING": FSU, ANL, MICH, TSUKUBA, LS

a) GROOVE QUALITY / INJECTION MOLD

* b) SHORTER OPTICAL PATH LENGTH ("SPIRAL")

c) LONGER WAVELENGTHS

* 3HF + O2 (SCSN81 + Y7) + R3 } ENHANCED GREEN

d) SILICA FIBER SPLICE

3. INEP/TSUKUBA/SACLAY:

a) ABSOLUTE GAIN: Am + SCINT (SHIELDED)

b) SILICA SPLICE TO CLEAR

c) GREEN/RED

d) "SPIRAL"

* e) NEW BICRON AND/OR KURARAY PLASTICS

* PRELIMINARY RESULTS SHOWN HERE

IF COLOR CENTER ABSORPTION
⇒ REDUCE OPTICAL PATH LENGTH
FOR BLUE LIGHT

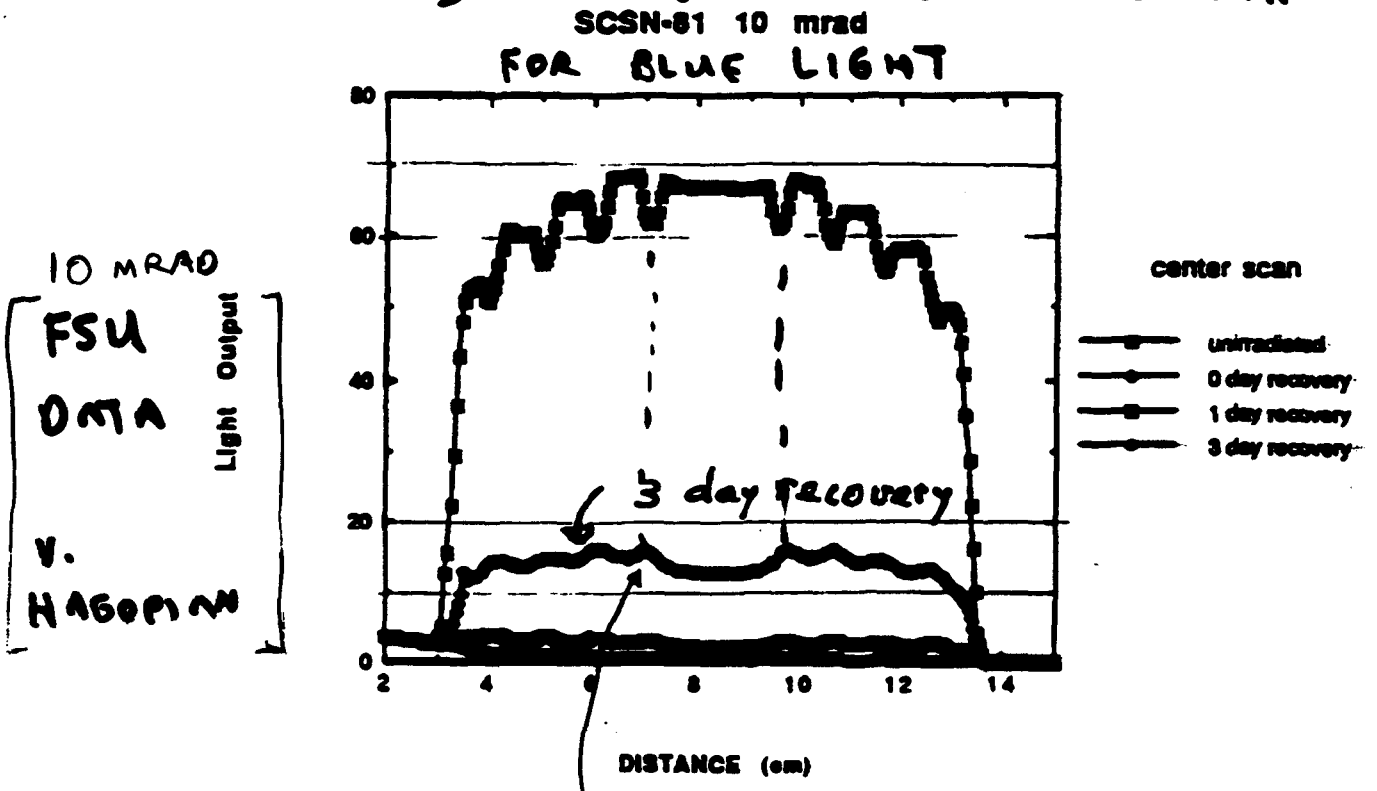

(LOOK LIKE TILE LOSS NOT FIBER SCSN81)

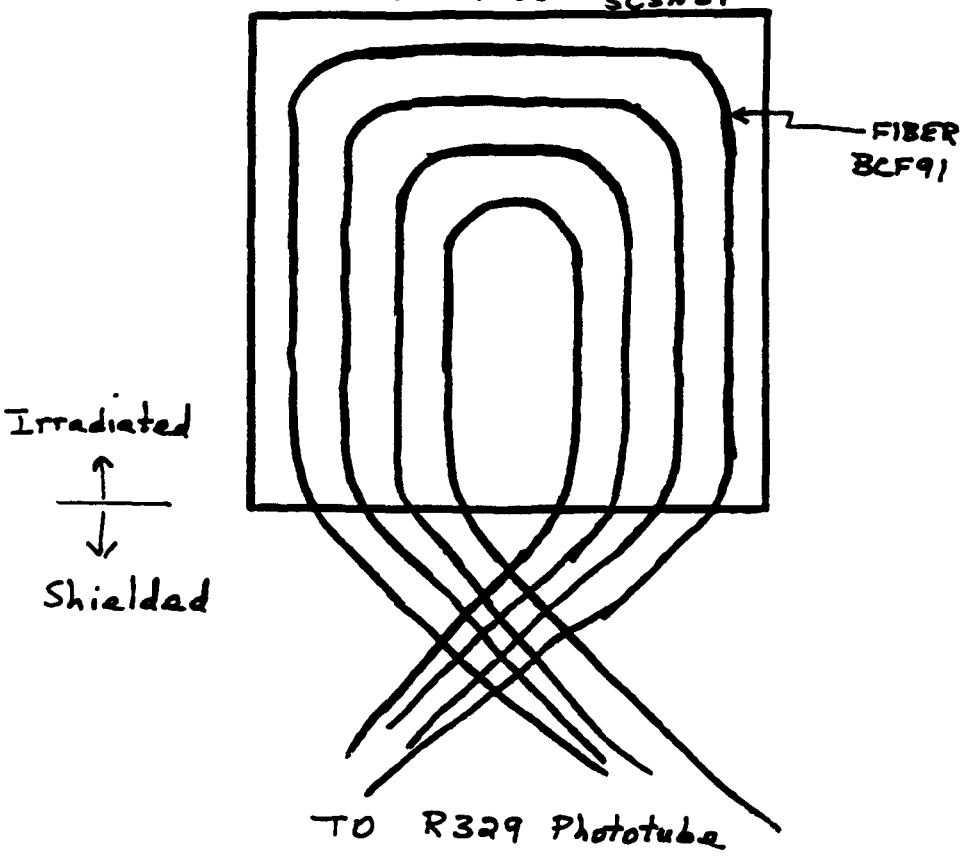

NEW BICRON PLASTIC
(J. PROVOFOOT)

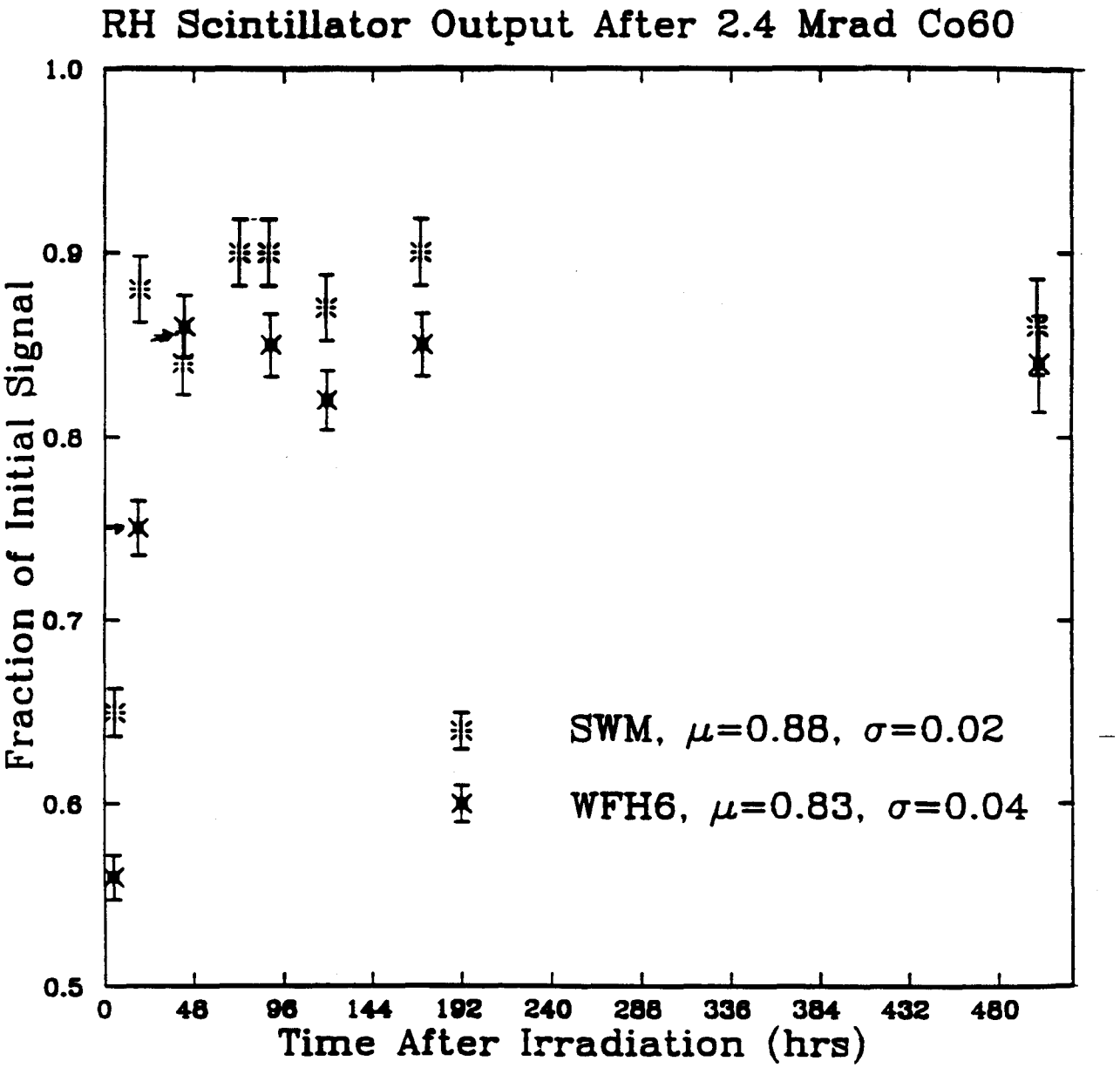

Figure 8.12 Average light output from 3 disks of 2 inches diameter read out using 2 wraps of 1 mm BCF91A.

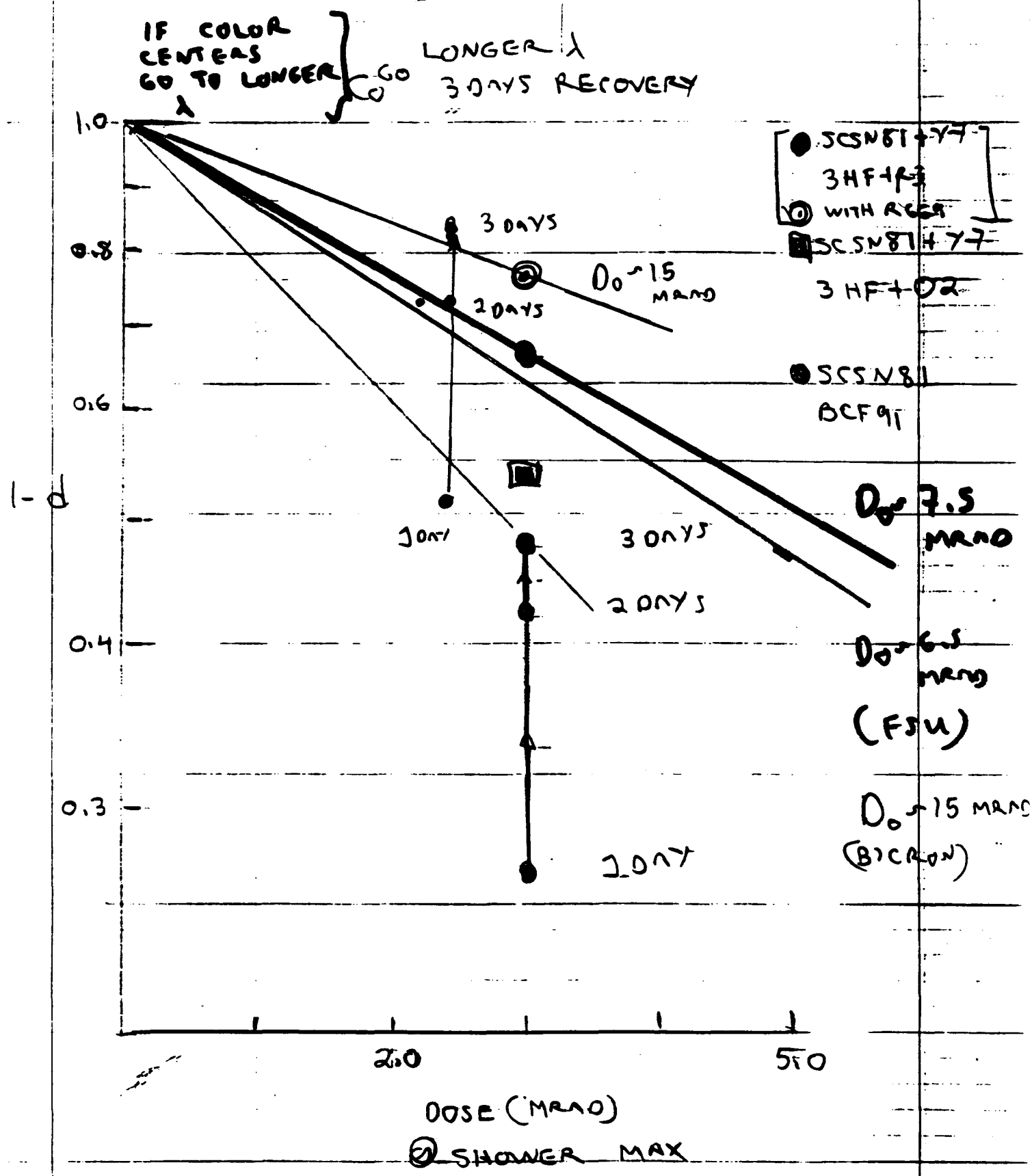
IF COLOR CENTERS GO TO LONGER λ
^{60}Co
LONGER λ
30 DAYS RECOVERY
1.0
0.8
0.6
0.4
0.3
1-d
3 DAYS
2 DAYS
1 DAY
$D_0 \sim 15$ MRAD
SCSN81+77
3HF+P3
WITH RCGR
SCSN81+77
3HF+02
SCSN81
BCF91
$D_0 \sim 7.5$ MRAD
$D_0 \sim 6.5$ MRAD
(FSU)
$D_0 \sim 15$ MRAD
(BICRON)
20
50
DOSE (MRAD)
SHOWER MAX

RADIATION DOSE IS DUE TO "MINBIAS" EVENTS WITH $\langle k_T \rangle_{\pi^0} \sim 0.6$ GeV

BARREL APPEARS TO ANNEAL WITH LITTLE DOSE RATE DEPENDENCE
∴ APPEARS TO BE OK

The SDC detector (100 YEARS AT DESIGN $\mathcal{L}$)

SPREAD OF D_0 FROM ~6 TO ~15 MRAD
∴
- SUPPOSE YOU GET D_0 = 10 MRAD THEN 1-d = 0.5 @ ~7 MRAD

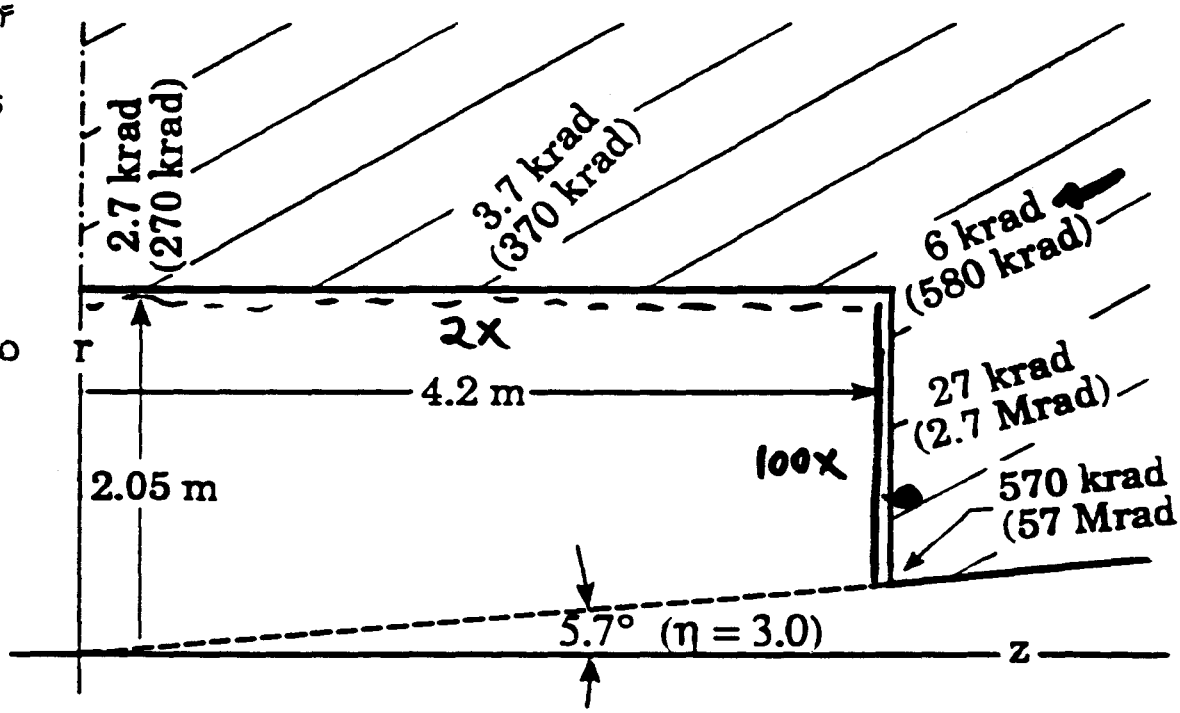

$$\text{DOSE} \sim \left(\frac{1}{\sigma}\frac{d\sigma}{d\eta}\right)\frac{\langle k_T \rangle}{\theta^3}$$

$1/\theta^3$ SCALING

⇒ DOSE IS VERY LIMITED IN ANGLE

REMASK (ENOUGH LIGHT?)
OR
REPLACE ?

IF $\theta_0 = 10$ MRAD
THEN $1-d > 0.5$
FOR $D < 7$ MRAD
EVERY 12 YEARS
AT DESIGN $\mathcal{L}$

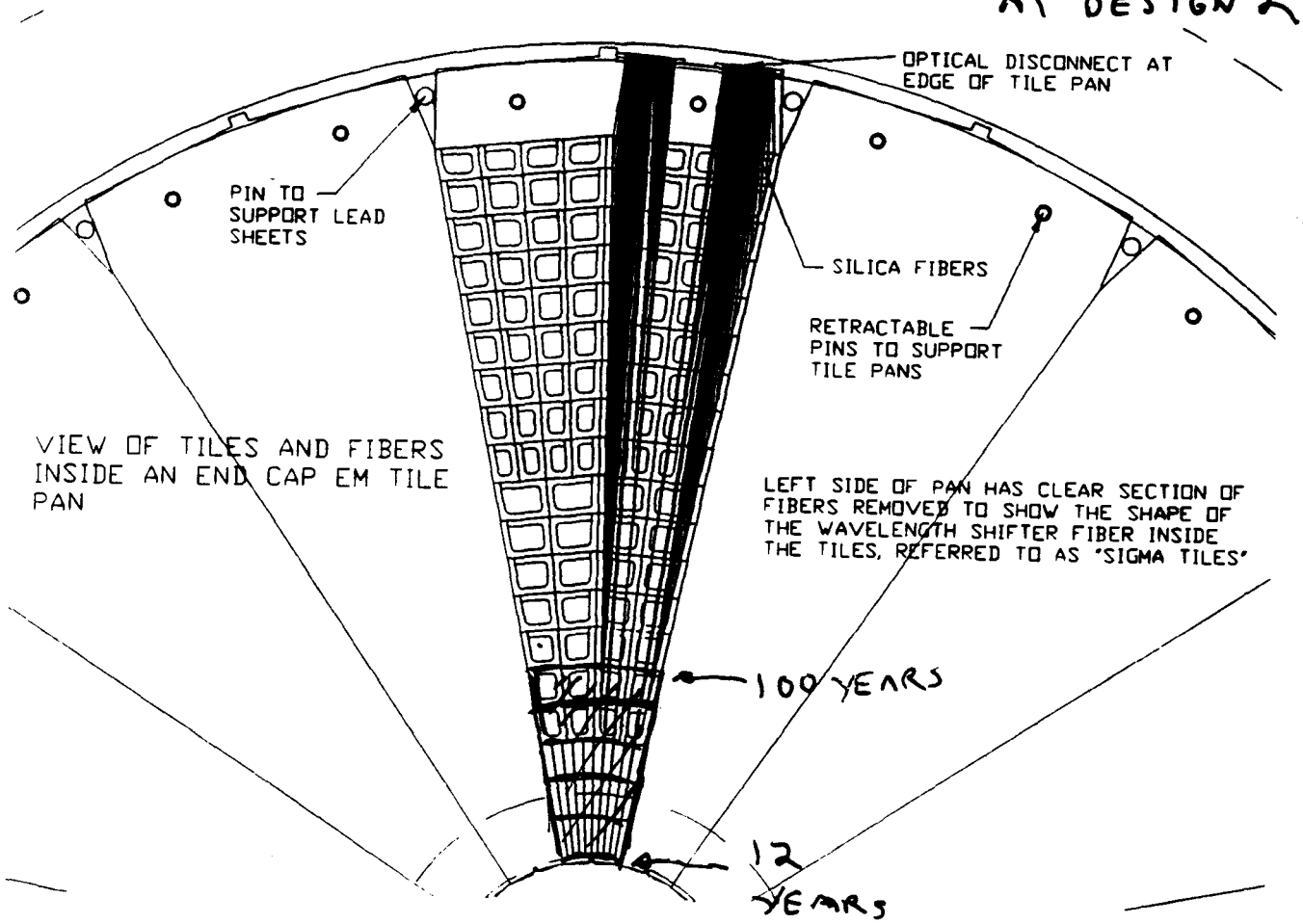

Figure 3.17 - View of tiles and fibers inside a "pizza pan" sector of the Endcap EM calorimeter. Each pan features an optical disconnect to aid in assembly. Note the "sigma tile" pattern in the outer tiles, and the high density of readout fiber in the inner tiles.

The EM absorber is a series of stainless-clad lead disks supported by posts at the outer circumference.

CDR [A DESIGN AND PROCEDURE NOW EXISTS FOR REPLACEMENT
⇒ CHANGE FROM BARREL STACK TO "PIZZA PAN" IN ENDCAP FOR EASE OF REPLACEMENT]

DOES REMASKING MAKE SENSE?

OPTICS
DESIGN IS > 2 PE / MIP ; AIR GAP QUICK DISCONNECT + NEUTRAL DENSITY FILTER

10 MIP / GeV AT SM

SM EXTENDS ~ $4 X_0$ ⟹ 8 TILES

∴ 160 PE / GeV

$E_T = 100$ GeV IS A REASONABLE SCALE

$\Theta > 15°$ DOES NOT REQUIRE REPAIR

$dE/E = 0.12/\sqrt{E} \oplus .01$

$= 0.0061 \oplus .01 \oplus 0.004$

$d \simeq 0.5$,
SUPPOSE IT TOOK 2X TO REFLATTEN THE RESPONSE OF DAMAGED SECTION ⟹

$\oplus$ 0.0057

⟹

CAN ACCEPT AT LEAST 1 REFLATTEN

∴ GOOD FOR 1 REPAIR EACH 24 YEARS

SOURCE SCAN → FIND DAMAGE PROFILE
GENERATE MASKS
STOP RUN
MAKE ACCESS, DROP IN NEW FILTERS
START RUN
SOURCE SCAN, FIND ±2% RELATIVE CALIBRATE
IN 1 WEEK HAVE 1% ABSOLUTE CALIBRATION
WITH IN SITU $Z \to ee$

"PIZZA PIE" REPLACEMENT
SCENARIO

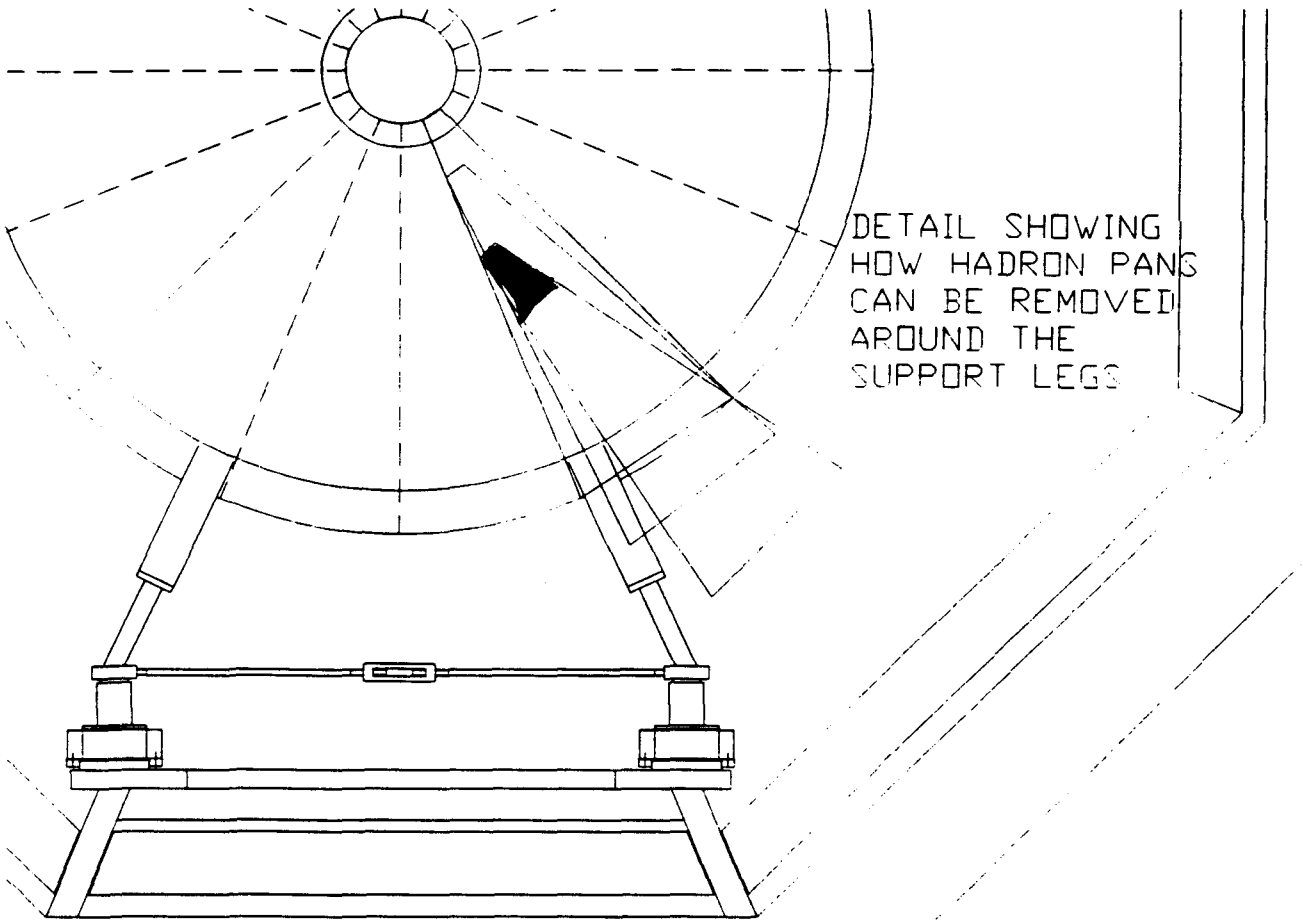

AFTER 24 YEARS OF CONTINUOUS
RUNNING, MAKE A "LONG SHUTDOWN"
PULL "PIZZA PANS"
REMOVE 15° TO 5.70 EM PLASTIC

Figure 3.21 - Endcap Hadron "Pizza-pie" scintillator segmentation. Detail showing how individual hadron pans can be removed in the area around the support legs.

SUMMARY OF TILE/FIBER CRITICAL ISSUES

1) FOR OPTICS THERE ARE 2 PROOFS OF PRINCIPLE FROM TESTBEAMS:

EM PROTOTYPE – ANL/WSTC

CDF PROTOTYPE – CDF

(HANGING FILE) – FNAL

2) WE HAVE OPERATIONAL EXPERIENCE WITH SOURCE CALIBRATIONS – USED IN QC AND IN RADDAM.

IN SITU $Z \to ee$ HAS BEEN USED AT THE TEVATRON COLLIDER

3) ANNEALING IS SEEN IN e BEAM TEST MODULES AND IN Co^{60} TEST TILES

LOW DOSE RATE EFFECTS APPEAR TO BE SMALL

$\Rightarrow$ BARREL OK WITH SOME SAFETY FACTOR

4) CLEAR SILICA + "SPIRAL" + GREEN/RED ALREADY $\Rightarrow$ $D_0 \gtrsim 10$ MRAD.

$\therefore$ ONLY $\theta \lesssim 15^\circ$ NEED EVER BE REPAIRED

@ $\gtrsim 12$ YEARS USE SYSTEM TO REMASK

@ $\gtrsim 24$ YEARS CHANGE $\theta \lesssim 15^\circ$ EM PLASTIC

$\gtrsim 48$ ⋮

$\gtrsim 72$ ⋮

CALORIMETER REVIEW AND TECHNICAL BOARD MEETING
SEPTEMBER 12 -14, 1991
SSCL

Presentation by:

Jim Freeman

Fermilab

Preliminary

Test Beam Results

- CDF plug prototype
- Hanging File Calorimeter

"HANGING FILE"
MT TEST

RAW DATA

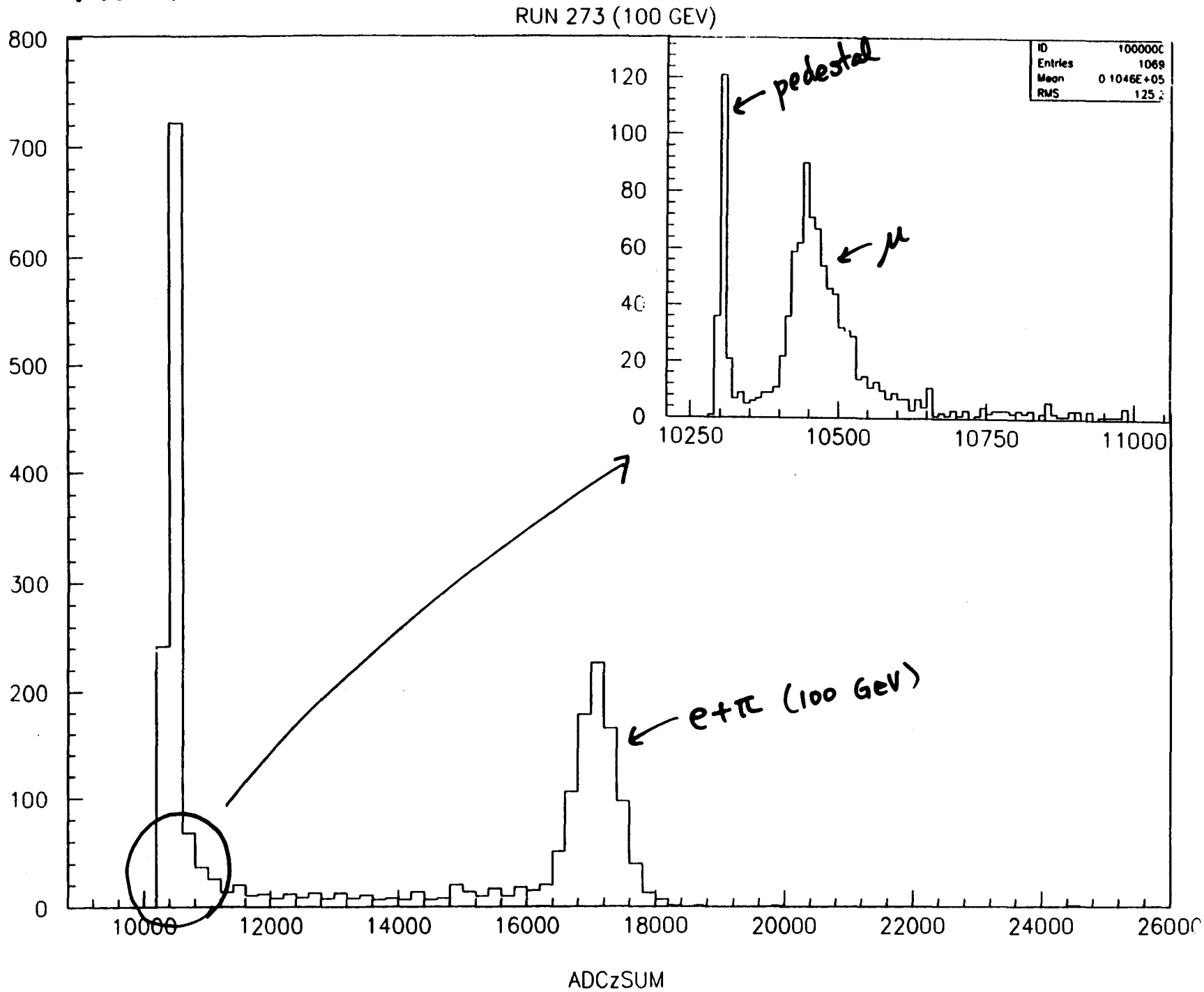

* RAW DATA *

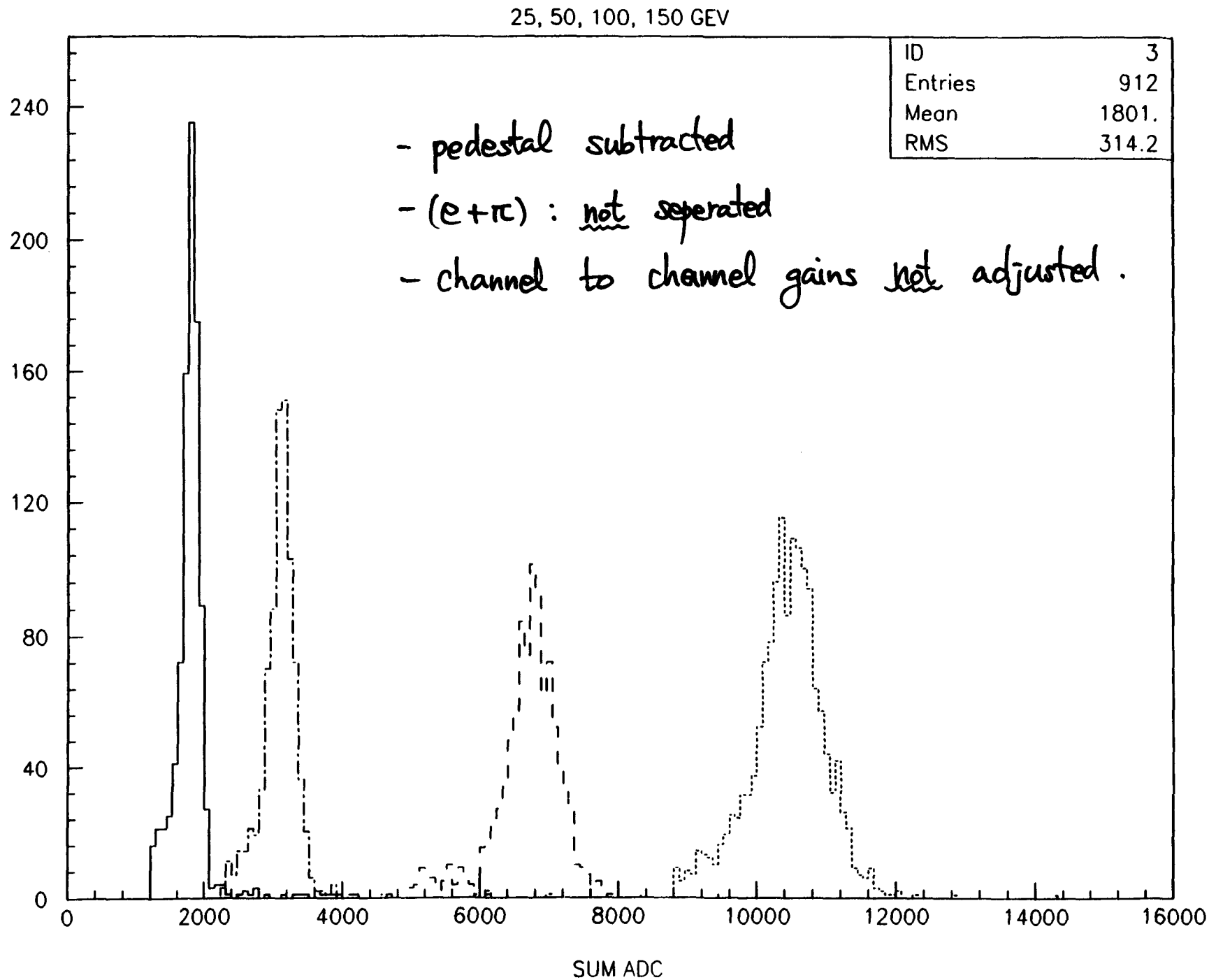
25, 50, 100, 150 GEV
ID 3
Entries 912
Mean 1801.
RMS 314.2
- pedestal subtracted
- (e+π) : not seperated
- channel to channel gains not adjusted.
0
40
80
120
160
200
240
0
2000
4000
6000
8000
10000
12000
14000
16000
SUM ADC

RAW DATA

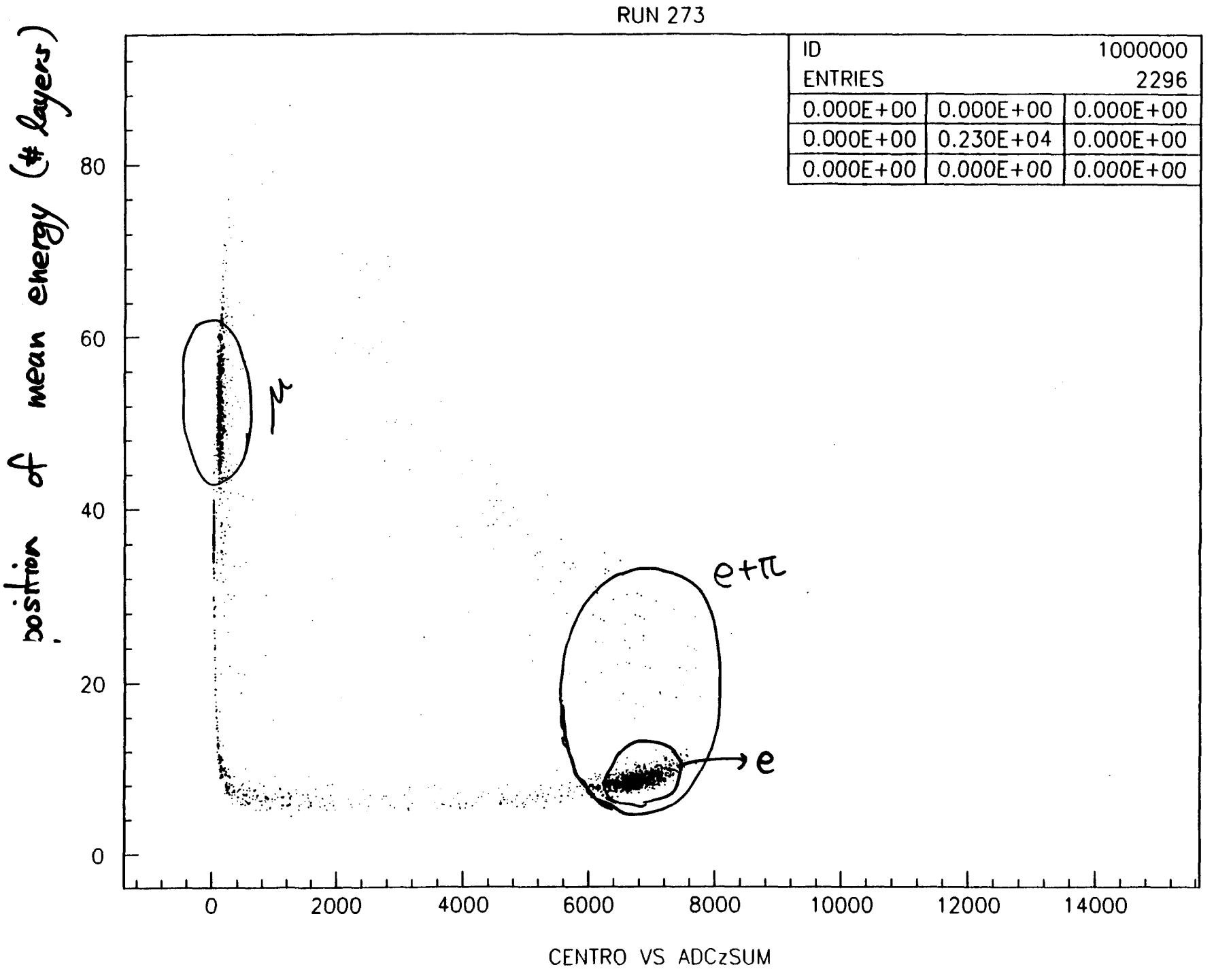
RUN 273
ID 1000000
ENTRIES 2296
0.000E+00 0.000E+00 0.000E+00
0.000E+00 0.230E+04 0.000E+00
0.000E+00 0.000E+00 0.000E+00
position of mean energy (# layers)
0
20
40
60
80
0
2000
4000
6000
8000
10000
12000
14000
CENTRO VS ADCzSUM
μ
e+π
e

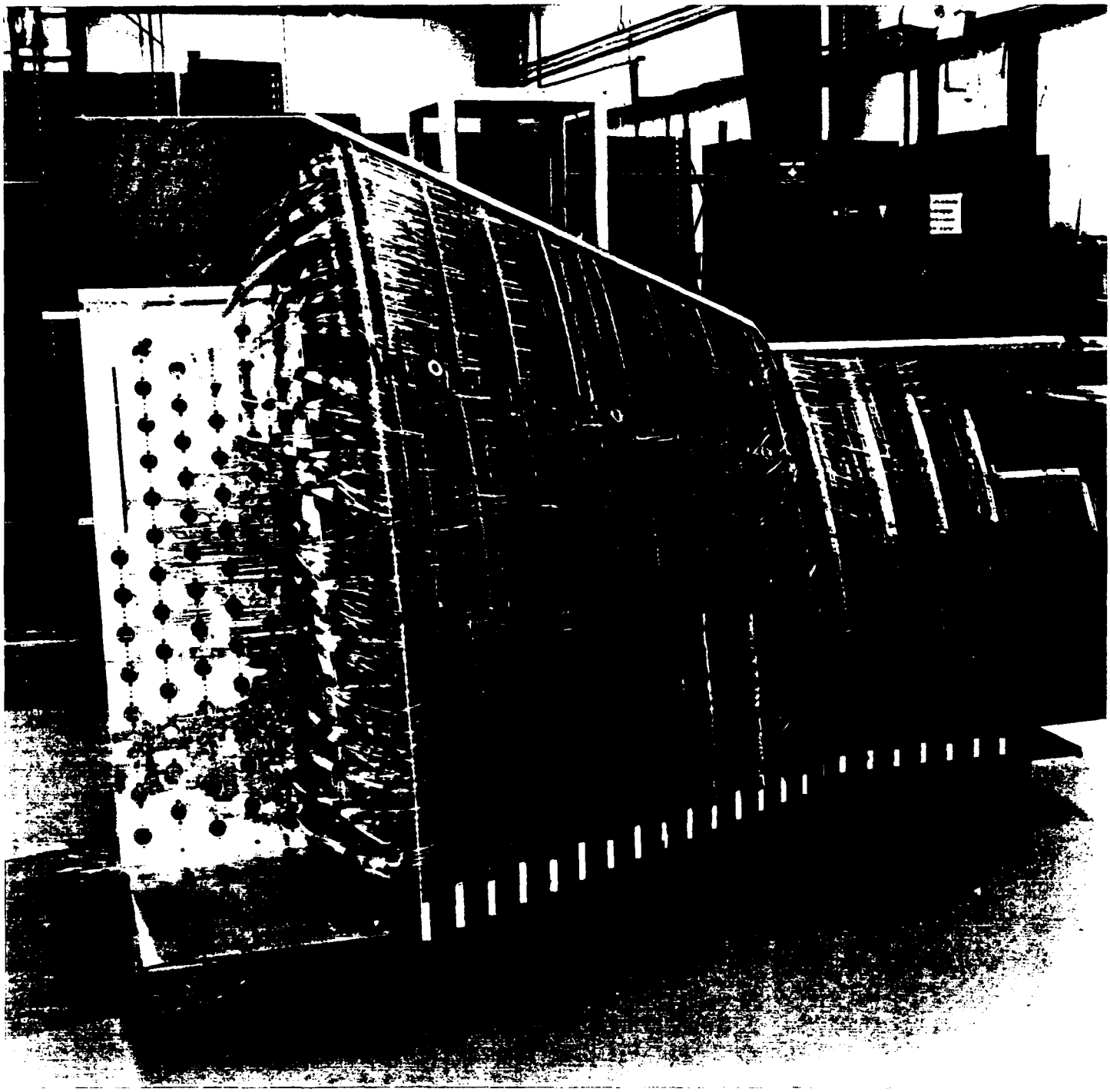

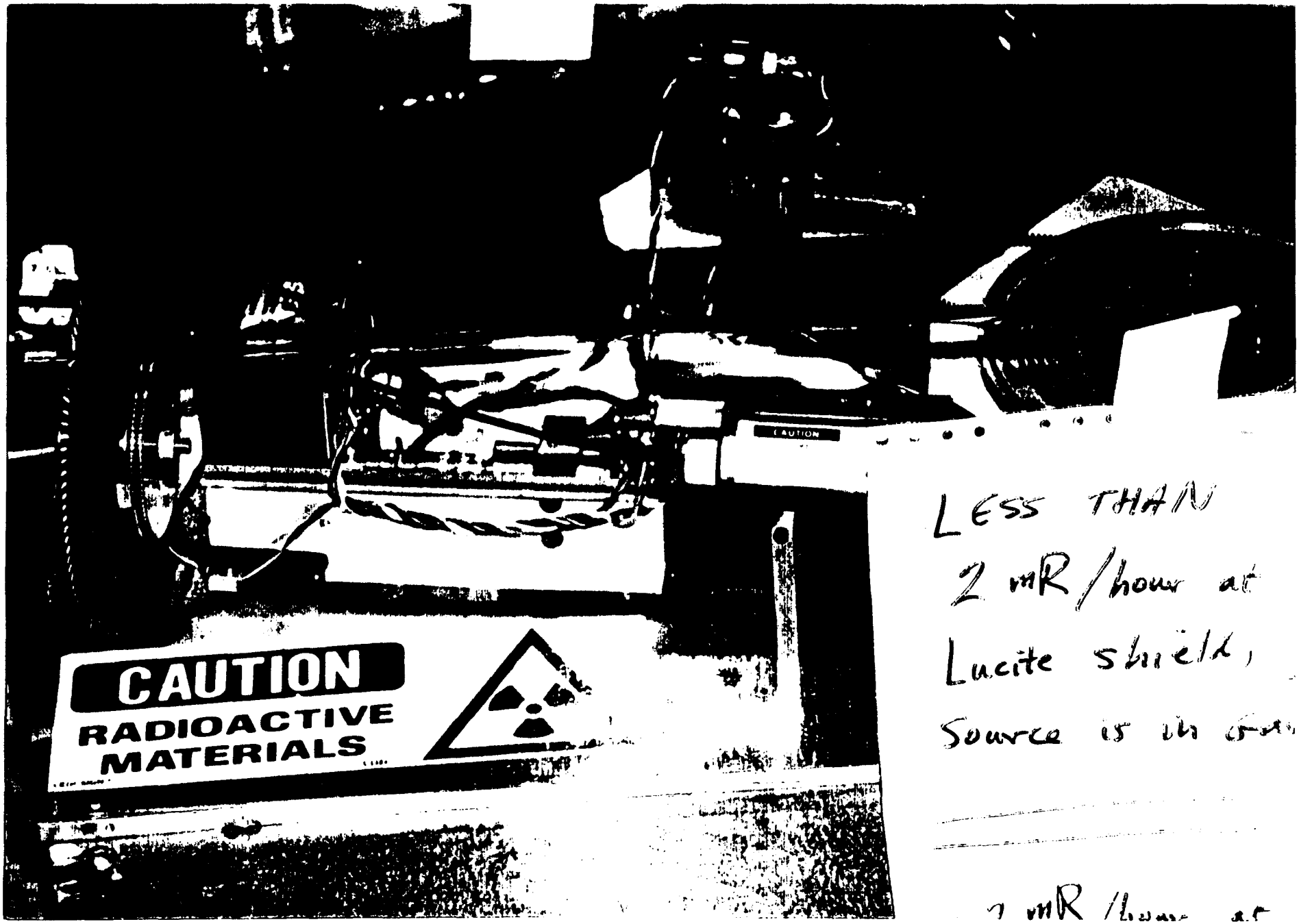

LESS THAN
2 mR/hour at
Lucite shield,
Source is in

1 mR/hour at

Prototype Design

desired energy res.

EM $\sim 19\%/\sqrt{E} + 1\%$

HAD $\sim 90\%/\sqrt{E} + 2\%$

light yield

EM $>$ 100 pe / GeV

HAD $>$ 10 pe / GeV

radiator

EM 4.8 mm Lead

HAD 2 inch Iron

observed light yield

EM 400 pe / GeV

4.3 pe/MIP/tile

(test bench expectation 4-5 pe/mip/tile)

HAD 39 pe / GeV

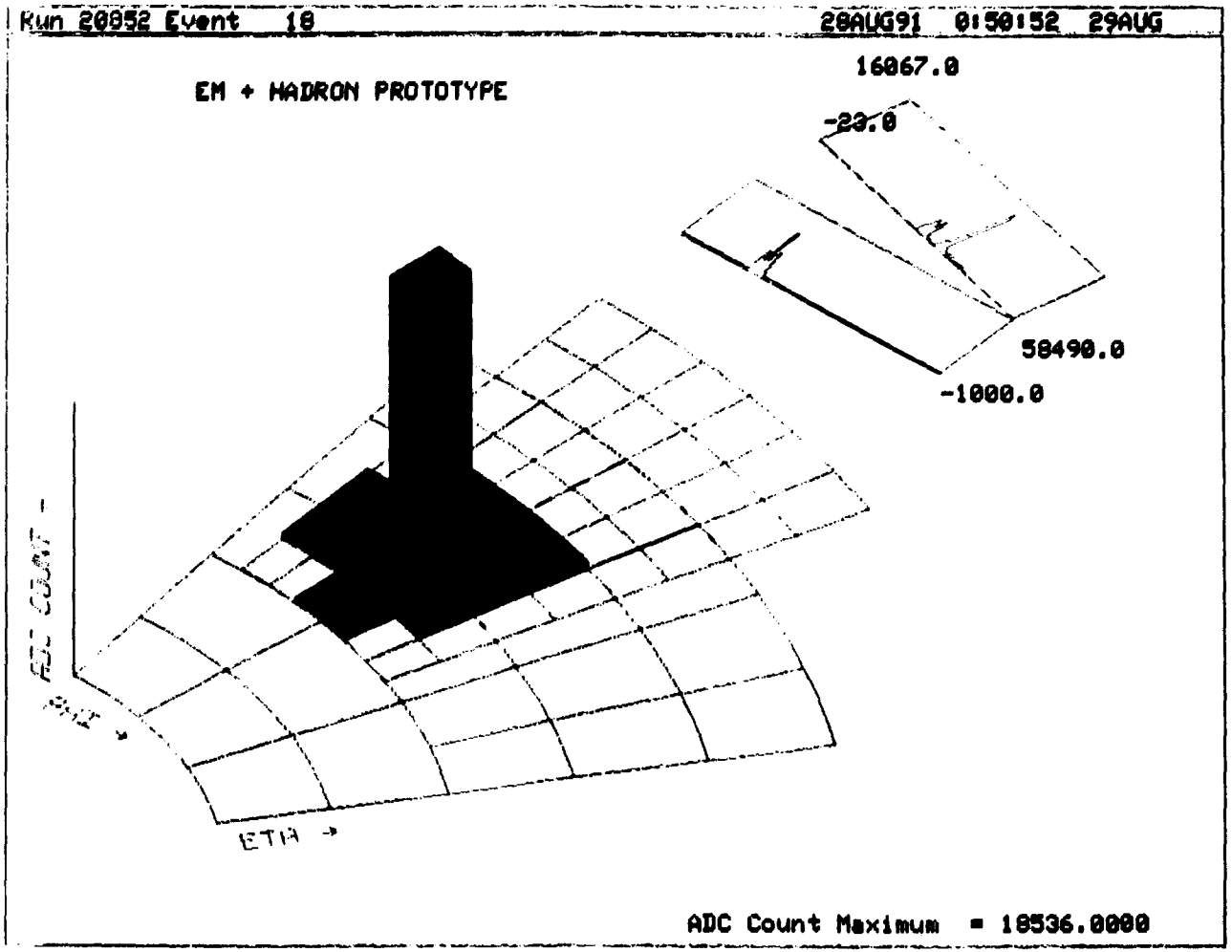
Run 20852 Event 18
28AUG91 0:50:52 29AUG
EM + HADRON PROTOTYPE
16067.0
-23.0
58490.0
-1000.0
ADC COUNT
ETA
ADC Count Maximum = 18536.0000

(8)

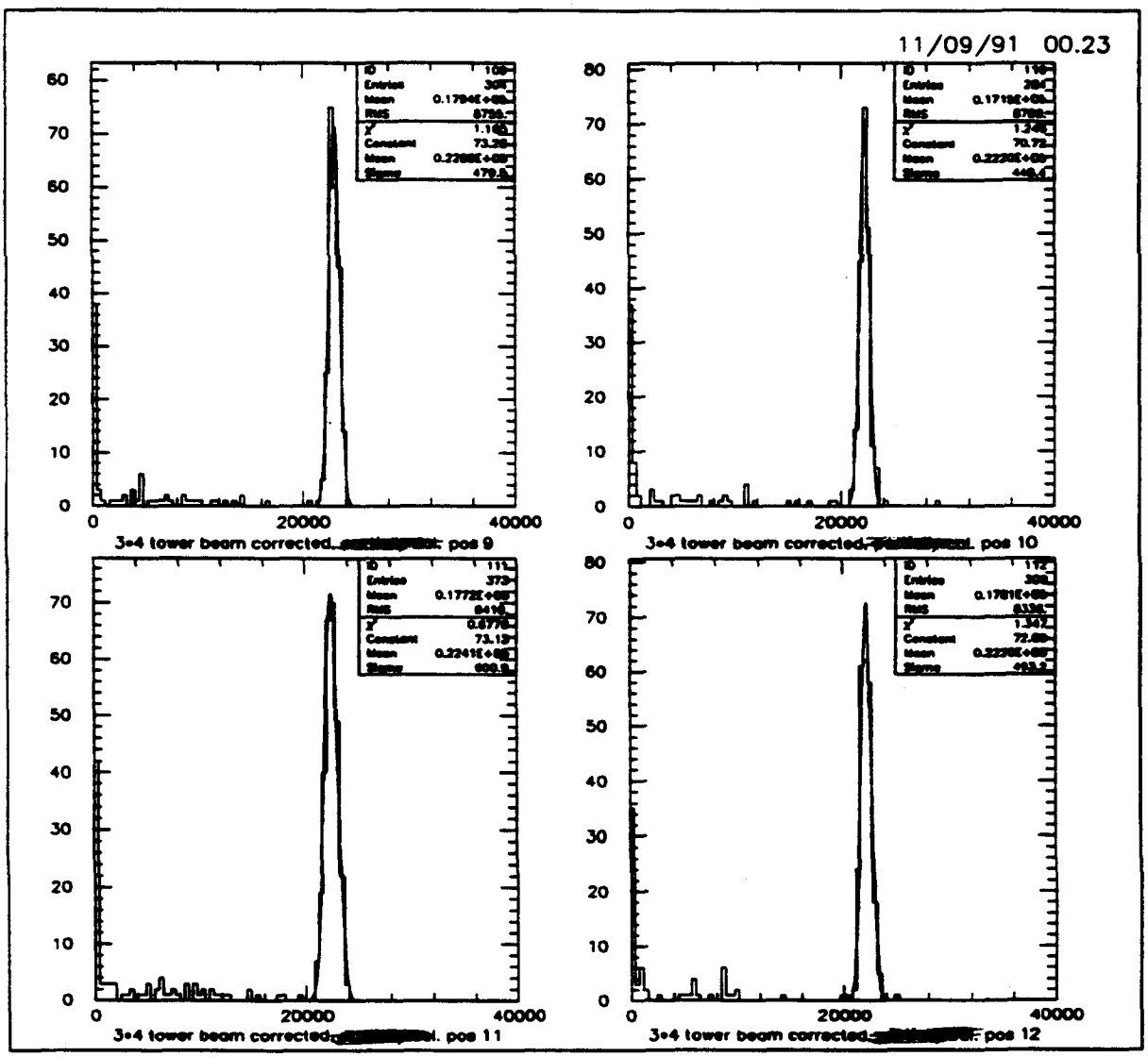
11/09/91 00.23
3+4 tower beam corrected. pos 9
3+4 tower beam corrected. pos 10
3+4 tower beam corrected. pos 11
3+4 tower beam corrected. pos 12

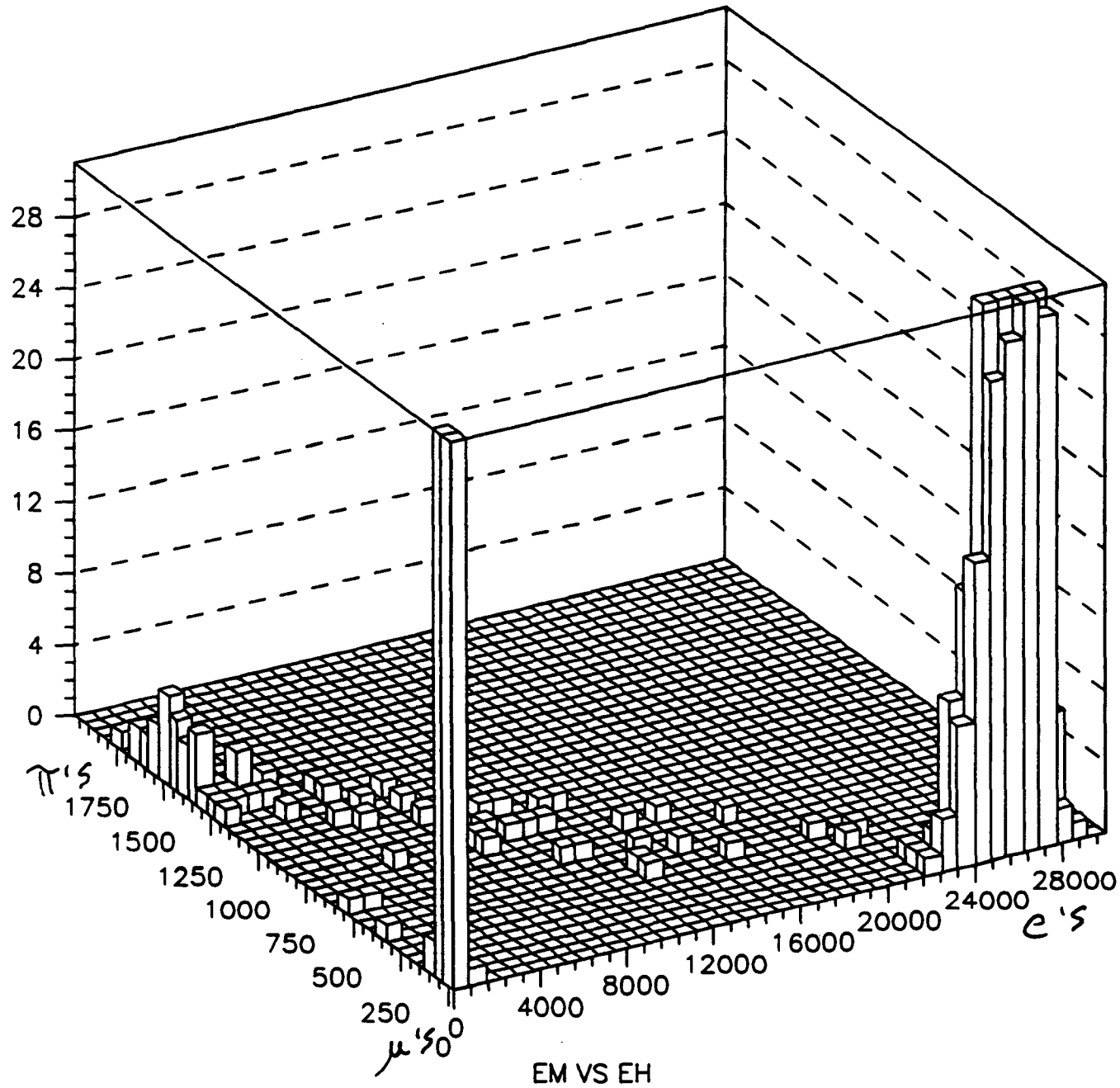
28
24
20
16
12
8
4
0
π's
1750
1500
1250
1000
750
500
250
μ's
0
4000
8000
12000
16000
20000
24000
28000
e's
EM VS EH

Summary of E_{cal}/P_{Beam}

Tower	$\langle E/p \rangle$	$\sigma(E/p)$ %
1	1.000 (By Definition)	1.6 %
2	1.002	1.65 %
3	1.008*	1.9 %
4	1.001	1.8 %
5	0.979*	1.8%
6	0.988	2.1 %
7	0.987*	1.8%
8	1.001	1.4%
9	0.993*	1.3%

Have uncalib. border towers.

* = 6 uncal. bc towers

3	4	5
2	1	6
9	8	7

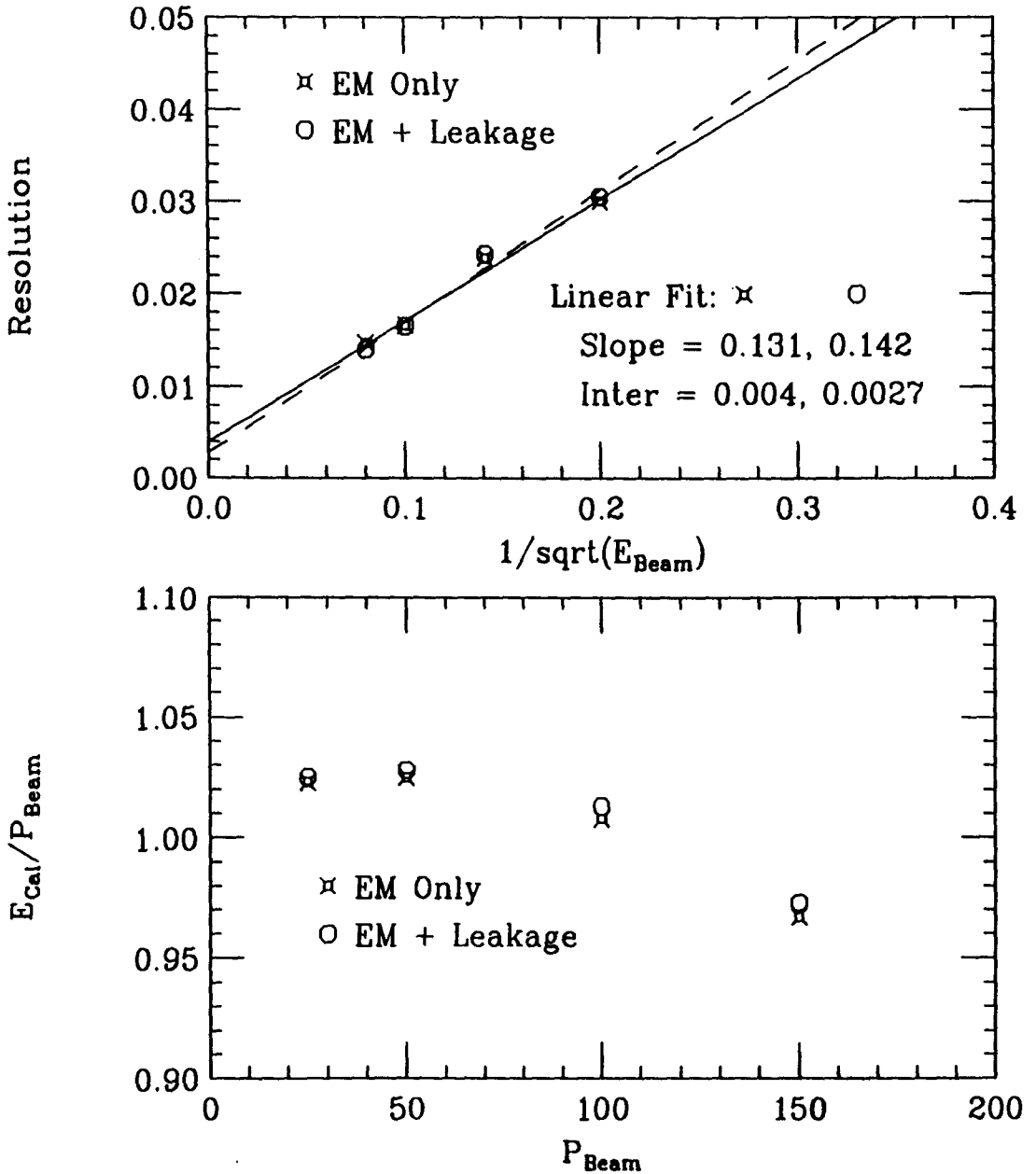
0.05
0.04
0.03
0.02
0.01
0.00
Resolution
EM Only
EM + Leakage
Linear Fit:
Slope = 0.131, 0.142
Inter = 0.004, 0.0027
0.0
0.1
0.2
0.3
0.4
1/sqrt(E_Beam)
1.10
1.05
1.00
0.95
0.90
E_Cal/P_Beam
EM Only
EM + Leakage
0
50
100
150
200
P_Beam

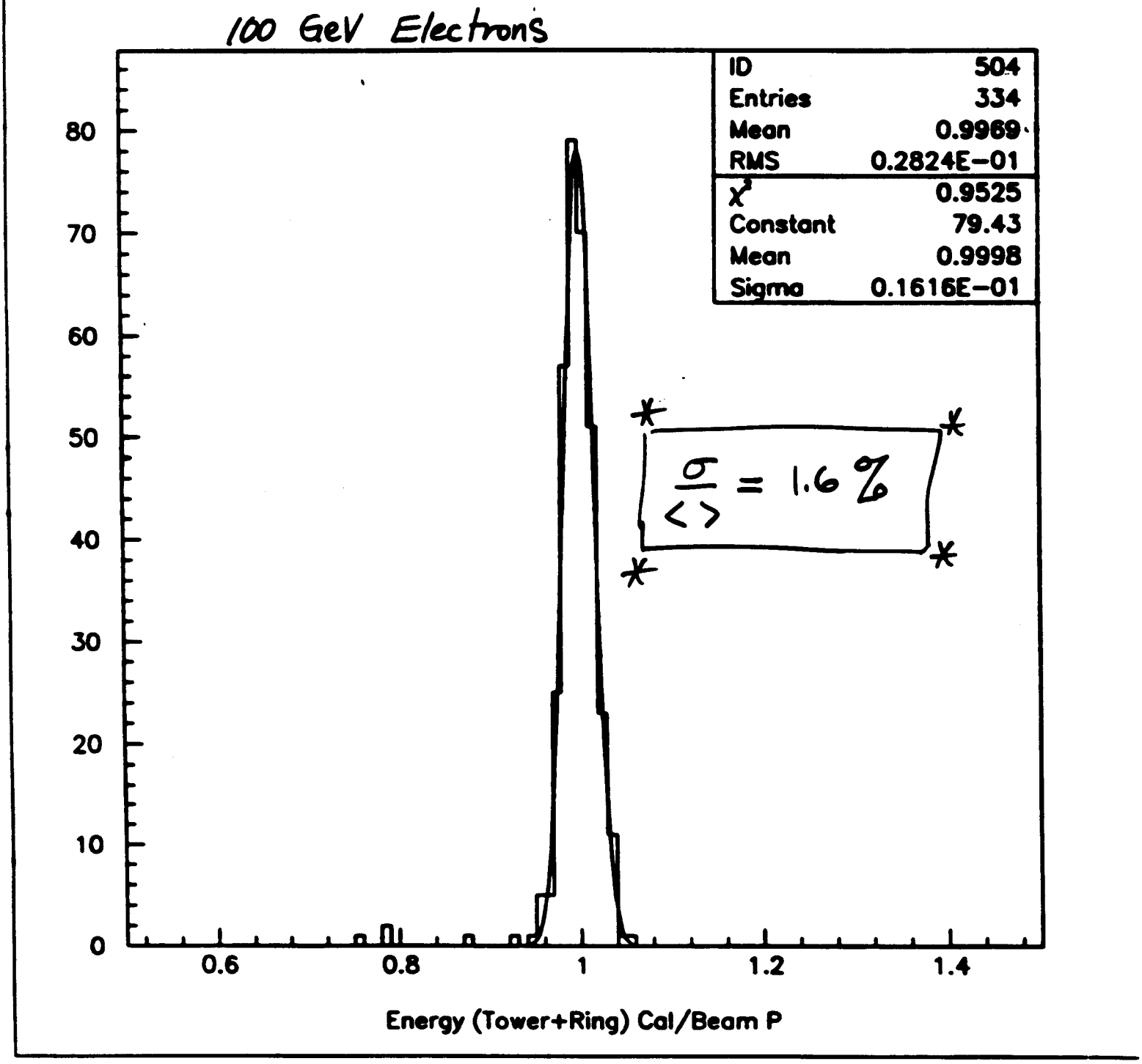
100 GeV Electrons
ID 504
Entries 334
Mean 0.9969
RMS 0.2824E-01
χ² 0.9525
Constant 79.43
Mean 0.9998
Sigma 0.1616E-01
σ/<> = 1.6 %
0
10
20
30
40
50
60
70
80
0.6
0.8
1
1.2
1.4
Energy (Tower+Ring) Cal/Beam P

layer 15

crack scan, 100 GeV e's

EM calorimeter $\sigma/\langle\rangle$ for E/p

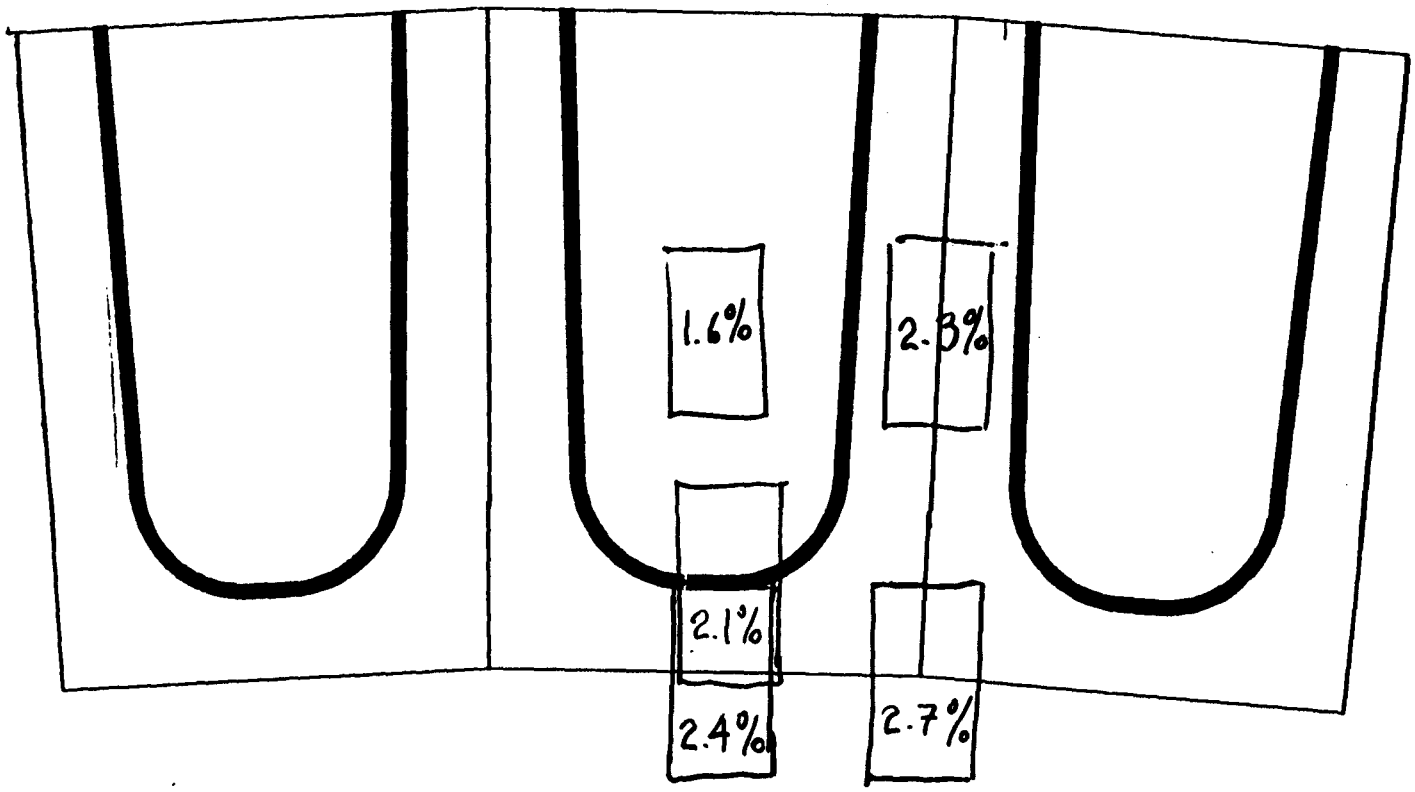

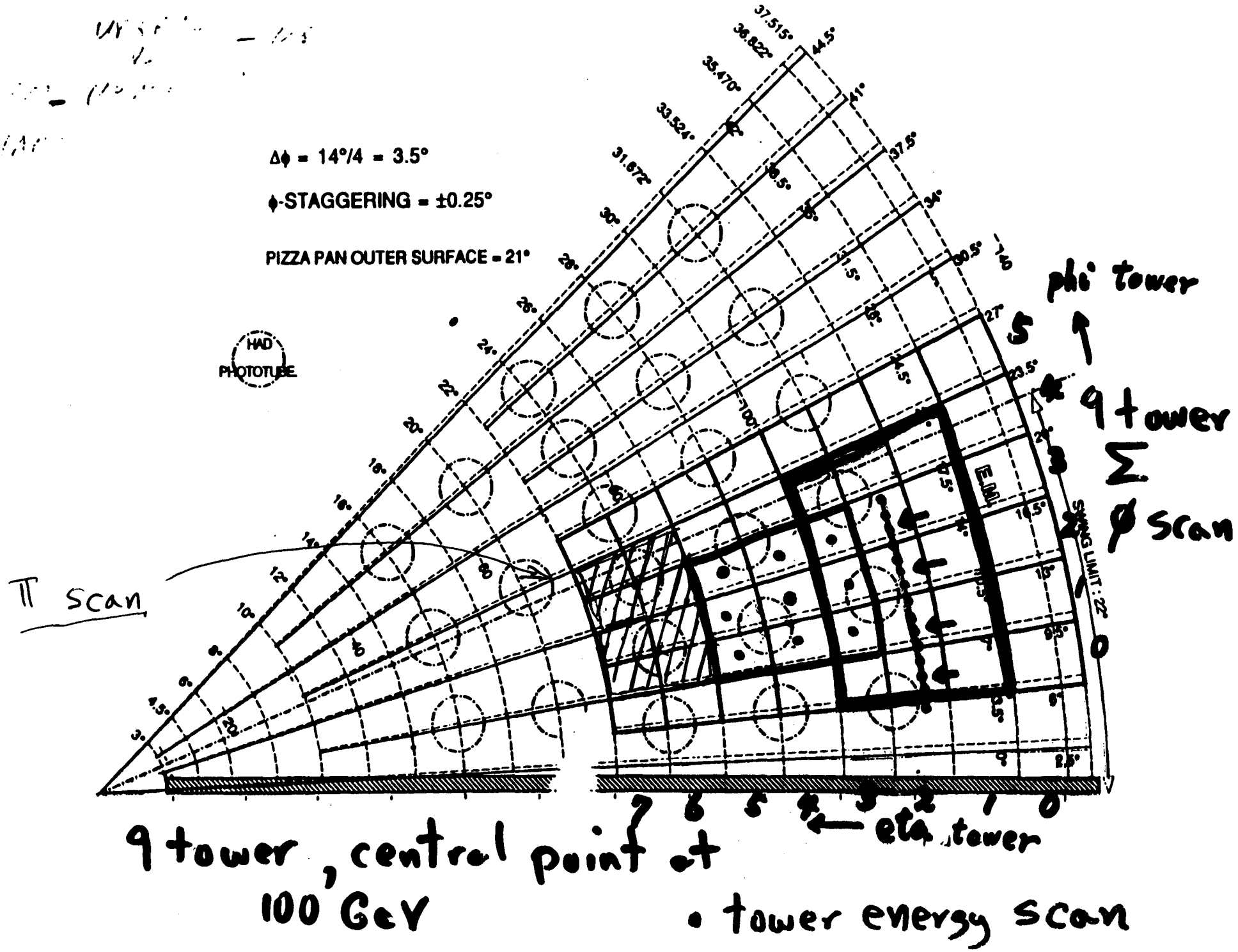
Δϕ = 14°/4 = 3.5°
ϕ-STAGGERING = ±0.25°
PIZZA PAN OUTER SURFACE = 21°
HAD PHOTOTUBE
EMU
SWING LIMIT : 22°
phi tower
9 tower Σ ϕ scan
π scan
eta tower
9 tower, central point at 100 GeV
• tower energy scan

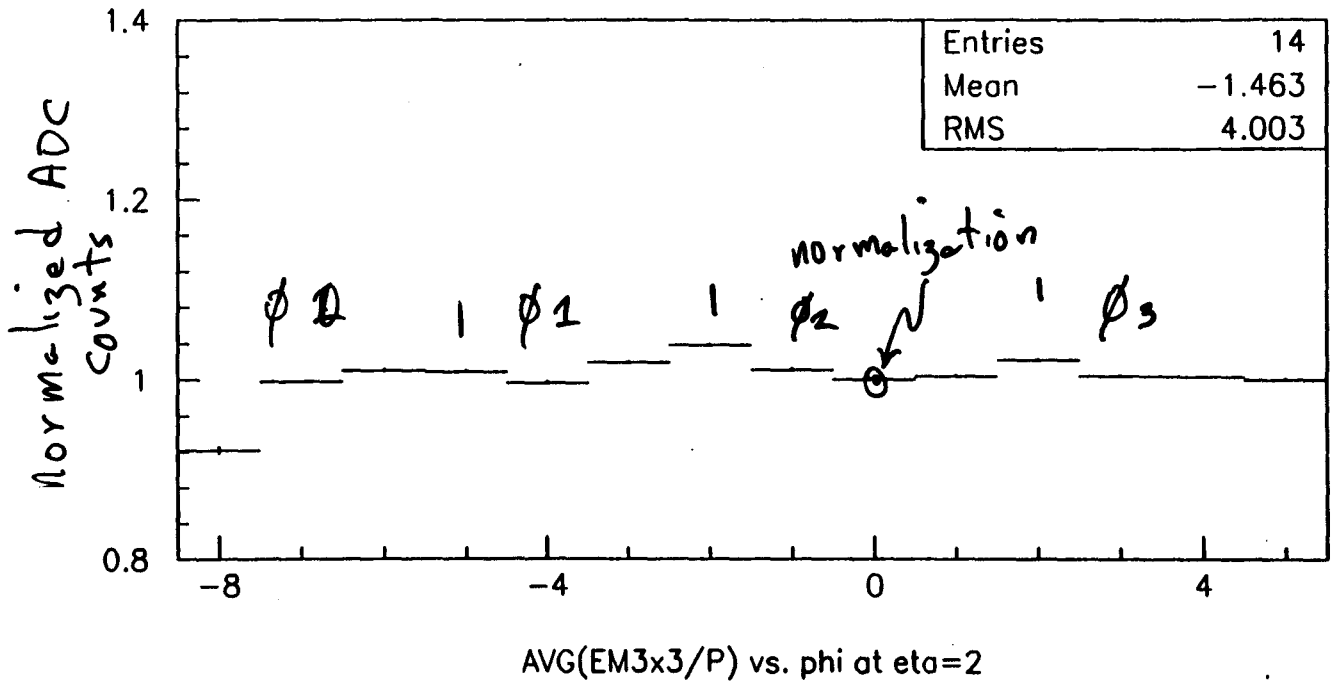
Entries 14
Mean −1.463
RMS 4.003
normalized ADC counts
normalization
φ 0
φ 1
φ 2
φ 3
AVG(EM3x3/P) vs. phi at eta=2

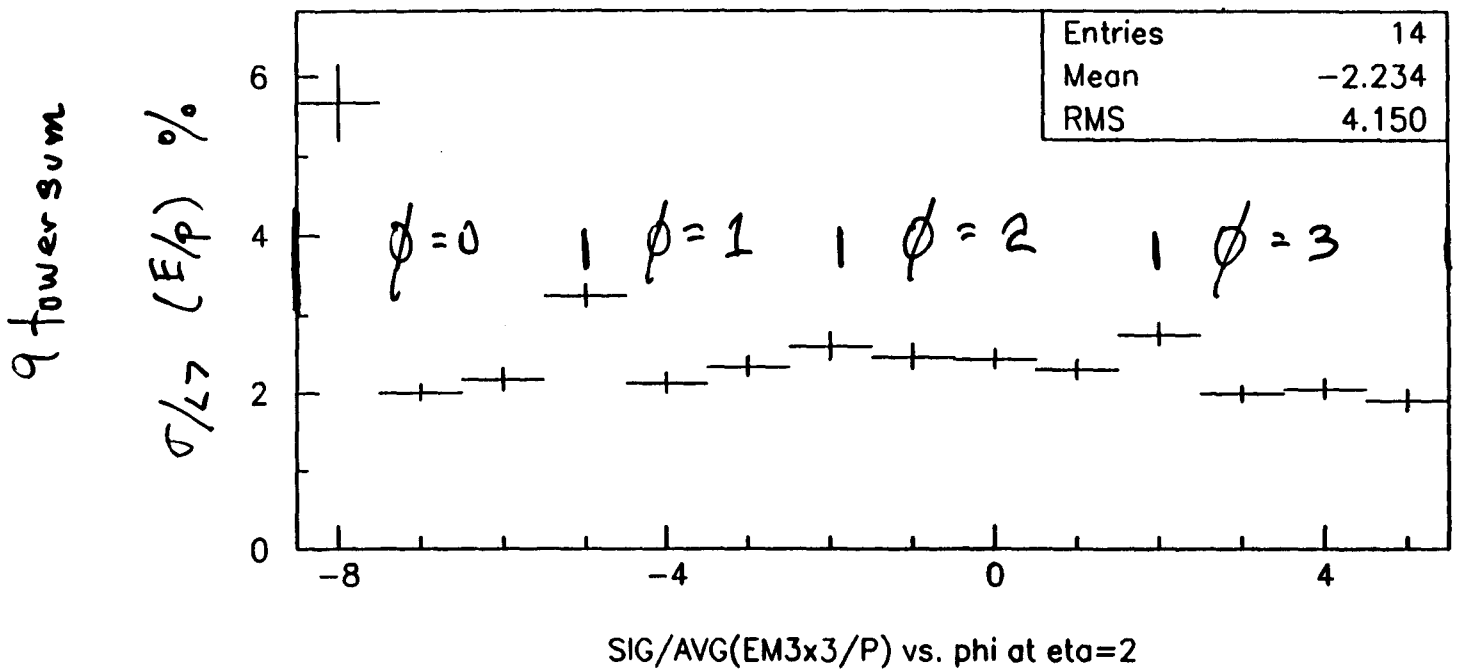
Entries 14
Mean −2.234
RMS 4.150
9 tower sum
σ/L7 (E/p) %
φ = 0
φ = 1
φ = 2
φ = 3
SIG/AVG(EM3x3/P) vs. phi at eta=2

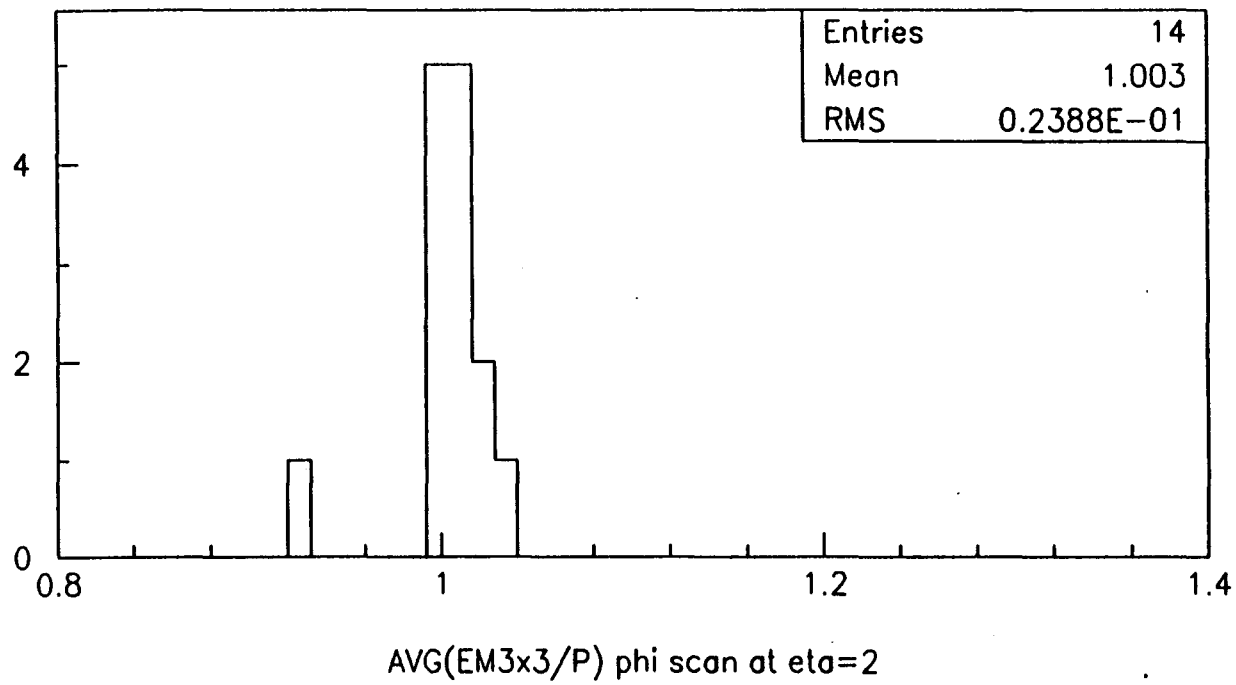
Entries 14
Mean 1.003
RMS 0.2388E-01
0
2
4
0.8
1
1.2
1.4
AVG(EM3x3/P) phi scan at eta=2

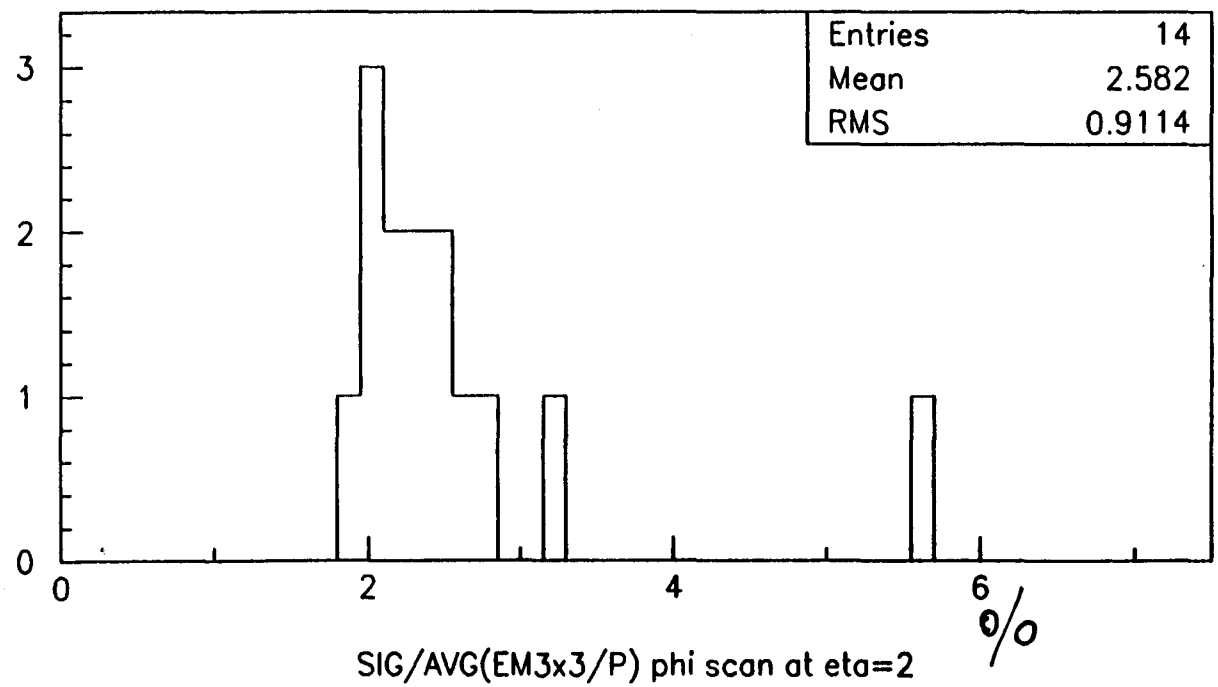
Entries 14
Mean 2.582
RMS 0.9114
0
1
2
3
0
2
4
6
%
SIG/AVG(EM3x3/P) phi scan at eta=2

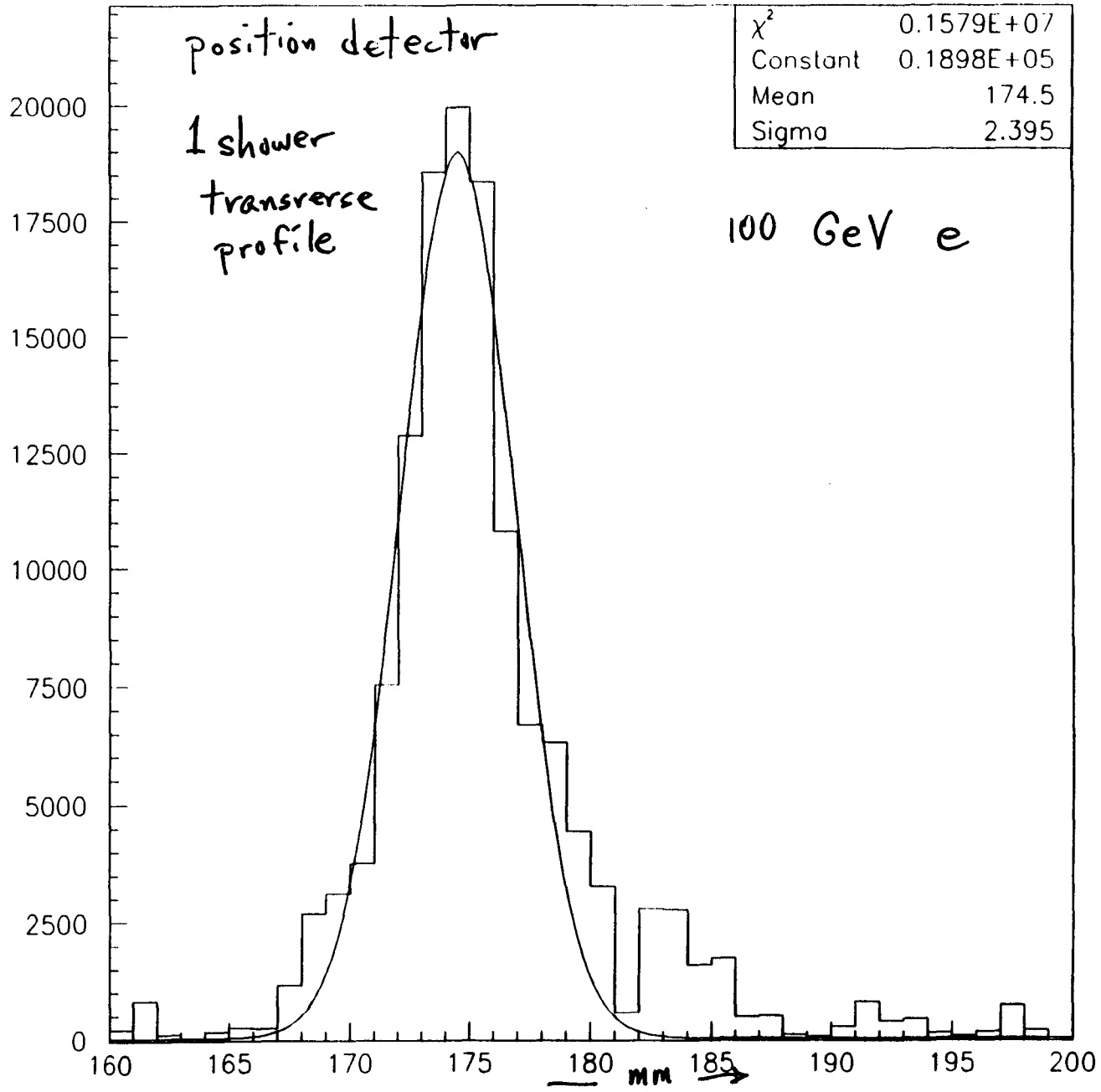
position detector
1 shower
transverse
profile
100 GeV e
χ^2 0.1579E+07
Constant 0.1898E+05
Mean 174.5
Sigma 2.395
20000
17500
15000
12500
10000
7500
5000
2500
0
160
165
170
175
180
185
190
195
200
mm
GAUSS FIT

11/09/91 10.46

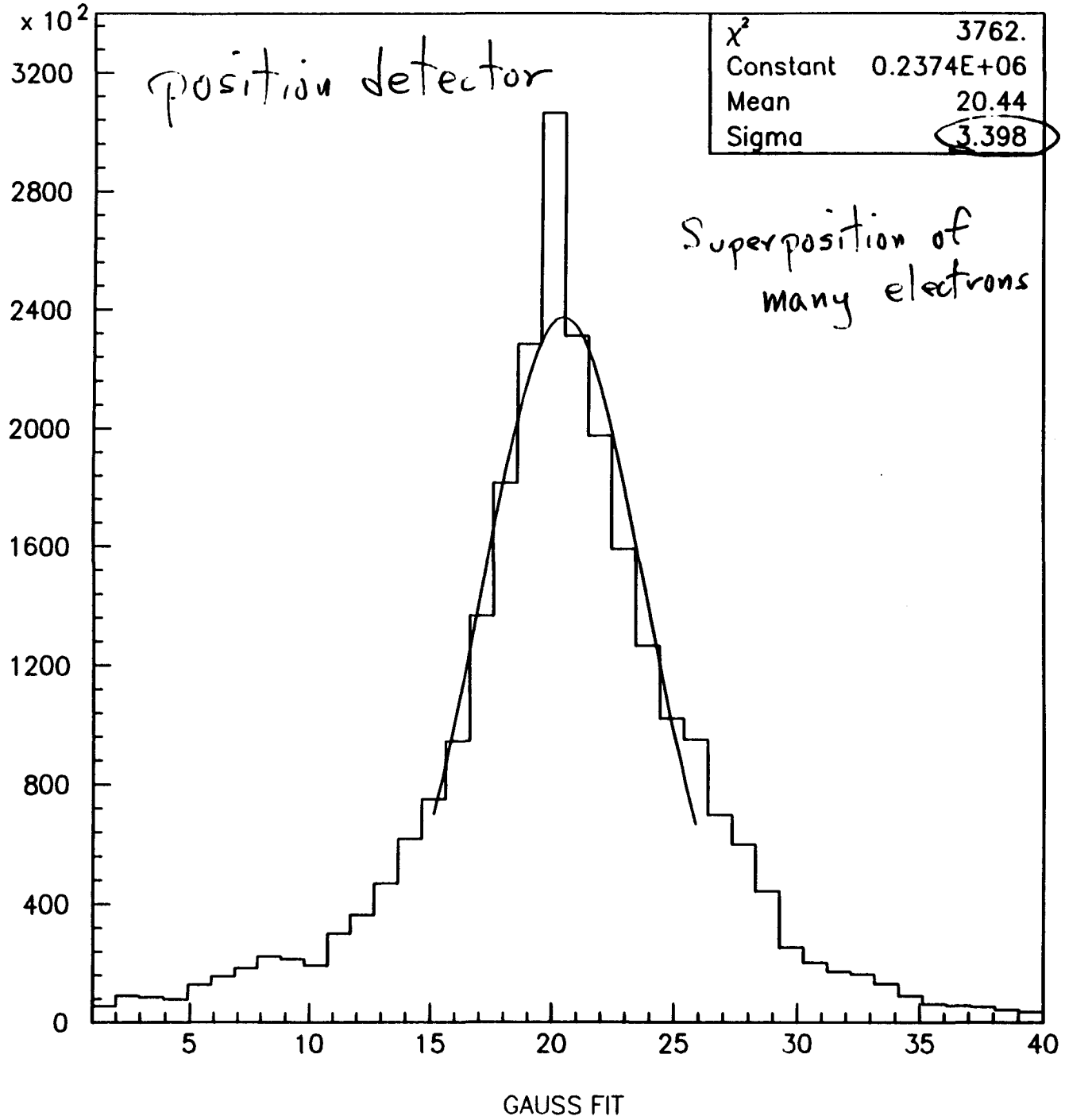
x 10^2
3200
2800
2400
2000
1600
1200
800
400
0
5
10
15
20
25
30
35
40
GAUSS FIT
χ² 3762.
Constant 0.2374E+06
Mean 20.44
Sigma 3.398
position detector
Superposition of many electrons

EM VDC vs HAD VDC
0
4000
8000
12000
16000
20000
24000
28000
0
2000
10000
12000
20000
22000
24000
HAD
EM
ID 204
ENTRIES 232
0.000E+00 0.000E+00 0.000E+00
0.000E+00 .228 0.81
0.000E+00 0.000E+00 0.000E+00

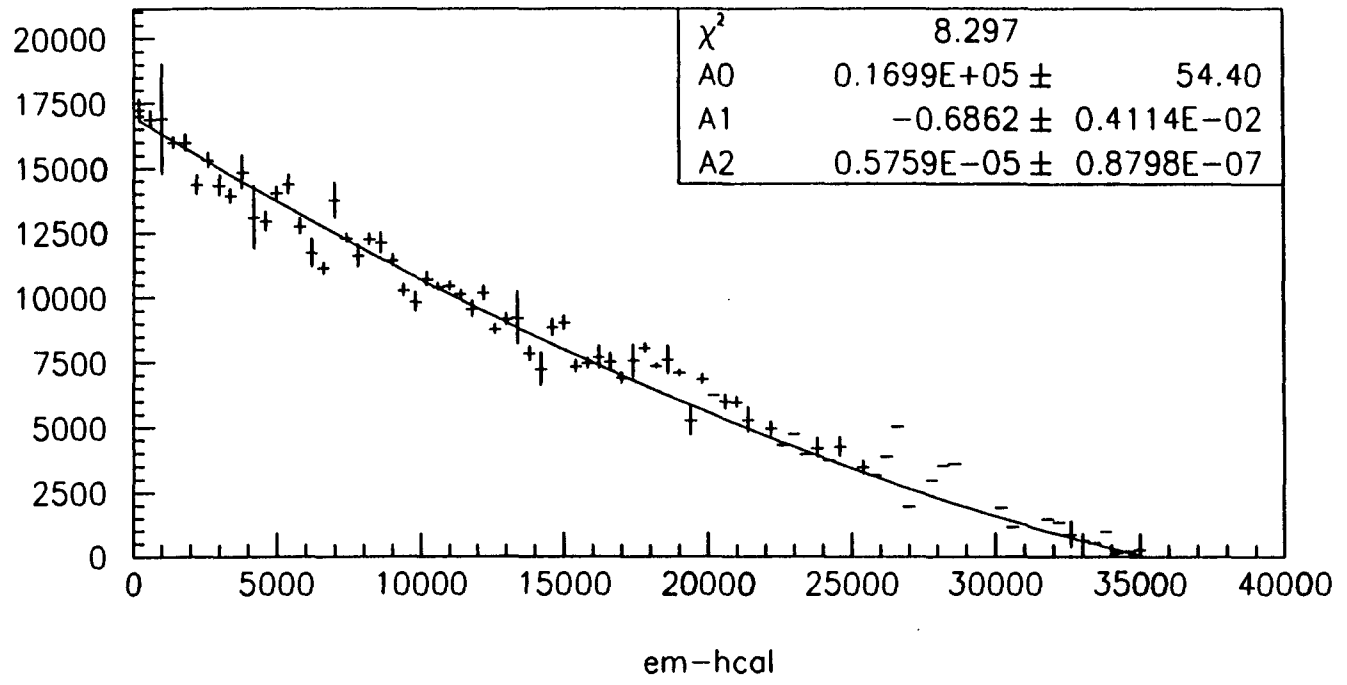

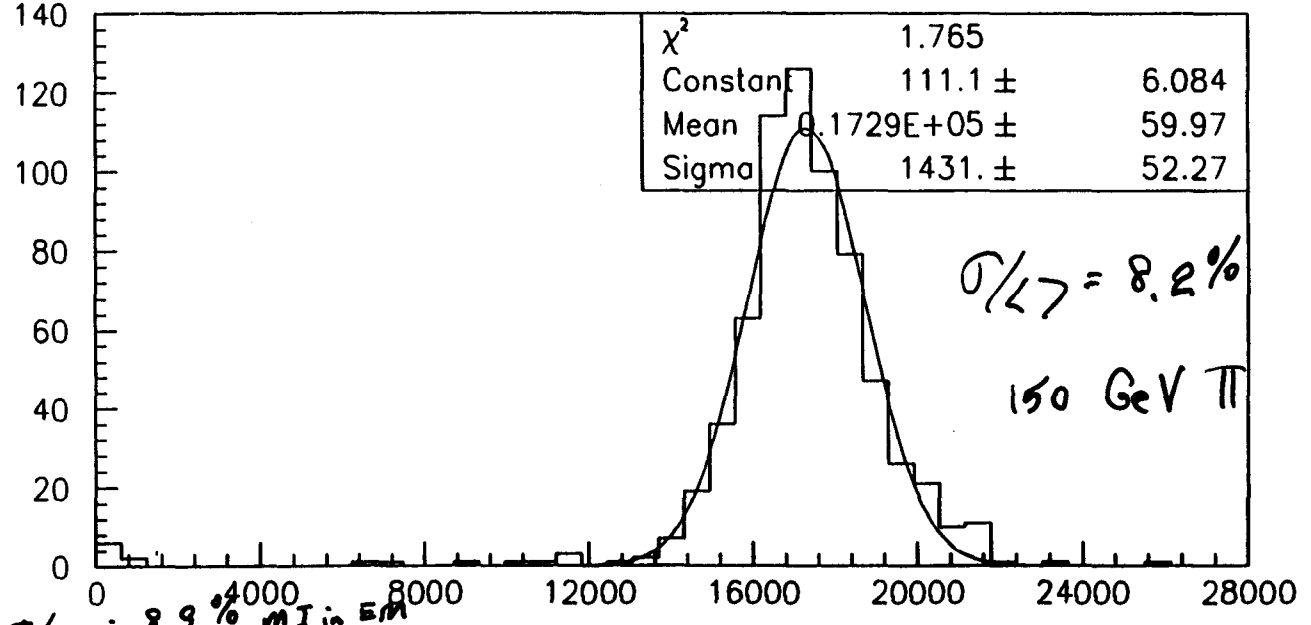

σ/⟨E⟩ = 8.9 %, MI in EM

HCAL resolution E/P, $E = E_{HAD} + (A_1 E_{EM} + A_2 E_{EM}^2)$

η	φ	layer	normalized light	
=12	1	11	10%	2
	2	2	50%	1
	2	11	10%	2
13	1	2	50%	1
	1	19	50%	1
	2	6	50%	1
14	2	23	30%	2
15	1	19	40%	1
	2	3	50%	1
	4	14	65%	1
16	2	19	50%	1
	3	19	40%	1
	4	6	50%	1
	4	18	60%	1
	4	19	65%	1
17	2	19	60%	1
	3	13	65%	1
	4	19	60%	1
	5	15	50%	1

broken fibers in EM
= 22/2208
= 1%

⇒ a problem
need to change
assembly techniq

Calibration System

- we have extensive system of tubes, source mover.

- we have not yet demonstrated its' utility.

- first set of EM longitudinal masks failed ($\sigma \sim 7\%$) (photographic process ?)

- plan : remake EM masks, target is $\sigma \sim 2\%$

  attempt to set tower-to-tower relative calibrations to 1% using source.

  purchase Sr^{90} wire source to evaluate

Test beam plans

- Complete mapping of this prototype
- retest with new masks on EM
- 9 tower prototype of mirrored fiber "σ" tiles installed in mid-October

CALORIMETER REVIEW AND TECHNICAL BOARD MEETING
SEPTEMBER 12 -14, 1991
SSCL

Presentation by:

Gerry Abrams

Lawrence Berkeley Laboratory

Liquid Argon Option for SDC Calorimetry

Design, Parameters, and Cost

Gerry Abrams

for the SDC LAC Group

Prepared for the SDC Calorimetry Review

September 12-14, 1991

SSC Laboratory

Summarizing the work of many others, but most especially -

Bill Pope, LBL

Nobu Unno, KEK

Tile/Fiber Technical Risks

Radiation Damage
Turn barrel corner ?

Optical System

Calibration

(Speed of response)

Outline

I. Design Overview

- A. Layout
- B. Design Parameters

II. Cryostat Design

- A. Barrel and Endcap Designs
- B. Dead Material
- C. Massless Gaps
- D. $\eta = 3$ Region
- E. Feedthroughs

III. Module Design

- A. Barrel EM and Hadronic
- B. Endcap Big Wheel
- C. Electrode Structure and Readout

IV. Integration

- A. Routing of Pipes and Cables
- B. Return Iron
- C. Access
- D. Safety
- E. Cost

Y.U 1991/6/18

Critical Issues for the LAC

Item	Status	Comment
Preamp (Rad.hard)		BNL hybrid: $>10^{13}$n/cm^2, >12Mrad
Speed		$\tau_{rise}\leq$30ns
Noise		τ_p=100(EM), 200ns(HAD) σ_{Et} (ΔR<0.15)
Pileup		3 meas., τ_p=50~200ns σ_{Et}~0.5GeV
e/h meas.		Hadron module beam test
e hermeticity		97%accept.(σ_E<25%/$\sqrt{E}$)
Reliability		<0.2% failure(SLD) in 10^8s
P/a cooling		KEK/Rochester test results
Safety		SSCL Safety committee
η=3,$\not{E}_t$		KHI, LBL
Integration		LBL
Cost		MMA

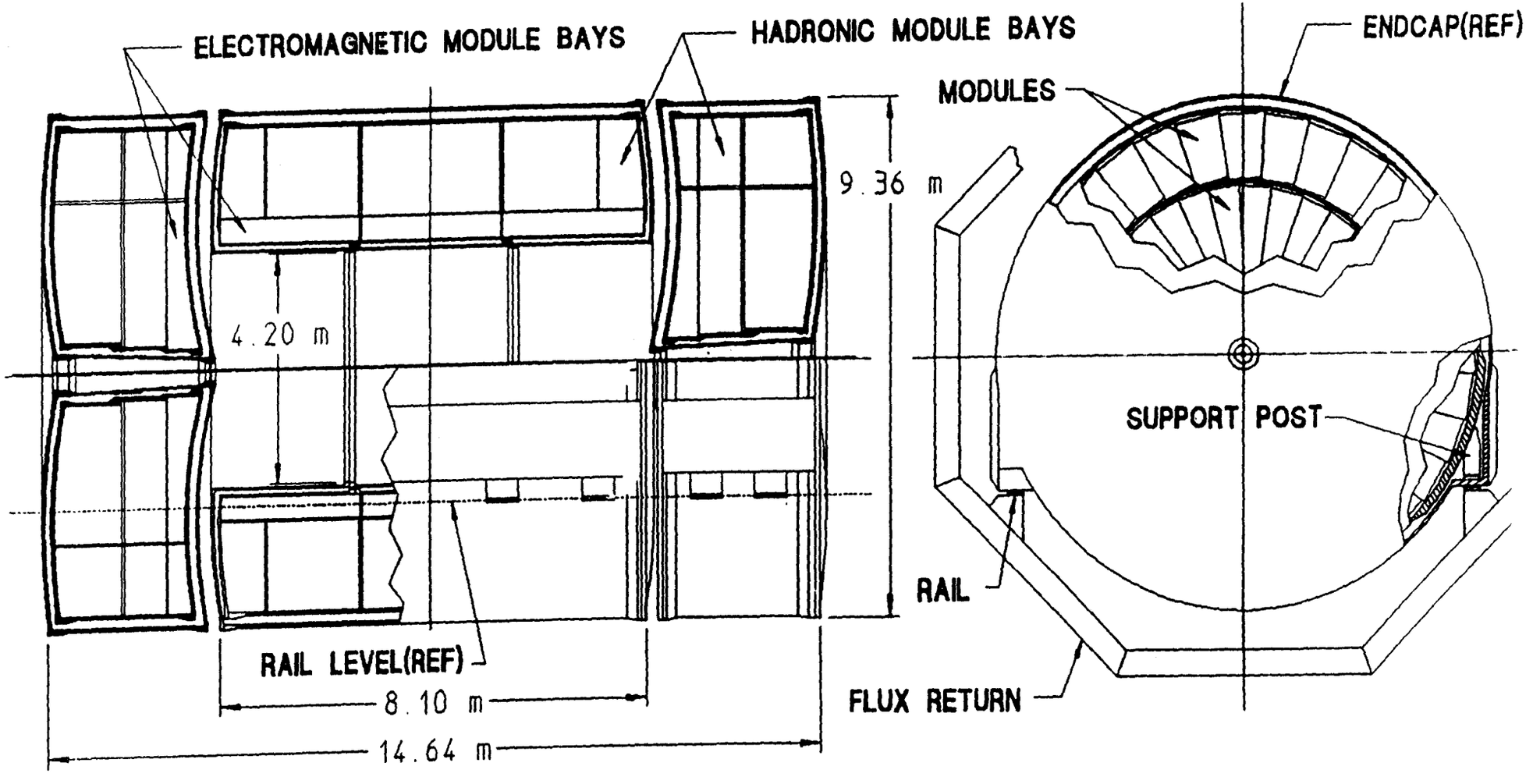
ELECTROMAGNETIC MODULE BAYS
HADRONIC MODULE BAYS
ENDCAP(REF)
MODULES
9.36 m
4.20 m
SUPPORT POST
RAIL
RAIL LEVEL(REF)
8.10 m
FLUX RETURN
14.64 m

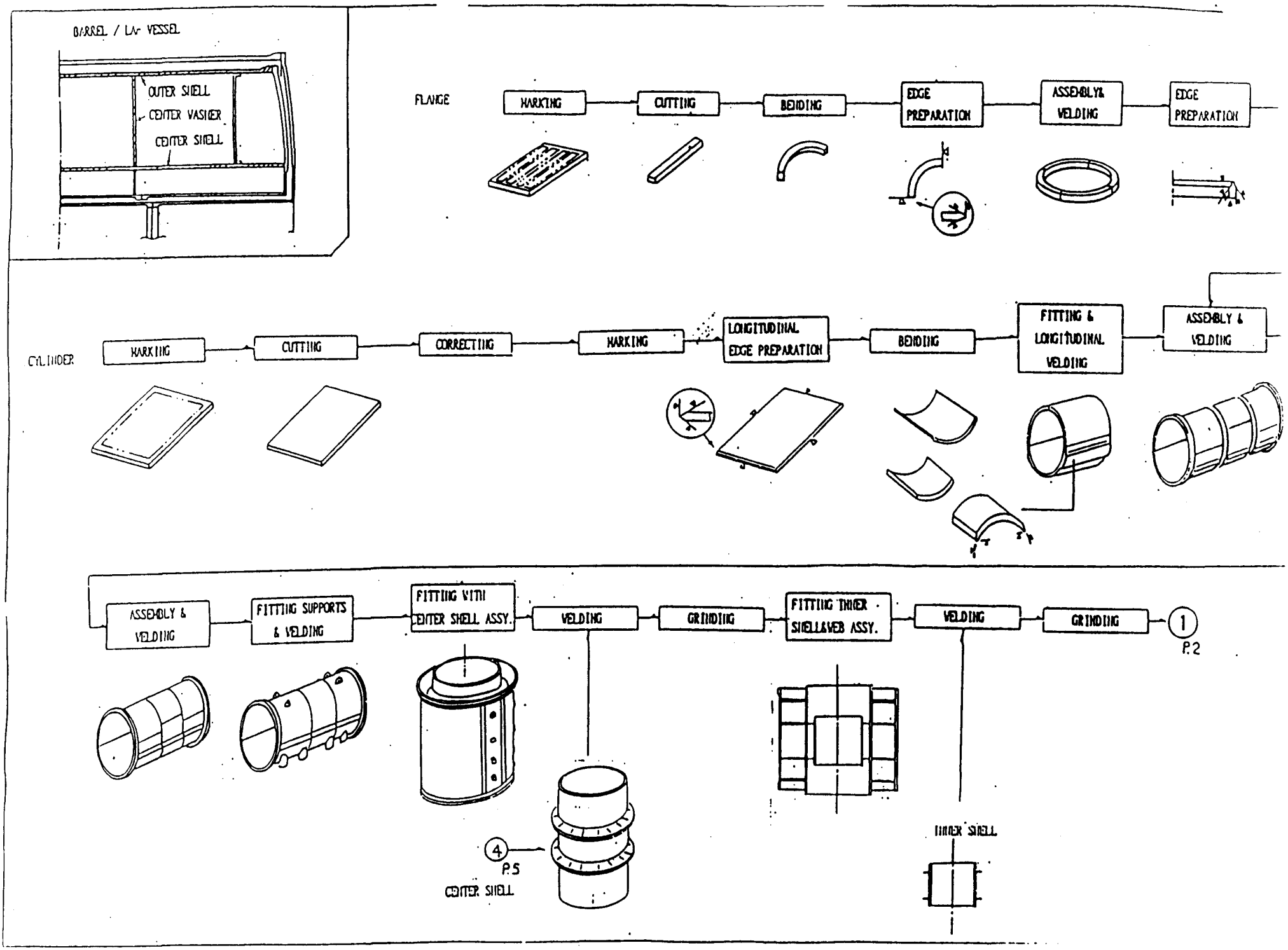
BARREL / LAV VESSEL
OUTER SHELL
CENTER WASHER
CENTER SHELL
FLANGE
MARKING
CUTTING
BENDING
EDGE PREPARATION
ASSEMBLY & WELDING
EDGE PREPARATION
CYLINDER
MARKING
CUTTING
CORRECTING
MARKING
LONGITUDINAL EDGE PREPARATION
BENDING
FITTING & LONGITUDINAL WELDING
ASSEMBLY & WELDING
ASSEMBLY & WELDING
FITTING SUPPORTS & WELDING
FITTING WITH CENTER SHELL ASSY.
WELDING
GRINDING
FITTING INNER SHELL&WEB ASSY.
WELDING
GRINDING
1
P.2
4
P.5
CENTER SHELL
INNER SHELL

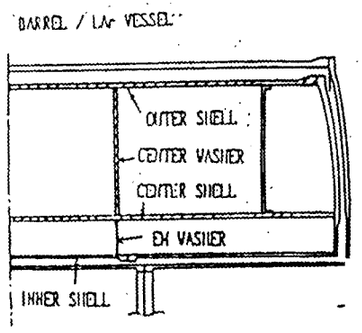
BARREL / LAP VESSEL
OUTER SHELL
CENTER WASHER
CENTER SHELL
END WASHER
INNER SHELL

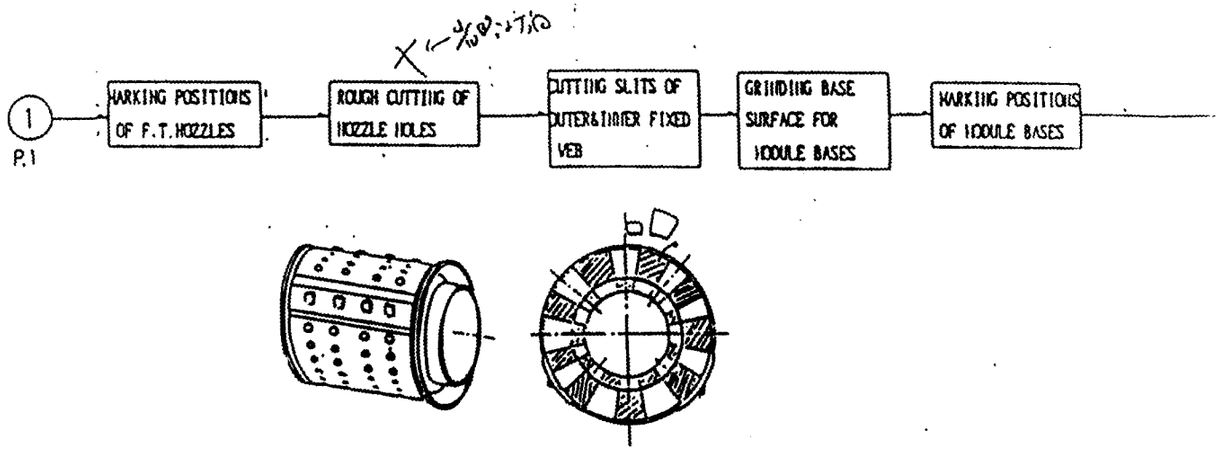
1
P.1
MARKING POSITIONS OF F.T. NOZZLES
ROUGH CUTTING OF NOZZLE HOLES
CUTTING SLITS OF OUTER&INNER FIXED WEB
GRINDING BASE SURFACE FOR NOZZLE BASES
MARKING POSITIONS OF NOZZLE BASES

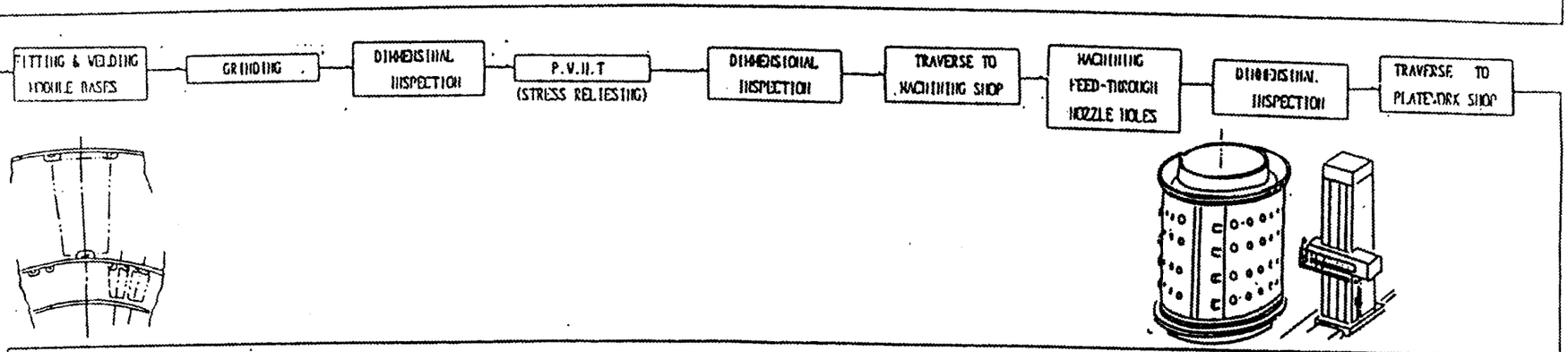
FITTING & WELDING NOZZLE BASES
GRINDING
DIMENSIONAL INSPECTION
P.W.H.T
(STRESS RELIEVING)
DIMENSIONAL INSPECTION
TRAVERSE TO MACHINING SHOP
MACHINING FEED-THROUGH NOZZLE HOLES
DIMENSIONAL INSPECTION
TRAVERSE TO PLATEWORK SHOP

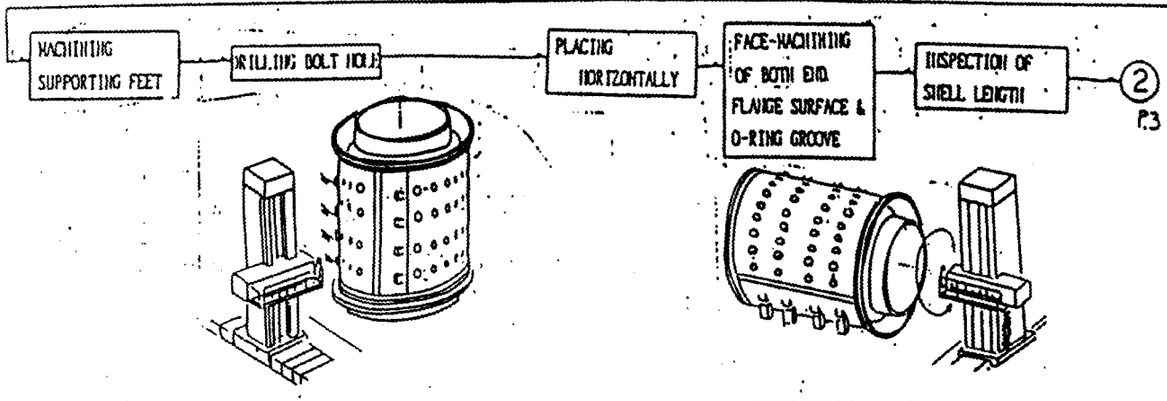
MACHINING SUPPORTING FEET
DRILLING BOLT HOLE
PLACING HORIZONTALLY
FACE-MACHINING OF BOTH END FLANGE SURFACE & O-RING GROOVE
INSPECTION OF SHELL LENGTH
2
P.3

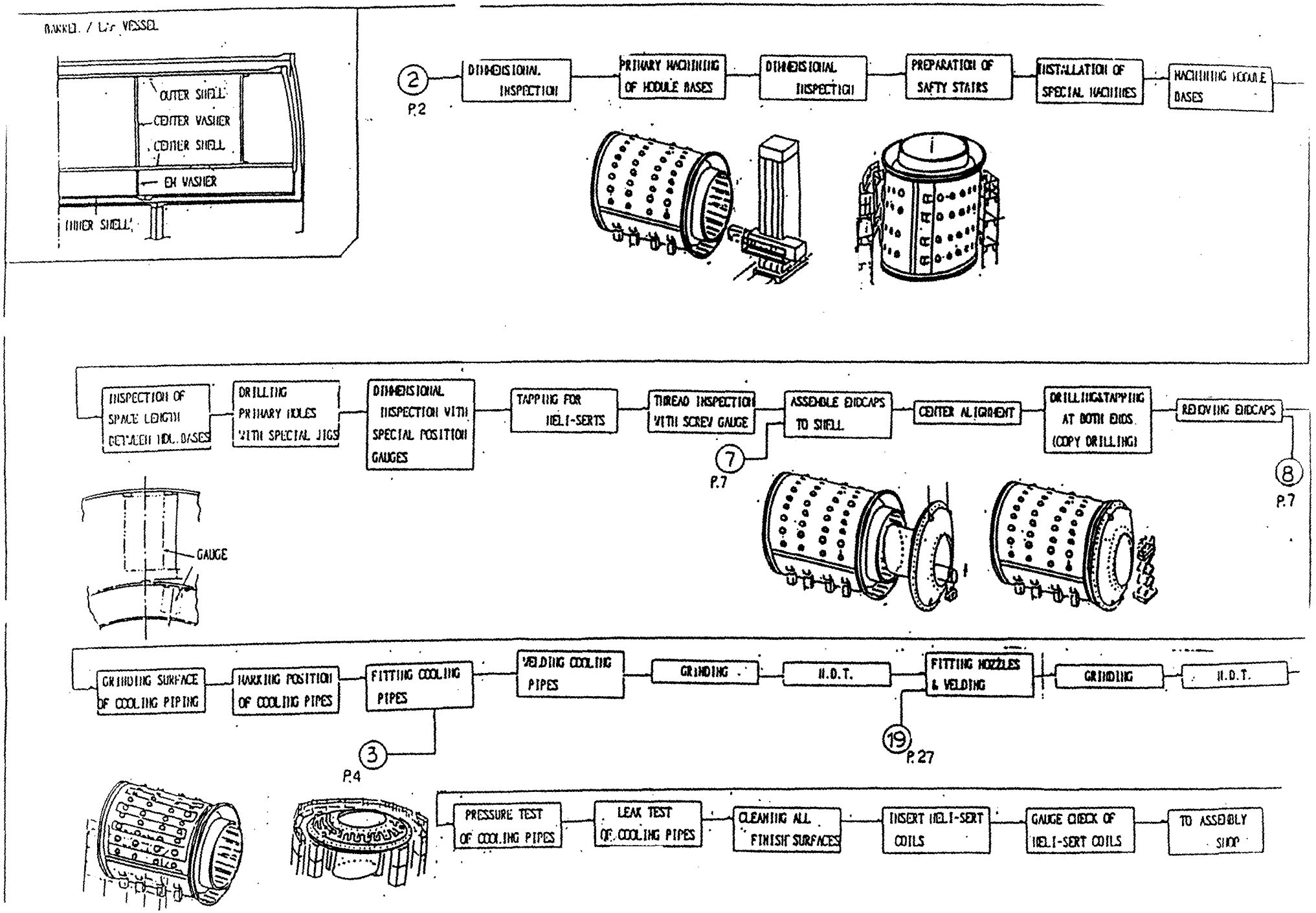
BARREL / L/r VESSEL
OUTER SHELL
CENTER WASHER
CENTER SHELL
EH WASHER
INNER SHELL
2
P.2
DIMENSIONAL INSPECTION
PRIMARY MACHINING OF MODULE BASES
DIMENSIONAL INSPECTION
PREPARATION OF SAFTY STAIRS
INSTALLATION OF SPECIAL MACHINES
MACHINING MODULE BASES
INSPECTION OF SPACE LENGTH BETWEEN MOD. BASES
DRILLING PRIMARY HOLES WITH SPECIAL JIGS
DIMENSIONAL INSPECTION WITH SPECIAL POSITION GAUGES
TAPPING FOR HELI-SERTS
THREAD INSPECTION WITH SCREW GAUGE
ASSEMBLE ENDCAPS TO SHELL
CENTER ALIGNMENT
DRILLING&TAPPING AT BOTH ENDS. (COPY DRILLING)
REMOVING ENDCAPS
7
P.7
8
P.7
GAUGE
GRINDING SURFACE OF COOLING PIPING
MARKING POSITION OF COOLING PIPES
FITTING COOLING PIPES
WELDING COOLING PIPES
GRINDING
N.D.T.
FITTING NOZZLES & WELDING
GRINDING
N.D.T.
3
P.4
19
P.27
PRESSURE TEST OF COOLING PIPES
LEAK TEST OF COOLING PIPES
CLEANING ALL FINISH SURFACES
INSERT HELI-SERT COILS
GAUGE CHECK OF HELI-SERT COILS
TO ASSEMBLY SHOP

(2) 応力評価

応力評価は、ASMEより以下の２式を満たすものとする。

一次応力　一般膜応力　$P_m < S_m$

二次応力　膜＋曲げ応力　$P_L + P_b + Q < 3S_m$

（参考資料）　ASME B&PV SecⅧ　Div.2 Appendix 4-130 より

4-131　　APPENDIX 4

応力分類	一次応力			二次応力	ピーク応力
	一般膜応力	局部膜応力	曲げ応力	膜応力＋曲げ応力	
代表的事例を表4-120.1に示す。	内部断面を横切る平均一次応力。構造不連続及び応力集中を除く。機械的荷重によって生じるものだけをとる。	内部断面を横切る平均応力。構造不連続は考慮するが応力集中は除く。機械的荷重によって生じるものだけをとる。	内部断面中心からの距離に比例する一次応力の成分。構造不連続及び応力集中を除く。機械的荷重によって生じるものだけをとる。	構造の連続性を満足するのに必要な自己平衡応力で構造不連続部に生じる。機械的荷重及び熱膨張により生じるものをとり、局部的応力集中を除く。	(1) 応力集中によって一次又は二次応力に付加される増加分（切欠きの場合） (2) 疲労のおそれはあるが容器の歪みを生じるおそれのない熱応力。
記号 4)	P_m	P_L	P_b	Q 2)	F 2)

応力成分の組合せ及び応力強さの許容限界

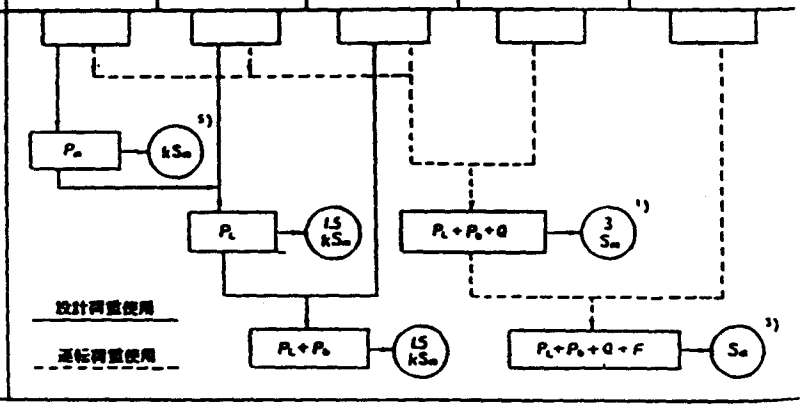

注　1) この制限は、応力強さの全変動範囲に適用する。$3S_m$ の値は、運転サイクル中の最高及び最低温度に対する S_m の平均値の３倍を示す。最大一次プラス二次応力強さ範囲を決める場合、個別サイクルよりも大きくなる重ね合わせサイクルを考慮する必要があろう。温度の低値は、各条件について異なる場合があるので、S_m の値は特定のサイクル又はサイクルの組合せによって変わる。したがって、各サイクル及びサイクルの組合せに対して、４－136.4で許容されているものを除いては、$3S_m$ の値を超えないことを確かめるよう留意すること。

2) 分類Qの応力は、温度こう配や構造不連続などによる応力の合計から同じ位置の一次応力を除いたものである。しかし、詳細解析による応力はしばしば（一次応力＋二次応力）を直接に示すことがあり、その場合は、Qだけではなく P_m（又は P_L）＋P_b＋Q の合計応力を表す。同様に分類Fの応力が応力集中によるものの場合には、Fはノッチによる公称応力以上の付加応力である。例えば、板が公称応力強さSと応力集中係数Kの切欠きを有するものである場合には、$P_m = S$、$P_b = 0$、$Q = 0$、$F = P_m(K-1)$ となり、ピーク応力強さは $P_m + P_m(K-1) = KP_m$ となる。

3) S_a は疲労曲線図５－110.1、110.2及び110.3から求められる。したがって、全変動範囲に対する許容限度界は $2S_a$ である。

4) 記号 P_m、P_L、P_b、Q及びFは単一応力値を表すのではなく、それぞれ六つの応力成分 σ_t、σ_l、σ_r、τ_{tl}、τ_{lr} 及び τ_{rt} の組合せからなる応力値を表す。

5) 係数kは表ＡＤ－150.1による。

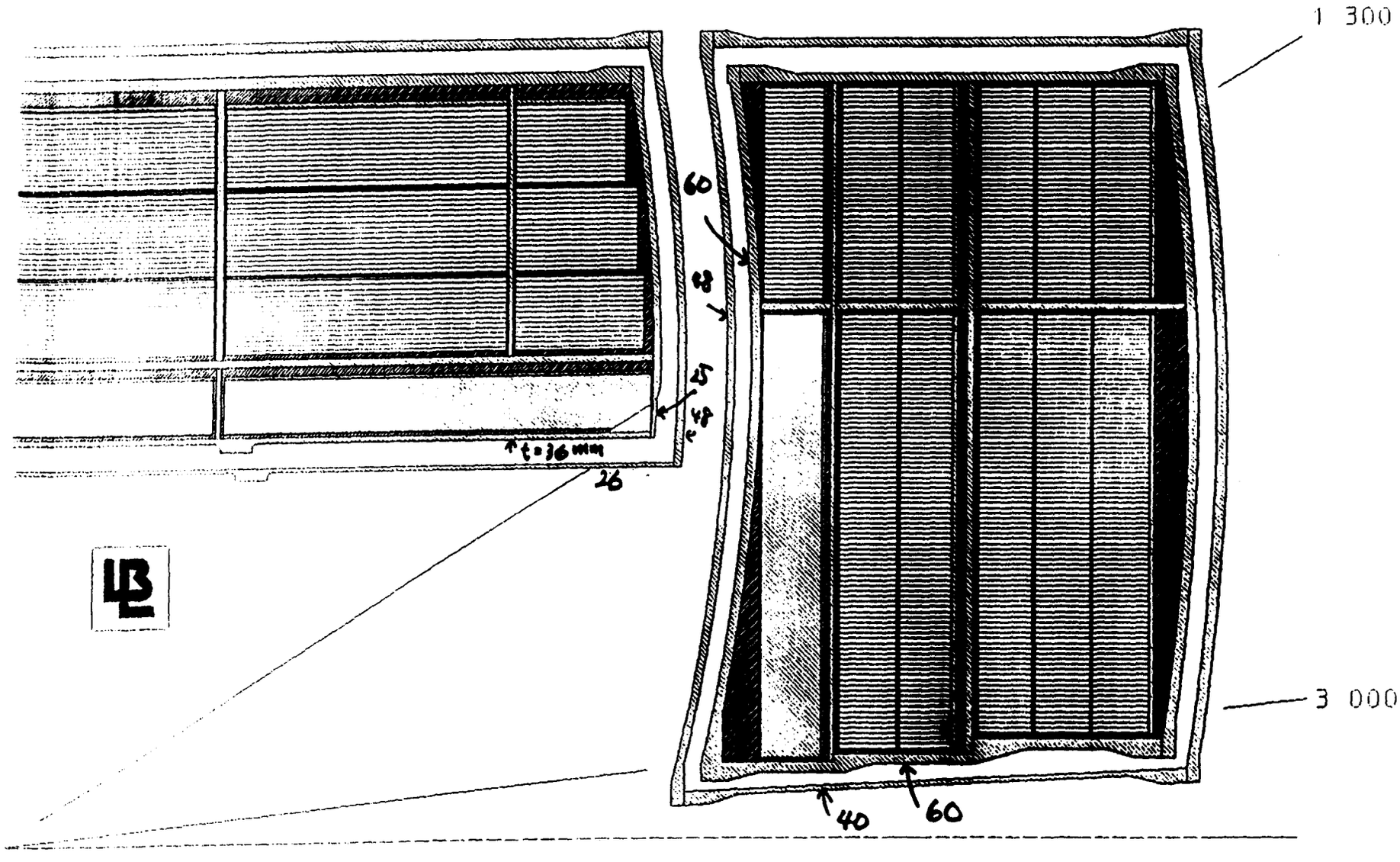

LAC NOV '90

DATE: 7-23-91

Cryostat Design

Curved heads and radial stays

The material budget for magnet coil, cryostat walls

The region of overlap between barrel and endcap - $\eta = 1.2$

Massless gaps and correction for dead material

$$E_{sum} = E_{LAr} + \alpha_{mg} E_{mg}$$

where we use use EGS to evaluate

$$\alpha_{mg} = \frac{E_{inc} \times s - E_{LAr}}{E_{mg}}$$

(s is the LAr sampling fraction)

The region of overlap between endcap and forward - $\eta = 3$

The design in Nov. 1990

No optimization near $\eta = 3$

3 cm thick walls traversed by particles at $\eta = 3$ appear to be 30 cm deep

The present design

	LBL	KEK
head shape	double conical	existing LAr heads
stays	EM penetrating cylinder	EM penetrating ro
inner cylinder	*thin*, no axial load	*thin*, has axial load
inner vacuum	cylinder close to beam pipe	study front head sh

FIGURE 4.12

lar_wmrsly3 (Rich Weidenbach)
color (David P. O'Neill)
7-24-91

ideal forward calorimete

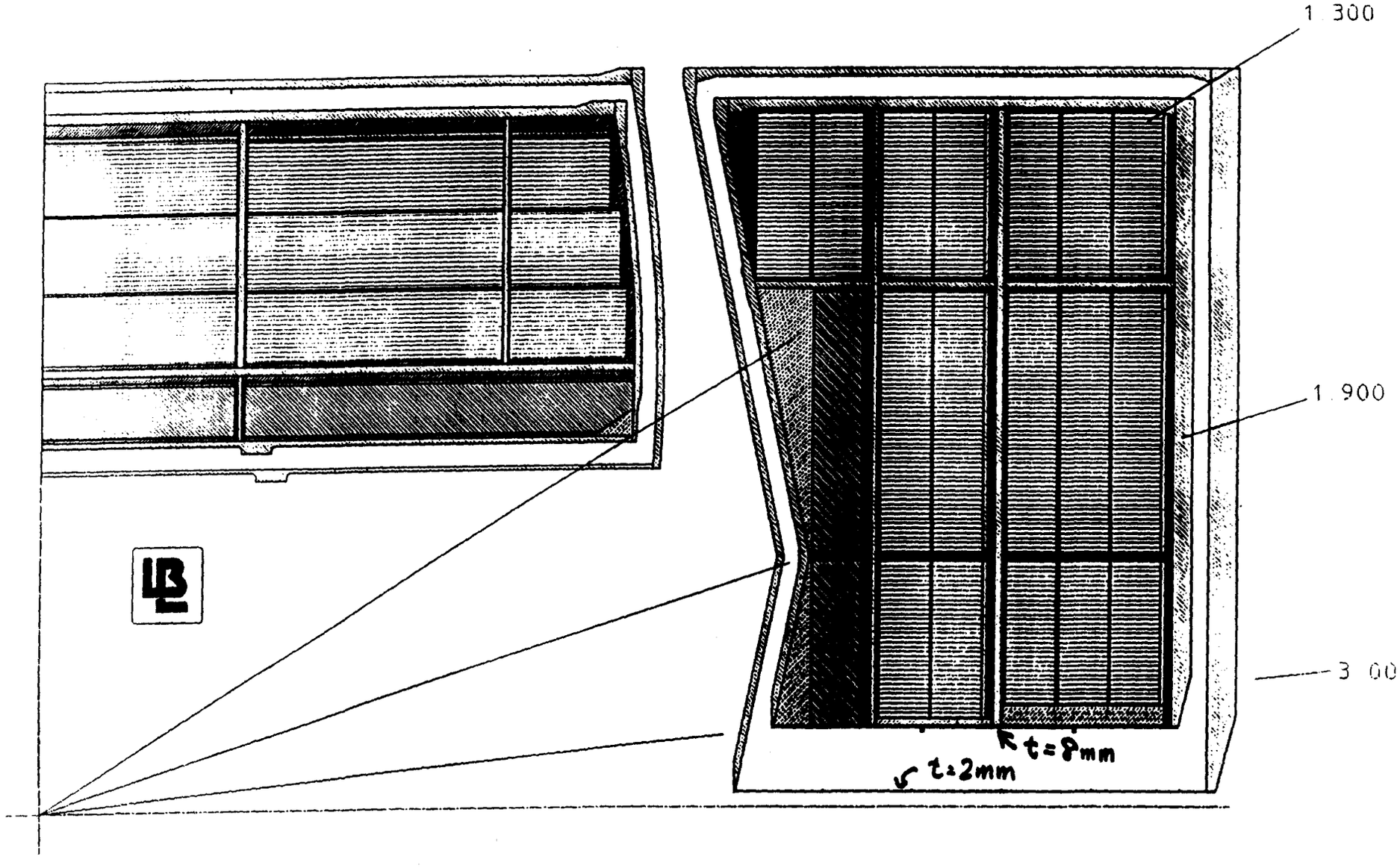

NEW LBL ENDCAP CONCEPT

DATE: 8-2-91

'HI ENDCAP VESSEL STUDIES

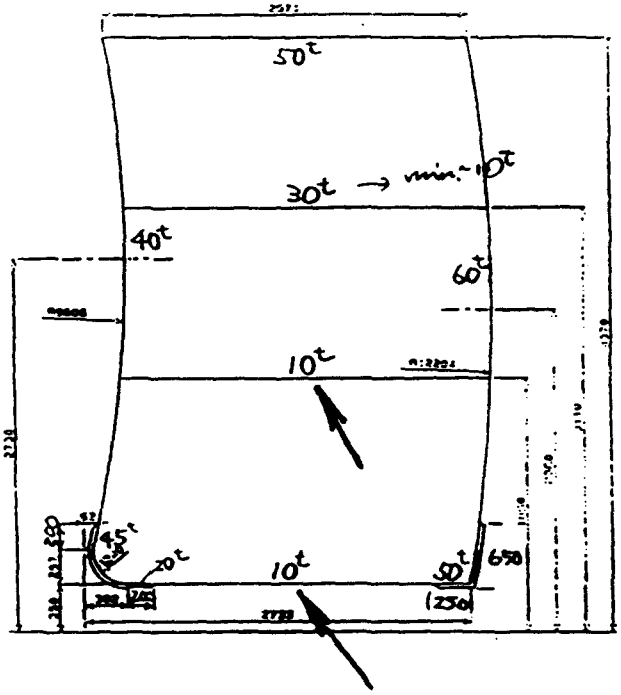

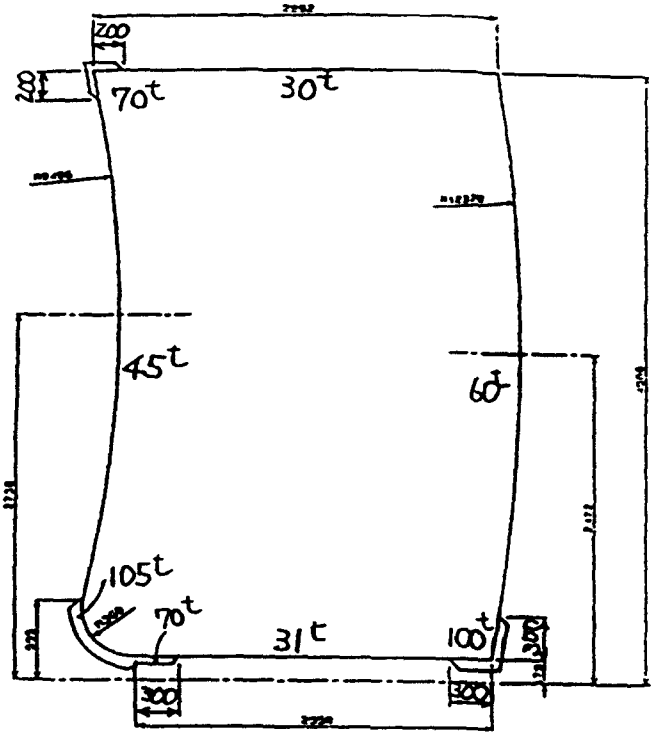

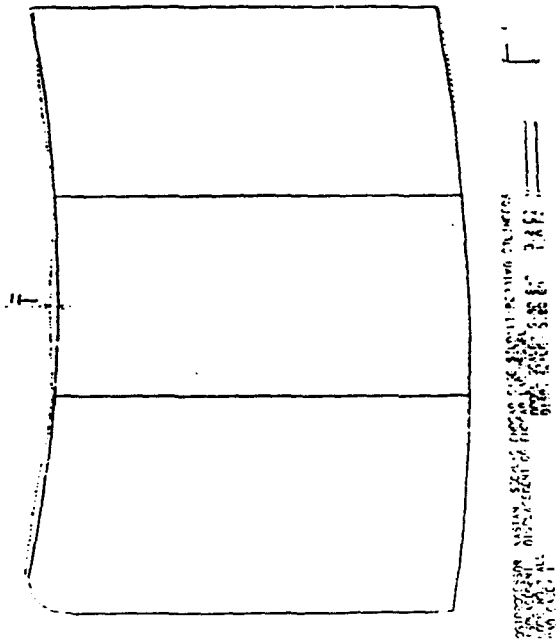

Type 3b

LAr

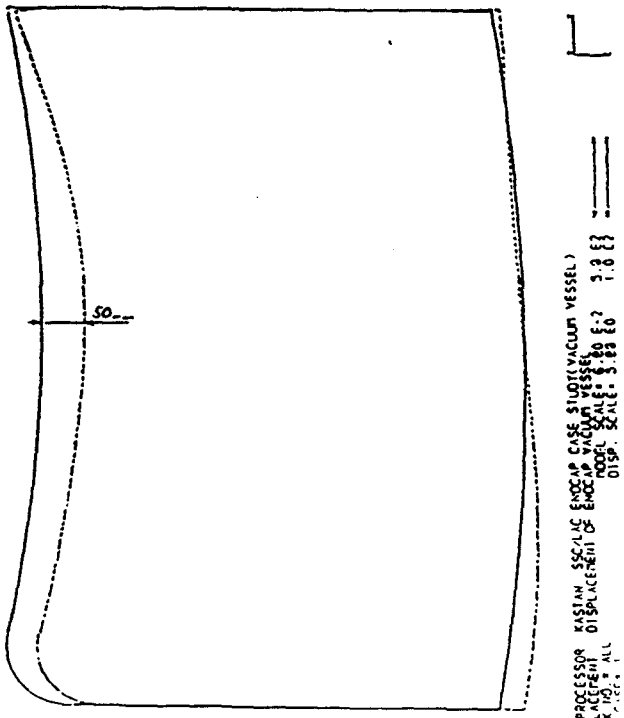

Type 2

VACUUM

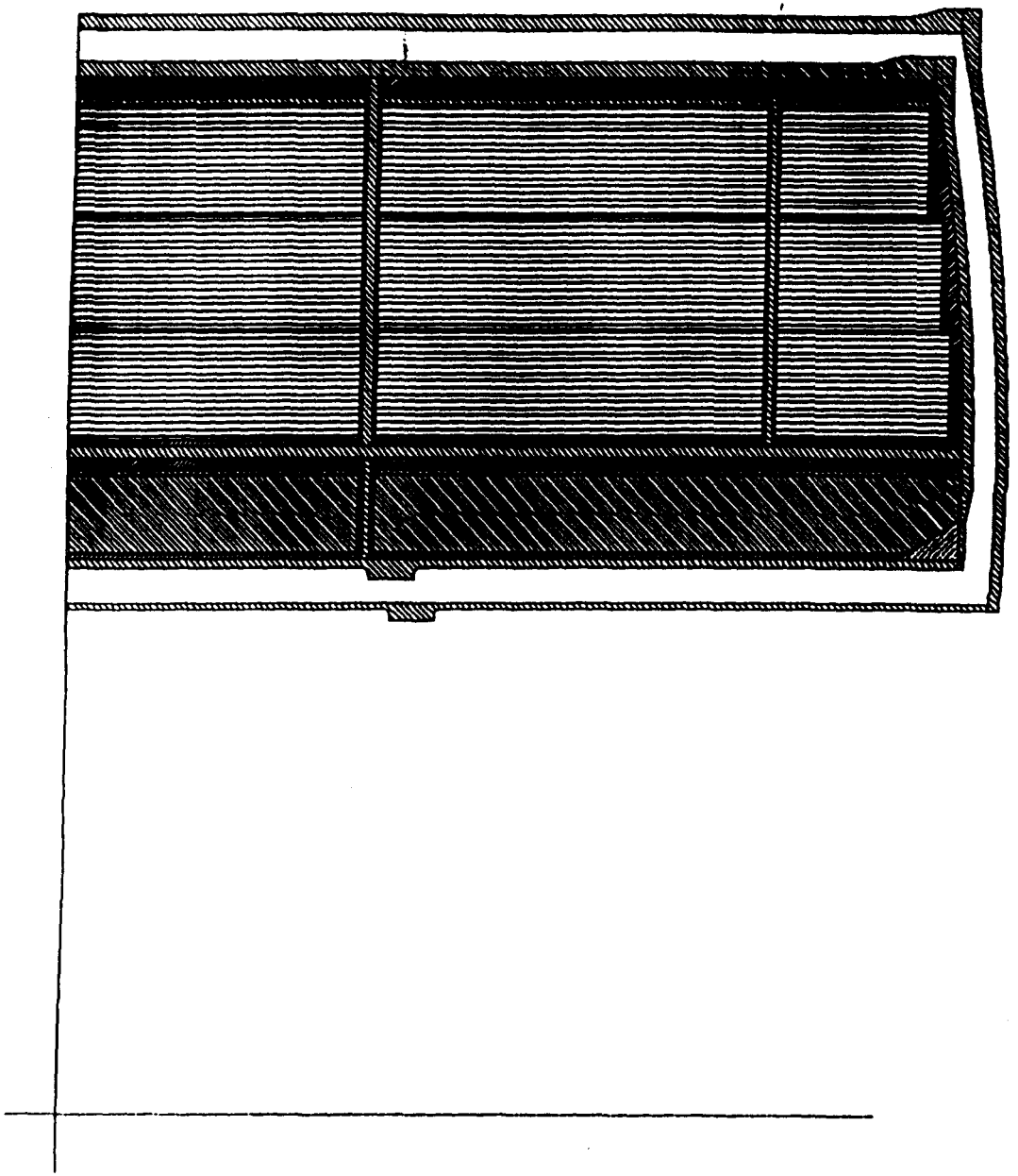

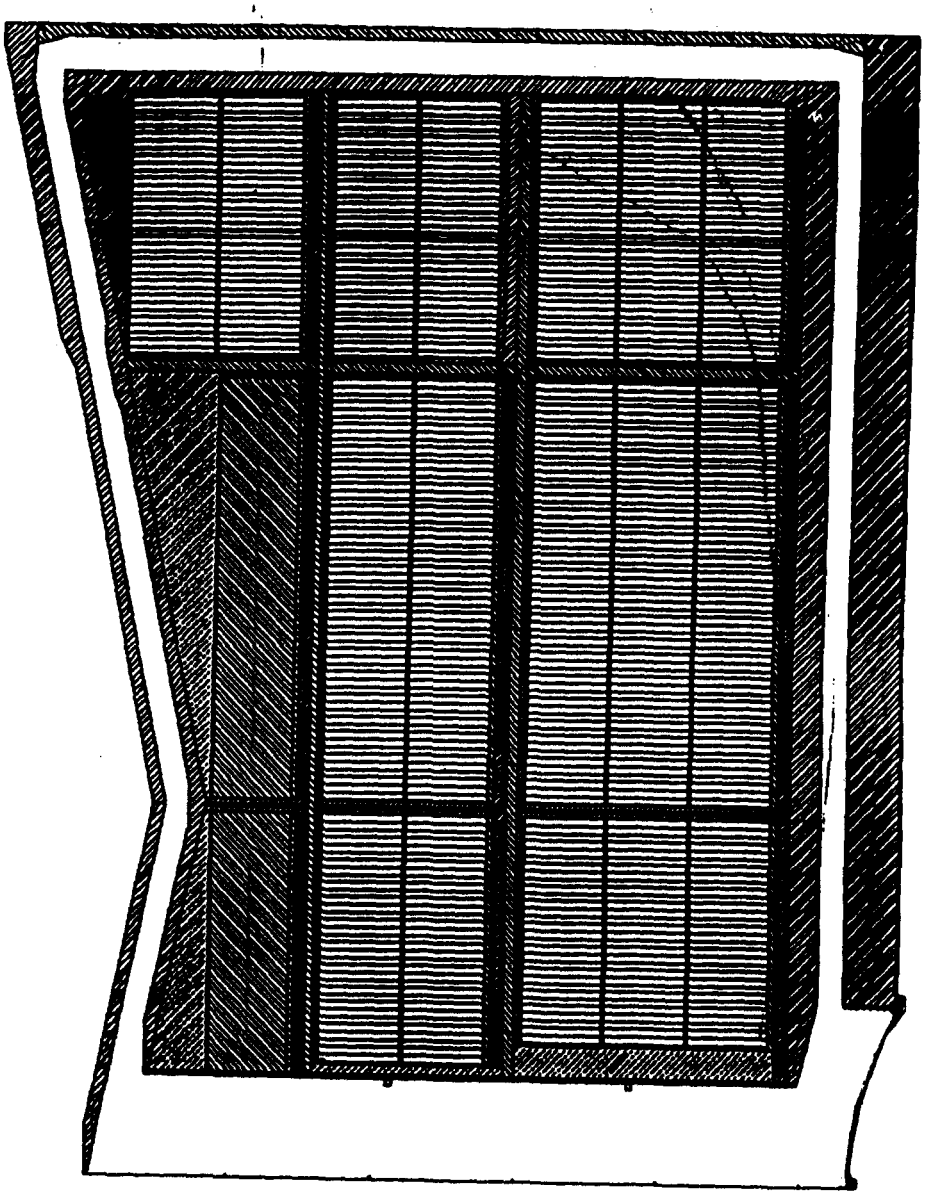

DATE: 8-27-91

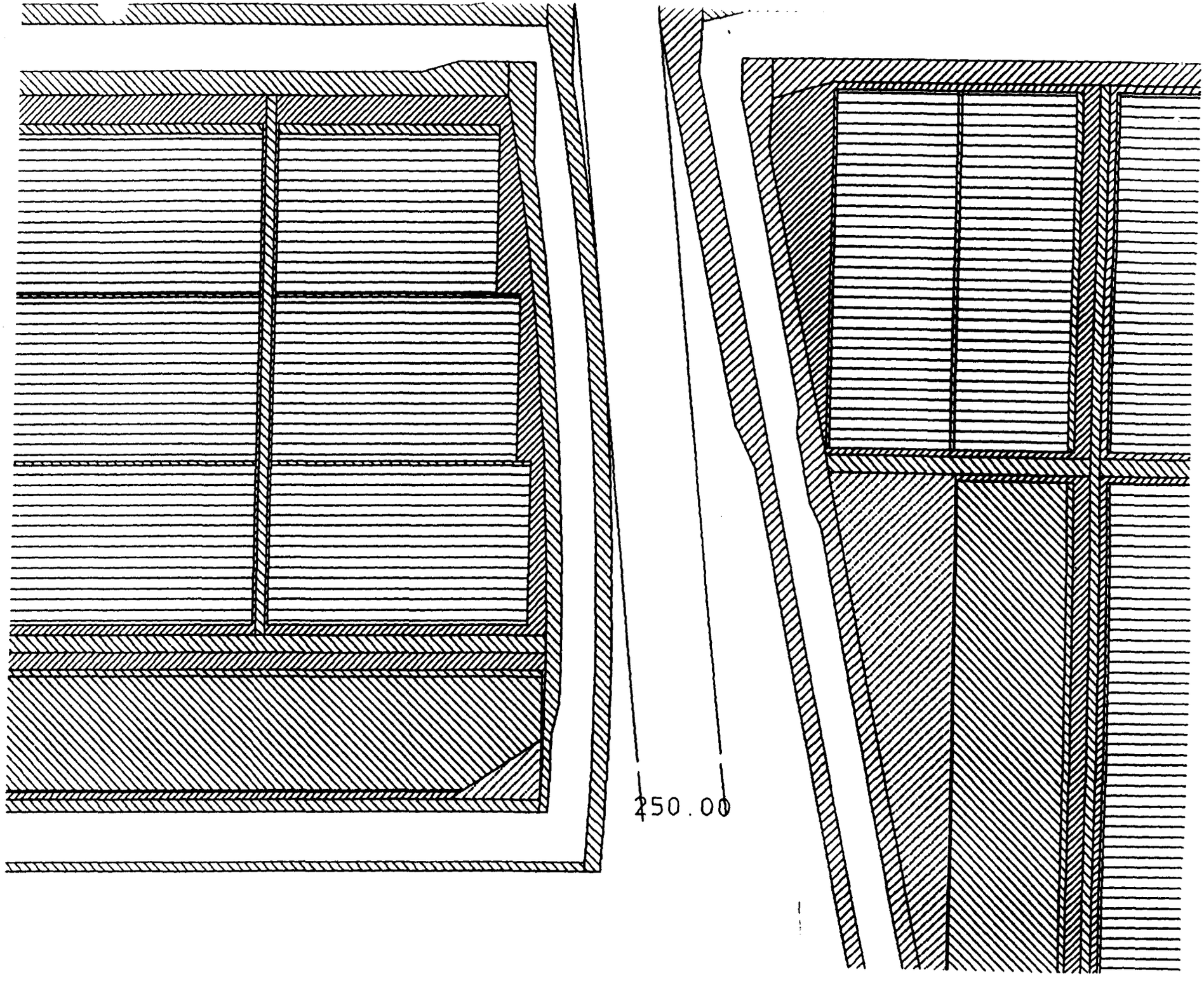
250.00

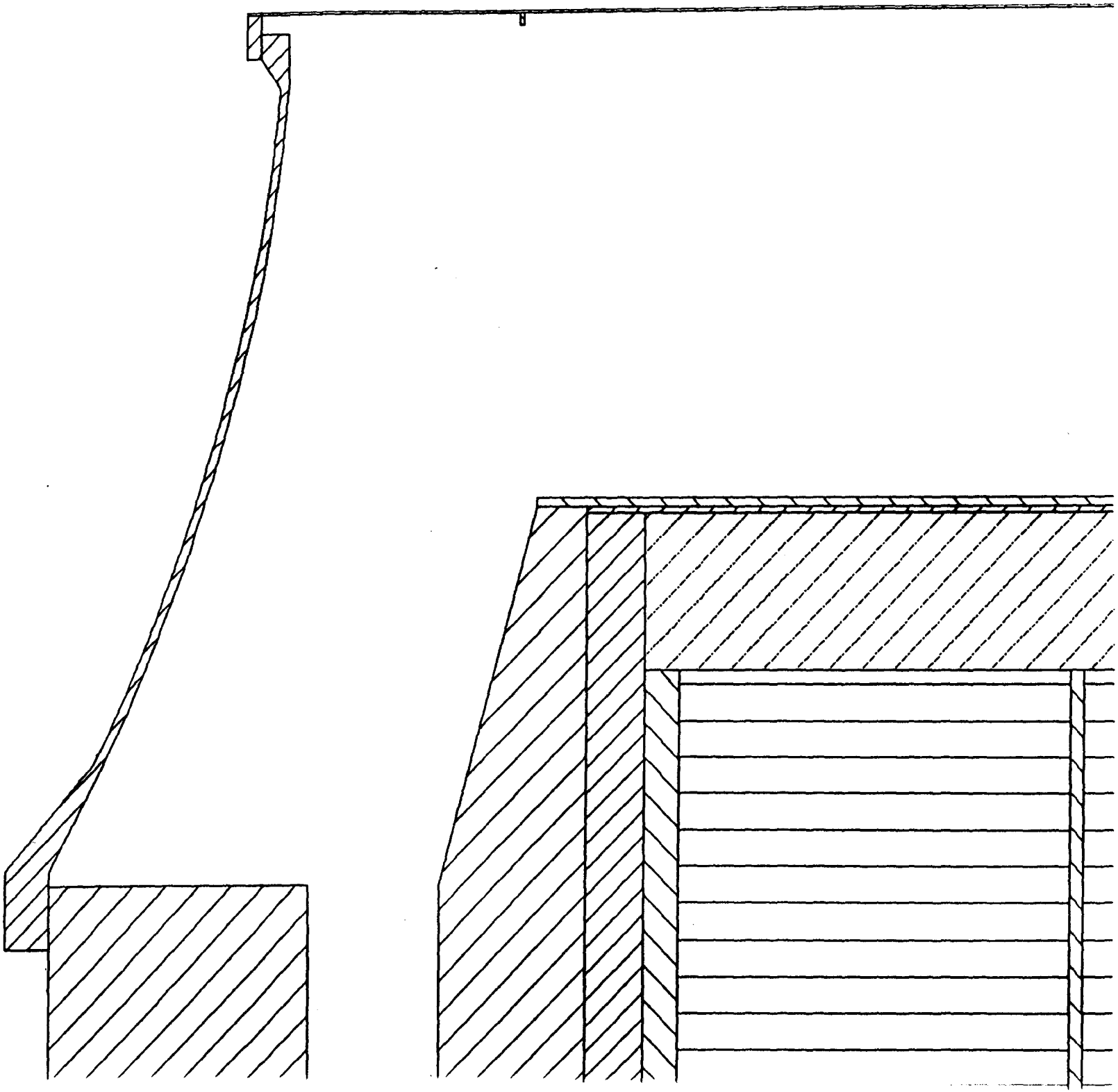

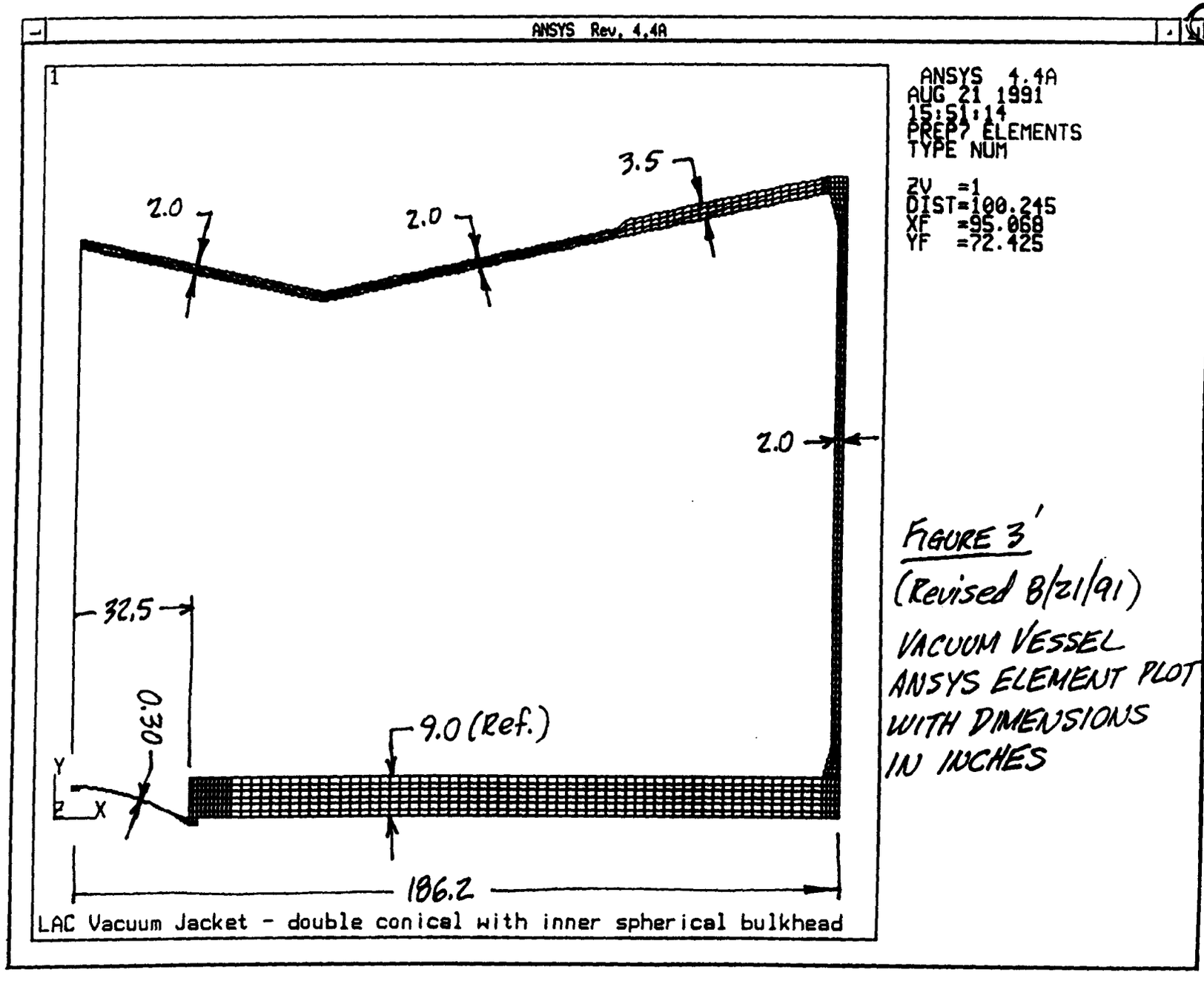

FIGURE 3'
(Revised 8/21/91)
VACUUM VESSEL
ANSYS ELEMENT PLOT
WITH DIMENSIONS
IN INCHES

G.A.

9/10/91

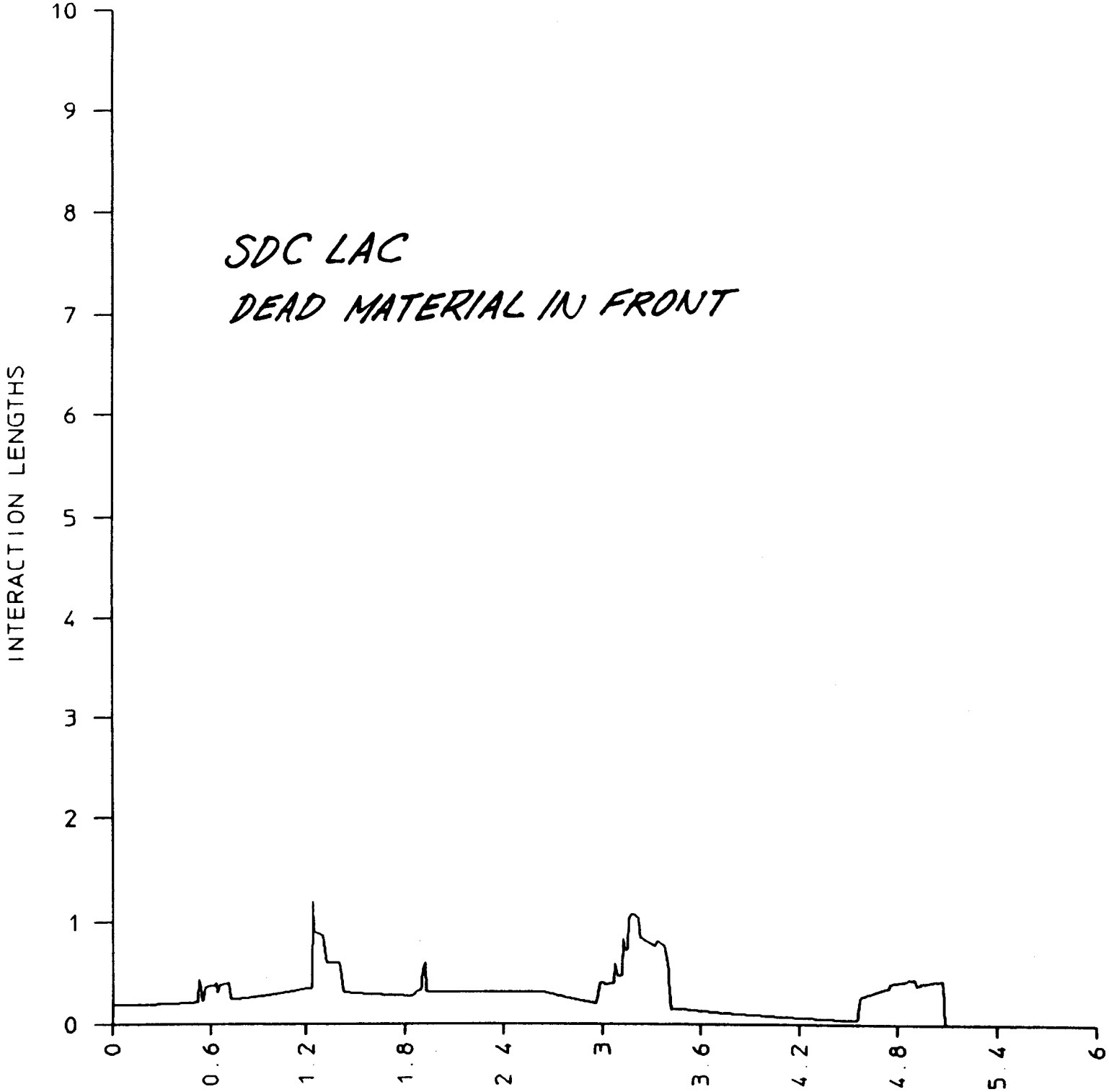
SDC LAC
DEAD MATERIAL IN FRONT
INTERACTION LENGTHS
0
1
2
3
4
5
6
7
8
9
10
0
0.6
1.2
1.8
2.4
3
3.6
4.2
4.8
5.4
6

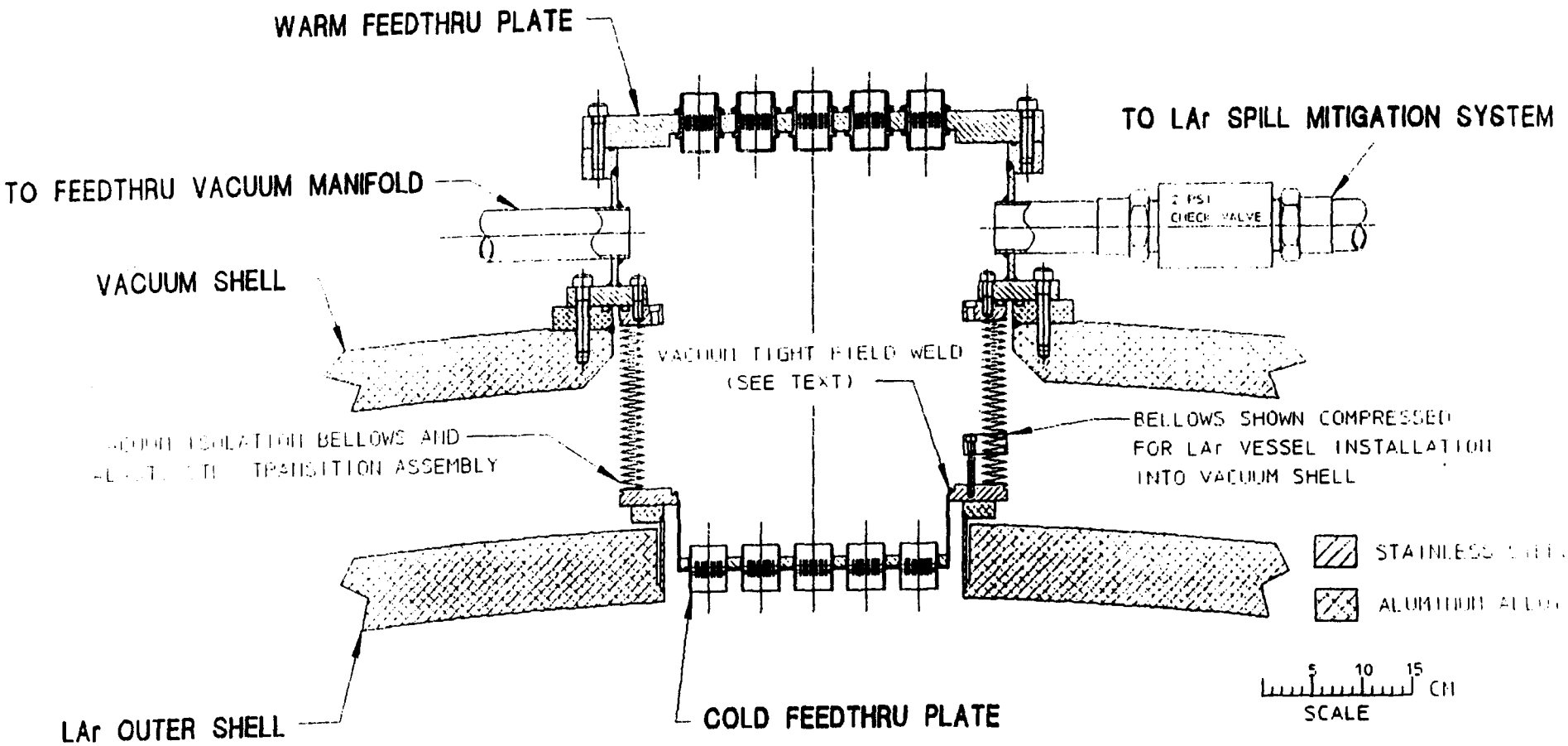

FIGURE 1. Cross-sectional details of the non-gas cooled signal cable Feedthru option. The SCFT utilities high pin density hermetic connectors, stainless steel bellows, and cryogenic fittings all of commercial design.

DATE JULY 16, 1991

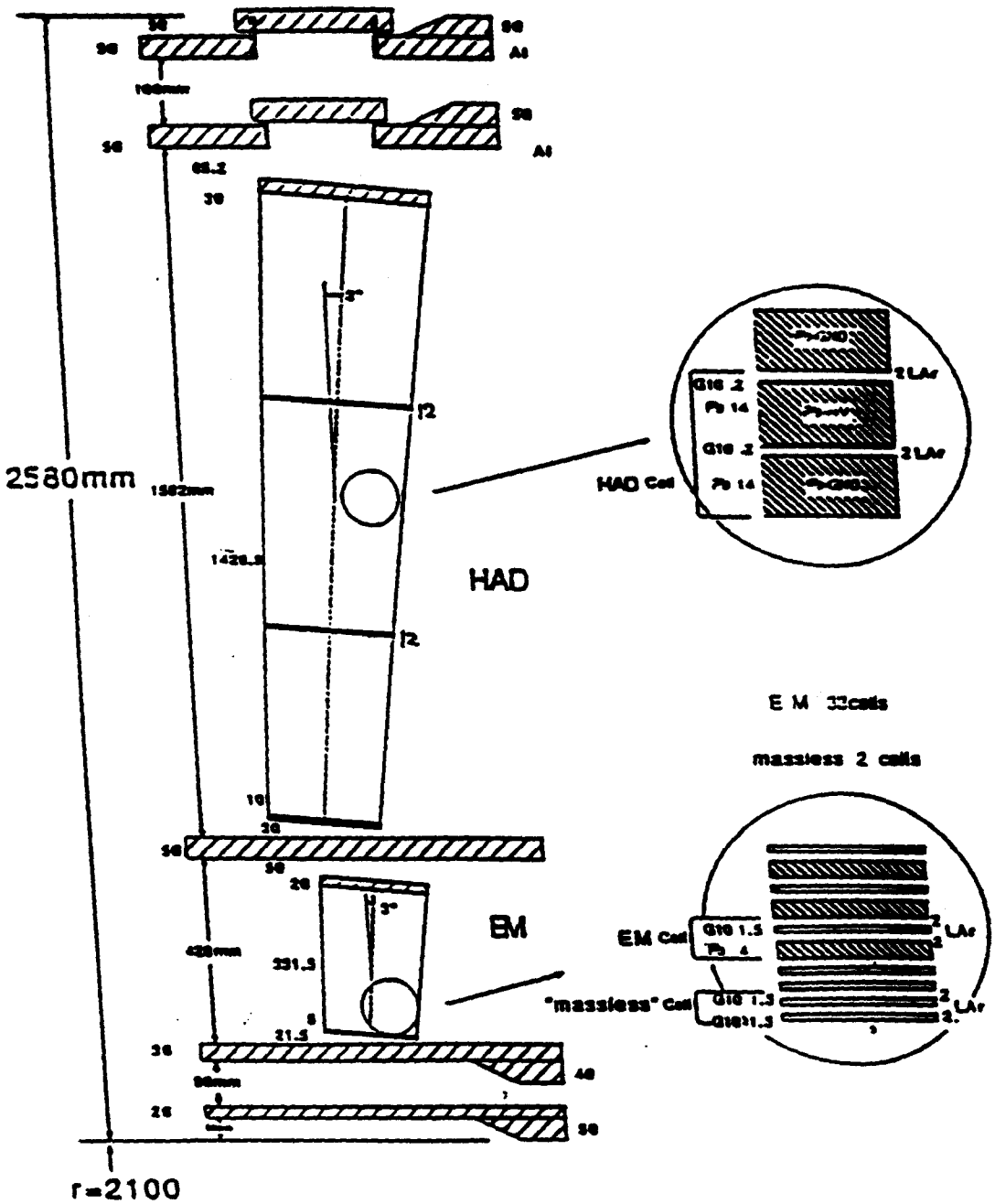

Fig 5.1 Radial dimensions and cell structures of the Barrel

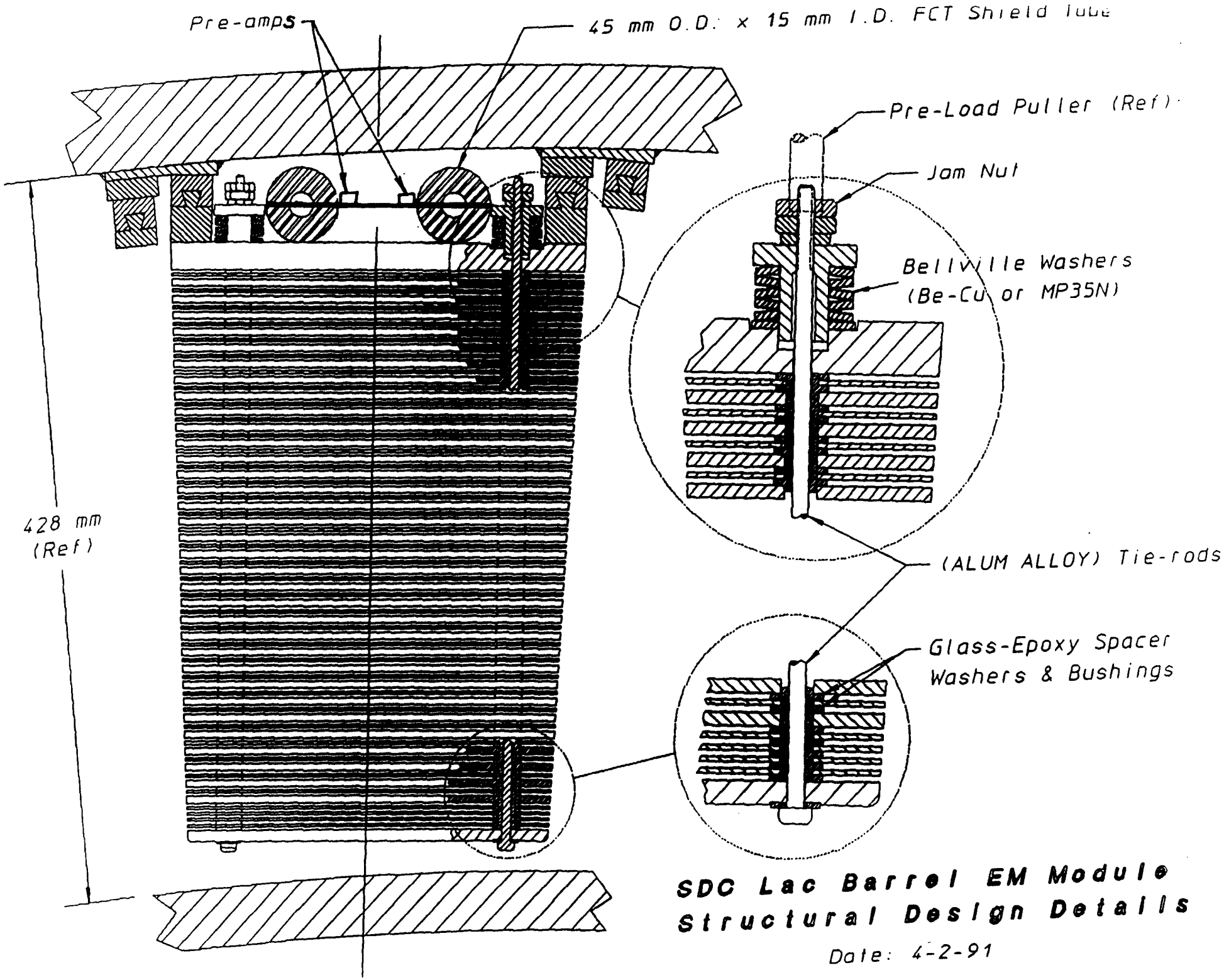

SDC Lac Barrel EM Module
Structural Design Details

Date: 4-2-91

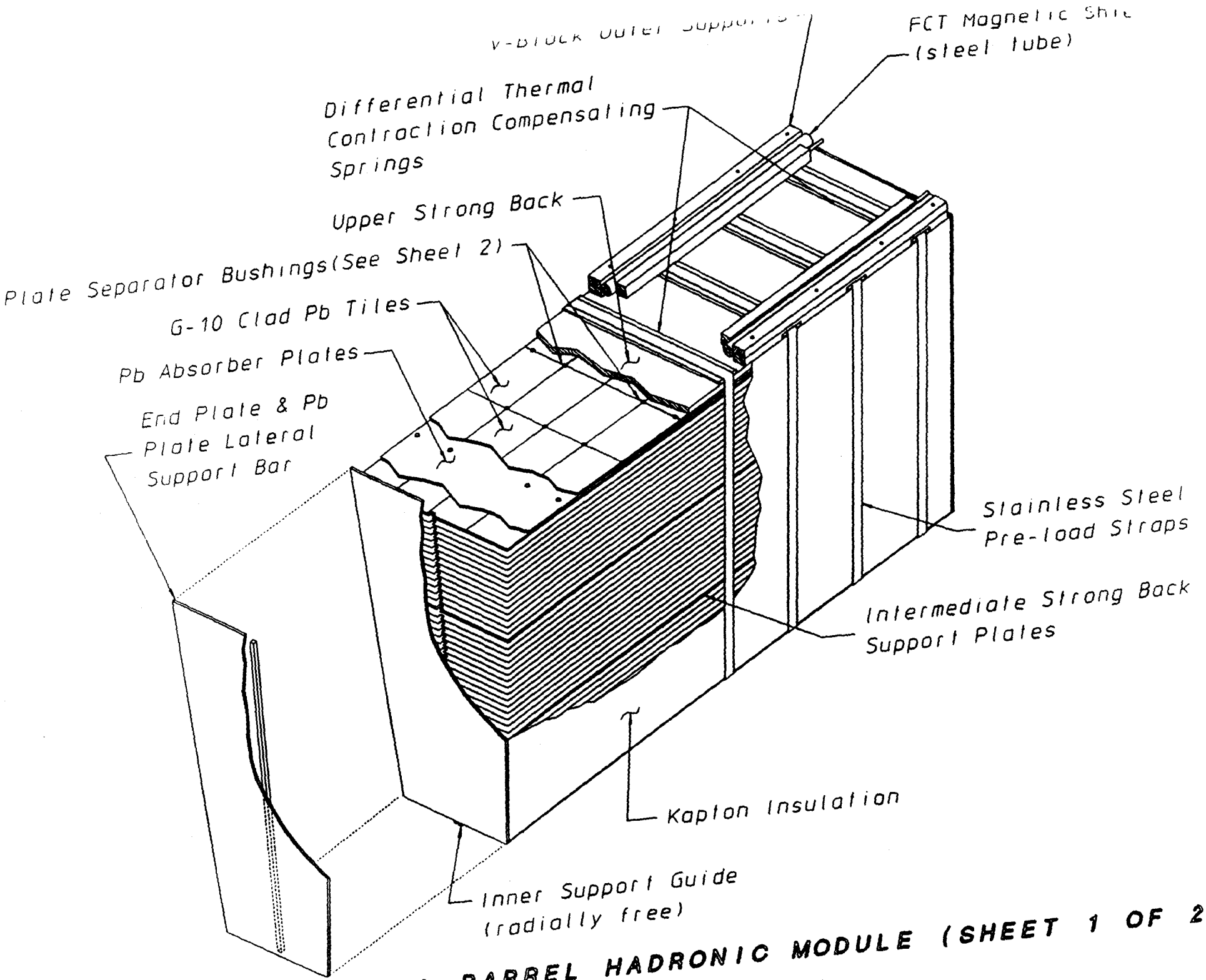

TYPICAL BARREL HADRONIC MODULE (SHEET 1 OF 2)

JUNE 28. 1991

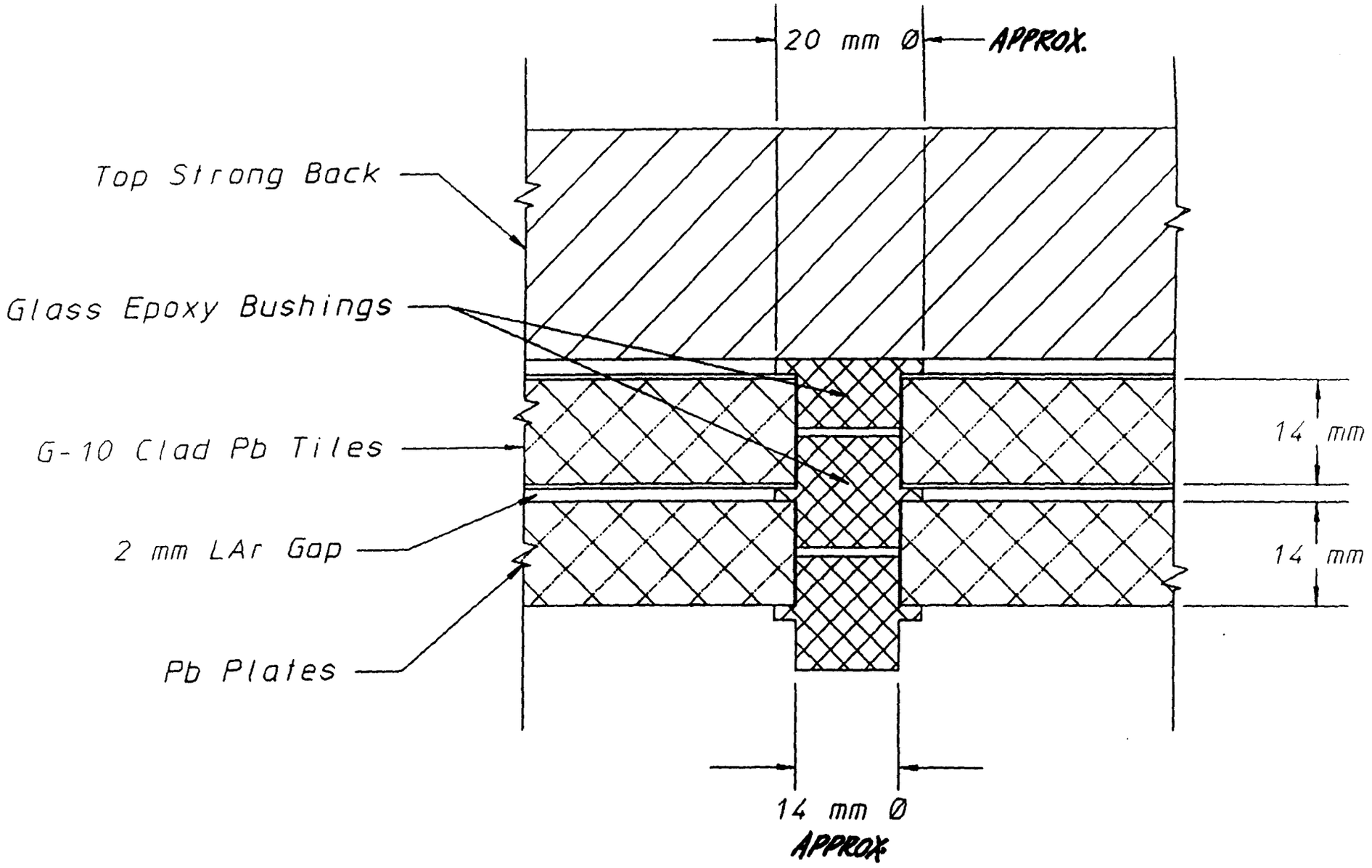

BARREL HAD MODULE (SHEET 2 OF 2)

(Typical Plate Separator Bushing Detail)

JUNE 28, 1991

"BIG WHEEL" ENDCAP MODULES

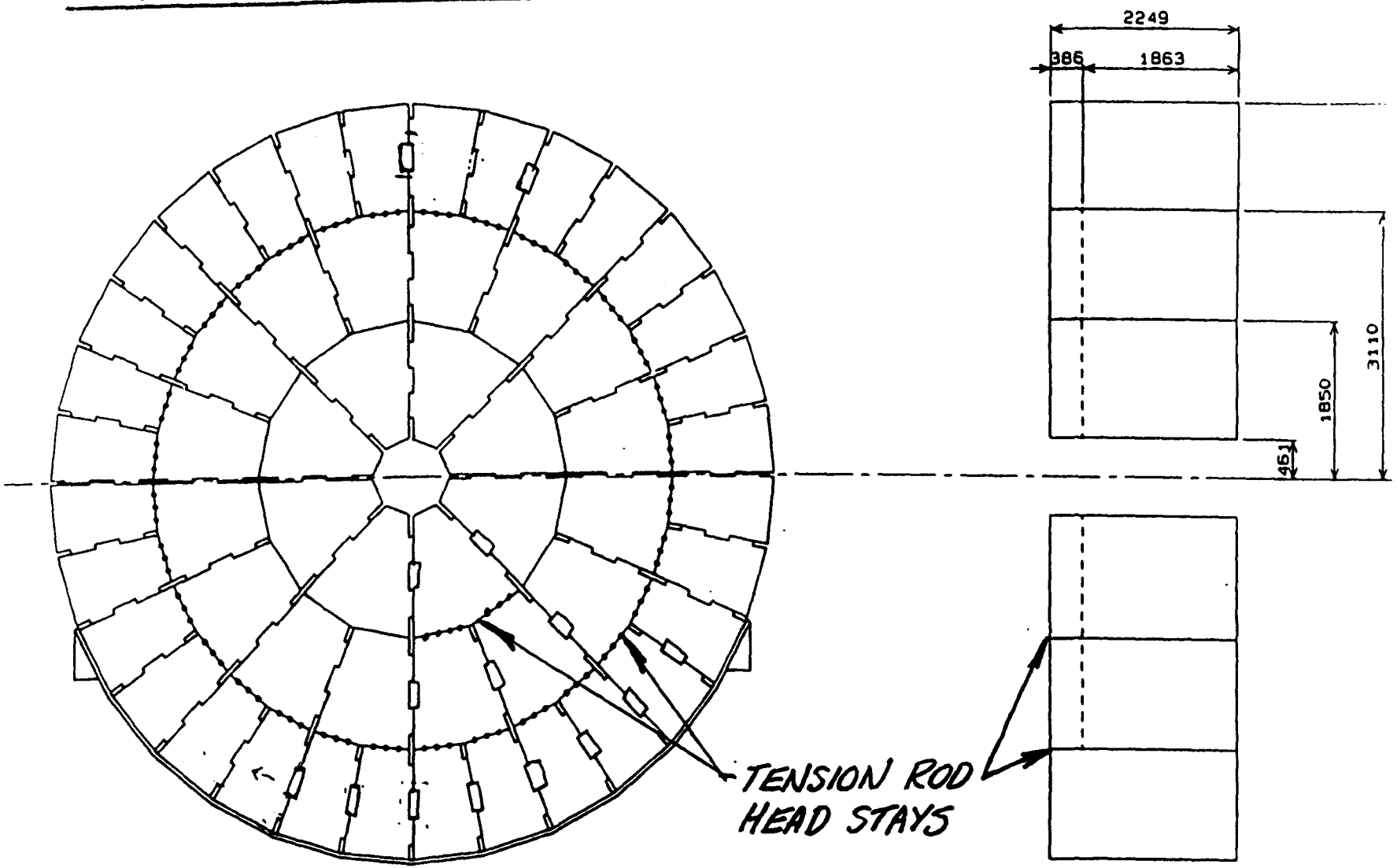

自立式モジュール

A部詳細

"BIG WHEEL" DETAILS

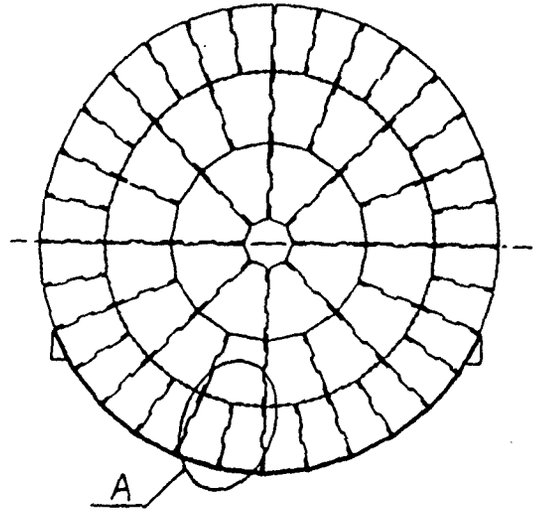

自立式モジュール

A部詳細

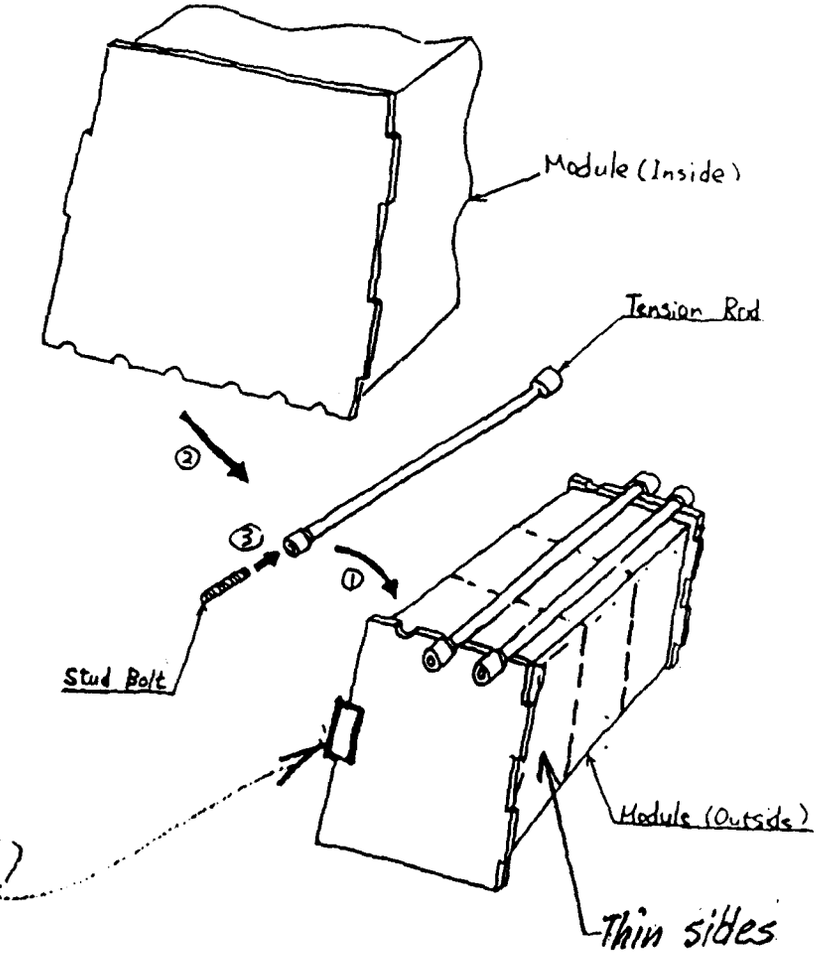

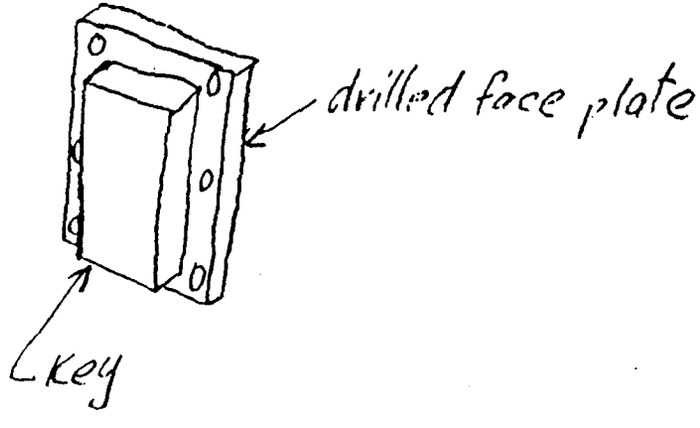

自立式モジュール組立手順

① Tension Rod と Module を溝に設置

② Module 組立

③ Stud Bolt ねじ込み

自立式モジュール組立手順

Section 7 Electronics

Section 7.1 Front End Electronics

The general schematic for the front end electronics of the liquid argon calorimeter is shown in Figure 7.1.1. The electrode gaps, represented by the capacitor Cd, are connected to the preamp boards by low impedance striplines. The preamp boards are located in the LAr at the outer radius of each module. They are multilayer printed circuit boards that hold damping resistors, shielded ferrite core transformers, protection diodes, calibration circuitry, and the preampifiers themselves. Layouts for the barrel EM and hadronic preamps boards are illustrated in Figures 7.1.2 and 7.1.3. The calibration electronics described in 7.6, while the remainder of the elements in Figure 7.1.1 are discussed below. Following the preamplifier is a shaping amplifier (section 7.3), summing and trigger electronics and the data acquistion system (section 7.5).

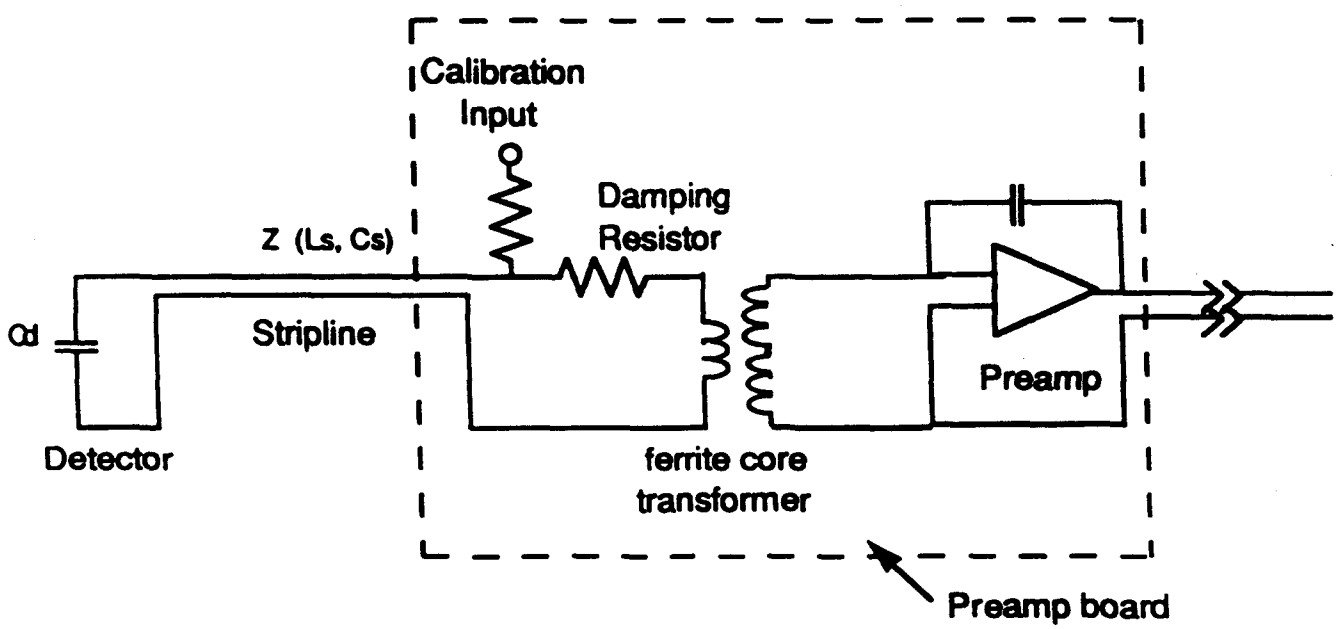

Figure 7.1.1 Schematic of the front end electronics. Channels without transformers have protection diodes at the preamp input.

Electrode Structure

a) Double gap Electrode Structure

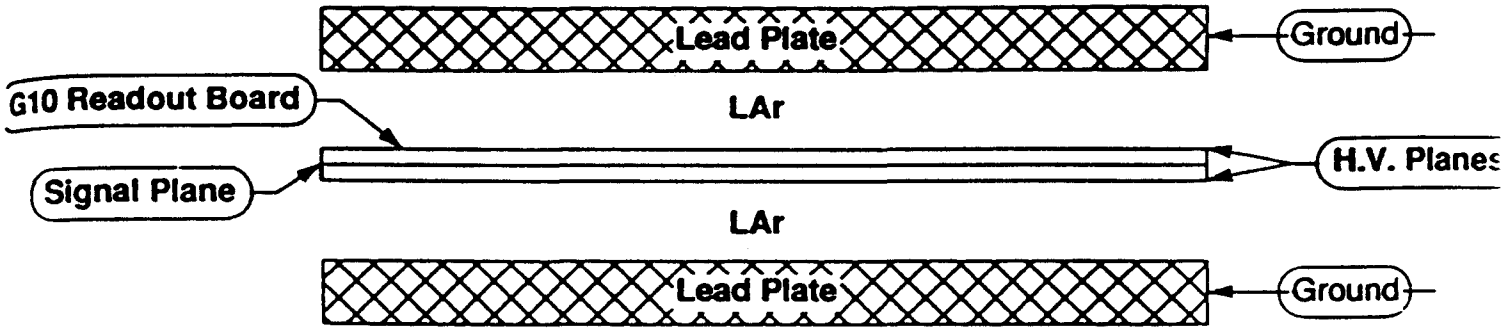

b) Single Gap Electrode Structure

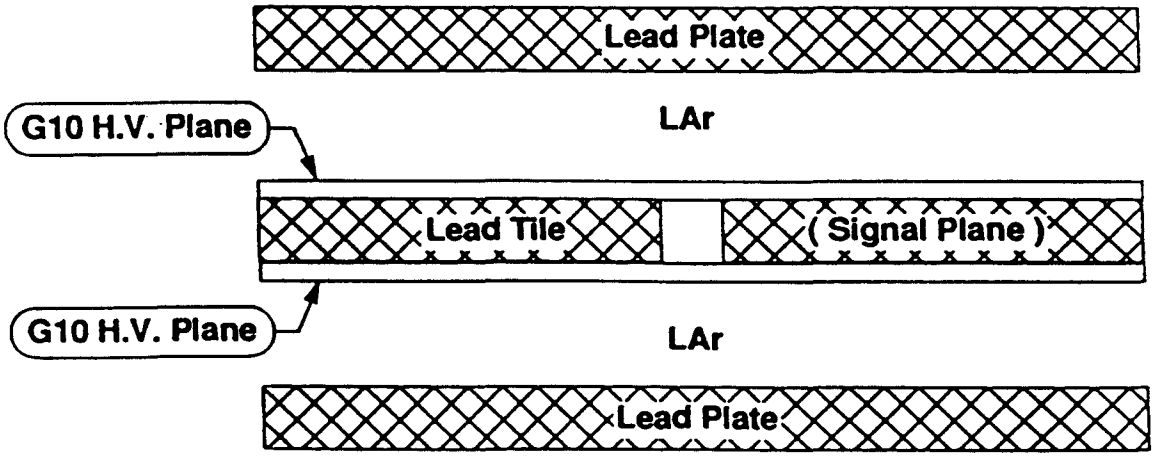

J.B. Hunter ✐ / C. Hearty
Original: 7-24-91
Updated: 7-24-91

E.M. Module Layout - Side View

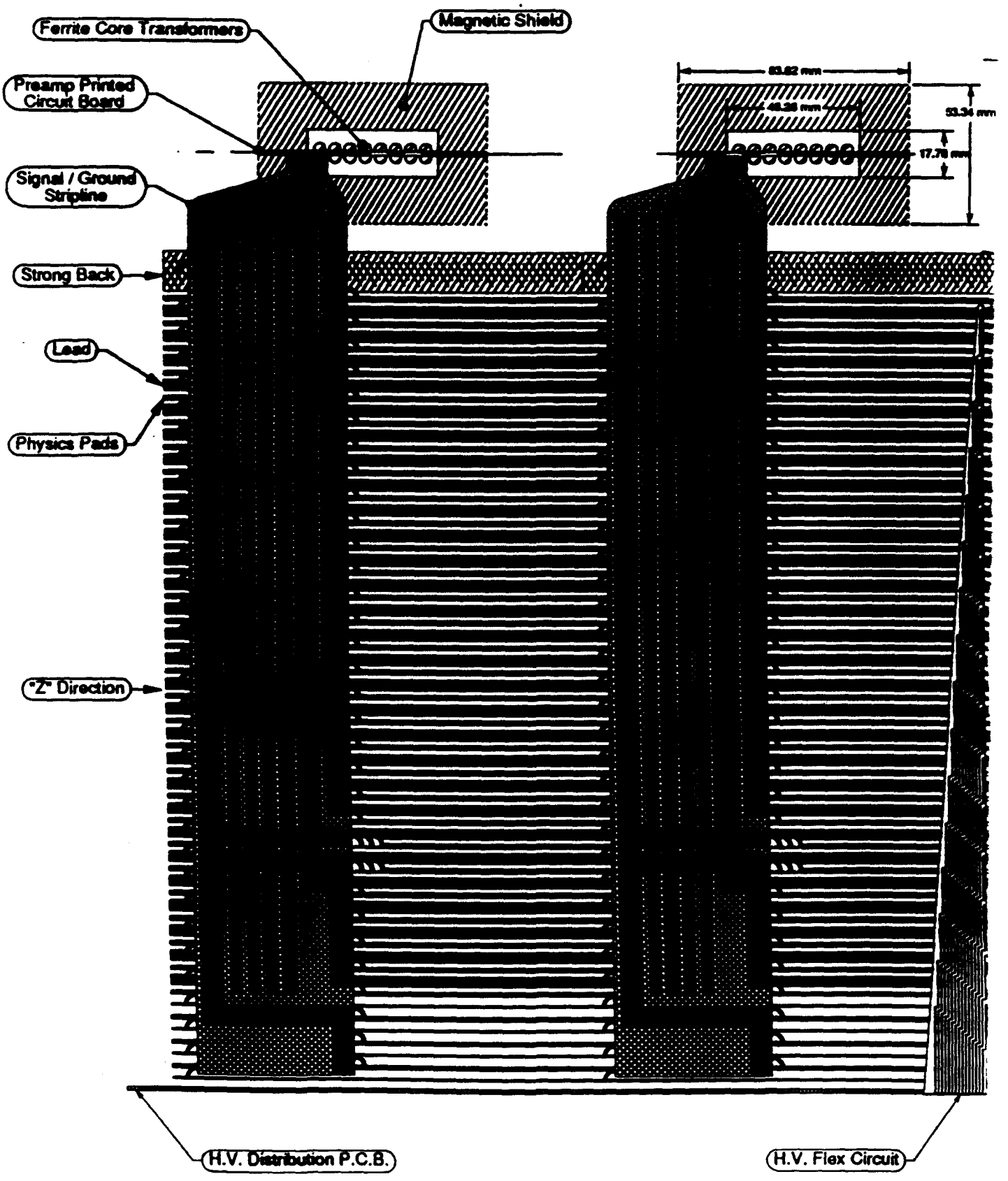

7.2.4

Physics Pad P.C.B.

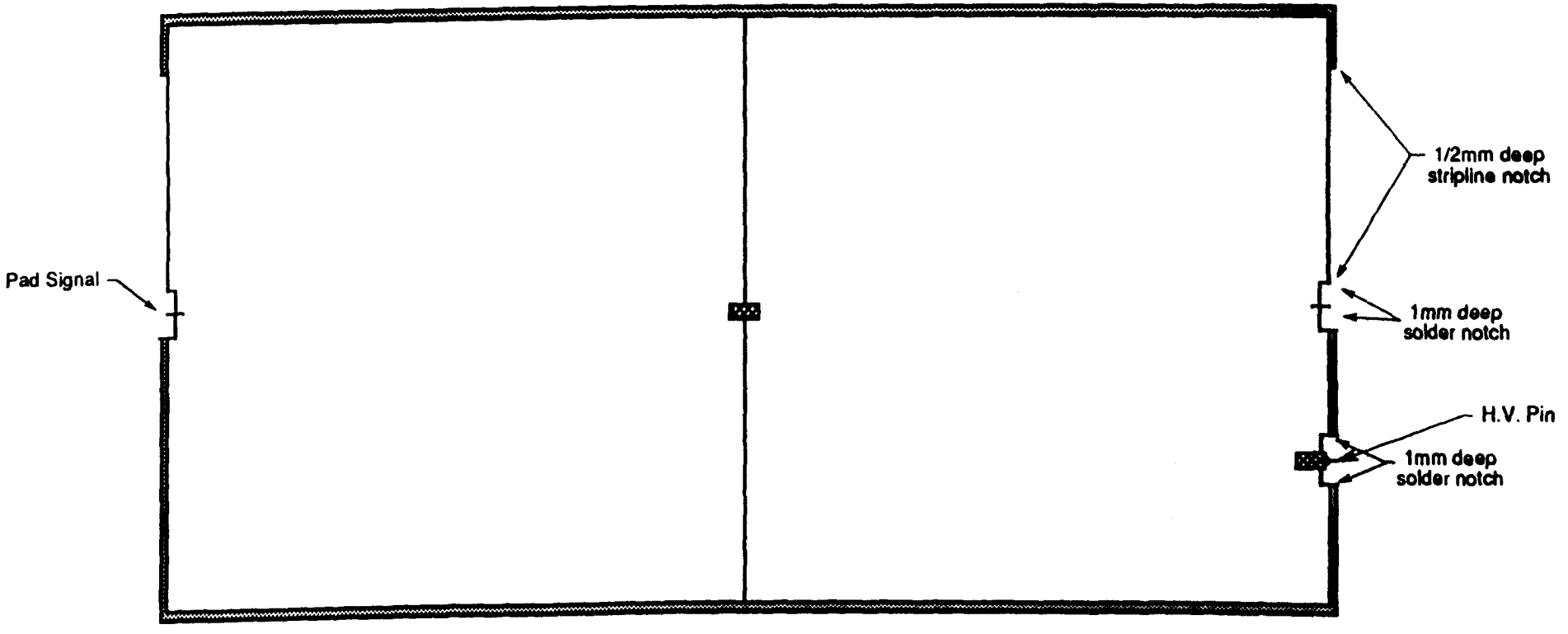

7.2.5a

A.A. Arthur / J.B. Hunter
1-16-91
Updated: 7-24-91

Lead Absorber Plate

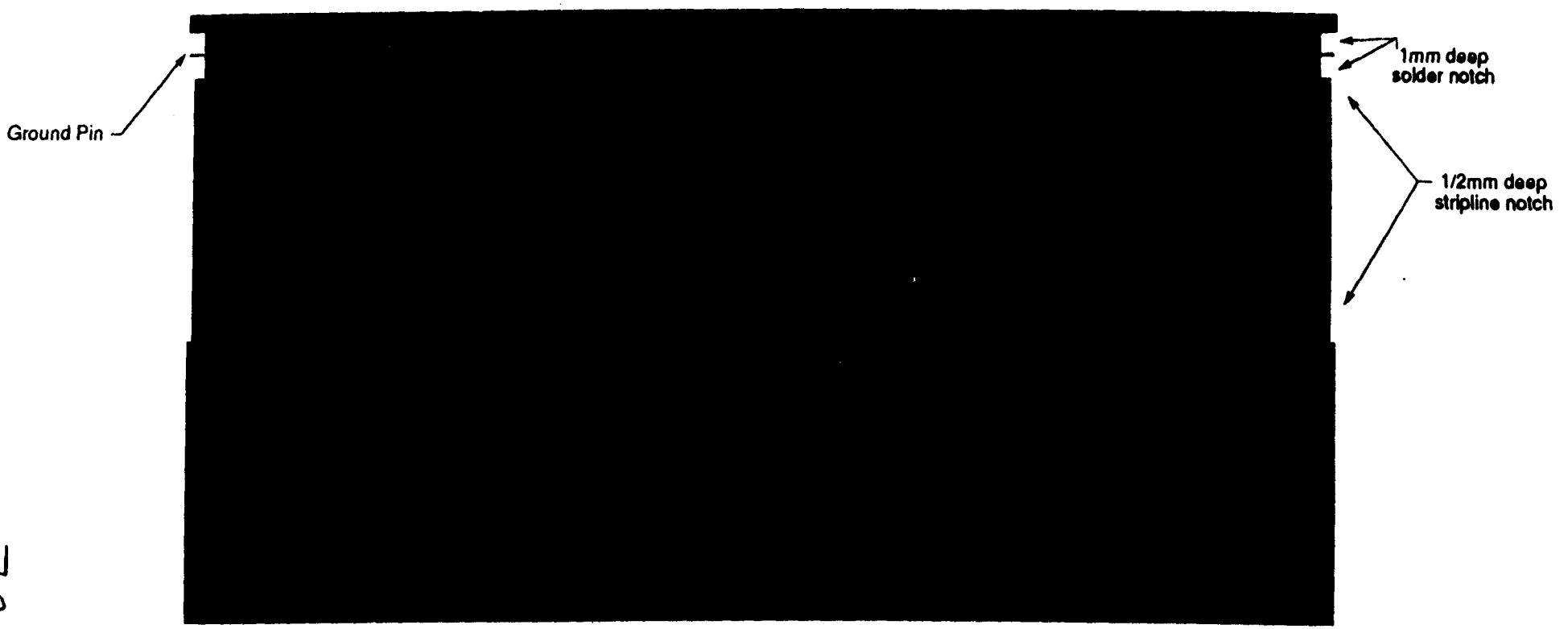

7.2.5b

SDC LAC P.C.B. Board & Electrical Connections

Three Layer P.C.B. Construction

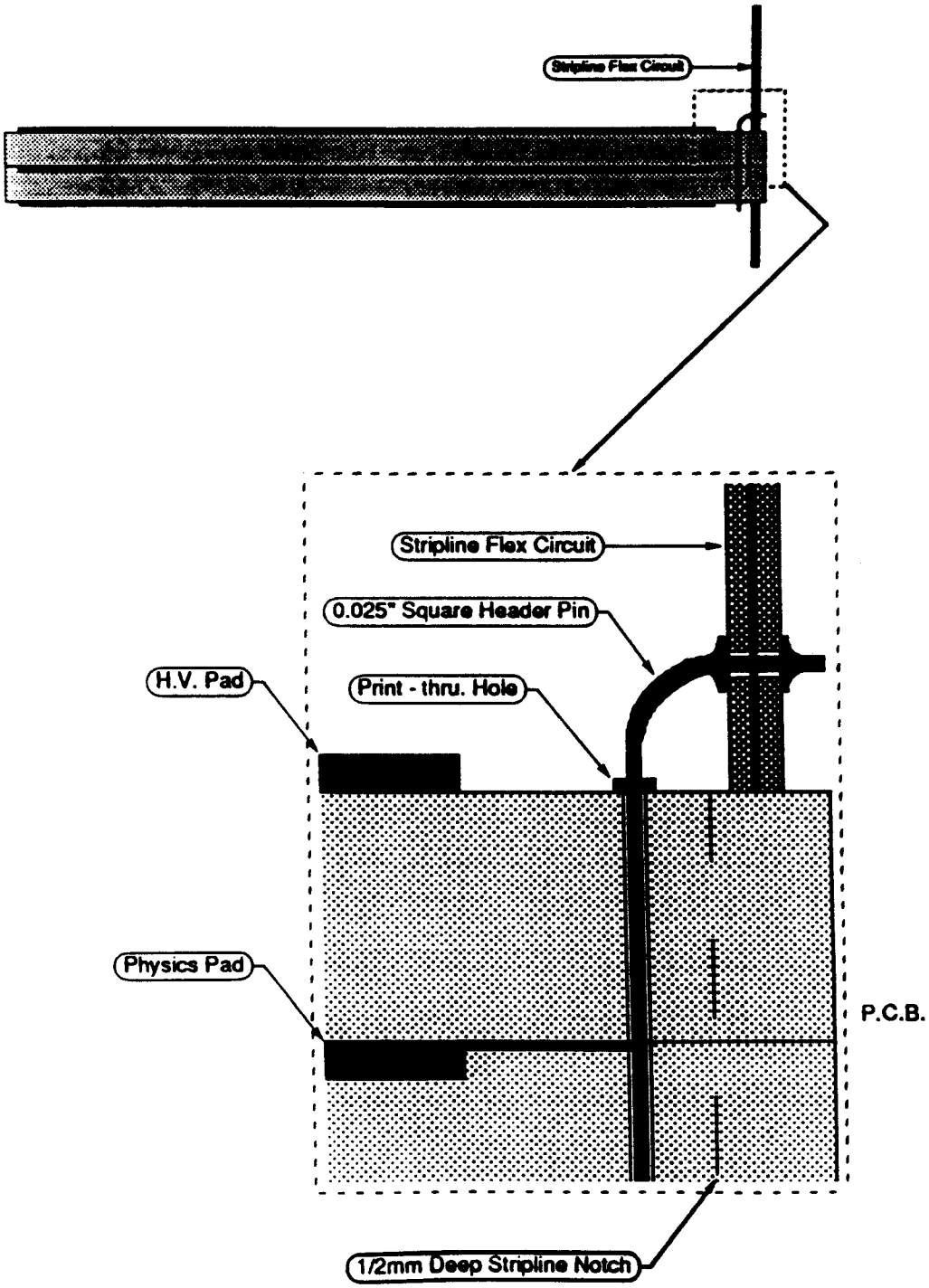

7.2.6

A.A. Arthur / J.B. Hunter
3-5-91
Updated: 3-6-91

EM Module Stripline

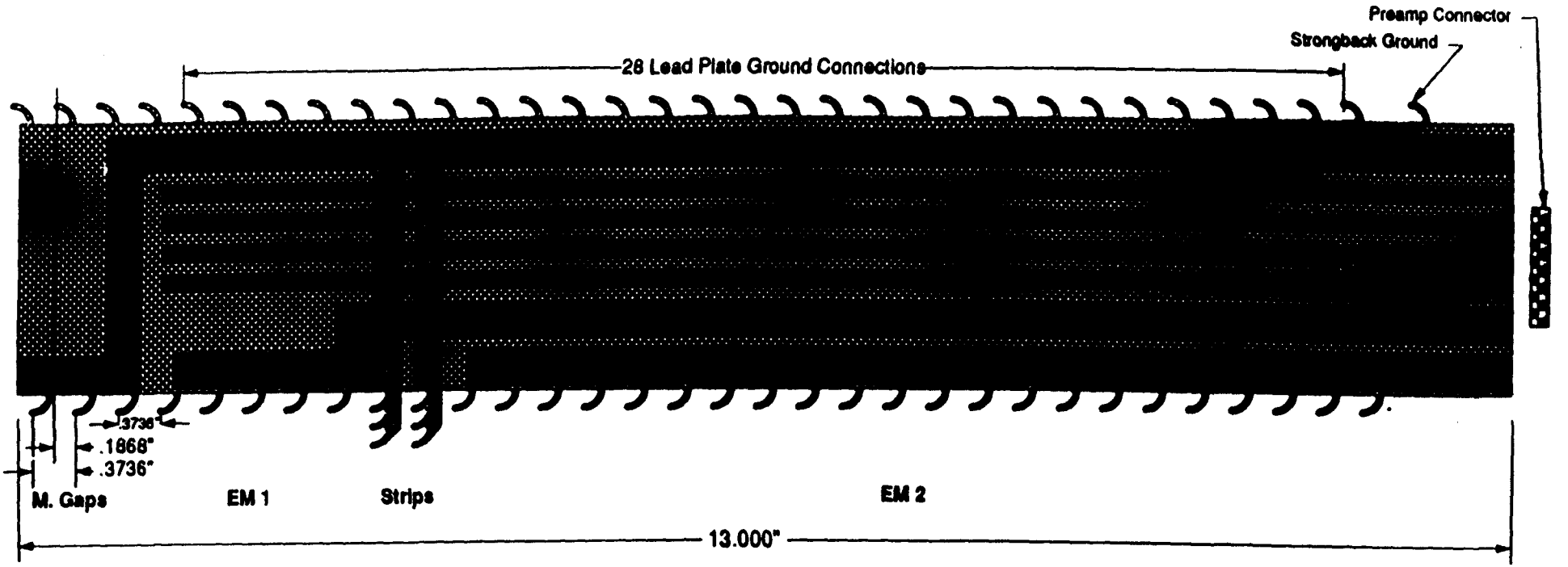

Data:

Absorber Thickness = 0.157" (4mm), 0.551" (14mm) *
Module Phi Gap (LAr) = 0.0788" (2mm), 0.197" (5mm) *
PC Board Thickness = 0.059" (1.5mm)

* **Note:** Dimensions for EM Modules 1, 2, & 6 are given first.

4 Layer Flex Circuit:
1 - Ground Plane
2 - M. Gaps, EM1, EM2 Traces
3 - Strips Traces
4 - Ground Plane

SCALE: 0.75" = 1"

J.B. Hunter / C. Hearty
Original: 1-22-91

7.1.4

High Voltage Distribution

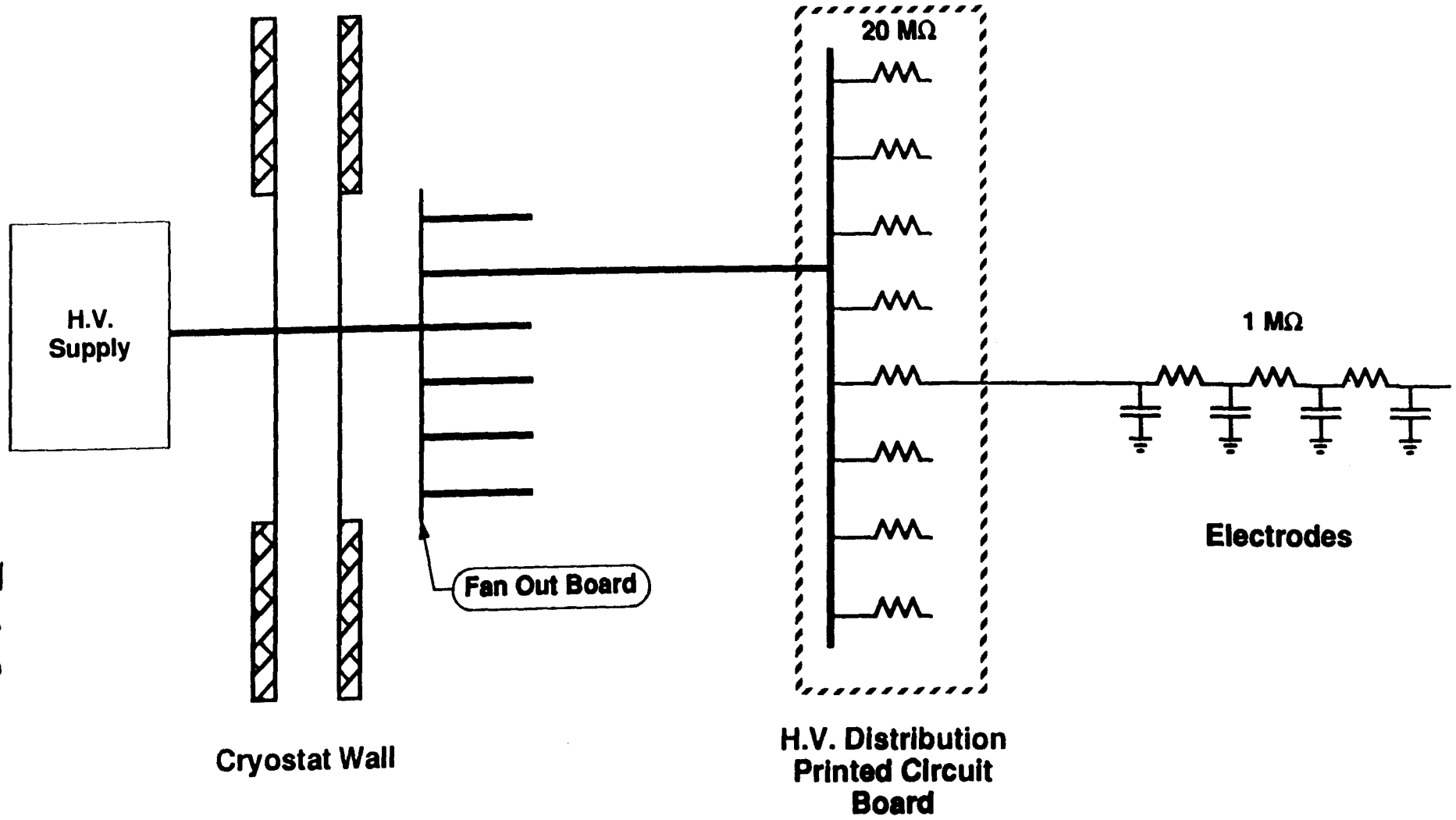

7.2.2

High Voltage Distribution Printed Circuit Board

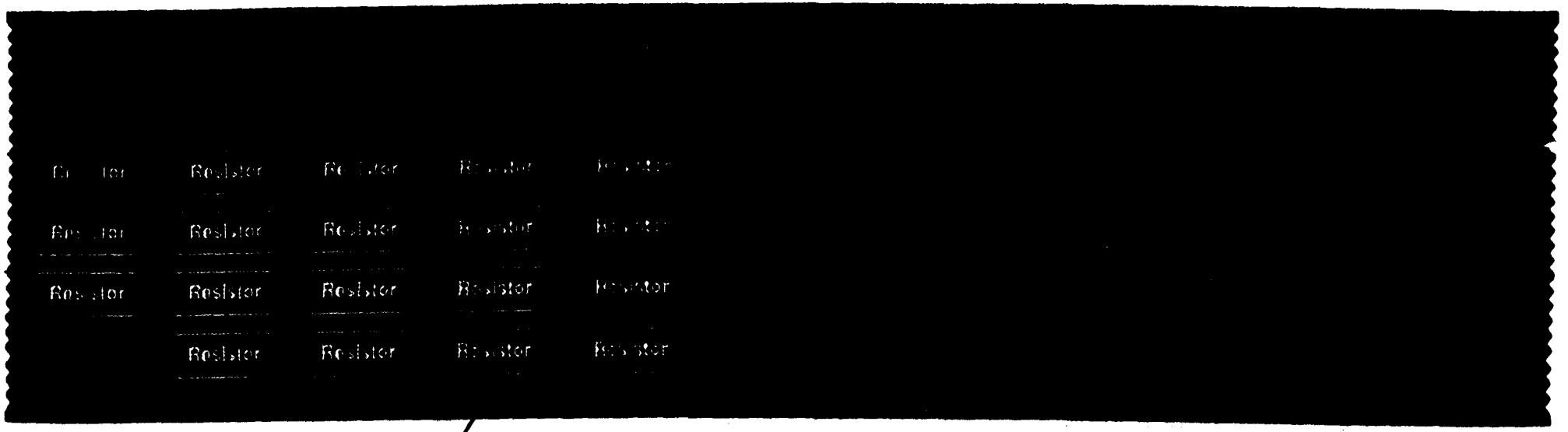

Inner Radius View

FULL SCALE

J.B. Hunter
Original: 4-22-91
Update: 4-24-91

7.2.3

EM Strips, Z Measuring 1 - 4

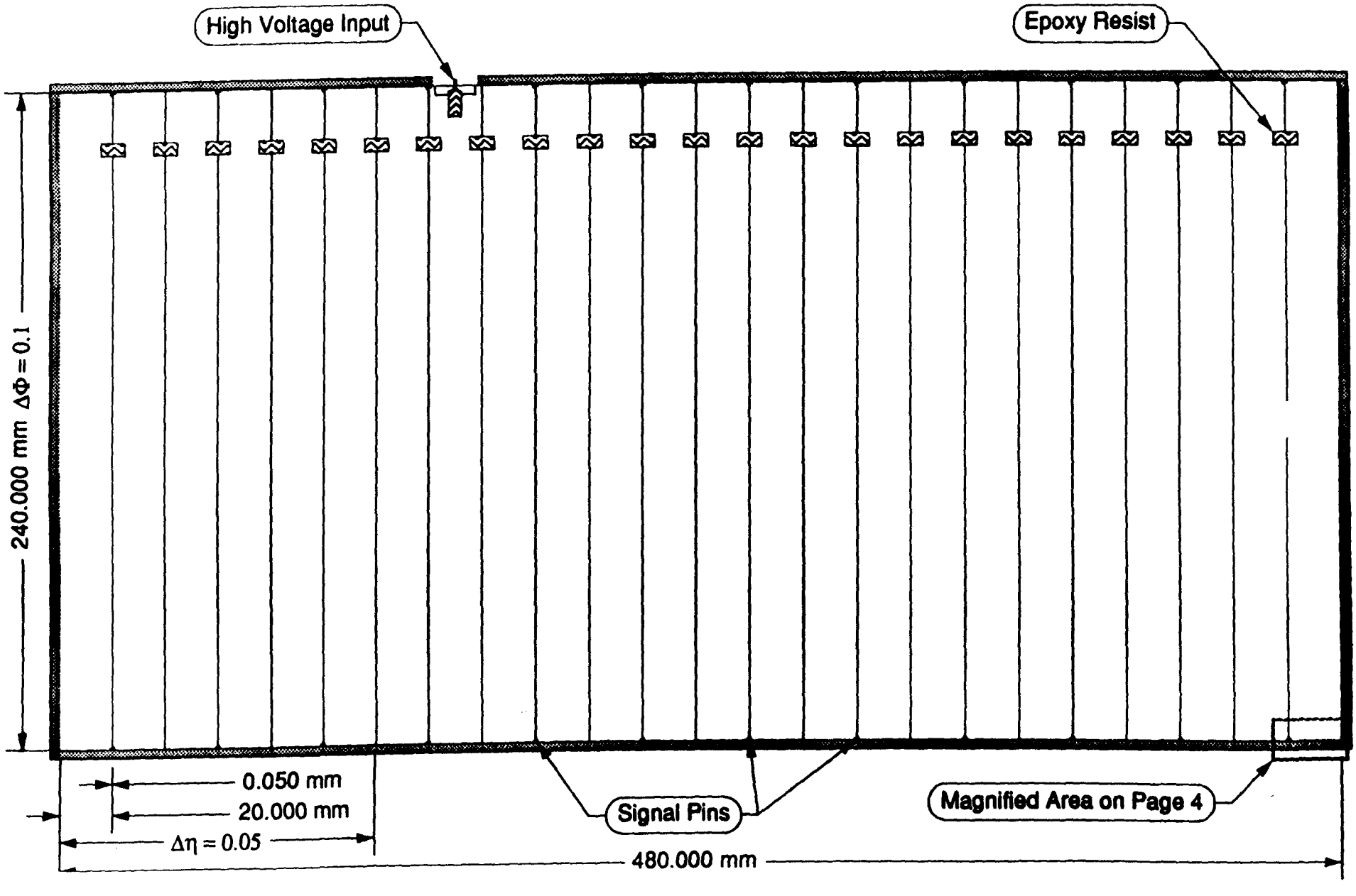

EM Strips, Φ Measuring, H.V. Plane 3 - 4

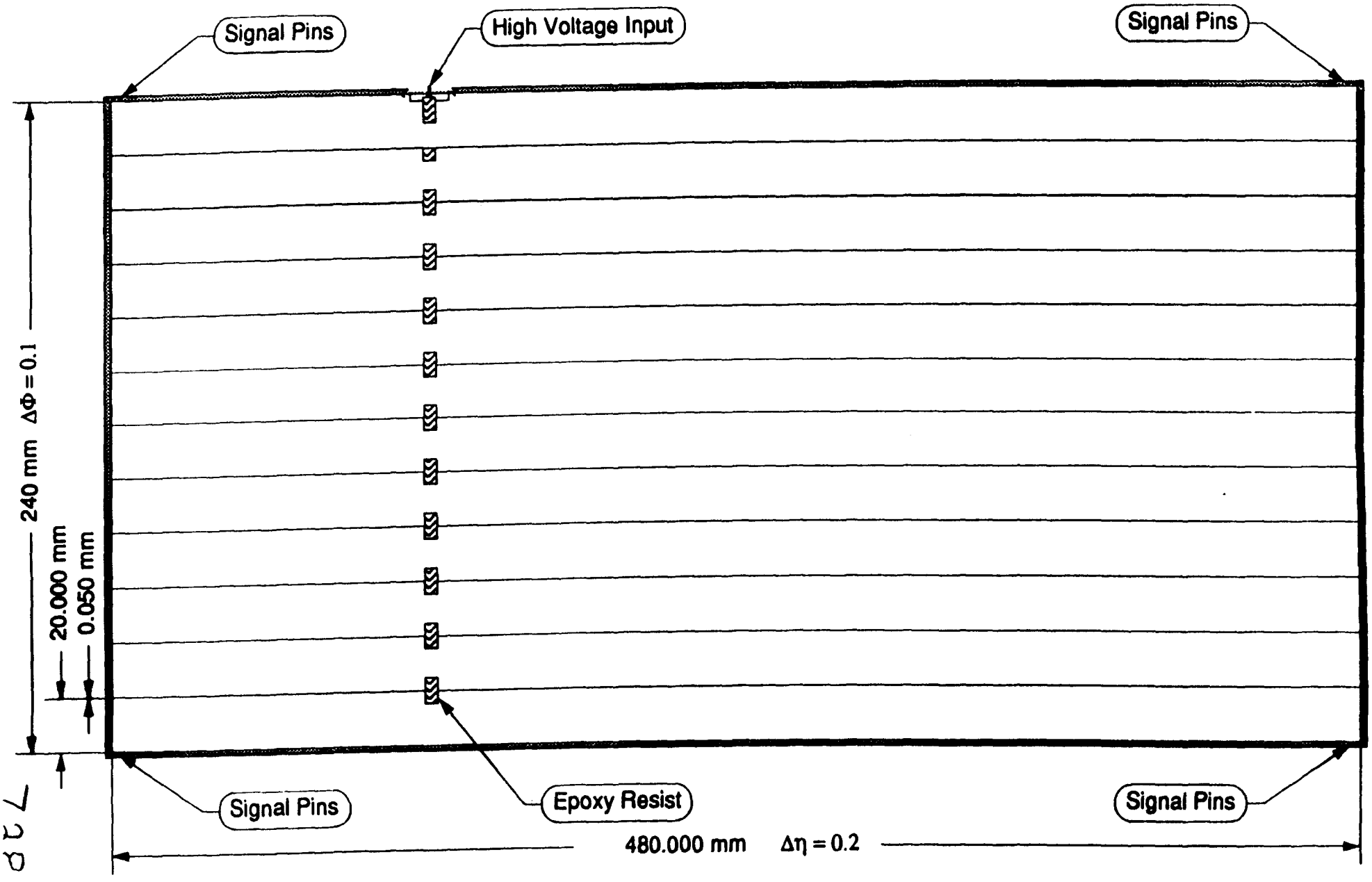

SCALE: 1mm = 2mm

J.B. Hunter / C. Hearty
Original: 7-23-91
Updated: 7-23-91

Barrel Hadronic: Lead Sheet 3 - 4

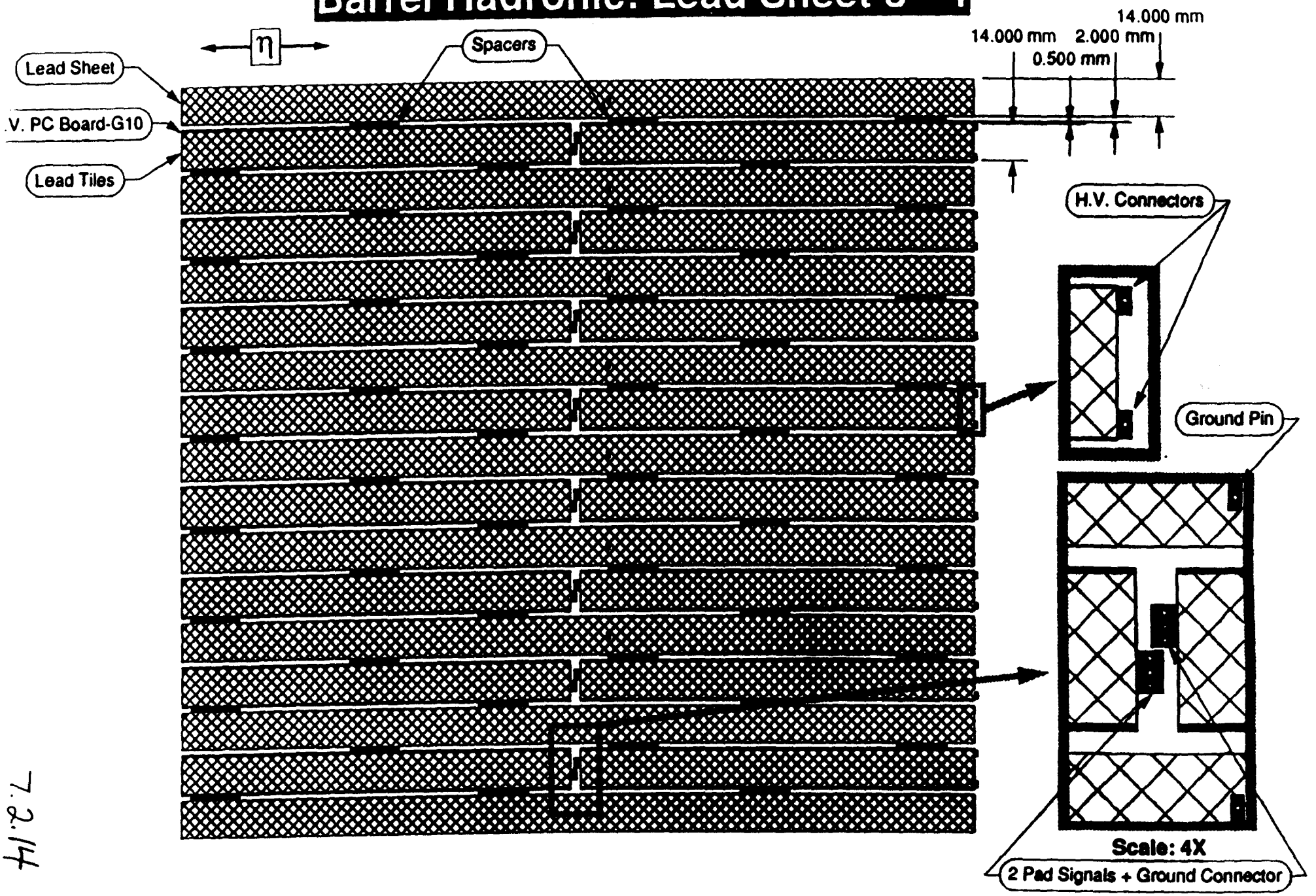

7.2.14

Cross Section
End View

SCALE:
2mm = 8.75mm

J.B. Hunter / C. Hearty
Original: 7-12-91

Barrel Hadronic: Lead Sheet 2 - 4

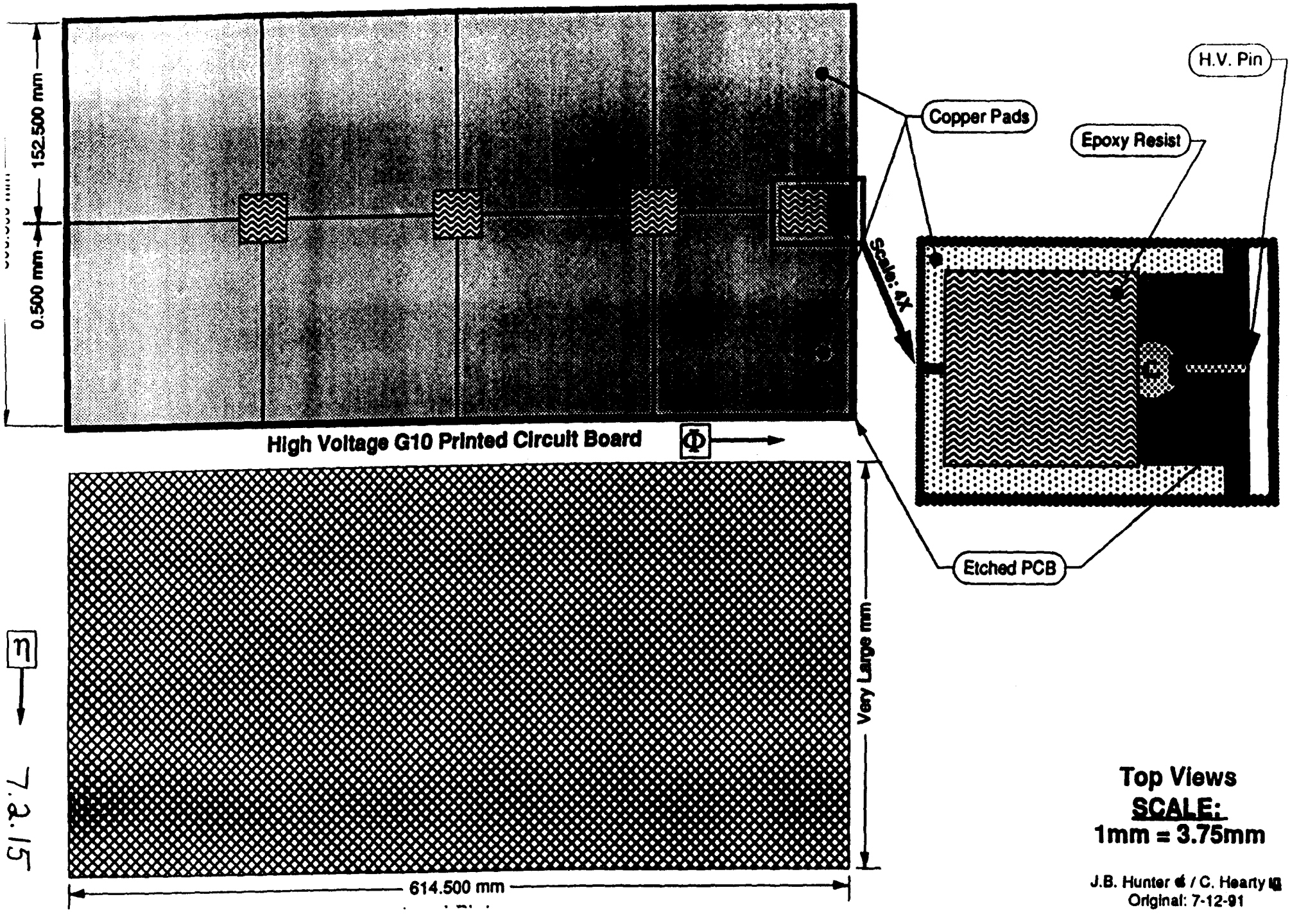

Top Views
SCALE:
1mm = 3.75mm

J.B. Hunter / C. Hearty
Original: 7-12-91

7.3.15

Barrel Hadronic: Lead Sheet 1 - 4

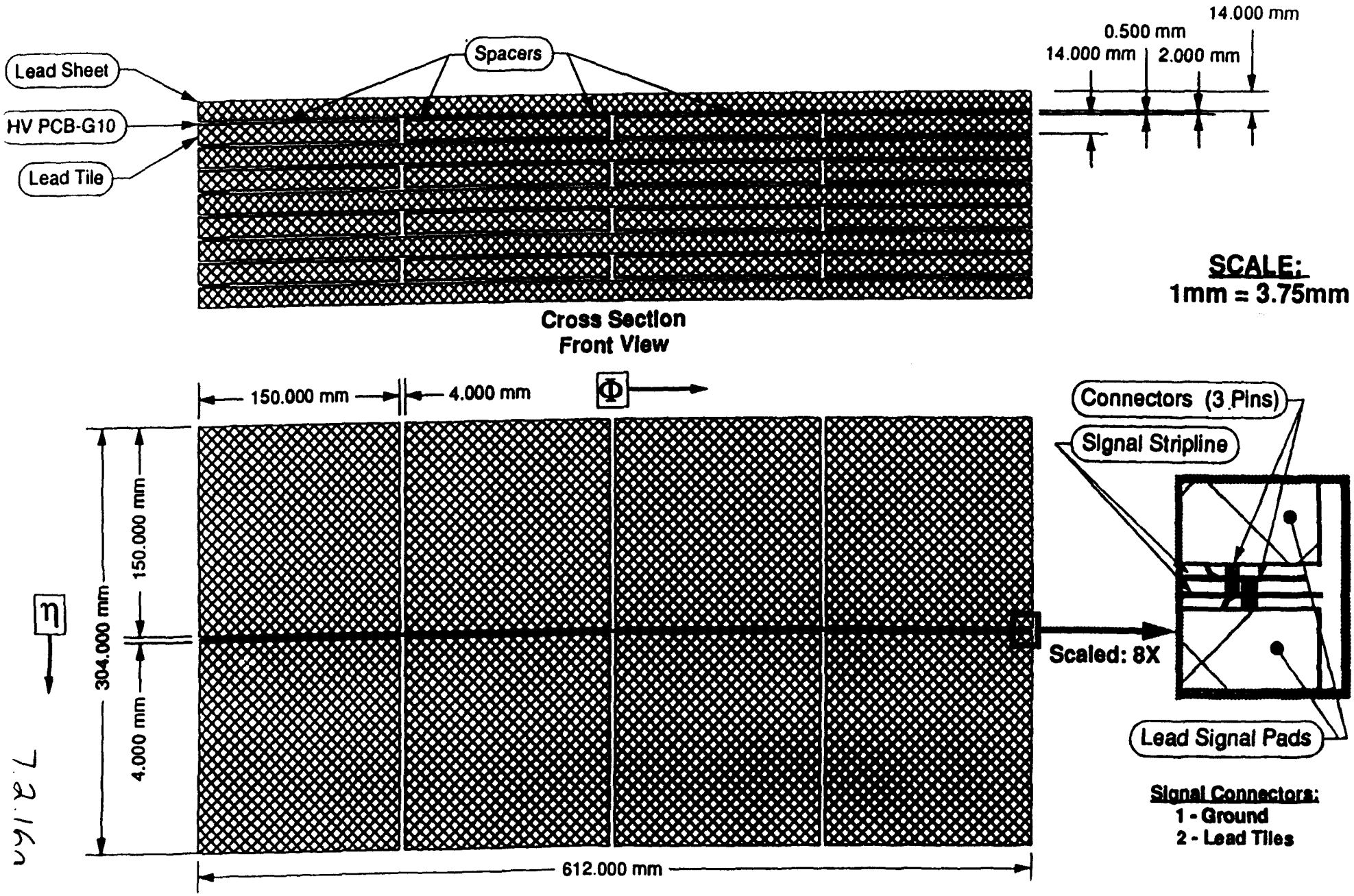

7.2.16n

Barrel Hadronic: Tile Flex Circuit

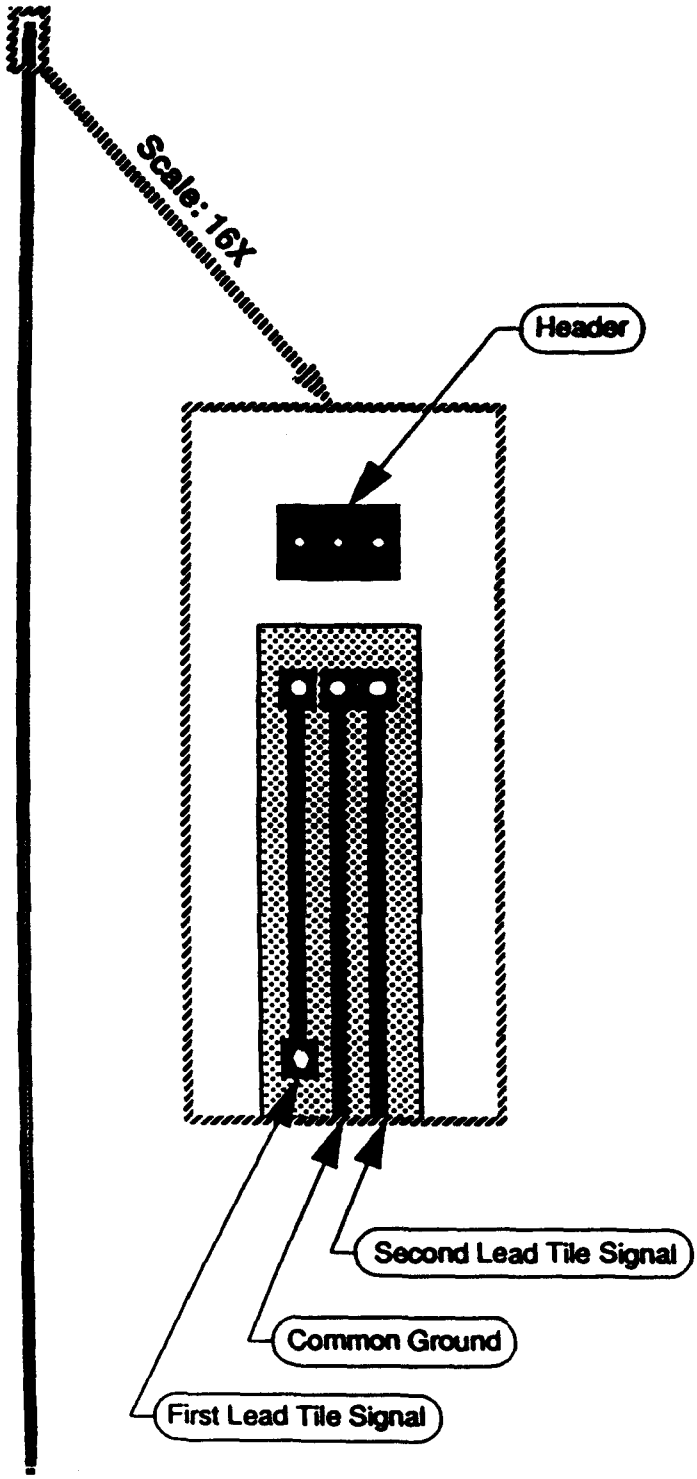

J.B. Hunter / C. Hearty
Original: 7-16-91
Updated: 7-16-91

7.2.16b

Barrel Hadronic: Flex Circuit

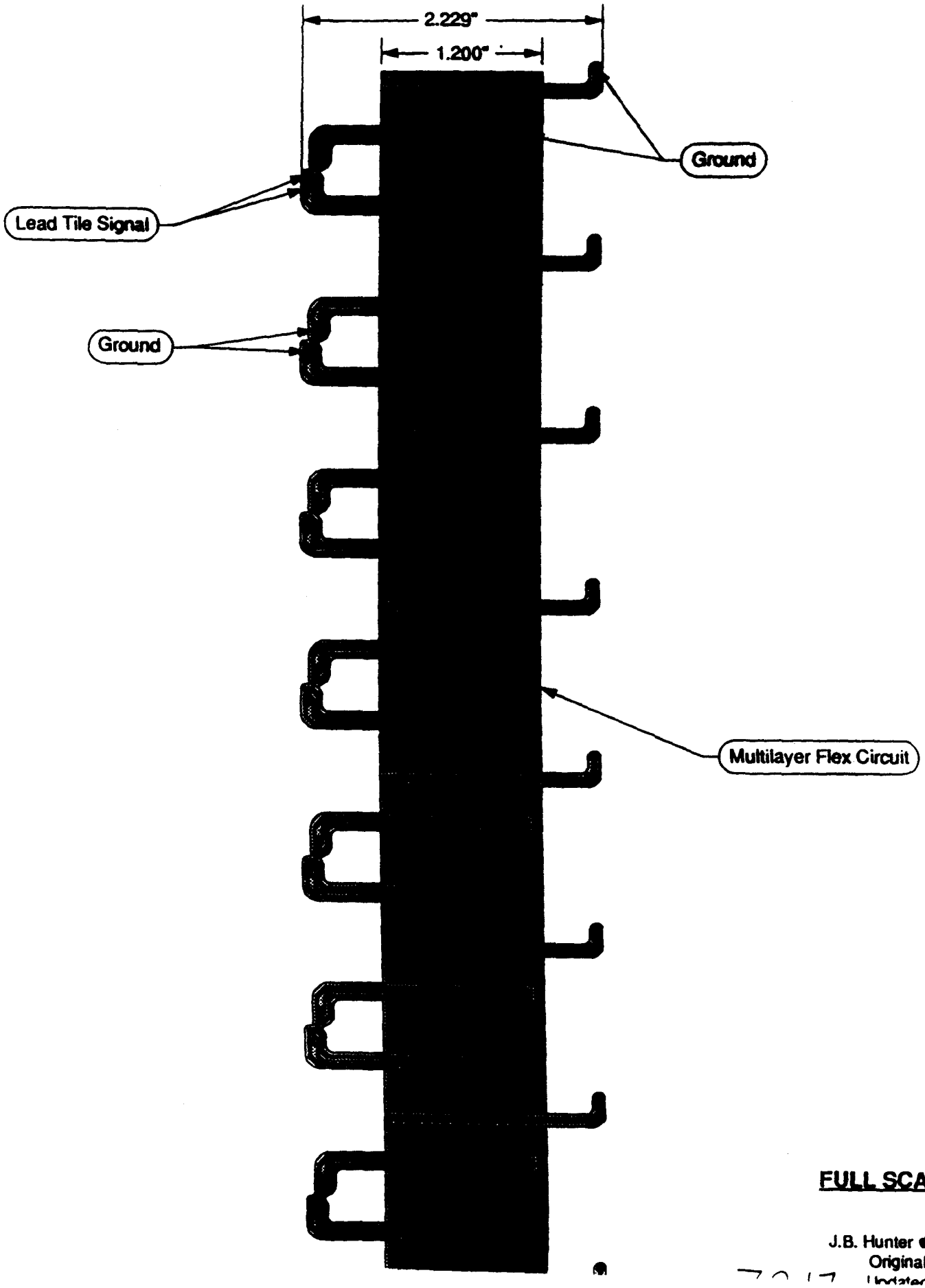

FULL SCAL

J.B. Hunter
Original:
Updated:

Hadronic Preamplifier Printed Circuit Board 1 - 2

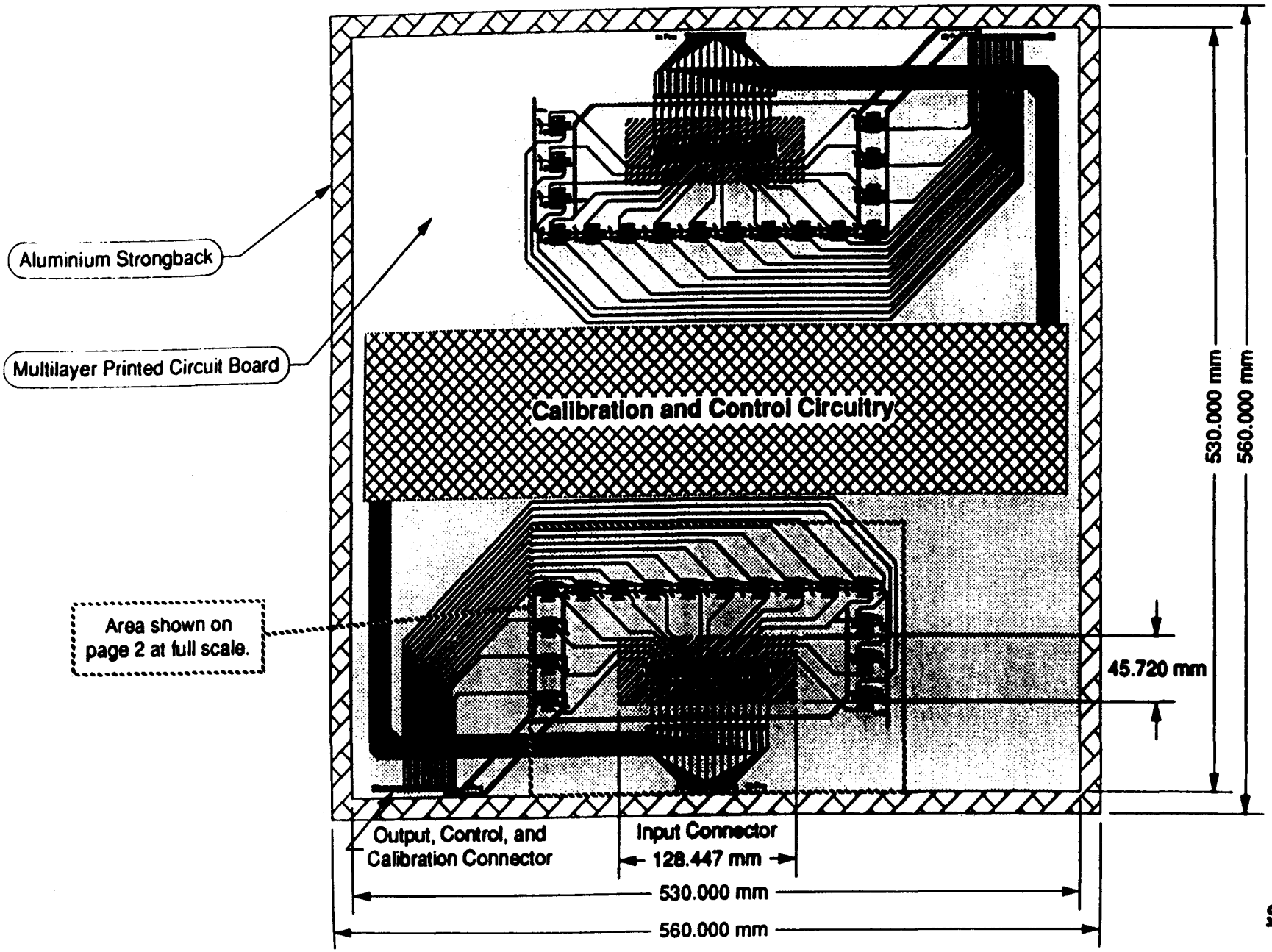

SCALE: 1 = 4

J.B. Hunter / C. Hearty

Hadronic Preamplifier Printed Circuit Board 2 - 2

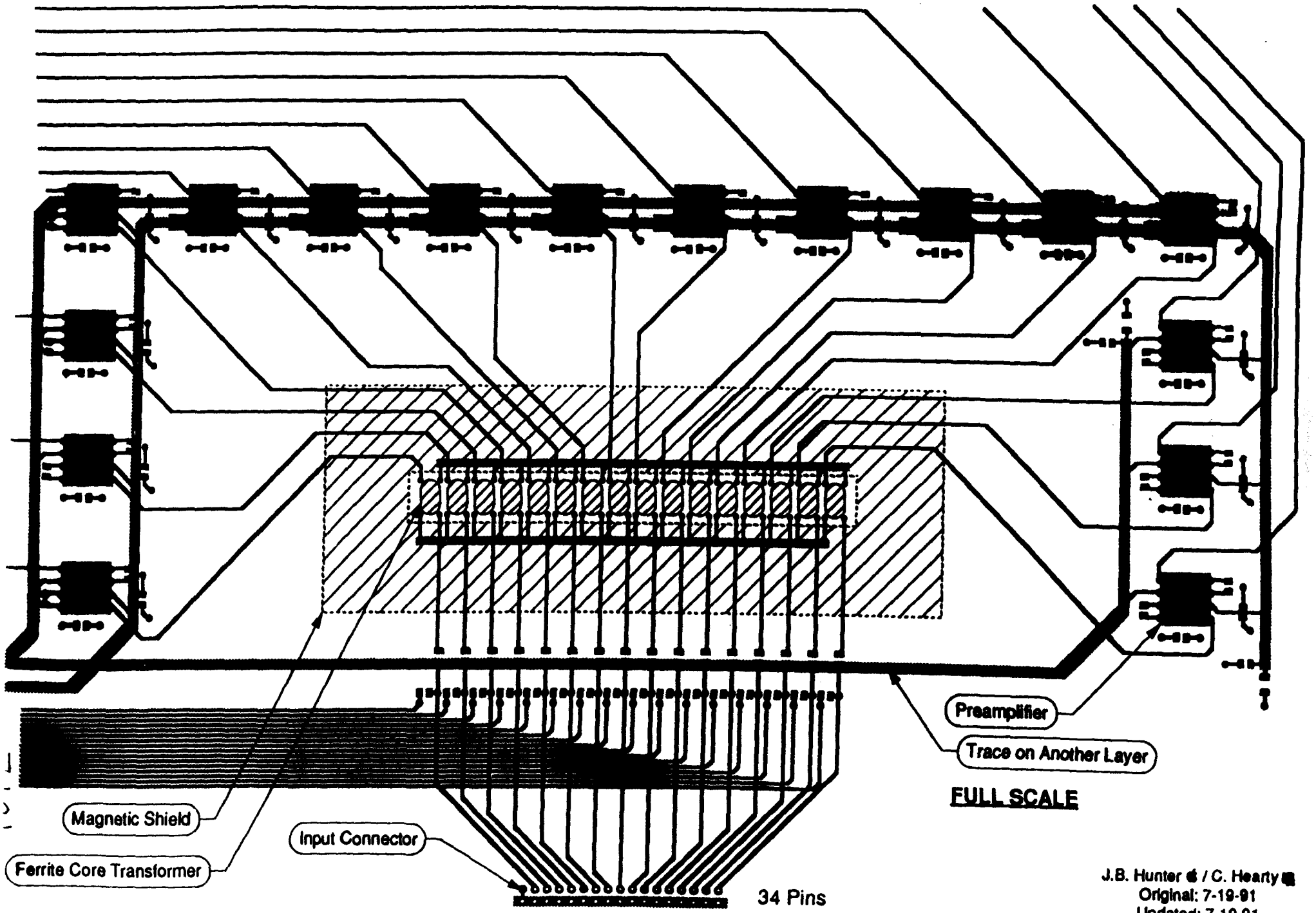

J.B. Hunter / C. Hearty
Original: 7-19-91
Updated: 7-19-91

End Cap Module - Side View

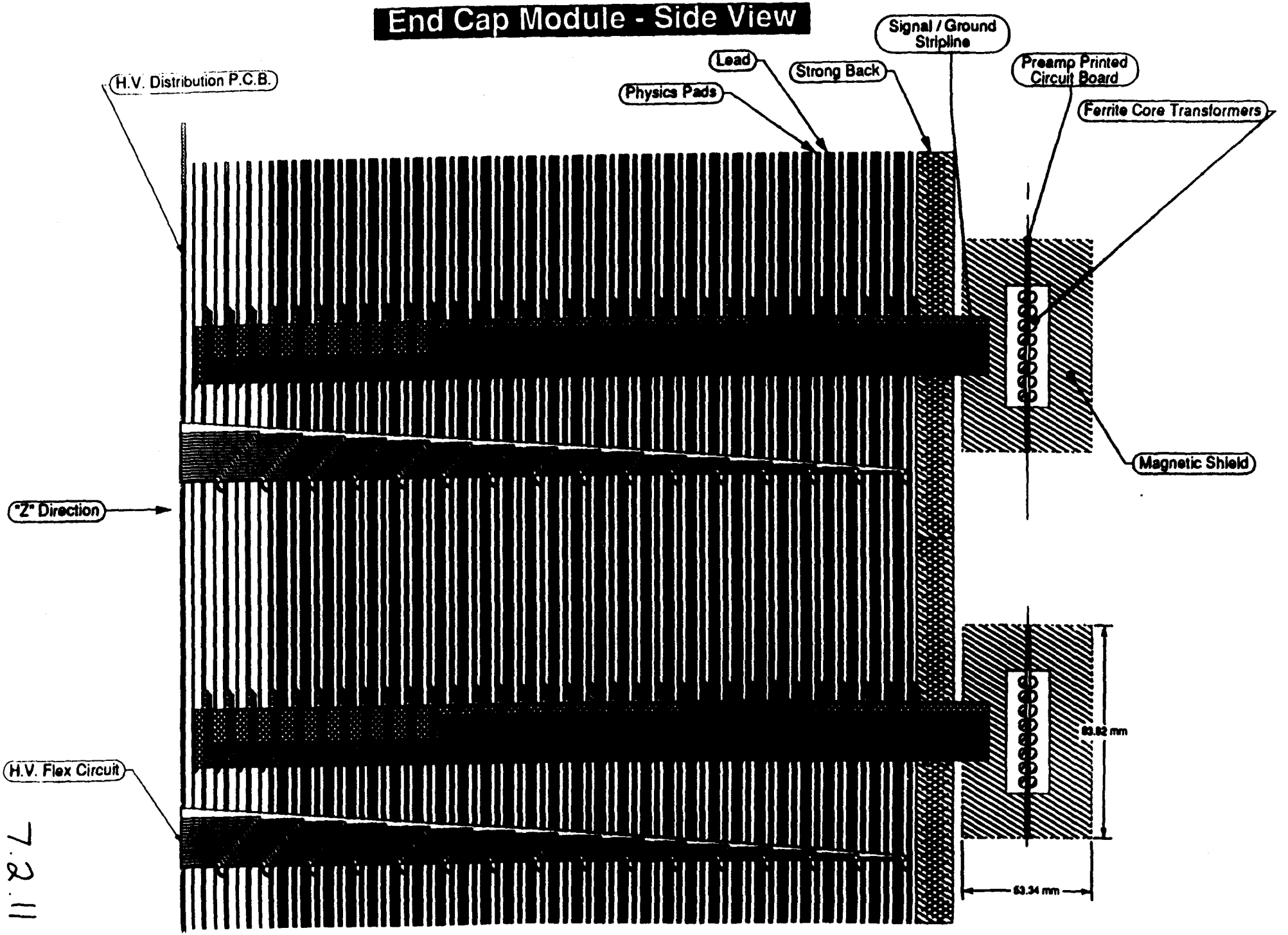

7.2.11

SDC / LAC End Cap E.M. Printed Circuit Board

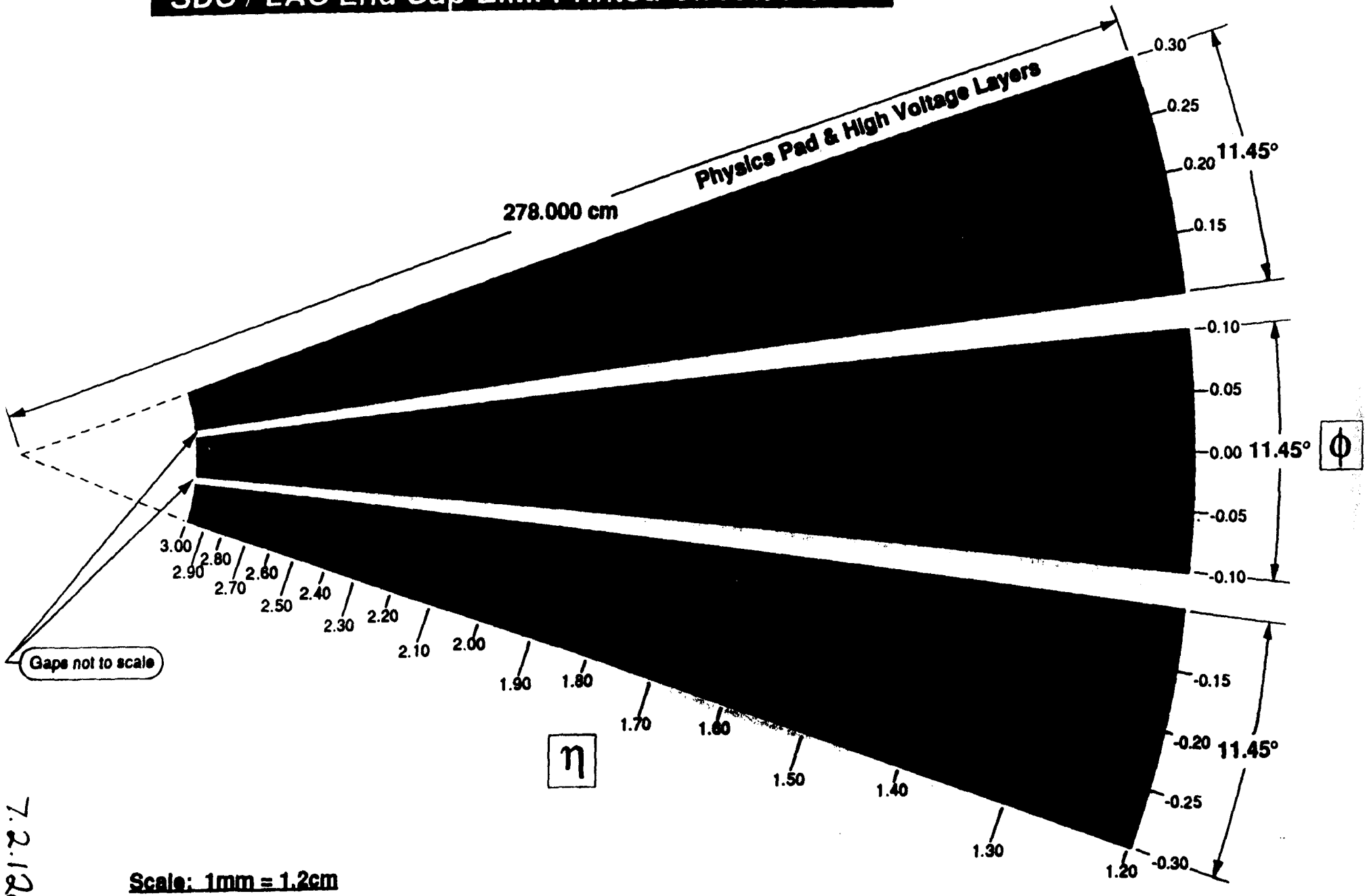

Scale: 1mm = 1.2cm

7.2.12a

J.B. Hunter / A.A. Arthur
Original: 5-7-91
Updated: 6-4-91

J.B. Hunter / A.A. Arthur
Original: 5-7-91

SDC / LAC End Cap E.M. Printed Circuit Board

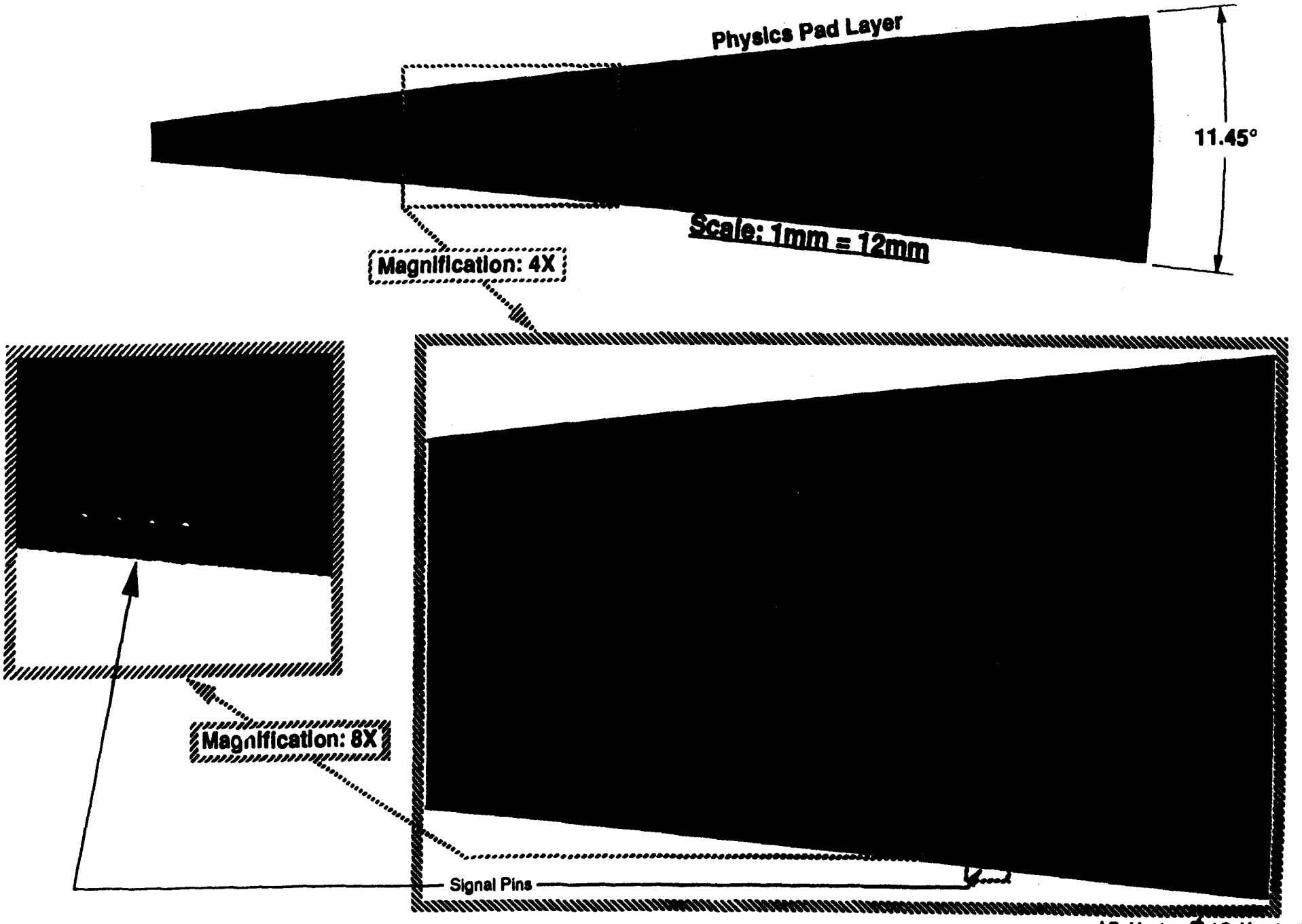

J.B. Hunter / C. Hearty III

7212

SDC / LAC End Cap E.M. Printed Circuit Board

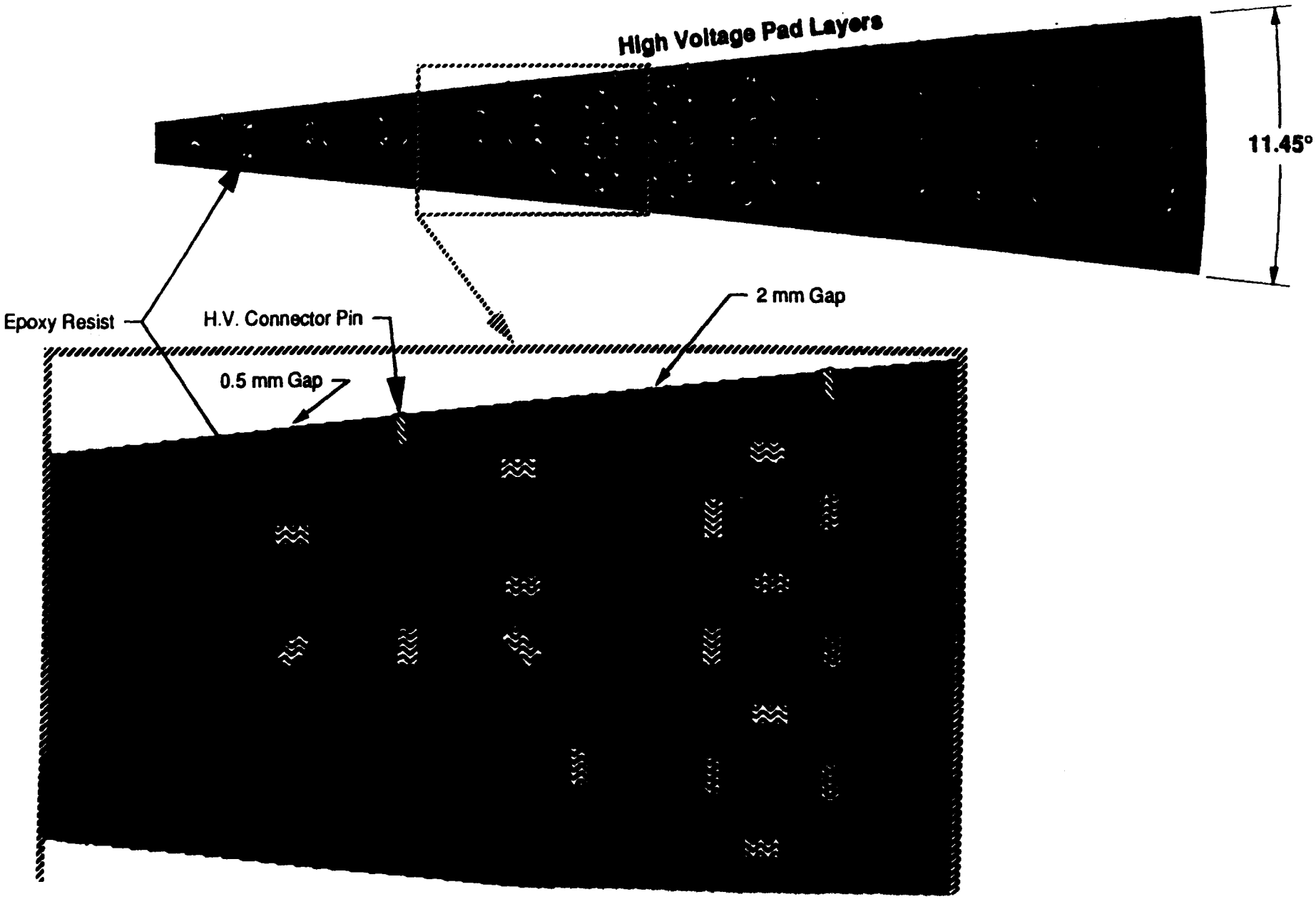

Liquid Argon Electronics Overview

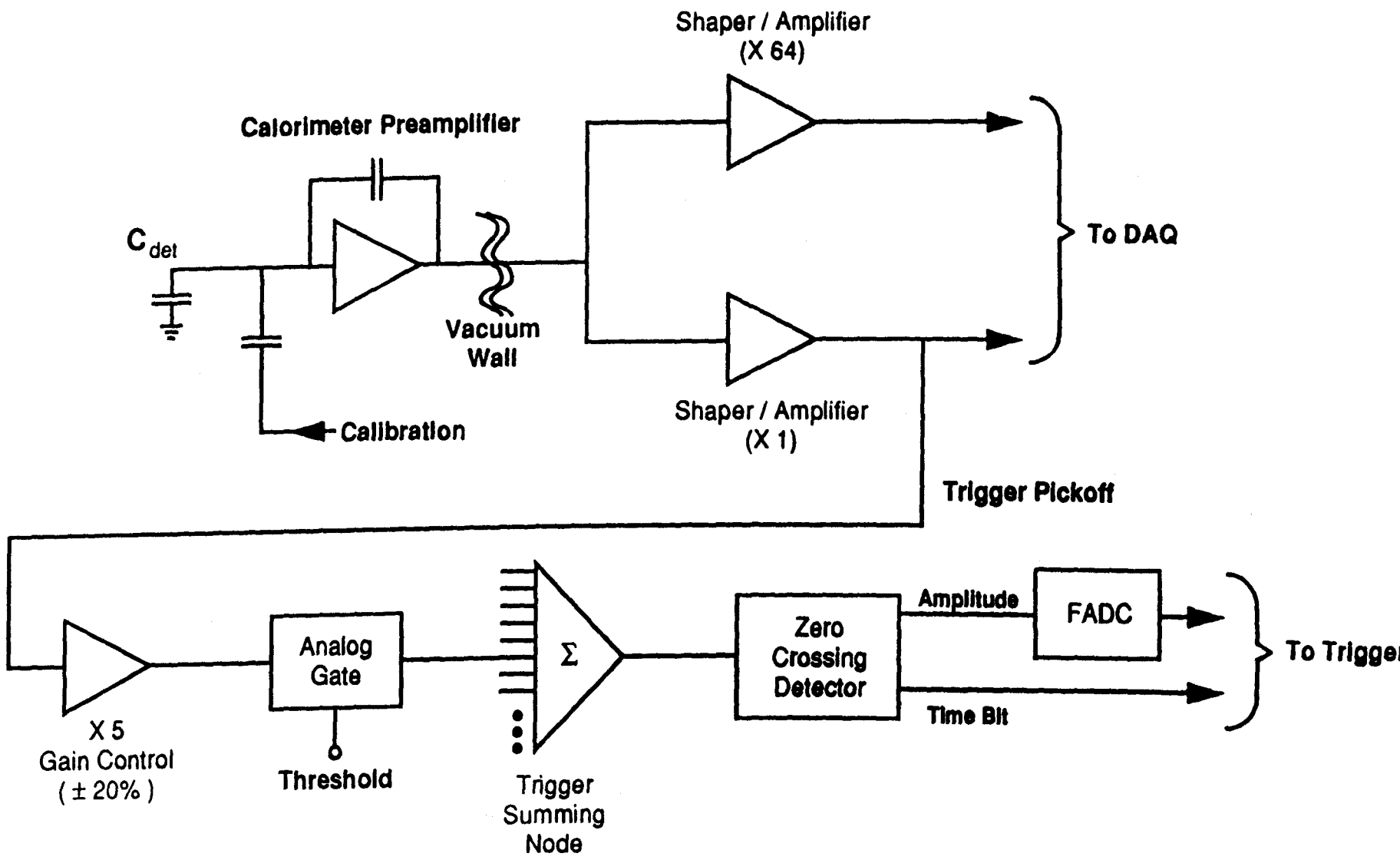

7.3.1

J.B. Hunter / C. Hearty
Original: 7-24-91
Updated: 7-25-91

CALORIMETER ELECTRONIC SYSTEM

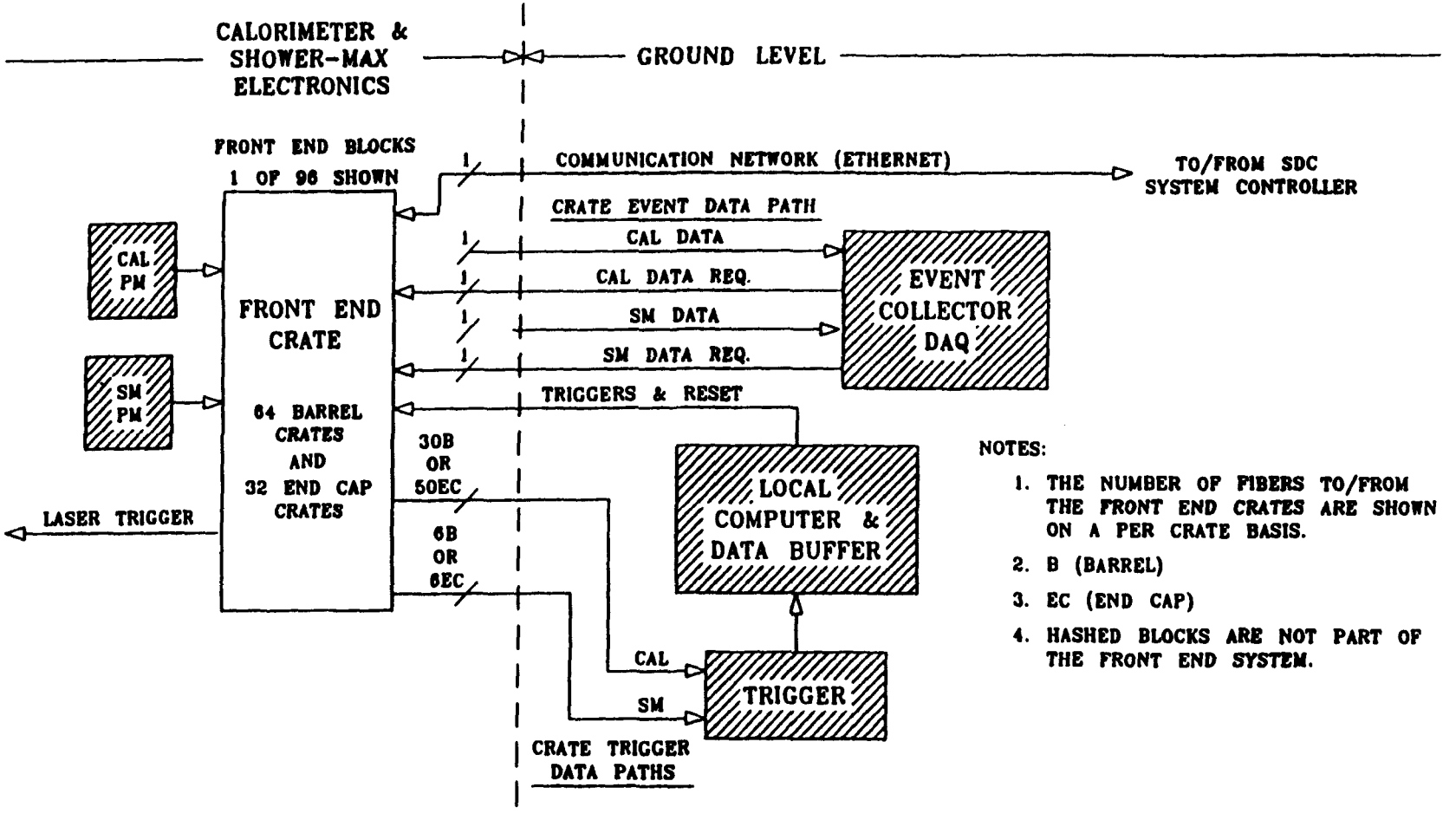

Figure 4.1

SIMPLIFIED CALORIMETER OR SHOWER-MAX FRONT END CRATE

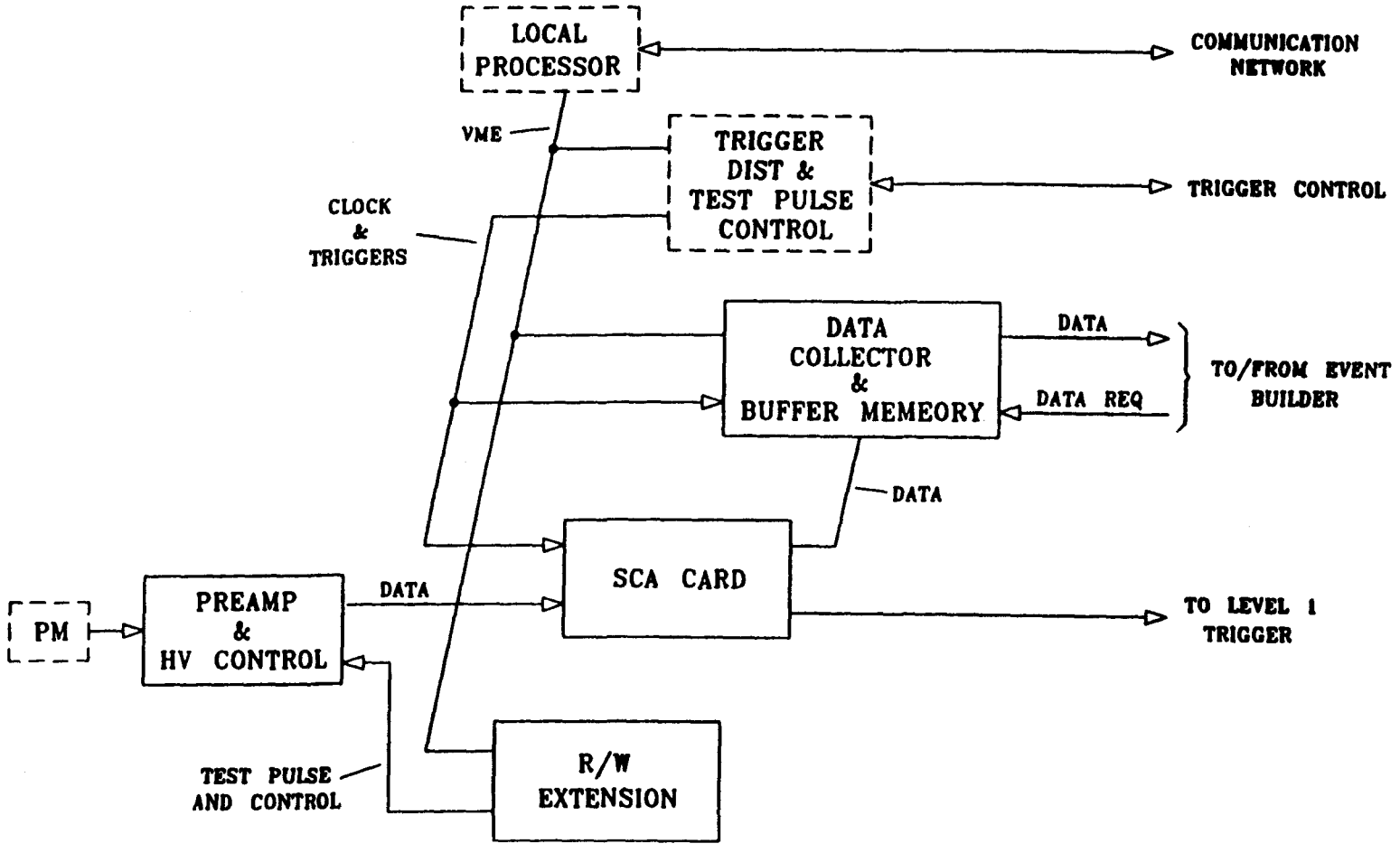

Figure 4.1.1

CALORIMETER PREAMP AND HV CONTROL CARD

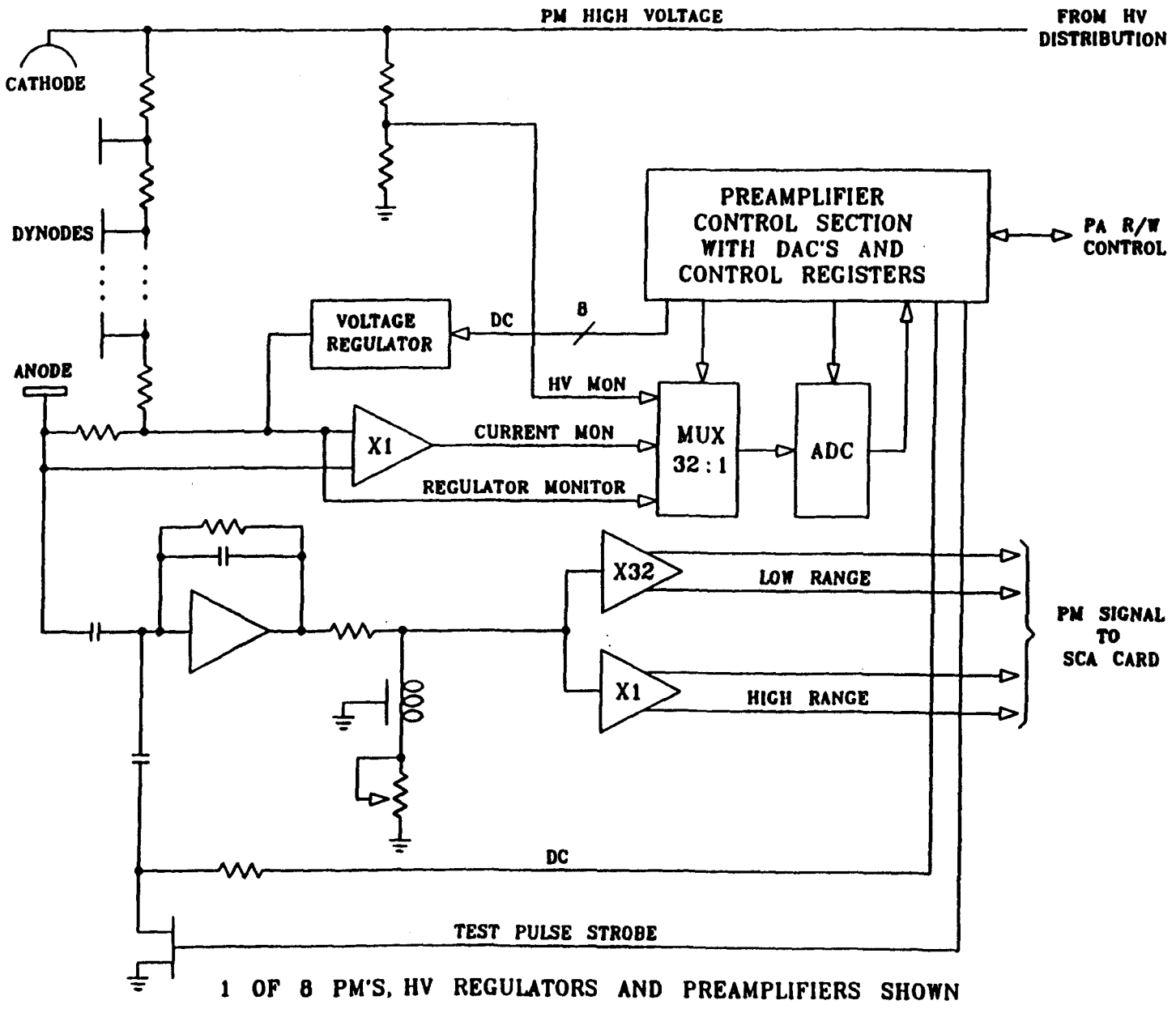

Figure 4.4a

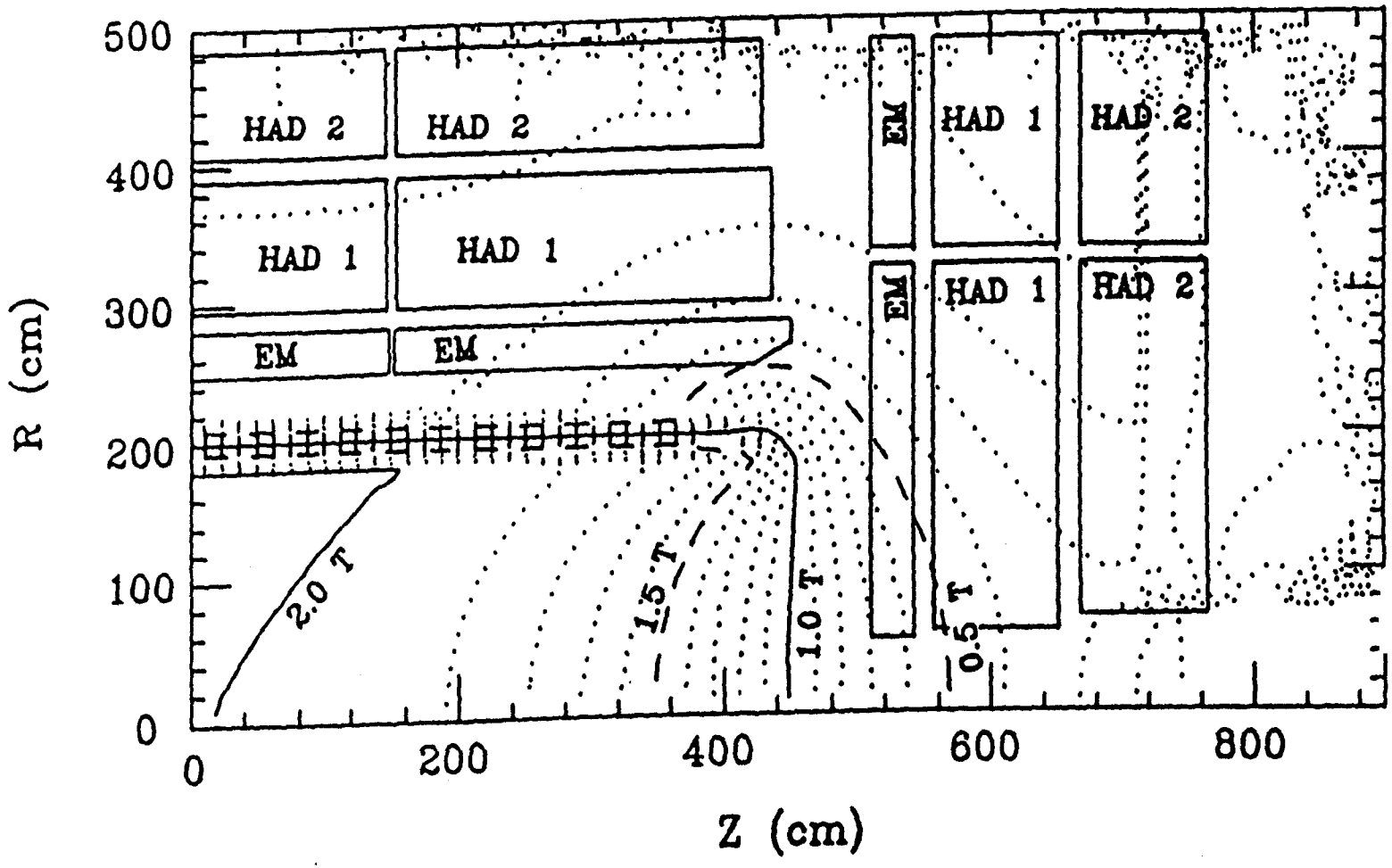
HAD 2
HAD 2
HAD 1
HAD 1
EM
EM
EM
EM
HAD 1
HAD 2
HAD 1
HAD 2
2.0 T
1.5 T
1.0 T
0.5 T
R (cm)
Z (cm)
0
100
200
300
400
500
0
200
400
600
800

LBL SDC 0049 Pg 3

8/20/91
RDS

- in all cases excitation = 6,562,500 Amperes
- $B_y(0,0)$ falls 0.6% case 1 → case 4; increasing excitation by this amount would keep $B_y(0,0)$ const.
- see Figs for Fields; Fields shown in FT1, FT2, BT1 are in addition to the 1.8T circum. Field (μ_R FT1, FT2, BT1 set to $\mu_R(B=1.8T)$ - good approx. since $(B_z^2 + B_\theta^2)^{1/2} = (\doteq 2340^2 + 18000^2)^{1/2}$ $= 18150 \approx 18000 = B_\theta$ ✓

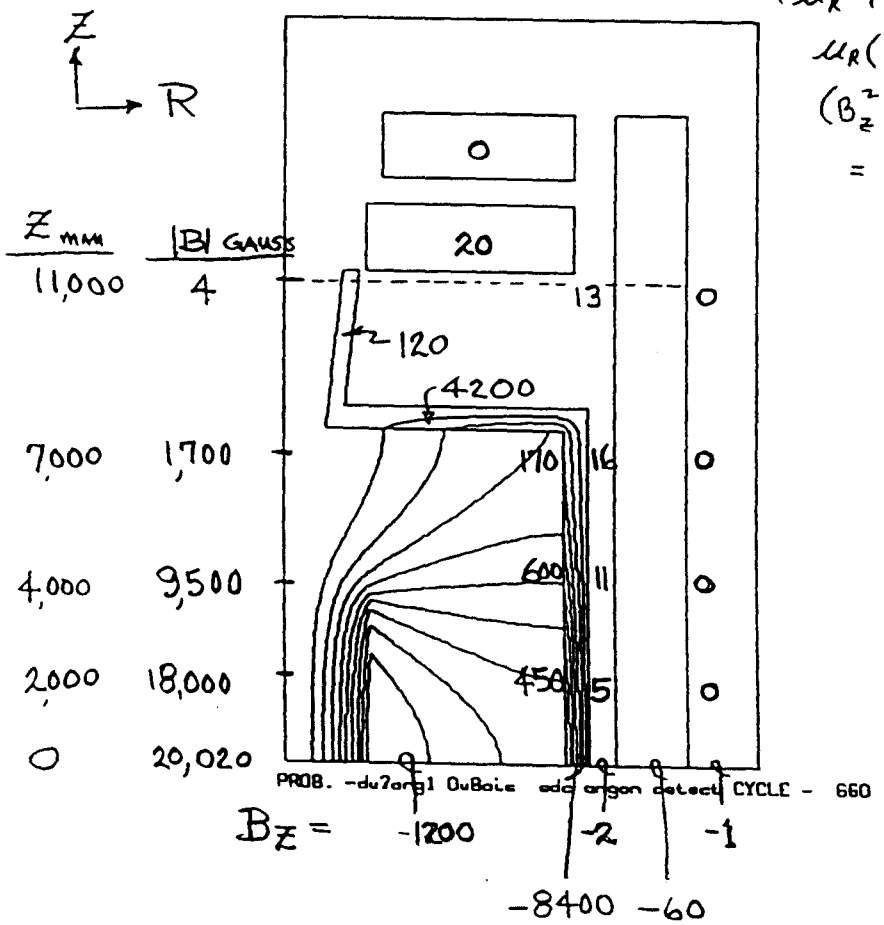

CASE 1

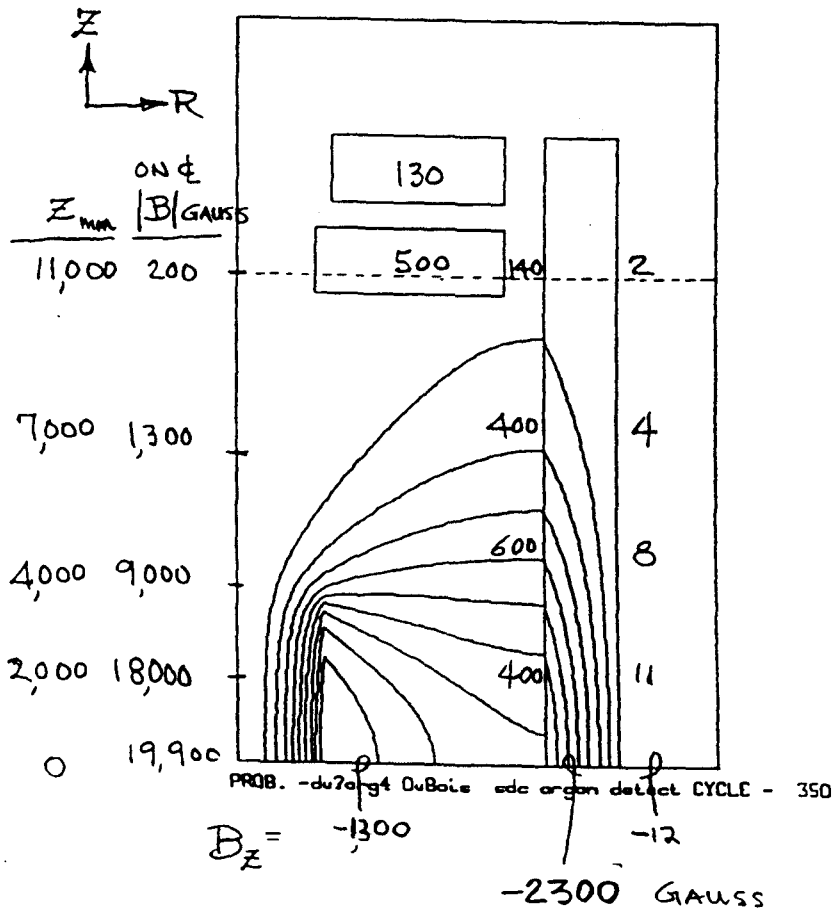
Z
R
ON ℄
Z_{MM}
$|B|$ GAUSS
11,000 200
7,000 1,300
4,000 9,000
2,000 18,000
0 19,900
130
500
140
2
400
4
600
8
400
11
PROB. -du2a-g4 DuBois sdc argon detect CYCLE - 350
B_Z =
-1300
-12
-2300 GAUSS

CASE 4

PREAMP COOLING

The LAC's preamps reside at the back of the modules in LAr. See Section 7 of the CDR for a complete description of their properties and expected performance.

1. Test & Analyses *strongly suggest* that boiling of LAr can be avoided in the *Baseline LAC*

2. Experimental Tests:

   2.1 University of Rochester

   2.2 KEK/KHI

3. Design Calculation Documentation:

   3.1 LLNL Analyses (Don Slack)

   3.2 KHI Analyses

4. Extension of the forgoing to Barrel modules:

   4.1 Sensible heat gain to LAr at HAD preamps can be removed by Watt's *existing* 2 *phase* N_2 *circuits* (in the vacuum annulus).

   4.2 Sensible heat gain to LAr at EM preamps can be removed by additional 2 phase N_2 circuits attached to the LAr vessel's mid-shell wall (2 circuits minimum; 4 circuits with 100 % redundancy).

HIGHLIGHTS OF PREAMPLIFIER COOLING

1. TESTING & ANALYSIS PROVE LOCAL BOILING OF LAr CAN BE MITIGATED

2. TESTING WAS AS FOLLOWS:

   2.1 COOLING BY DIRECT COUPLING TO LN_2

   2.2 COOLING BY INDIRECT COUPLING TO LN_2

   2.3 COOLING BY CONVECTION IN LAr

   2.4 CONCLUSION: NO LOCAL BOILING OCCURRED AT OPERATING POWER LEVELS IN ANY TEST

3. CALCULATIONS: PRELIMINARY CALCULATIONS INDICATE THAT IN THE LAC THE LAr IS SUBCOOLED AND DOES NOT BOIL

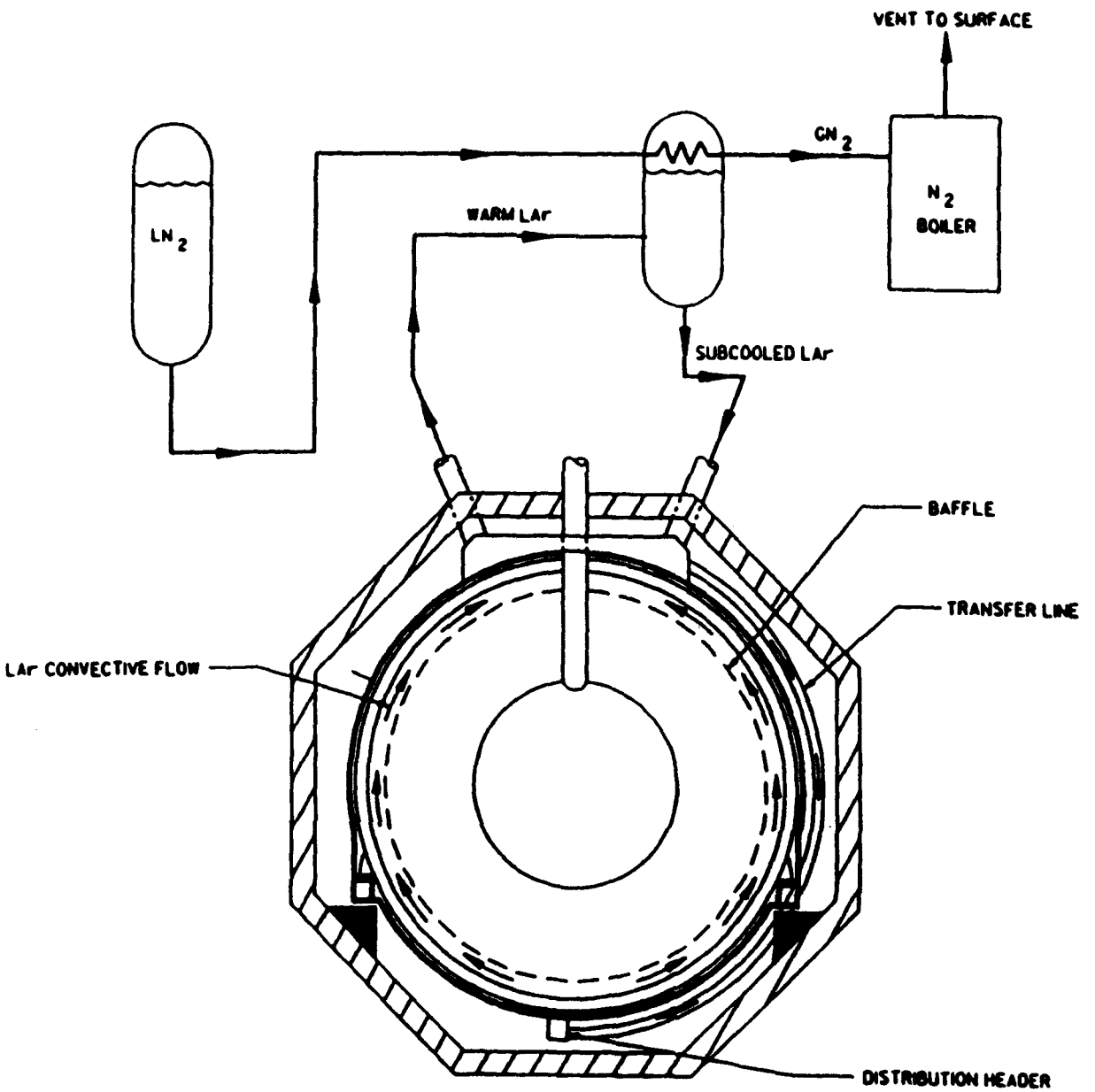

Fig. 6.11 Convective Cooling with Liquid Argon

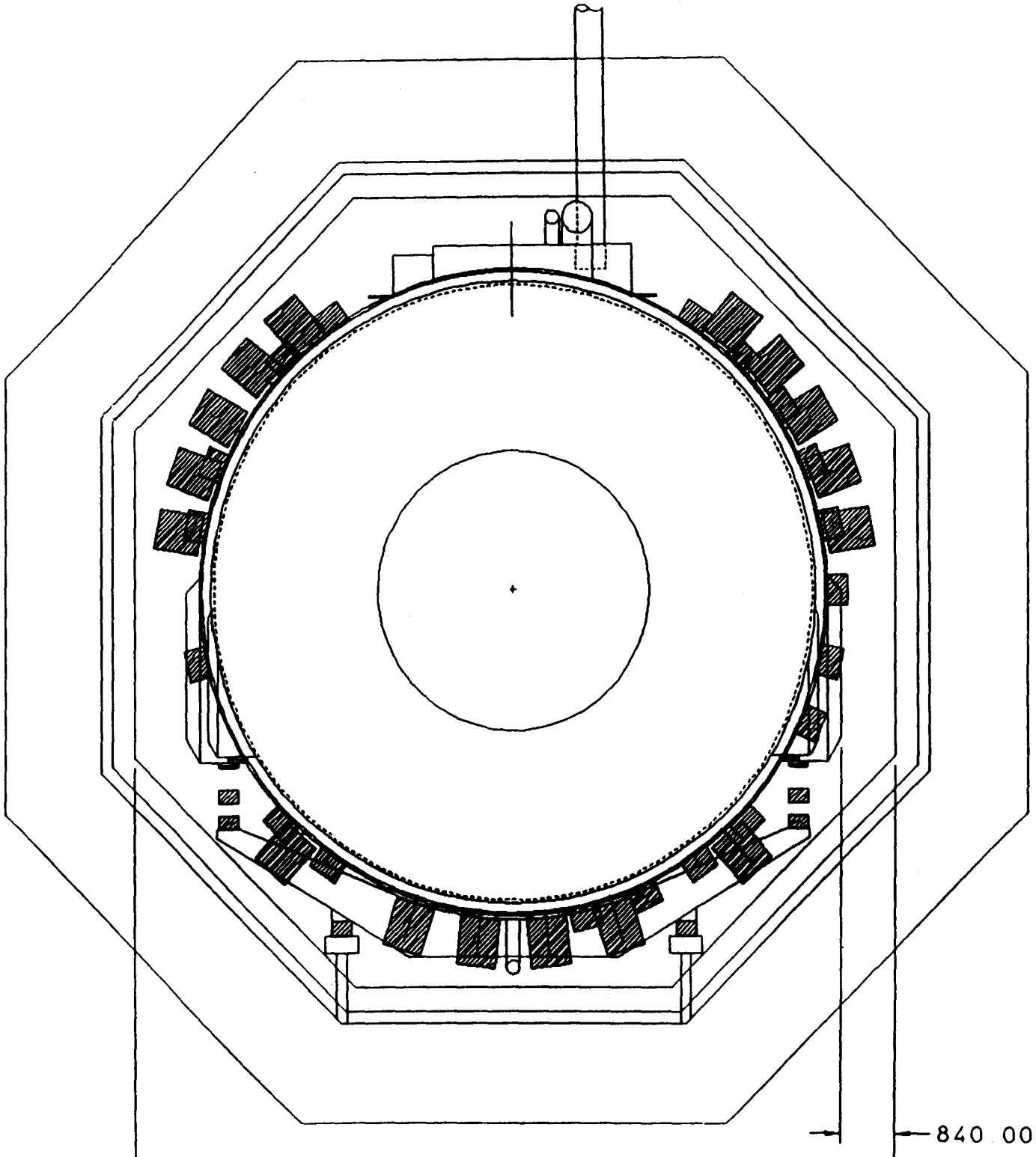
840 00

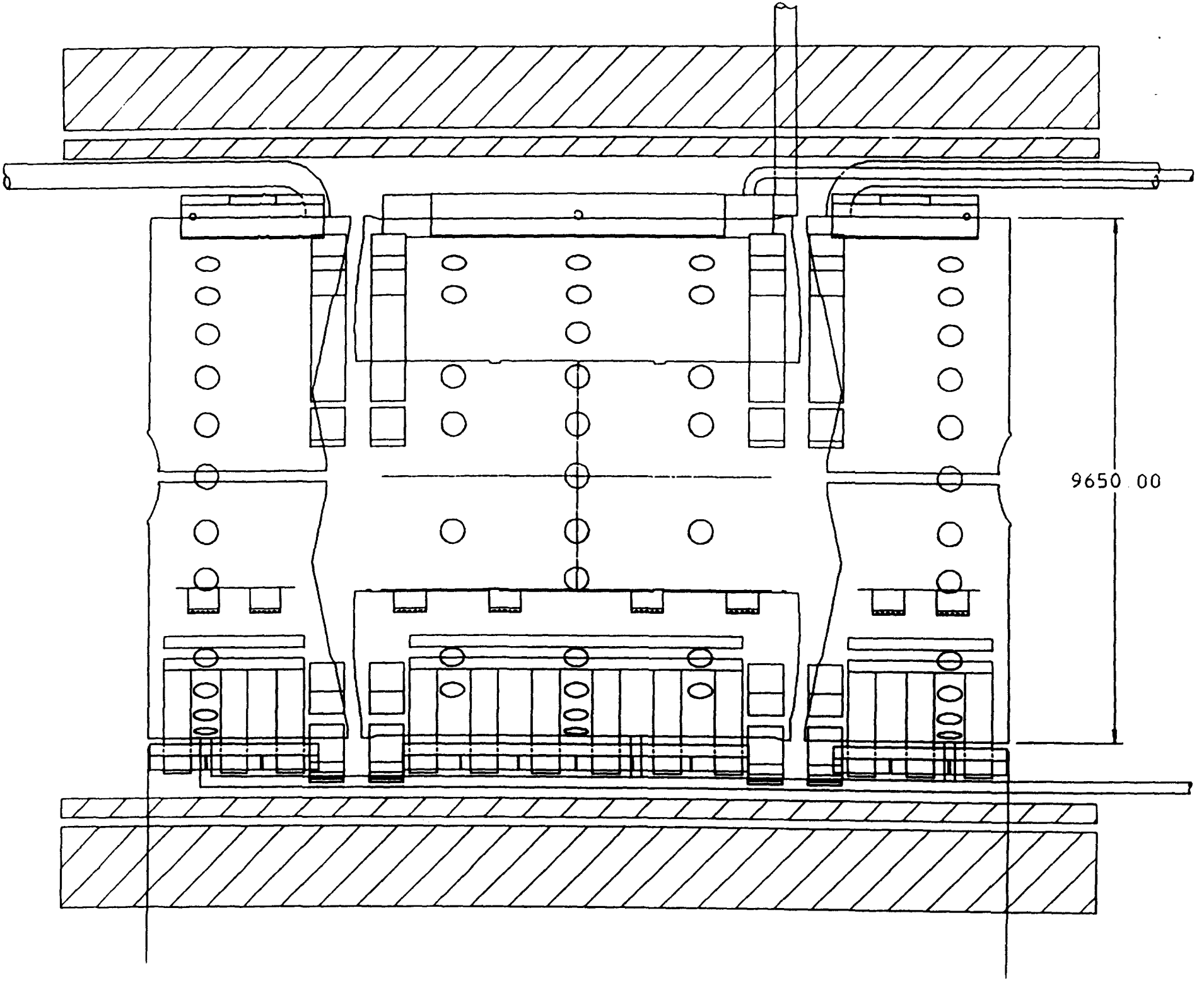
9650.00

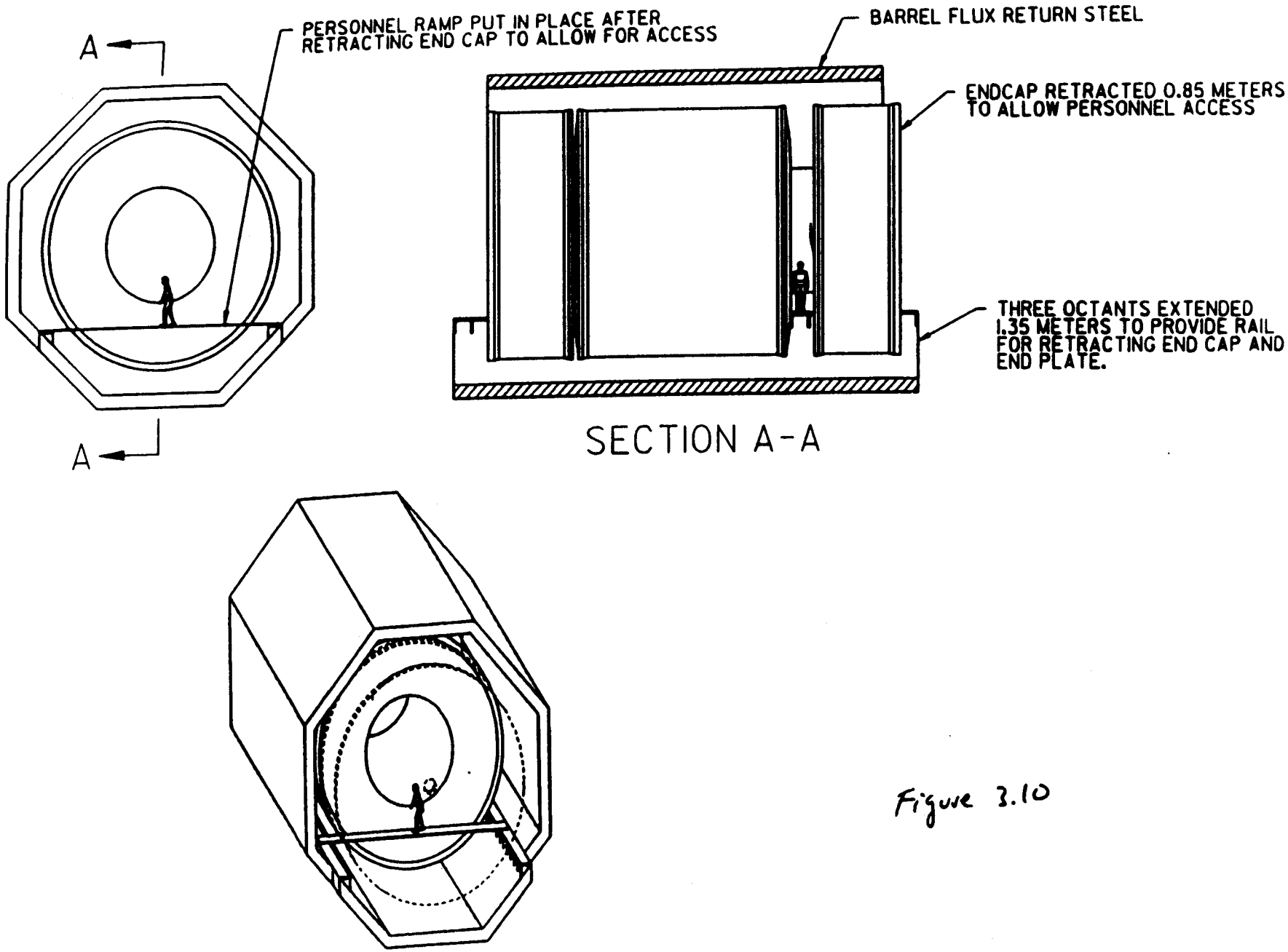
A
A
PERSONNEL RAMP PUT IN PLACE AFTER RETRACTING END CAP TO ALLOW FOR ACCESS
BARREL FLUX RETURN STEEL
ENDCAP RETRACTED 0.85 METERS TO ALLOW PERSONNEL ACCESS
THREE OCTANTS EXTENDED 1.35 METERS TO PROVIDE RAIL FOR RETRACTING END CAP AND END PLATE.
SECTION A-A

Figure 3.10

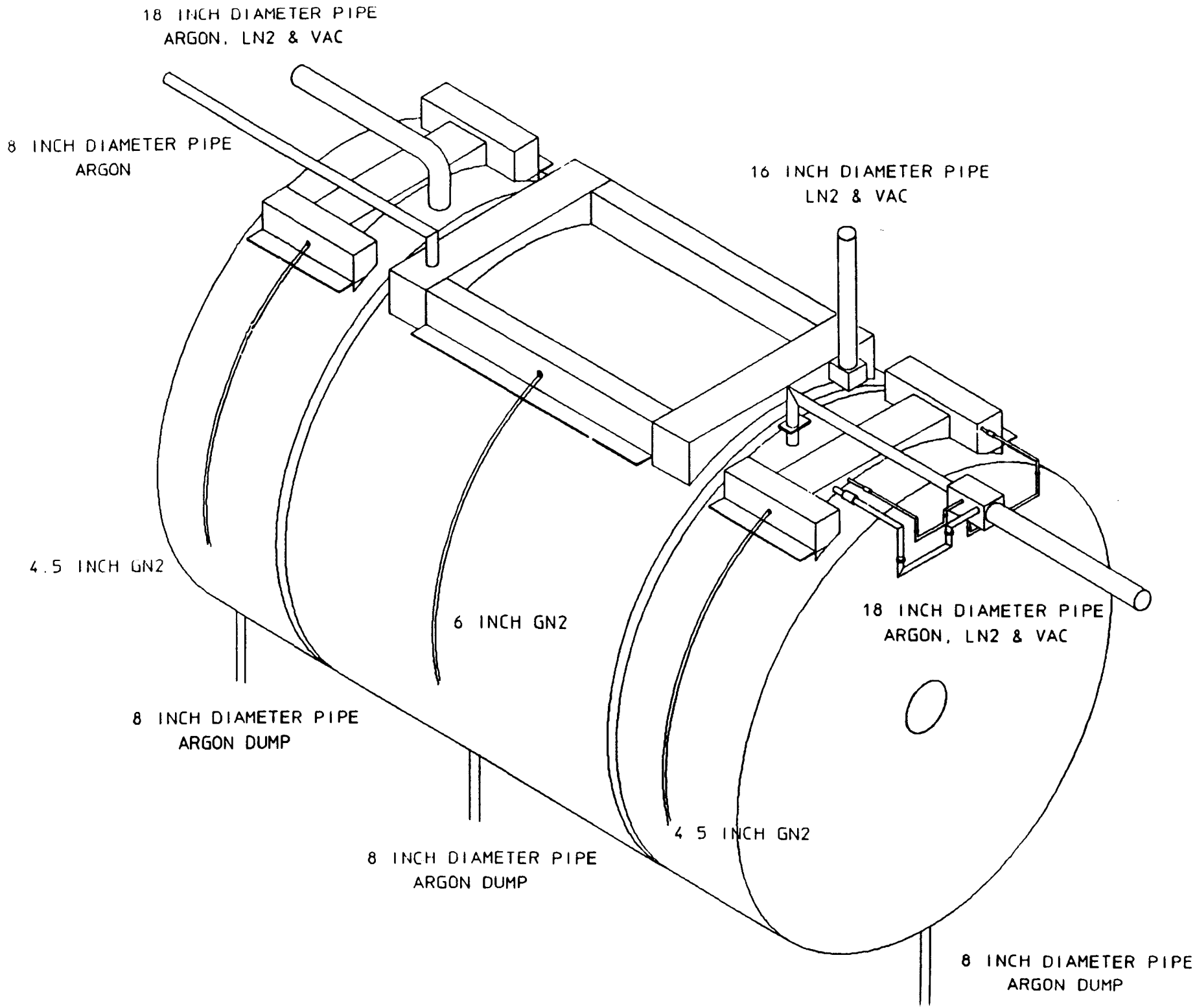
18 INCH DIAMETER PIPE
ARGON, LN2 & VAC
8 INCH DIAMETER PIPE
ARGON
16 INCH DIAMETER PIPE
LN2 & VAC
4.5 INCH GN2
6 INCH GN2
18 INCH DIAMETER PIPE
ARGON, LN2 & VAC
8 INCH DIAMETER PIPE
ARGON DUMP
4 5 INCH GN2
8 INCH DIAMETER PIPE
ARGON DUMP
8 INCH DIAMETER PIPE
ARGON DUMP

4/11/91

Fig. 16

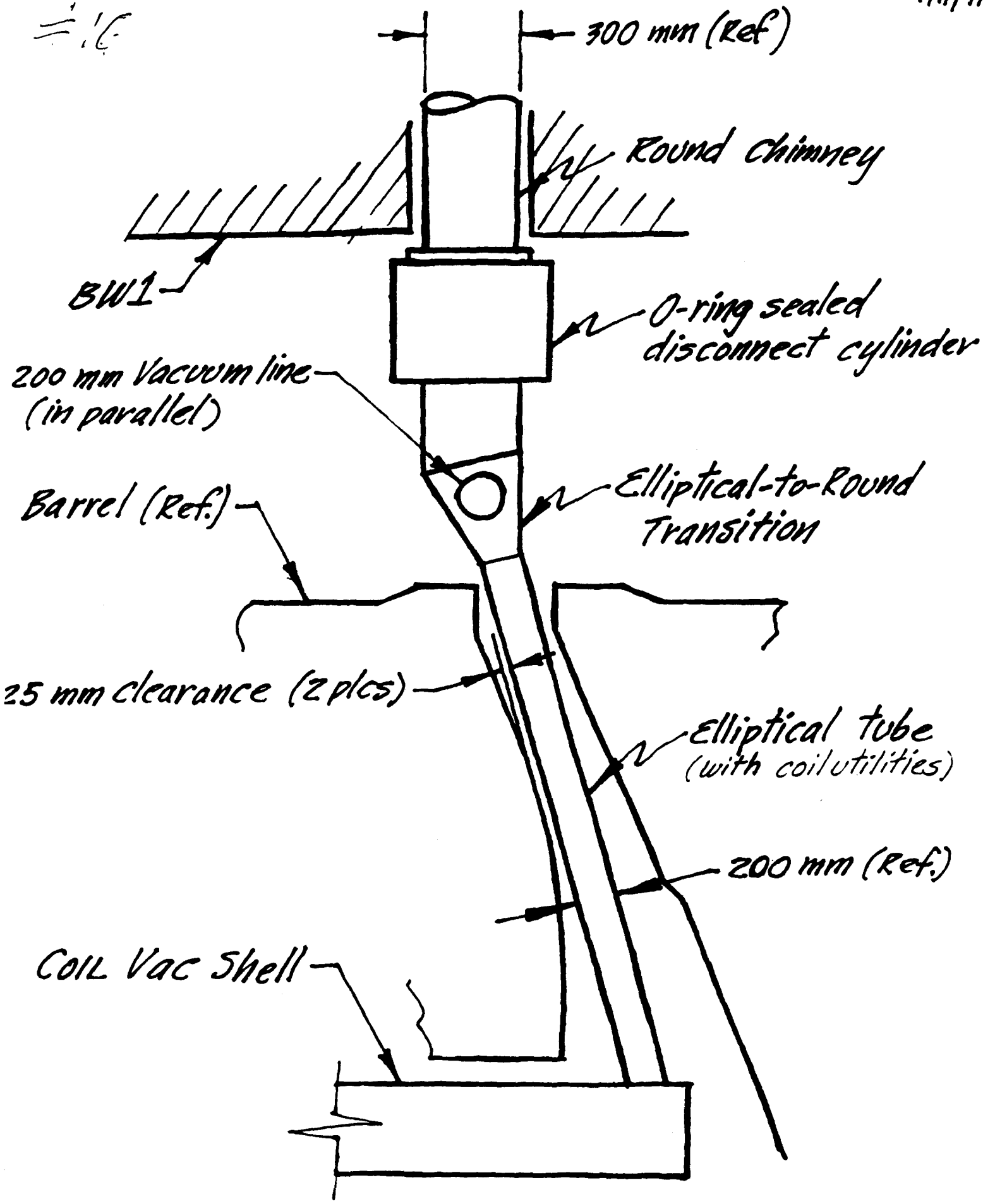
300 mm (Ref)
Round Chimney
BW1
O-ring sealed disconnect cylinder
200 mm Vacuum line (in parallel)
Elliptical-to-Round Transition
Barrel (Ref.)
25 mm clearance (2 plcs)
Elliptical tube (with coil utilities)
200 mm (Ref.)
Coil Vac Shell

SDC LAr Calorimeter Cost Summary

Modules	30,916
Cryostat	21,879
Feedthrus	5,010
Calorimeter Assembly	2,905
Fixtures	10,135
Test Equipment	1,640
Transportation	1,152
Cryogenic System	7,900
Facilities	2,000
Return Iron	4,681
EDIA	17,516
Total	105,734
Contingency (28.0%)	29,602
Total w/Contingency	135,336
Derived $/lb	11.74

7/31/91

Appendix A - SDC LAr Calorimeter Cost Roll-Up

	Procurement ($k)	Mfg Labor ($k)	EDIA ($k)	WBS Base ($k)	Cont. ($k)	WBS Total ($k)
Modules	16,141	14,775	4,652	35,568	8,537	44,105
Cryostat	4,949	16,930	4,800	26,679	6,877	33,556
Feedthrus	4,362	647	356	5,366	1,445	6,811
Calorimeter Assembly	0	2,905	2,666	5,571	1,448	7,019
Tooling/Fixtures	6,326	3,809	4,028	14,164	5,043	19,207
Test Equipment	1,640	0	89	1,729	588	2,316
Transportation	1,152	0	136	1,289	438	1,727
Cryogenic System	7,900	0	428	8,328	2,831	11,159
Facilities	2,000	0	108	2,108	717	2,825
Return Iron	4,681	0	253	4,934	1,678	6,612
Total	49,152	39,066	17,516	105,734	29,602	135,336

SDC LAC Downsizing Options (Barrel Only)

LAC Barrel Baseline

	Material ($k)	Mfg Labor ($k)	EDIA ($k)	WBS Base ($k)	Cont. ($k)	WBS Total ($k)
Modules	9,505	7,655	2,235	19,395	4,566	23,961
Cryostat	2,003	5,847	2,087	9,937	2,556	12,493
Feedthrus	2,394	304	192	2,890	776	3,667
Calorimeter Assem	0	1,378	1,287	2,665	693	3,358
Tooling/Fixtures	3,566	3,809	2,731	10,107	3,257	13,364
Test Equipment	1,640	0	89	1,729	588	2,316
Transportation	620	0	68	689	234	923
Cryogenic System	7,900	0	428	8,328	2,831	11,159
Facilities	2,000	0	108	2,108	717	2,825
Return Iron	4,681	0	253	4,934	1,678	6,612
Total	34,309	18,993	9,479	62,782	17,896	80,678

Calorimeter Location Sensitivity

	Outside Rad. (cm)	Inside Rad. (cm)	Surface Area (cm^2)	% of Baseline Volume	Total Cost ($k)	Delta Cost ($k)	
Baseline	428.5	233.1	406,135	100%	80,678	0	
Option 1	418.5	223.1	393,857	97%	78,872	-1,806	move LAC in 10 cm
Option 2	398.5	203.1	369,303	91%	75,261	-5,417	move LAC in 20 cm
Option 3	368.5	173.1	332,470	82%	69,844	-10,834	move LAC in 40 cm

1. length of calorimeter stays constant
2. material costs decrease by volume
3. number of layers is constant (no impact to module assembly labor)
4. cryostat/calorimeter assembly scales by volume

Calorimeter Inside Radius Cost Sensitivity

	Outside Rad. (cm)	Inside Rad. (cm)	Surface Area (cm^2)	% of Baseline Volume	Total Cost ($k)	Delta Cost ($k)	
Baseline	428.5	233.1	406,135	100%	80,678	0	
Option 1	428.5	209.8	438,568	108%	86,213	5,535	move inside radius in 10%
Option 2	428.5	188.8	464,838	114%	90,077	9,399	move inside radius in 20%
Option 3	428.5	169.9	486,118	120%	93,206	12,529	move inside radius in 40%

1. length of calorimeter stays constant
2. material costs increase by volume
3. number of layers increases with depth (module assembly labor)
4. cryostat/calorimeter assembly scales by volume

SDC LAC Downsizing Options (Barrel Only)

Calorimeter Length Cost Sensitivity

	Outside Rad. (cm)	Inside Rad. (cm)	Length (cm)	Volume (m^3)	% of Baseline Volume	Total Cost ($k)	Delta Cost ($k)	
Baseline	428.5	233.1	802.0	326	100%	80,678	0	
Option 1	428.5	233.1	702.0	285	88%	73,230	-7,448	move ends in 0.5 m
Option 2	428.5	233.1	602.0	244	75%	65,783	-14,895	move ends in 1 m
Option 3	428.5	233.1	402.0	163	50%	50,887	-29,791	move ends in 2 m

1. radius of calorimeter stays constant
2. material costs decrease by volume
3. number of layers is constant (no impact to module assembly labor)
4. cryostat/calorimeter assembly scales by volume

Channel Count Sensitivity

	# of Feedthrus	# of Channels	Feedthru ($k)	Electronics ($k)	LAC Total ($k)	Delta Cost ($k)	
Baseline	102	93,696	3,667	23,424	80,678	0	
Option 1	92	84,326	3,300	21,082	80,311	-367	10% decrease in channels
Option 2	77	70,272	2,750	17,568	79,761	-917	25% decrease in channels
Option 3	51	46,848	1,833	11,712	78,844	-1,833	50% decrease in channels

1. feedthru costs scale by channel count
2. signal handling scales by channel count
3. assume $250/channel

Pb Cast Modules

	Materials ($k)	Mfg Labor ($k)	EDIA ($k)	Base ($k)	WBS Total ($k)	Delta Cost ($k)
Baseline	16,141	14,775	4,652	35,568	44,105	0
Cast	21,822	8,370	3,763	33,955	41,067	-3,038

1. Pb $/lb changes from $0.77/lb (sheets) to $1.66/lb (hadronic), $1.26/lb (tiles) to $2.53/lb (EM)
2. Pb stacking steps eliminated
4. Straps eliminated
5. Module Assembly steps revised

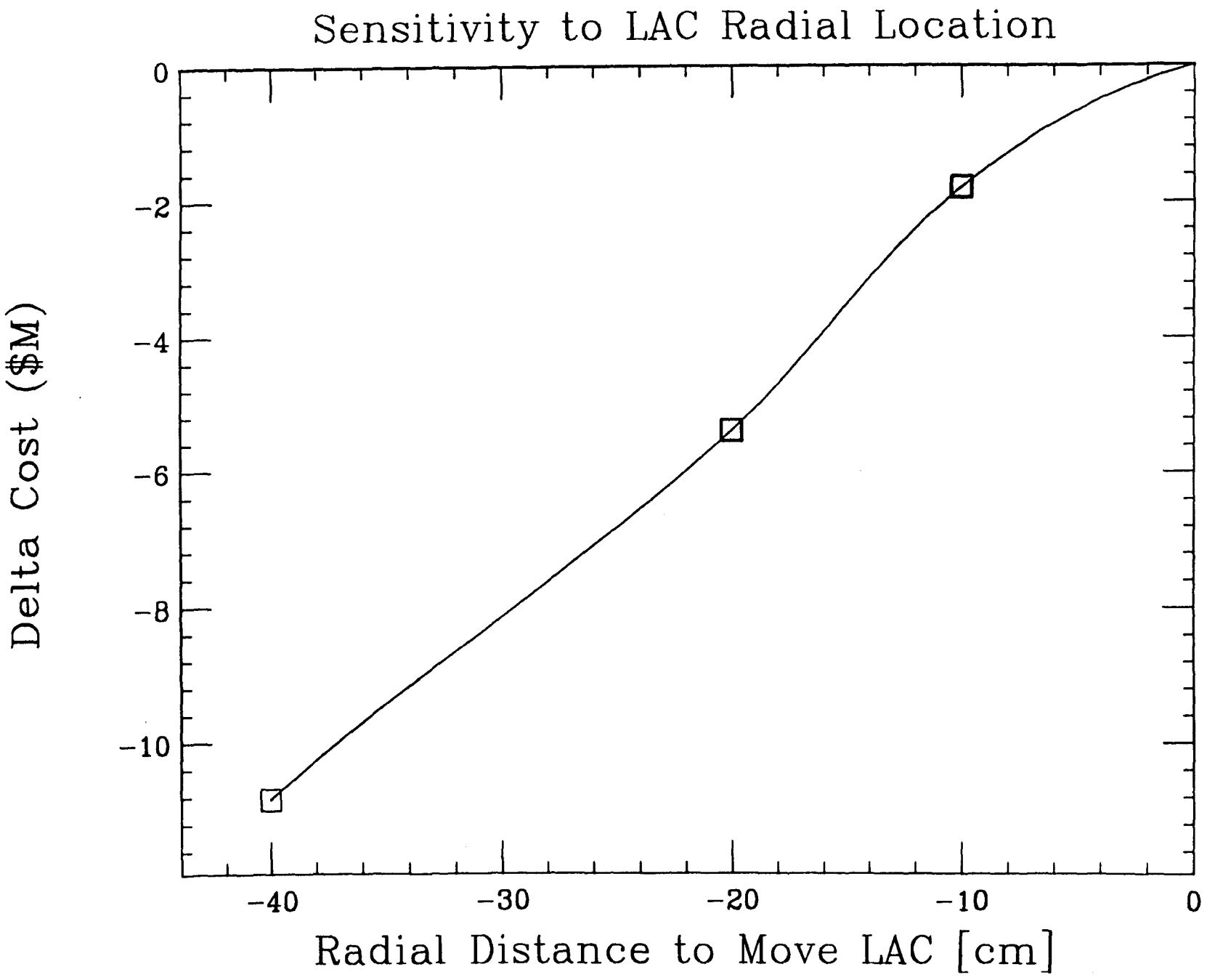
Sensitivity to LAC Radial Location
Delta Cost ($M)
0
-2
-4
-6
-8
-10
-40
-30
-20
-10
0
Radial Distance to Move LAC [cm]

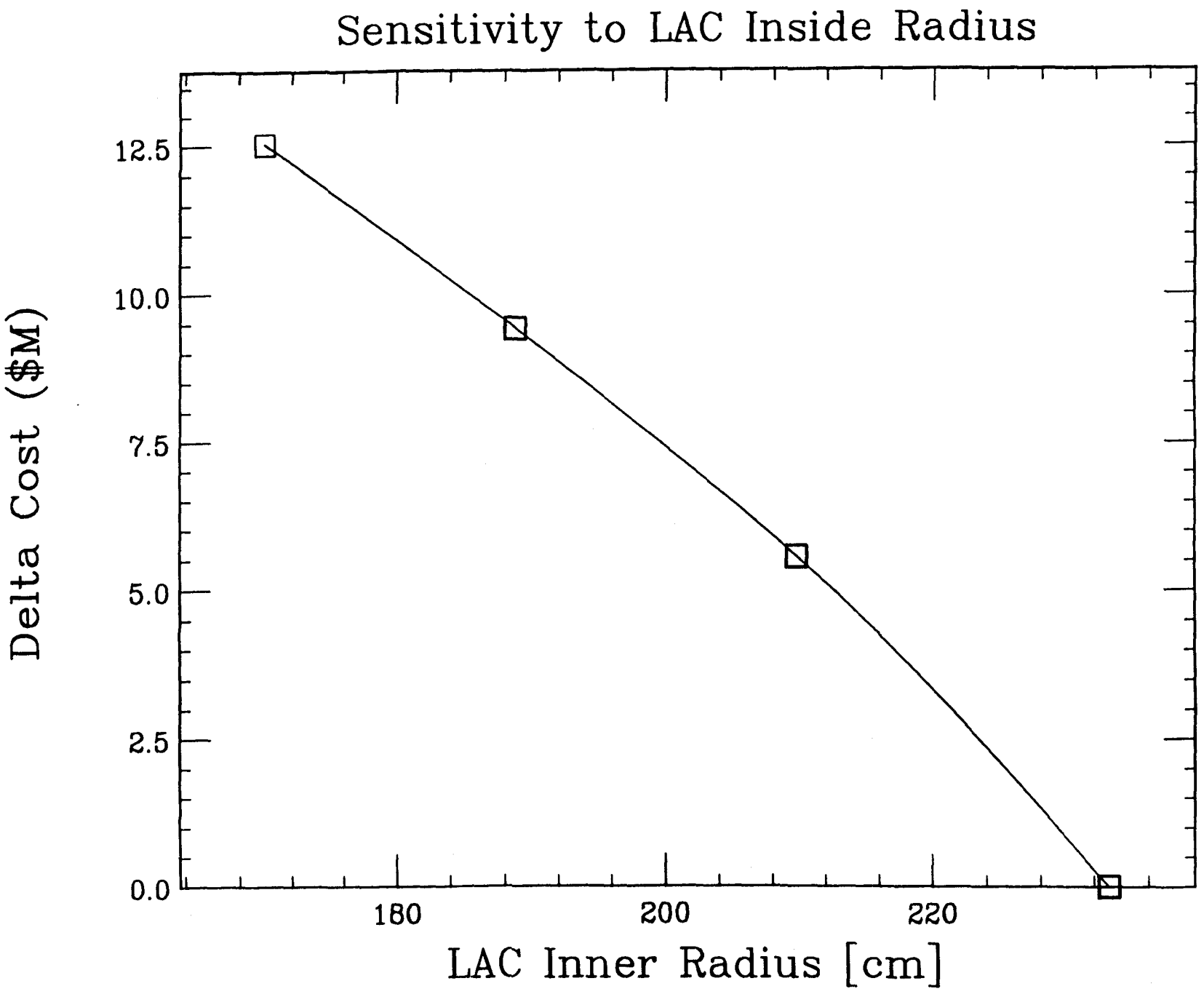
Sensitivity to LAC Inside Radius
Delta Cost ($M)
12.5
10.0
7.5
5.0
2.5
0.0
180
200
220
LAC Inner Radius [cm]

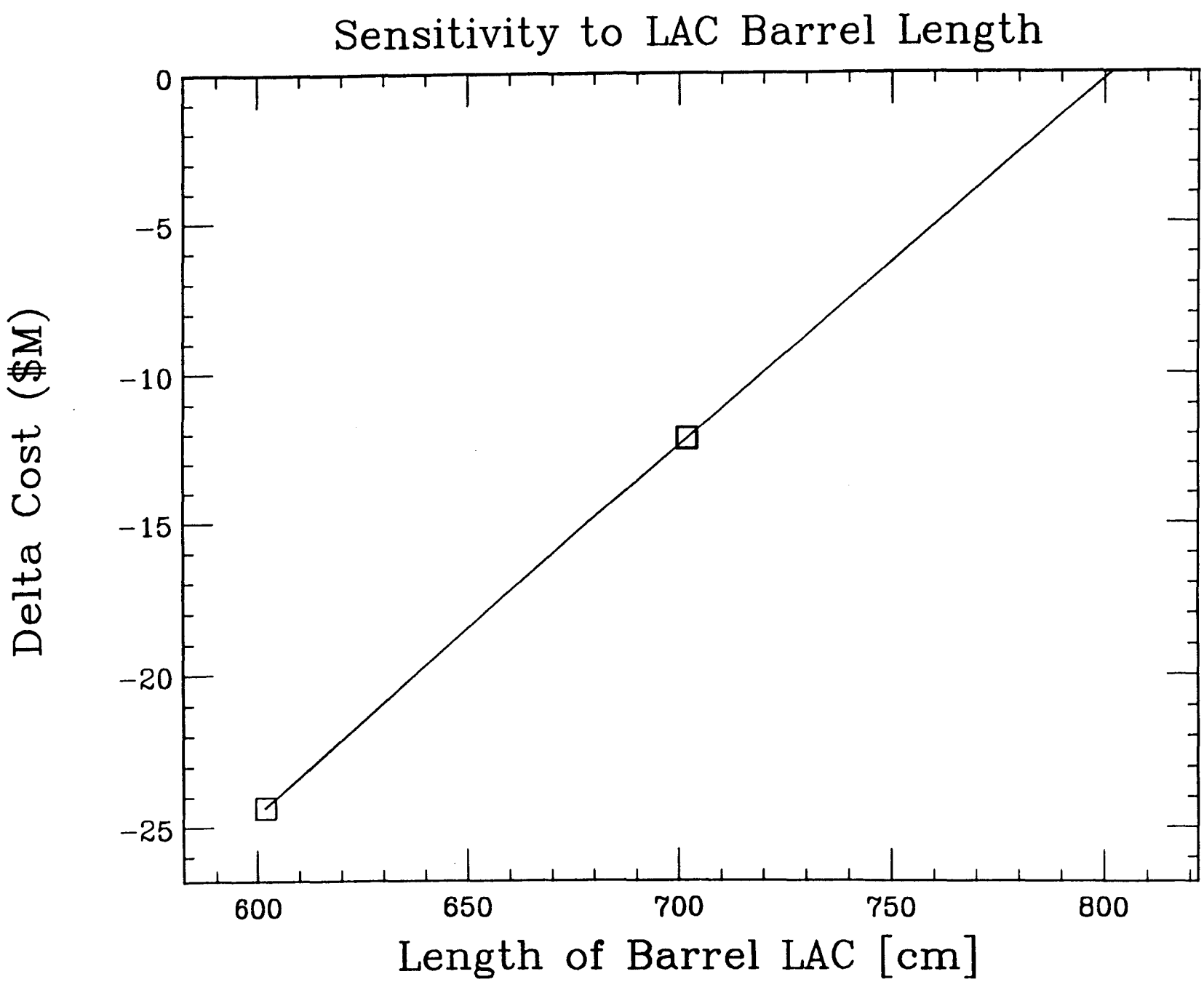
Sensitivity to LAC Barrel Length
Delta Cost ($M)
0
-5
-10
-15
-20
-25
600
650
700
750
800
Length of Barrel LAC [cm]

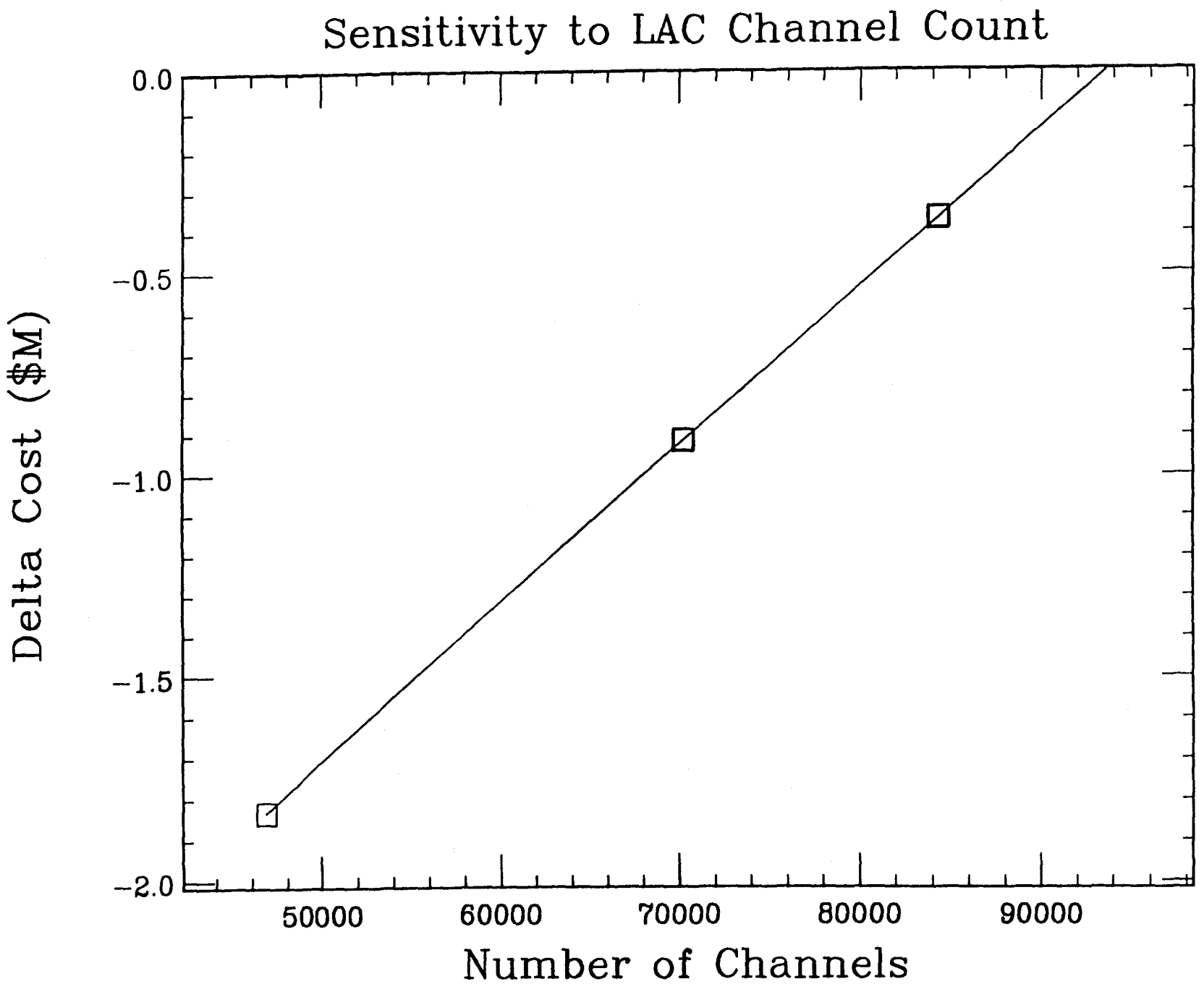
Sensitivity to LAC Channel Count
0.0
−0.5
−1.0
−1.5
−2.0
Delta Cost ($M)
50000
60000
70000
80000
90000
Number of Channels

Liquid Argon Calorimeter, Current Weight Summary 9/10/91

Module Details (See sketch below for Module I.D. Number)

Module I. D. No.	Outer Radius (mm)	Inner Radius (mm)	Avg. Z Length (mm)	No. of Modules per ring	No. of Absorber plates*	Module Phi Gap (mm)	Module weight each (tonn)
1	2808.0	2451.5	2650.0	64	33	3.00	1.43
2	2808.0	2451.5	2580.3	64	33	3.00	1.39
3	4429.8	2938.0	2630.0	32	87	5.00	26.90
4	4429.8	2938.0	1740.0	32	87	5.00	17.80
5	4429.8	2938.0	732.9	32	87	5.00	7.50
6	3135.0	461.0	356.5	16	33	3.00	3.80
7	3135.0	508.0	728.0	32	42	5.00	6.11
8	3135.0	593.0	1078.0	32	63	5.00	9.09
9	4495.0	3300.0	363.0	32	21	5.00	2.97
10	4495.0	3300.0	728.0	32	42	5.00	6.10
11	4495.0	3300.0	1078.0	32	63	5.00	9.10

* Absorber plates in EM Modules (1,2 & 6) are 4.0 mm thk. The rest are 14 mm thk.

Total Number of Electromagnetic Modules	224
Total Number of Hadronic Modules	480
Total Number of Modules	704

Module Weight

Barrel Modules	2749	(tonn)
Endcap Modules	2258	(tonn)
Total Modules	5007	(tonn)

Cryostat Weight (not changed)

Barrel Cryostat	206	(tonn)
Endcap Cryostat (2)	123	(tonn)
Total Cryostat	452	(tonn)

Calorimeter Weight (not including LAr)

Barrel Calorimeter	2955	(tonn)
Endcap Calorimeter	2504	(tonn)
Total Calorimeter	5459	(tonn)

≅ 4.4 % increase since L0

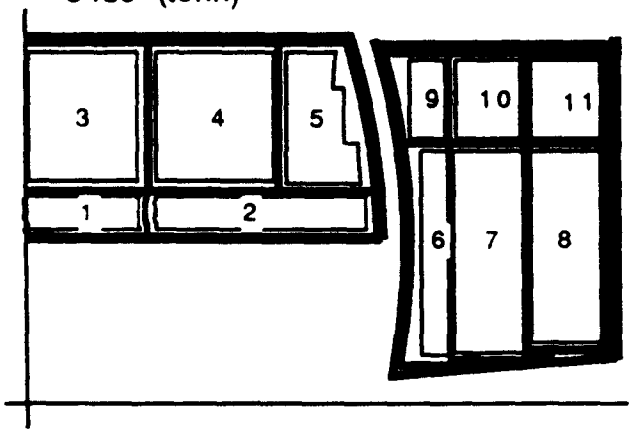

LAC Module Numbering

Parameters for the SDC Liquid Argon Calorimeter

Gerry Abrams
Sept. 11, 1991

<u>Mechanical Parameter</u>	
Barrel	
Volume	$4.2 \times 9.7 \times 8.4\ m^3$ (id × od × length)
Weight	2955 tonne
Total Depth (at 90°)	9 λ
Had Depth	8 λ
Endcap	
Volume (each)	$0.1 \times 9.7 \times 3.9\ m^3$ (id × od × length)
Weight (each)	1252 tonne
Total Depth	11 λ
Had Depth	10 λ
Both Barrel and Endcap	
Lateral Segmentation	0.05×0.05 ($\delta\eta \times \delta\phi$), coarser for $\eta > 1.9$
EM Pb absorber thickness	4 mm
EM Depth	25 X_0 (33 layers)
Had Pb absorber thickness	14 mm
Longitudinal Segmentation	
EM gap structure	Pb / 2mm LAr / 1.6mm G10 / 2mm LAr
EM Section	2 depths, 5 layers ($1 \rightarrow 5$), 26 layers ($8 \rightarrow 33$)
Had gap structure	Pb / 2mm LAr
Had Section	2 depths, HAD1 3.2 λ, HAD2 4.8 λ
Massless Gap	Standard 0.05×0.05, Separate readout
Shower Max Detector	2 layers, η and ϕ, 0.05/6 segmentation (at layers 6 and 7, $\approx 5\ X_0$)
Channel Count total)	97,024
Region immune from radiation damage	$\eta < 5$

LAC R&D

FY92

Had prototype

Convective preamp cooling

Front End Electronics -

- Calibration
- Rad Hard Preamp
- Shaper
- Trigger unit - bunch tagging

FY93

More Front End

CALORIMETER REVIEW AND TECHNICAL BOARD MEETING
SEPTEMBER 12 -14, 1991
SSCL

Presentation by:

Yoshinobu Unno

KEK

SDC Central Calorimeter Liquid Argon Option

- Performance at design and higher luminosity -

Y.Unno
KEK

and

The SDC Liquid Argon Group

- Electron hermeticity
- Electromagnetic Calorimeter Thickness
- η=3 issue, and missing E_T ; Gluino production
- Induced hadronic resolutions with the (dead) iron for the magnetic shielding
- Beam tests of EM and Hadronic prototype
- Summary

Y.Unno 1991/9/12

Critical Issues for the LAC

Item	Status	Comment
Speed	**solved**	$\tau_{rise} \leq 30$ns
Noise	**solved**	τ_p=60(EM), 200ns(HAD1) σ_{E_t}~0.7GeV (ΔR<0.15)
Pileup	**solved**	τ_p=60(EM), 200ns(HAD1) σ_{E_t}~0.9GeV(ΔR<0.15)
e hermeticity	**solved**	97%accept.(σ_E<25%/$\sqrt{E}$)
η=3,$\not{E}_t$	**solved**	LBL, KHI
e/h	**solved**	beam test; *e/h*~1.25
Preamp (Rad.hard)	**solved**	BNL hybrid: >10^{13}n/cm^2, >12Mrad
Reliability	**solved**	<0.2% failure(SLD) in 10^8s
P/a cooling	**solved**	KEK/Rochester test results
Safety	**solved**	SSCL Safety committee
Integration	in progress	LBL
Cost	**solved**	MMA; $135M(undescoped)

• Electron hermeticity

Wall thickness around η=1.2~1.3 for electron acceptance

- Thining the Barrel walls→Cryostat cut-view
- Utilization of the extra Massless gap(MLG) for the η=1.2~1.3 region→EGS modeling
- Dead material in front of the EM calorimeter without the extra MLG
- EM resolution with the MLG correction

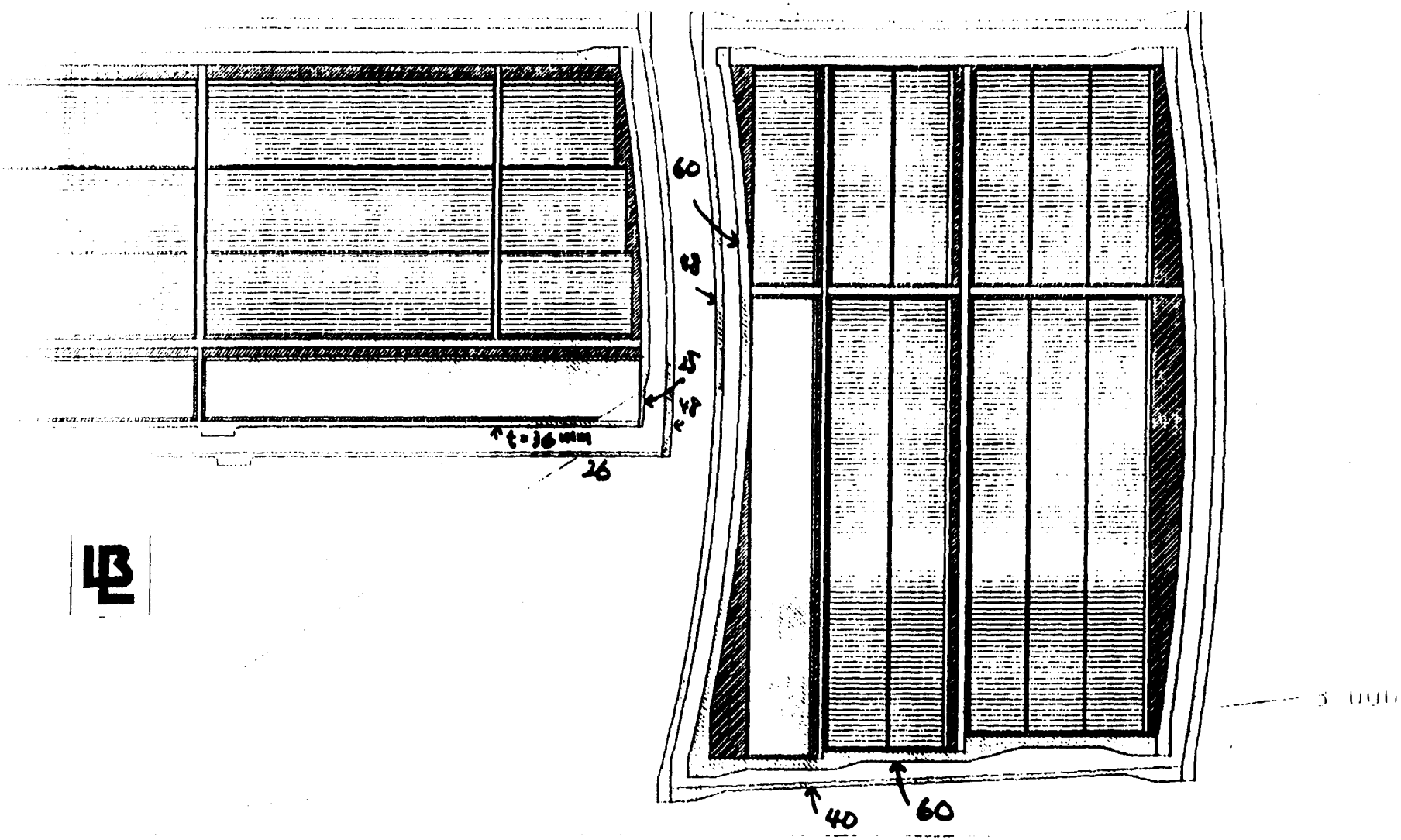

LAC NOV '90

DATE: 7-23-91

C. Hearty

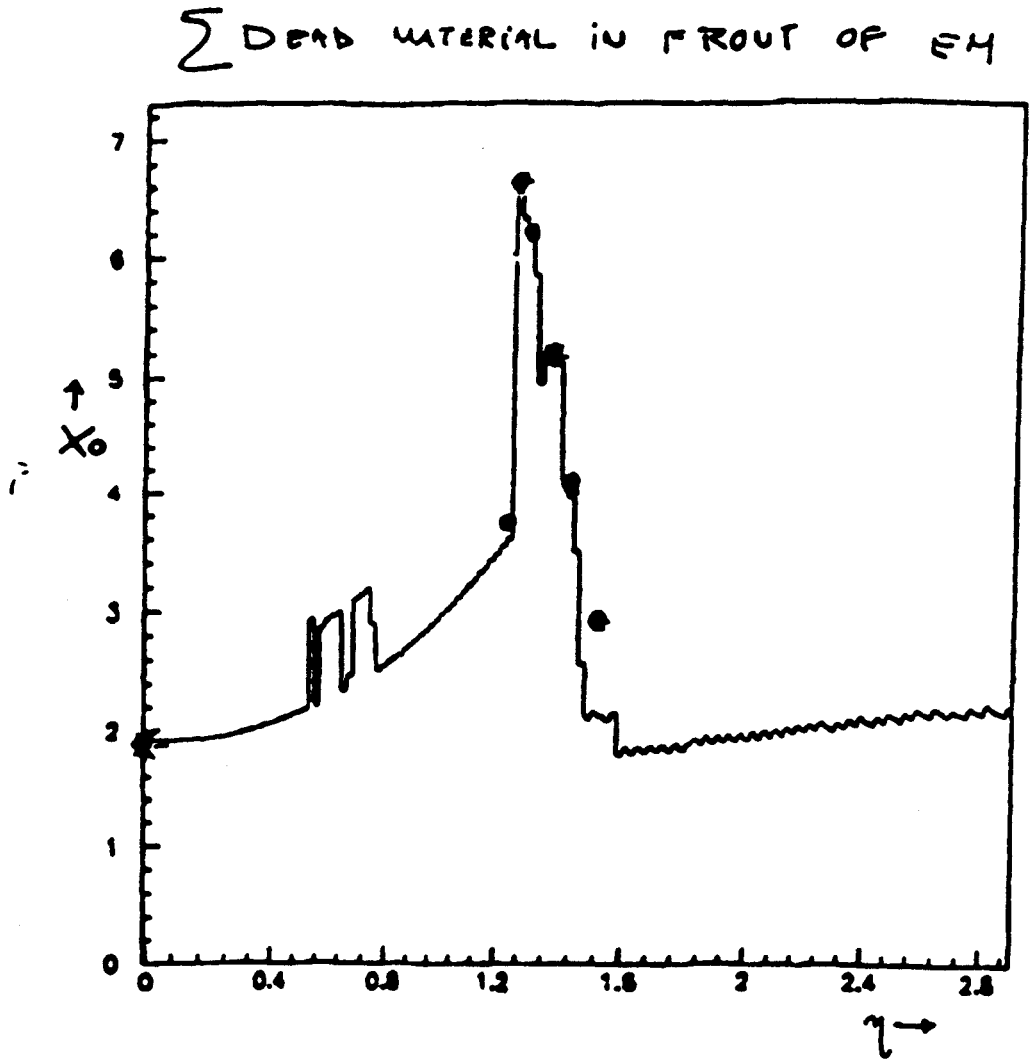

Figure 2

Massless Gap (MLG) correction

- Massless gap is commonly used when there exits a fair amount of dead material in front of the active EM calorimeter.

- The idea is to use the dead material in front as the calorimeter absorber and to make the actual first active sensing medium without an absorber (massless gap).

- Because the thickness of the dead material is usually not equal to the absorber thickness of the calorimeter, there need a weight to the response of the massless gap to the rest of the calorimeter response to equalize. The weight can be "hardwired" by thickening the medium thickness or "software" factored.

$$E_{TOTAL}=\varepsilon(\alpha E_{MLG}+E_{EM})$$

ε: energy scale

α: Massless gap weight

- The weight is obtained to recover the incident energy; peak value of the shower fluctuation.

- With the usage of MLG, the dead material is not really "dead". However, the "dead" material in front become very thick and showering tracks are started absorbed, resolution is getting increased; resolution is still recovered from the one without MLG.

C. Hearty

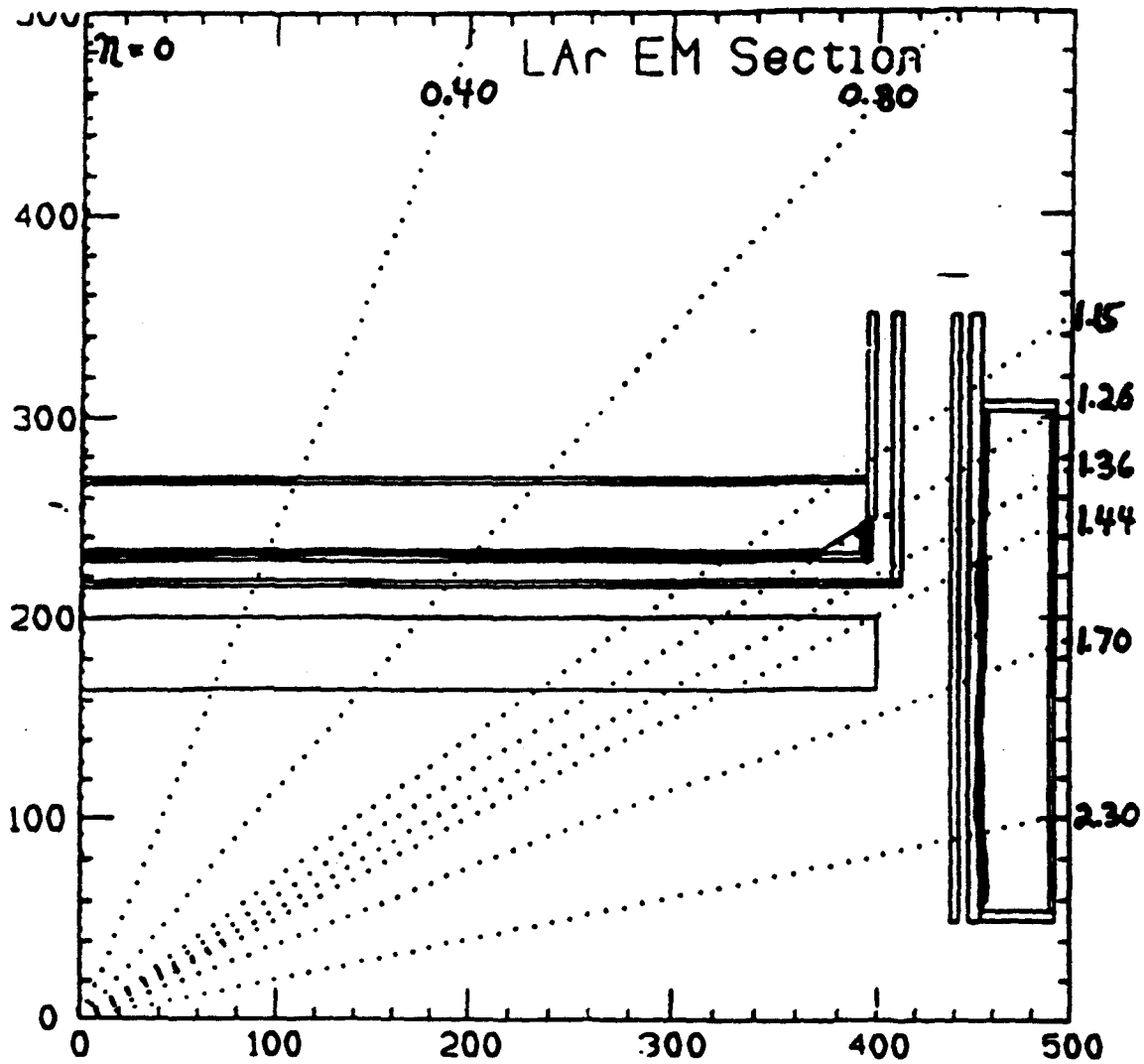

Figure 1

—Massless Gap

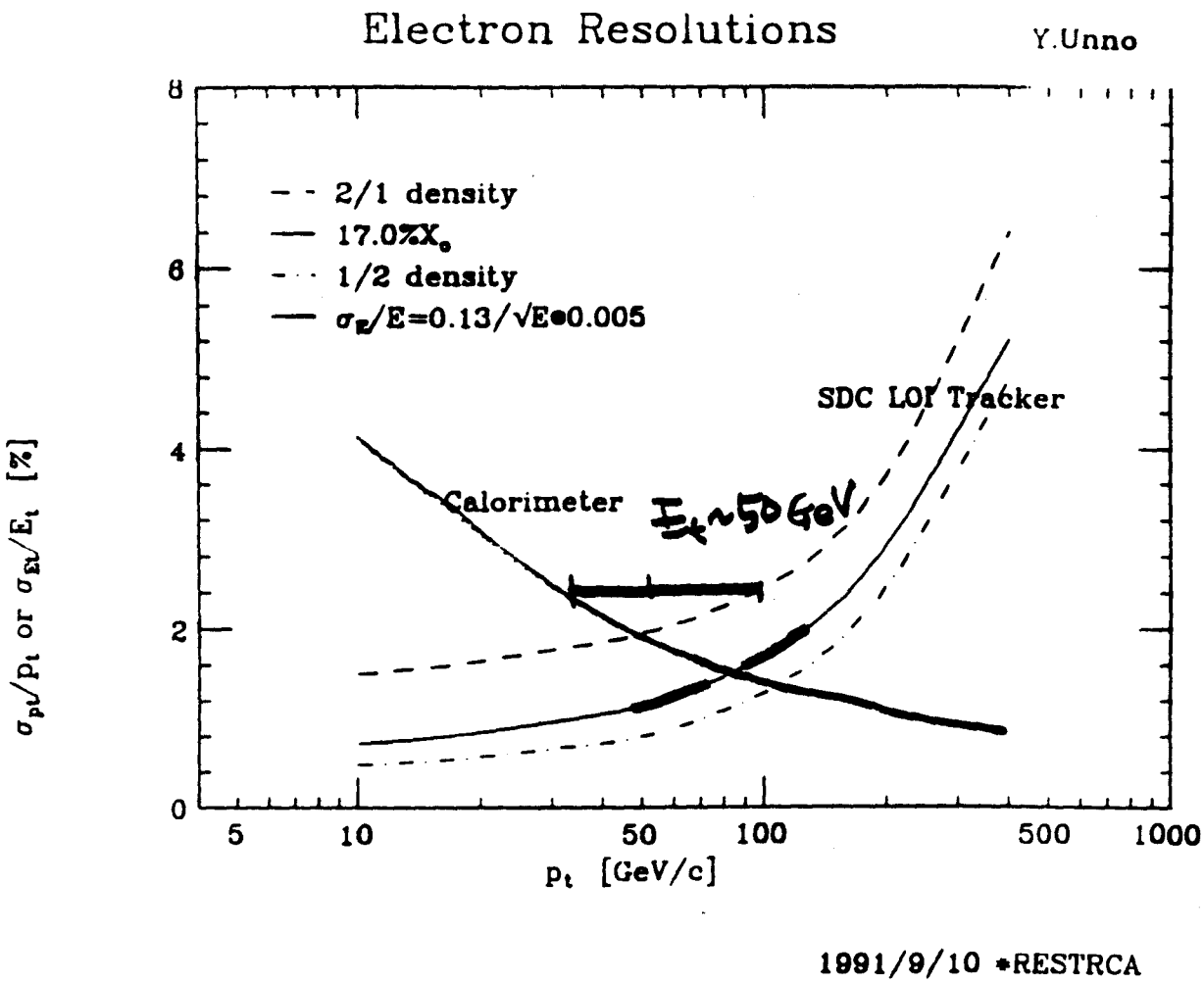

Ref. Y. Unno, "Impact of Material in the tracking volume (EGS4 simulations), SDC meeting at LBL, Aug. 1991

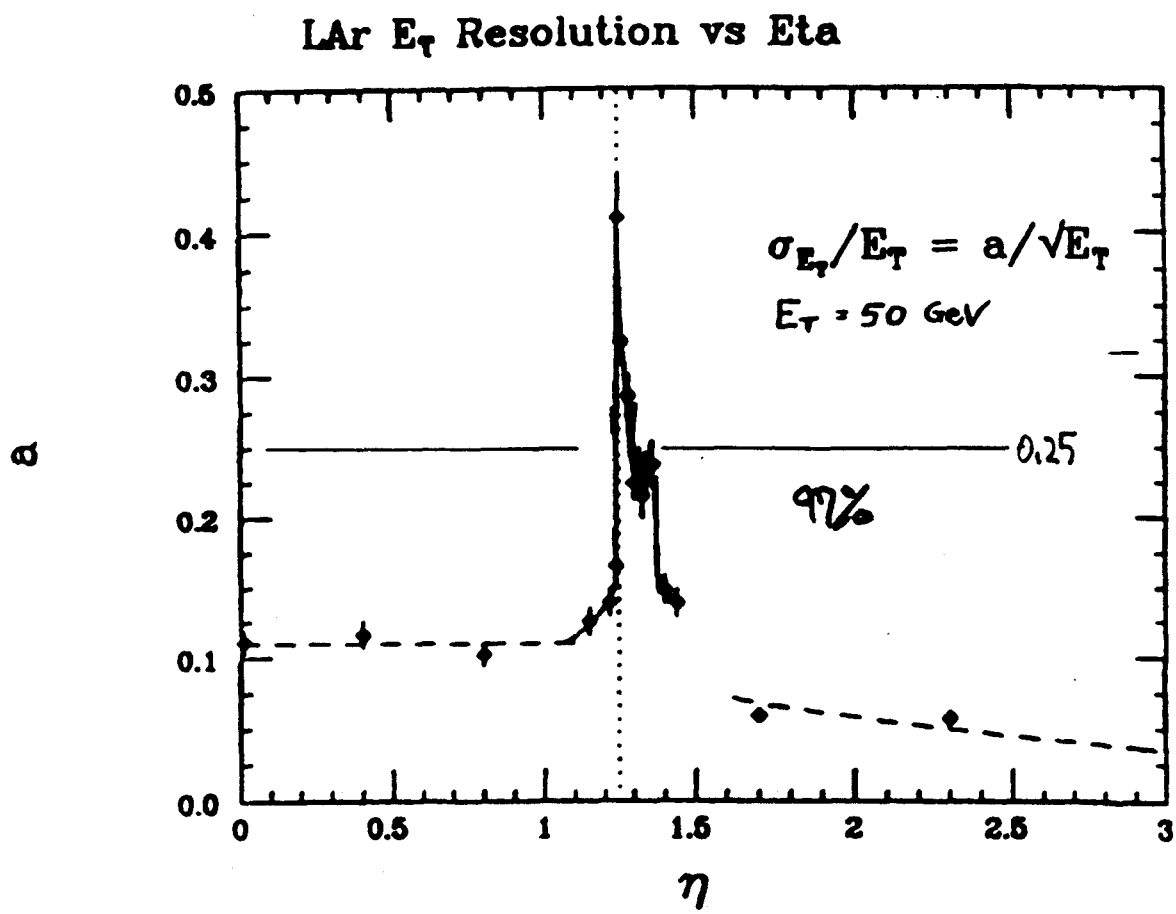
LAr E_T Resolution vs Eta
$\sigma_{E_T}/E_T = a/\sqrt{E_T}$
E_T = 50 GeV
0.25
97%
a
η
0.0
0.1
0.2
0.3
0.4
0.5
0
0.5
1
1.5
2
2.5
3

Figure 5b

Electromagnetic Calorimeter Thickness

C.Hearty (LBL), SDC-91-00084

- EGS4: (4mmPb+4mmLAr)x70 ≥ 50 Xo
  Cutoffs: 0.7 MeV for electrons; 0.1 MeV for γ's

- Split into "EM" and "HAD" sections:

  "EM": 20.4, 21,9, 23.3, 24.8, 26.2, 27.7, 29.2, 30.6
  and the rest was "HAD"

- Calculated

  leakage, linearity, resolution,...
  and induced constant term

  with and without "HAD"

  (Because of electronic noise, LAC may not use
  leakage energy into "HAD" section)

SEP 10 '91 09:10 SLAC/SLD 415 926 2923

Leakage vs EM Thickness

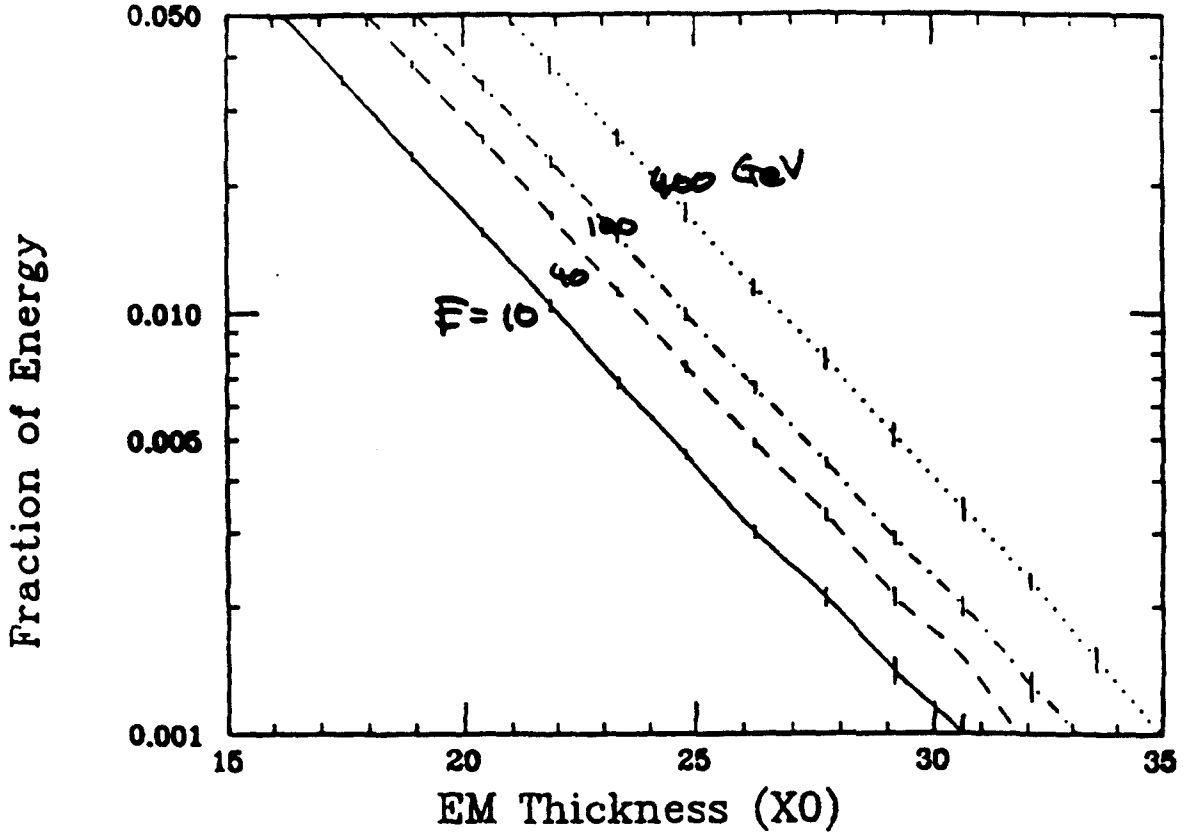

Fig. 1a

Resolution vs EM Thickness, 40 and 400 GeV

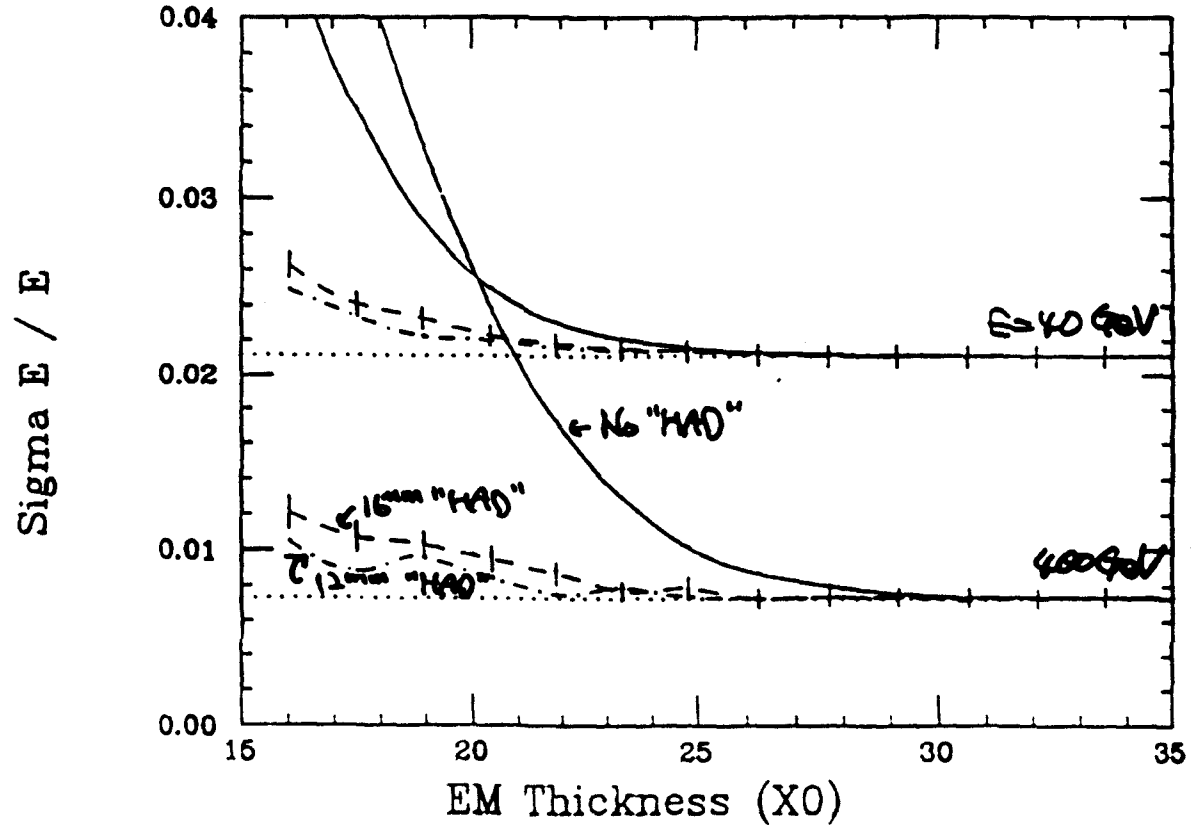

SEP 10 '91 09:11 SLAC/SLD 415 926 2923

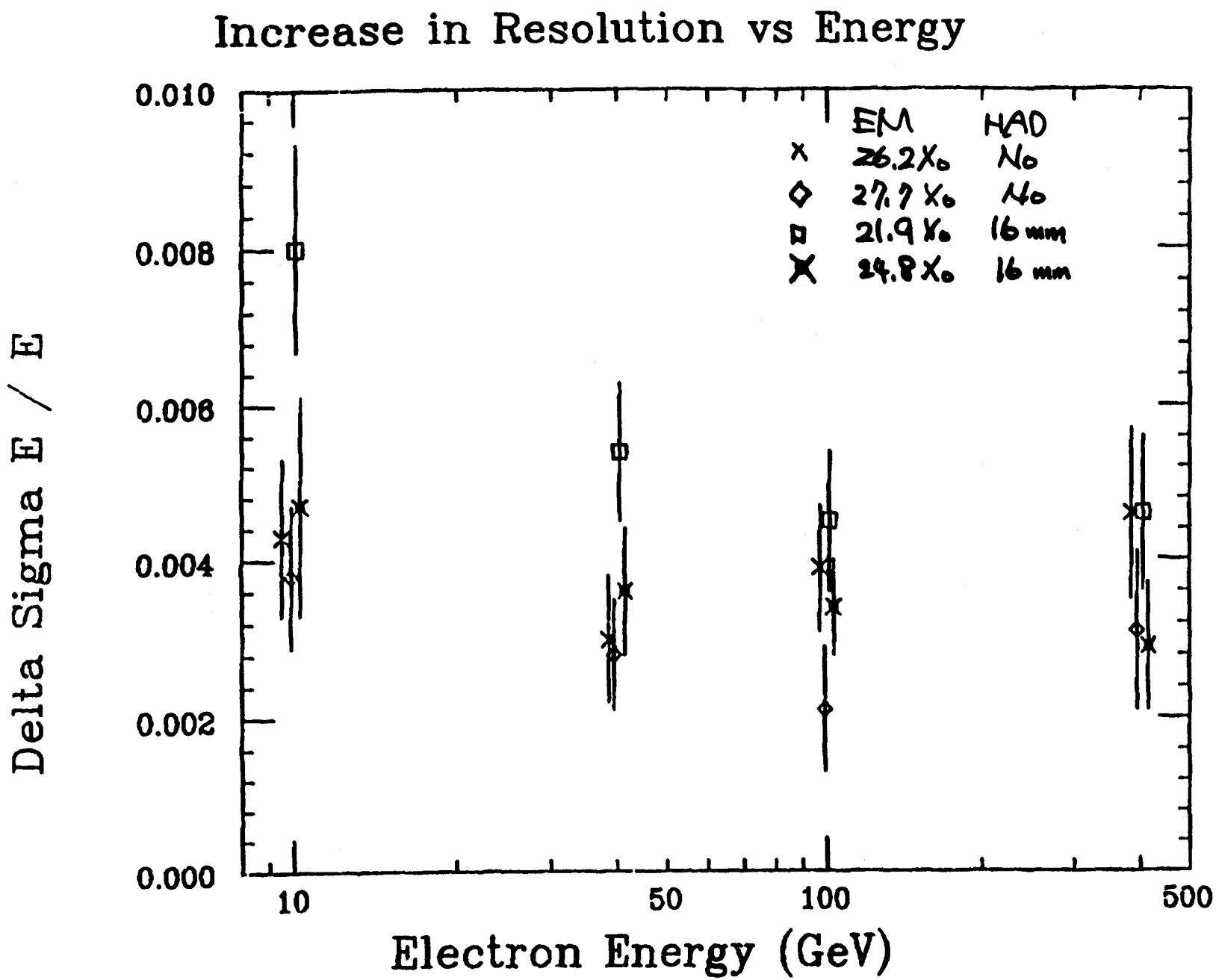
Increase in Resolution vs Energy
EM
HAD
26.2X₀
No
27.7 X₀
No
21.9 X₀
16 mm
24.8 X₀
16 mm
0.010
0.008
0.006
0.004
0.002
0.000
10
50
100
500
Delta Sigma E / E
Electron Energy (GeV)

Fig. 5

Summary of the EM thickness

- To get <0.5% constant term, the thickness must be

  ≤26 Xo if "HAD" is not used
  ≤22 Xo if "HAD" is used

  Note: Dead material preceding the calorimeter counts towards the required material.

  LAC : 25 Xo not including the dead material in front.

• η=3 issue

Wall thickness around η=3 for hadron acceptance

• The LOI design was not optimized for the issue. LBL worked out a design to thining the inner walls of the Endcap cryostat (LAr and Vacuum vessels). KEK/KHI also figured out a design for the LAr vessel.

• Dead masses in front of the calorimeter for the LOI and for the new LBL design

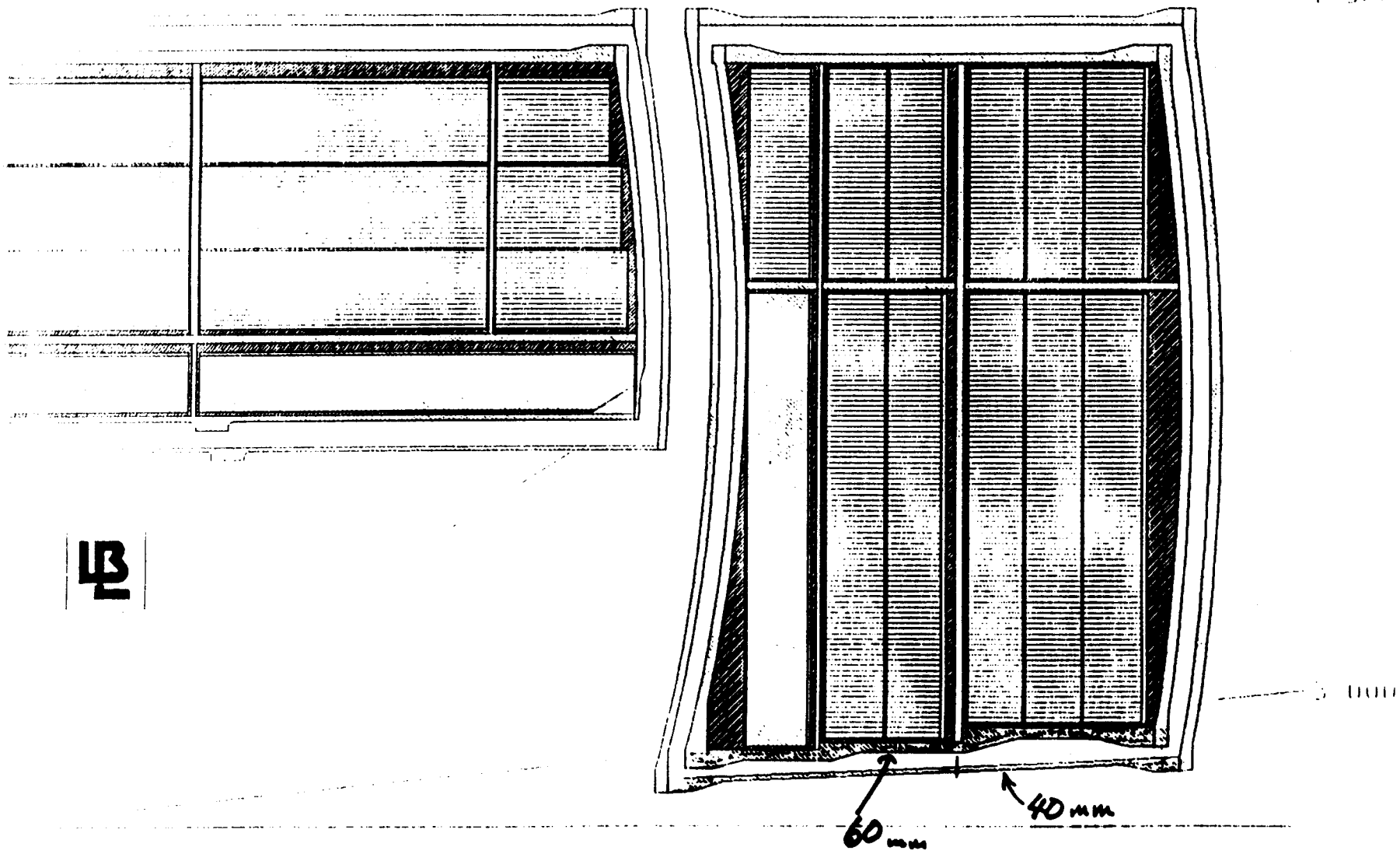

LAC NOV '90

DATE: 7-23-91

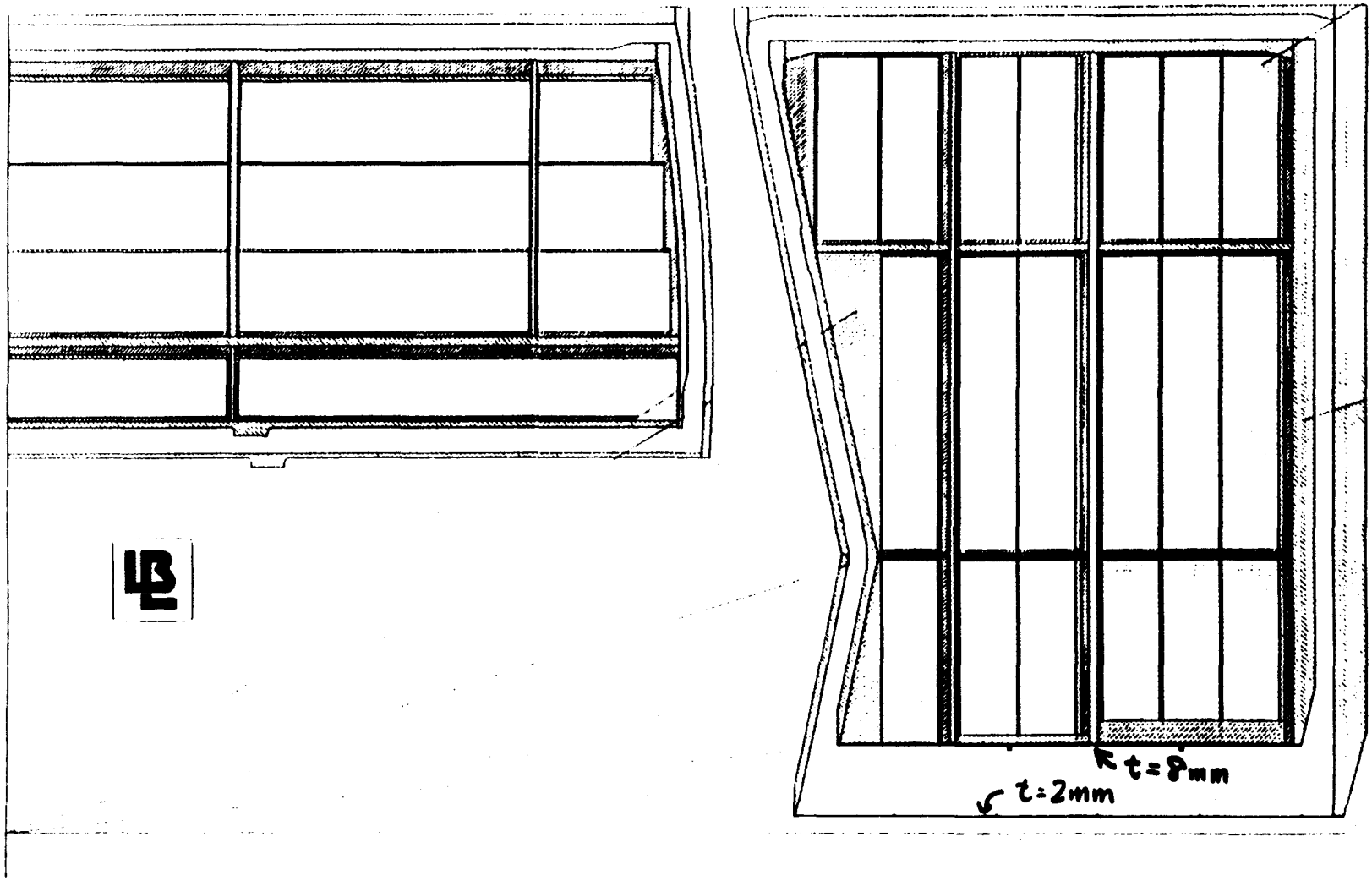

NEW LBL ENDCAP CONCEPT

DATE 8-2-91

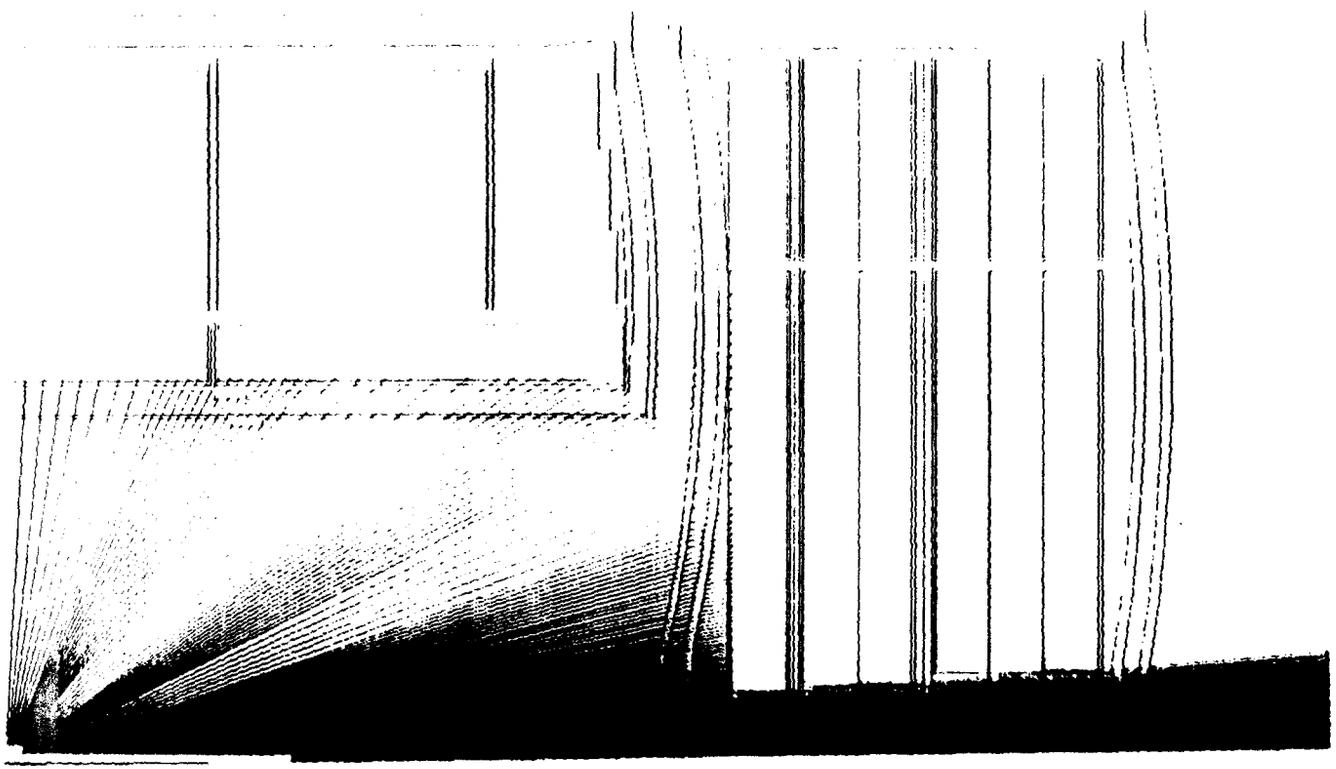

kek_wmrsly3 (Rich Weidenbach)
color (David P. O'Neill)
7-24-91

ideal foward calorimeter

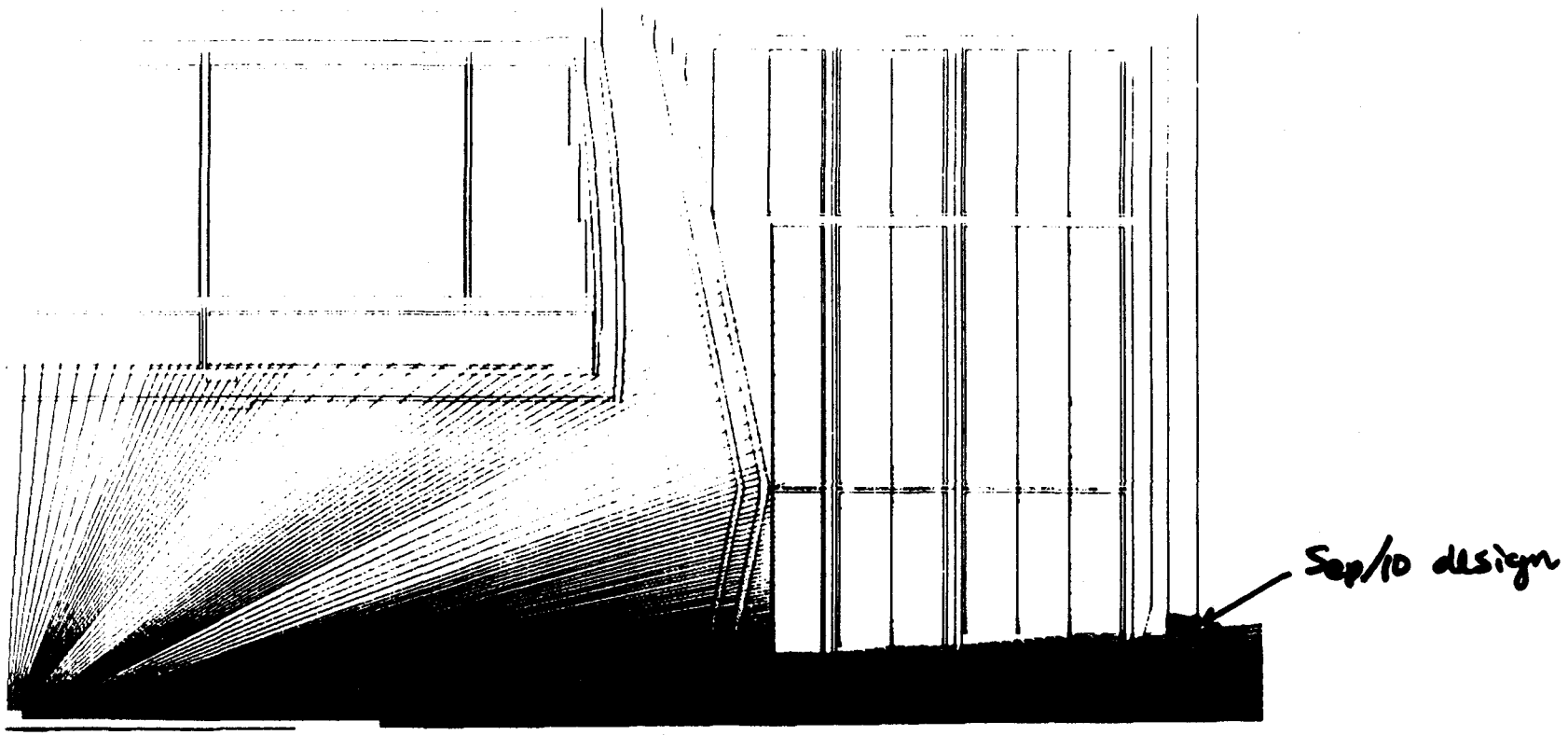

lar_wmrsly3 (Rich Weidenbach)
color (David P O'Neill)
7-24-91

ideal foward calorimeter

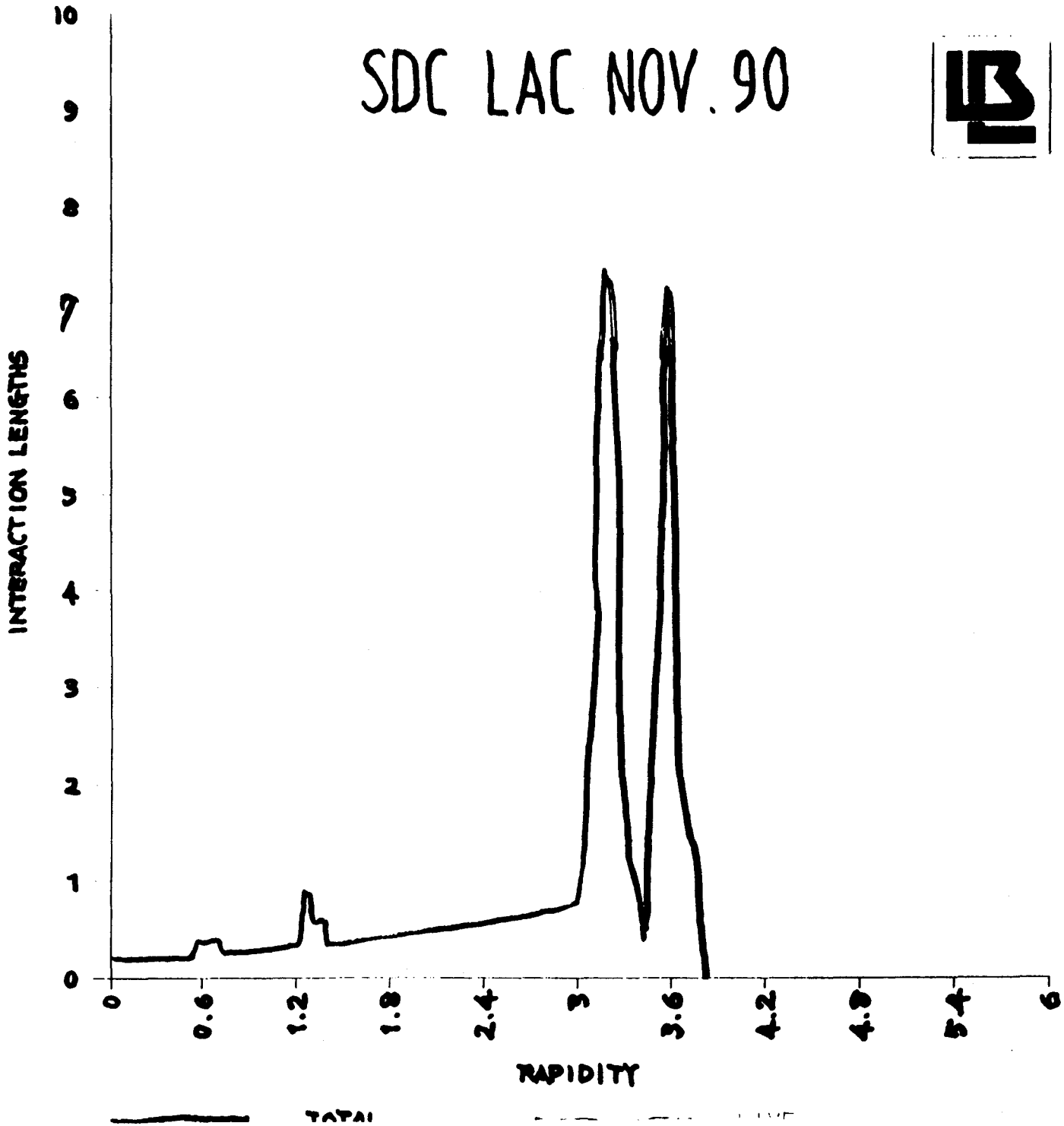
SDC LAC NOV. 90
INTERACTION LENGTHS
0
1
2
3
4
5
6
7
8
9
10
0
0.6
1.2
1.8
2.4
3
3.6
4.2
4.8
5.4
6
RAPIDITY

NEW LBL DESIGN

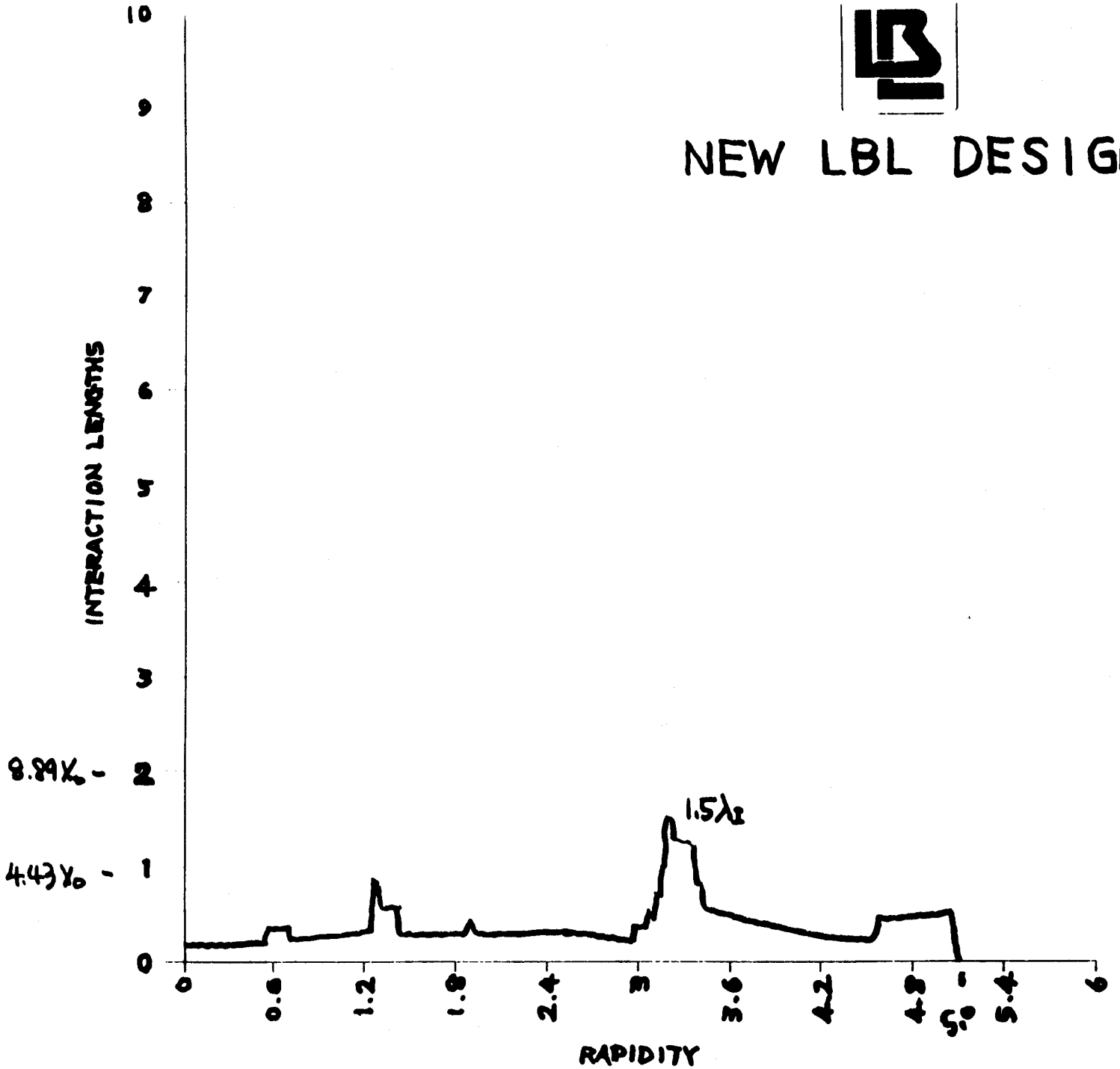

9/10/91

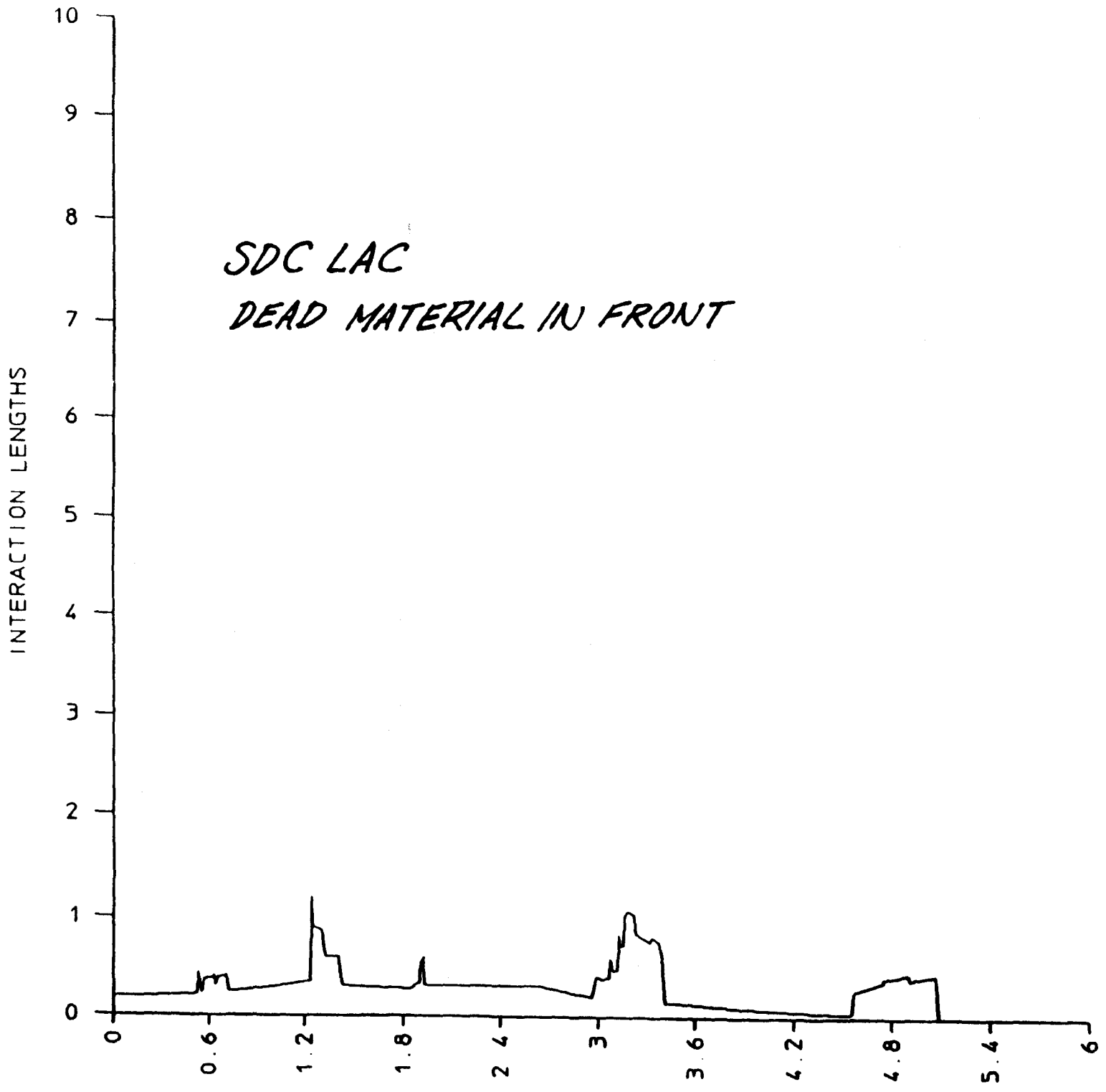
SDC LAC
DEAD MATERIAL IN FRONT
INTERACTION LENGTHS
0
1
2
3
4
5
6
7
8
9
10
0
0.6
1.2
1.8
2.4
3
3.6
4.2
4.8
5.4
6

NEW LBL DESIGN

Wormersly parameterization

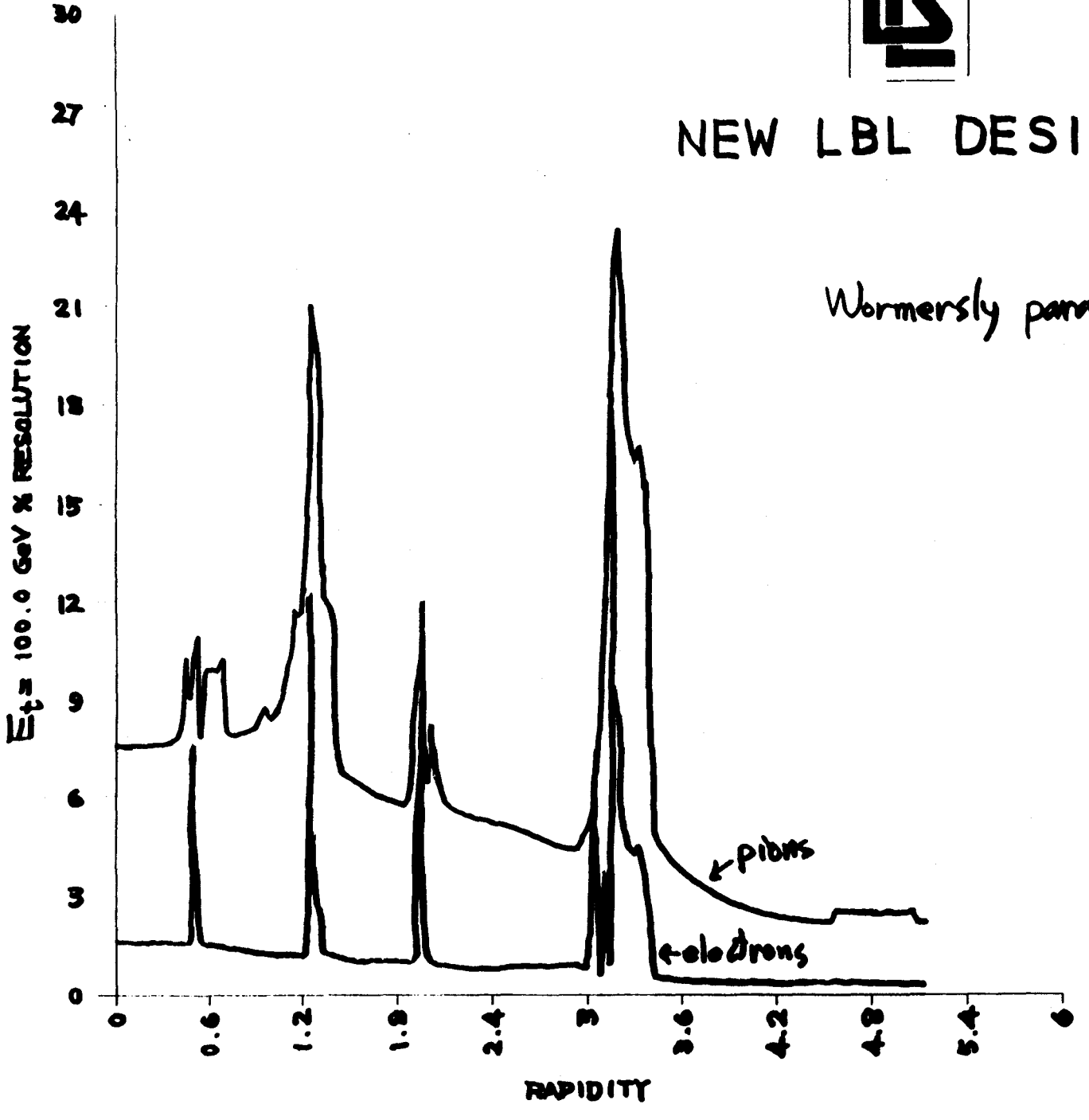

• Summary of the η=3 issue

• The material in front of the first active region of the new LBL design is

$\leq 1.5\,\lambda_I$. → $\leq 1.0\,\lambda_I$ (1991/9/10)

• There is a common ground in the LBL and KHI design and a (to be developed) KBL design will have the mass $\leq 2\,\lambda_I$ in front of the active region for $\eta \leq 5$.

$\leq 8\,X_0$ → $4\,X_0$ (1991/9/10)

missing E_T ; Gluino production

- M. Pang took the new LBL design, approximated in GEANT, and tested the effect of dead material in the η=3~5 region with a perfect forward calorimeters.

- u-quark jets of 200-900 GeV energies were generated uniformly from η=2.5 to 6.

- He made distributions of the "bias" and its sigma for the cases with and without dead materials.

  "bias"=$(E_{t\_}measured - E_{t\_}jet)/E_{t\_}jet$

- M. Barnett calculated the background from QCD jet events with mismeasurement of one or more jets. He put a conservative resolution of

  $80\%/\sqrt{E}\oplus 20\%$ for $|h|>3$

  ($80\%/\sqrt{E}\oplus 5\%$ in the LOI)

in addition with non-Gaussian smearing. In this region, the constant term is relevant.

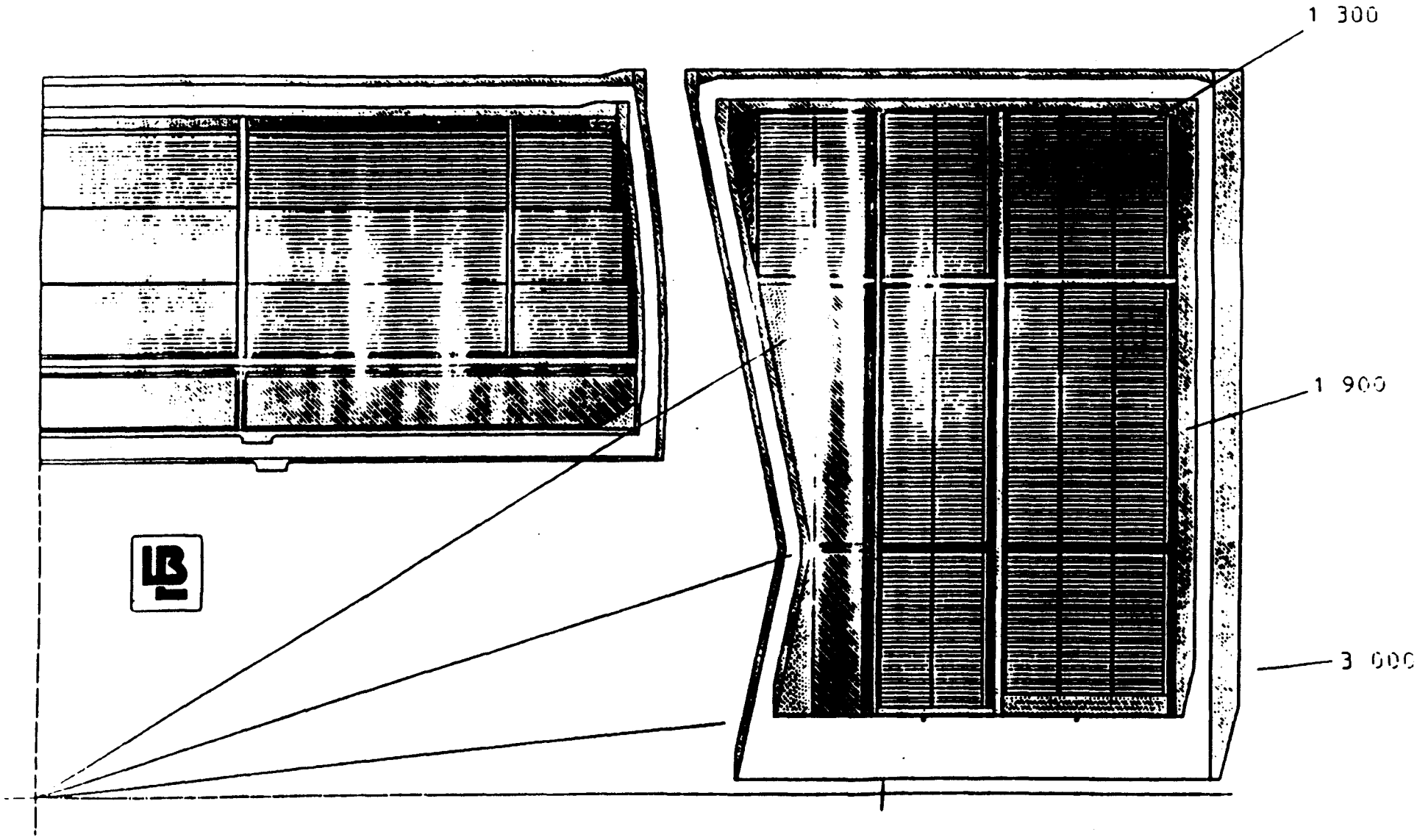

Figure 1. NEW LBL ENDCAP CONCEPT

DATE: 8-2-91

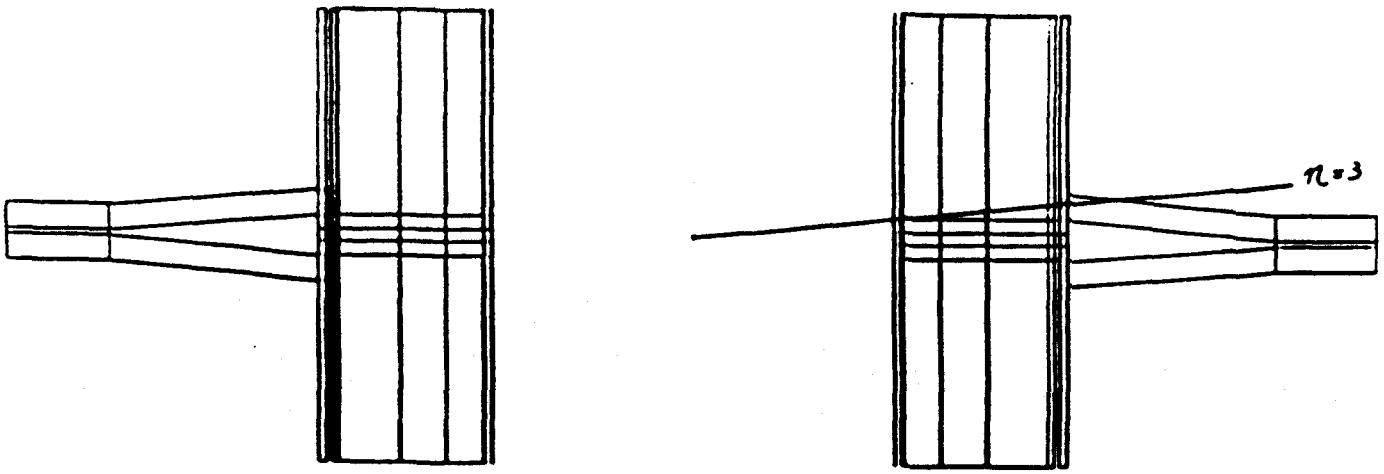

Figure 2. The geometry of the endcap and forward calorimeter with dead material in endcap calorimeter.

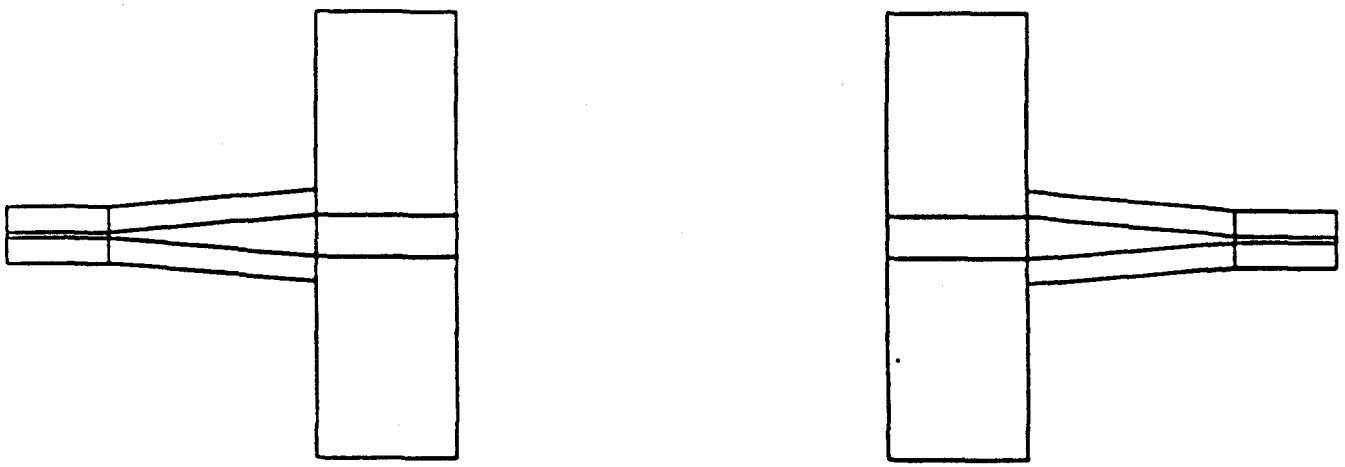

Figure 6. The geometry of the endcap and forward calorimeter without dead material in endcap calorimeter.

With dead material

Figure 5. Sigma and bias of E_t as a function of rapidity. (with dead material)

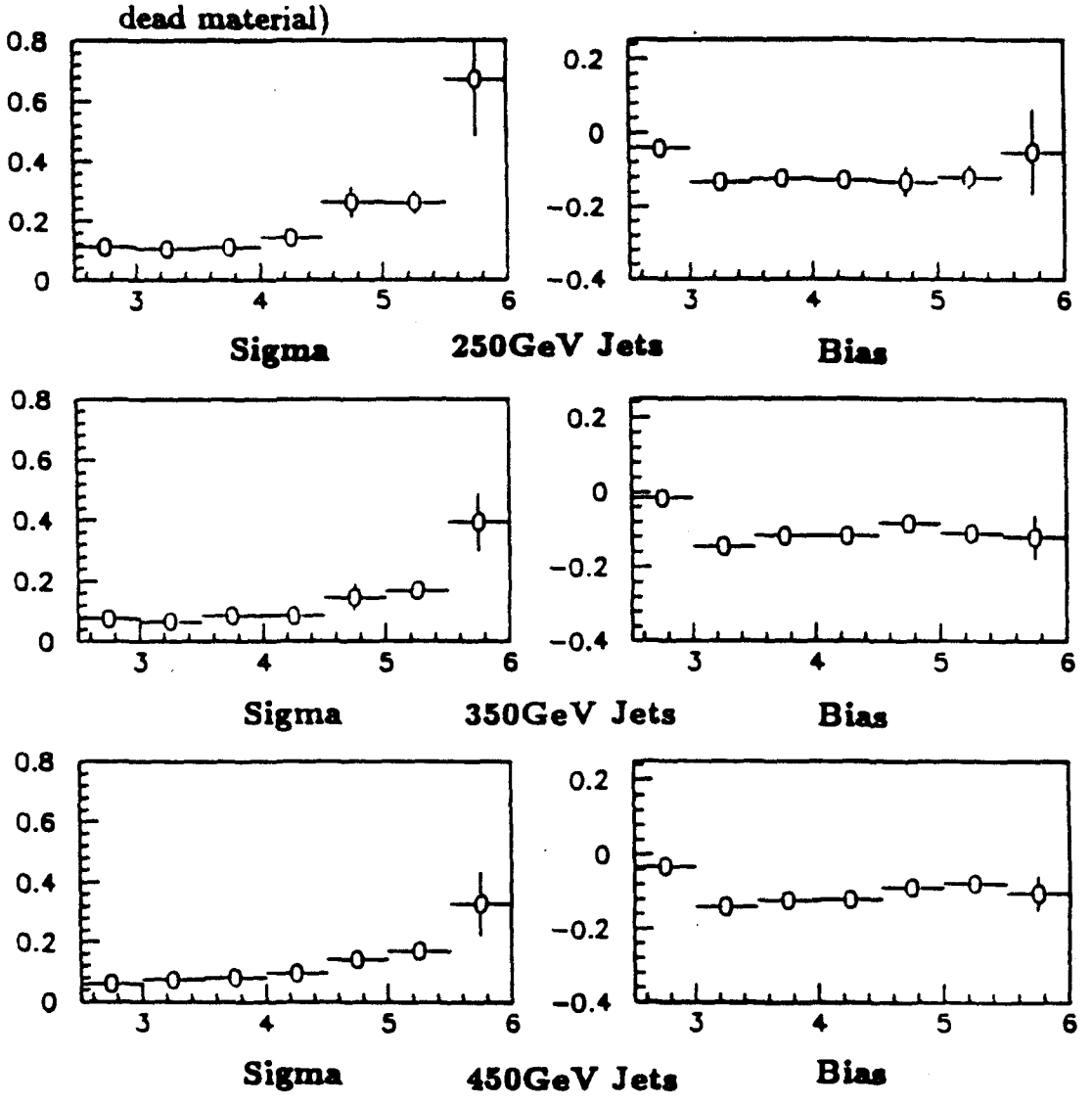

Without . . .

Figure 8. Sigma and bias of E_t as a function of rapidity. (without dead material)

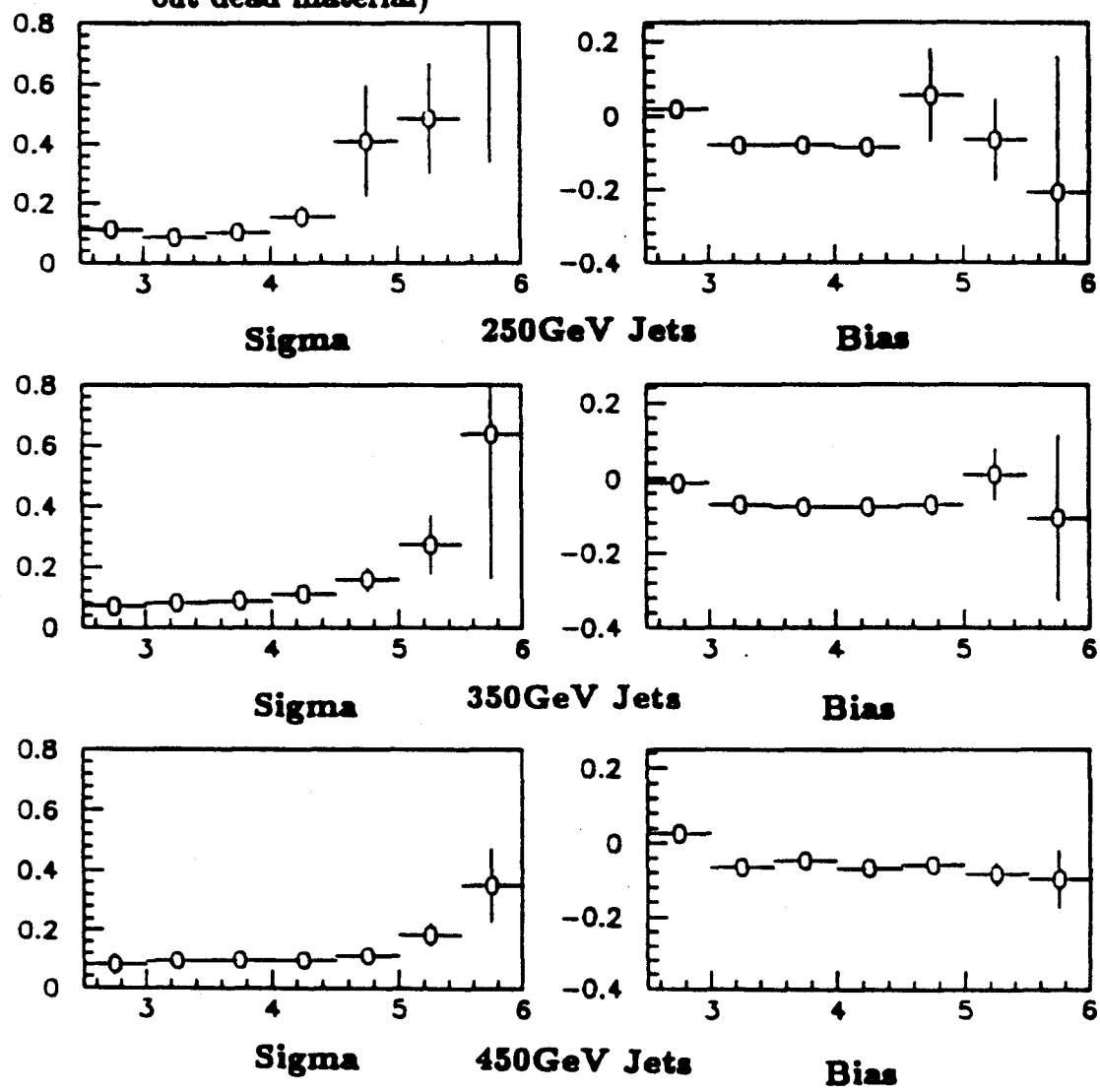

With dead material

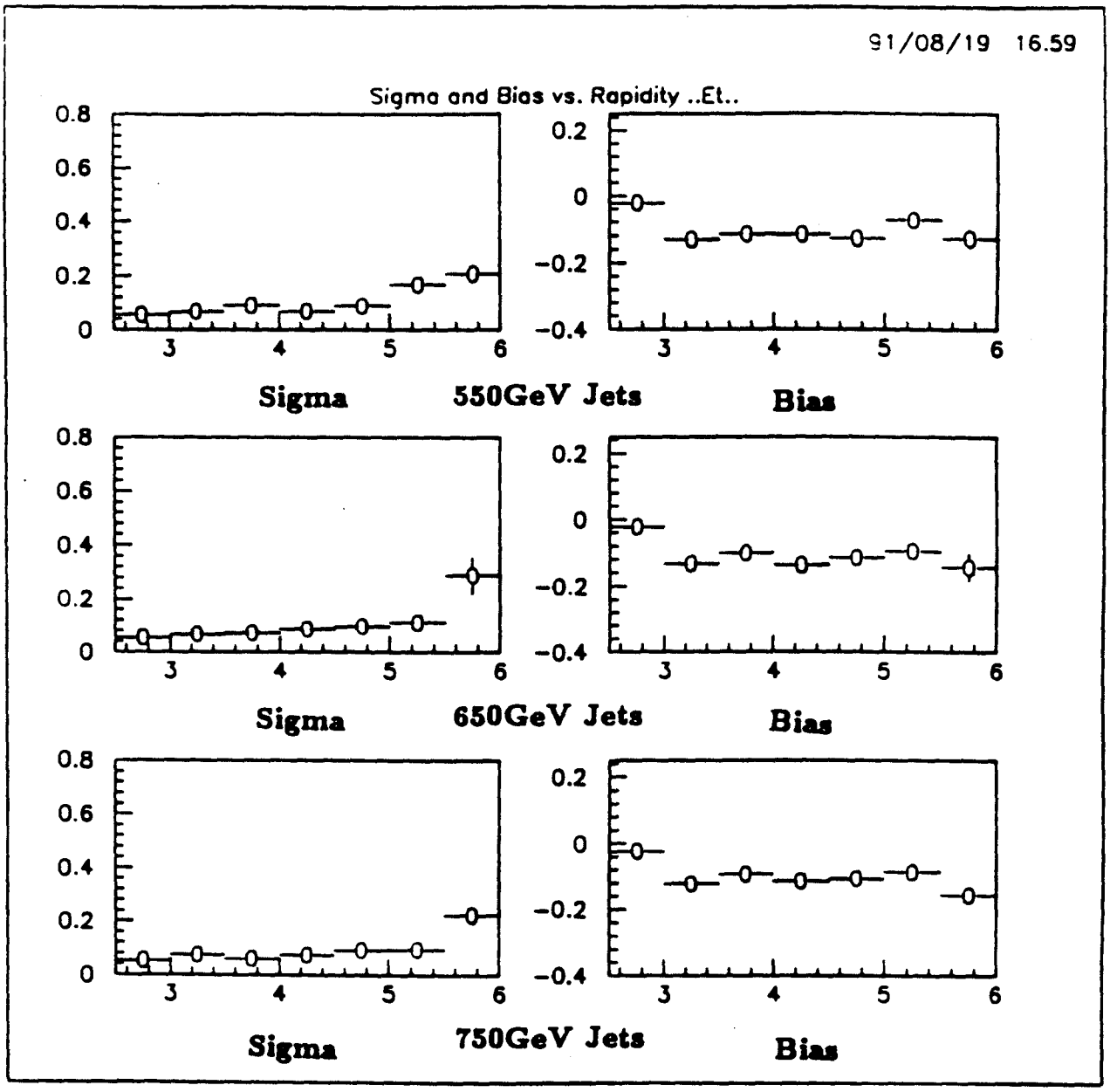

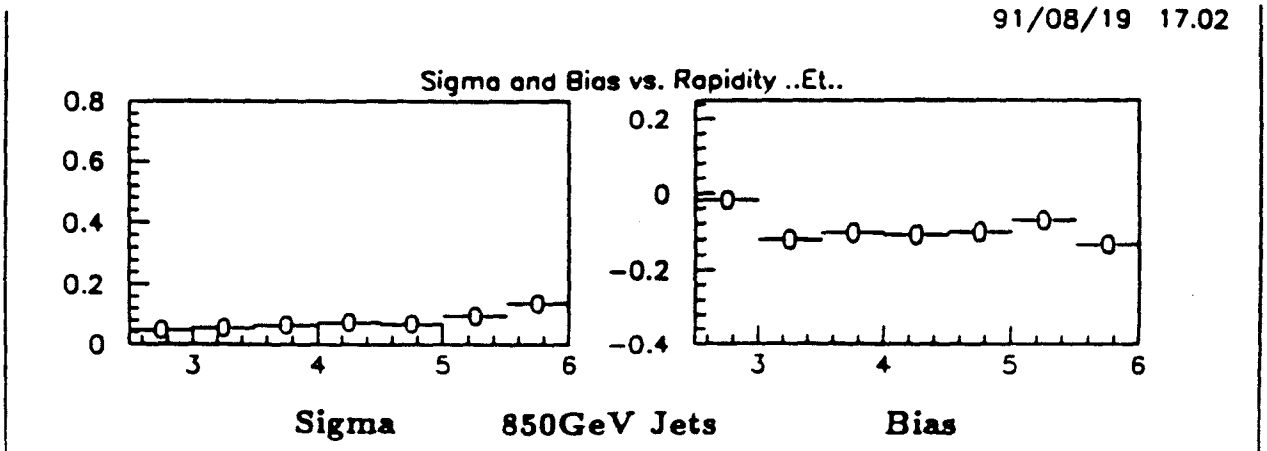

without...

91/08/19 17.04

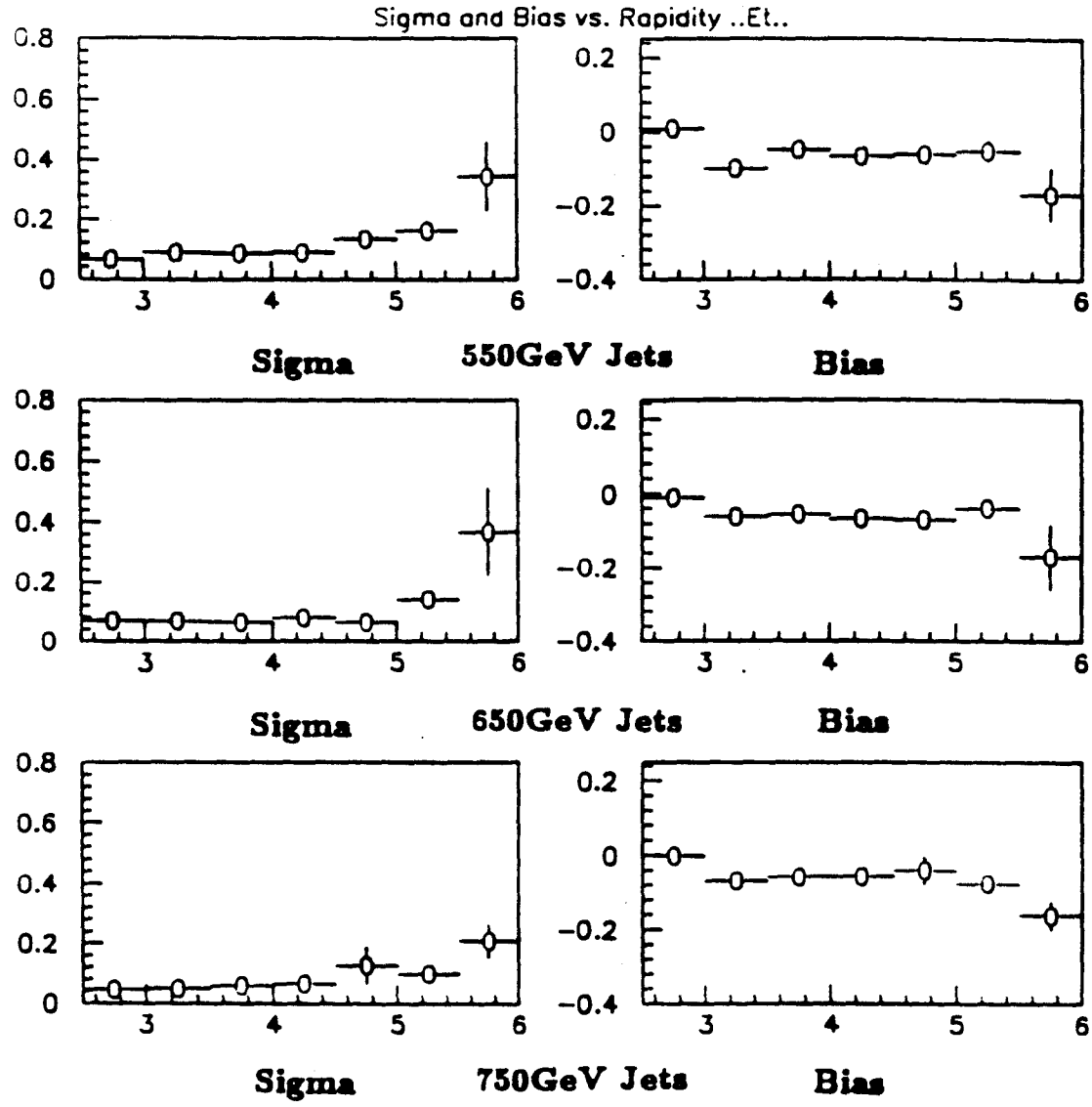

91/08/19 17.05

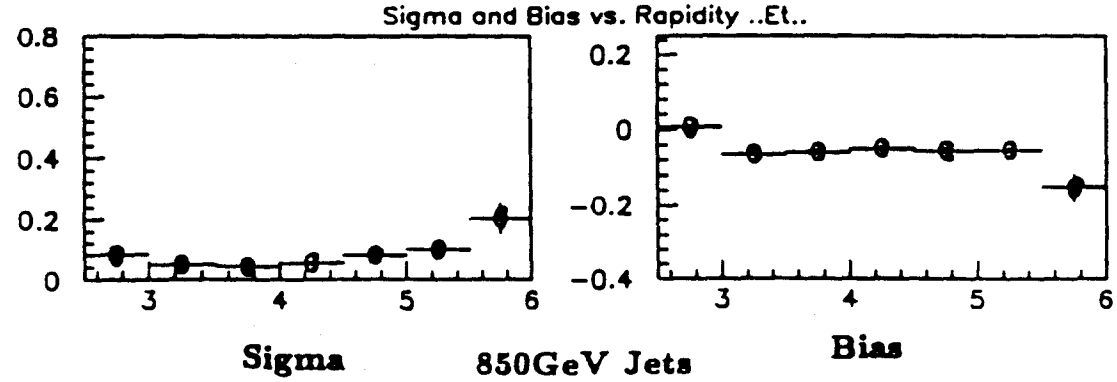

Jets>70. ϕ>40. $\Delta E/E$= 0.05, 0.2

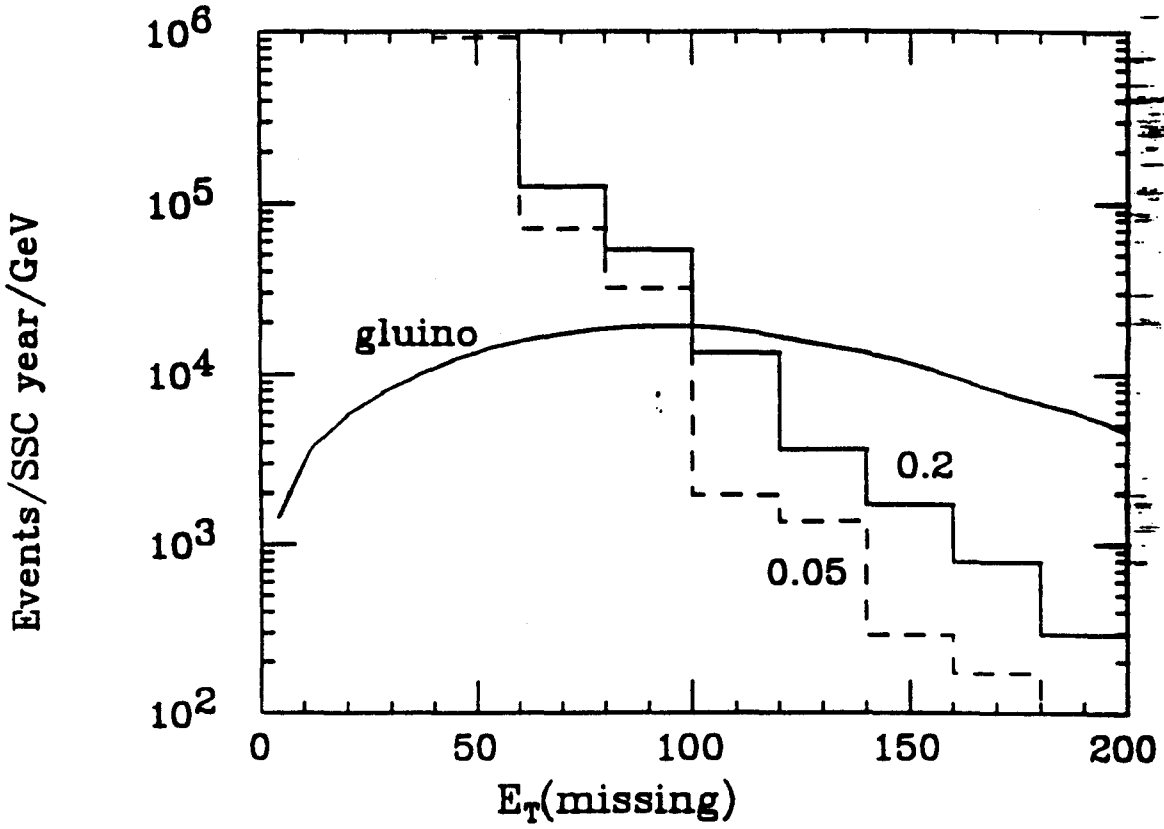

$M_{Gluino} \simeq 300$ GeV/c²

Summary of Gluino production

- The "bias" was further biased by <5% with the dead material, but the degradation of sigma was barely visible.

- The QCD background was almost an order of magnitude smaller than the signal beyond $E_t(missing)$=120 GeV (used to be 100 GeV). Considering that the bad regions are a part of the range of $|\eta|>3$, the difference is expected further small.

Induced hadronic resolutions with the (dead) irons for the magnetic shielding

N.Kanematsu (KEK), SDC-91-00082

- The SDC Liquid Argon calorimeter is designed to include magnetic transformers inside the cryostat and they must be shielded magnetically by placing them in an iron pipes. Because they are dead material, they may induce errors to the hadronic resolutions.

- With GEANT/GHEISHA simulation program, with cut-off energies of 0.1 MeV for e/g and 1 MeV for others, induced stochastic and constant terms (added in quadrature) were evaluated.

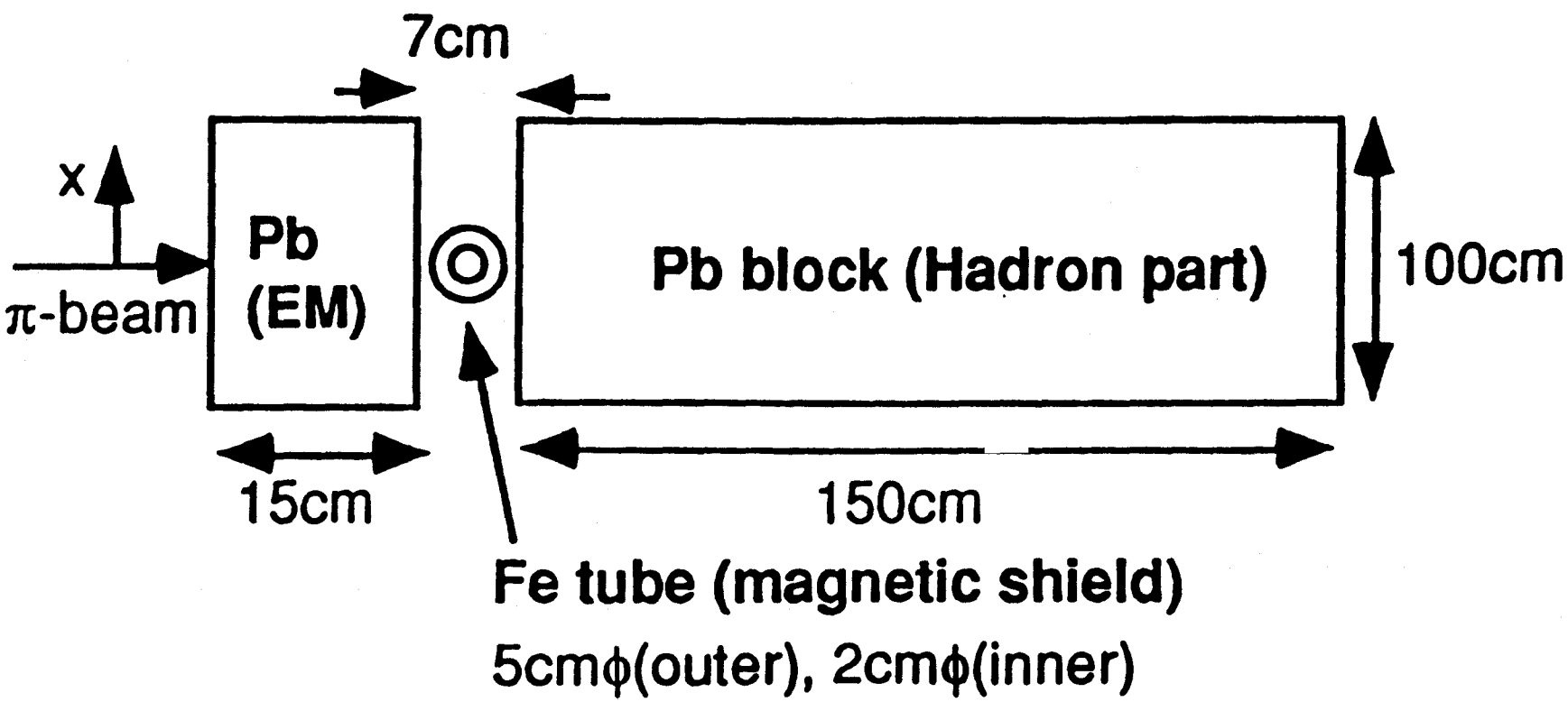

Figure 1: detector configuration in the simulation

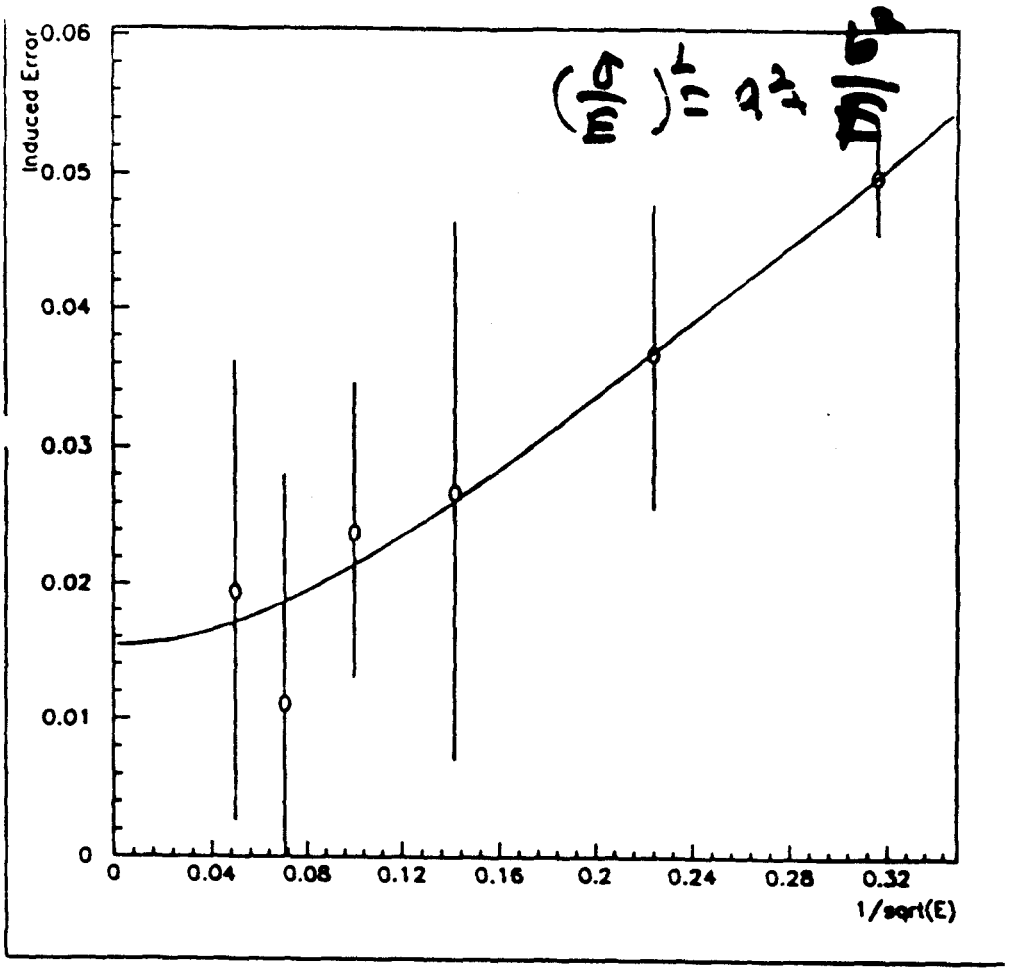
Induced Error
0.06
0.05
0.04
0.03
0.02
0.01
0
0
0.04
0.08
0.12
0.16
0.2
0.24
0.28
0.32
1/sqrt(E)

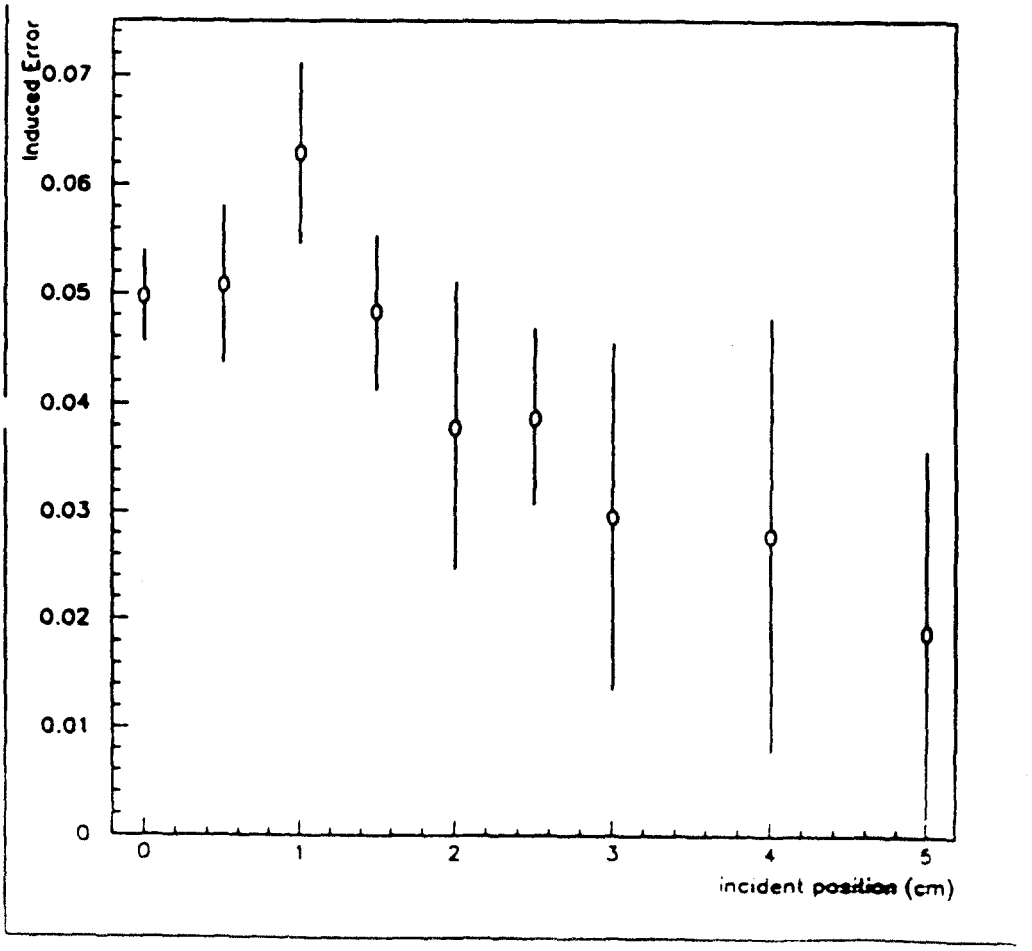
Induced Error
0.07
0.06
0.05
0.04
0.03
0.02
0.01
0
0
1
2
3
4
5
incident position (cm)

Summary of effect of Mag. shield iron

- The irons induced a stochastic term of $15\%/\sqrt{E}$ and a constant term of 1.5% when aimed at the center of the pipes.

- They also induced non-uniformity of response, 0.7%, which should be added to the constant term.

- These numbers were very small compared with the intrinsic hadronic resolutions;

$$60\%/\sqrt{E} \oplus 4\% \rightarrow 62\%/\sqrt{E} \oplus 4.3\% \ .$$

Beam tests of EM and Hadronic prototype

Y.Unno 1991/9/12
SDC cal TB at SSCL

Objectives of the beam test

(1) Drift velocity of electrons in the Liquid Argon is said to be slow. However, what we need is the signal, and fast-readout can be achieved by fast charge transfer time and by shaping the signal for an appropriate peaking time (detail will be discussed by C.Hearty).

The objective of the beam test is to test the fast-readout with bipolar shaping with the peaking times of 50, 100, and 200 ns, for HADRONIC and ELECTROMAGNETIC calorimetry.

(2) e/π (e/h) measurement with Pb absorber in HADRONIC calorimetry with the fast-readout.

(3) Uniformity of response across the module crack in ELECTROMAGNETIC calorimetry of the SDC design.

HADRONIC MODULE

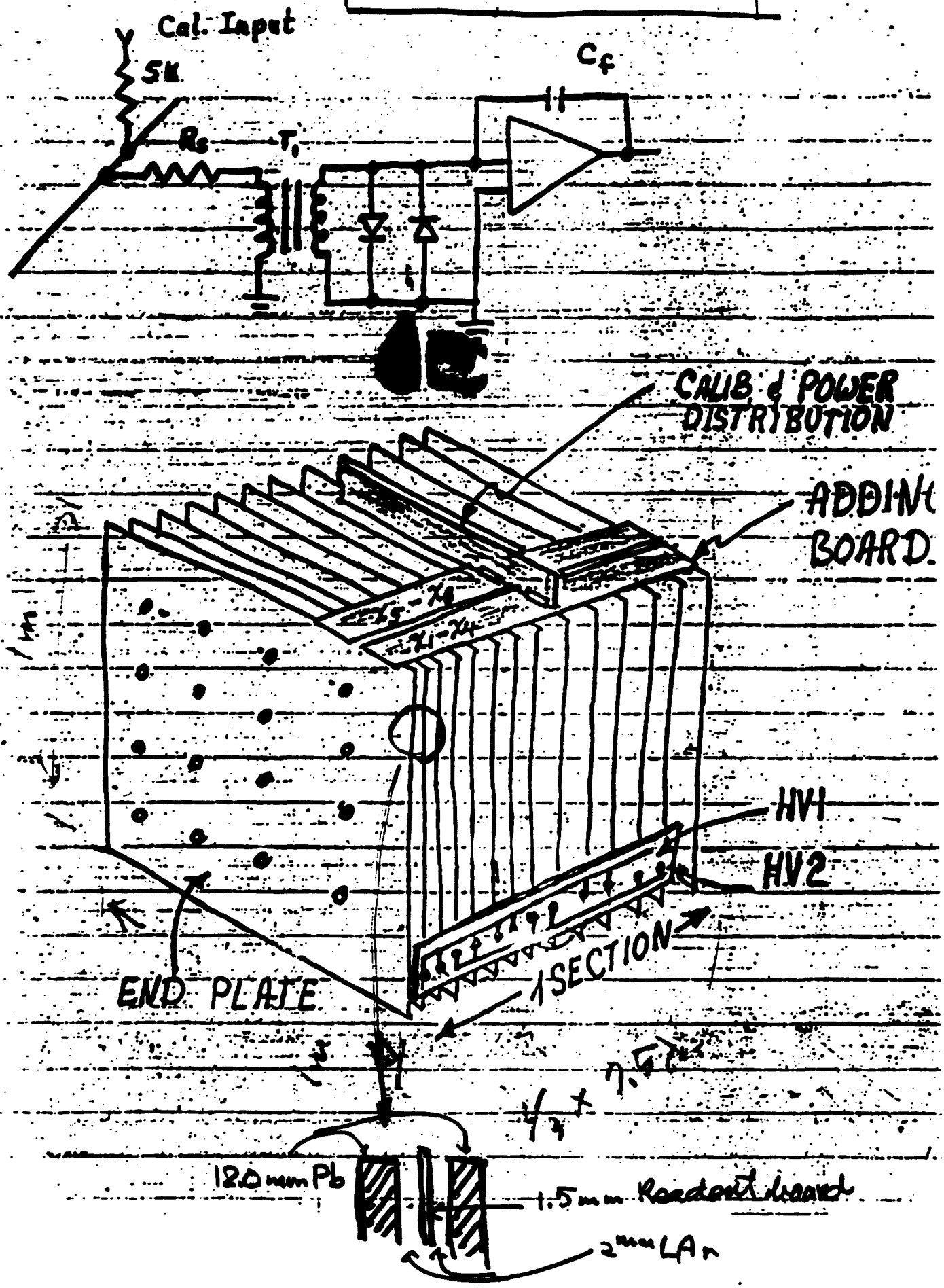

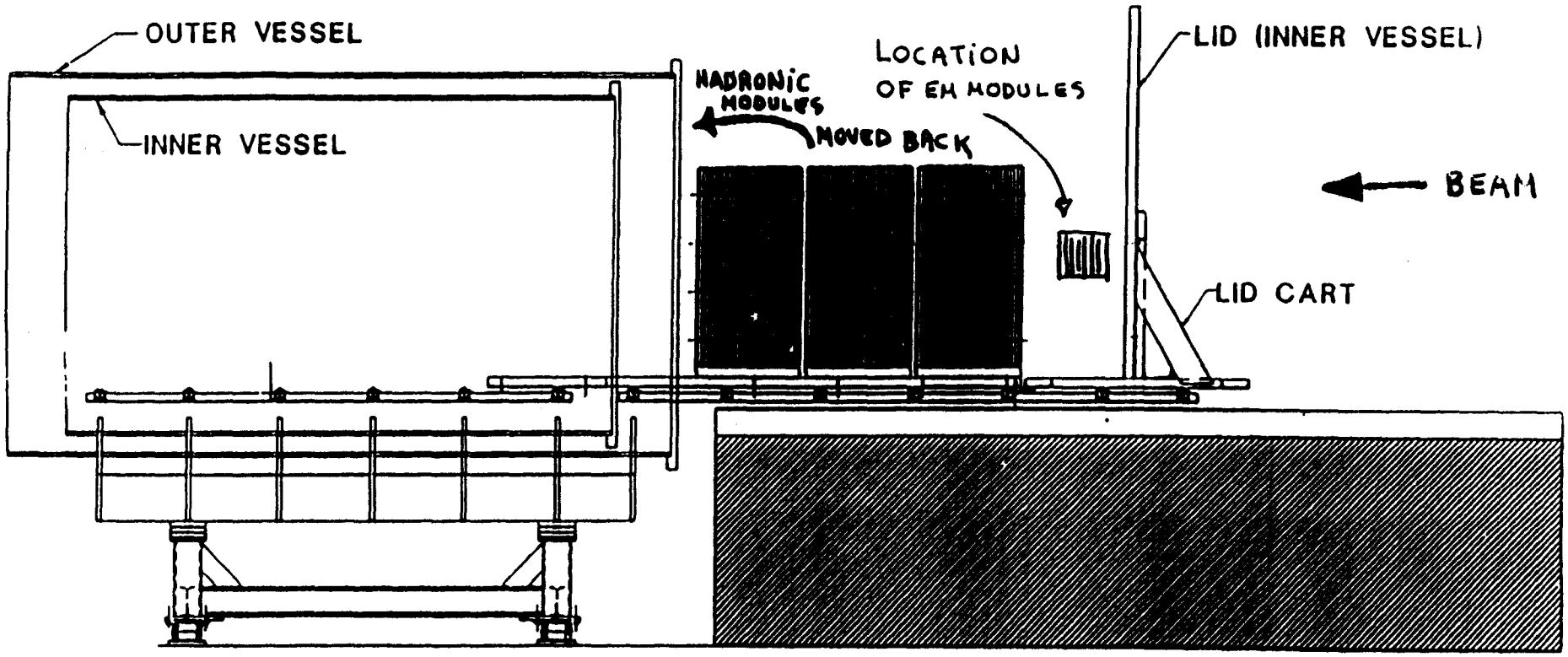
OUTER VESSEL
INNER VESSEL
HADRONIC MODULES
MOVED BACK
LOCATION OF EM MODULES
LID (INNER VESSEL)
BEAM
LID CART

FIGURE 8·17

SDC LAC EM PROTOTYPE

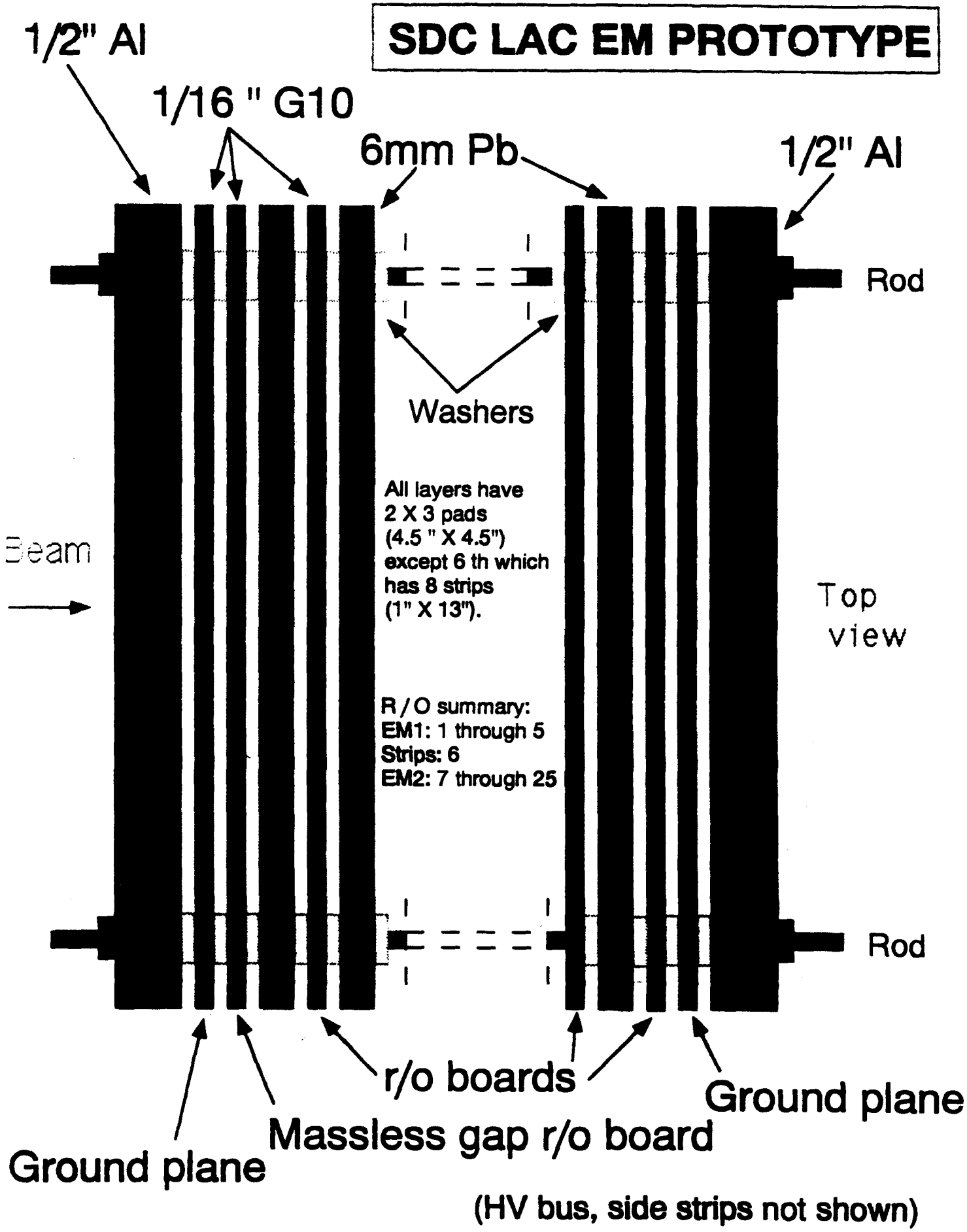

(HV bus, side strips not shown)

SDC LAC EM PROTOTYPE

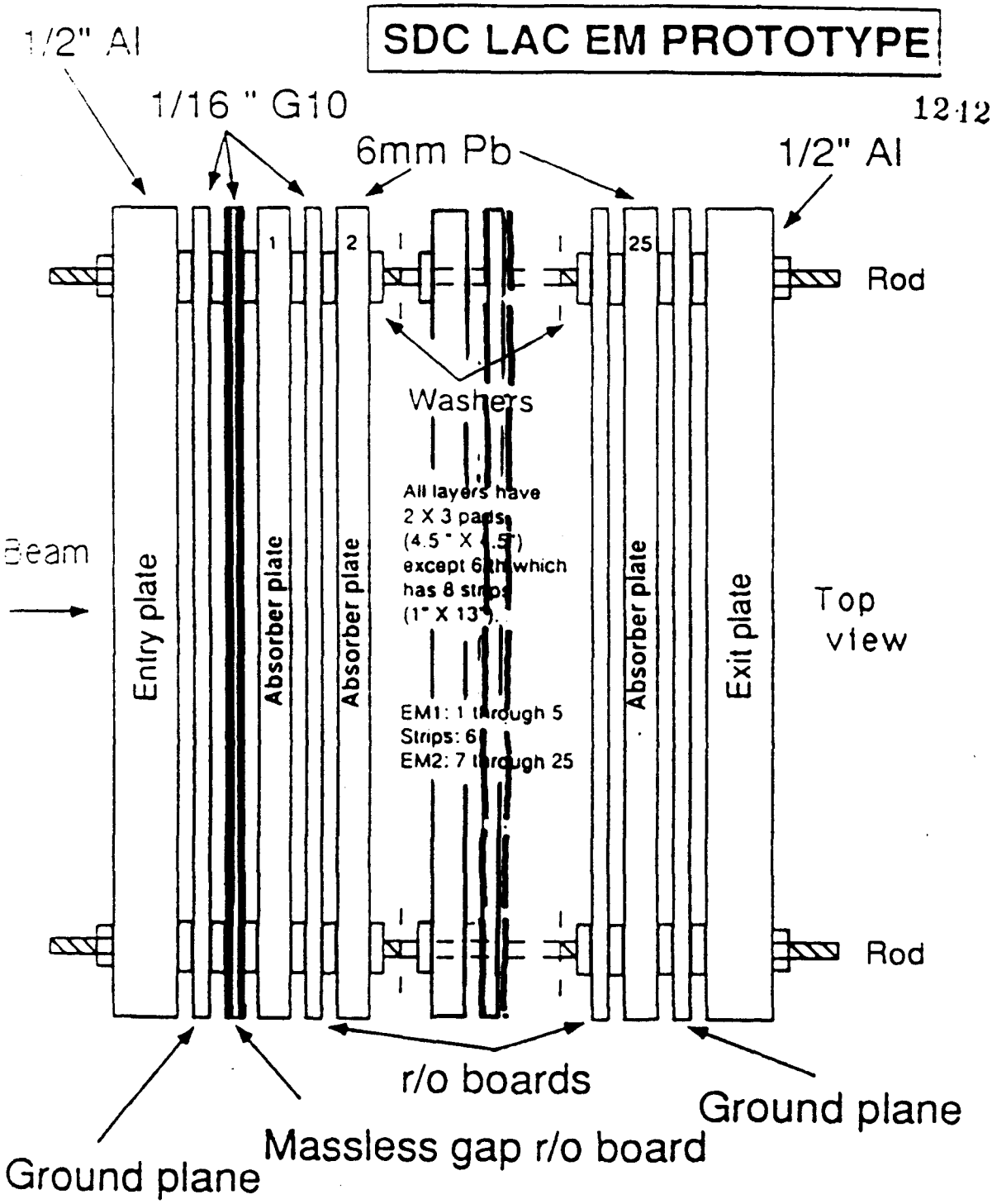

(HV bus, side strips not shown)

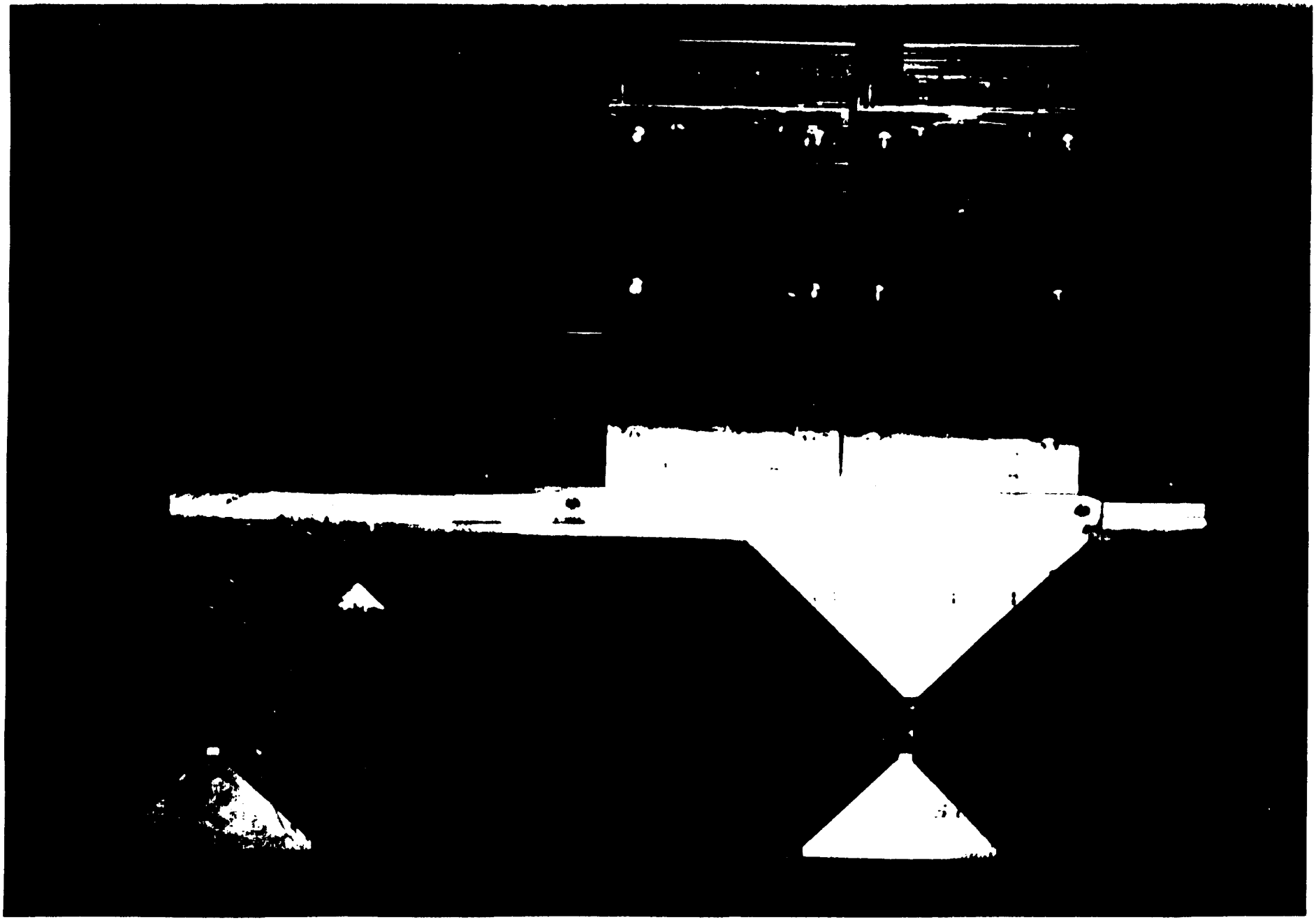

SSC LABORATORY

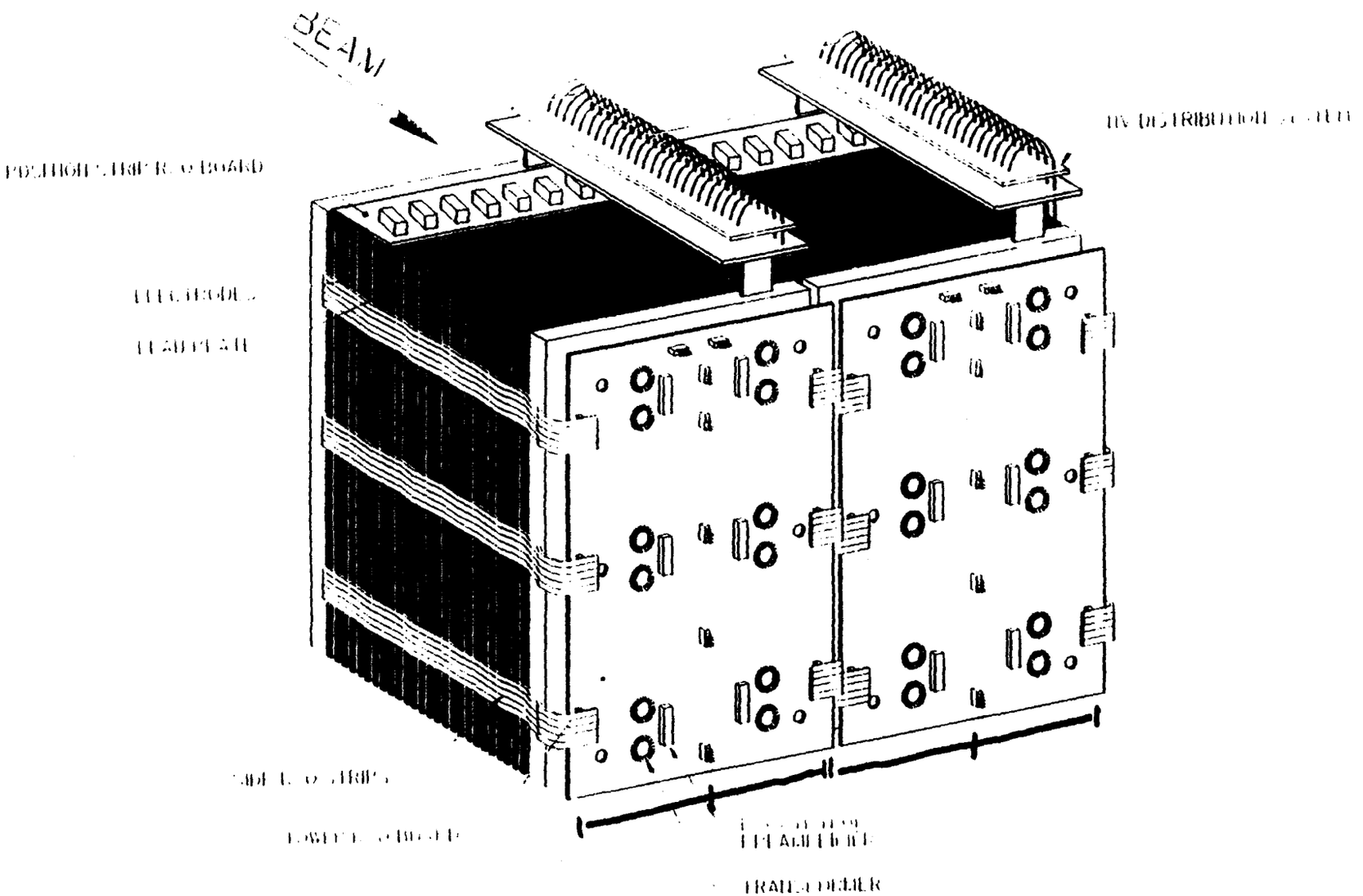

KURT PENNINGTON
8/2/91
F3000001

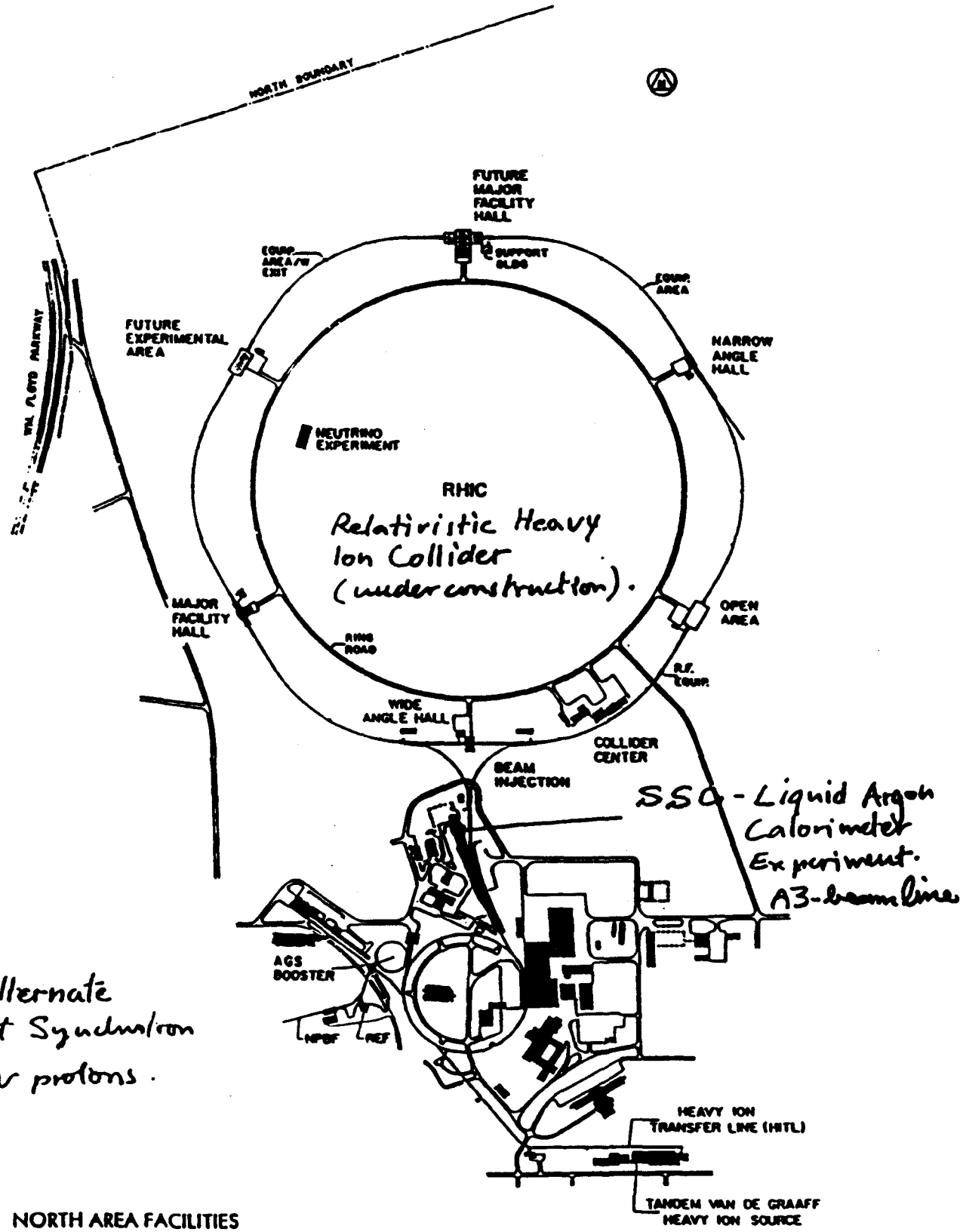

NORTH AREA FACILITIES

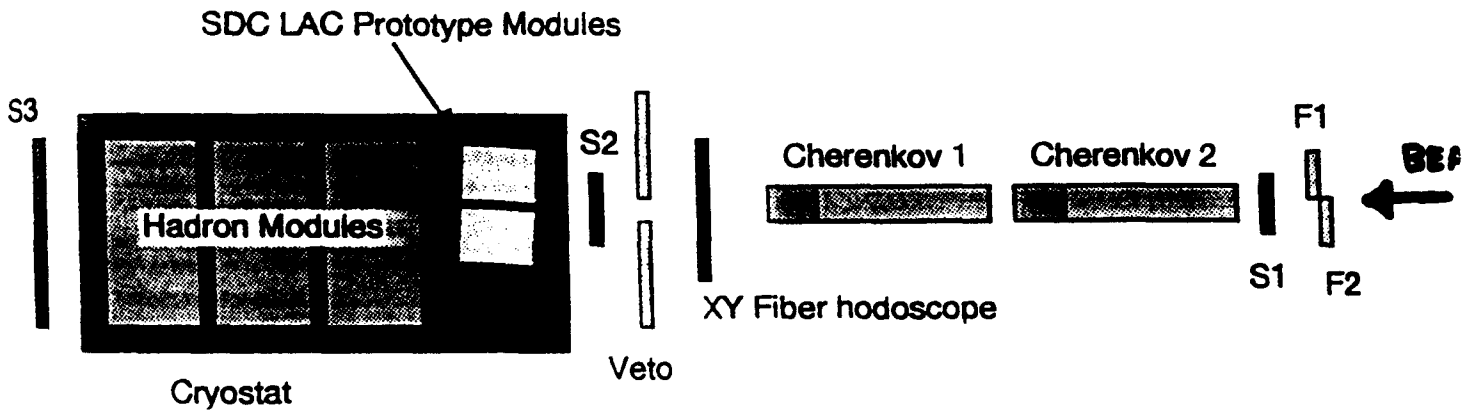

Figure 8.16

Schematic view of the BNL Spring '91 test

Summary of the BNL A3 beam line

- Triggers:

$$S_1 \cdot S_2 \cdot \bar{V} \cdot C_1 \cdot C_2 \cdot \bar{S} \quad \rightarrow \quad e^-$$

$$S_1 \cdot S_2 \cdot \bar{V} \cdot \bar{C}_1 \cdot \bar{C}_2 \cdot \bar{S} \quad \rightarrow \quad \pi^-$$

$$S_1 \cdot S_2 \cdot \bar{V} \cdot \bar{C}_1 \cdot \bar{C}_2 \cdot S \quad \rightarrow \quad \mu^-$$

F_1, F_2, and XY Fiber hodoscope were used to define better parallel beams and positions for the EM module.

- Momentum: 0.5~20 GeV/c
- Intensity: 10^3~10^6 particles/spill
- Extraction: ~0.8 sec
- Electron concentration: ~1% at 10 GeV/c

Readout Electronics chain

Very much like the proposed electronics chain of the SDC LAC option other than Analog memory (or more correctly, we follow the readout chain in the beam test laid by the Liquid Argon subsystem R&D).

- Preamp in the Liquid Argon
- Intermediate amp on the feedthru (outside)
- Variable Gain Amp in the counting hut:

  (1) t_p=100 ns Bipolar shaping to individual ADC's
  (2) Analog sum to a shaper with t_p=50, 100, 200 ns shaping, then to an ADC or a transient recorder

- Calibration chain

Liquid Argon Calorimeter

Electronics Chain Block Diagram

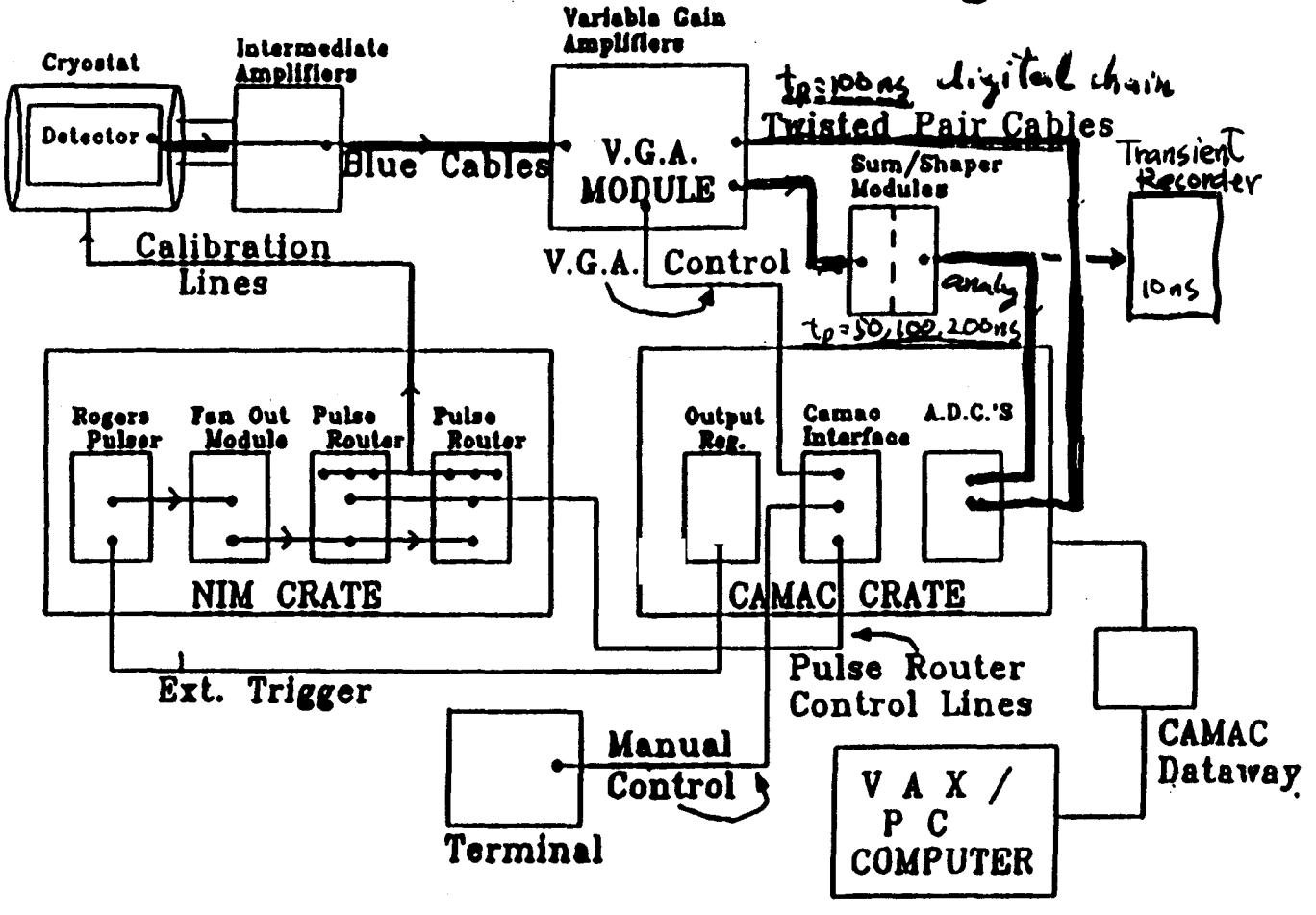

–Bold lines indicate signal path.

Results

The beam test data are under rigorous analysis among collaborators. The results being presented here are one of many and also should be taken as preliminary. More and better-understood results will be available by the time of the Corpus Christi Conference.

- EM module:

  Energy sum of EM1 and EM2

- Hadronic module:

  Hadron energy resolution at t_p=100 ns (individual digital channel sum)

  Responses of electrons and pions t_p=100 ns and e/π ratios

Resolution away from crack

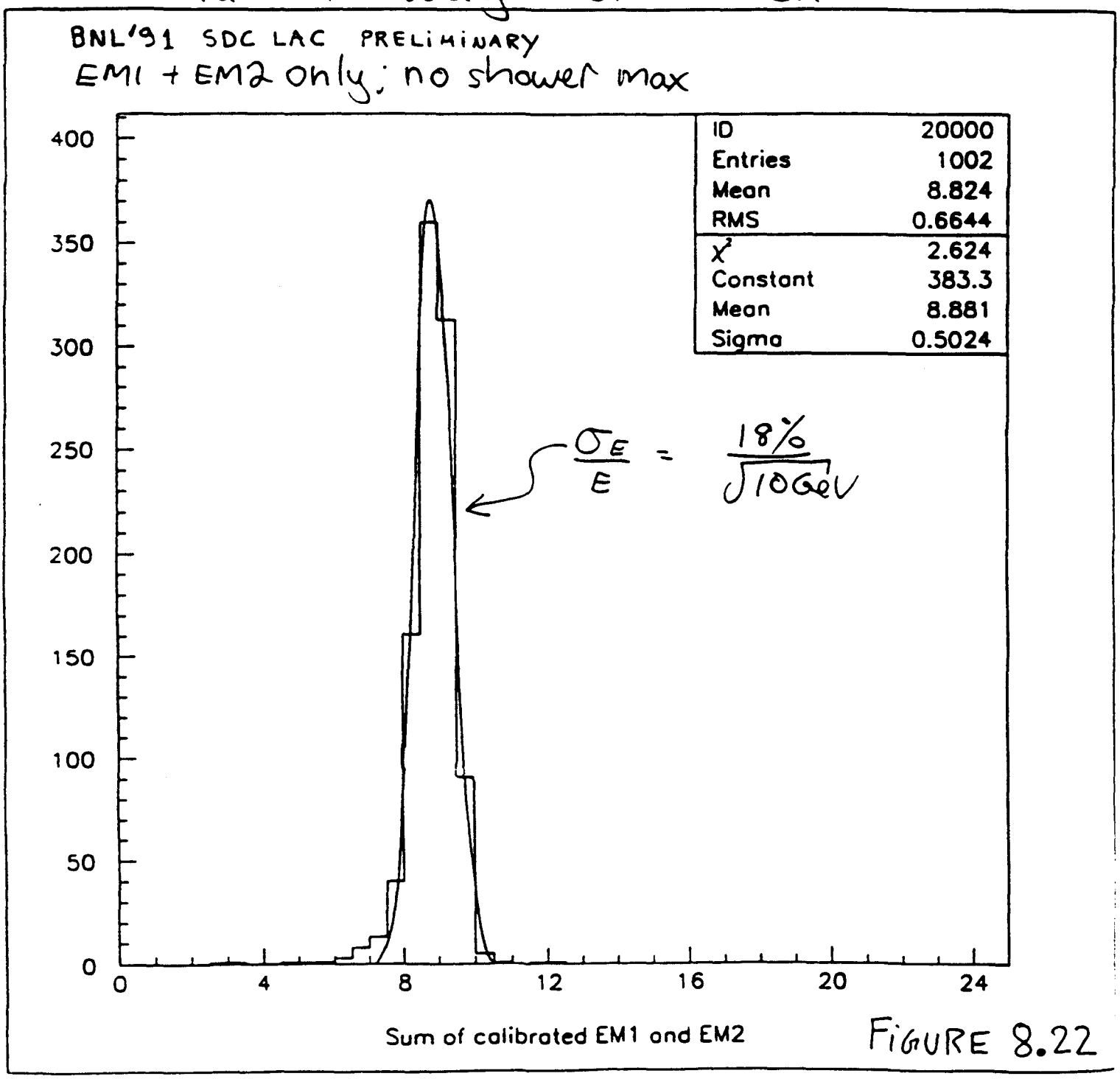

FIGURE 8.22

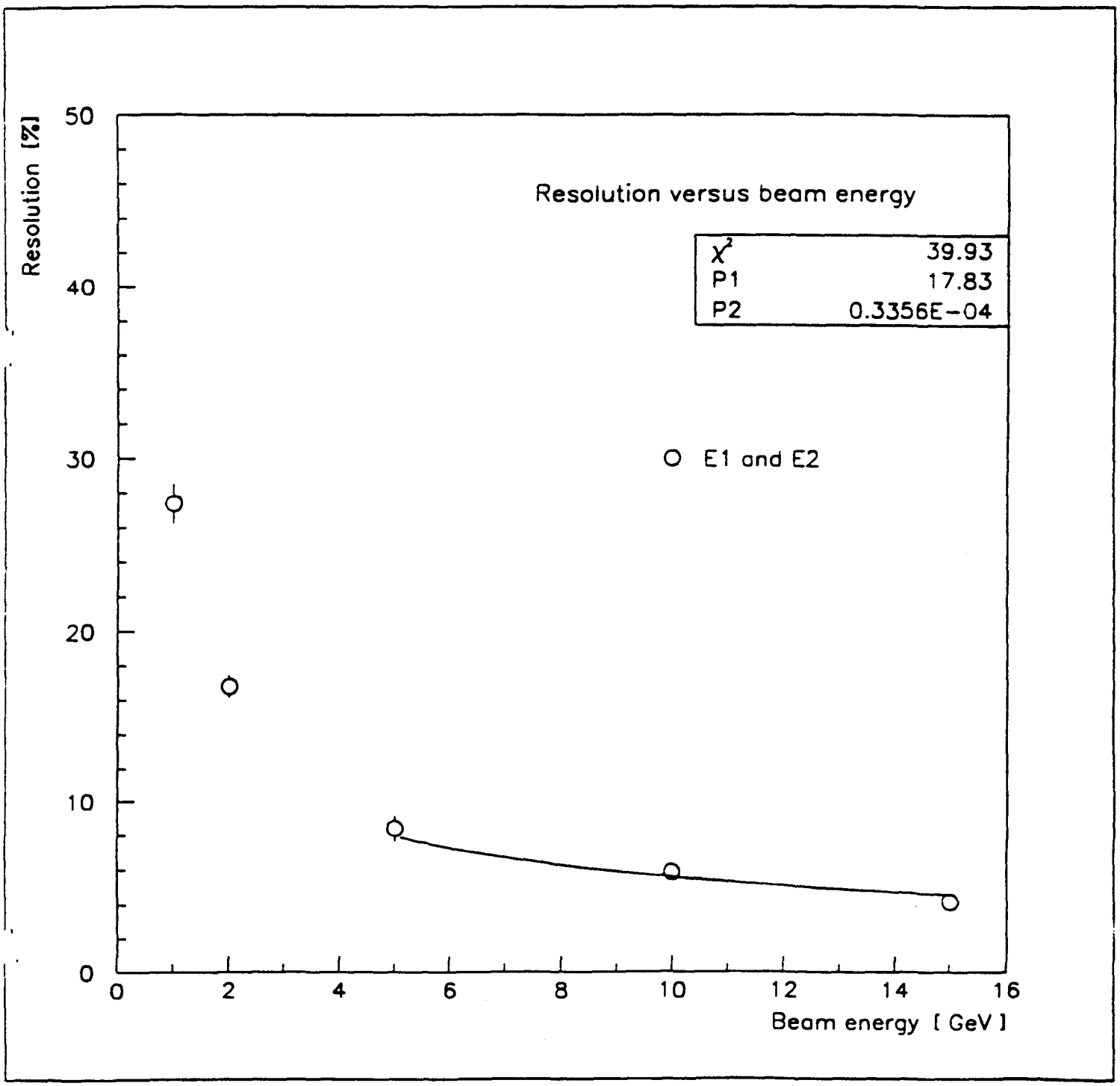
Resolution versus beam energy
χ^2 39.93
P1 17.83
P2 0.3356E-04
E1 and E2
Resolution [%]
Beam energy [GeV]
0
10
20
30
40
50
0
2
4
6
8
10
12
14
16

BNL '91 SDC LAC PRELIMINARY

FIGURE 8.30

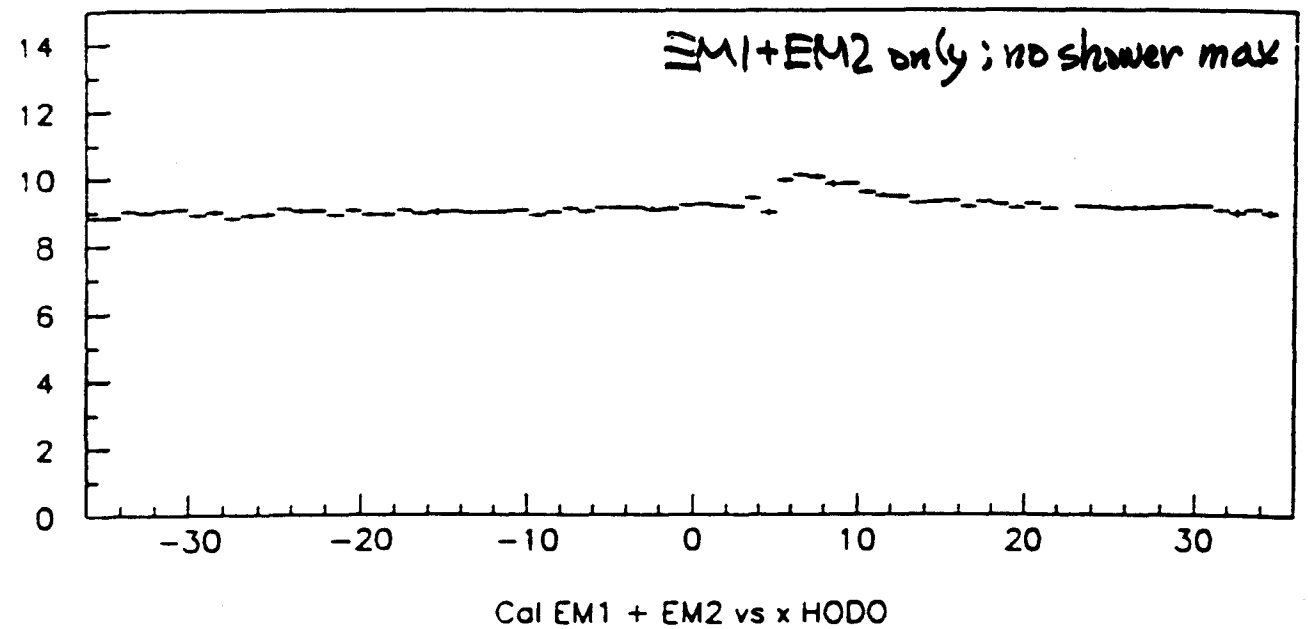

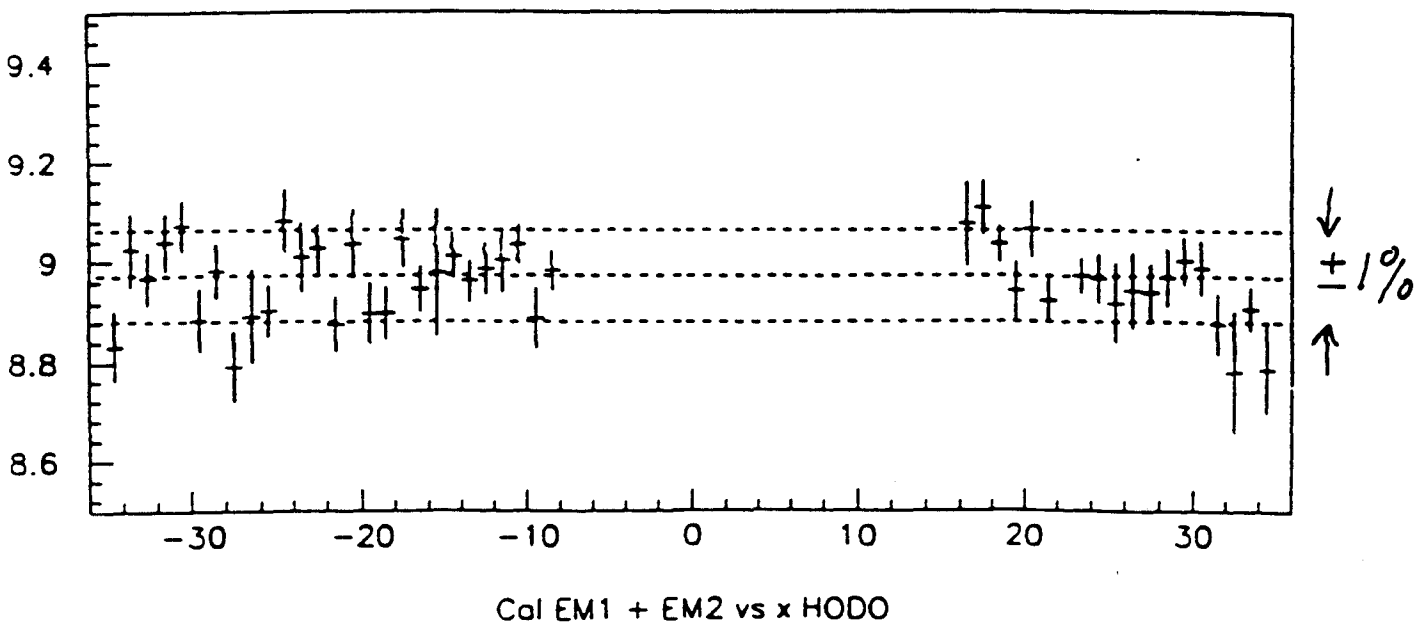

Histogram of $(r_i - \langle r \rangle)/\sigma_i$;
r_i = response at scan point i

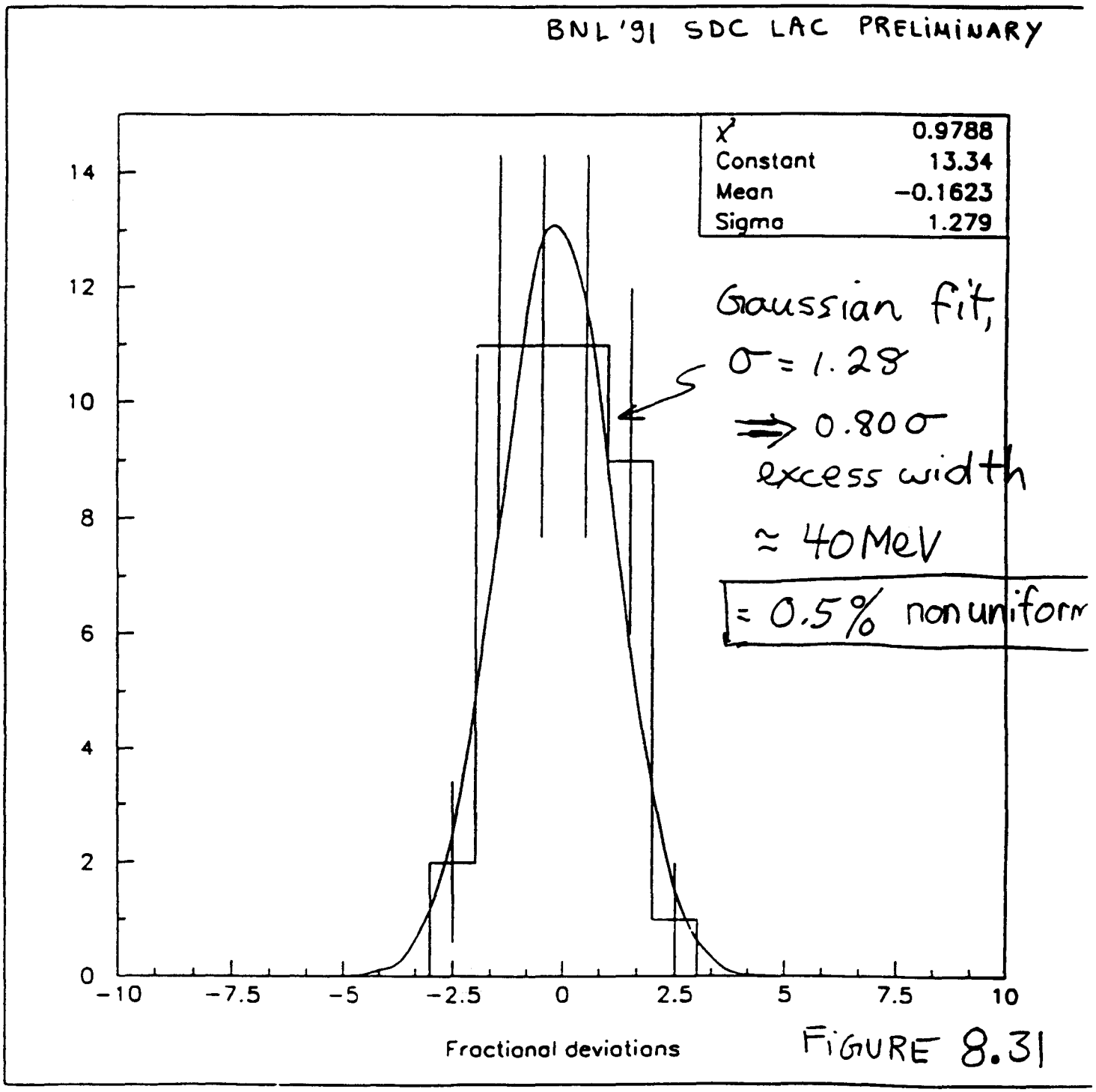

FIGURE 8.31

Hadronic Section

Y.Unno 1991/9/12
SDC Cal TB at SSCL

e

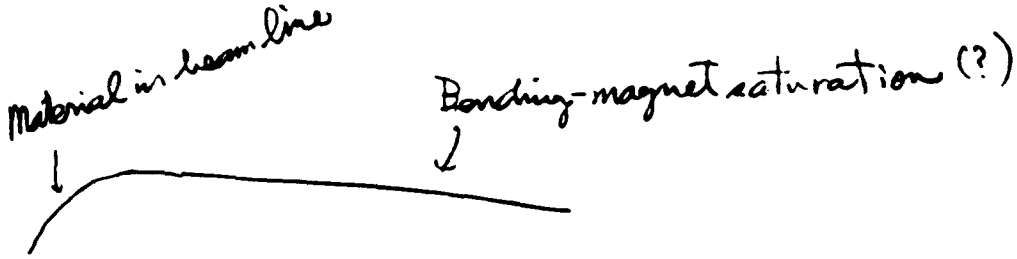

Preliminary

digital $\tau_p = 100ns$

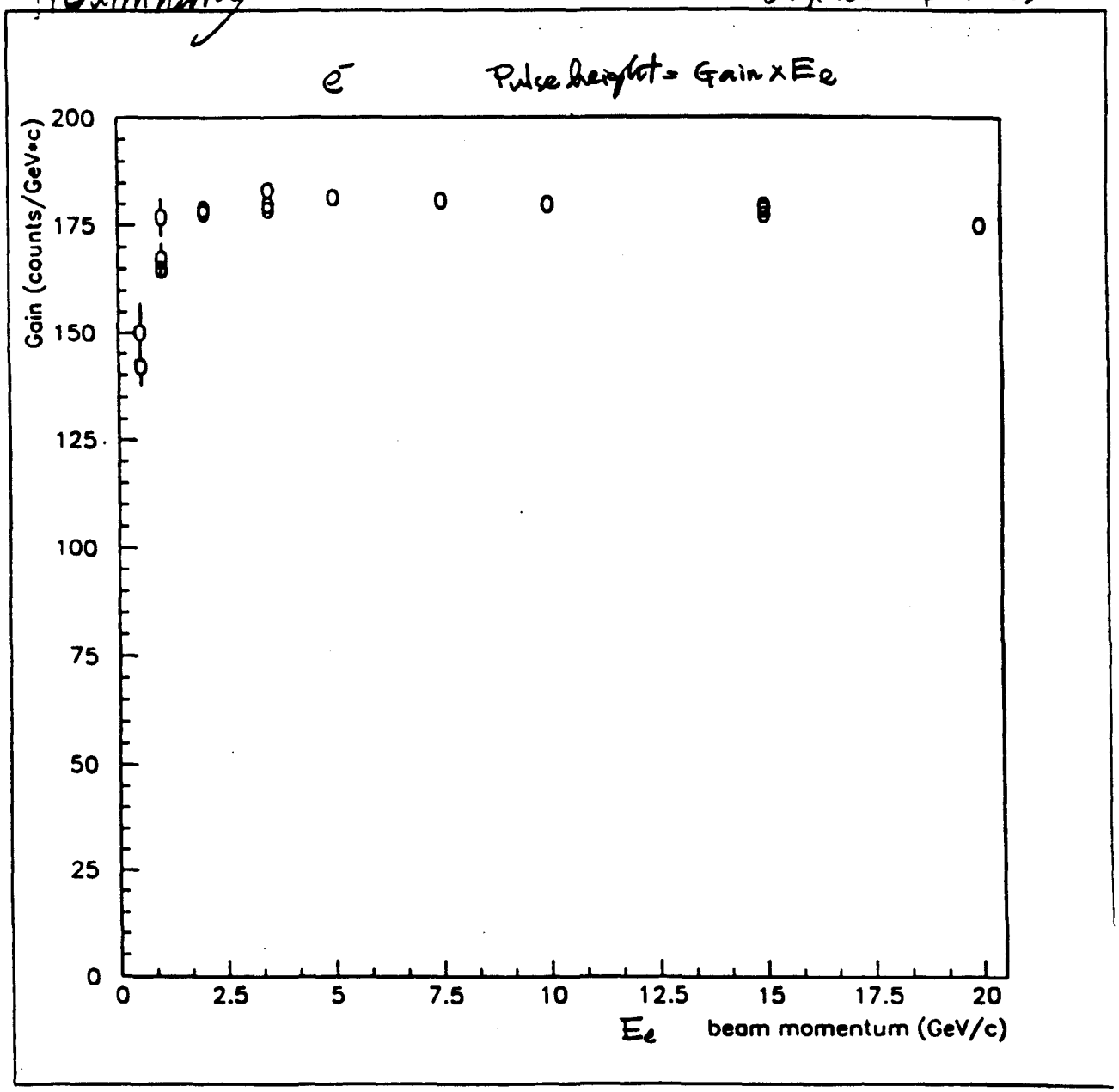

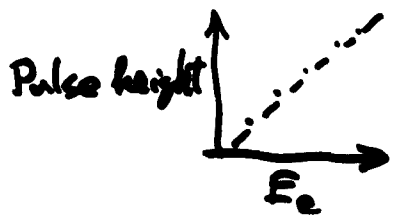

Preliminary

100ns

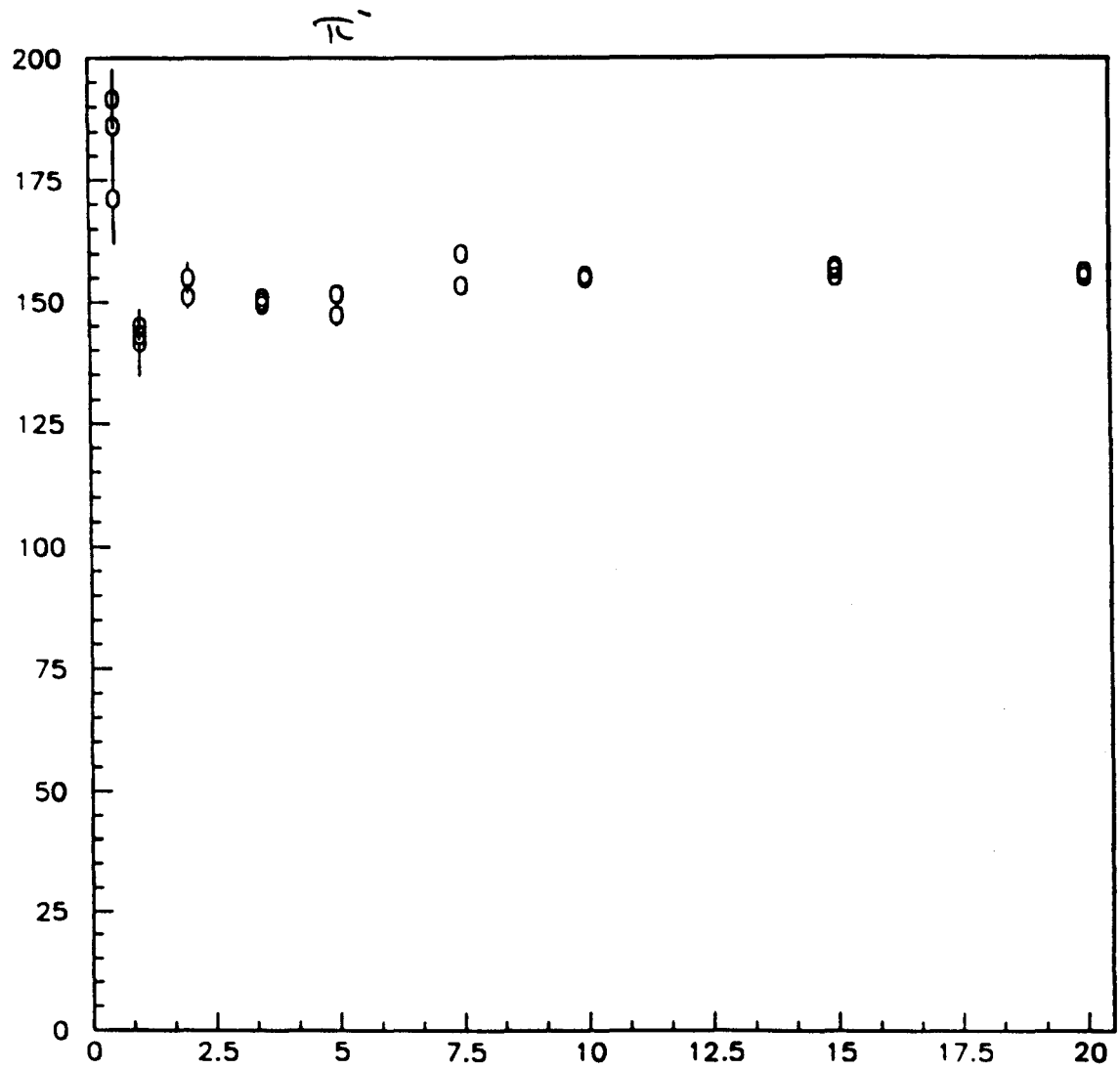

To $\frac{\sigma}{E} = \sqrt{(0.00 \pm 0.48)^2 + (63.77 \pm 0.17)^2/E}$ %

(P2 3.5 GeV/c)

Preliminary

100ns

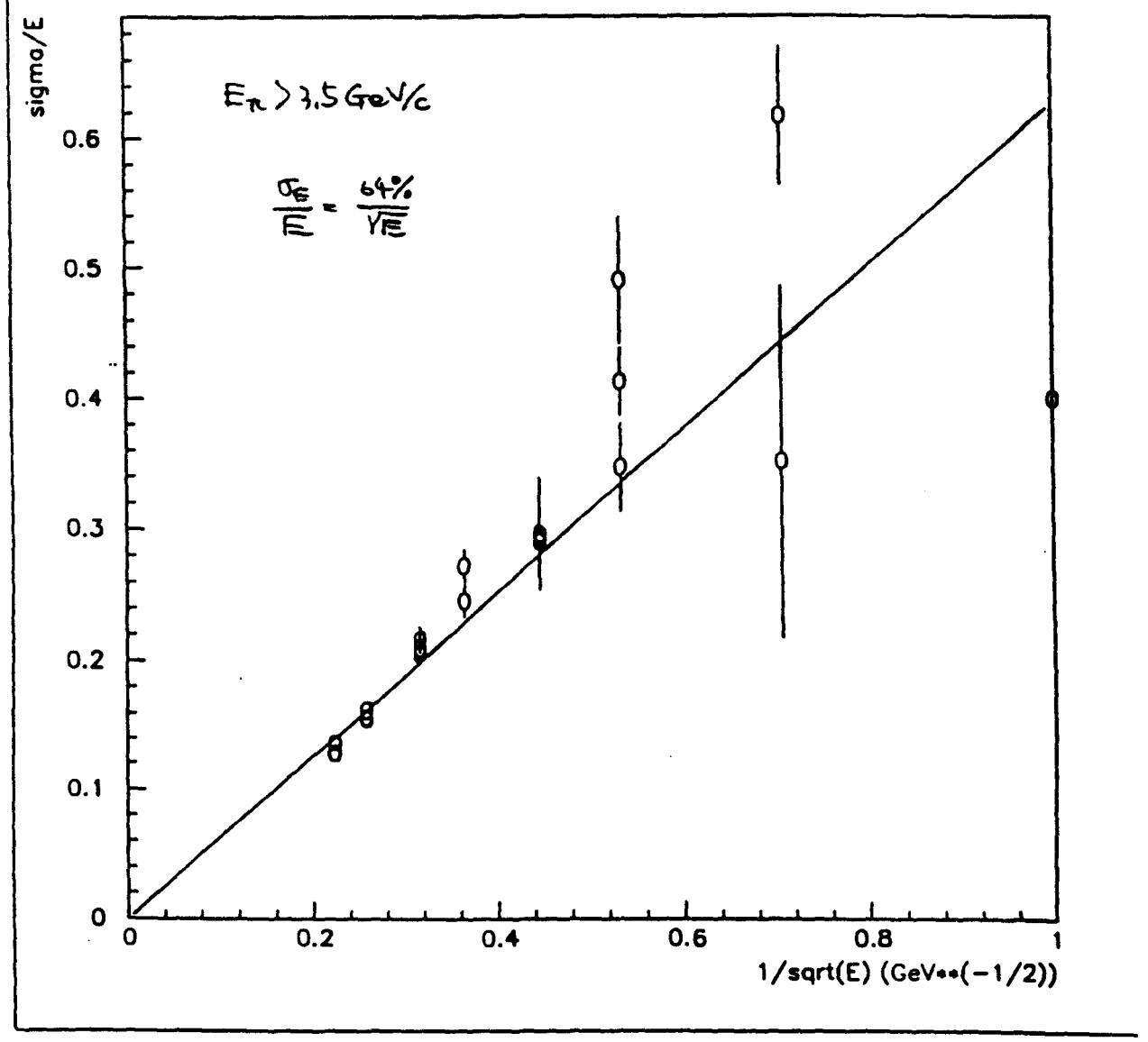

e $\frac{\sigma}{E} = \sqrt{(0.00 \pm 0.44)^2 + (22.19 \pm 0.17)^2/E}$ %

r-χ^2 = 3.8 dof = 14. (P23.5)

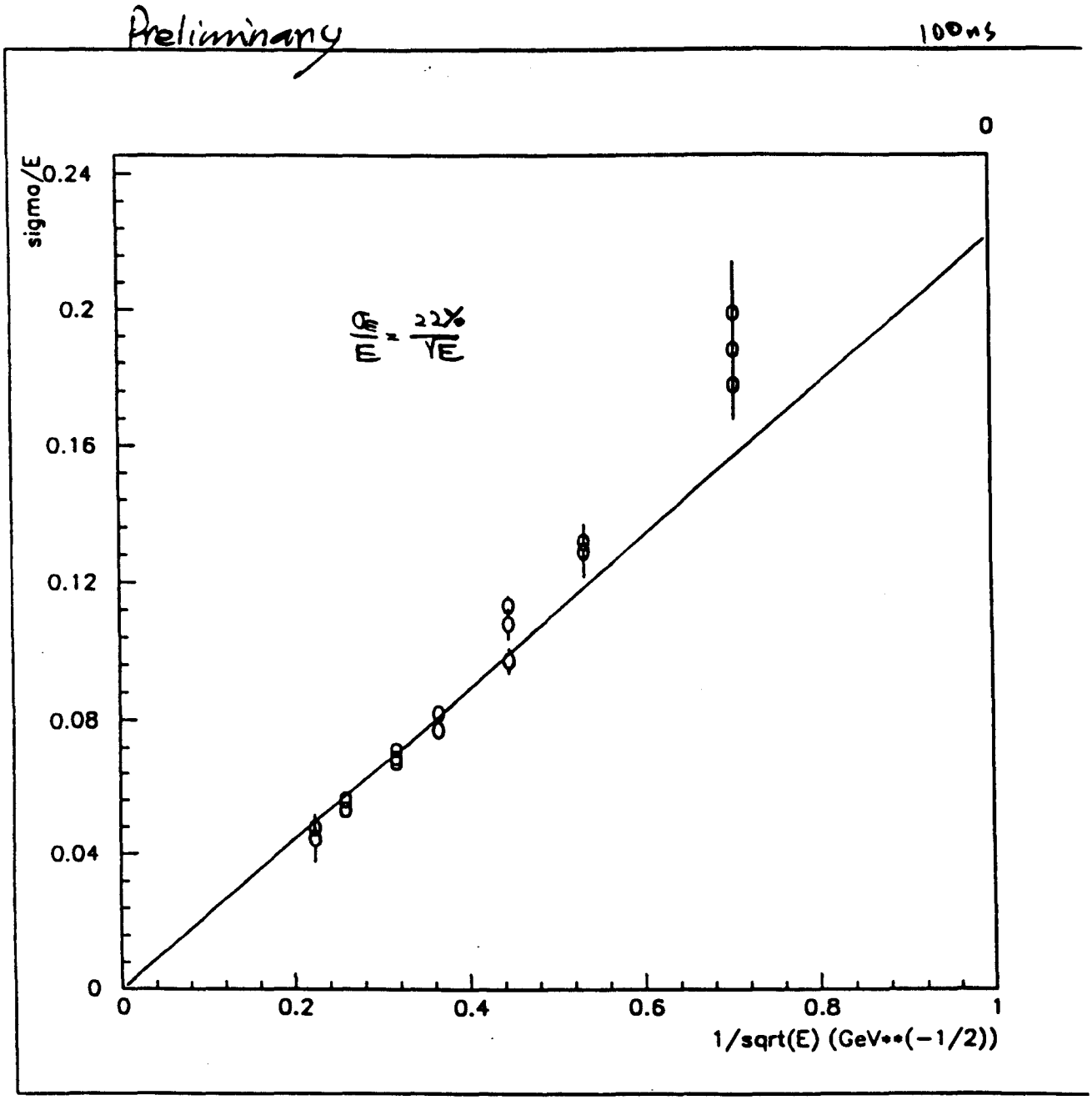

Preliminary Results of Liquid Argon Test at BNL

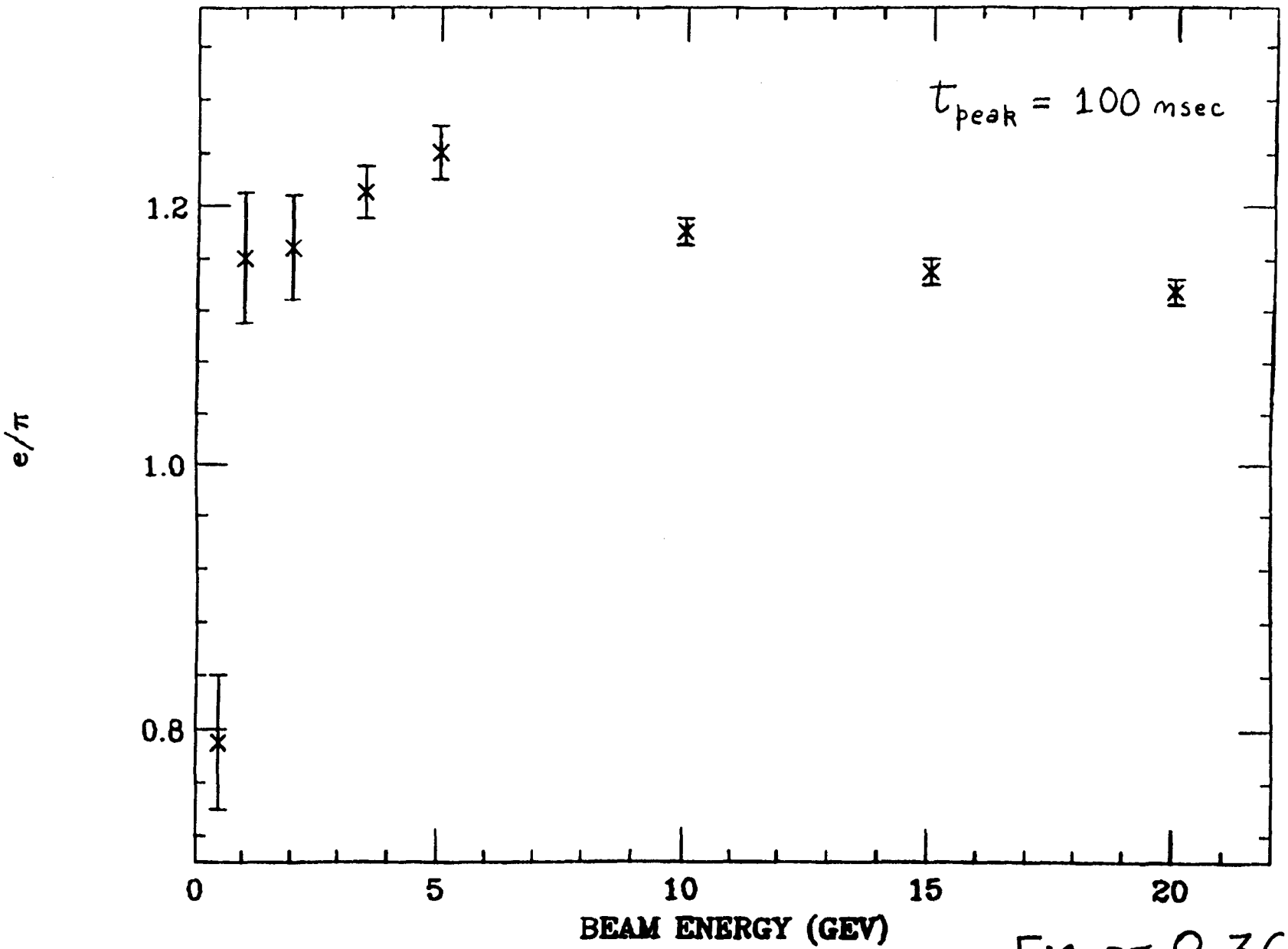

FIGURE 8.36

f_{π^0} simulation

$$f_{\pi^0} = 1 - (E/E_0)^{m-1}$$

$E_0 = 1.08 \pm 0.10$ GeV

$m = 0.8457 \pm 0.0062$

Preliminary

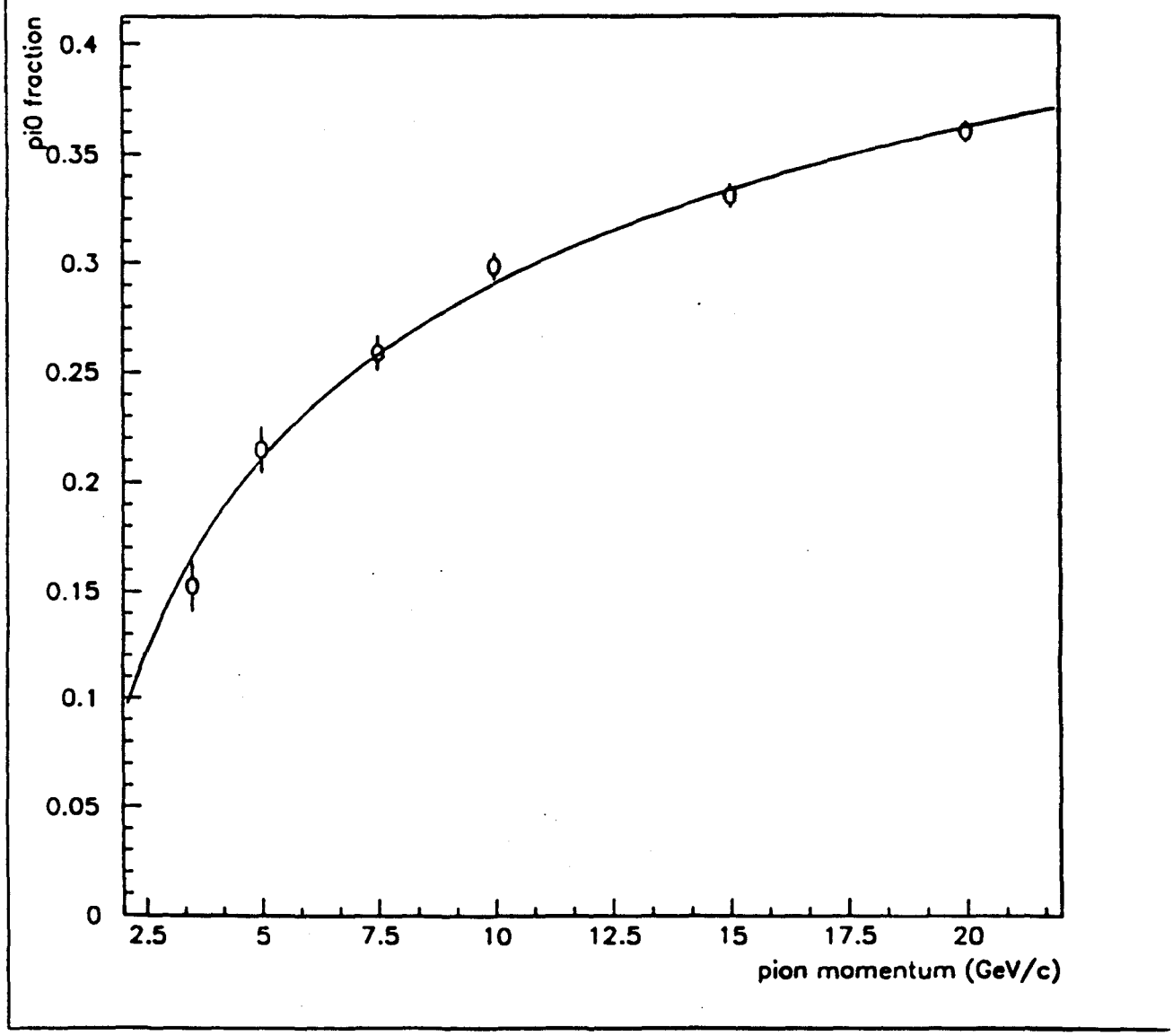

From the e/π to the e/h ratio

- The pion response(π) can be expressed by the electron response(e) and the hadron response(h) as

$$\pi = f\pi^{o}\, e + (1 - f\pi^{o})\, h \qquad (1)$$

where the factor, $f\pi^{o}$, is the (average) π^{o} fraction in the hadronic shower. Then the electron response over the pion response ratio is

$$e/\pi = e/(\, f\pi^{o}\, e + (1 - f\pi^{o})\, h) \ . \qquad (2)$$

After some manipulation, we have the e/h ratio as

$$e/h = (1 - f\pi^{o})/(1/(e/\pi) - f\pi^{o}) \ . \qquad (3)$$

- D.Groom's ansatz is

$$\pi/e = 1 - (1 - h/e)(E/E_{0})^{-0.15} \qquad (4)$$

where E_{0}~1GeV.

- Non-unity e/h induces a constant term in the hadronic resolution, parametrized as

$$\sigma_{E}/E(\text{const. by } e/h) = 0.14 \times |1 - e/h| \ . \qquad (5)$$

$$e/\pi = \frac{e/h}{(1-(1-e/h)f_{\pi^0})} \qquad f_{\pi^0} = 1-(E/E_0)^{m-1}$$

$m = 0.847$

$e/h = 1.232 \pm 0.0022$ $\qquad E_0 = 1.08$

$\chi^2 = 5.5 \times$ dof $\quad$ dof $= 13$

fit : $P \geq 3.5$

Preliminary

100 ns

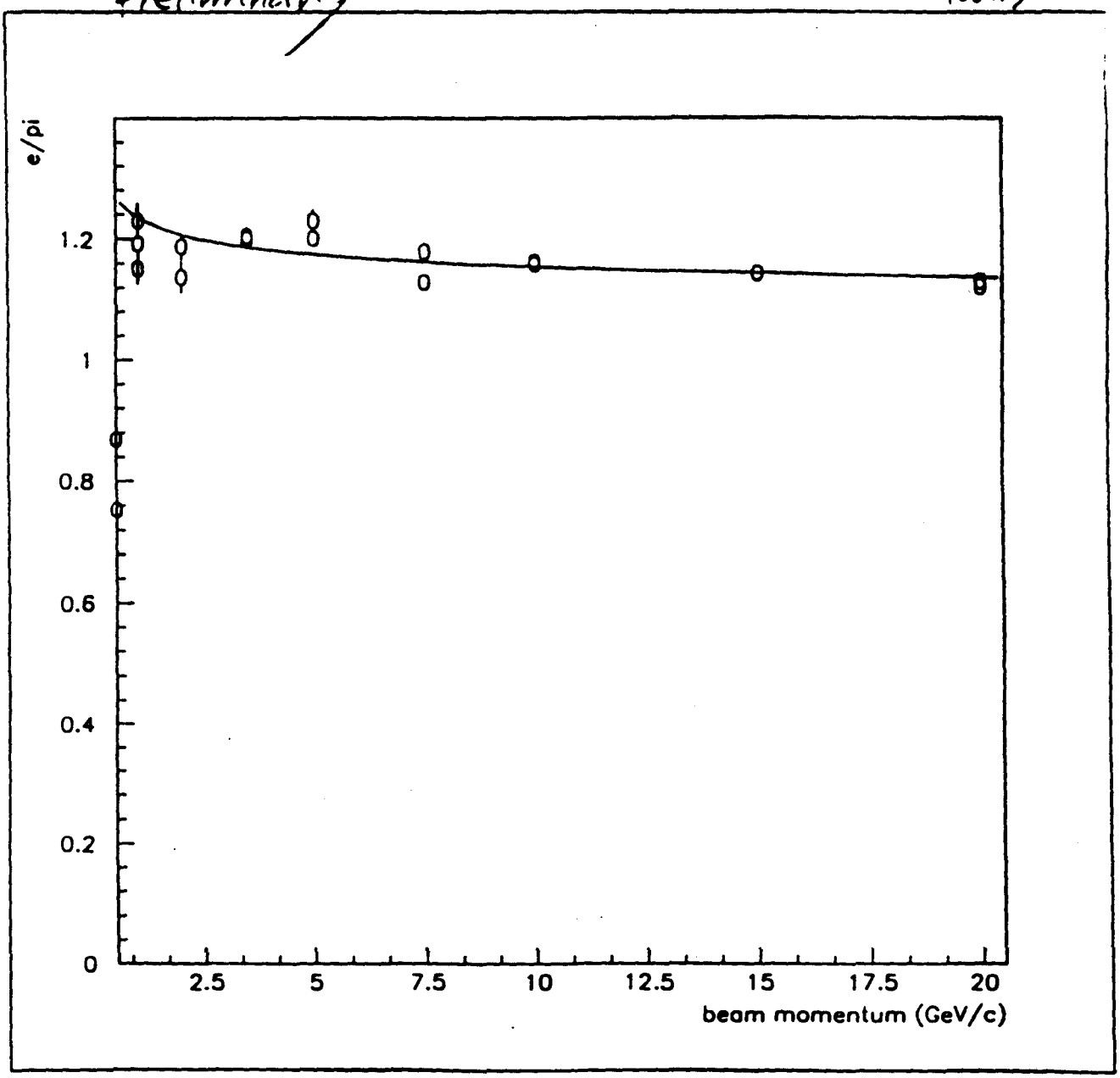

Summary

Y.Unno 1991/9/12
SDC cal TB at SSCL

(1) Electron Hermeticity

- 97% @ $sE/E<25\%/\sqrt{E}$
- In the remaining 3%, electrons is still sensitive and not lost

(2) Electromagnetic calorimeter thickness

- LAC(25Xo) is enough to get <0.5% constant term

(3) h=3~5

- Dead material $\leq 1\ \lambda_I\ (4X_O)$
- No severe degradation for jet resolutions
- No severe degradation on the missing E_t signal of the gluino production

(4) Iron shield for the magnetic transformer

- Very small contribution to the stochastic and constant terms of the hadronic resolution, e.g.

$$60\%/\sqrt{E}\oplus 4\% \rightarrow 62\%/\sqrt{E}\oplus 4.3\%$$

(5) Beam test of EM and Hadronic prototype

- Critical issues of the LAC with fast-readout have been demonstrated in the beam test at BNL

- Preliminary results are:

EM:	$\sigma_E/E=18\%/\sqrt{E}$	(t_{Pb}=6mm)
HAD:	$\sigma_E/E_\pi=64\%/\sqrt{E}$	(t_{Pb}=12mm)
	$\sigma_E/E_e=22\%/\sqrt{E}$	

e/π(HAD)=1.15@20GeV

$\rightarrow$ e/h=1.23~1.25

(These values are as expected by the simulation programs: EGS, GEANT)

- These results lead us to expect for the Pb absorber thickness of the SDC LAC (supplemented with separate estimation for the constant terms)

EM:	$\sigma_E/E=13\%/\sqrt{E}\oplus 0.5\%$	(t_{Pb}=4mm)
HAD:	$\sigma_E/E_\pi=68\%/\sqrt{E}\oplus 4\%$	(t_{Pb}=14mm)

Final words...

- We have demonstrated that LAC can be build to satisfy the SDC calorimeter requirements with its intrinsic and proven fact:

  STABILITY,

which is concentrated in the small constant term of the EM resolution and is in hand straightway.

Timing resolution			
EM	~5ns, ET>15GeV	<5ns, >1GeV	Beam test
HAD	~5ns, >100GeV	~5ns, >10GeV	Beam test
Signal peaking time	<200ns	60, 200ns	HAD(200ns)
Baseline rest.	100ns-6ms	400, 800ns	Bipolar shap.
Noise	<5GeV, ΔR=0.3	3GeV	EM+HAD1
Pileup	<5GeV, ΔR=0.3	1.2GeV	
Noise+Pileup	<5GeV, DR=0.3	3.3GeV	

Appendix: Effect of non-uniform magnetic field

T.Kondo, Task force note

Y.Unno 1991/9/12
SDC cal TB at SSCL

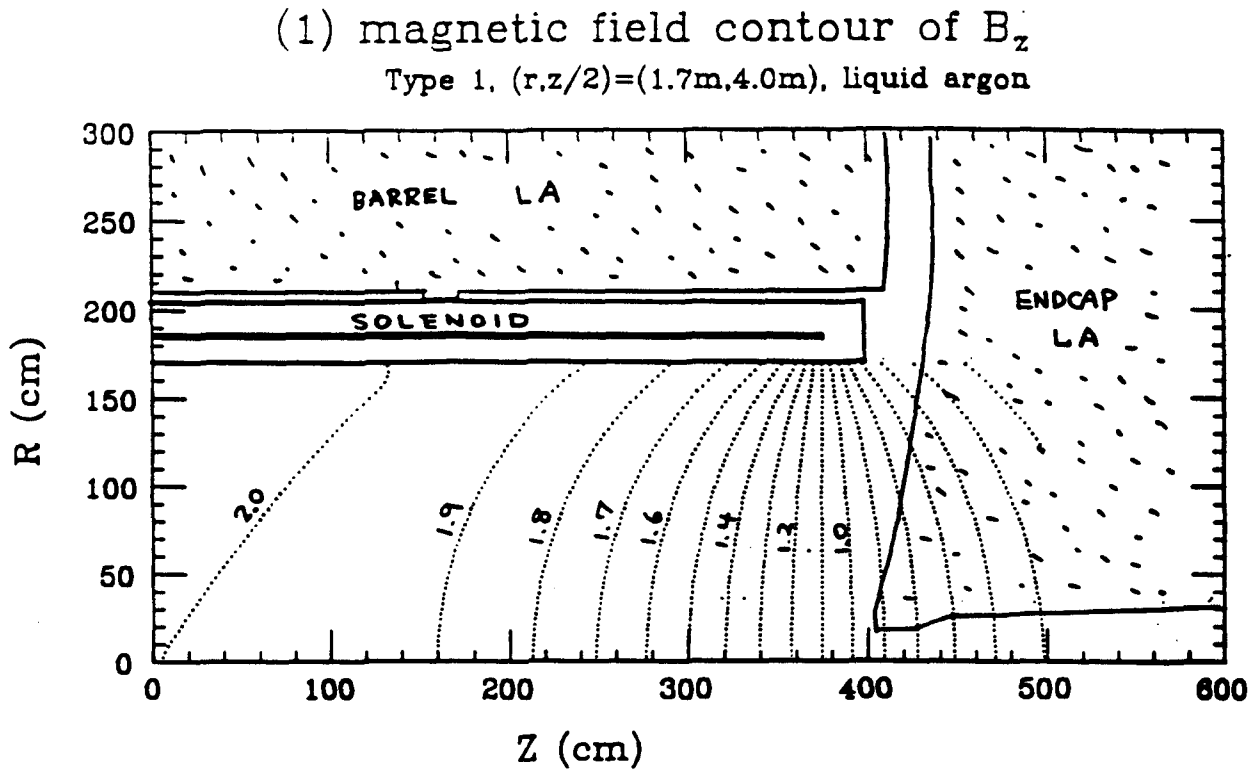
(1) magnetic field contour of B_z
Type 1, (r,z/2)=(1.7m,4.0m), liquid argon
BARREL LA
SOLENOID
ENDCAP LA
2.0
1.9
1.8
1.7
1.6
1.4
1.3
1.0
R (cm)
Z (cm)
0
50
100
150
200
250
300
0
100
200
300
400
500
600

Fig. 1

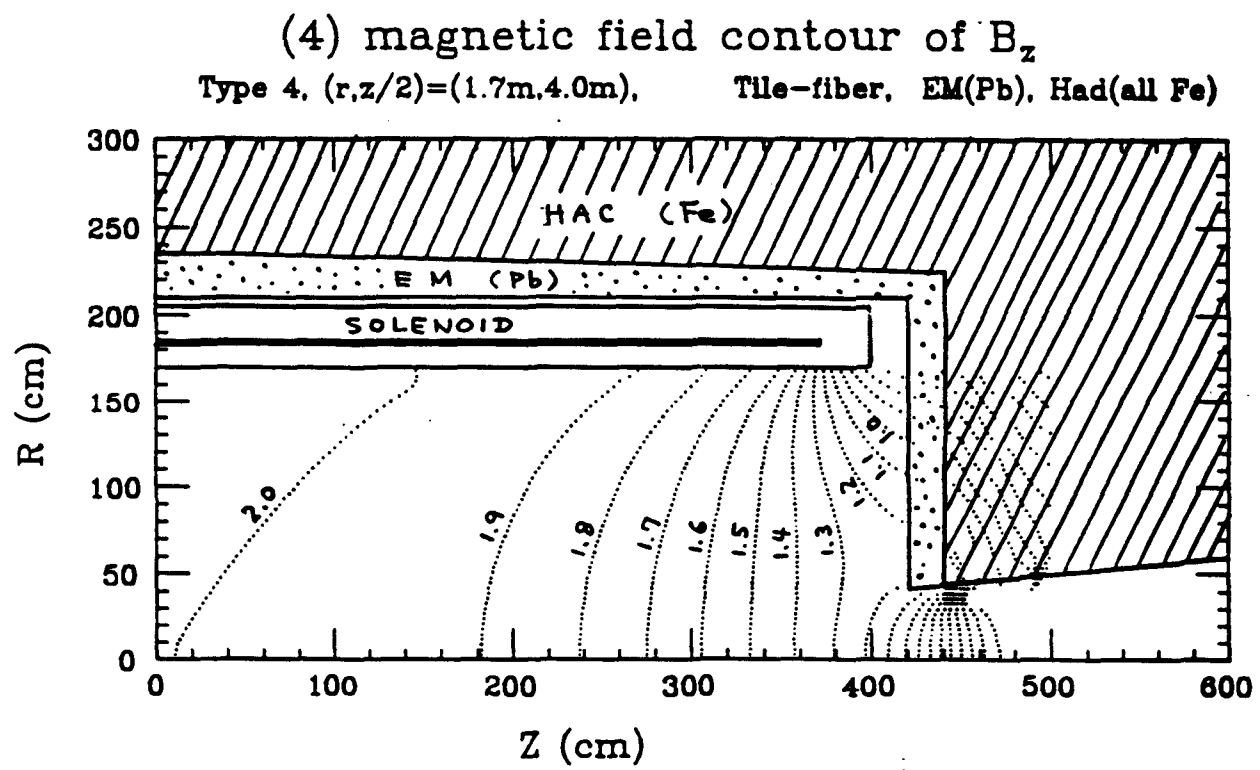
(4) magnetic field contour of B_z
Type 4, (r,z/2)=(1.7m,4.0m), Tile-fiber, EM(Pb), Had(all Fe)
HAC (Fe)
EM (Pb)
SOLENOID
2.0
1.9
1.8
1.7
1.6
1.5
1.4
1.3
R (cm)
Z (cm)
0
50
100
150
200
250
300
0
100
200
300
400
500
600

Fig. 2

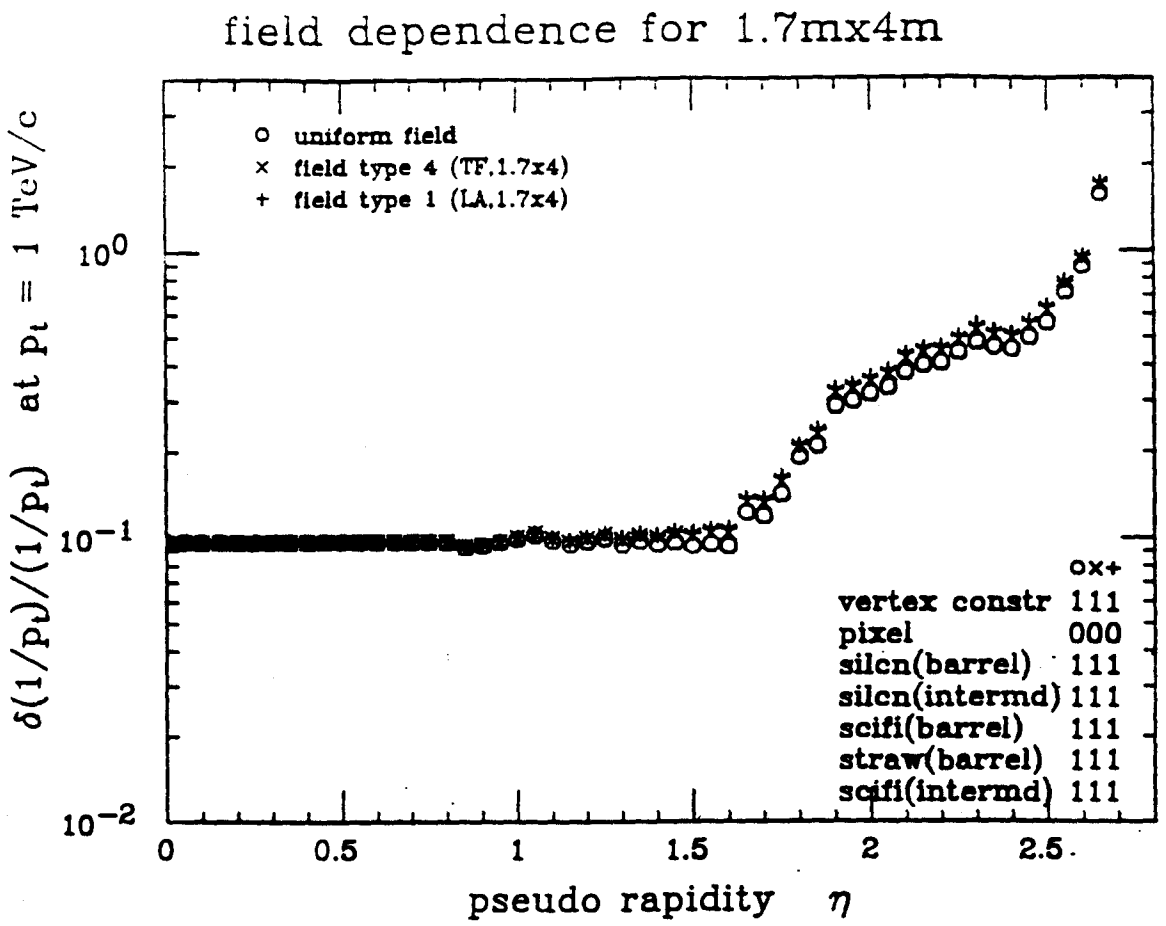
field dependence for 1.7mx4m
o uniform field
× field type 4 (TF,1.7x4)
+ field type 1 (LA,1.7x4)
δ(1/pt)/(1/pt) at pt = 1 TeV/c
10^0
10^-1
10^-2
0
0.5
1
1.5
2
2.5
pseudo rapidity η
ox+
vertex constr 111
pixel 000
silcn(barrel) 111
silcn(intermd) 111
scifi(barrel) 111
straw(barrel) 111
scifi(intermd) 111

Fig. 3

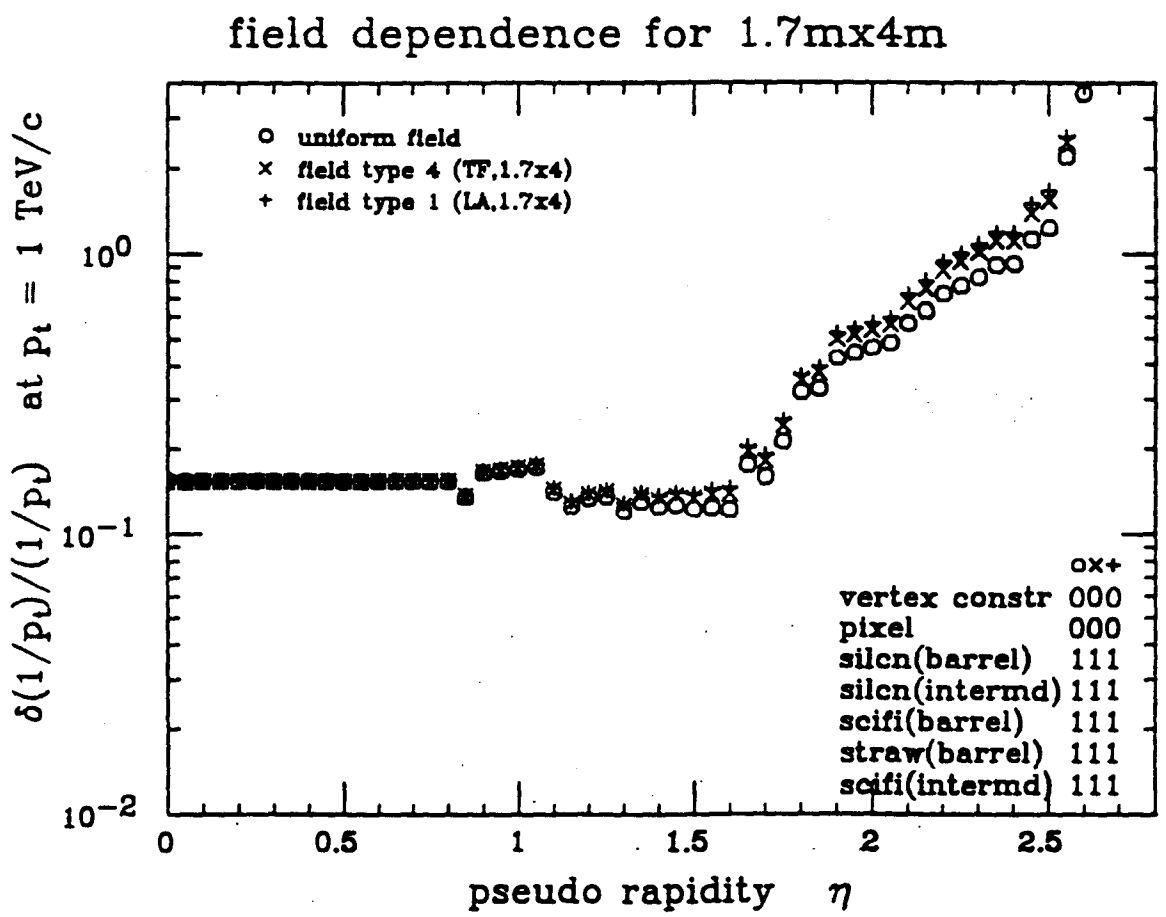
field dependence for 1.7mx4m
o uniform field
× field type 4 (TF,1.7x4)
+ field type 1 (LA,1.7x4)
δ(1/pt)/(1/pt) at pt = 1 TeV/c
10^0
10^-1
10^-2
0
0.5
1
1.5
2
2.5
pseudo rapidity η
ox+
vertex constr 000
pixel 000
silcn(barrel) 111
silcn(intermd) 111
scifi(barrel) 111
straw(barrel) 111
scifi(intermd) 111

$$\frac{\sigma}{E} = \sqrt{a^2 + b^2/E}$$

EM shower.

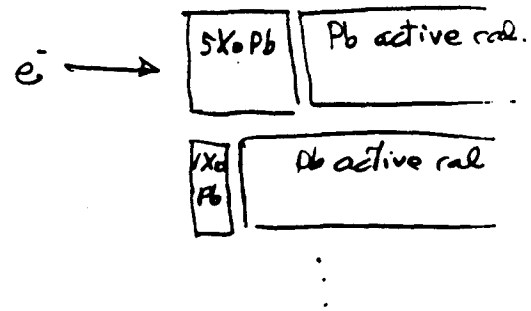

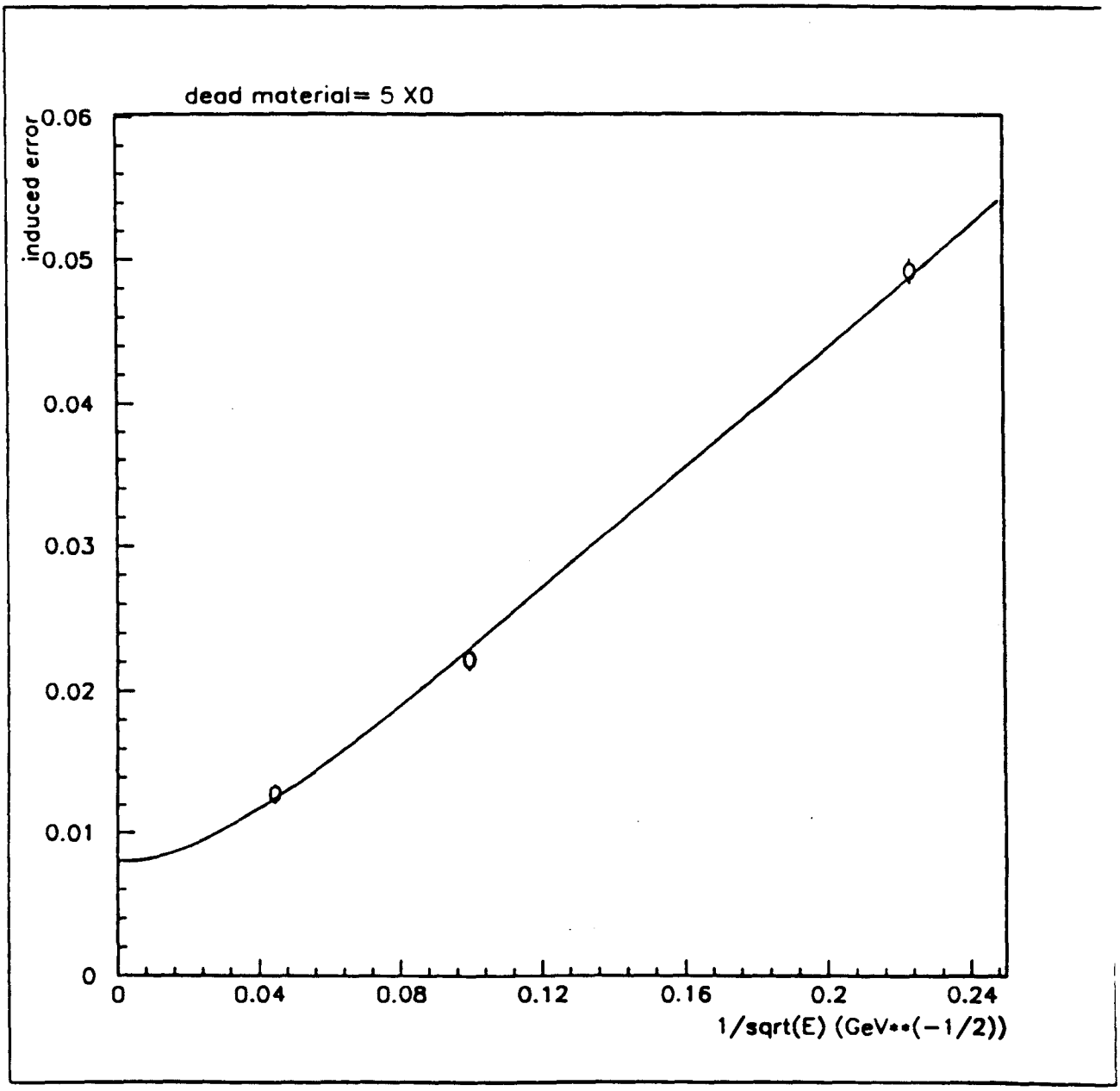

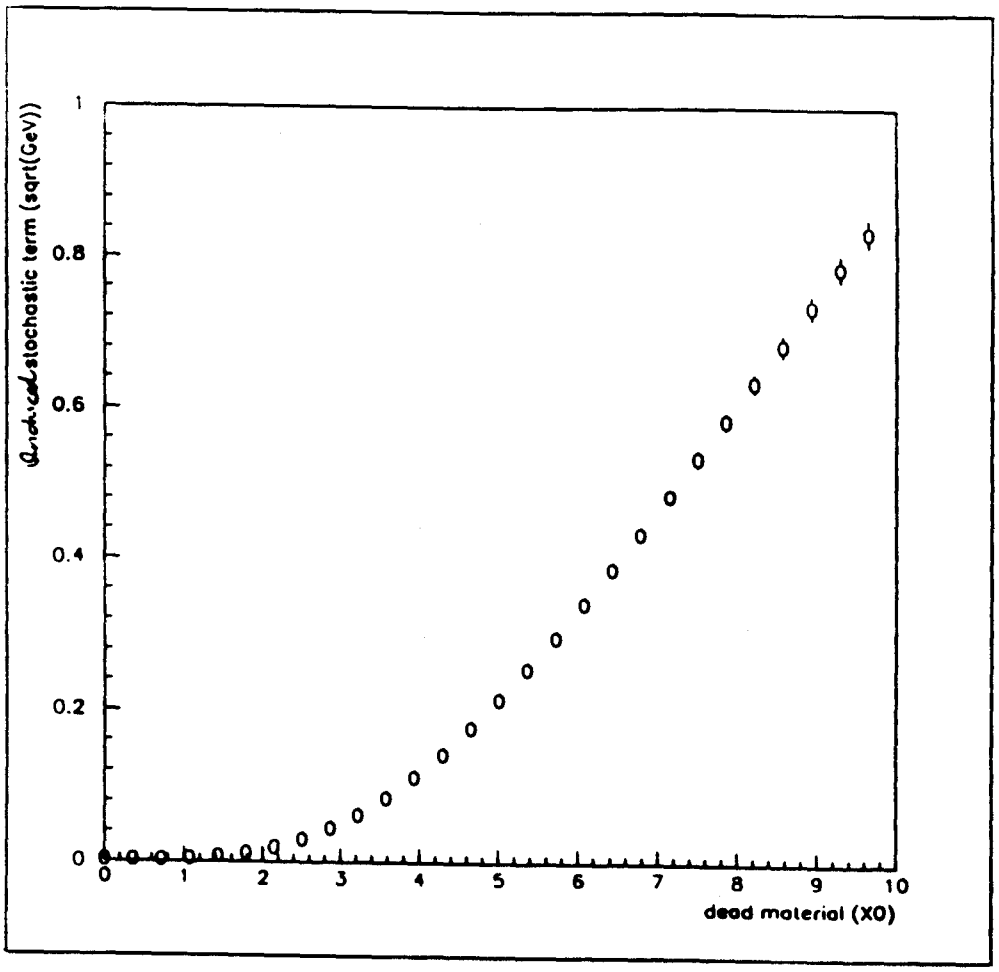
stochastic term (sqrt(GeV))
1
0.8
0.6
0.4
0.2
0
0
1
2
3
4
5
6
7
8
9
10
dead material (X0)

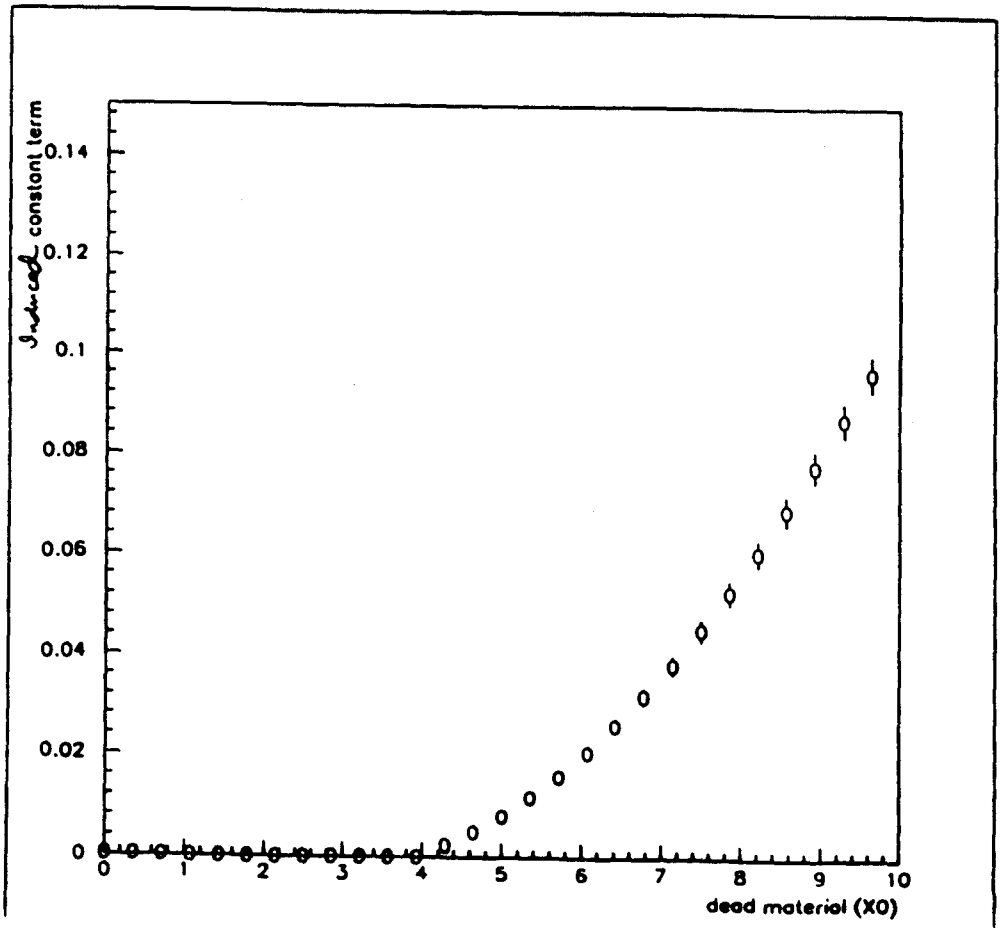
constant term
0.14
0.12
0.1
0.08
0.06
0.04
0.02
0
0
1
2
3
4
5
6
7
8
9
10
dead material (X0)

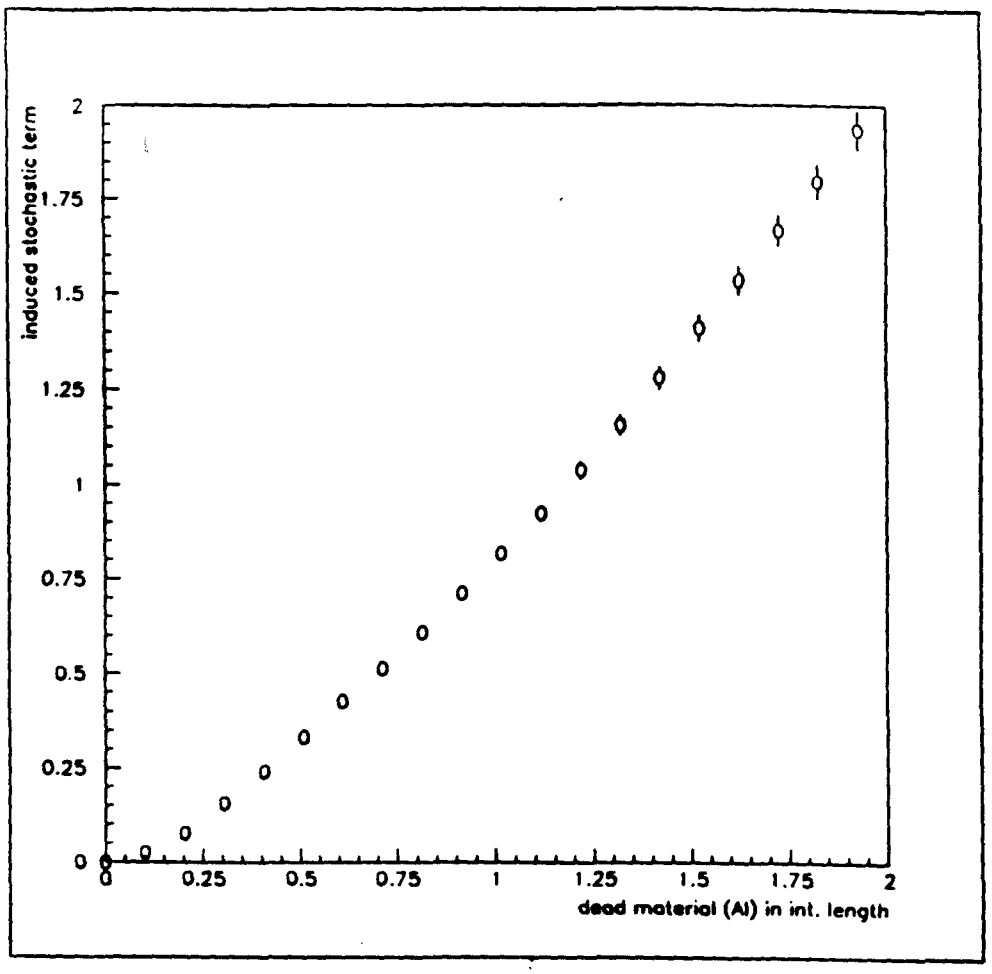
induced stochastic term
0
0.25
0.5
0.75
1
1.25
1.5
1.75
2
dead material (Al) in int. length

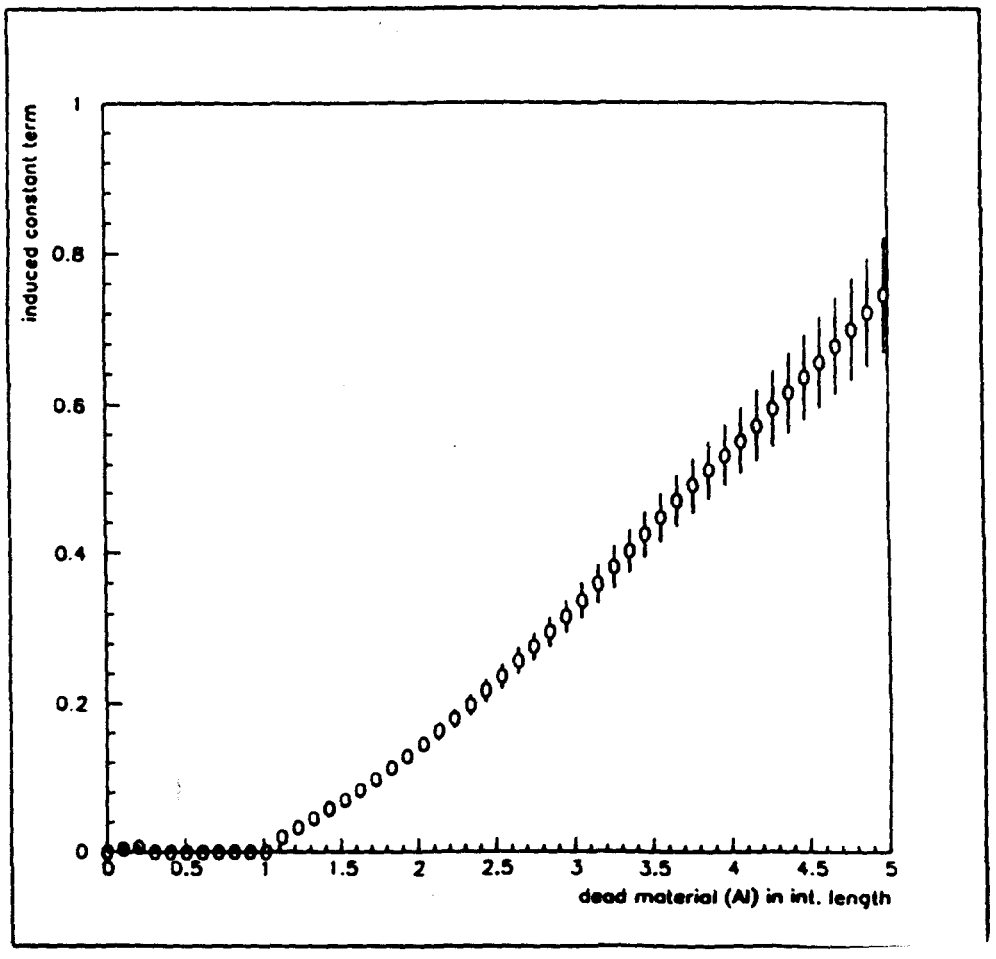
induced constant term
0
0.2
0.4
0.6
0.8
1
0.5
1.5
2
2.5
3
3.5
4
4.5
5
dead material (Al) in int. length

CALORIMETER REVIEW AND TECHNICAL BOARD MEETING
SEPTEMBER 12 -14, 1991
SSCL

Presentation by:

Chris Heartly

Lawrence Berkeley Laboratory

Liquid Argon Performance: Speed, Noise and Pileup

Christopher Hearty

Sept. 12, 1991
Technical Board Meeting

OUTLINE

1. Speed
   - speed of response
   - timing resolution

2. Electronic Noise

3. Pileup
   - impact on measurements of Higgs decay
   - impact on isolated e- ID
   - impact on jet measurements

4. Summary

Speed of Response

Current in LAr gap has very fast rise time:

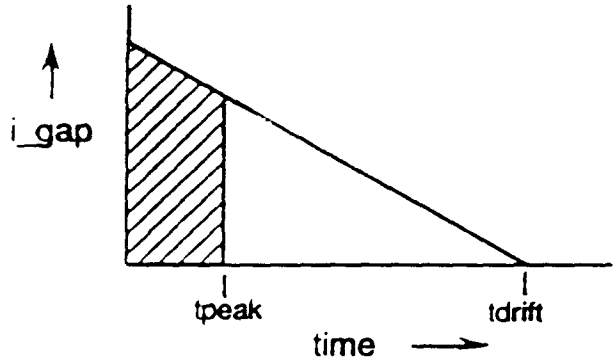

Charge transfer time and preamp response time slow leading edge.

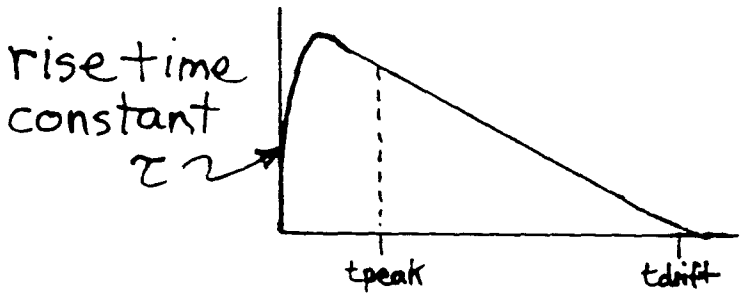

- $\tau \approx \sqrt{L \cdot C_D}$ ==> need to keep inductance low

- noticable signal loss for tau ≥ tpeak
  (signal loss <==> increase in noise)

Time Resolution

- bucket tag using zero cross of bipolar shape

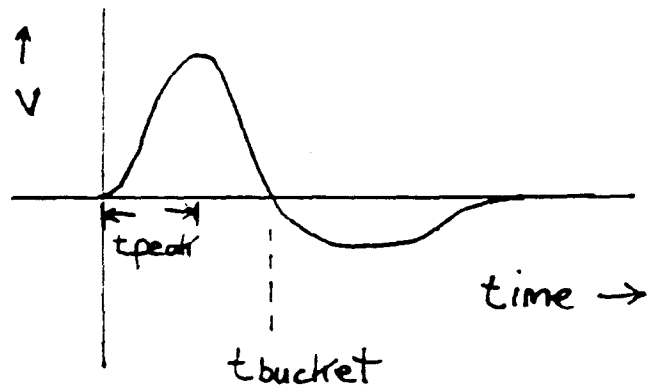

$$\sigma_t \approx t_{peak} \cdot \frac{N}{S}$$

For 10 GeV e- into test beam module,

EM2: S = 5.1 GeV
N = 0.067 GeV
tpeak = 100 ns

==> sigma_t (expected) = 1.3 ns

Measured: sigma_t = 1.5 +/- 0.2 ns

Timing: Trigger

Use ~5 waveform samples to measure amplitude and zero cross, and to tag significant pileup.

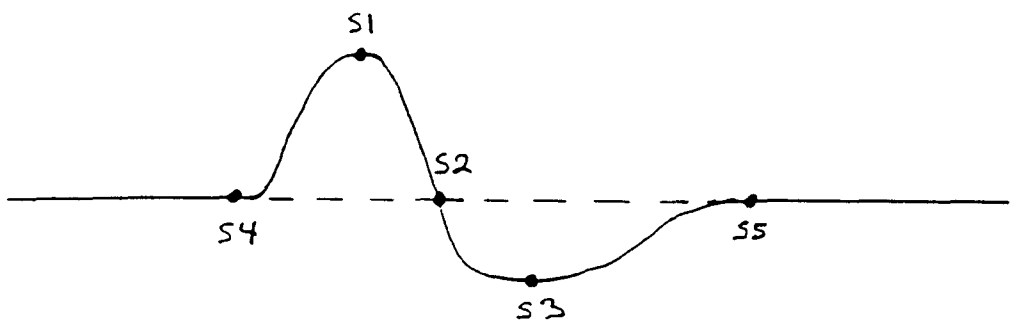

Level 1 may be simpler

Timing: Readout

Trigger determines the bucket of interest

For each channel, record waveform at expected location of peak and zero cross (s1,s2)

==> timing information is preserved

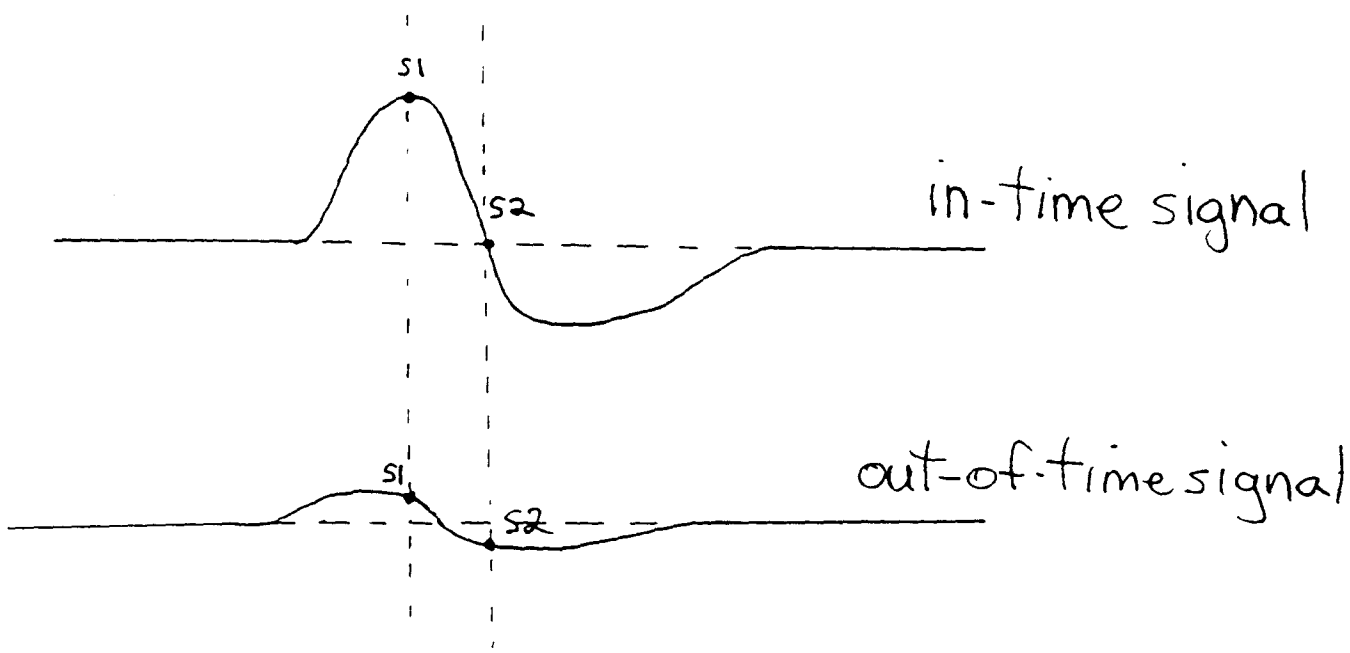

Maybe more (five?) samples for EM

Effect of Timing Resolution

Electron Isolation

Expect small signals, so do not apply bucket tag to isolation cone (just sum s1 for each channel)

==> never create "isolated" electron by mistiming accompanying energy

Missing-Et/ Fake Signal

Probability of placing a ≥80 GeV Et jet in the adjacent bucket is 2E-5.

==> <1 Hz at 10**33

Level 1/2 trigger issue only; easy to spot at level 3 or offline

80 GeV Jet Timing Resolution vs Eta

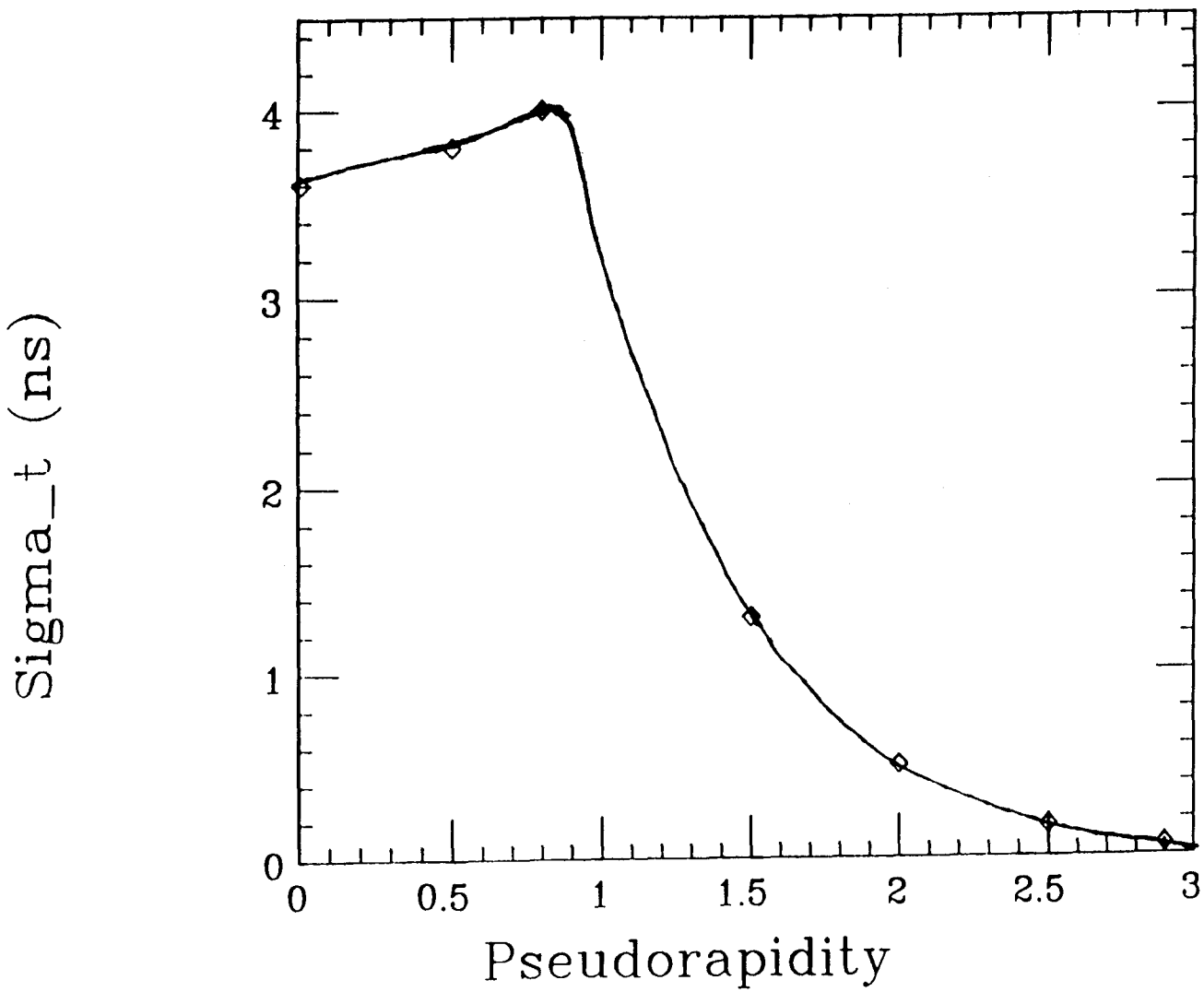

For SDC, at eta = 0,

Sigma_t < 5 ns for

- E > 1 GeV in EM channel
- E > 5 -- 10 GeV in hadronic channel

(See summary table later)

Electronic Noise

Equivalent Noise ~~Energy~~ Charge

ENC is the impulse charge on the signal pads of the electrodes that gives the same response after the shaper as the electronic noise

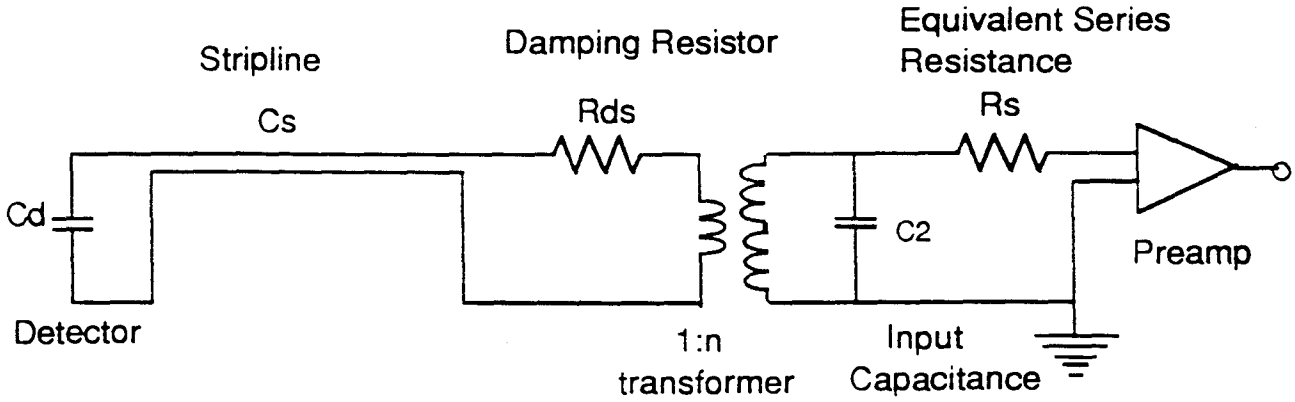

Schematic diagram of front end for calculating noise. Rds and Rs are the two significant noise sources.

Only series noise is important for JFET:

$$ENC^2 = \frac{8k}{t_{peak}}\left[R_{ds}\cdot T_{ds}C_1^2 + R_s T_s\left(\frac{C_1}{n} + n\cdot C_2\right)^2\right]$$

Rds is damping resistor at temperature Tds
Rs is the equivalent series resistance of the JFET at temperature Ts
C1 = Cd + Cs is the total capacitance upstream of transformer
C2 = Cfet + Cstray is the total capacitance downstream

Transformer matches C1 to C2, so ENC depends linearly on C1 in 1st term and on sqrt(C1) in second term.

For SDC, Rds = 2 ohms, Tds = 88 K
Rs = 17 ohms, Ts = 300K (equiv)
Cfet = 40 pF, Cstray = 10 pF

Choose stripline so Cstrip = Cdet/3, but Zstrip ≥ 4 ohms

Equivalent Noise Energy

Relate energy deposited in the calorimeter to charge collected during the effective integration time (tpeak).

- Ballistic deficit:

$$\frac{Q}{Q_0} = \frac{2\, t_{peak}}{t_{drift}}\left(1 - \frac{1}{2}\frac{t_{peak}}{t_{drift}}\right) = \begin{cases} 0.28 & t_{peak} = 60\,ns \\ 0.44 & t_{peak} = 100\,ns \end{cases}$$

- Sampling fraction:
  fraction of energy in LAr from dE/dx.
  s = 0.13 EM
  = 0.023 hadronic

- p/mu: fraction of energy deposited in LAr by showers is less by
  e/mu = 0.66
  pi/mu = 0.53

$$\frac{dQ}{dE} = 3.03 * S * \frac{Q}{Q_0} * \frac{P}{\mu} * B_{block} \quad \left[\frac{fC}{MeV}\right] \quad \frac{\text{charge on sig.f}}{\text{energy in calo}}$$

- 3.03 is LAr ionization
- Bblock = 0.9 for charge lost on blocking C

(finite rise time effects would decrease Q/Q0)

Electronic Noise: Test Beam Module

EM2-A Pedestal Width and Muon Peak

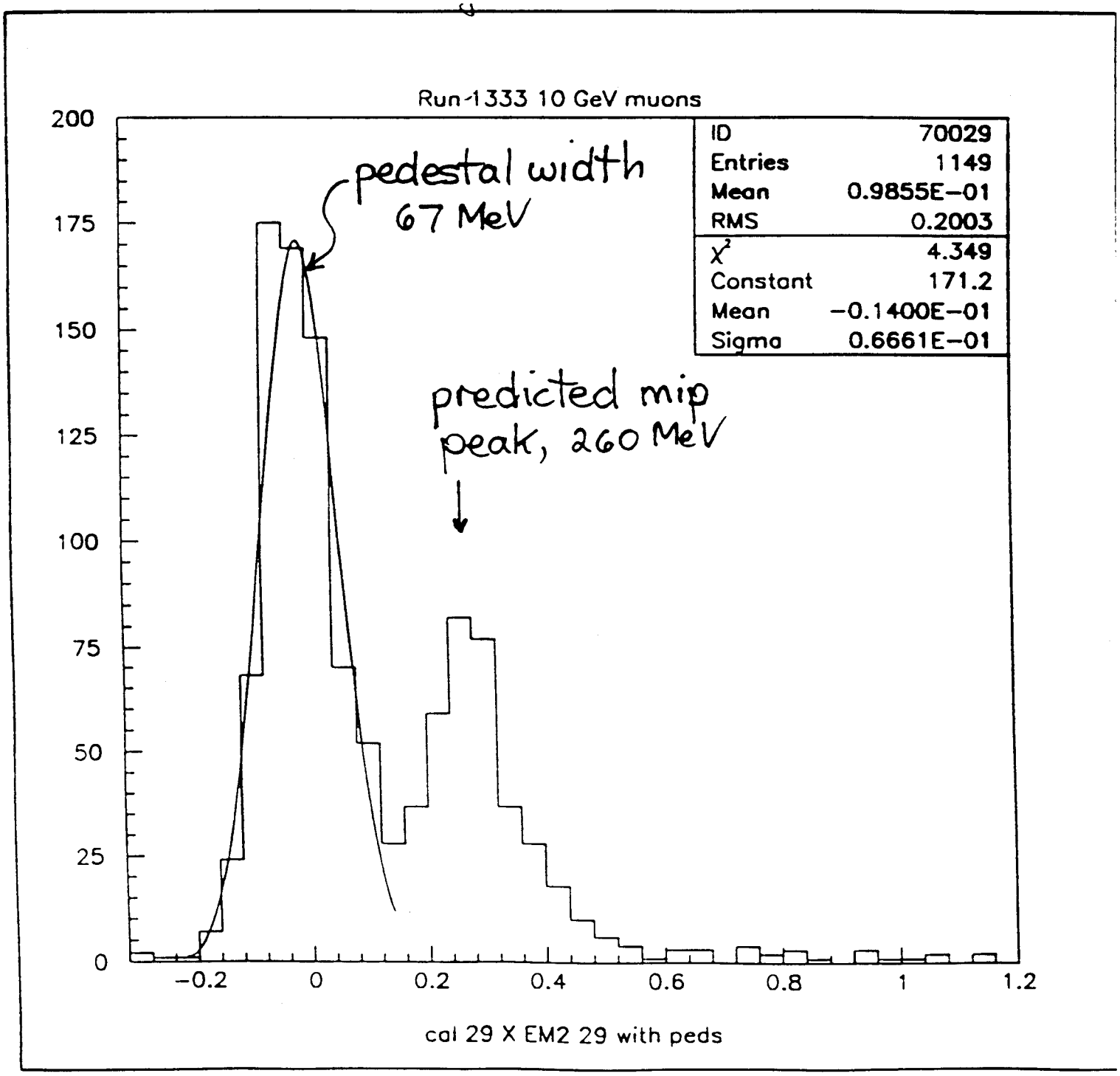

EM2-A Pedestal width

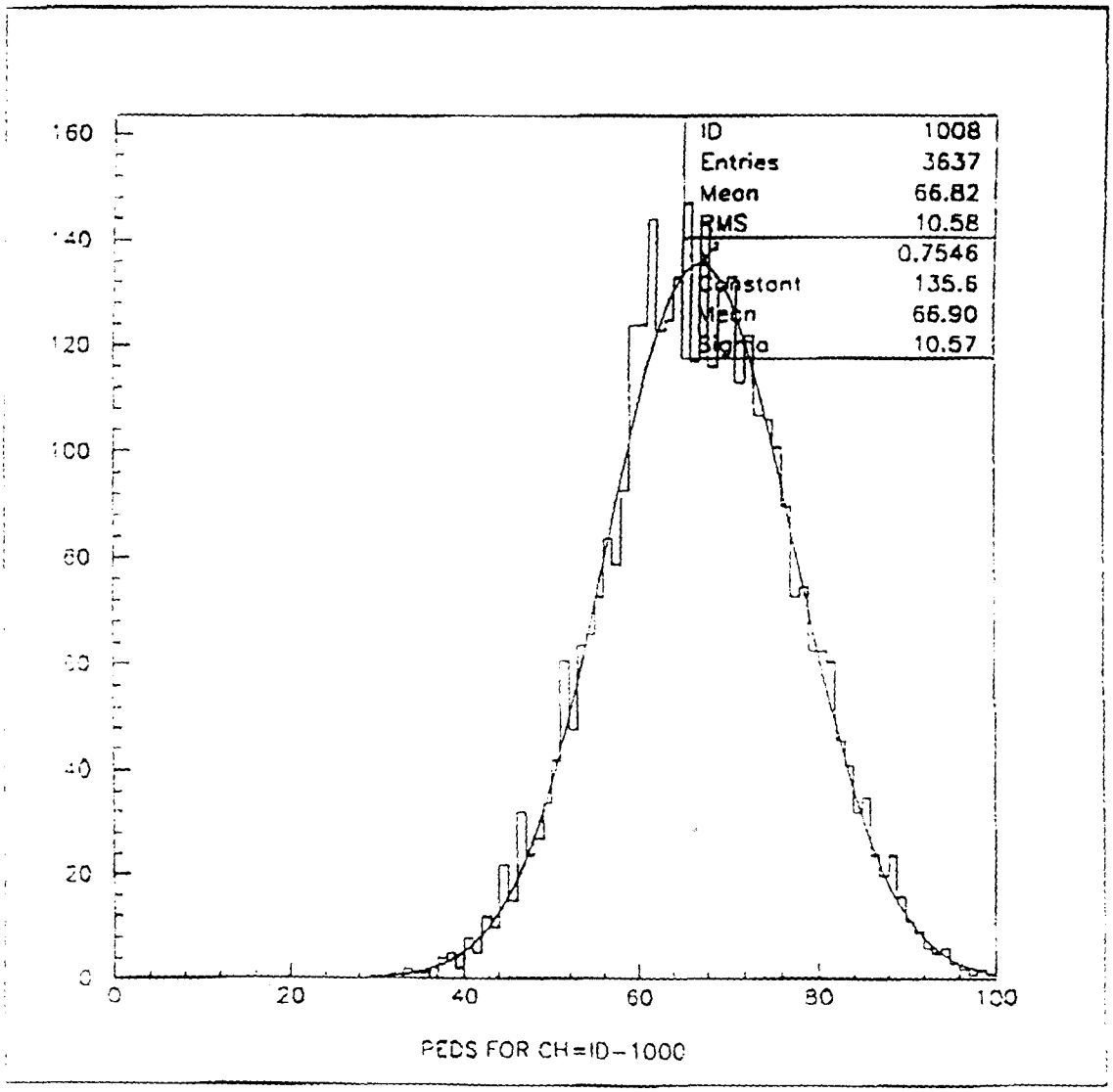

Figure 1. Pedestal width (ADC counts) for Channel 5 (EM2) VGA gain = 10.

Comparison between measured and predicted ENE (MeV), BNL test beam module:

Channel	Measured	Predicted
EM1-A	16 +/- 2	23 +/- 5
EM1-B	17 +/- 2	23 +/- 5
EM2-A	67 +/- 7	50 +/- 10
EM2-B	50 +/- 7	50 +/- 10

Measured values are consistent with expected thermal noise (not a surprise).

No significant pickup. (EM2 pedestal width corresponds to preamp output voltage of 150μV)

SDC conceptual design

Preamp output voltage vs deposited energy in EM2

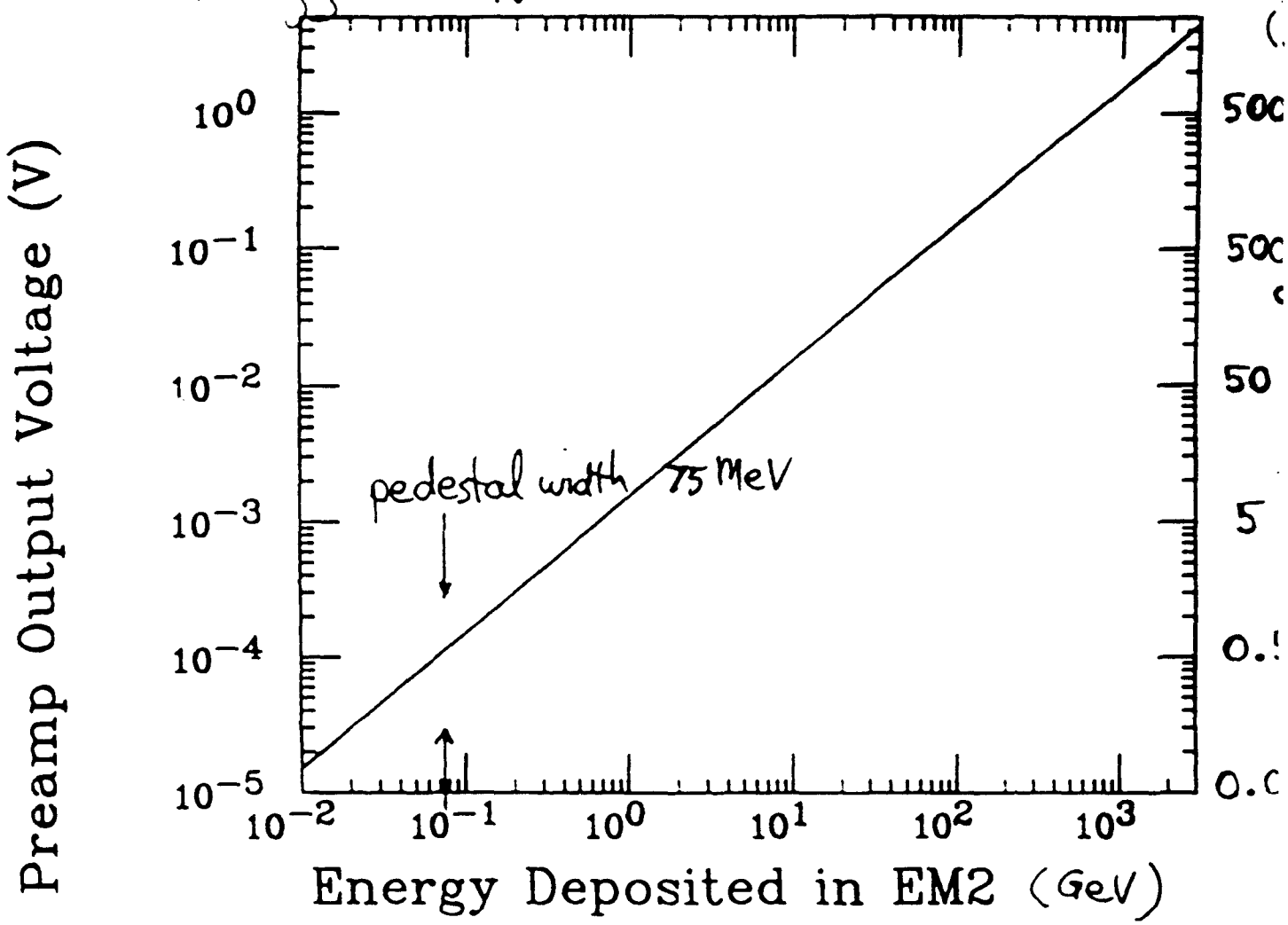

Summary of Noise per Channel

- eta = 0
- pileup for 10**33
- Mip = energy deposited by mip; mip S/N is signal-to-noise for mip
- sigma_t is timing resolution for 10 GeV in channel
- two preamps per hadronic section; sum before readout

		per Preamp									per Channel					
Section	N_{amp}	N_{gap}	$< r >$	C_D	C_s	C_{tot}	n	t_{peak}	ENC	ENE	ENE	Pileup	Total	Mip	Mip	
			cm	pF	pF	pF		ns	fC	MeV	MeV	MeV	MeV	MeV	S/N	
EM1	1	5	236	970	340	1310	5	60	1.7	27	27	30	40	32	0.8	<
EM2	1	26	255	5680	460	6140	11	60	4.9	75	75	54	92	161	1.7	<
HAD1	2	18	314	3100	1030	4130	9	100	2.8	194	274	44	278	662	6.3	2
								200	2.0	80	113	63	129		5.1	2
HAD2	2	27	387	7070	1530	8600	13	100	4.9	337	477	3	477	993	2.1	4
								200	3.5	139	197	4	197		5.0	3

- Total EM noise essentially constant for $60 \leq$ tpeak ≤ 100 ns. 60 ns selected to minimize pileup at 10**34.

- EM noise increases 2.4X for 10**34 (proportional to Lum**0.38)
  EM+HAD1 noise increases 1.6X for 10**34
  (proportional to Lum**0.20)

- Noise insensitive to details of pileup calculation:
  +/- 30% in sigma(inelast) or Lum
  ==> +/- 5% in EM+HAD1 noise

- 200 ns tpeak for hadronic clearly closer to optimum than 100 ns. tpeak limited by pipeline and level 1 trigger time.

- separation between ENE and Mip
  ==> threshold per channel before sum
  (not used in results next section)

Noise in Cones

tpeak (EM) = 60 ns
tpeak (had) = 100 or 200 ns

Cone Radius	Excluded Section	Electronic Noise (GeV) t_{peak} = 100 ns	200 ns	Pileup Noise (GeV) 100 ns	200 ns	Total Noise (GeV) 100 ns	200 ns
Single Tower	—	0.56	0.24	0.13	0.15	0.57	0.28
	HAD2	0.29	0.14	0.13	0.15	0.31	0.20
0.15	—	2.9	1.3	0.83	0.96	3.1	1.6
	HAD2	1.5	0.73	0.81	0.93	1.7	1.2

Electronic Noise E_t vs η ; cone radius 0.15

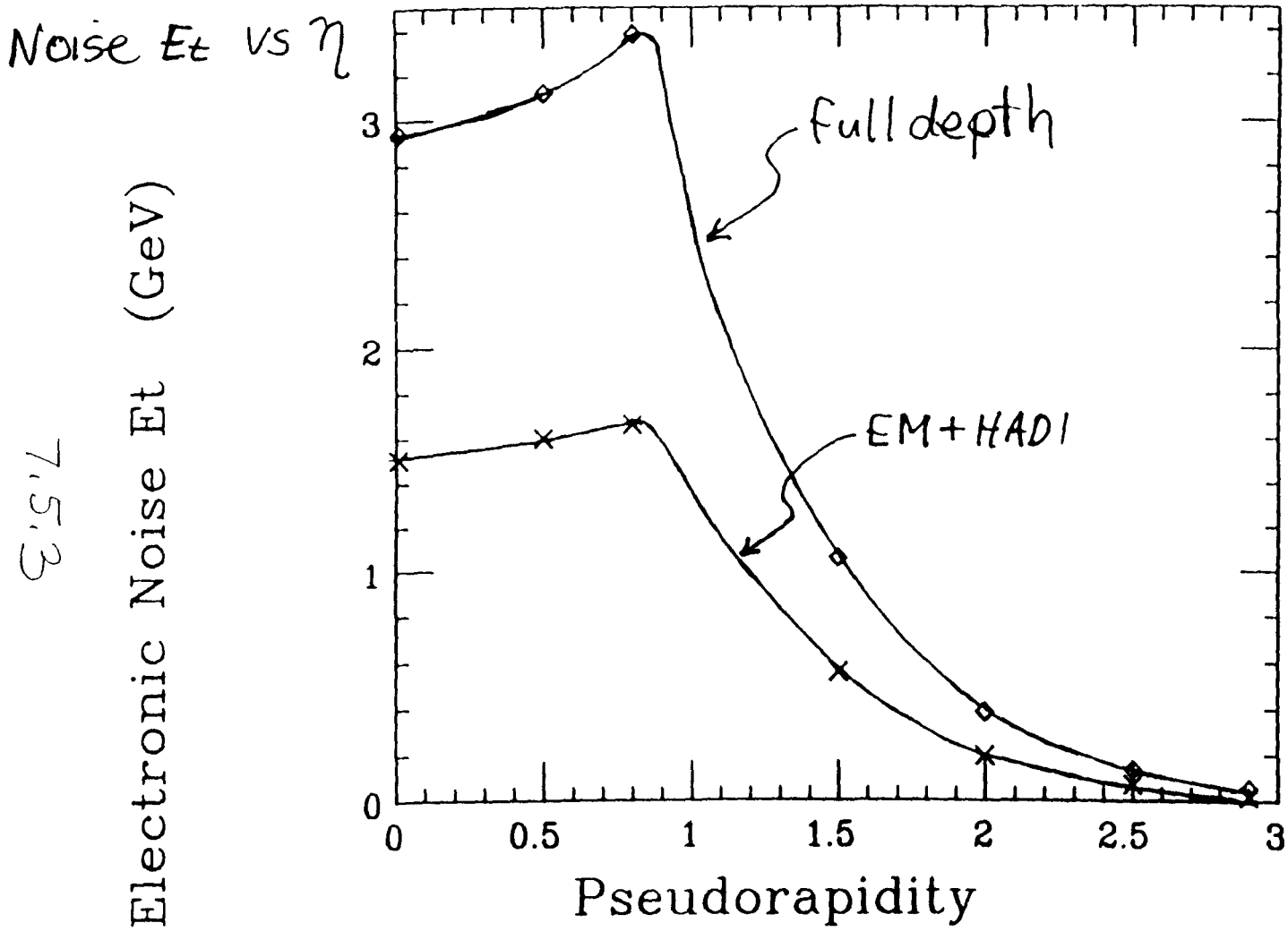

7.5.3

Pileup

Convolution of shaper and triangular input current:

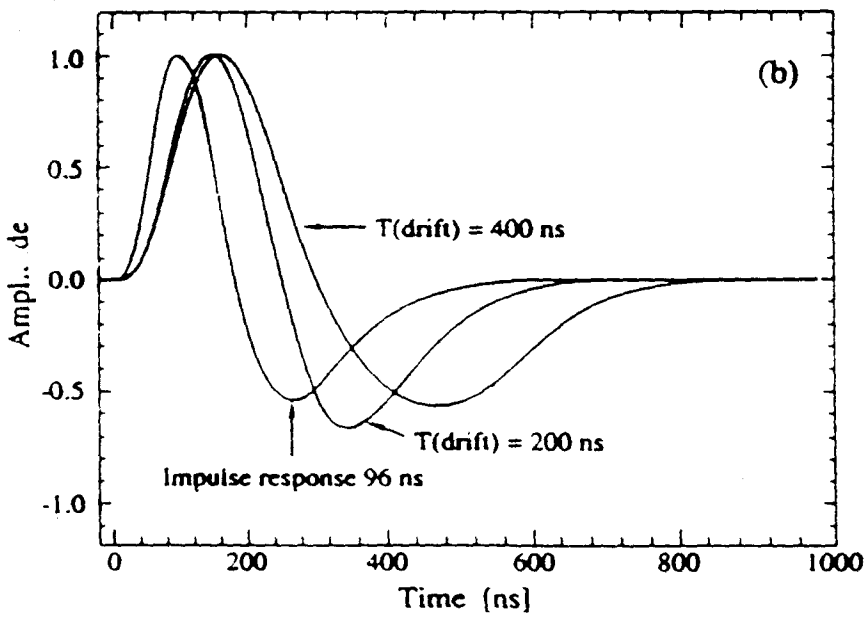

Resulting shape has long, low amplitude negative tail and no net amplitude
==> average observed energy is zero

Observed pileup E_t in cell 0.2×0.2 @ 10^{33}

- $\langle E_t \rangle = 0$
- asymmetric tails from asymmetric bipolar sh

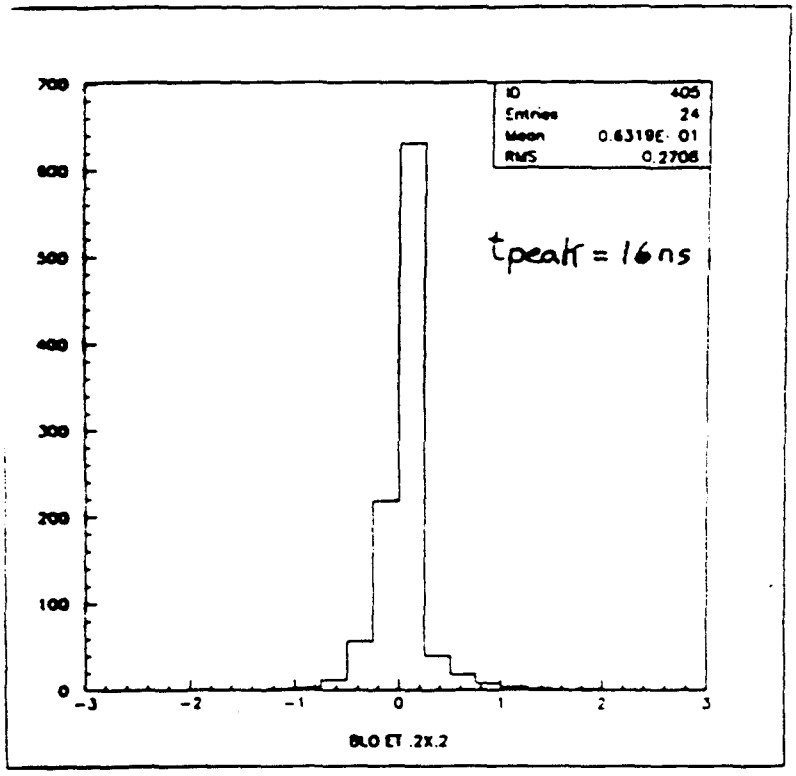

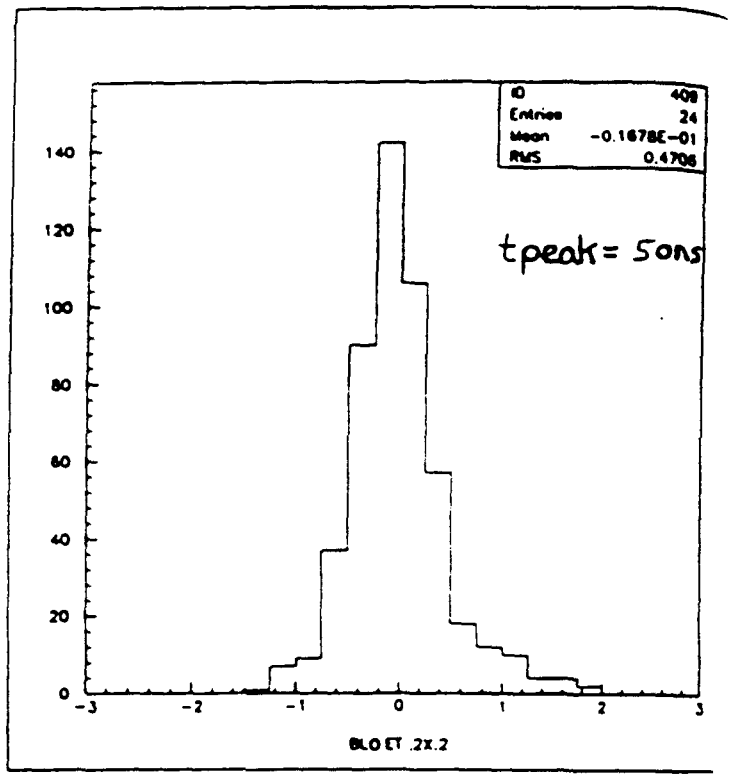

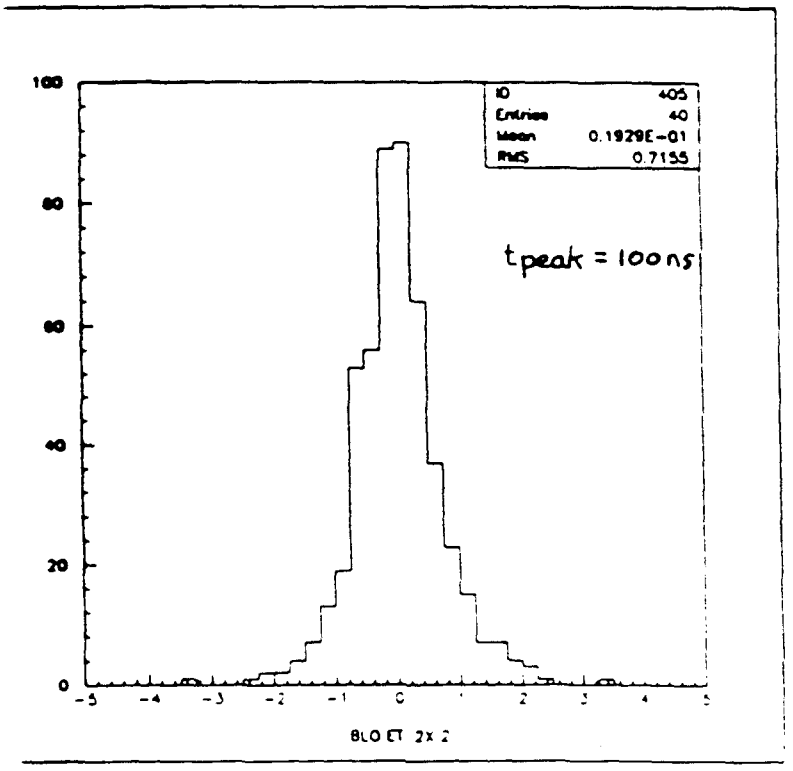

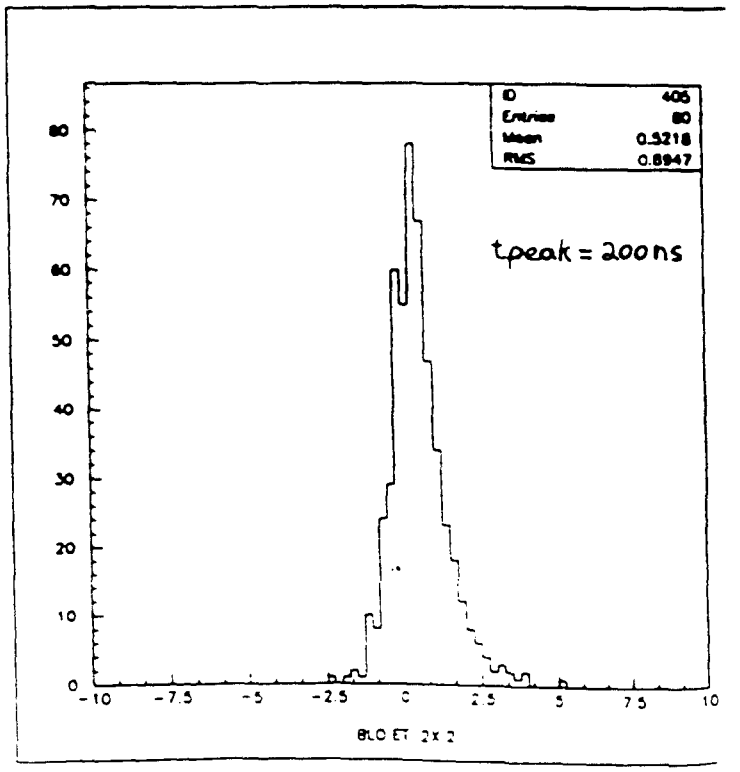

Pileup "noise" from non-zero rms:

$$\sigma_p^2 = \sigma^2(E_t) \cdot W$$

σ^2(Et) = variance of Et deposited per crossing

W = effective duration in number of beam crossings of observed shaper output

$$= \sum_{i=-\infty}^{\infty} h^2(t_i)$$

(W ≈ 7.4 tpeak = 60ns
24 200ns)

$\propto$ tpeak (approx)

$$\sigma_p \propto \sqrt{\mathcal{L} \cdot \Delta\Omega \cdot t_{peak}} \quad \text{(approx.)}$$

Effect of Pileup and Noise on Higgs Measurement

Overlap minbias events, including drift and shaping time, with photons from associated production of 80 GeV Higgs.

Compare resulting energy resolution, e- ID efficiency, and mass resolution to fast calorimeter case.

Simulation

Calculate signal observed after shaper for every cell for a long sequence of crossings.

- cells 0.1 by 0.1, no shower spread
- hadrons deposit 30% of energy in EM compartment
- average of 1.6 [16] low-pt jets per crossing
- No B field, no energy loss in coil
- tdrift = 400ns; tpeak = 60 ns [EM], 200 ns [HAD]; bipolar shaping
- no thresholds applied before sums, no attempt to reject out-ot-time energy.

Fast calorimeter response is a delta-function

ID= 110

Et deposited in 0.1×0.1 cell per crossing

ET IN 0.1 BY 0.1 $10^{3/3}$

<(X)=(1753 +- 7)E-5 SD=(1077 +- 1)E-4

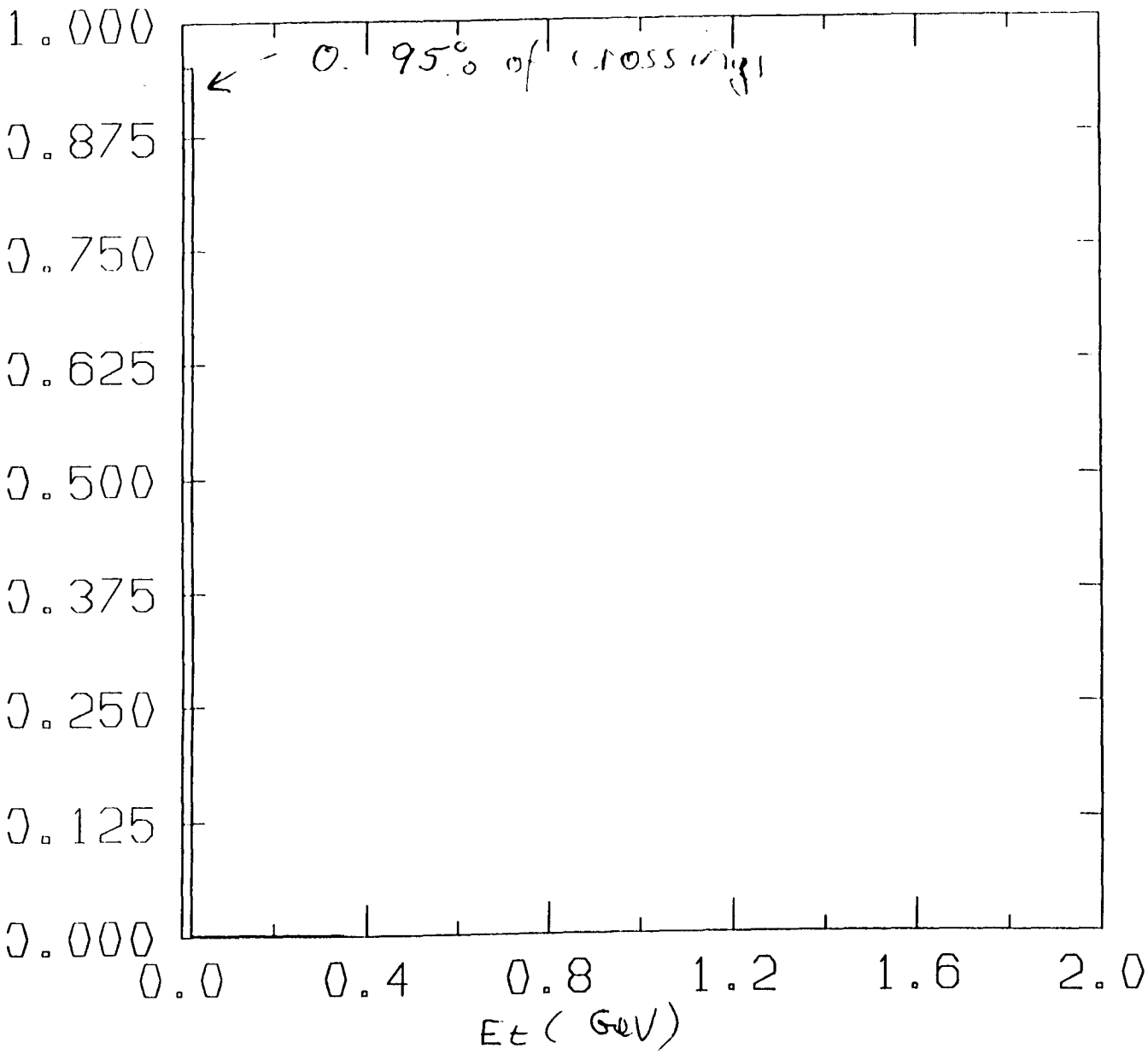

ID= 110

Et deposited per crossing

ET IN 0.1 BY 0.1 10^{3}

<(X)=(1753 +- 7)E-5 SD=(1077 +- 1)E-4

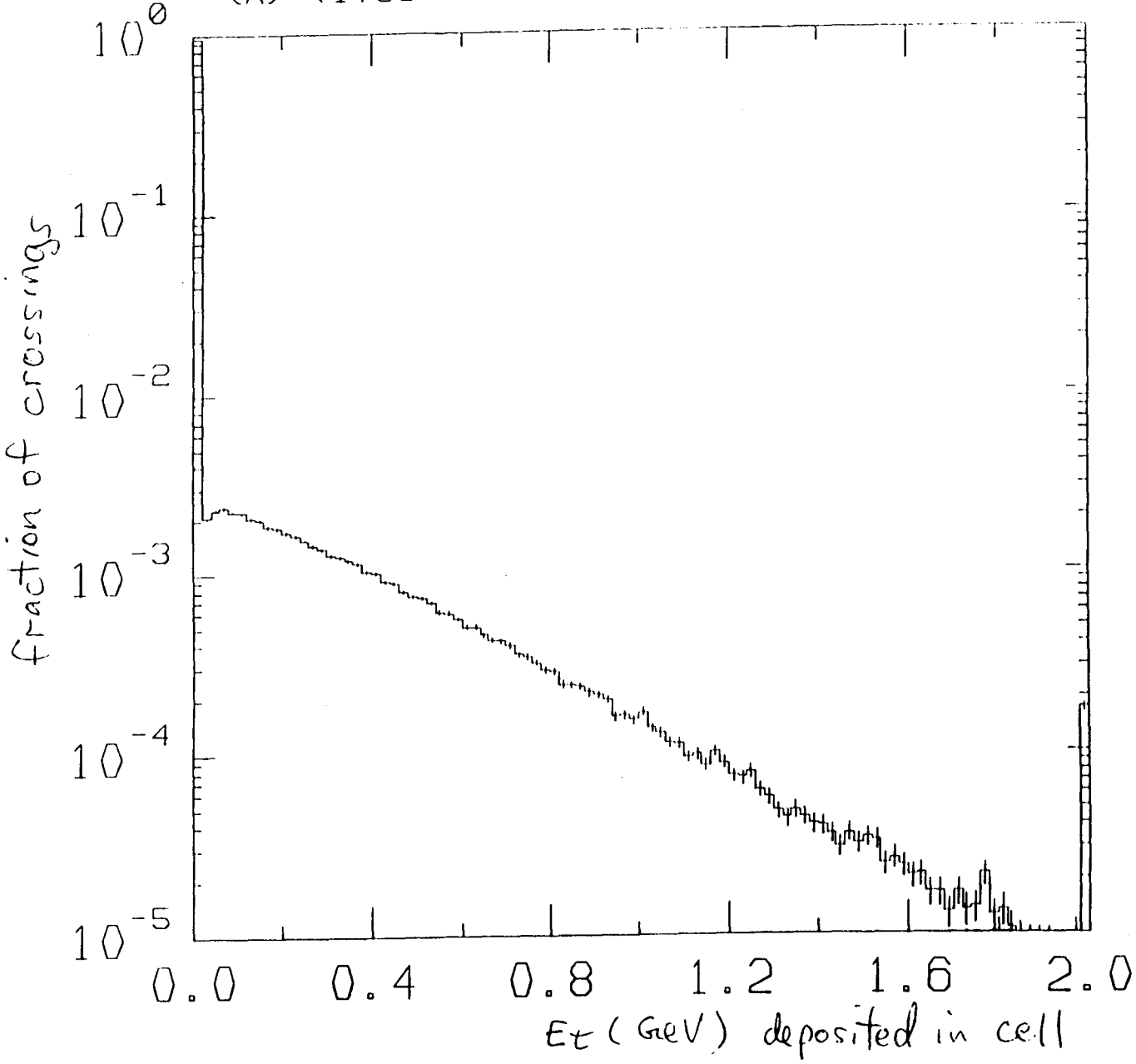

Shaper Output, tpeak=60 ns, tdrift=400ns

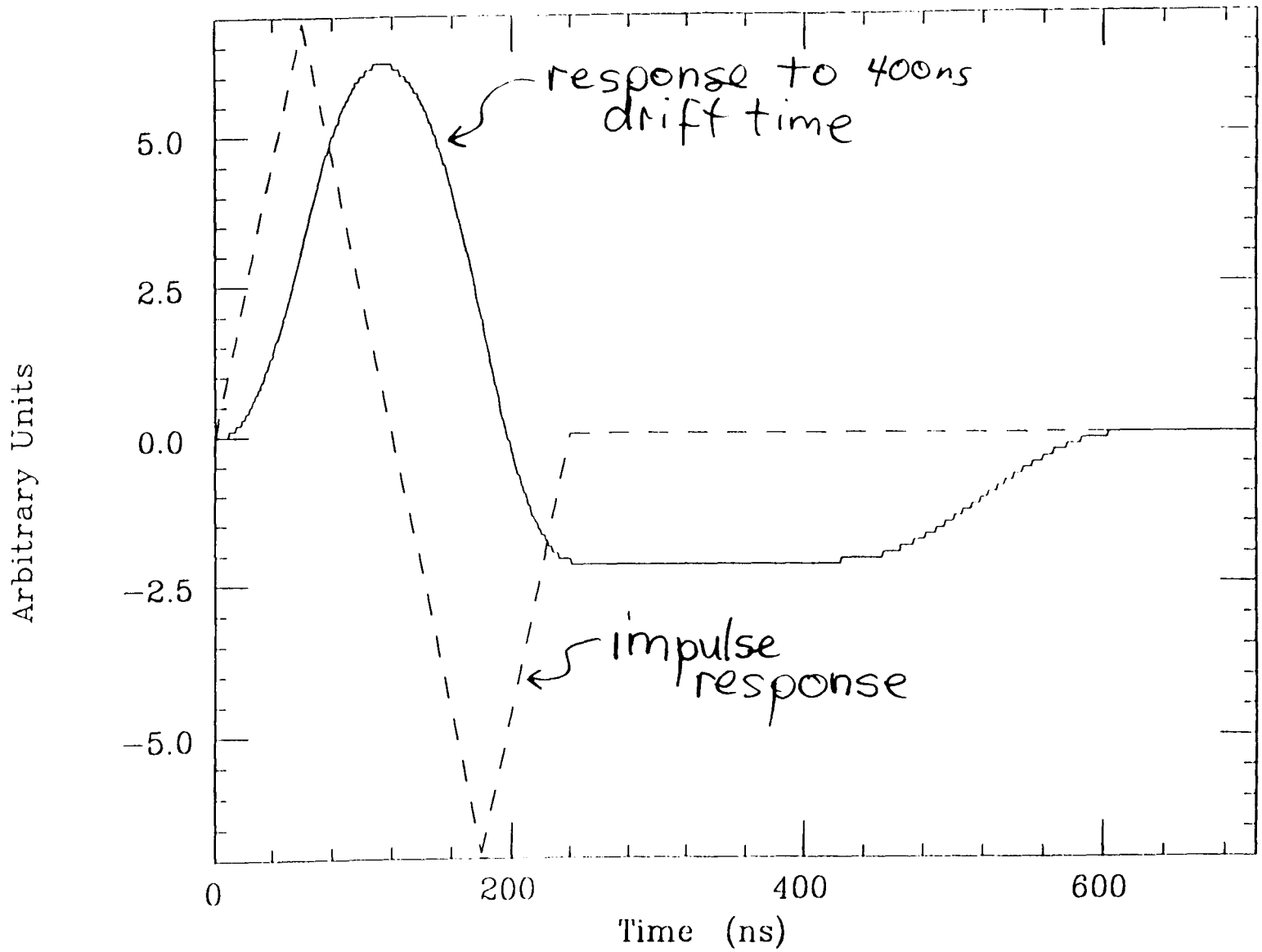

Before/After Shaping

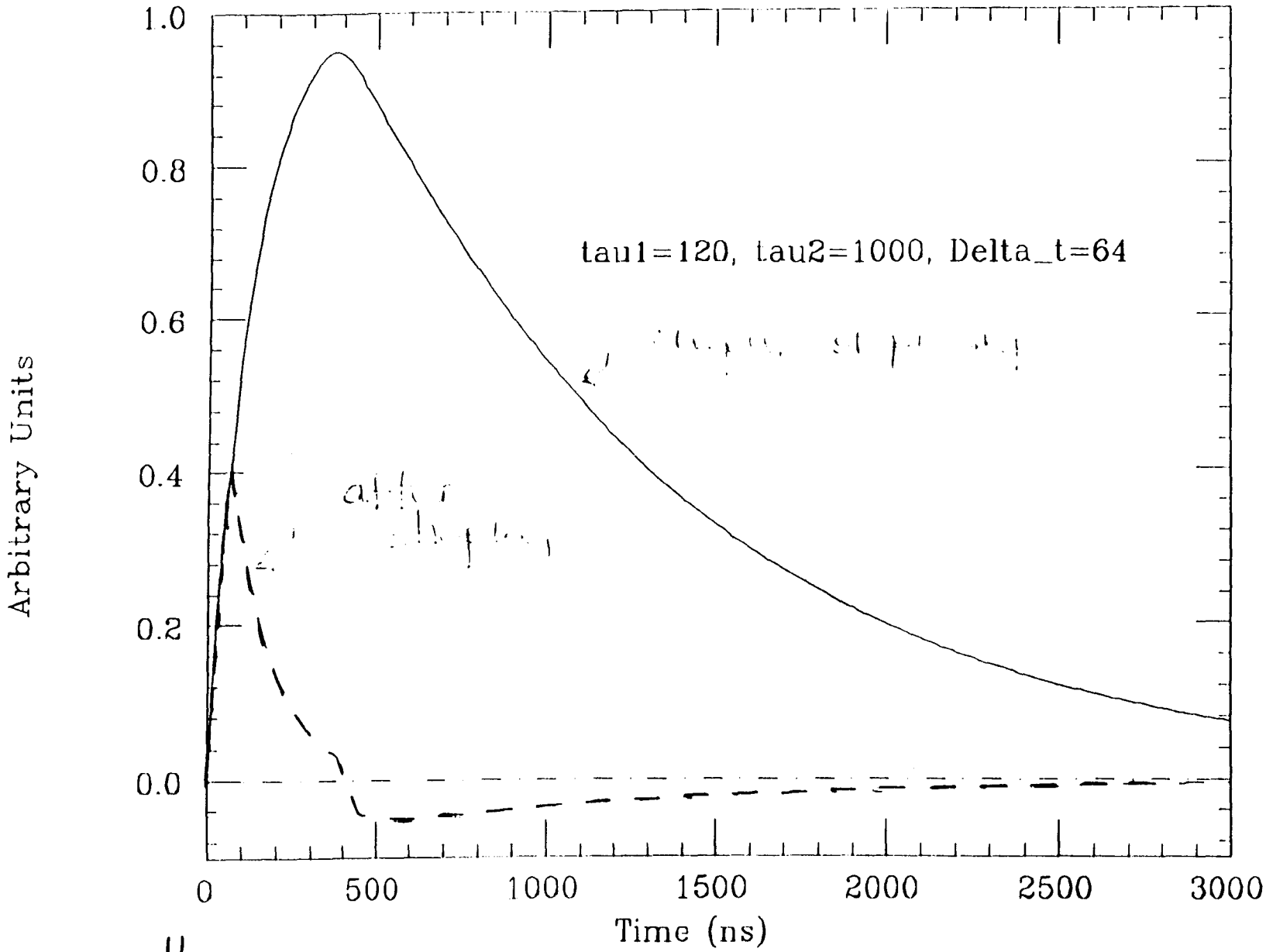

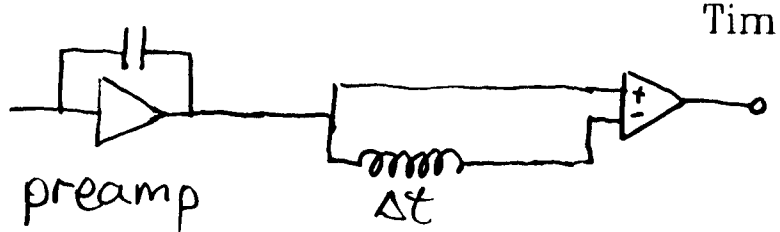

ID- 121

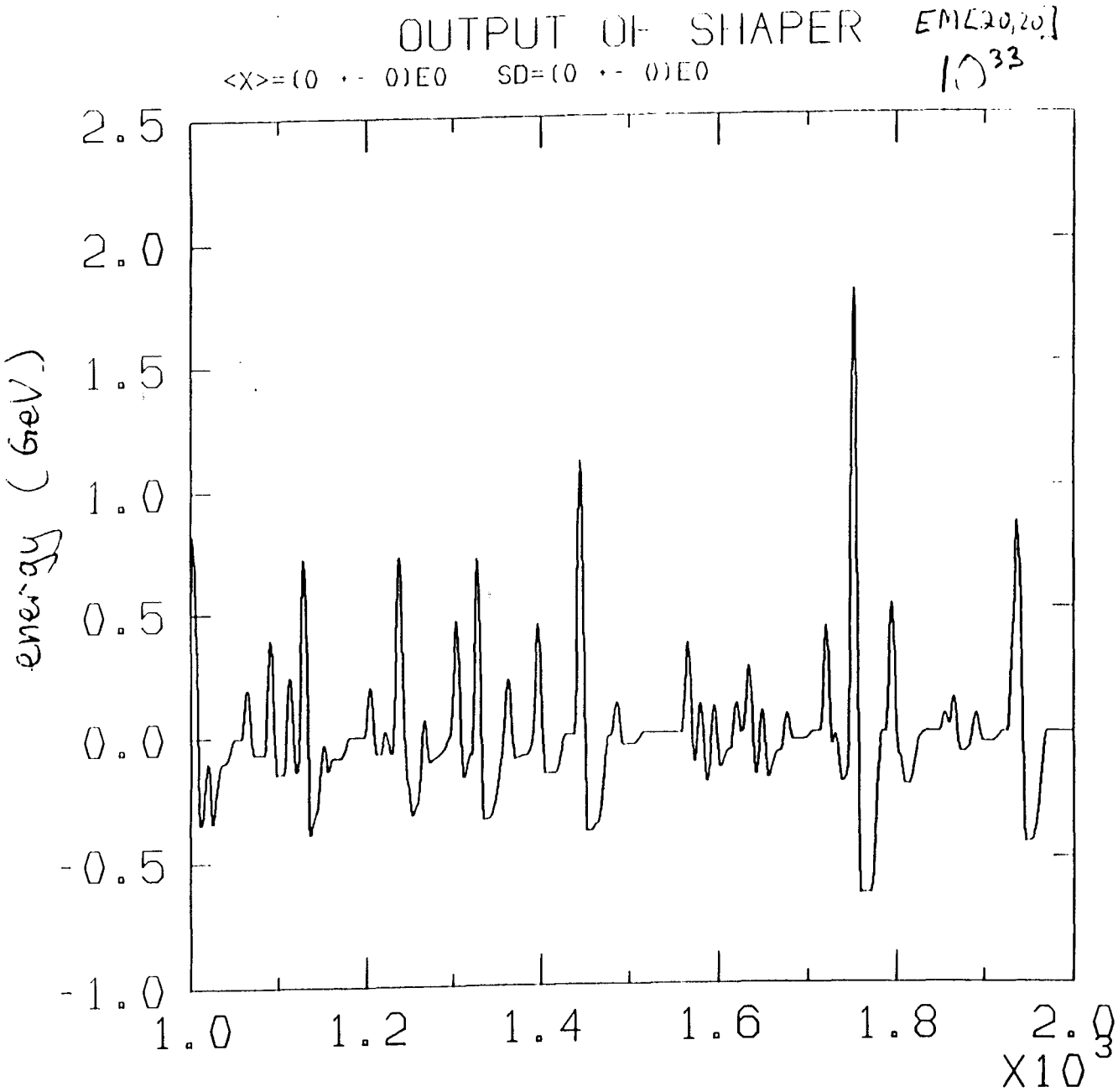

HEA09:54 10SEP91

ID= 200

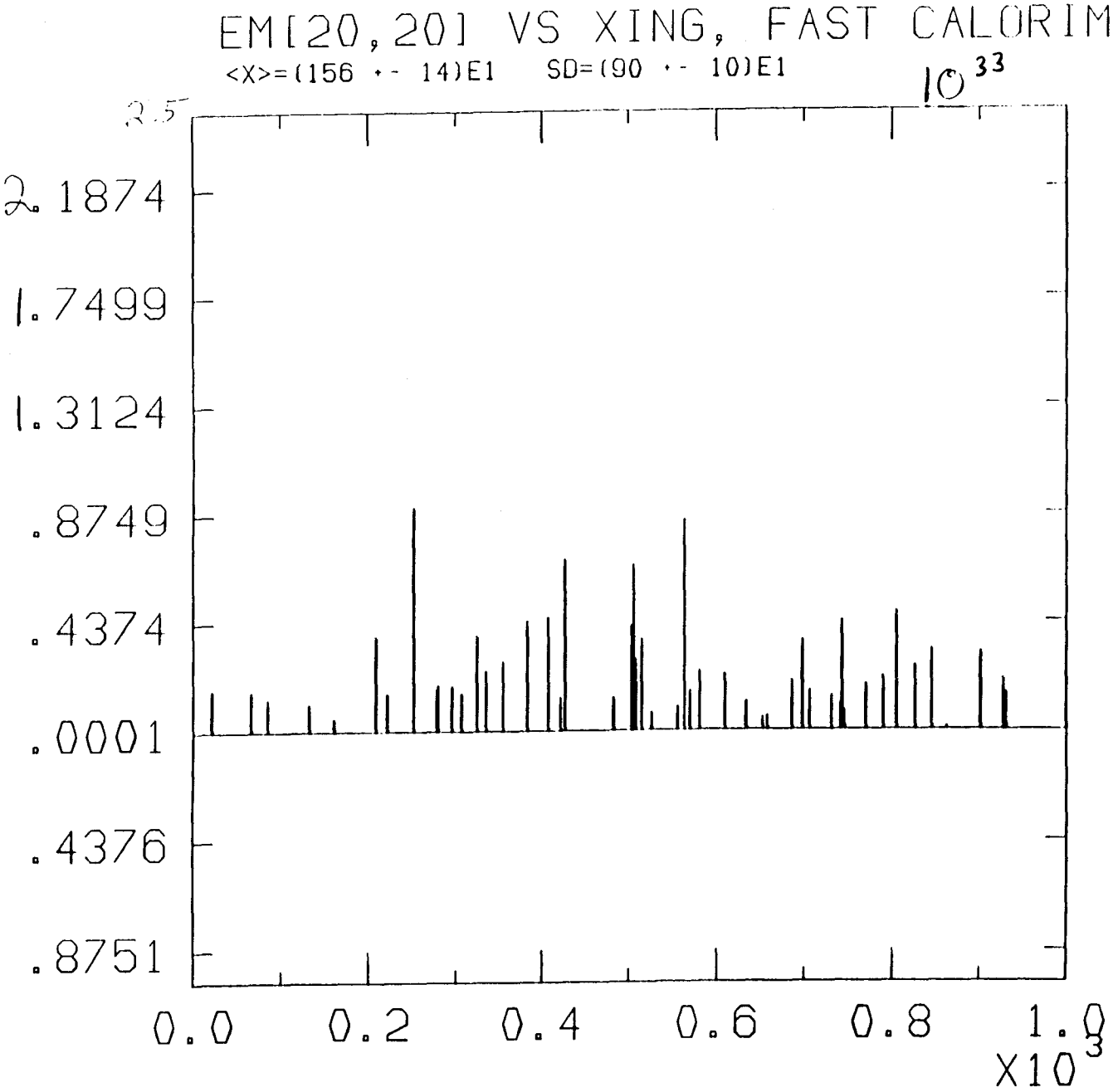

HEA11:06 10SEP91

ID= 115

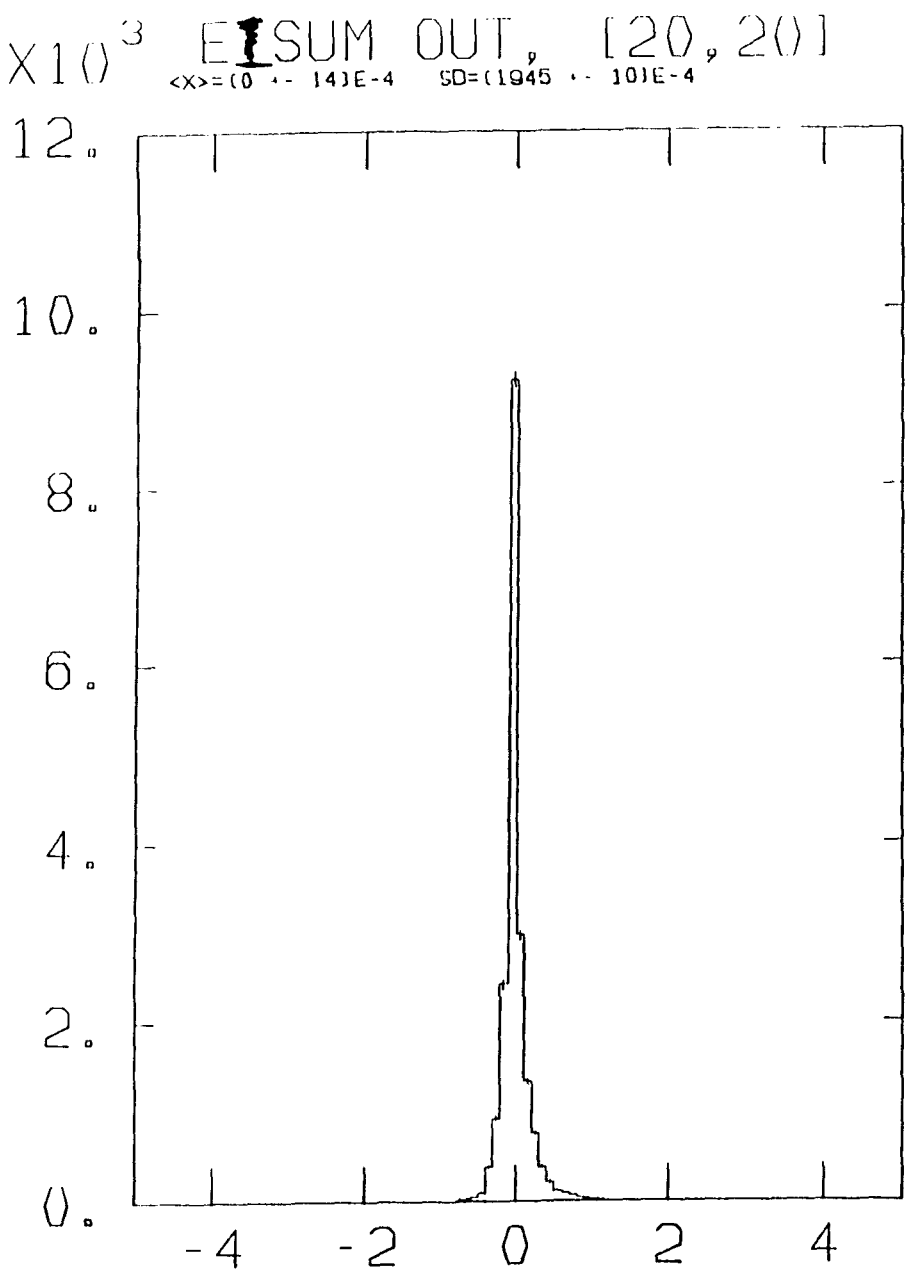
X10^3 E SUM OUT, [20,20]
<X>=(0 +- 14)E-4 SD=(1945 +- 10)E-4
12.
10.
8.
6.
4.
2.
0.
-4
-2
0
2
4

ID= 131

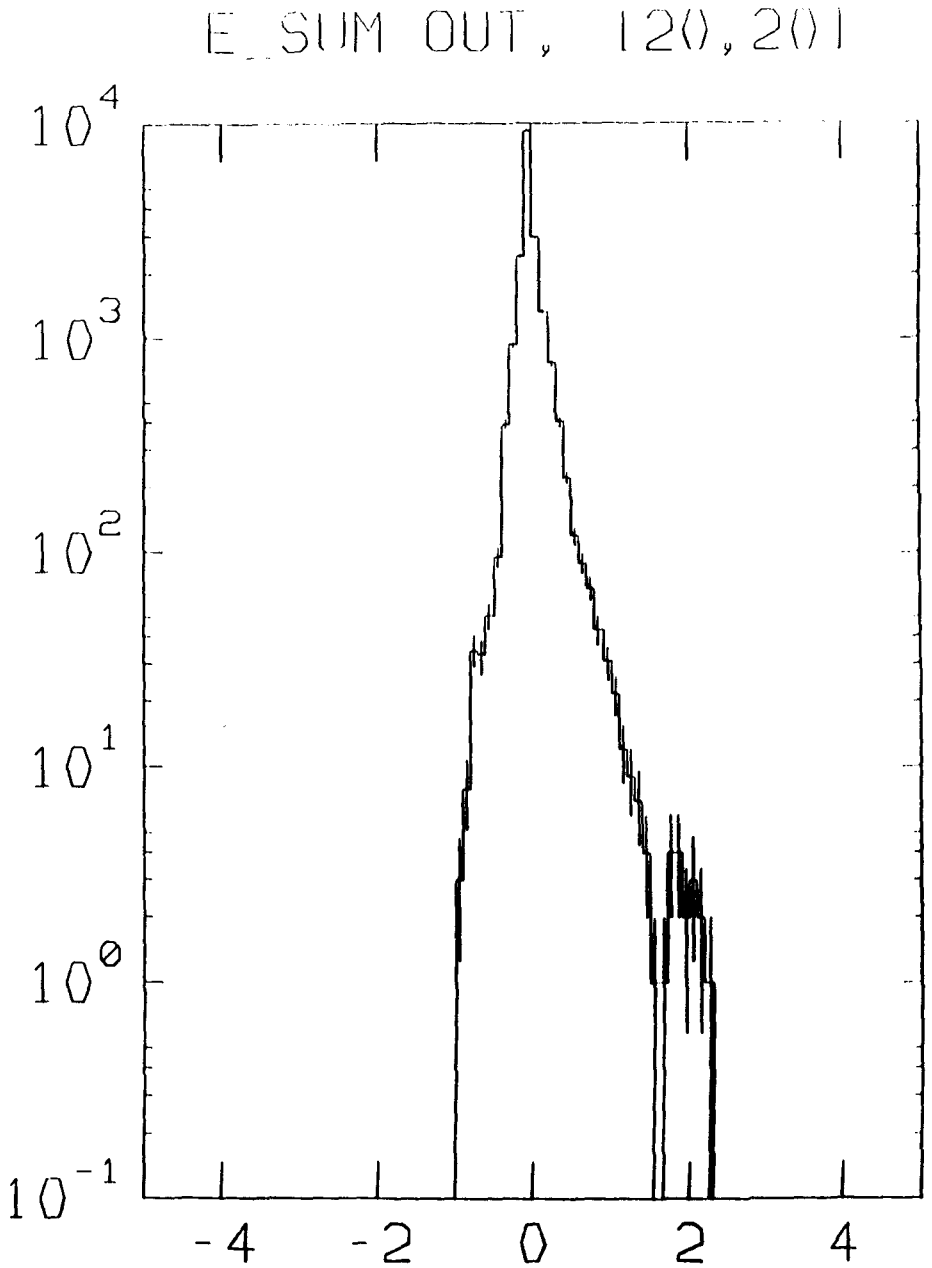
E SUM OUT, [20,20]
10^4
10^3
10^2
10^1
10^0
10^-1
-4
-2
0
2
4

Higgs --> Gamma Gamma Events

Associated production: $H t\bar{t}$, $H \to \gamma\gamma$

$t\bar{t}$ included in background, but effect of pileup on tagging efficiency is not included.

1000 Higgs decays supplied by Kevin Einsweiler.

- full photon energy deposited in a single 0.1X0.1 cell.

- detector resolution is 13%/Sqrt(Et) in barrel, 13%/Sqrt(E) in endcap.

- Gaussian electronic noise added; sigma_n=0.16 GeV in EM section at eta=0.

photons from H->bb

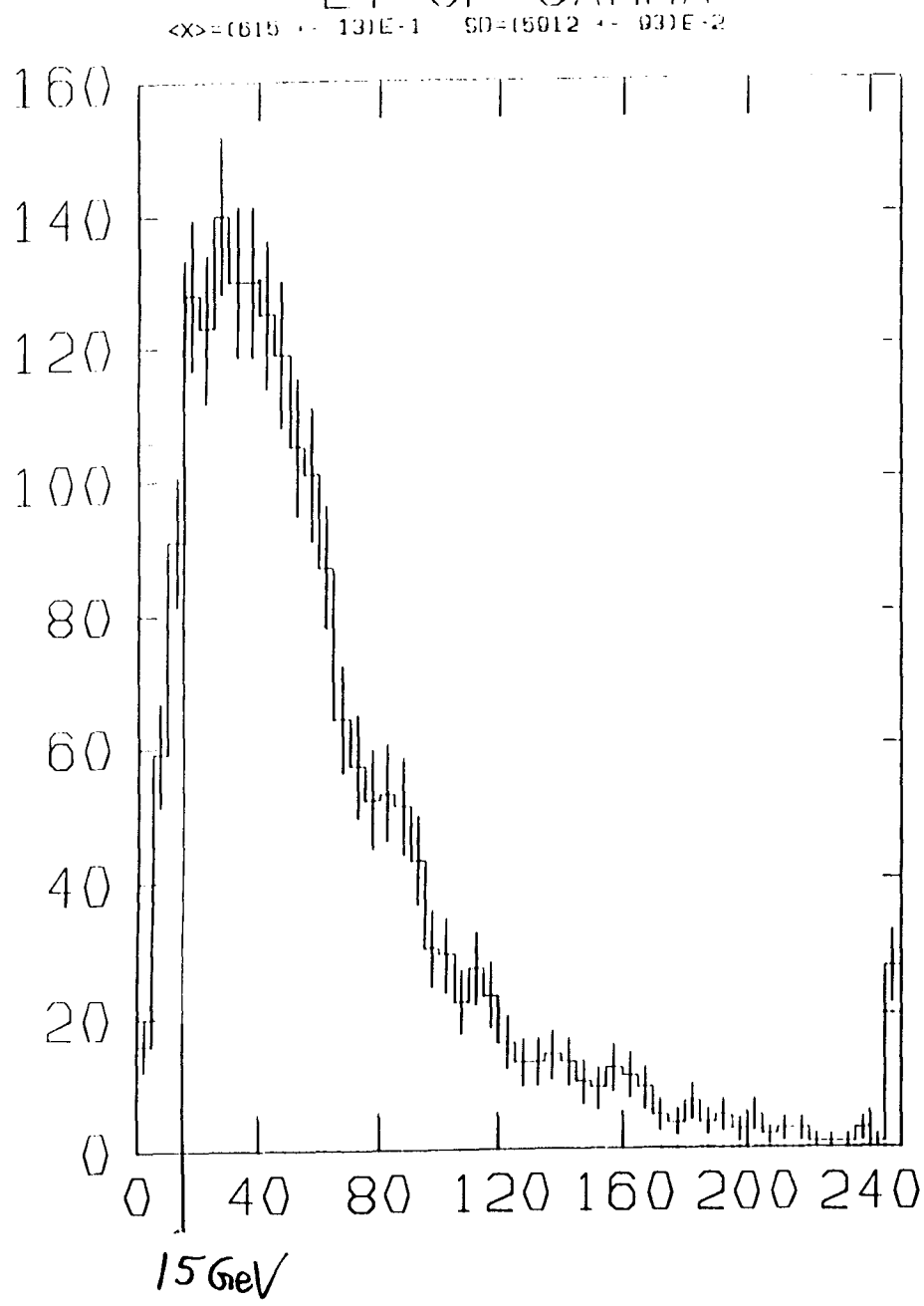

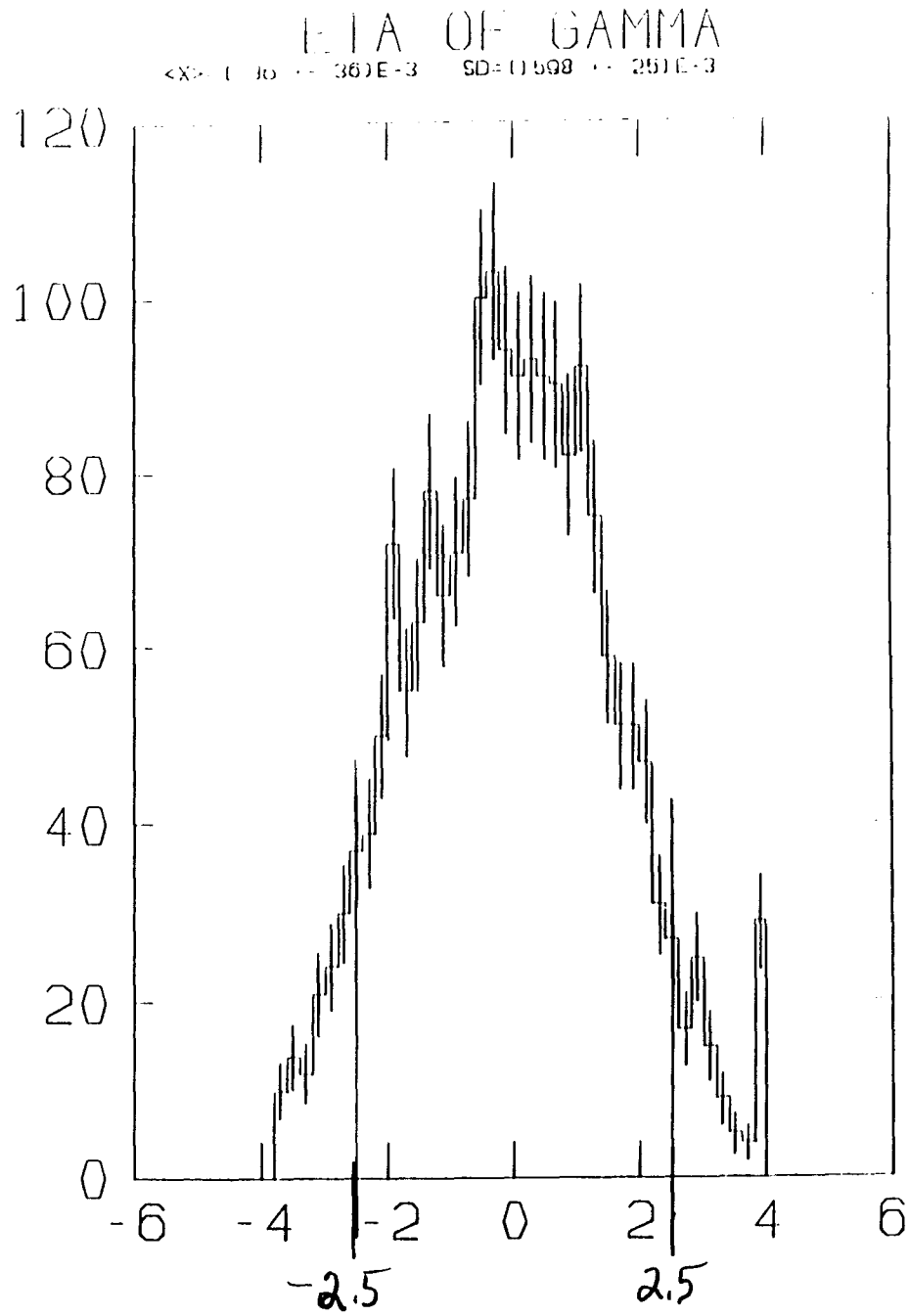

Impact on Energy Resolution

For barrel region, expect

$$\left(\frac{\sigma_{E_t}}{E_t}\right)^2 = \frac{a^2}{E_t} + \cancel{b^2}^{\,0} + \frac{c^2}{E_t^2}$$

stochastic pileup, electronic noise

$$\Rightarrow \sigma_{E_t}^2 = c^2 + a^2 E_t \qquad \text{linear in } E_t$$

(following plots for |eta|<1.3)

Results of simulation

$$\frac{\sigma_{E_t}}{E_t} = \frac{0.13}{\sqrt{E_t}} \oplus \frac{0.22}{E_t} \qquad (10^{33})$$

pileup & electronic noise ~ equal contributions

$$= \frac{0.13}{\sqrt{E_t}} \oplus \frac{0.52}{\sqrt{E_t}} \qquad (10^{34})$$

In endcap, stochastic term is smaller, pileup the same:

$$\sigma_{E_t}^2 = 0.13^2 \times E_t \cdot \sin\theta + \sigma_{pile}^2$$

Contributions to Et resolution LAr, 10^{33}

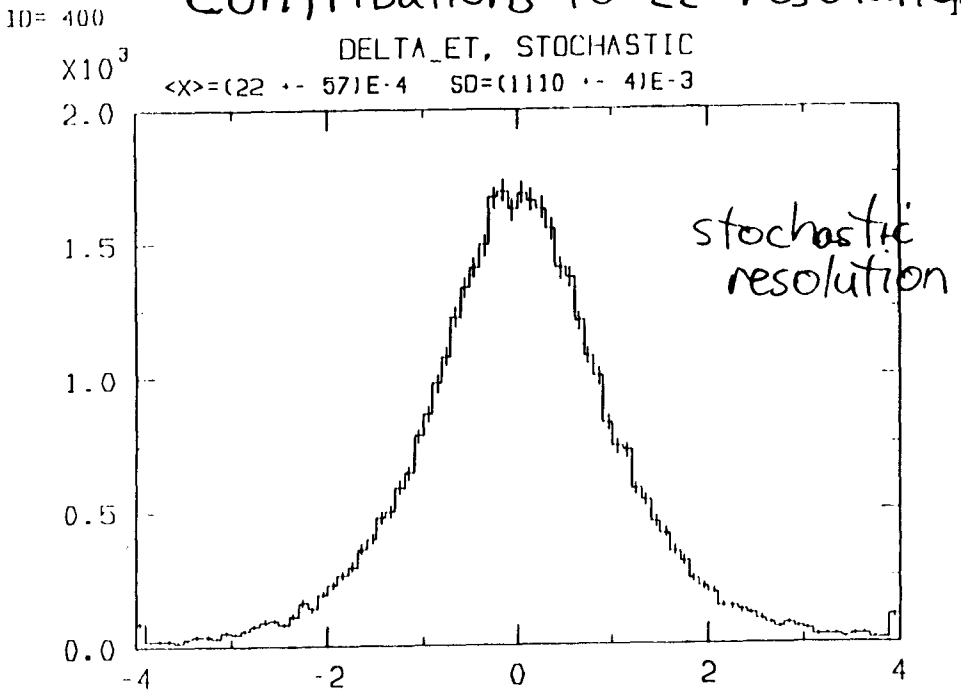

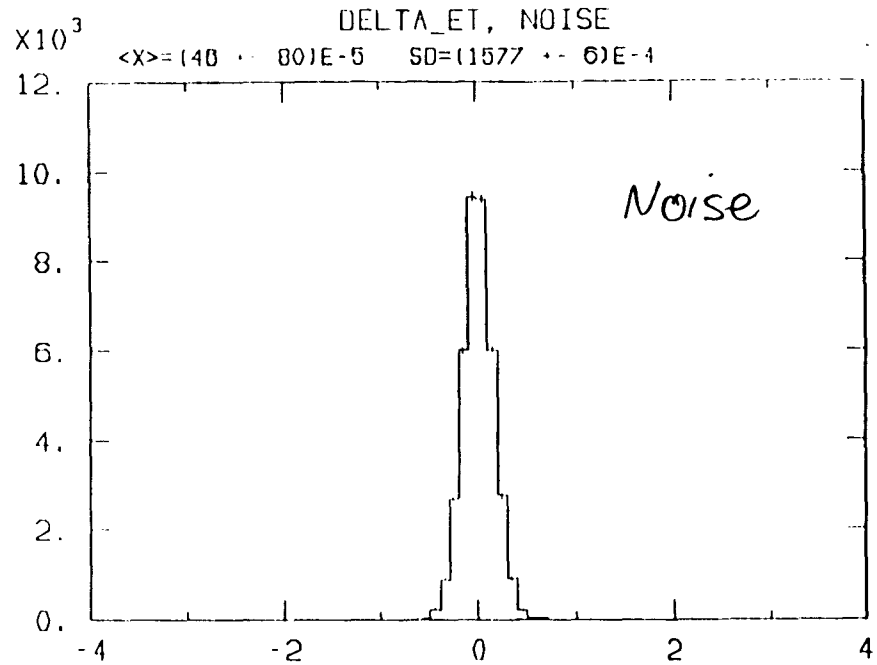

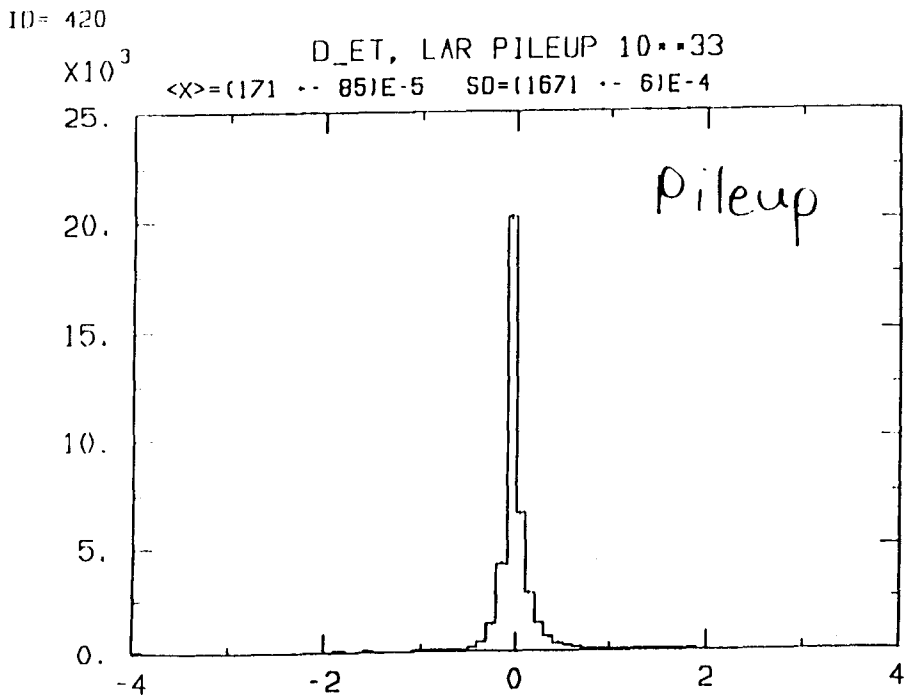

σ_Et**2 vs Et, Stochastic + Pileup + Noise 10^{33}

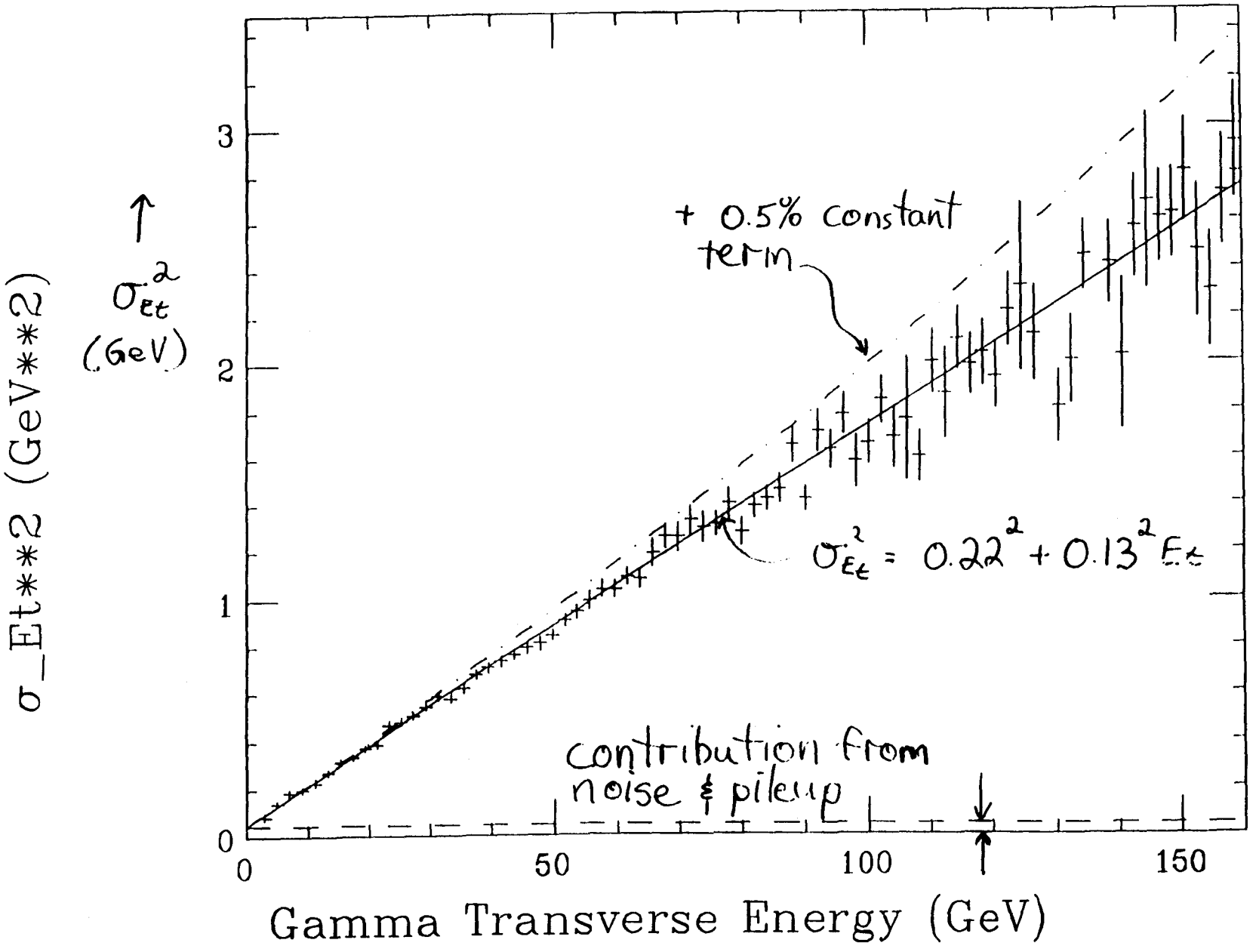

contributions to resolution

ID= 400

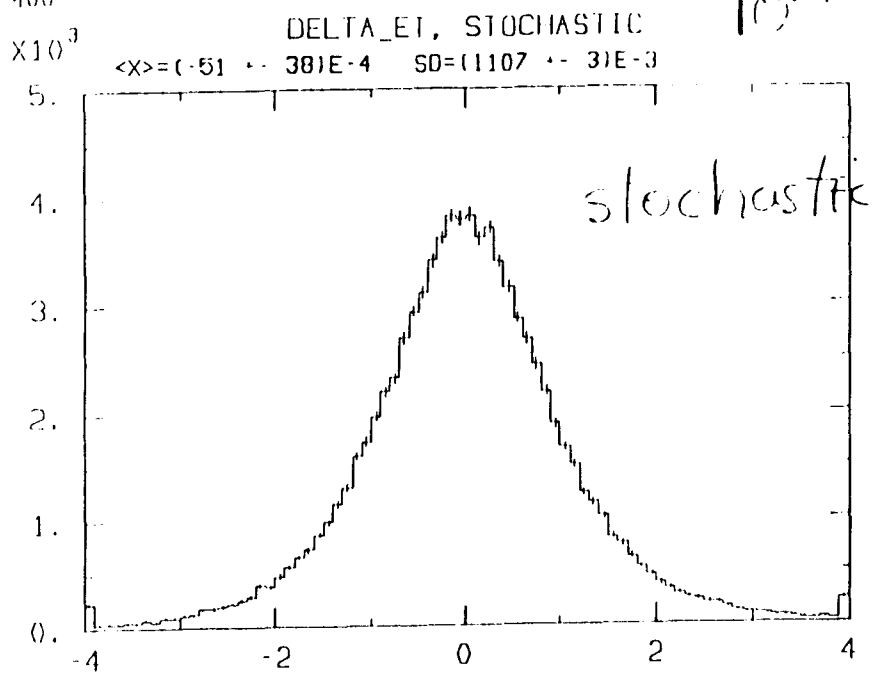

ID= 410

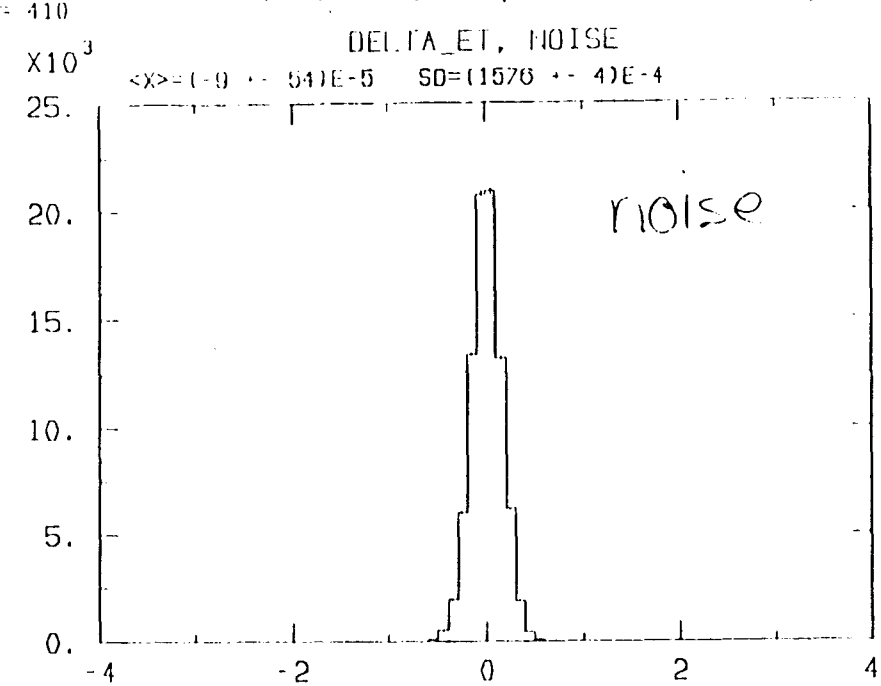

ID= 420

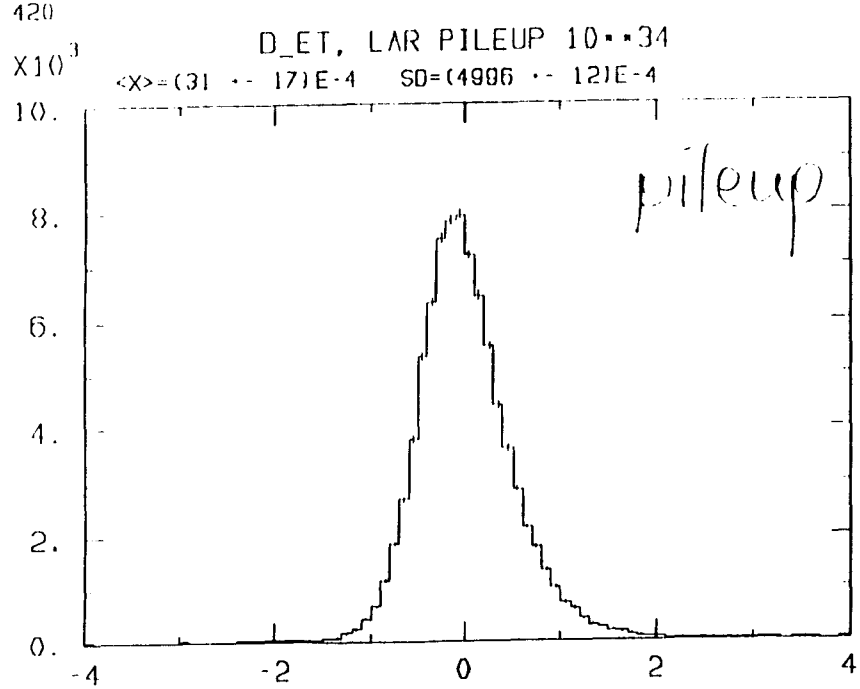

σ_Et**2 vs Et, Stochastic+Pileup+Noise, 10**34

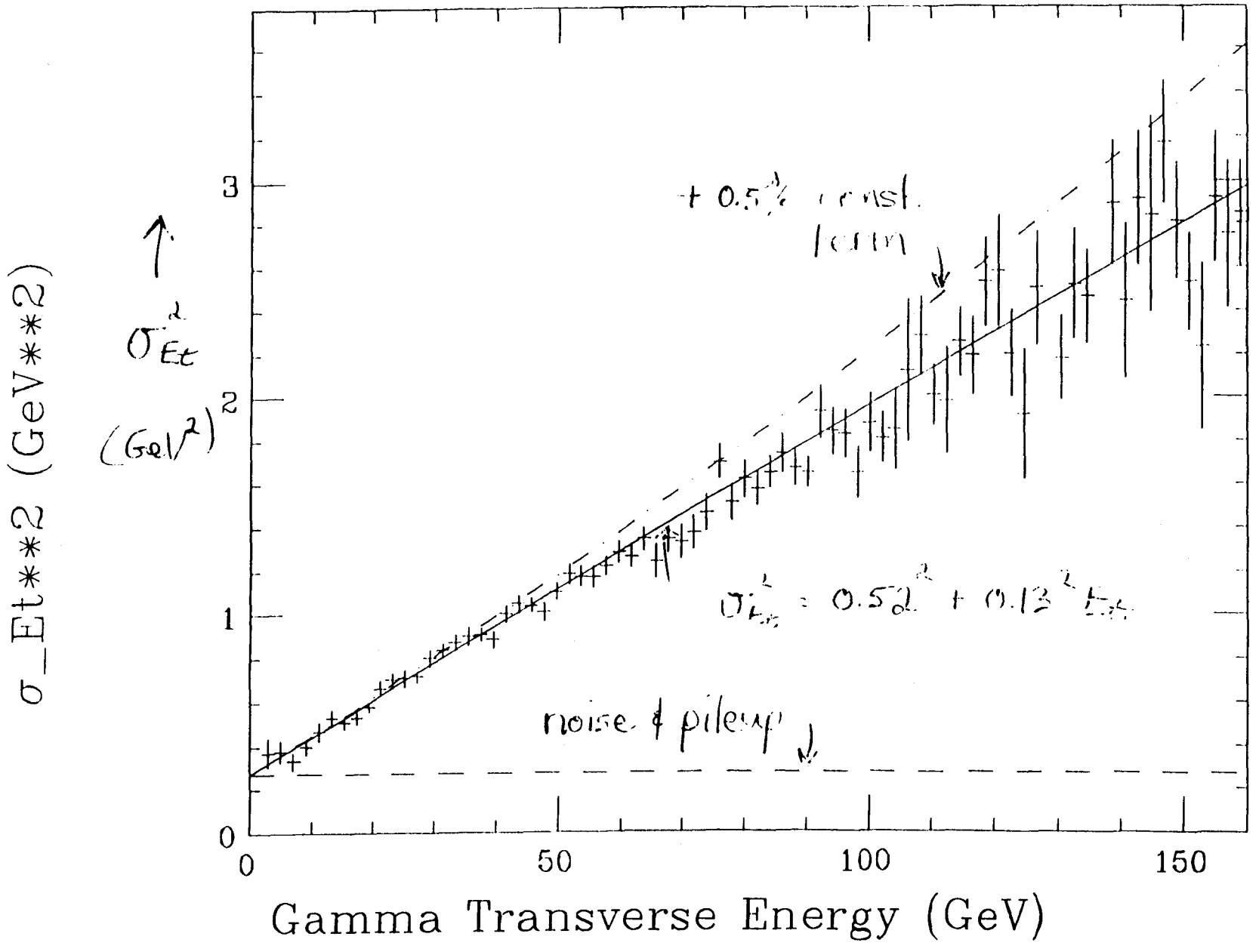

ID= 402

measured E_t - true E_t

DELTA_ET, 40<ET<45, ST

<X>=(2 +- 11)E-3 SD=(8522 +- 77)E-4

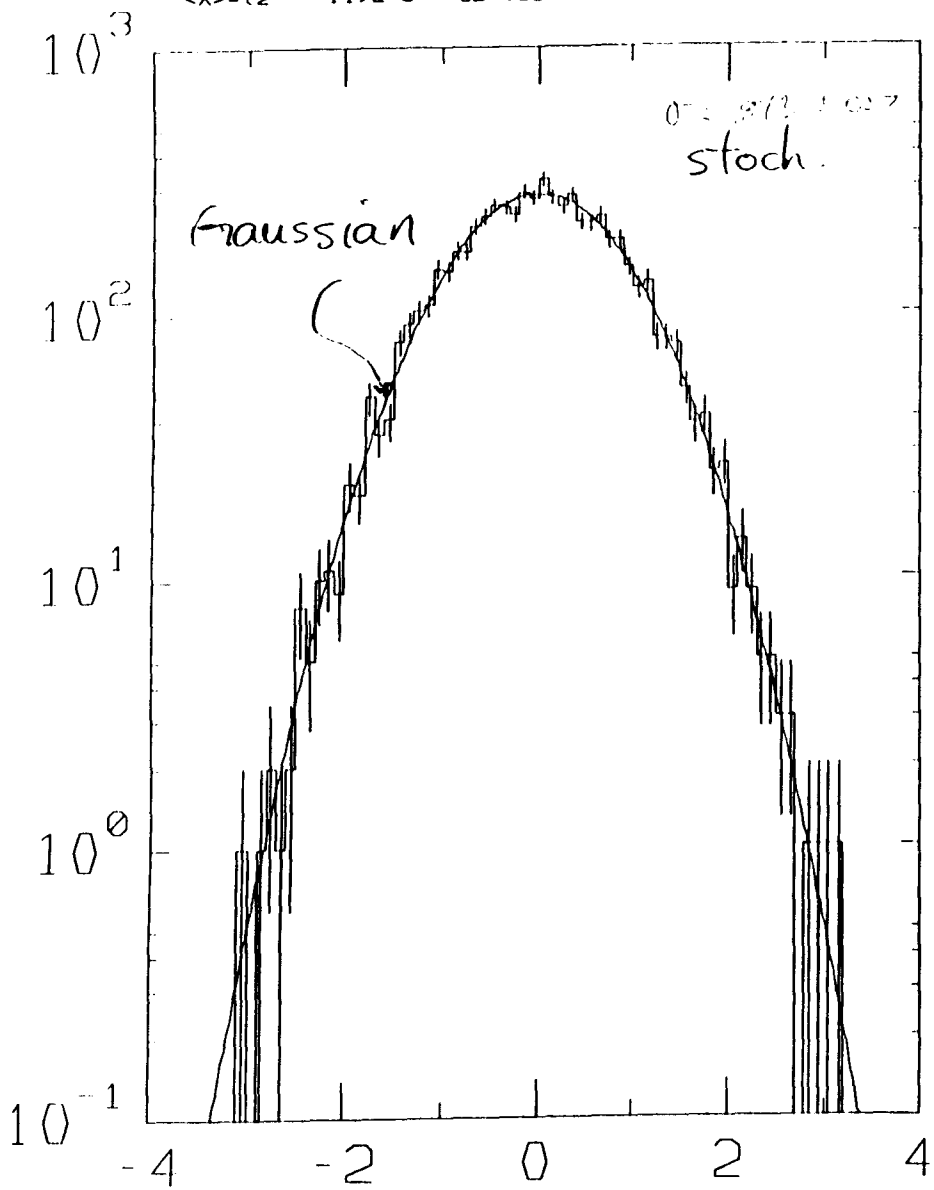

ID= 432

D_ET, 40<ET<45, STOCH+P

<X>=(3 +- 13)E-3 SD=(9872 +- 90)E-4

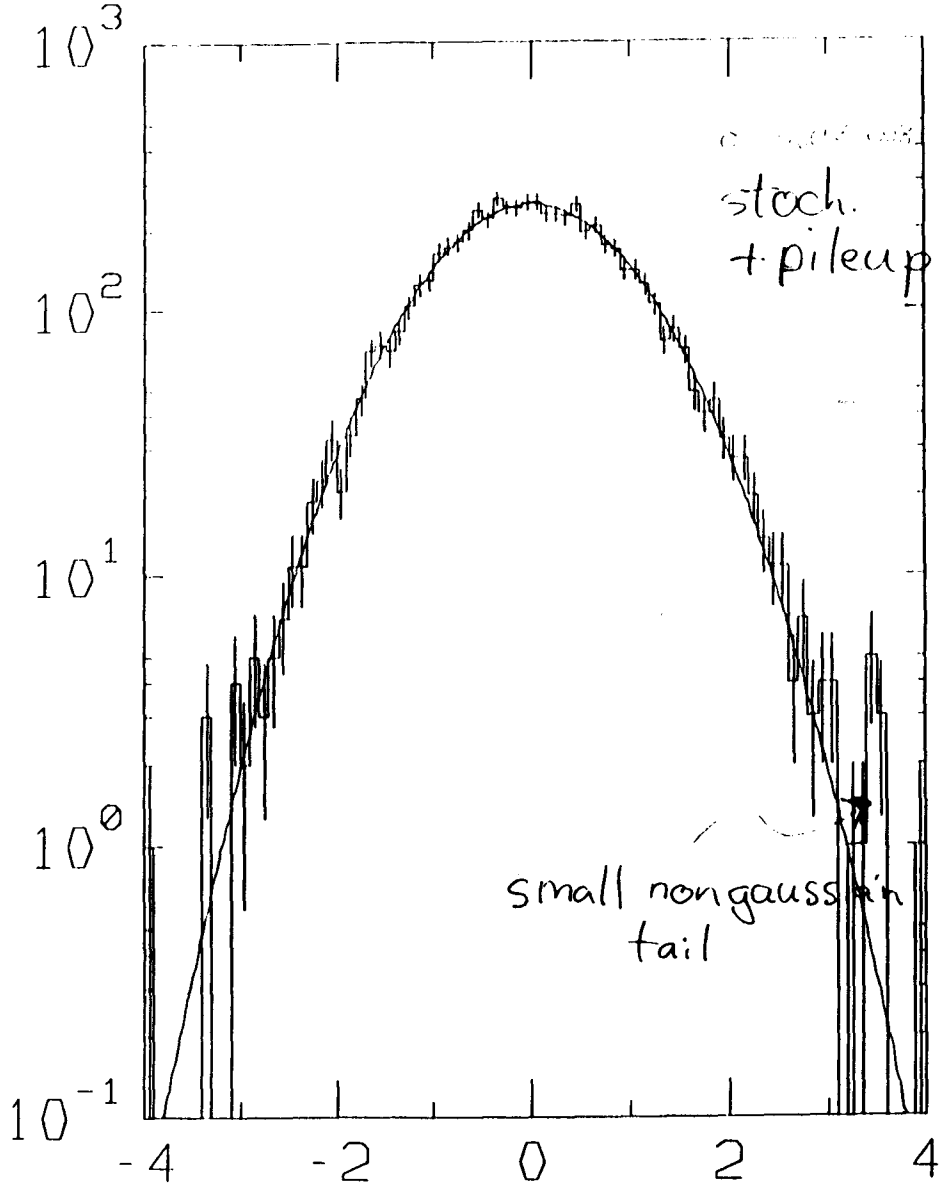

Impact on Electron Identification

Photon selection:

- pt > 15 GeV
- Et in isolation cone <5 GeV [10 GeV] (cone = 0.3X0.3, EM+HAD1)
- had/EM < 0.06

Isolation cone included minbias pileup background plus underlying energy from $Ht\bar{t}$ event.

Compare LAr case to fast calorimeter case (delta-function response, no electronic noise).

E_t in 0.3×0.3 isolation cone from underlying event, Htt

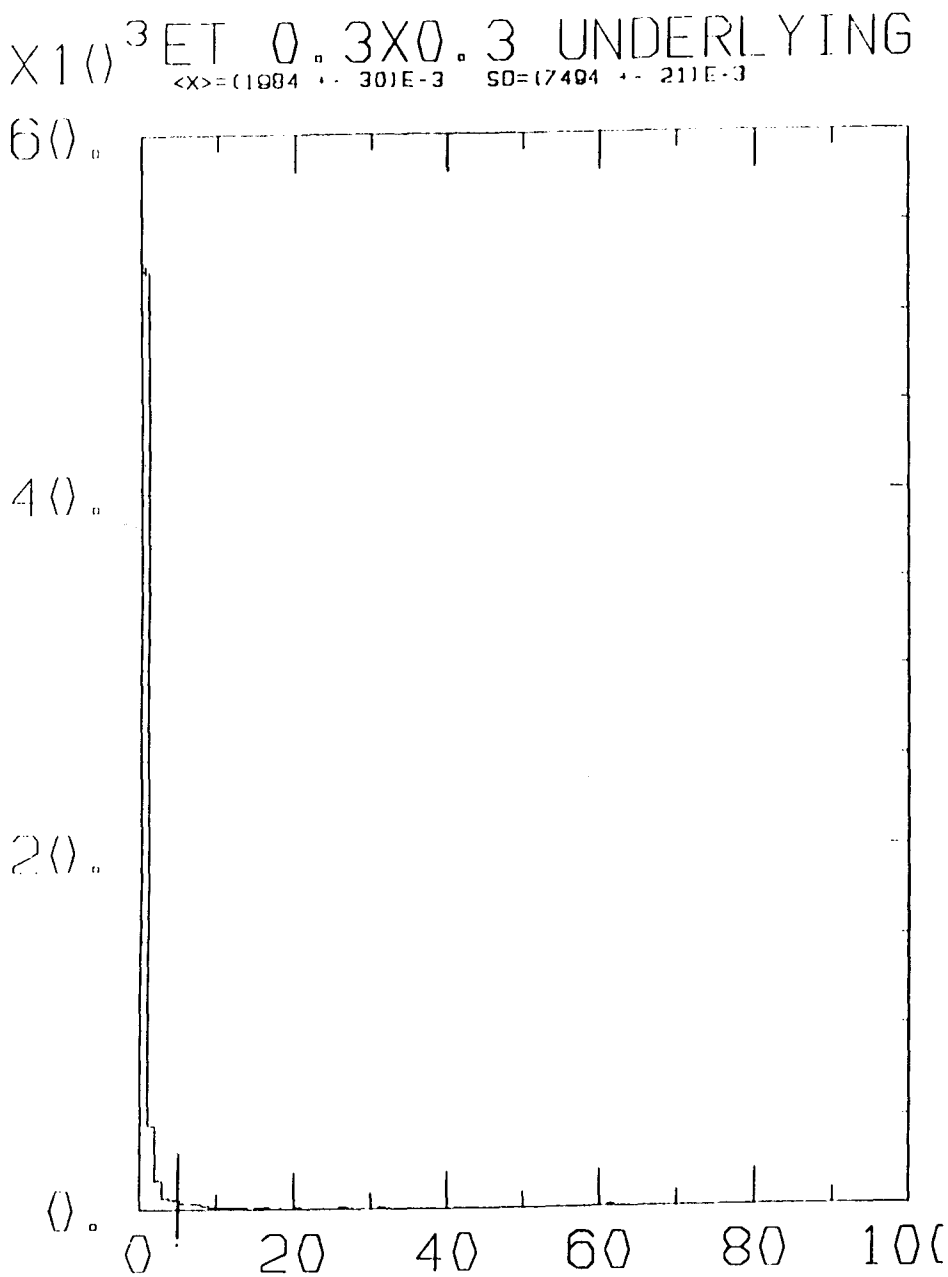

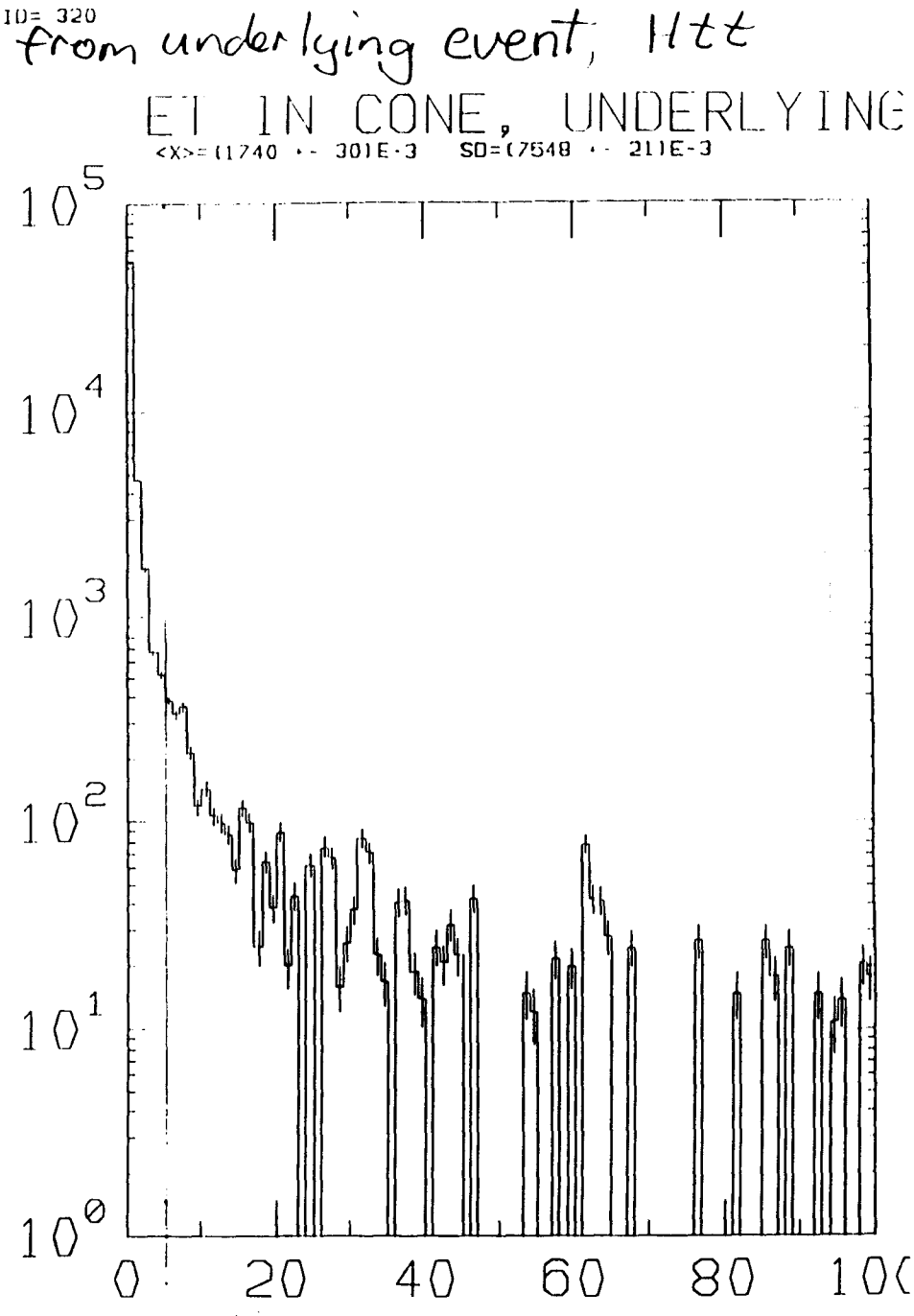

Pileup contributions to isolation cone

ID= 832

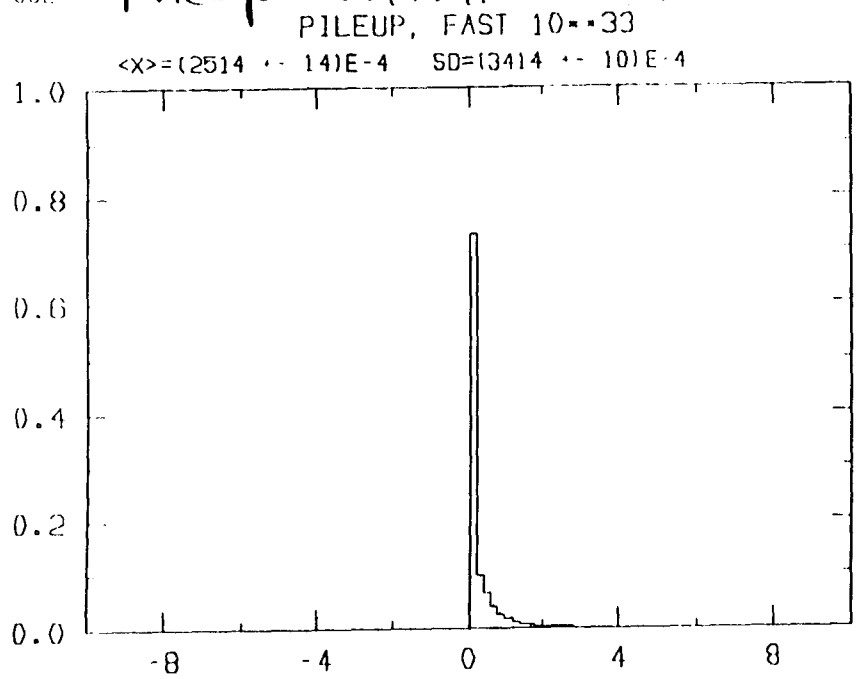

ID= 831

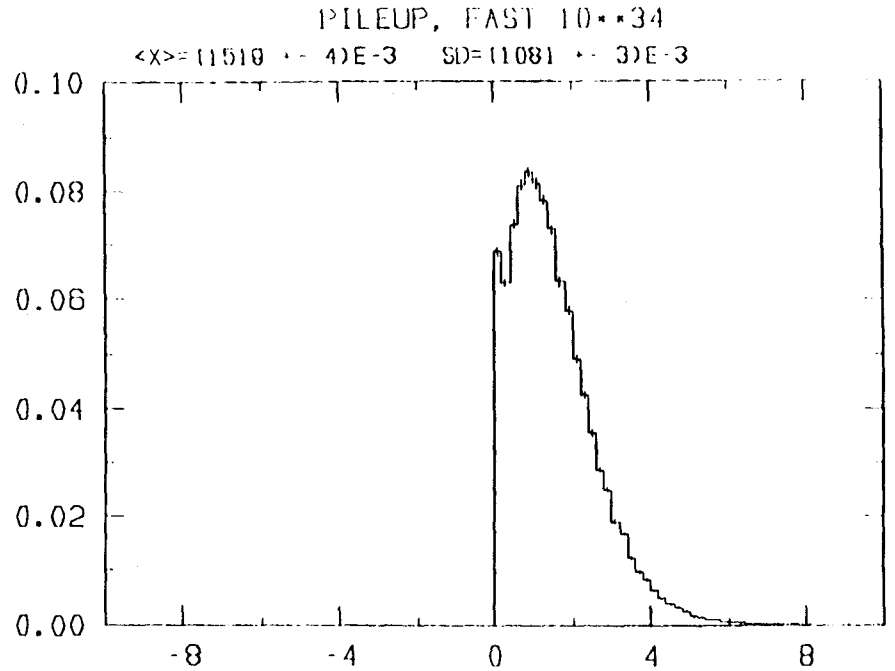

ID= 833

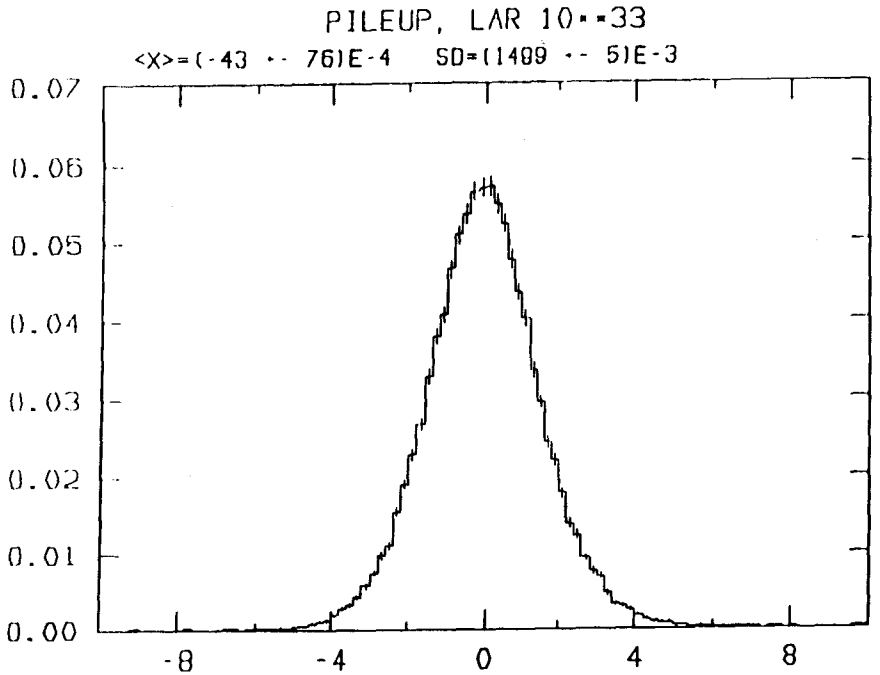

ID= 834

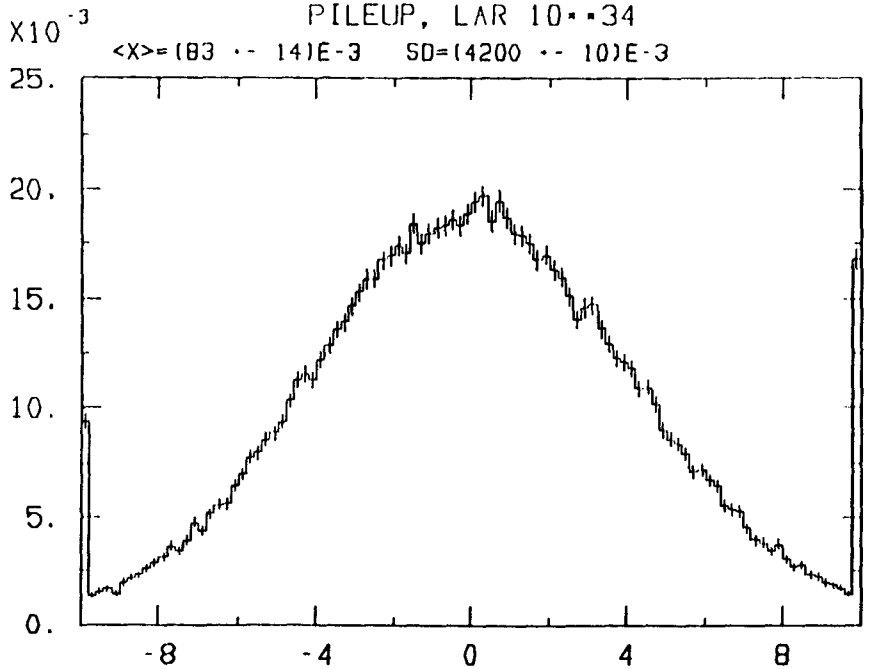

ID= 800

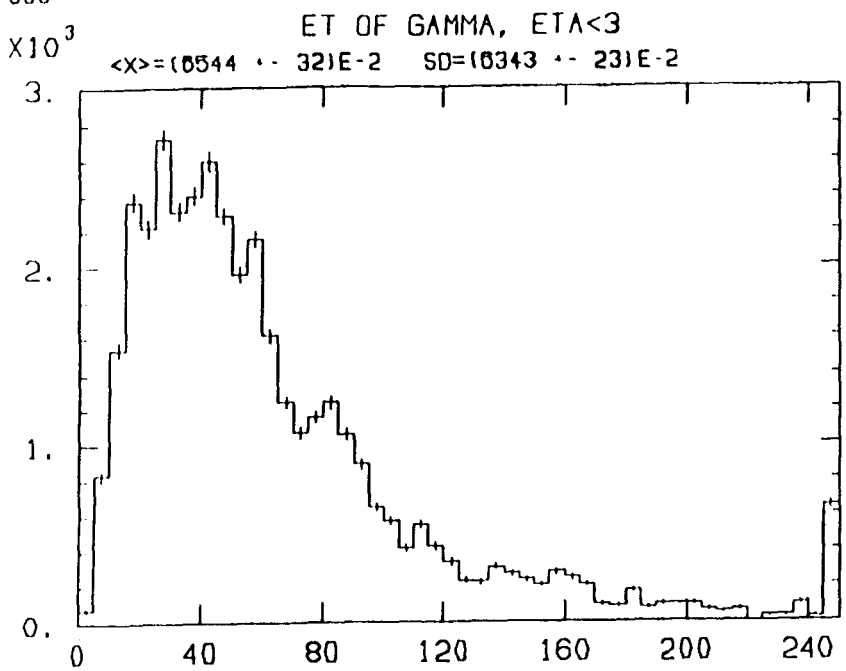

ID= 810

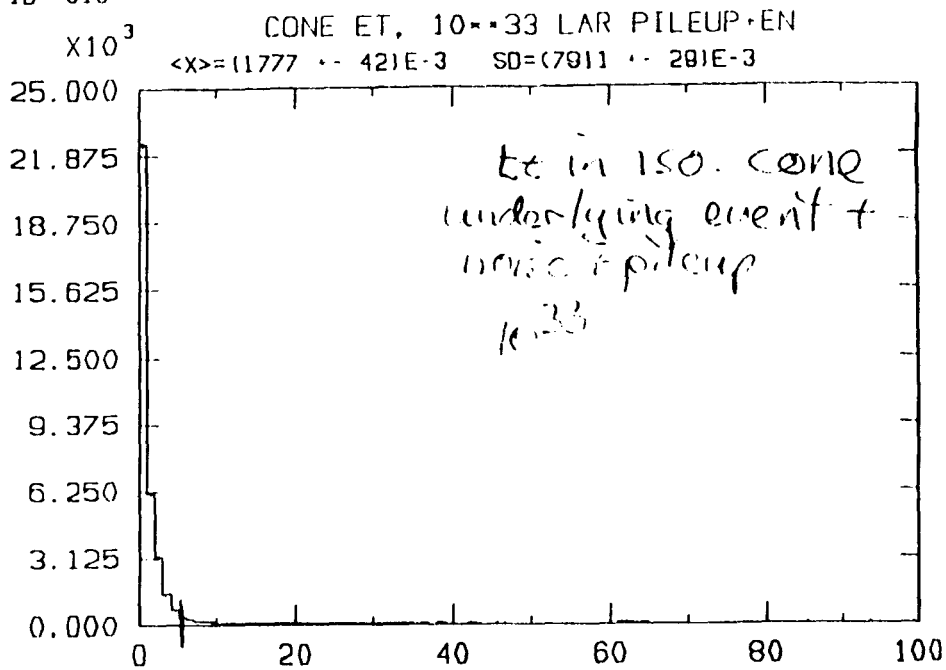

ID= 820

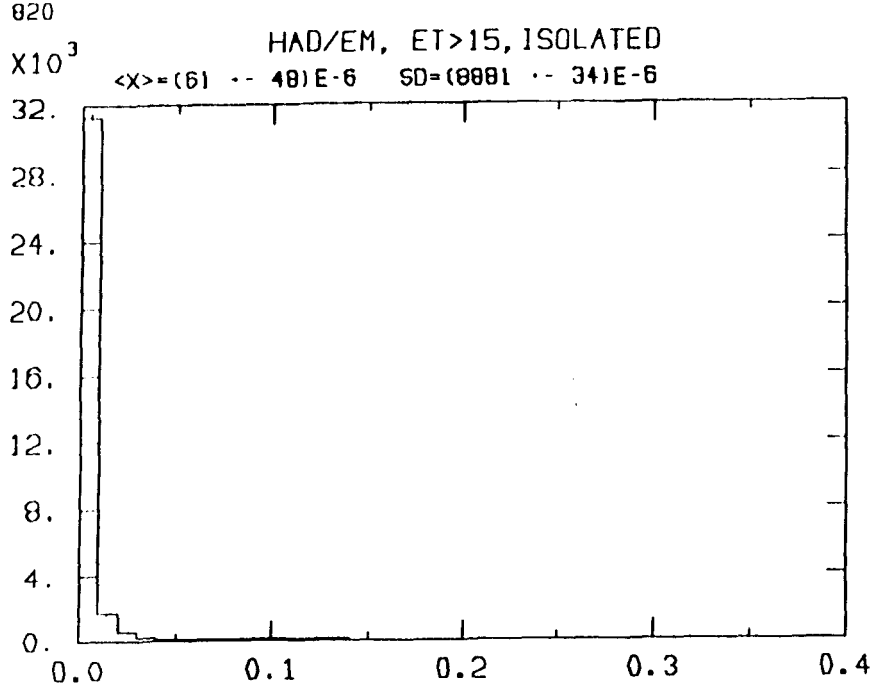

ID= 830

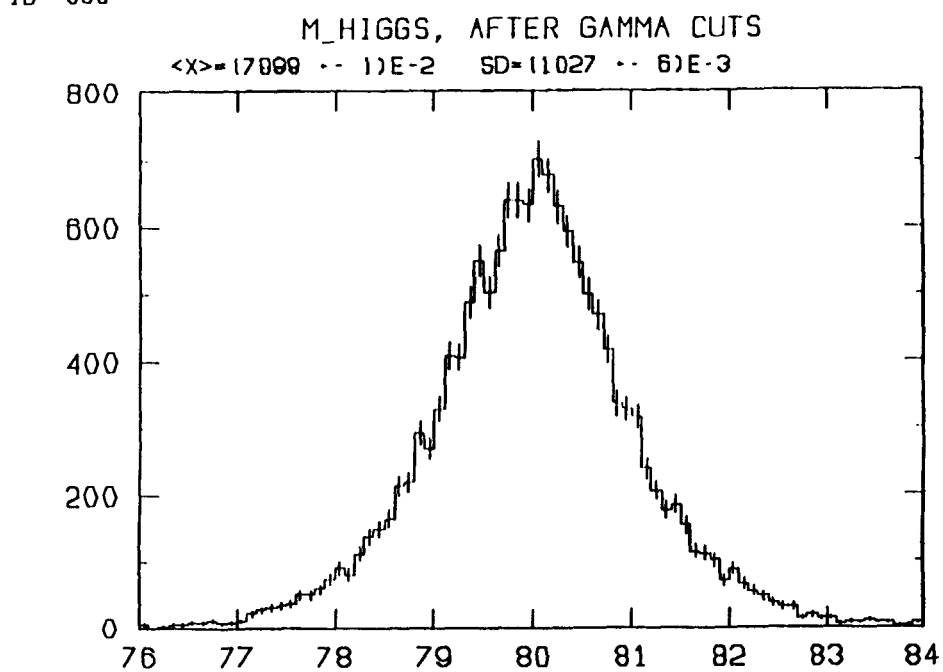

UEA16:04 QSERP1

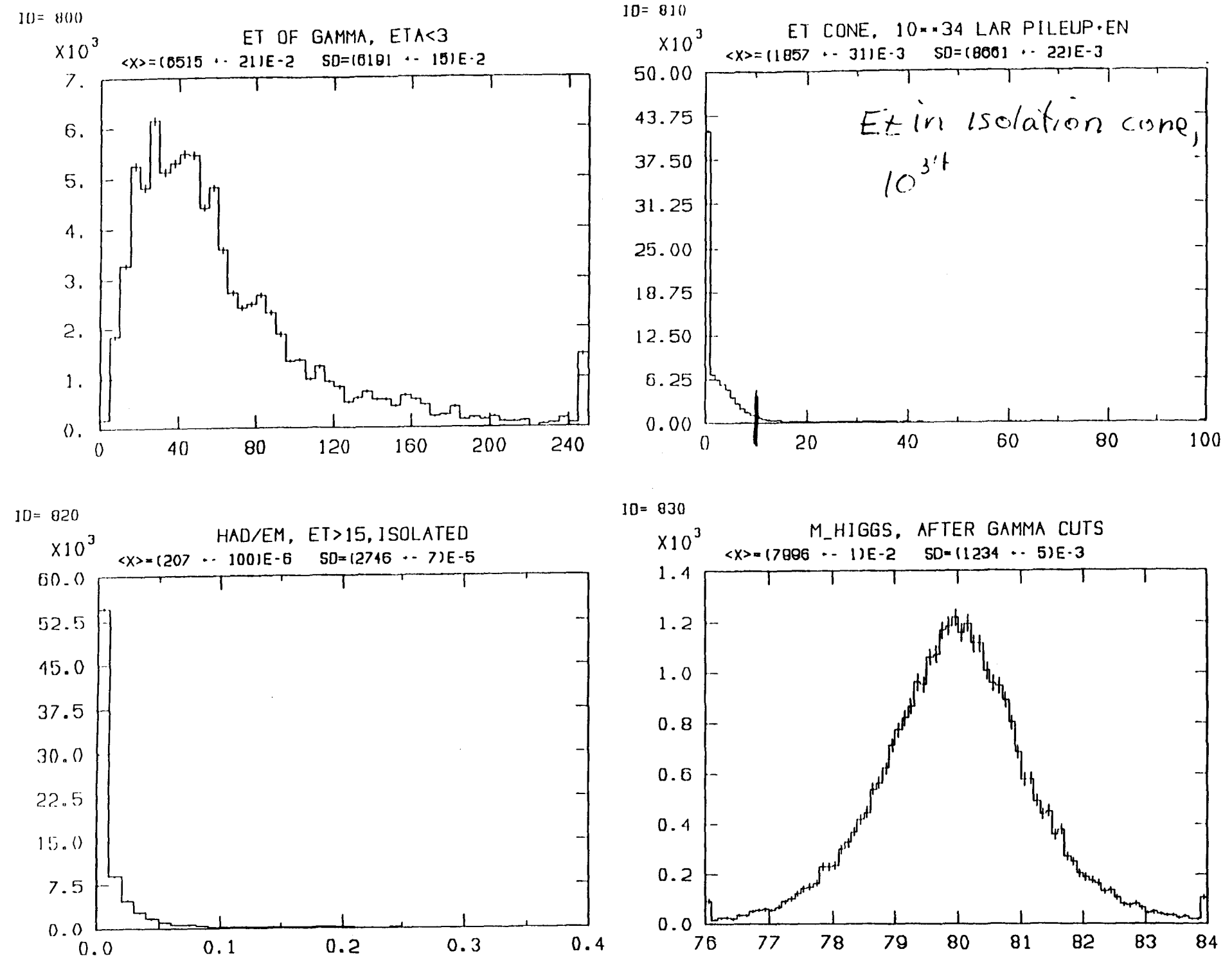
ID= 800
ET OF GAMMA, ETA<3
<X>=(6515 +- 21)E-2 SD=(6191 +- 15)E-2
X10^3
ID= 810
ET CONE, 10**34 LAR PILEUP*EN
<X>=(1857 +- 31)E-3 SD=(8661 +- 22)E-3
X10^3
Et in isolation cone, 10^34
ID= 820
HAD/EM, ET>15,ISOLATED
<X>=(207 +- 100)E-6 SD=(2746 +- 7)E-5
X10^3
ID= 830
M_HIGGS, AFTER GAMMA CUTS
<X>=(7896 +- 1)E-2 SD=(1234 +- 5)E-3
X10^3
HEA16:04 9SEP91

Photon Selection Efficiency

cut	10^{33} LAr	10^{33} fast	10^{34} LAr	10^{34} fast
• $E_t > 15$ GeV	0.937	0.937	0.937	0.937
• E_t in 0.3×0.3 cone < 5 GeV (10^{33}) < 10 GeV (10^{34})	0.935	0.941	0.943	0.960
• had/Em < 0.06	0.999	1.000	0.976	0.999
single γ efficiency*	0.875	0.882	0.863 (0.729)	0.900 (0.858)

* parentheses for 5 GeV isolation cut

$|\eta_\gamma| < 2.5$

Et in isolation cone, backgrounds

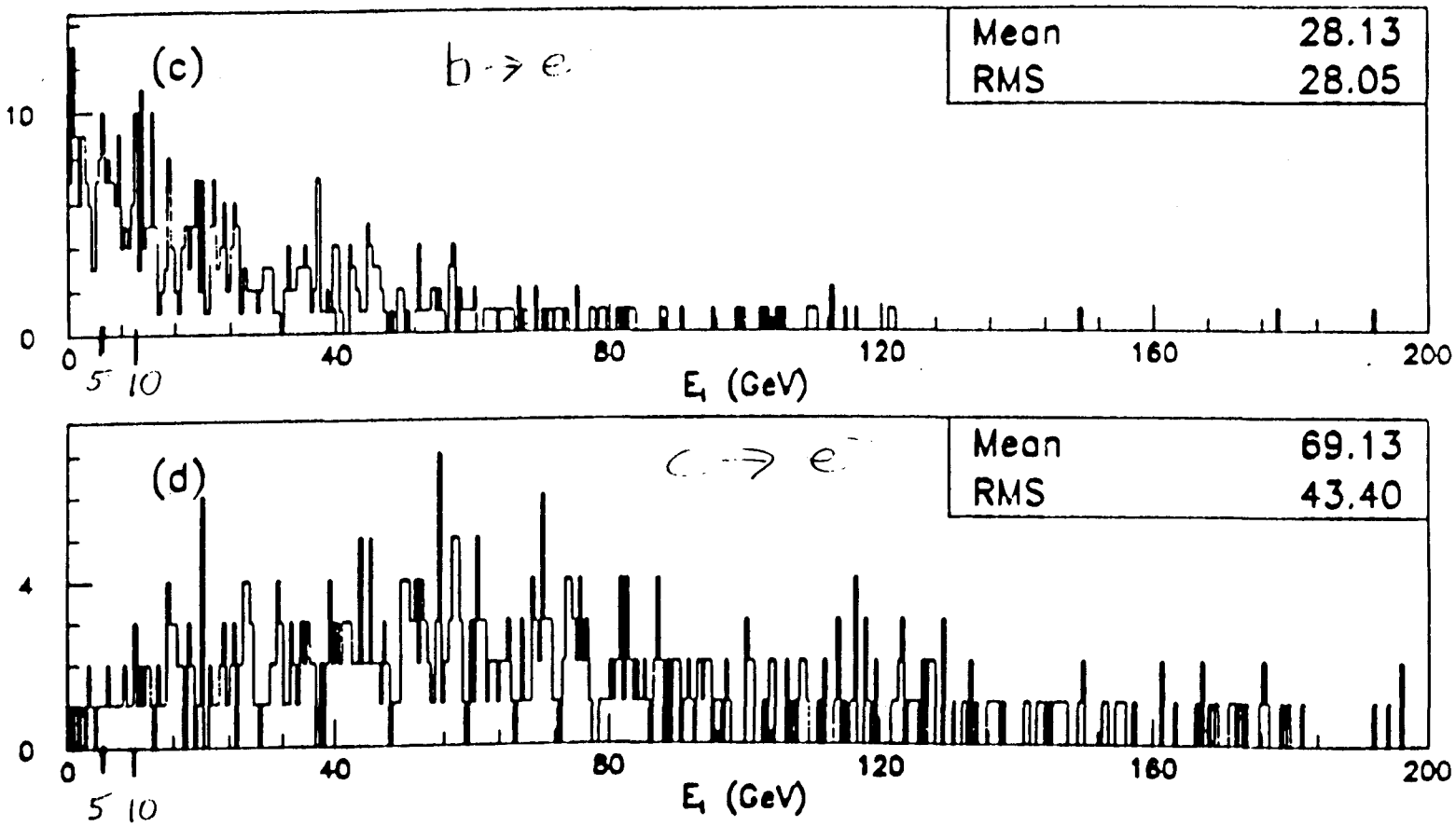

Figure 3: The distribution of E_t in a cone of radius $R = 0.2$ for different classes of electrons. The electrons are all in the range $10 < p_t < 20$ GeV.

(a) Electrons from $H \to ZZ^*$ for $M_H = 140$ GeV.

(b) W electrons coming from t quark decays ($M_{top} = 150$ GeV).

(c) b electrons coming from t quark decays.

(d) c (or u, d) electrons coming from t quark decays.

Isolation E_t from $b \to e$ & $c \to e$

Impact on Mass Resolution

(after γ cuts)

	10^{33}		10^{34}	
	LAr	fast	LAr	fast
σ_M (GeV)	1.03	0.98	1.23	1.02
fraction with $78 < M_H < 82$	0.938	0.949	0.896	0.940

ID= 8332

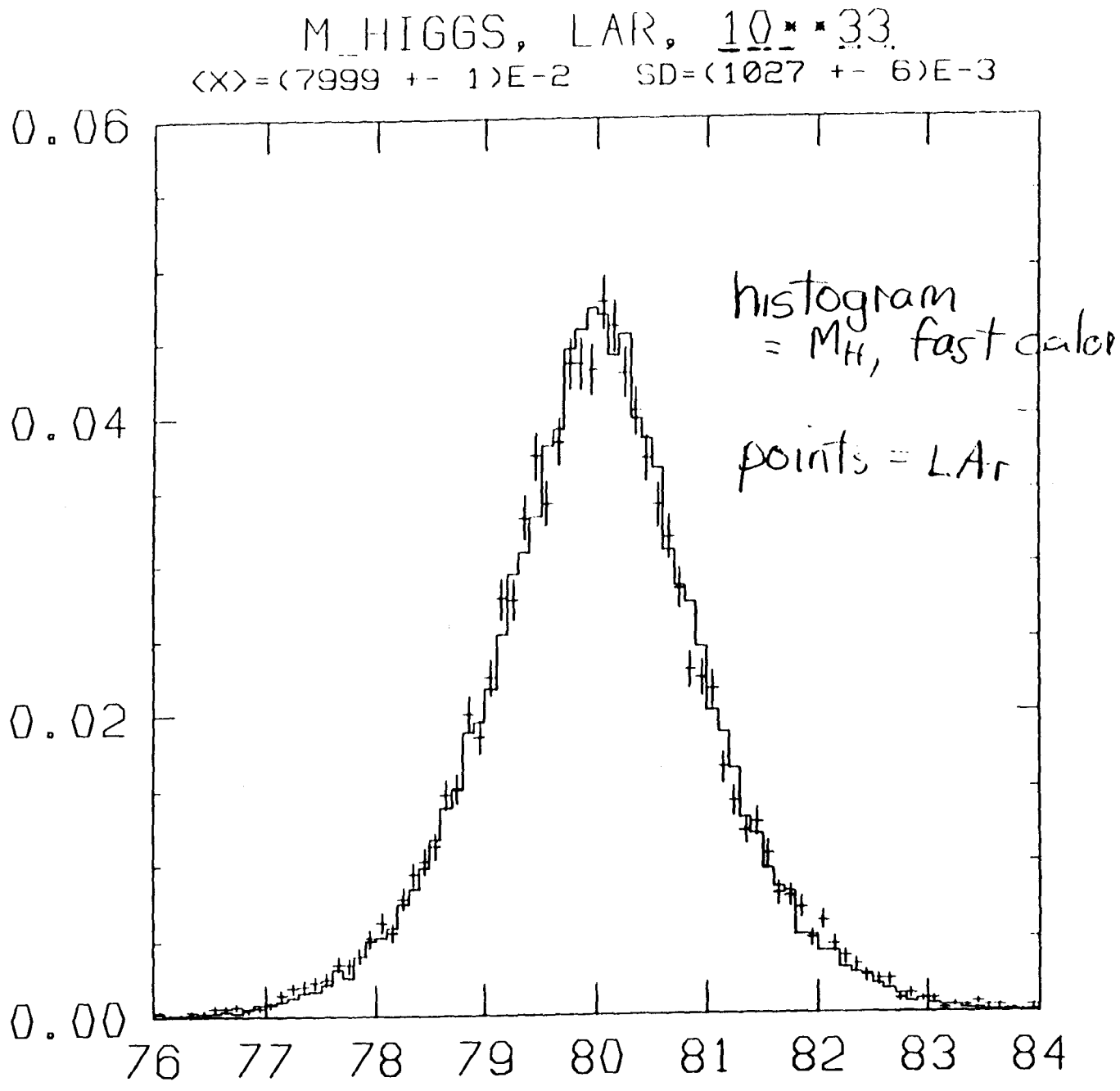
M_HIGGS, LAR, 10**33
<X>=(7999 +- 1)E-2 SD=(1027 +- 6)E-3
0.06
0.04
0.02
0.00
76
77
78
79
80
81
82
83
84
histogram
= M_H, fast calor.
points = LAr

ID= 835

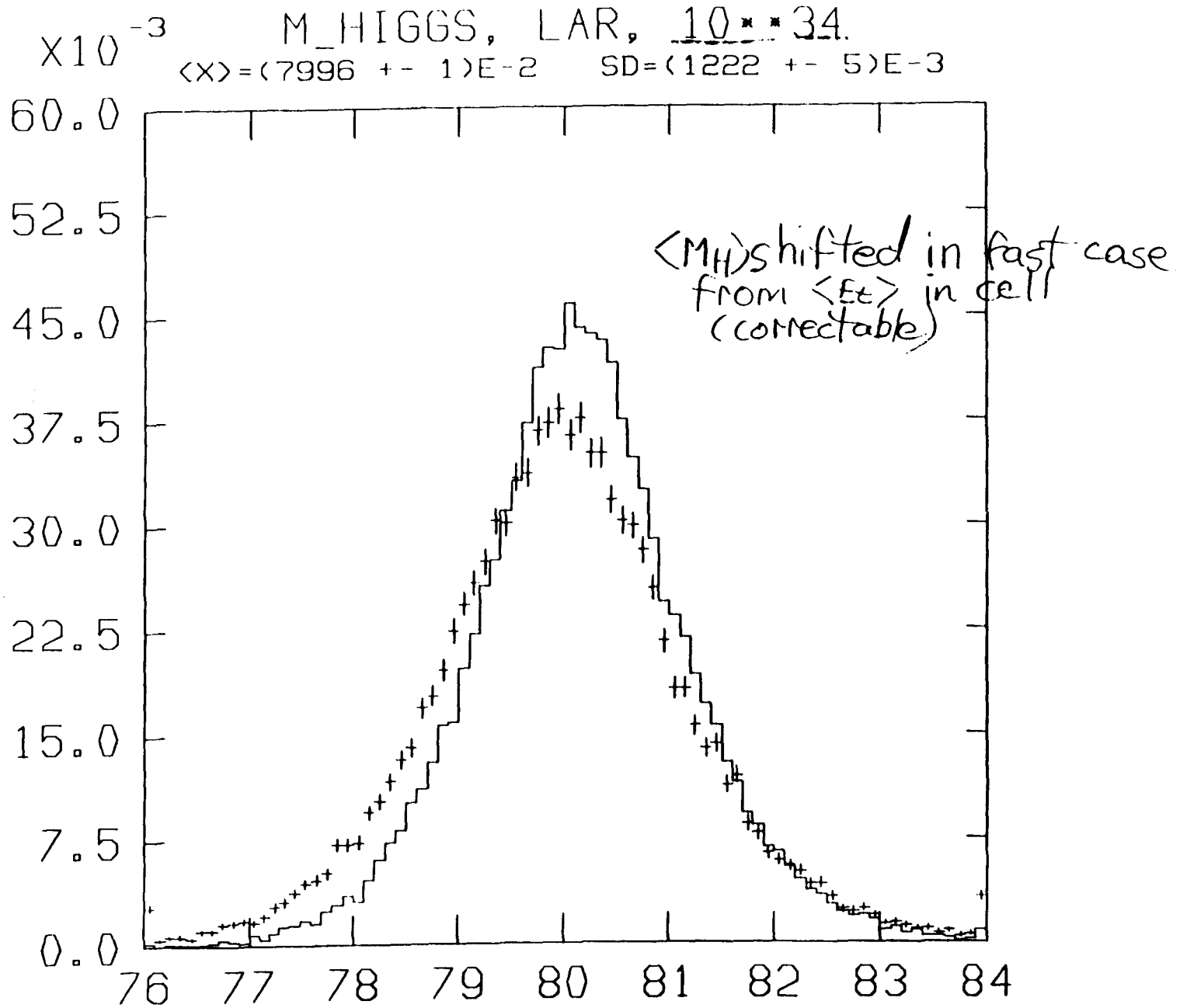
M_HIGGS, LAR, 10**34.
X10^-3
<X>=(7996 +- 1)E-2 SD=(1222 +- 5)E-3
60.0
52.5
45.0
37.5
30.0
22.5
15.0
7.5
0.0
76 77 78 79 80 81 82 83 84
<M_H> shifted in fast case
from <E_t> in cell
(correctable)

Overall Event Efficiency

$H \to \gamma\gamma$, $M_H = 80$ GeV

	10^{33}		10^{34}	
	LAr	fast	LAr	fast
both γ's, $\lvert\eta\rvert < 2.5$	0.786	0.786	0.786	0.786
2-γ efficiency*	0.763	0.775	0.743	0.809
$78 < M_H < 82$ GeV	0.938	0.949	0.896	0.940
Overall efficiency*	0.56	0.58	0.52 (0.39)	0.60 (0.54)

* 5 GeV isolation cut at 10^{33}, 10 GeV for 10^{34}.
values in parentheses for GeV cut

(excludes $t\bar{t}$ tagging efficiency)

Y.Sakai
KEK

Effect of Pileup on Efficiency of Isolated Electron

- Signal events : H(400GeV) -> WW -> ev+jet
- Pile up events: ISAJET "TOWJET" (P_T>3 GeV)

- Wave Form Simulation;
  τ_p=100, 200 nsec: T_d=400 nsec, Bipolar(m=3)
  * Electric Noise: (per tower, in rms)
    EM: 0.05, HAD1: 0.274 GeV for τ_p=100 nsec
    EM: 0.02, HAD1: 0.113 GeV for τ_p=200 nsec
  τ_p=0 (No wave form): no electric noise

- Cal Segmentation: 0.05 x 0.05
  e, photon, pizero --> EM ($15\%/E^{1/2}$)
  hadrons --> HAD ($50\%/E^{1/2}$)
- Magnetic Field: Bz = 2 Tesla
- Cal Energy: Pulse Hight at peak of signal
  Readout both positive and negative signal

- Electron ID: $E_{HAD1}/E_{EM} < 0.05$
- Isolation: ΣE_T (EM+HAD1) within cone $\Delta R < 0.3$
  (all tower or $|E_T(\text{tower})| > 1$ GeV in sum)
- Efficiency vs Luminosity:
  L = 0(no pileup), (1-10)x10^{33} (1.6-16ev/xing)
  Signals only

• Effects of pileup to the electron efficiency and to the isolation efficiency were evaluated by using the physics process

$$\text{Higgs}(400\text{GeV}/c^2) \rightarrow W^+W^- \rightarrow e\nu + \text{jets}$$

for the design luminosity of $10^{33}cm^{-1}s^{-1}$ and 10^{34} for the two shaping times of τ_p=100 and 200 ns. In the analysis, only HAD1 was used to suppress the electronics noise. (The simulation simplified the calorimeter vastly and more sophisticated full simulation should be performed to finalize the following results.)

• Because the electronics noise and the pileup noise interplayed for the short and long shaping times, the longer shaping time did not help to improve the efficiencies (Fig. (a), (c), and (e)).

• From Figs. (a) and (c), efficiencies of "electron ID" and "isolation<5GeV" at τ_p=100 ns were:

	$10^{33}cm^{-1}s^{-1}$	10^{34} $cm^{-1}s^{-1}$
"electron ID"	96%	95%
"isolation<5GeV"	92%	72%

The decrease of "isolation" efficiency means we lose isolated electrons as non-isolated; we have effectively 7 times the luminosity when we increase 10 times.

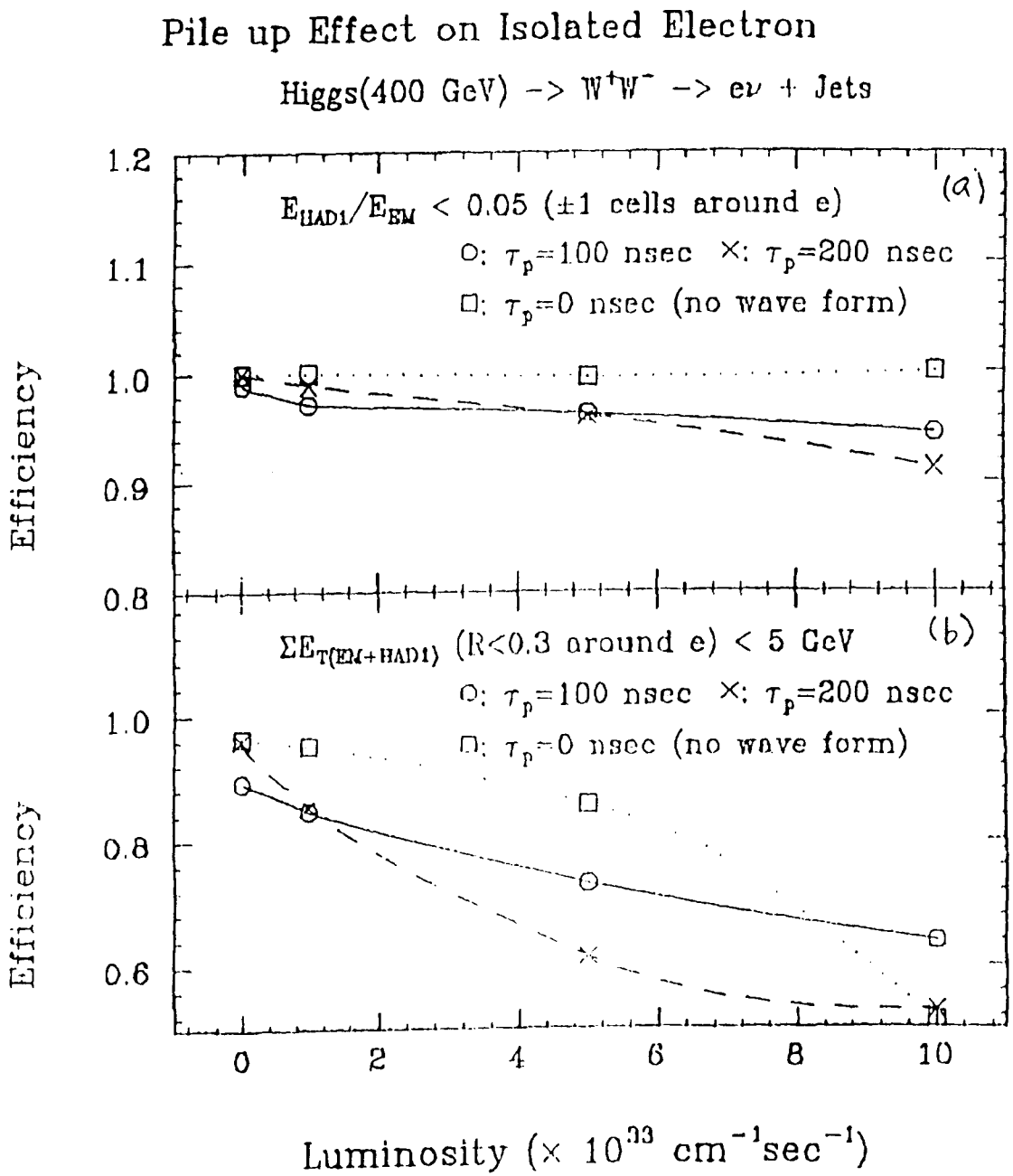
Pile up Effect on Isolated Electron
Higgs(400 GeV) -> W+W- -> eν + Jets
(a)
E_HAD1/E_EM < 0.05 (±1 cells around e)
O: τp=100 nsec ×: τp=200 nsec
□: τp=0 nsec (no wave form)
(b)
ΣE_T(EM+HAD1) (R<0.3 around e) < 5 GeV
O: τp=100 nsec ×: τp=200 nsec
□: τp=0 nsec (no wave form)
Efficiency
Efficiency
1.2
1.1
1.0
0.9
0.8
1.0
0.8
0.6
0
2
4
6
8
10
Luminosity (× 10^33 cm^-1sec^-1)

Impact on Jet Measurements

For cone of radius 0.7, sigma_Et = 8 GeV (pileup+noise, EM+HAD1, 60ns/200ns tpeak)

- comparable to resolution for Et = 100 GeV (for $\frac{\sigma_{E_t}}{E_t} = \frac{0.70}{\sqrt{E_t}} \oplus 0.04$)

ID= 300

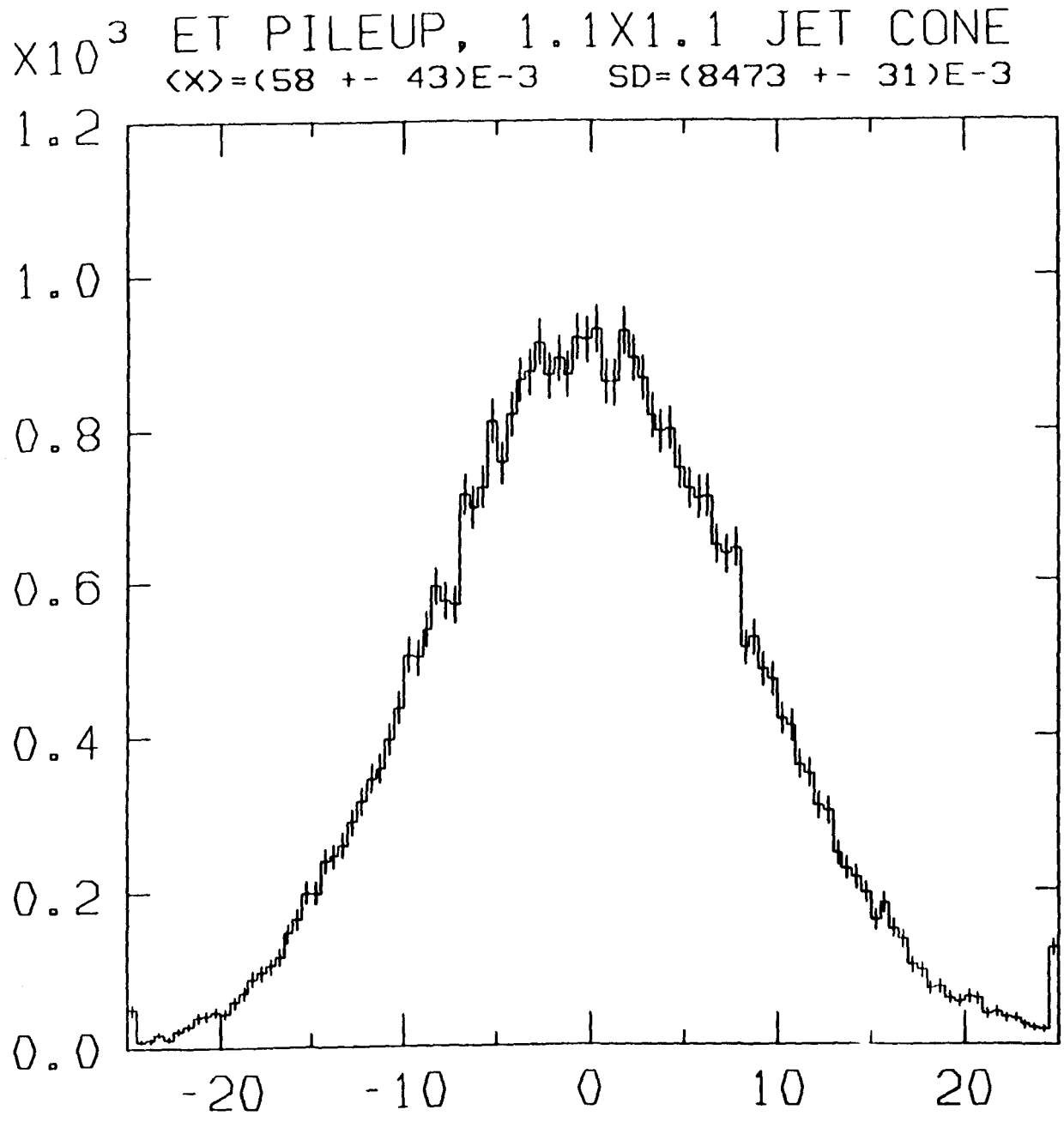

HEA12:01 11SEP91

SUMMARY

- Fast LAr risetime preserved by electrode structure

- $\sigma t < 4$ ns for >2 GeV in EM tower
  $\sigma t < 4$ ns for >80 GeV jet
  (both are better in endcap)

- Effect of noise and pileup on EM resolution:

$$\frac{\sigma}{Et} = \frac{0.13}{\sqrt{Et}} \oplus \frac{0.22}{Et} \qquad @\ 10^{**}33$$

- H --> $\gamma\gamma$ efficiencies
  - single γ efficiency reduced 1% [4%]
  - mass resolution worse by 5% [20%]
  - event efficiency 0.58 (fast) --> 0.56 (LAr)
    0.60 (fast) --> 0.52 (LAr)

- H --> WW --> $e\nu$ + jets; isolated e-
  efficiency 0.92 [10**33] --> 0.72 [10**34]
  (tighter cuts)

CALORIMETER REVIEW AND TECHNICAL BOARD MEETING
SEPTEMBER 12 -14, 1991
SSCL

Presentation by:

Kenneth Einsweiler

Lawrence Berkeley Laboratory

KFE 9/12/91

K. Einsweiler

EM Calorimeter Requirements

have a preliminary "requirements" document (rough but useful ...)

- EM Hermeticity
- ✓ EM Resolution
- EM Linearity
- ✓ EM Transverse Segmentation
- EM Depth + Longitudinal Segmentation
  + Preshower / Shower Max

GOAL: Overall electron efficiency ~85-90% for "clean" events

Caveat: real, interesting questions in e, γ ID too hard for simulation ⇒ "everything looks like CD

EM Hermeticity | $|\eta| \leq 2.5$ only ...

- cracks and holes
- regions with non-Gaussian tails
- regions with large spatial non-uniform

from CDR's :

LAr claims ~97% coverage
(area where $\frac{\sigma_E}{E} \lesssim \frac{25\%}{\sqrt{E}}$)

- azimuthal ϕ crack 3mm, 3° tilt
- tie rods $\lesssim 1\%$ of area
- real problem = "30° crack"

Sci-Ti claims ~100% coverage

- azimuthal ϕ crack 2mm, 5.7° tilt
- claim "30° crack" ~ invisible

Believe : arguments about < 5% of solid angle are basically "religious"...

EM Linearity

→ major factor is large amount of material (coil, ...)

1) loss in response, function of E since shower max moves

LAr ~4% at 10 GeV, ~15% at 2 GeV

2) deterioration of resolution

D. Green :

$$\frac{\Delta E}{E} \sim \frac{0.019}{\sqrt{E}} e^{t/1.58}$$

without massless gap correction

⇒ for $\sigma_0 = \frac{.12}{\sqrt{E_T}} \oplus .5\%$

at $\eta = 0$, coil ~ ½ of σ_0

at $\eta = 1.5$, coil ~ equal to σ_0

⇒ massless gap with readout [correction = f(E

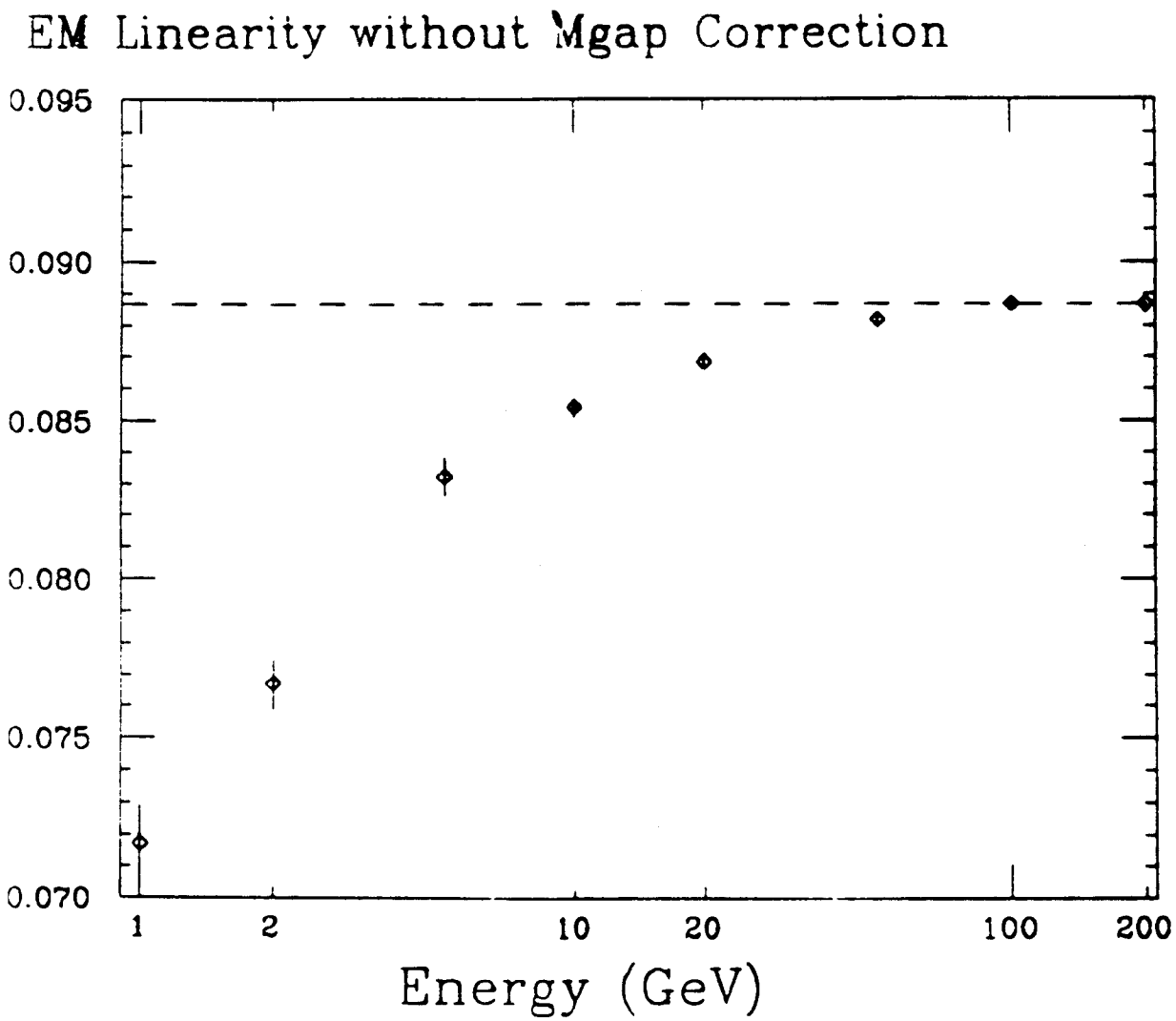

EGS study by C. Hearty
of response vs E for LAr model

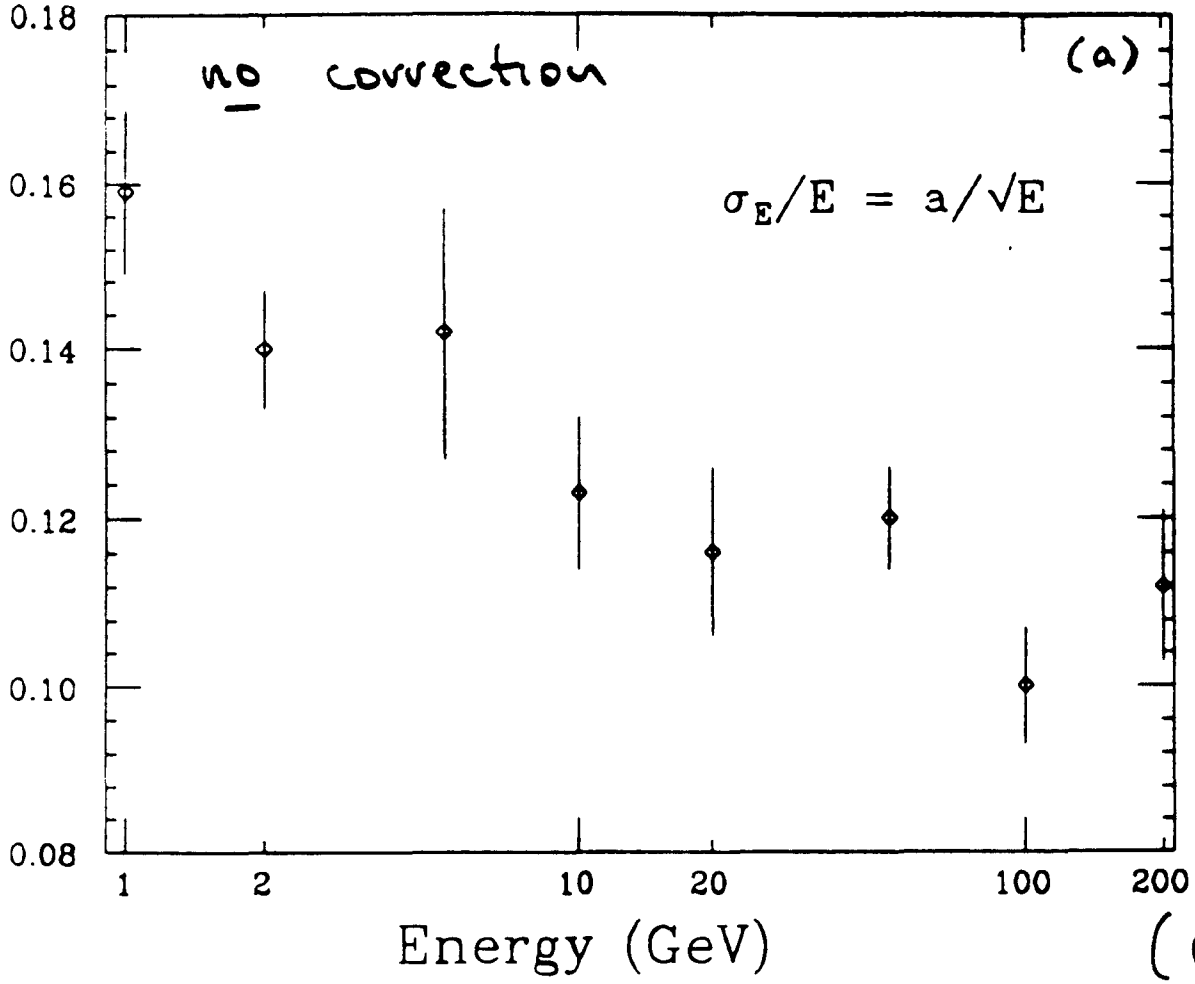

Ebs study of stocha term in resolu

(C. Hear

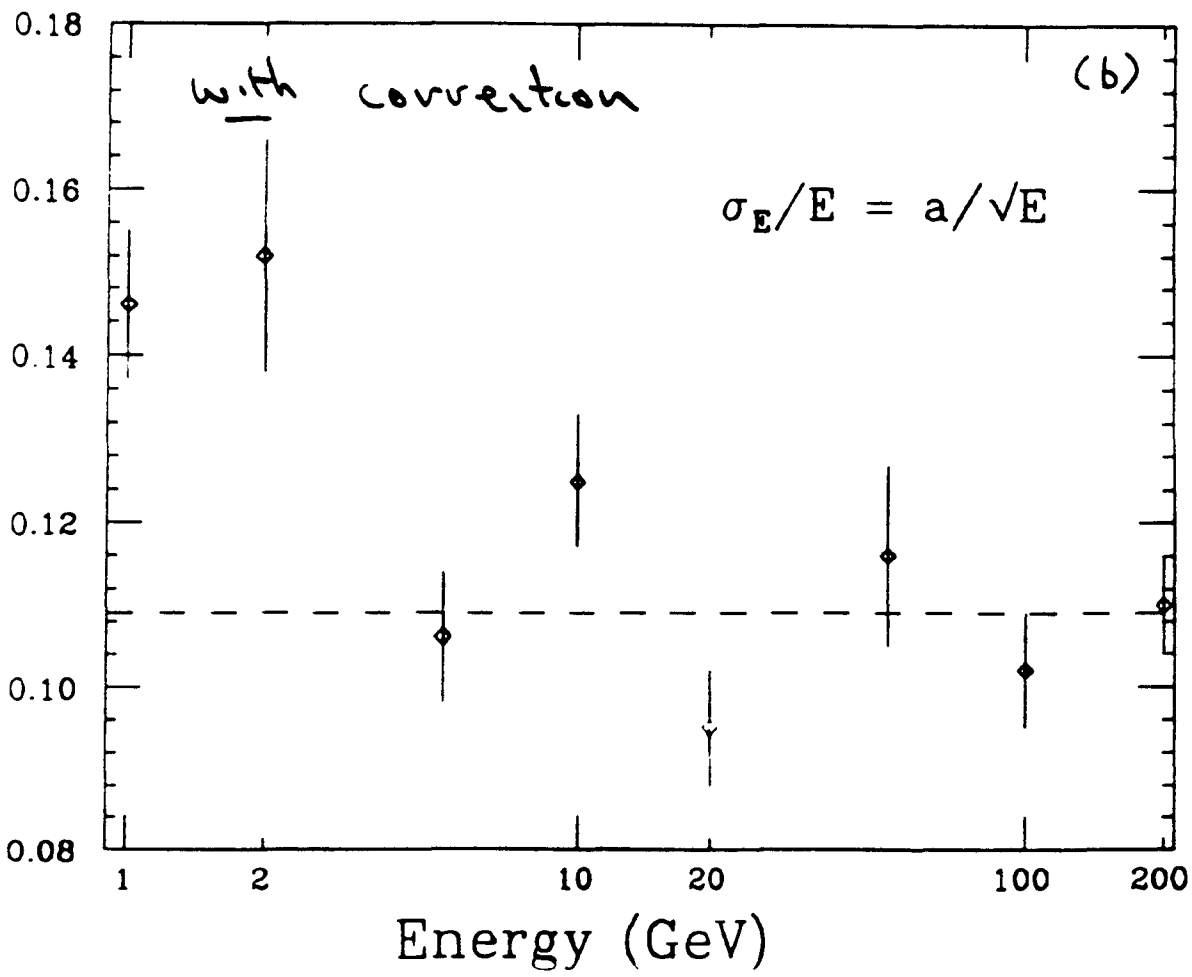

EM Depth + Longitudinal Segmentation

considering: 20 X_0
22 X_0
25 X_0

depending on:
- HAD1 material
- correction schem

Conflicting requirements:

- HAD/EM cut for e/π separation at low E is less effective if calorimeter is "too thick"

  but: HAD/EM strongly correlated with preshower pulse height
  $\Rightarrow$ redundant (B. Wickland)

- different radiator thickness (and material?) in HAD 1 will induce non-linearity at high E if calorimeter is "too thin"

In order to keep effects under control, prefer 2 EM depth segment

?

Also: Sci-T: needs depth segmentation to help correct longitudinal non-uniformities which come with large damage coefficients

EM Transverse Segmentation

roles:

- electron / photon ID
- electron / photon E measurement
- isolation

.05 x .05 ~ 10 cm x 10 cm at $\eta = 0$

R_m ~ 2 cm 99% of E in cylinder of 3.5 R_m

Scales:

1) shower max segmentation

~ .006 x .006 at $\eta = 0$ (~ R_m)

shower profile uses ~ 7-11 strips

⇒ occurs in roughly an area of .05 x .05 (cone with R ~ 0.0

2) E measurement

- want larger area to collect all e/γ energy
- want smaller area to minimize pileup effects

→ SDC towers same physical size as those of UA2 (but ~ factor 25 in $\Delta\eta \times \Delta\phi$

⇒ 2x2 tower sum works well

| typically use only those towers which are predicted to contain more than some fraction of E, based on electron impact point

⇒ measurement area ~ .1 x .1
(cone with R ~ .05)

3) isolation = topological cut

typical cone size for SSC physics R ~ 0.2, 0.

| driven by jet size, energy flow around b leptons above P_T ~ 10-20 GeV, ...

Note : real scales for (1) & (2) are cm
not $\Delta\eta$, $\Delta\phi$

$\eta = 2$ 1/sin θ ~ 3 ; $\eta = 2.5$ 1/sin θ ~ 6

segmentation implications :

(1) Shower max detectn = thin slice through shower ⇒ lots of fluctuations

CDF data (Wickland) ⇒ $\lesssim 1$ GeV additional E deposition in measurem region has ~ no effect on transve profile of 50 GeV electron

(2) E measurement : goal is measuremen of precision 1-2%

⇒ additional energy deposit in measurement region $\lesssim 1\%$

or $\lesssim 500$ MeV

(3) Isolation cones are large on scale of proposed segmentations

⇒ ignore for now

Address issues using Associated Higgs production $W+H$, $t\bar{t}+H \longrightarrow \ell + \gamma\gamma + \nu$

- PYTHIA simulation
- $B=0$, no shower shapes, no materia

look at energy density in cones around ℓ and γ

W+H events at 10^{31}

ratio of : $\frac{\text{excess } E_T \text{ in cone}}{E_T \text{ of } \gamma}$

$R = 0.05$

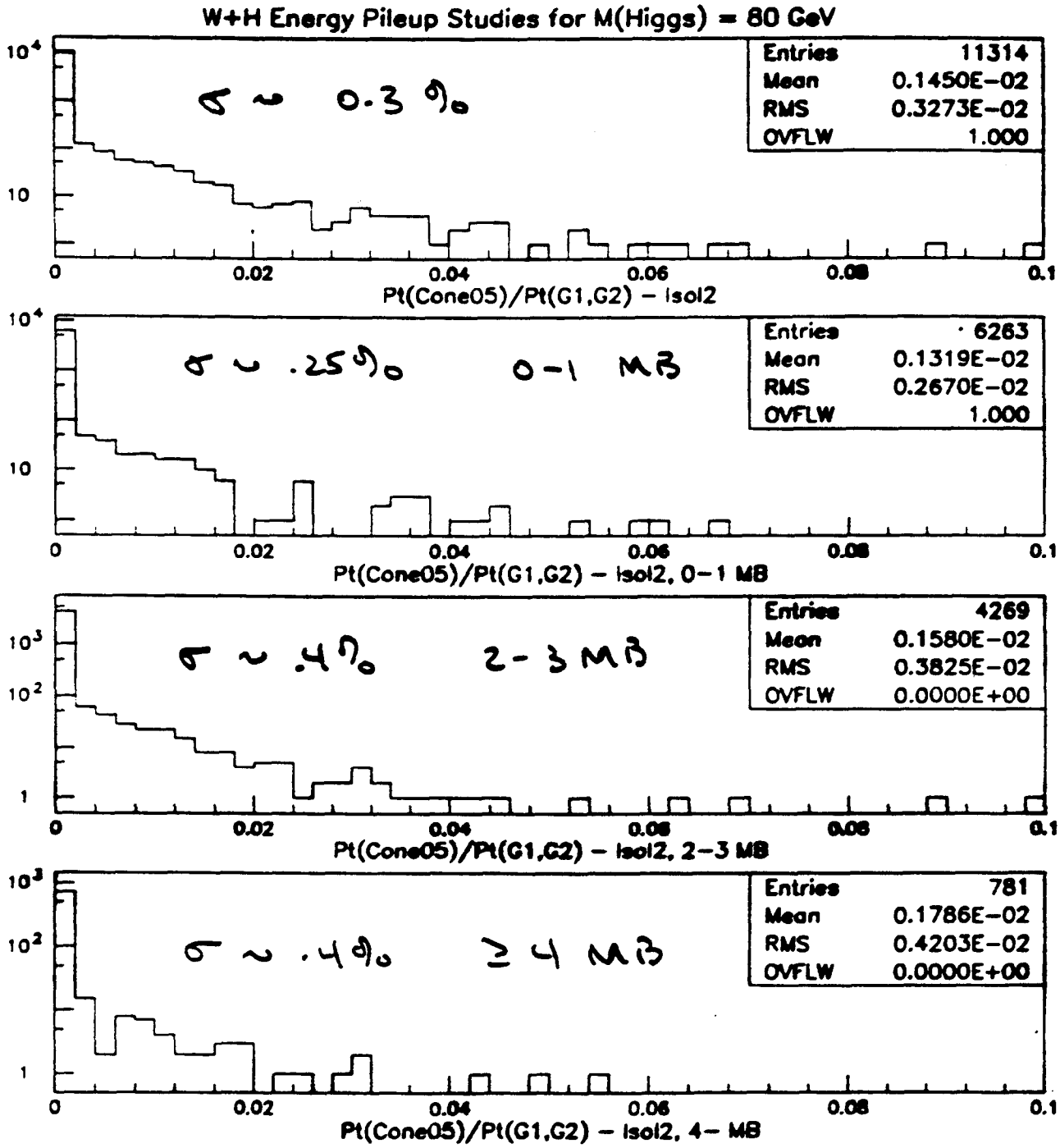

R = 0.1

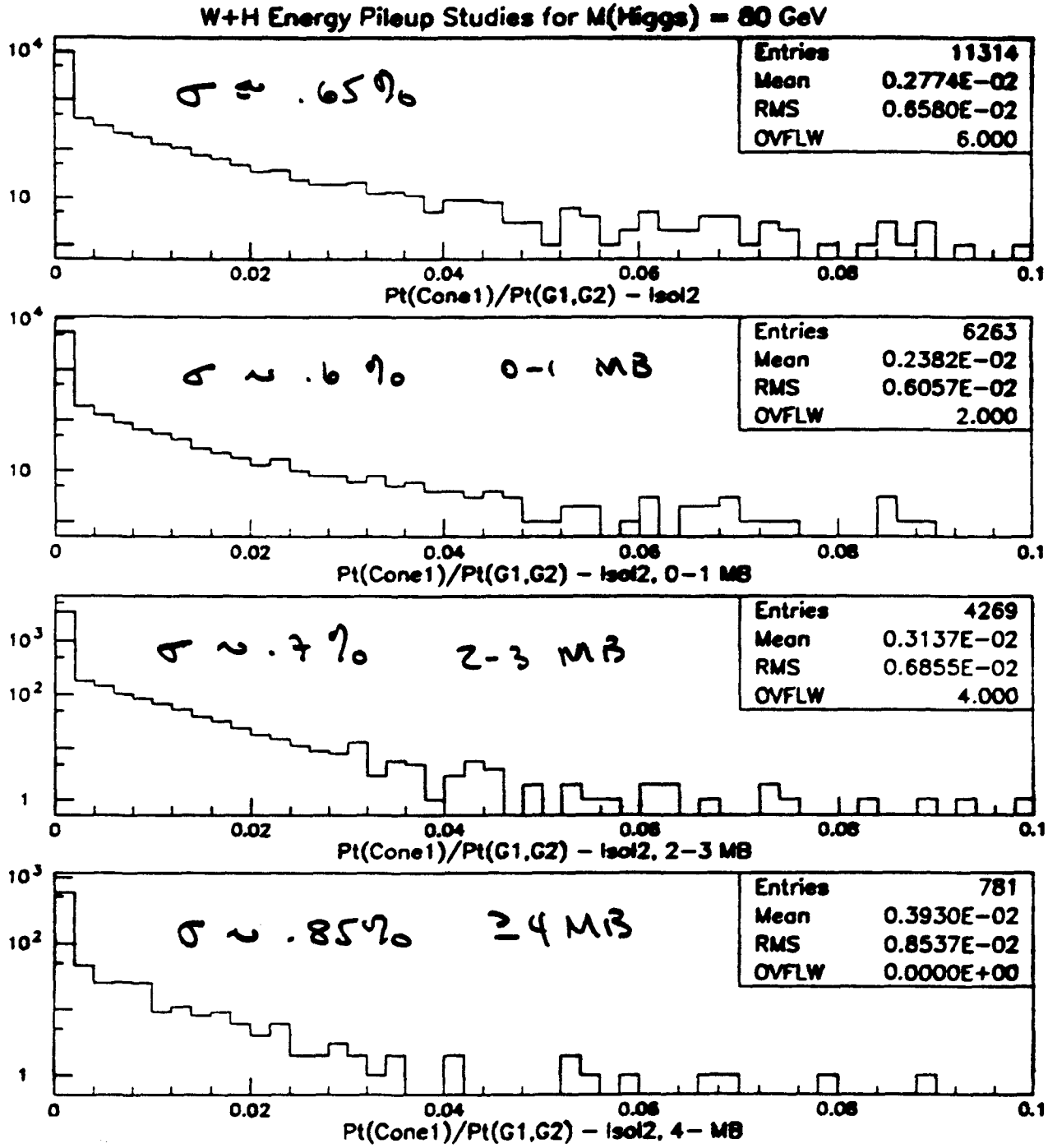
W+H Energy Pileup Studies for M(Higgs) = 80 GeV
Entries 11314
Mean 0.2774E-02
RMS 0.6580E-02
OVFLW 6.000
σ ≈ .65%
Pt(Cone1)/Pt(G1,G2) – Isol2
Entries 6263
Mean 0.2382E-02
RMS 0.6057E-02
OVFLW 2.000
σ ~ .6%
0-1 MB
Pt(Cone1)/Pt(G1,G2) – Isol2, 0–1 MB
Entries 4269
Mean 0.3137E-02
RMS 0.6855E-02
OVFLW 4.000
σ ~ .7%
2-3 MB
Pt(Cone1)/Pt(G1,G2) – Isol2, 2–3 MB
Entries 781
Mean 0.3930E-02
RMS 0.8537E-02
OVFLW 0.0000E+00
σ ~ .85%
≥4 MB
Pt(Cone1)/Pt(G1,G2) – Isol2, 4– MB

Fraction of events with

fraction < x

R = 0.05

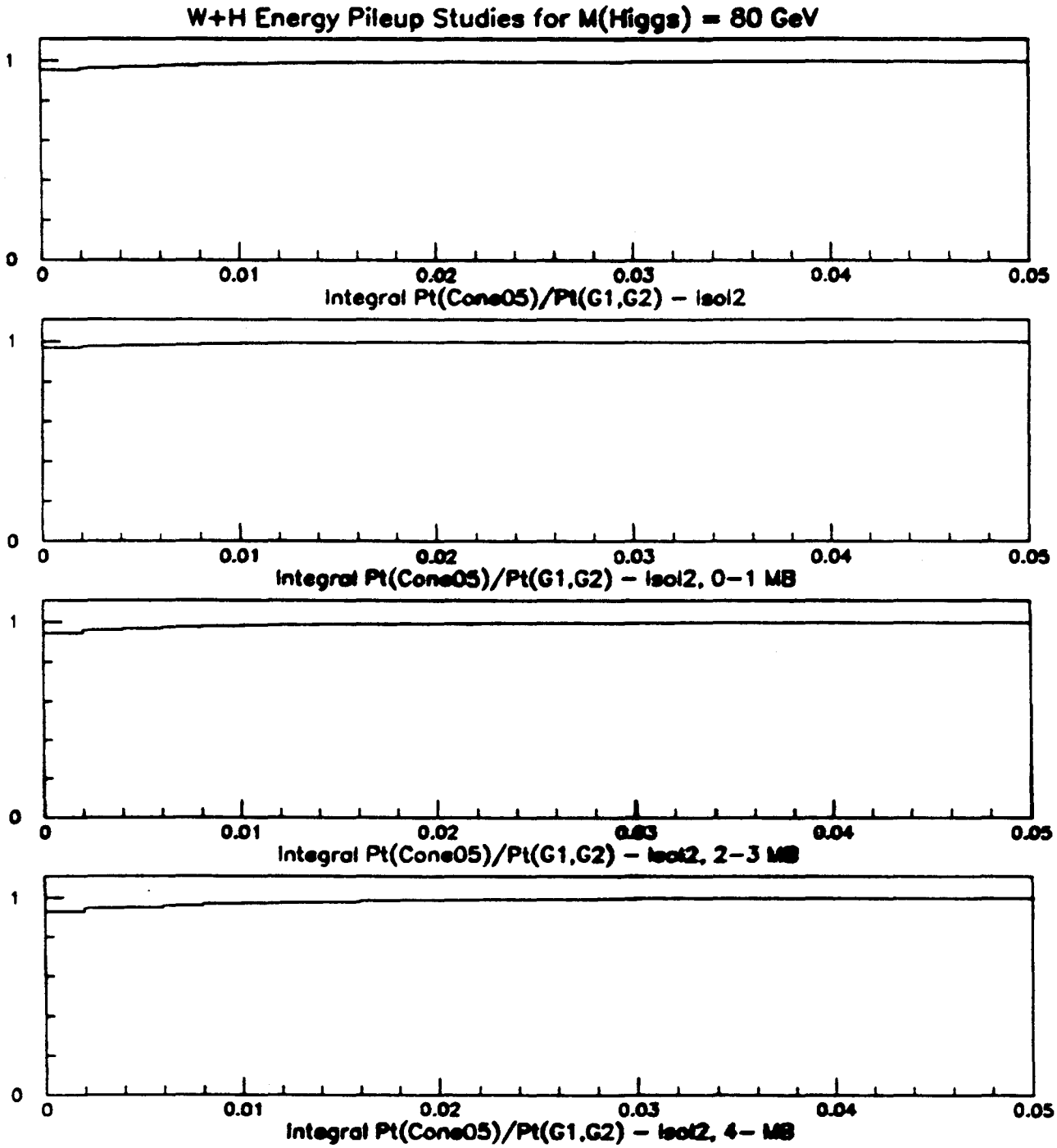

tt+H Energy Pileup Studies for M(Higgs) = 80 GeV

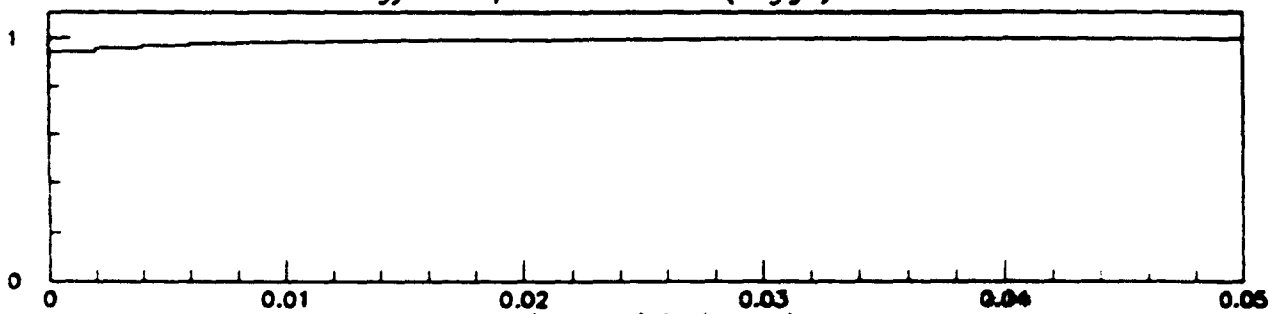

Integral Pt(Cone05)/Pt(G1,G2) – Isol2

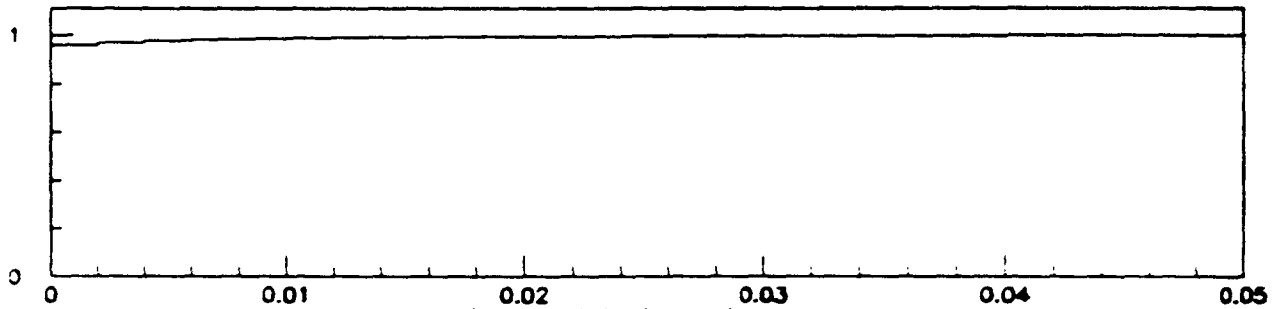

Integral Pt(Cone05)/Pt(G1,G2) – Isol2, 0–1 MB

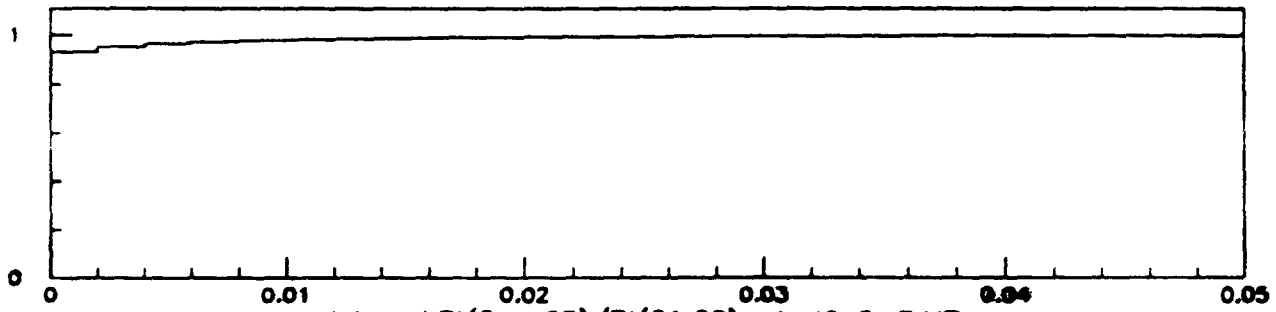

Integral Pt(Cone05)/Pt(G1,G2) – Isol2, 2–3 MB

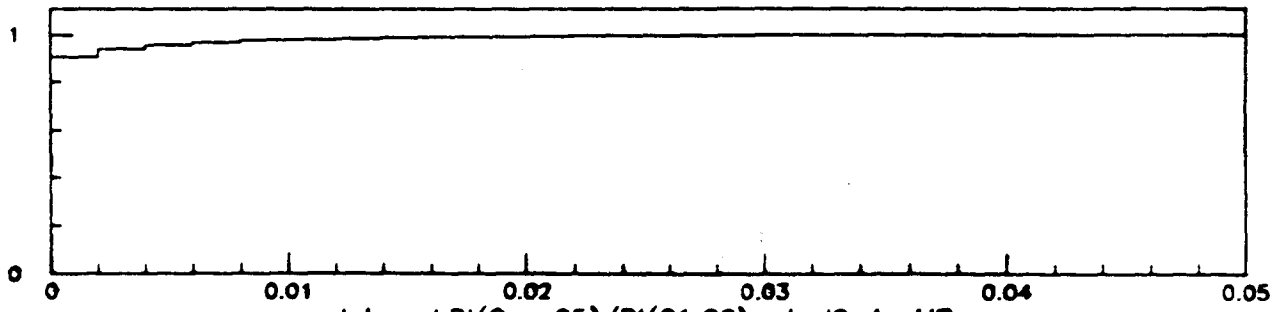

Integral Pt(Cone05)/Pt(G1,G2) – Isol2, 4– MB

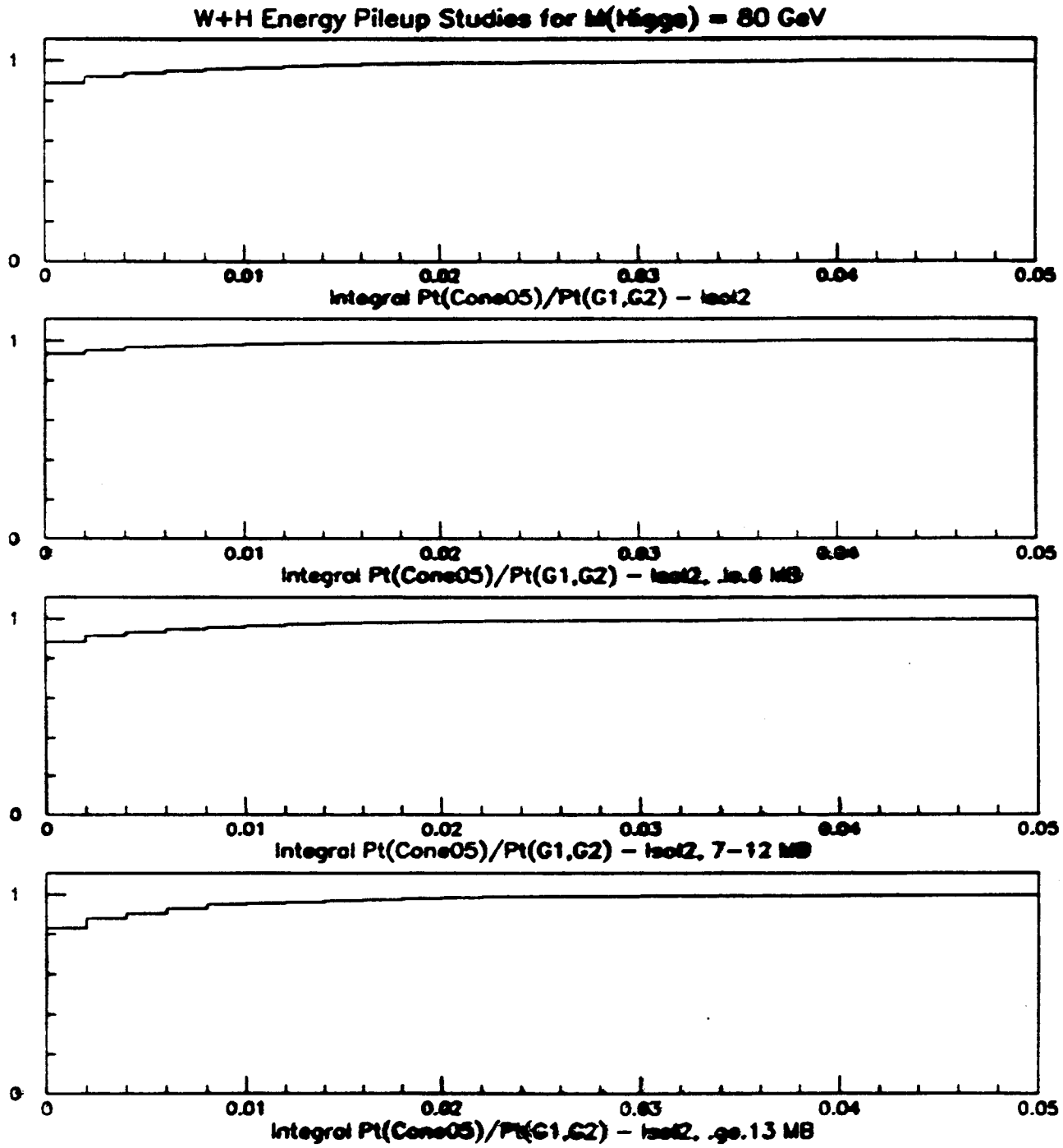
W+H Energy Pileup Studies for M(Higgs) = 80 GeV
1
0
0
0.01
0.02
0.03
0.04
0.05
Integral Pt(Cone05)/Pt(G1,G2) – Isol2
Integral Pt(Cone05)/Pt(G1,G2) – Isol2, .le.6 MB
Integral Pt(Cone05)/Pt(G1,G2) – Isol2, 7–12 MB
Integral Pt(Cone05)/Pt(G1,G2) – Isol2, .ge.13 MB

R = 0.1

W+H Energy Pileup Studies for M(Higgs) = 80 GeV

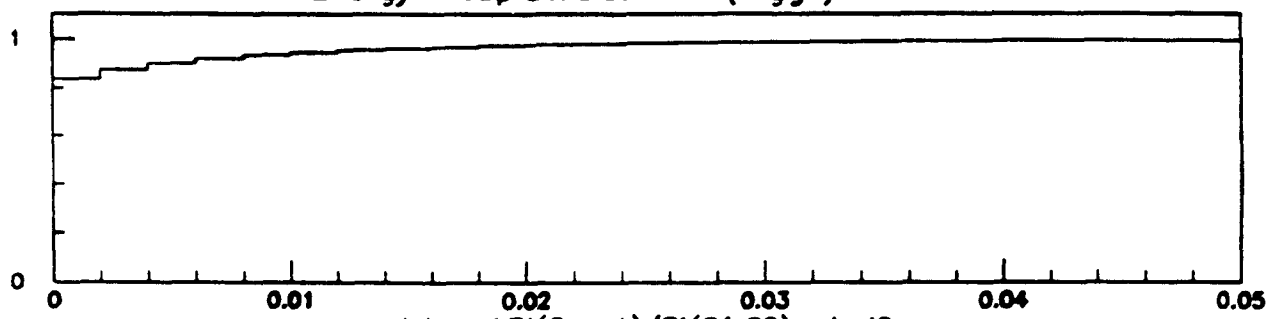

Integral Pt(Cone1)/Pt(G1,G2) – Isol2

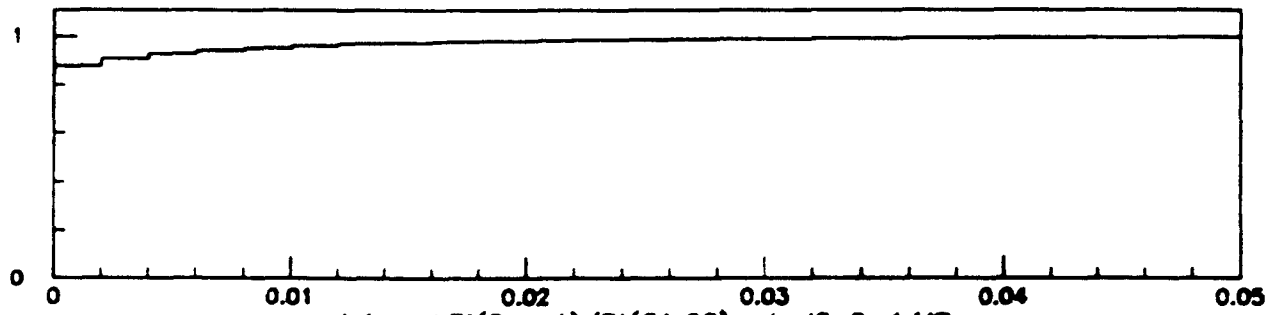

Integral Pt(Cone1)/Pt(G1,G2) – Isol2, 0–1 MB

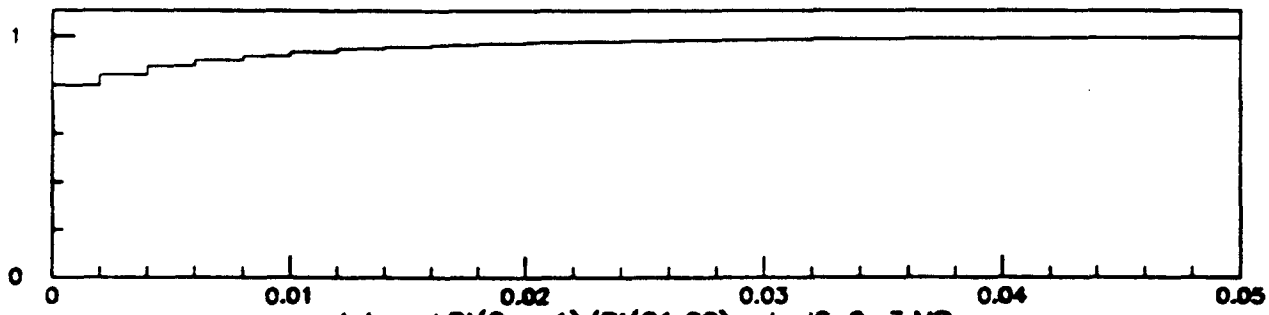

Integral Pt(Cone1)/Pt(G1,G2) – Isol2, 2–3 MB

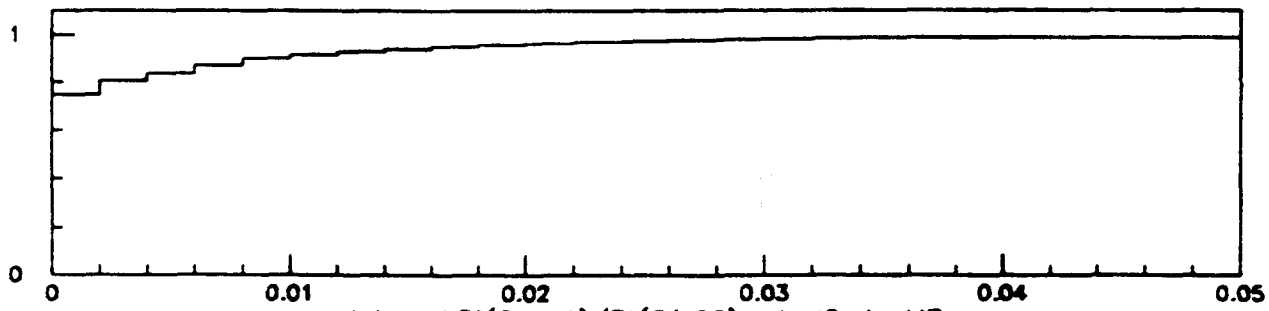

Integral Pt(Cone1)/Pt(G1,G2) – Isol2, 4– MB

tt+H Energy Pileup Studies for M(Higgs) = 80 GeV

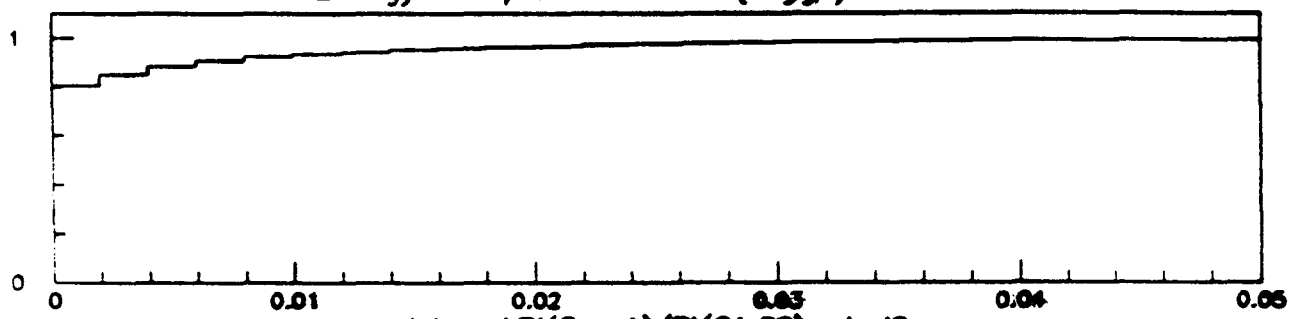

Integral Pt(Cone1)/Pt(G1,G2) – Isol2

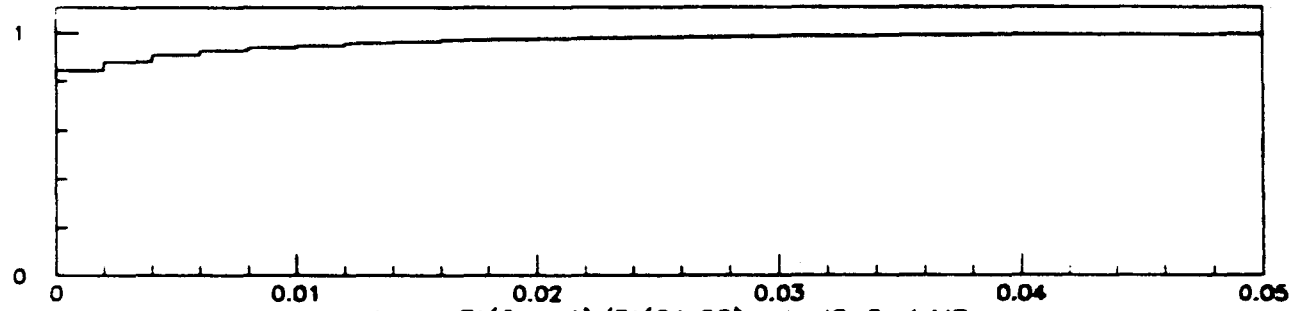

Integral Pt(Cone1)/Pt(G1,G2) – Isol2, 0–1 MB

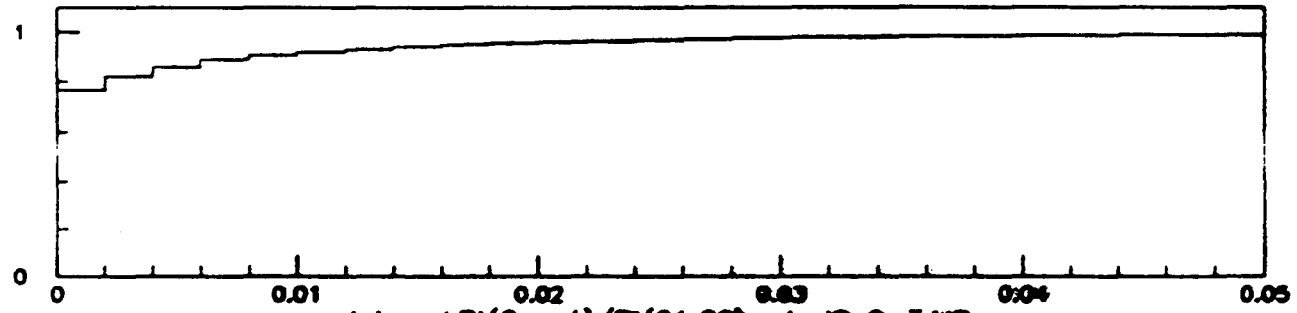

Integral Pt(Cone1)/Pt(G1,G2) – Isol2, 2–3 MB

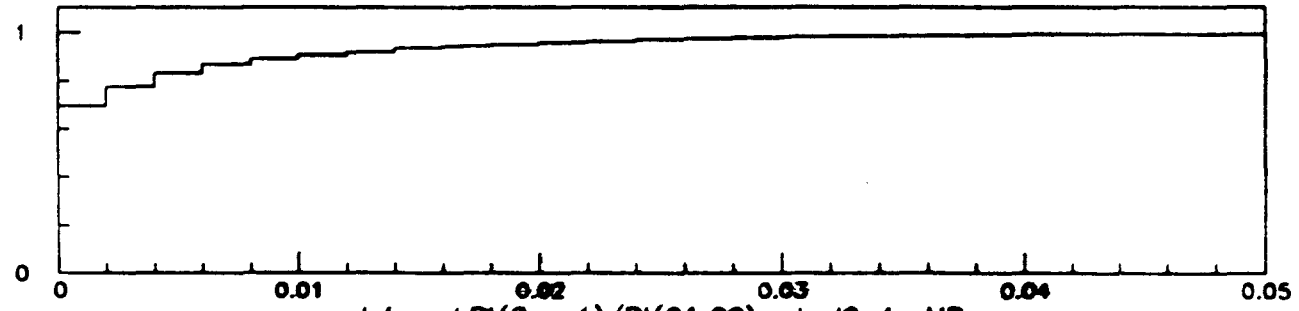

Integral Pt(Cone1)/Pt(G1,G2) – Isol2, 4– MB

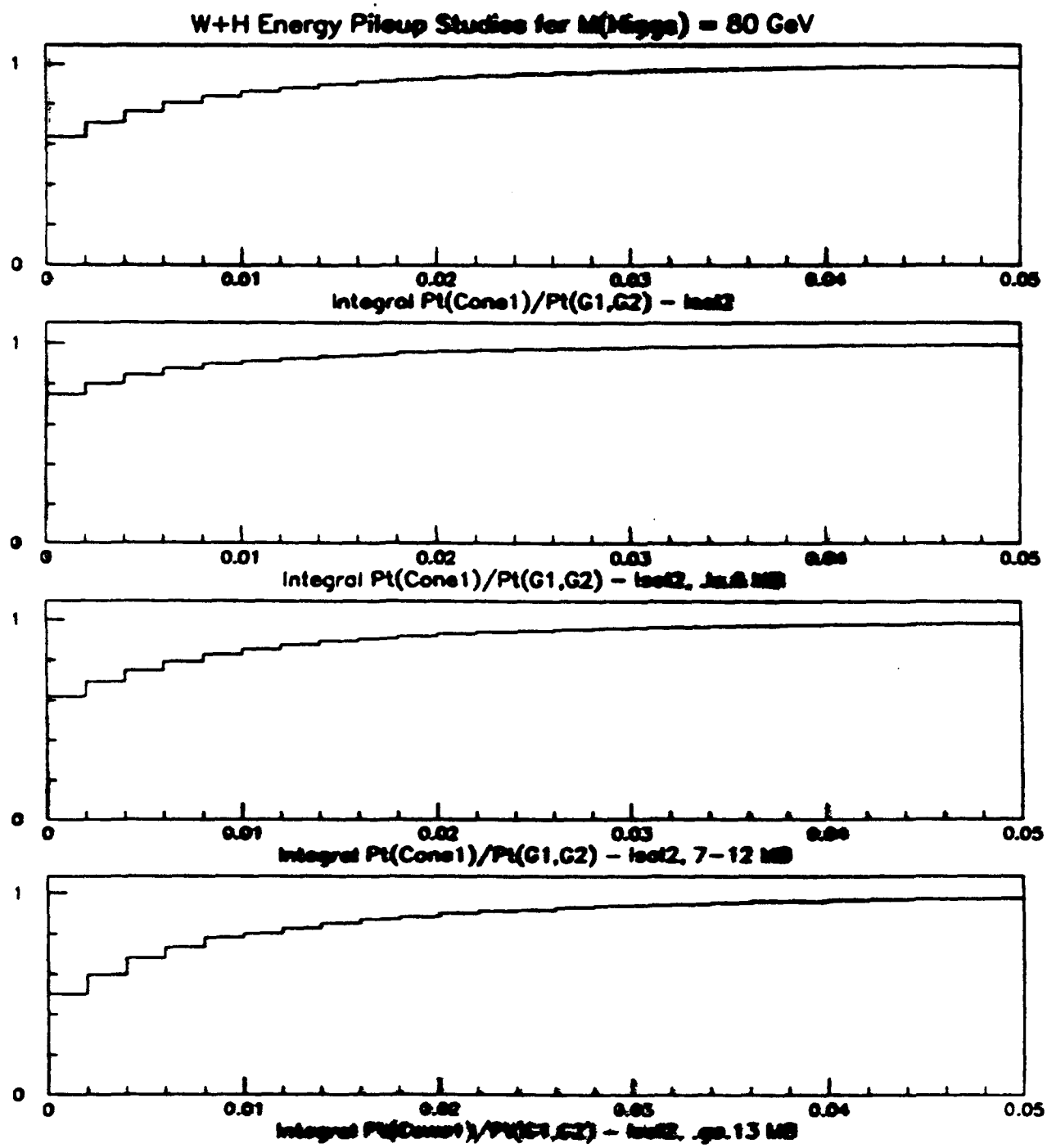
W+H Energy Pileup Studies for M(Higgs) = 80 GeV
1
0
0
0.01
0.02
0.03
0.04
0.05
Integral Pt(Cone1)/Pt(G1,G2) – Isol2
Integral Pt(Cone1)/Pt(G1,G2) – Isol2, Jan.8 MB
Integral Pt(Cone1)/Pt(G1,G2) – Isol2, 7–12 MB
Integral Pt(Cone1)/Pt(G1,G2) – Isol2, ge.13 MB

EM Resolution

assume cylindrical design

$$\Rightarrow \frac{\sigma_E}{E} \sim \frac{a}{\sqrt{E_T}} \oplus b \qquad \text{barrel}$$

$$\frac{a}{\sqrt{E_L}} \oplus b \qquad \text{endcap}$$

consider:

3-4 mm Pb plates in barrel $a = 12-13\%$

6-8 mm Pb plates in endcap $a = 17-18\%$

this morning's results are somewhat worse ?

assume $b \lesssim 2\%$

<u>note</u>: segmentation <u>will</u> play a role at higher $\mathcal{L}$ or in complex events due to pileup smearing

i) stochastic term only important at "low E" $\Rightarrow$ $\lesssim$ 100 GeV

$\Rightarrow$ intermediate Higgs is a good probe

ii) constant term important at "high E" $\Rightarrow$ $\gtrsim$ 50 GeV

$\Rightarrow$ still important for intermediate Higgs width of high mass $Z' \to ee$

Intermediate Mass Higgs:

<u>$H \to ZZ^*$</u>

- tracking gives better resolution (beware of brem
- Z width sets natural scale
  - $\Rightarrow$ all SDC resolutions are acceptable:
    $\sigma(m_Z) \lesssim 3\%$

$\underline{H \to \gamma\gamma}$

- produce in association with W or t $\Rightarrow$ tag on lepton

- natural line width $\underline{\underline{\sim 0}}$

  ($\Gamma(H) \sim 10$ MeV for $m_H \sim 140$ GeV

better resolution $\Rightarrow$ better S/N ...

Analysis:

<u>signal</u> = $W + H$, $t\bar{t} + H$

$t\bar{t} + H$ ~ factor 5 larger at SSC
(after acceptance ...)

~ independent of m_t if $100 < m_t < 2$

<u>backgrounds</u> = $W + \gamma\gamma$

$b\bar{b} + \gamma\gamma$

$t\bar{t} + \gamma\gamma$

Backgrounds to $\ell + \gamma\gamma + X$

Note: $tt\gamma\gamma$ strongly m_t dependent:

$\times 3$ for $m_t = 100$ $\div 3$ for $m_t = 200$

Combined ttbar + Higgs and W + Higgs Final State

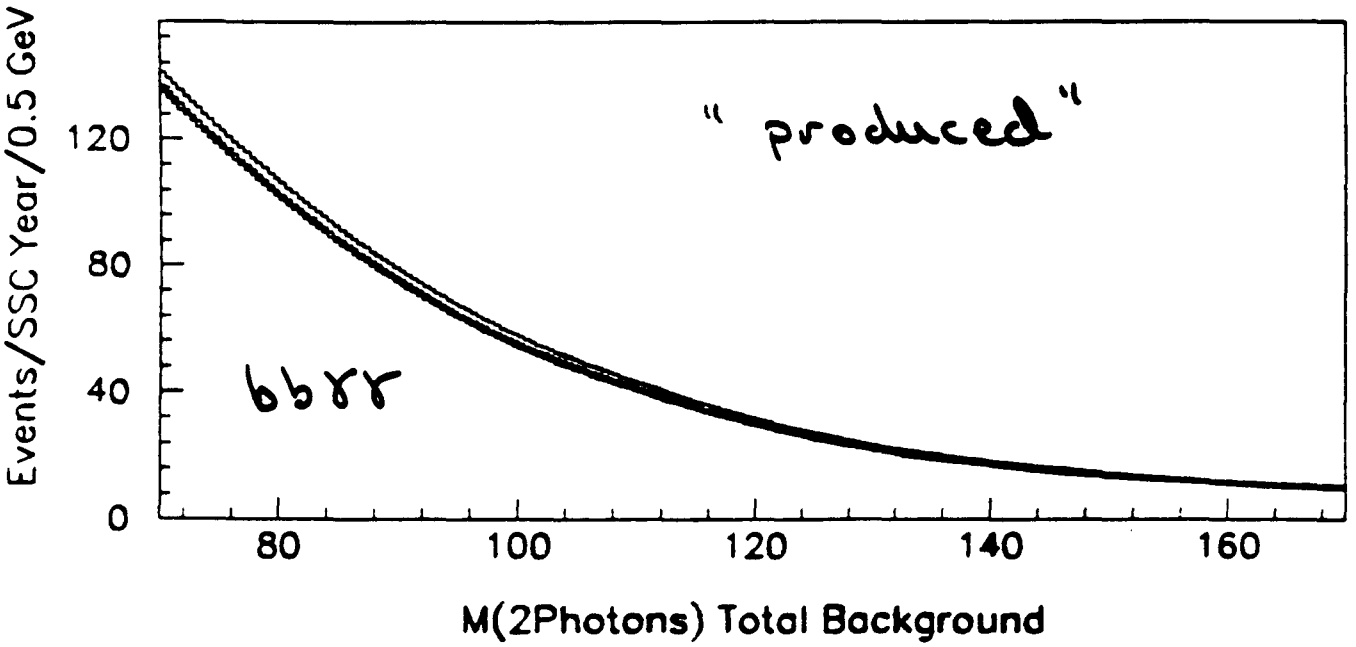

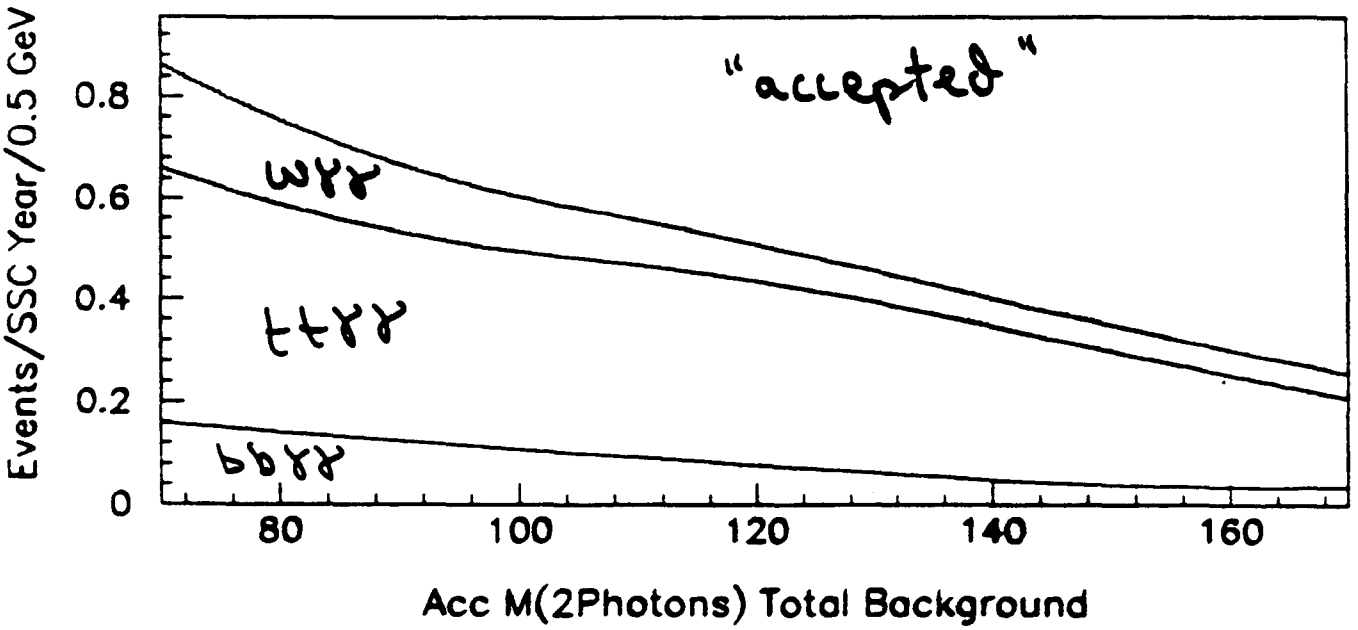

studies of background kinematics
$\Rightarrow$ little reduction possible

Analyze S/N for set of resolutions

"Good" $= .10/\sqrt{E}$

"Base" $= .12/\sqrt{E_T} \sim .18/\sqrt{E_L}$

with constant $= 0, .5, 1, 2\,\Omega_0$

"Poor" $= .20/\sqrt{E_T} \sim .20/\sqrt{E_L}$

constant $= 2.0\,\Omega_0$

Photon E resolution vs η

for $t\bar{t}+H$ events, $m_H = 80$ GeV

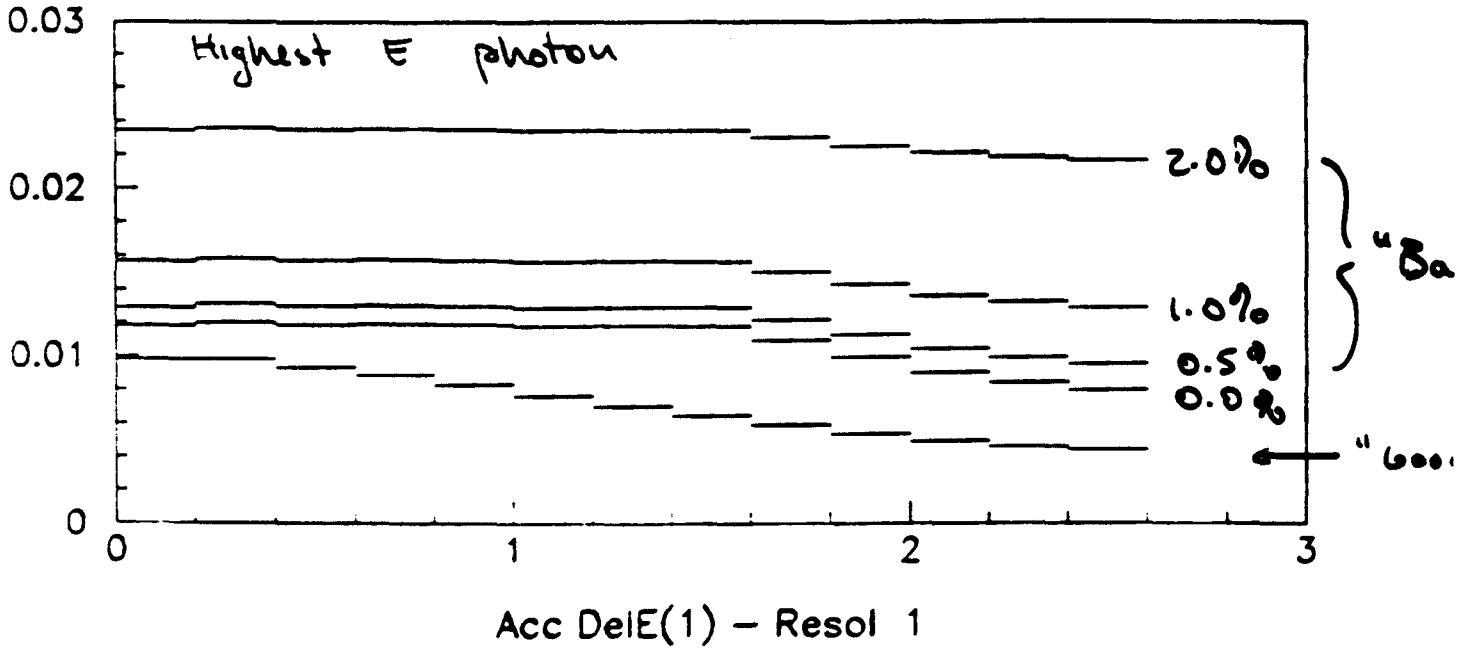

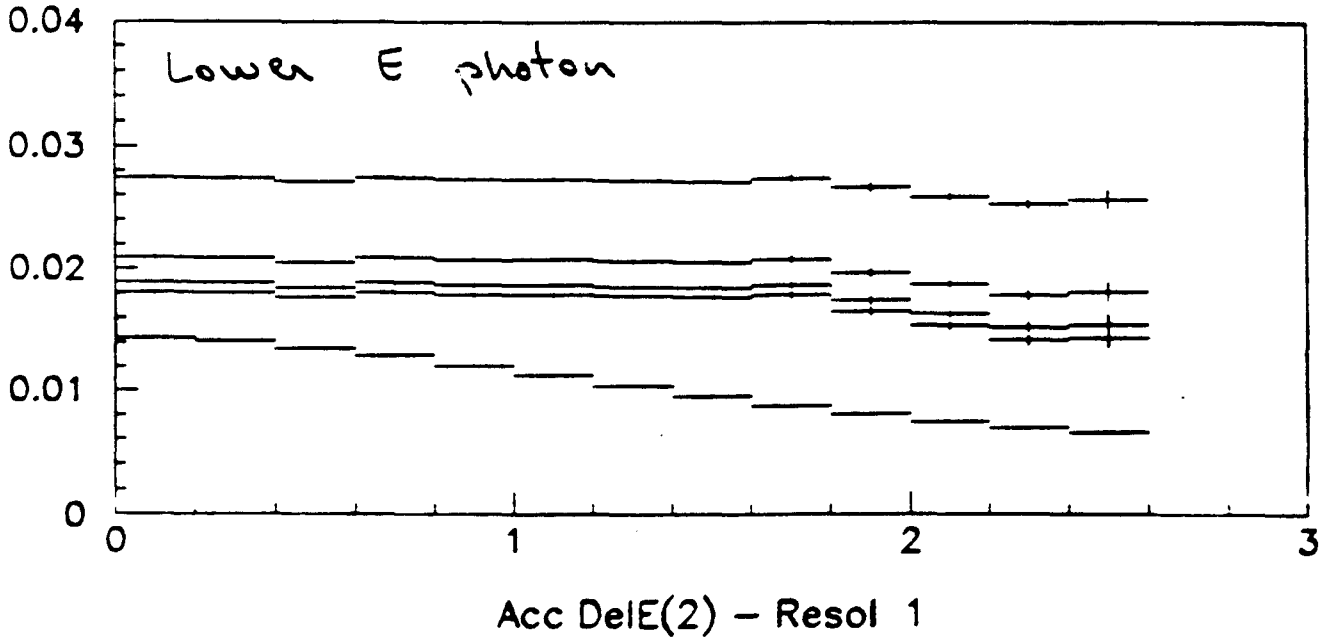

Mass resolution for $t\bar{t} + H$ $\hookrightarrow \gamma\gamma$

versus m_H

$\Rightarrow$ factor of $\underline{3}$ variation

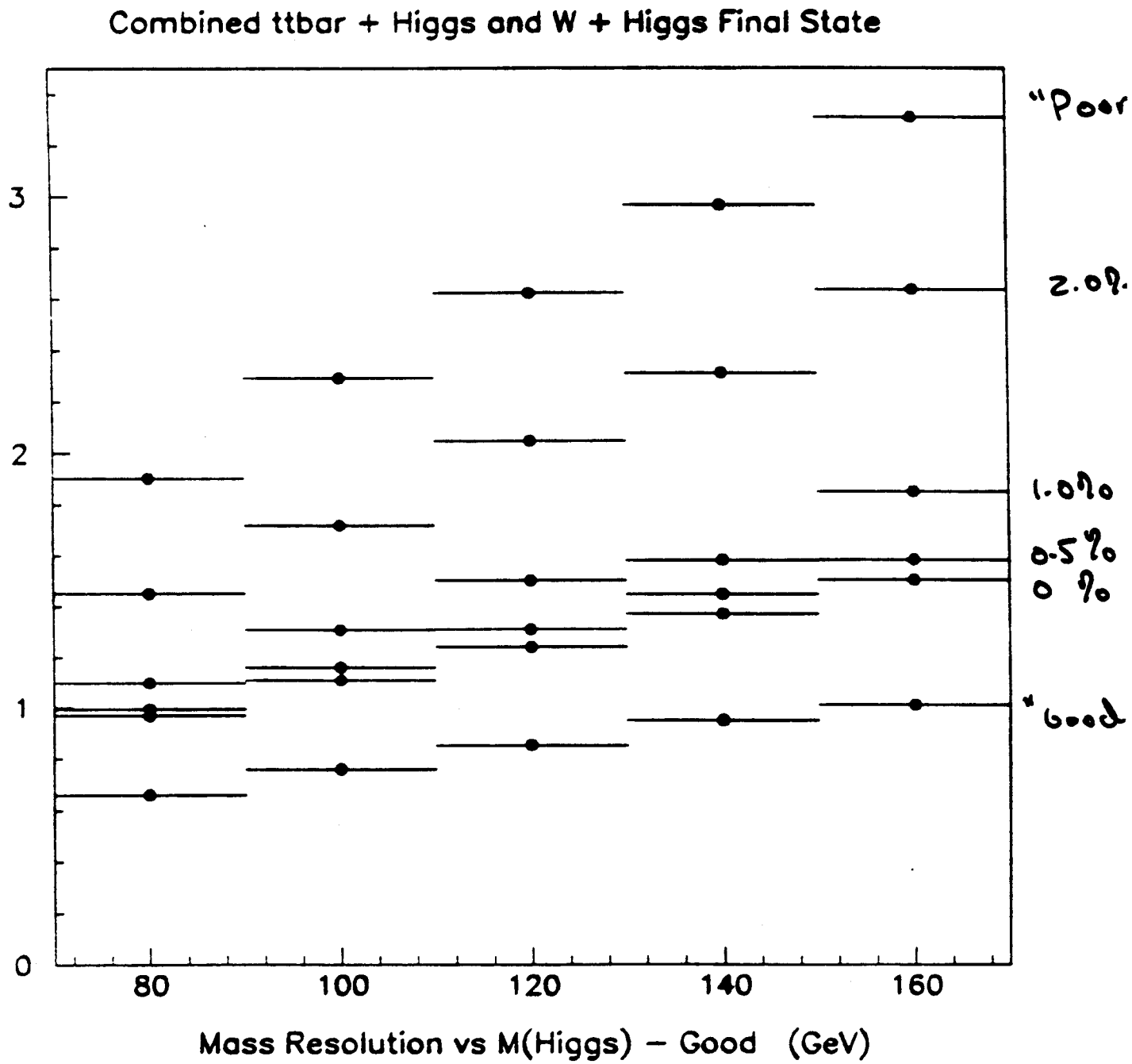

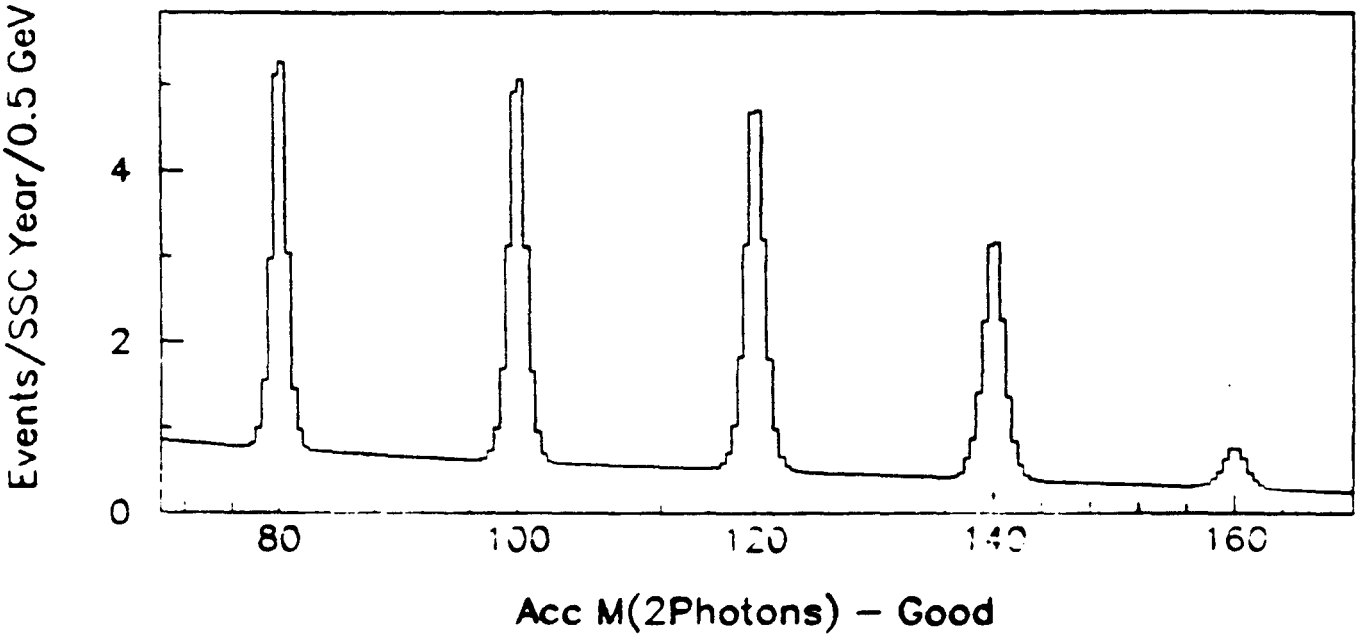
Events/SSC Year/0.5 GeV
0
2
4
80
100
120
140
160
Acc M(2Photons) – Good

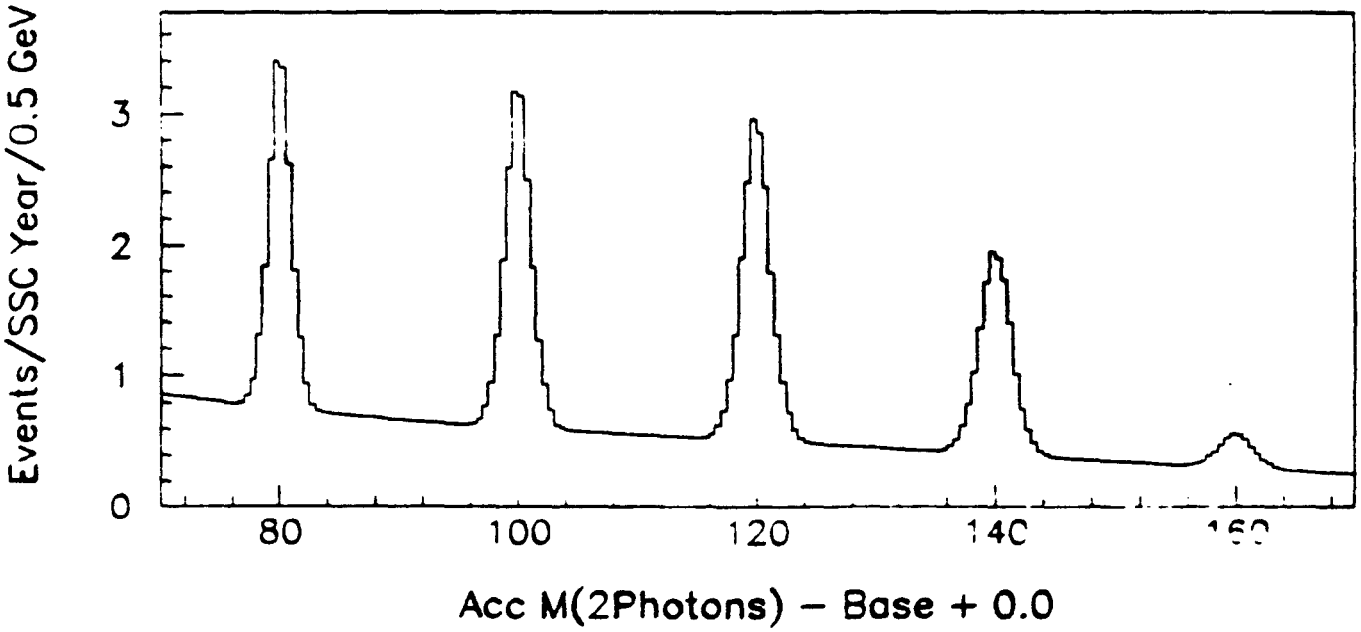
Events/SSC Year/0.5 GeV
0
1
2
3
80
100
120
140
160
Acc M(2Photons) – Base + 0.0

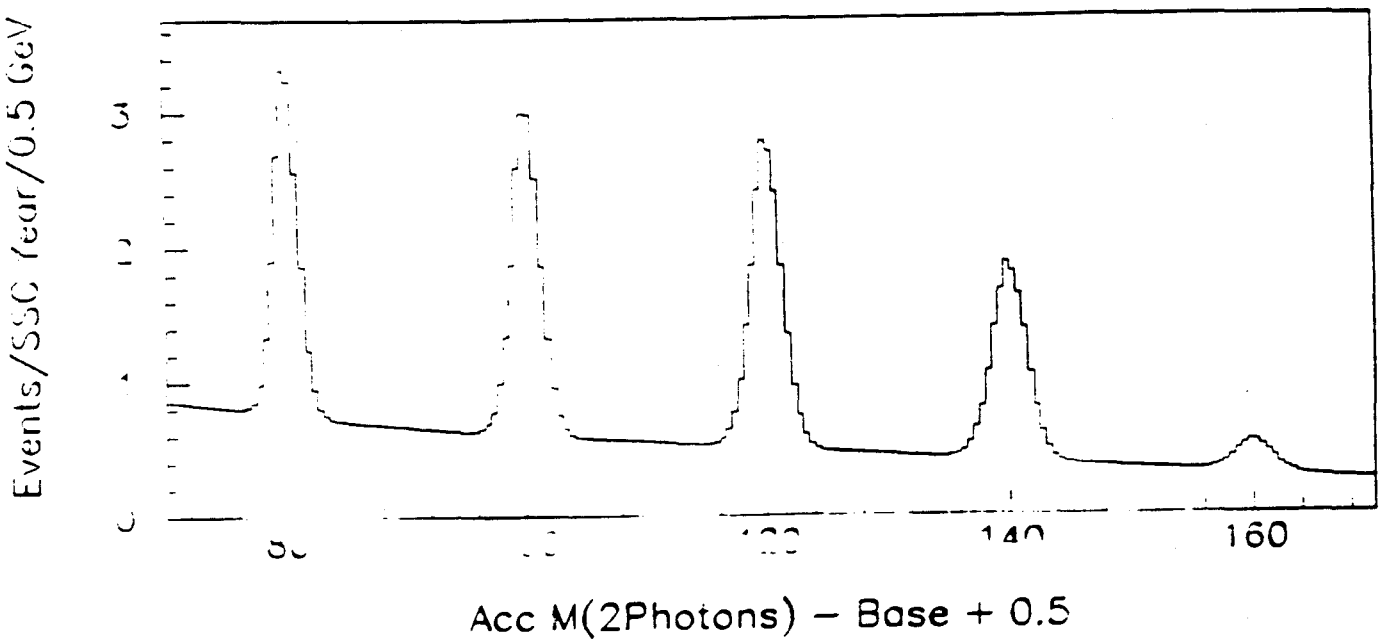
Events/SSC Year/0.5 GeV
140
160
Acc M(2Photons) − Base + 0.5

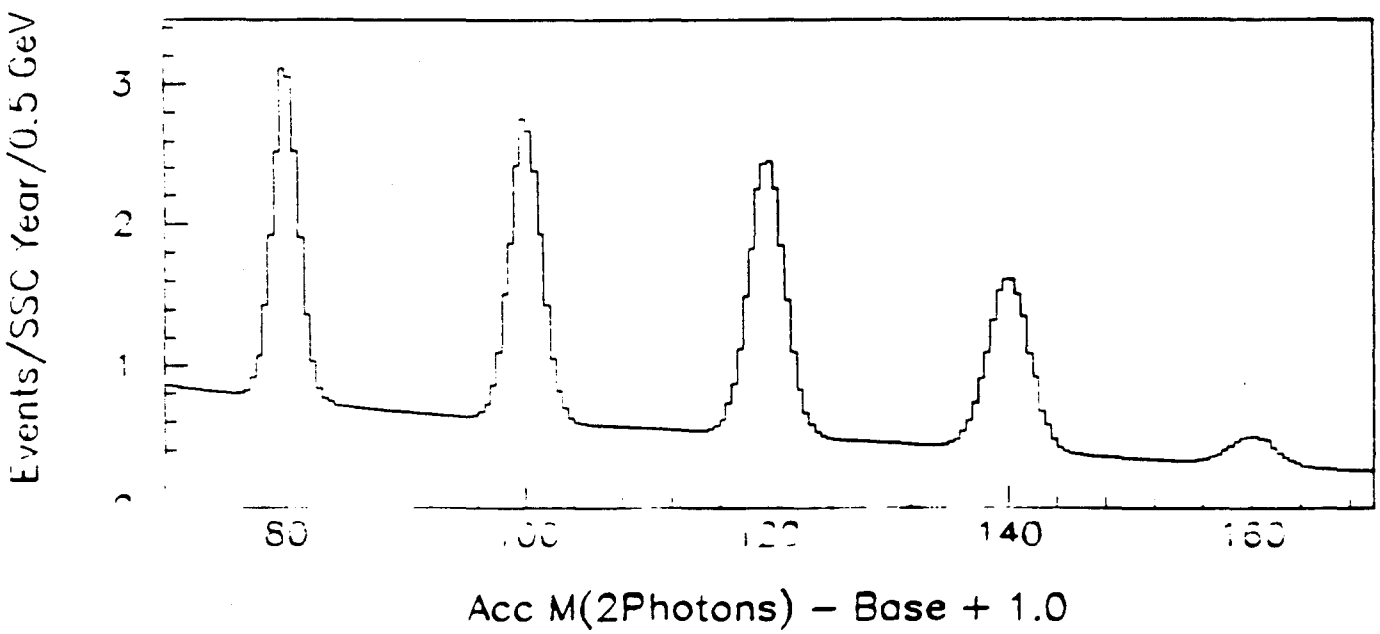
Events/SSC Year/0.5 GeV
3
2
80
140
Acc M(2Photons) − Base + 1.0

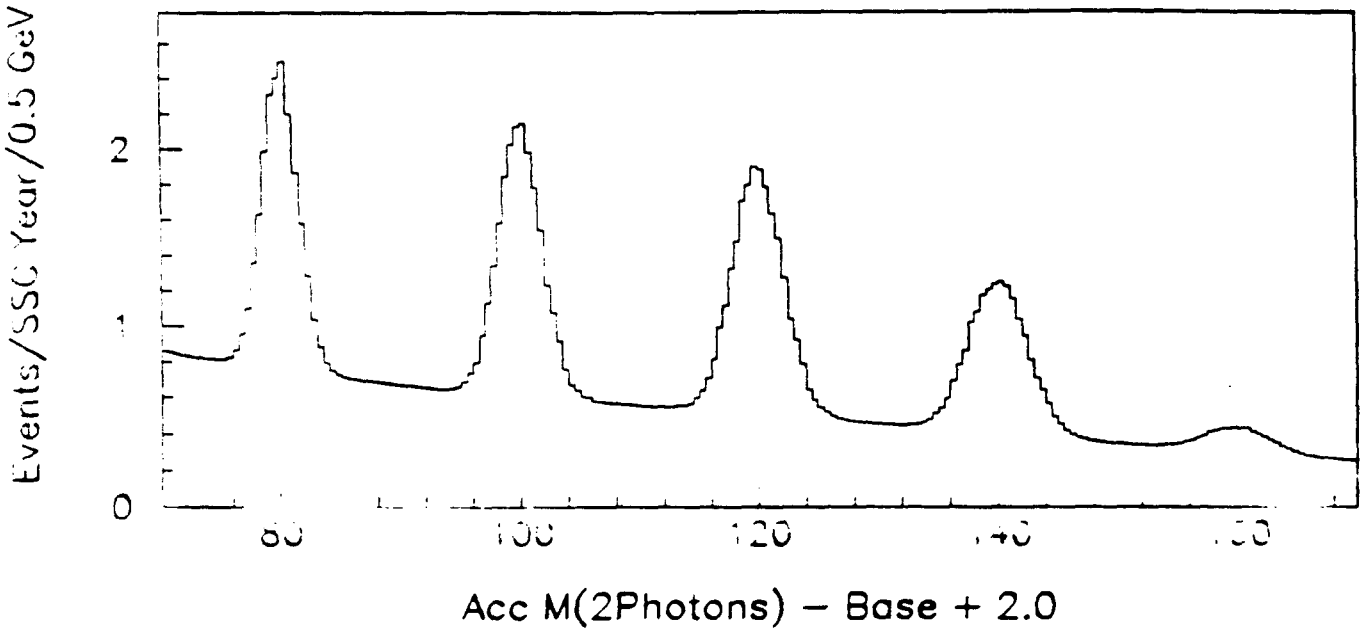
Events/SSC Year/0.5 GeV
2
1
0
80
100
120
140
160
Acc M(2Photons) – Base + 2.0

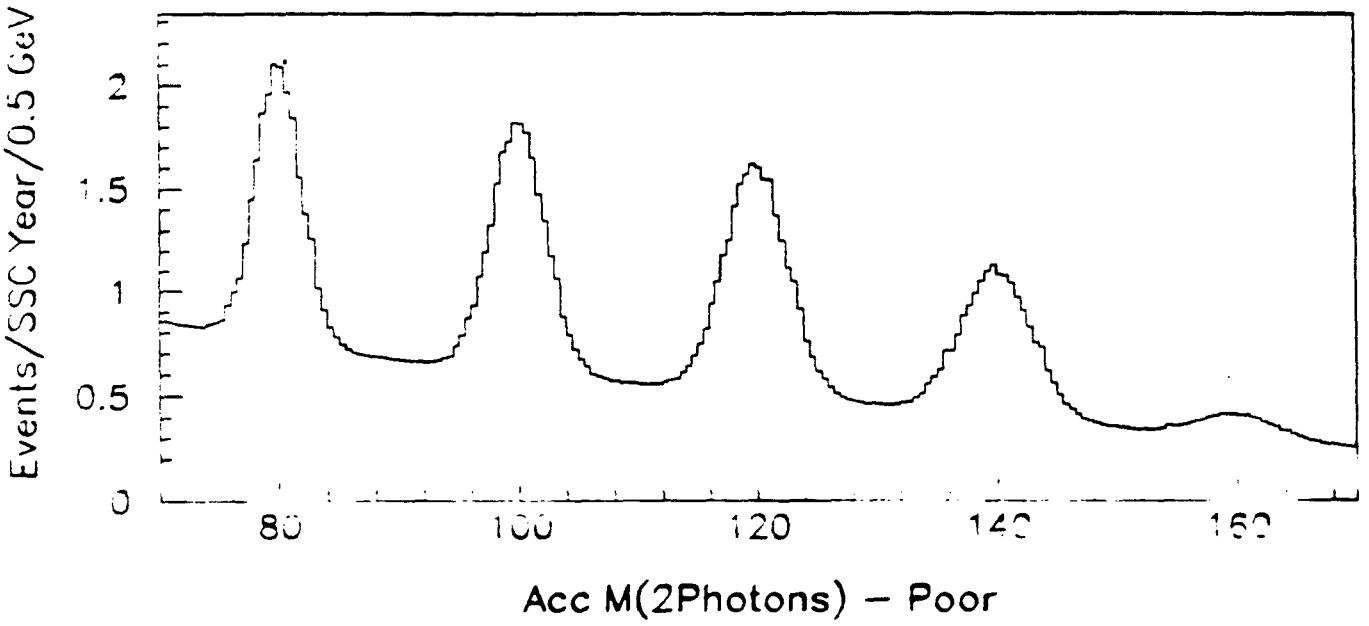
Events/SSC Year/0.5 GeV
2
1.5
1
0.5
0
80
100
120
140
160
Acc M(2Photons) – Poor

Naive significance of signal :

$d = S/\sqrt{B}$

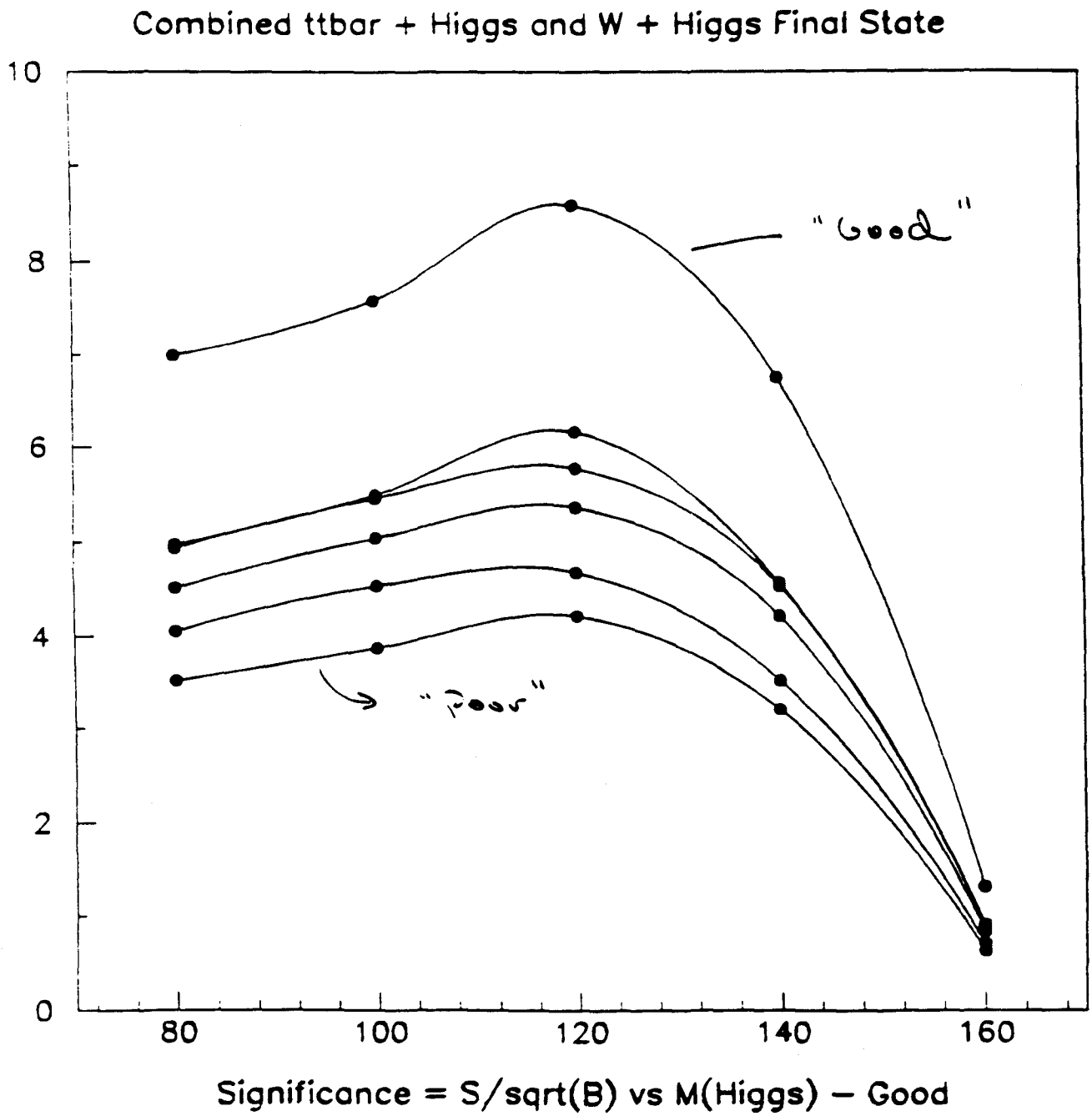

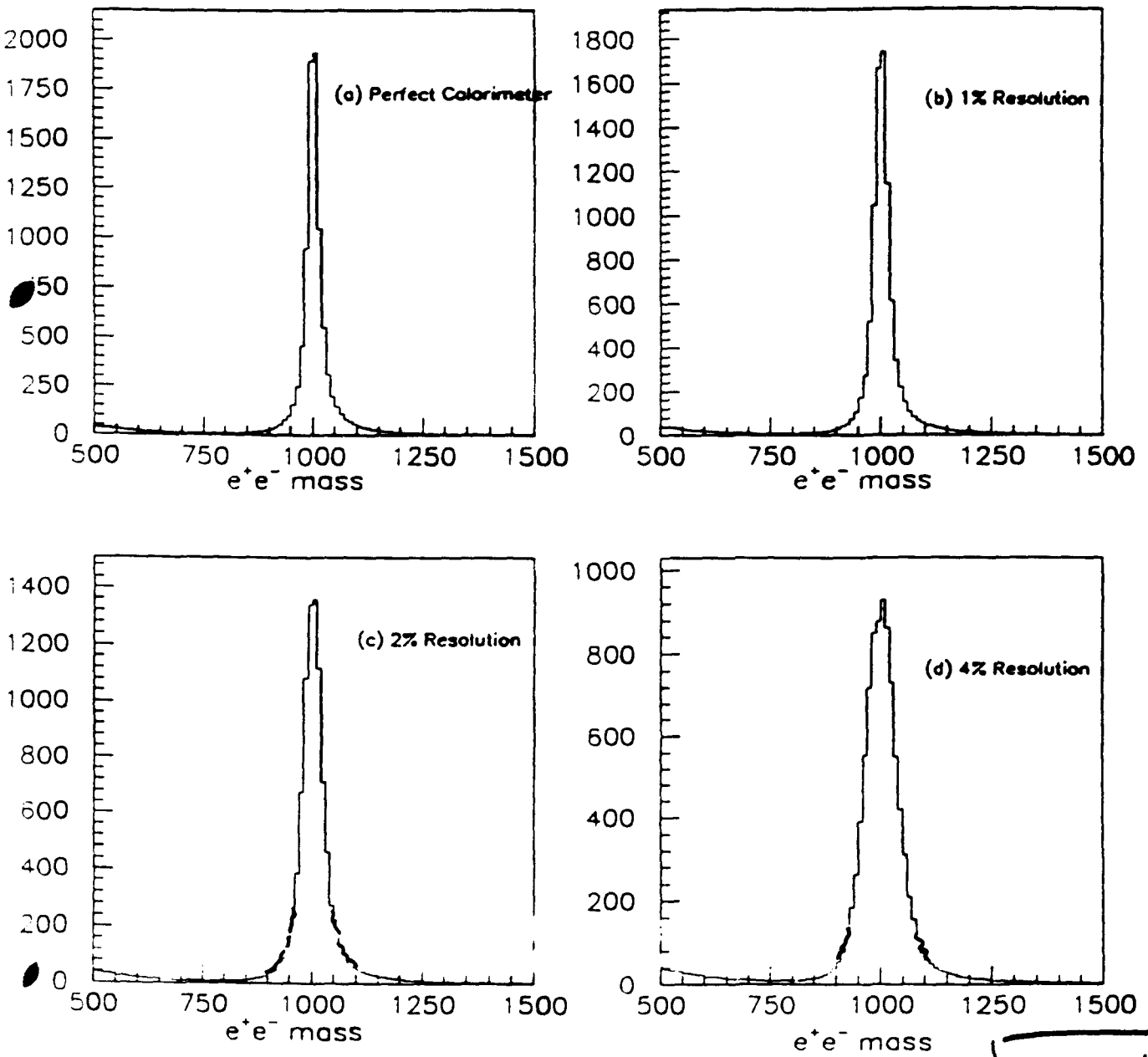

Hinchliffe
SDC 91-85

Measure $\Gamma(Z')$

Standard Model Z'

$m = 1$ TeV

<u>Claim</u> : $\lesssim 2\%$ constant term OK

missing statistical analysis of

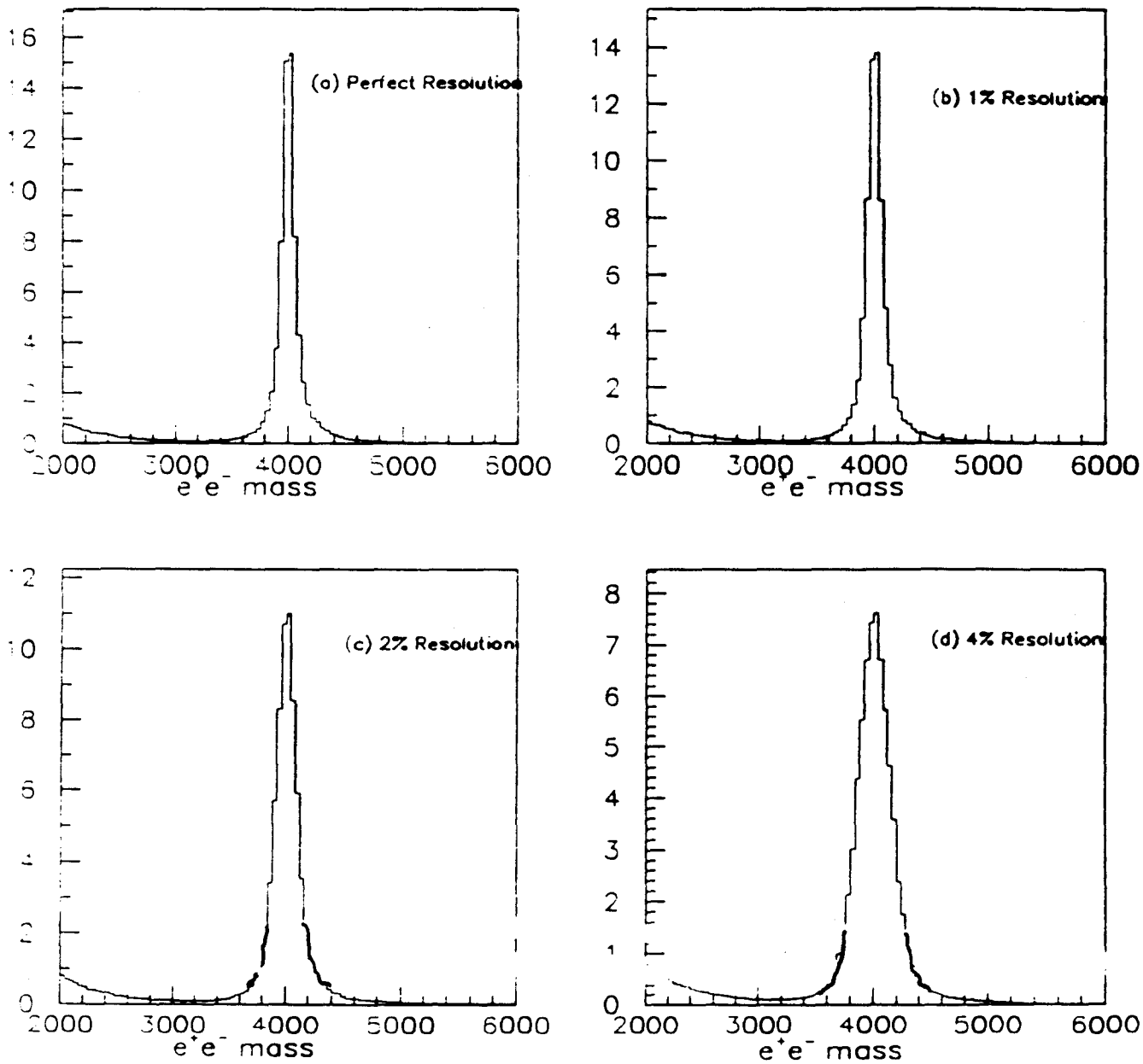

Standard Model Z'

4 TeV

constant $\lesssim 2\%$ still "ok"

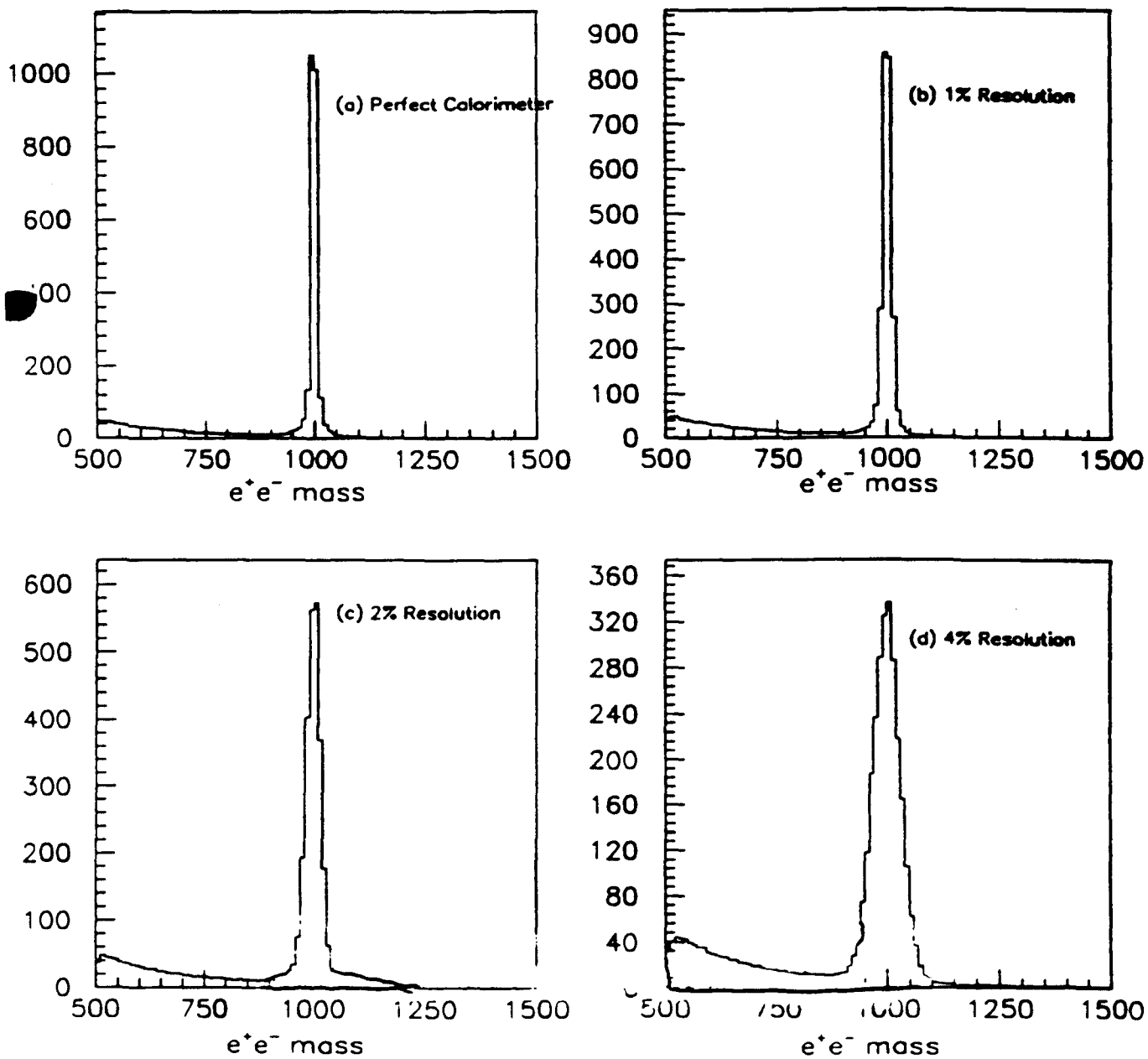

$E(6)$ Z_η $m = 1$ TeV

- narrower
- smaller cross section

$\Rightarrow$ 10% constant term preferred

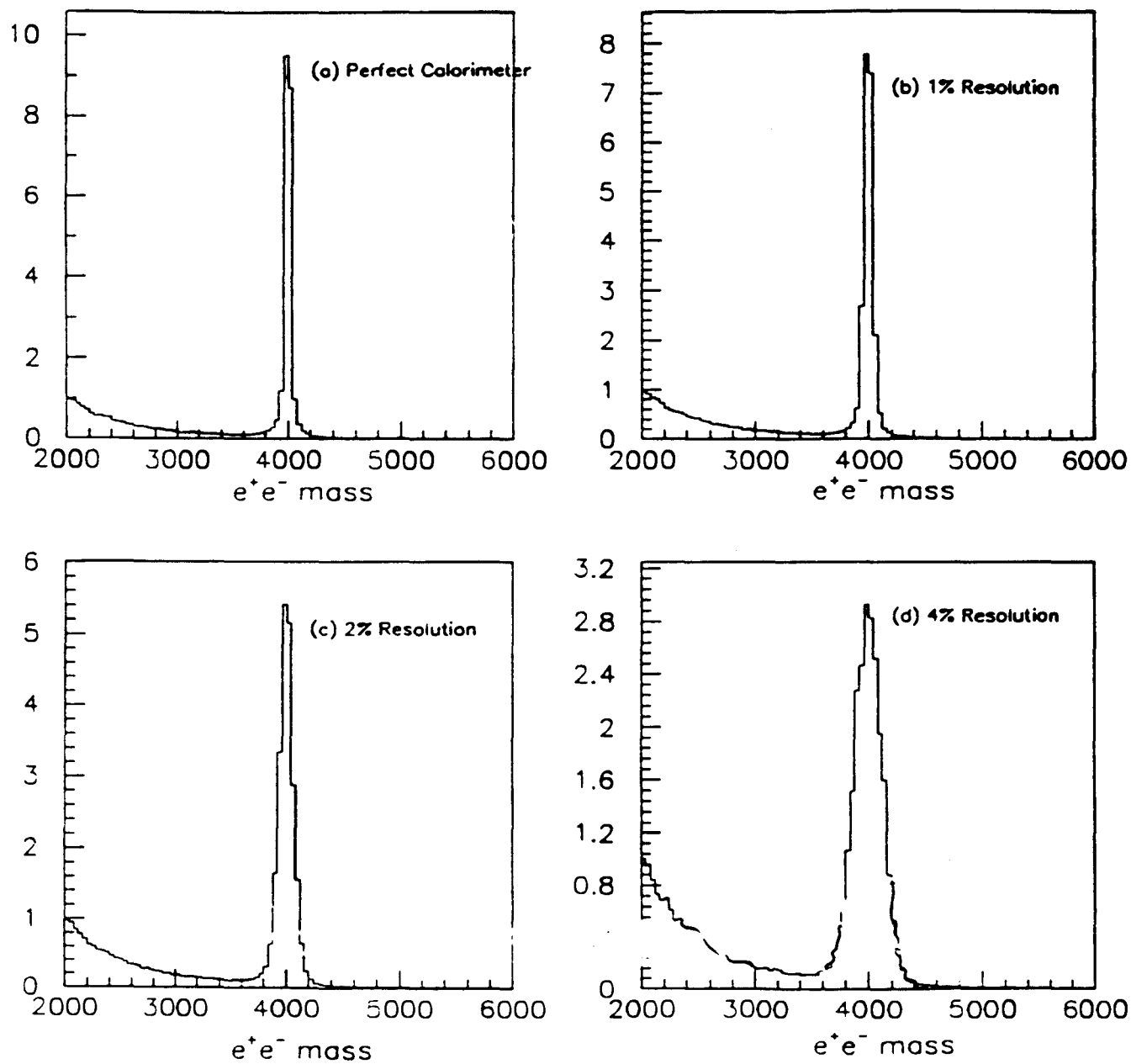

E(6) Z_χ m = 4 TeV

Conclusions :

- Hermeticity OK
- Linearity Massless Gap
- Depth + Long. Segmentation
  - → understand what you lose with deep EM and Fe HAD1
- EM resolution
  - → $\frac{.12}{\sqrt{E_T}}$ preferred over $\frac{.20}{\sqrt{E_T}}$
  - → constant term $\lesssim$ .5 - 1.0 %
- EM segmentation

  .05 × .05 important for E measurem

  | includes HAD1 ? |

<u>remark</u>:

I believe we want:

- massless gap / preshower
- 2 EM } .05 x .05 EM, HAD 1
- 2 HAD

+ 8 x 8 strip (strip ~ R_M) shower M

<u>Resist</u> the tendency to modify this ...

CALORIMETER REVIEW AND TECHNICAL BOARD MEETING
SEPTEMBER 12 -14, 1991
SSCL

Presentation by:

Dan Green

Fermilab

"HADRONIC" CALORIMETRY

ORG 9/94

Dan Green

Standard Model Components

$\begin{pmatrix} u \\ d \end{pmatrix}$ $\begin{pmatrix} c \\ s \end{pmatrix}$ $\begin{pmatrix} t \\ b \end{pmatrix}$ → JETS

$\begin{pmatrix} e \\ \nu \end{pmatrix}$ $\begin{pmatrix} \mu \\ \nu \end{pmatrix}$ $\begin{pmatrix} \tau \\ \nu \end{pmatrix}$

γ, g, W+, Z^0, H

↳ JET

1

μ → M.I.P. IN HAC2 (REDUNDANCY!)

τ → τ + ν LOW MULT JET

ν → $\not{E}_T$ IN HAC + EM

e → HAC/EM

Detector Subsystem Contributions

	STANDARD MODEL COMPONENT					
SYSTEM	u,d,s, g = Jet	c,τ, b g= Jet vertex, lepton tag	ν	γ	e	μ
Track	✓-	✓			✓	✓
CAL	✓	✓	✓	✓	✓	✓-
Mu		✓				✓

HAC IS INVOLVED IN ALL STANDARD MODEL COMPONENTS

Table 2.2
Requirements on the Measurement of the Magnitude of the Energy

Parameter	Particle Type	Requirement	Physics or Technical Basis	Ref. Section
Energy Resolution EM stochastic term	e,γ	15-25%/ √ E_t	low mass Z'→ee width ttH→γγ	3
EM constant term	e,γ	< 1-2%	high mass Z' width	3
HAD stochastic term	π	50-75% /√E_t	Jet resolution	4
HAD constant term	π	<4%	Jet resolution	4
Time stability of response	e,π	<1% after correction	Small EM constant term	3
e/h response	π	<1.3	Jet resolution	4
EM linearity	e	<4%, >10 GeV uncorrected <1% after correction	Good linearity - correct via massless gap	3
HAD linearity	π	<2%	Compositeness	4
Non-gaussian tails EM HAD	 e π	<5% loss*	e acceptance missing E_t tails?	 3 4
Spatial uniformity EM HAD	 e π	<5% loss*	e acceptance	3
Dynamic range EM HAD	 e π	 20 Mev-2 TeV 50 MeV-5 TeV	 4 TeV Z' 10 TeV jets	 3 4

*total electron acceptance >.9 inside η max for all losses.

JETS AND HADRONIC RESOLUTION

(LOI STUDY)

$\frac{dM_Z}{M_Z}$

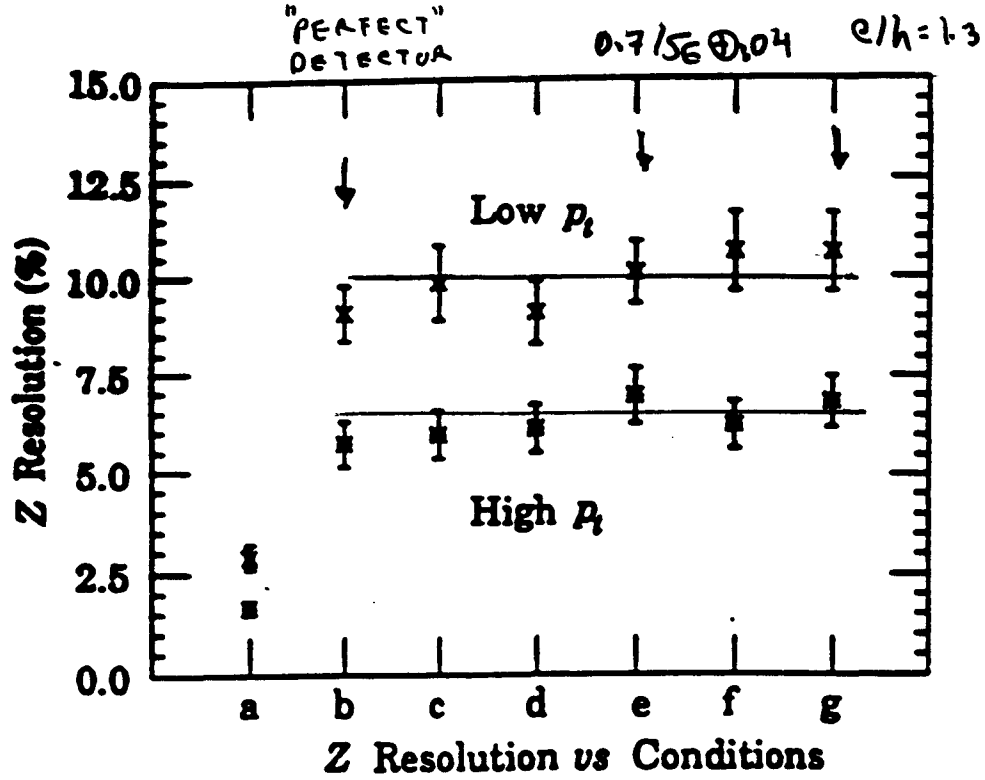

UNDERLYING EVENT + FRAGMENTATION CONE FLUCTUATIONS

FIG. 33. Summary of mass resolution calculations for reconstructed Z's for the two p_t ranges described in the text. The first two points show the effect of detector-independent contributions to the resolution. The following points show the effect of variations in detector performance. The values plotted represent the sigma from the fits described in the text. The error bars correspond to the statistical error on the sigma. See the text for explanations of each entry.

$< 0.75/\sqrt{E} \oplus 0.04$

(a) The original quark direction is used as the center of a clustering cone of radius 0.7, within which the energy from all detectable tracks in the generated event is combined as a jet. Extra tracks from the underlying event are included. No simulation of showers is performed. This shows the contribution to the mass resolution of basic physics processes, including fluctuations in fragmentation energy outside the cone, effects of the underlying event, missing neutrinos, and gluon radiation.

(b) Our detector simulation distributes the shower energy with a realistic shape, but perfect energy resolution is assumed. Clustering is now done with seed towers as described above. This point represents a minimum resolution for a perfect detector with a reasonable tower geometry.

(c) Same as (b) with the addition of energy resolution in the calorimeter cells of $0.3/\sqrt{E} \otimes 0.02$ for individual hadrons and $0.15/\sqrt{E} \otimes 0.01$ for photons and electrons.

(d) Same as (c) with a hadronic calorimeter resolution of $0.5/\sqrt{E} \otimes 0.03$.

(e) Same as (c) with a hadronic calorimeter resolution of $0.7/\sqrt{E} \otimes 0.04$

(f) Same as (d) with an electromagnetic calorimeter resolution of $0.25/\sqrt{E}$.

(g) Same as (d) with calorimeter noncompensation corresponding to $e/h = 1.3$. The resulting overall constant term of about 4% in the hadronic energy resolution is in addition to the 3% constant term introduced in (d) for each hadron. The nonlinear response of the hadron calorimeter due to imperfect compensation is simulated using an ansatz of Groom (4.2).

JJ MASS RESOLUTION

- CALOR $.5/\sqrt{E} \oplus .03$
- FRAG
- V

[DIFFICULTIES IN DEFINING A JET MAKE CALORIMETER REQUIREMENTS LESS SEVERE]

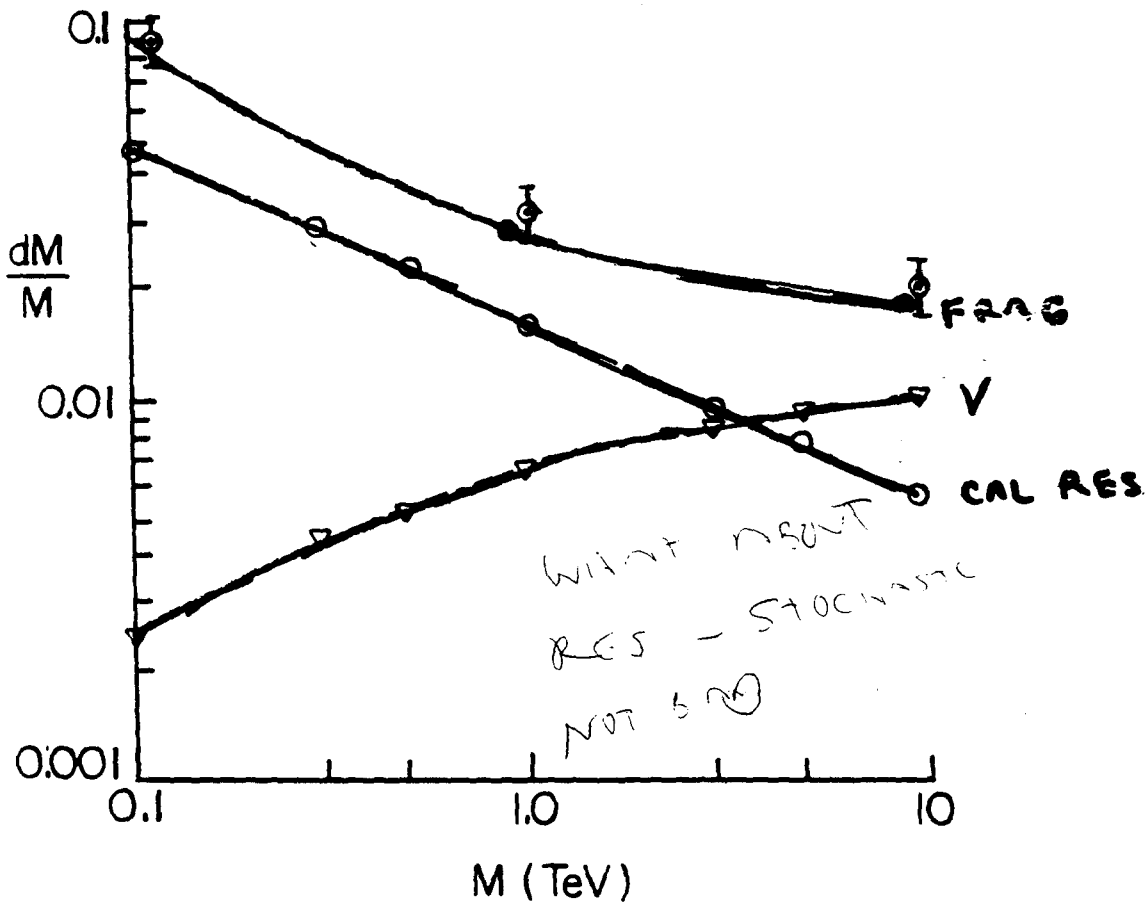

$$\left(\frac{dM}{M}\right)_V \sim \frac{2}{\sqrt{2}}\left(\frac{\alpha_s}{\pi}\right)\ln\left[\frac{2M_Q}{p}\right] 2B$$

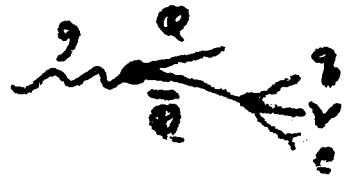

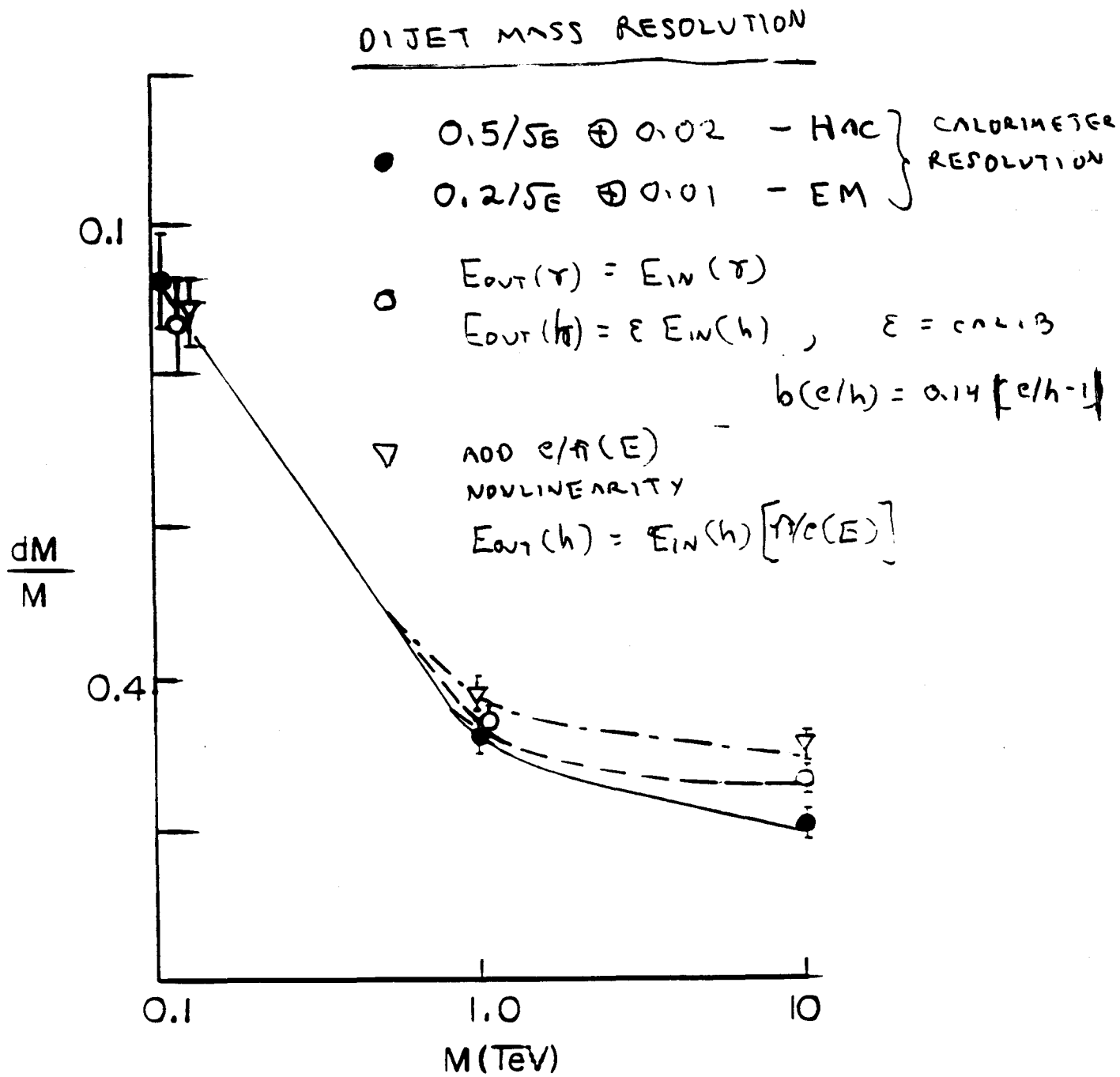

Figure 2.18 Dijet mass resolution as a function of mass. The points are for the "default" SDC calorimeter, . ,a calibrated calorimeter with e/h = 1.3, o , and a calorimeter with e/h = 1.3 which is only calibrated at asymptotic energies, V.

10 TeV DIJETS

→ e/h ?

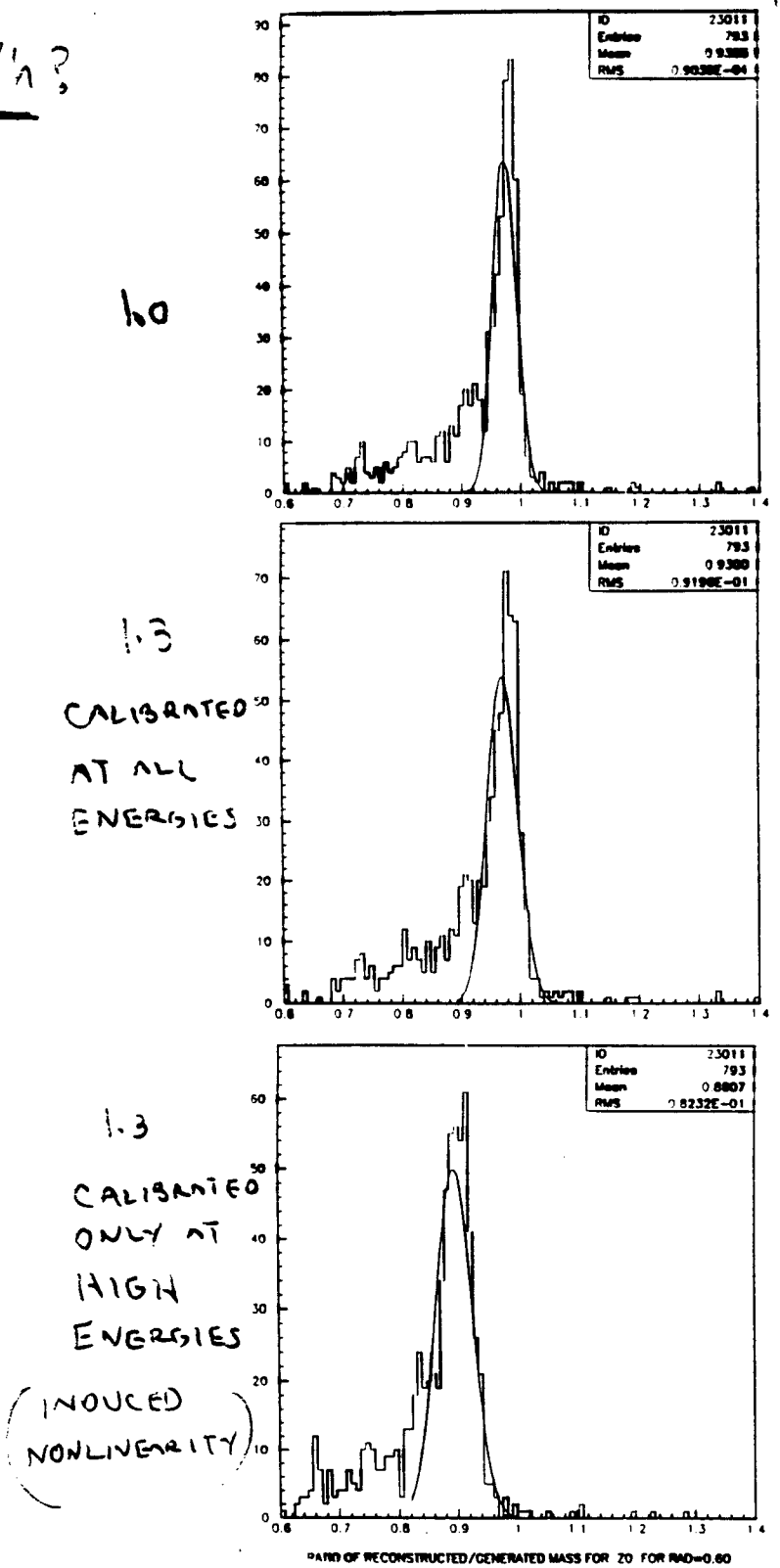

Figure 2.19 10 TeV dijet resolution, dM/M for a) e/h = 1, b)e/h = 1.3 calibrated at all energies, c) e/h calibrated only at asyptotic energies.

Table 2.3
Requirements on the Position Measurement and Particle ID

Parameter	Particle Type	Requirement	Physics or Technical Basis	Ref. Section
EM transverse segmentation	e,γ	.05 x .05	e isolation	3
Transverse seg. HAD 1 HAD 2	 e π	 .05 x .05 .1 X .1	 e isolation angular res.	 3 4
EM depth	e,γ,π	22 X_0	adequate containment to 100 GeV	3
HAD Depth	π	10±1 λ	good high energy jet measurement	4
EM longitudinal segmentation	e,γ	Two compartments + massless gap	needed to correct radiation damage	3
HAD longitudinal segmentation	π	Two compartments	needed for leakage correction	4
SM position res r-φ direction strip length ΔΦ η direction strip length Δη	e,γ	 40 cm 3 mm	good track shower match	 3
Trigger transverse granularity				
Cross Talk	e,π			

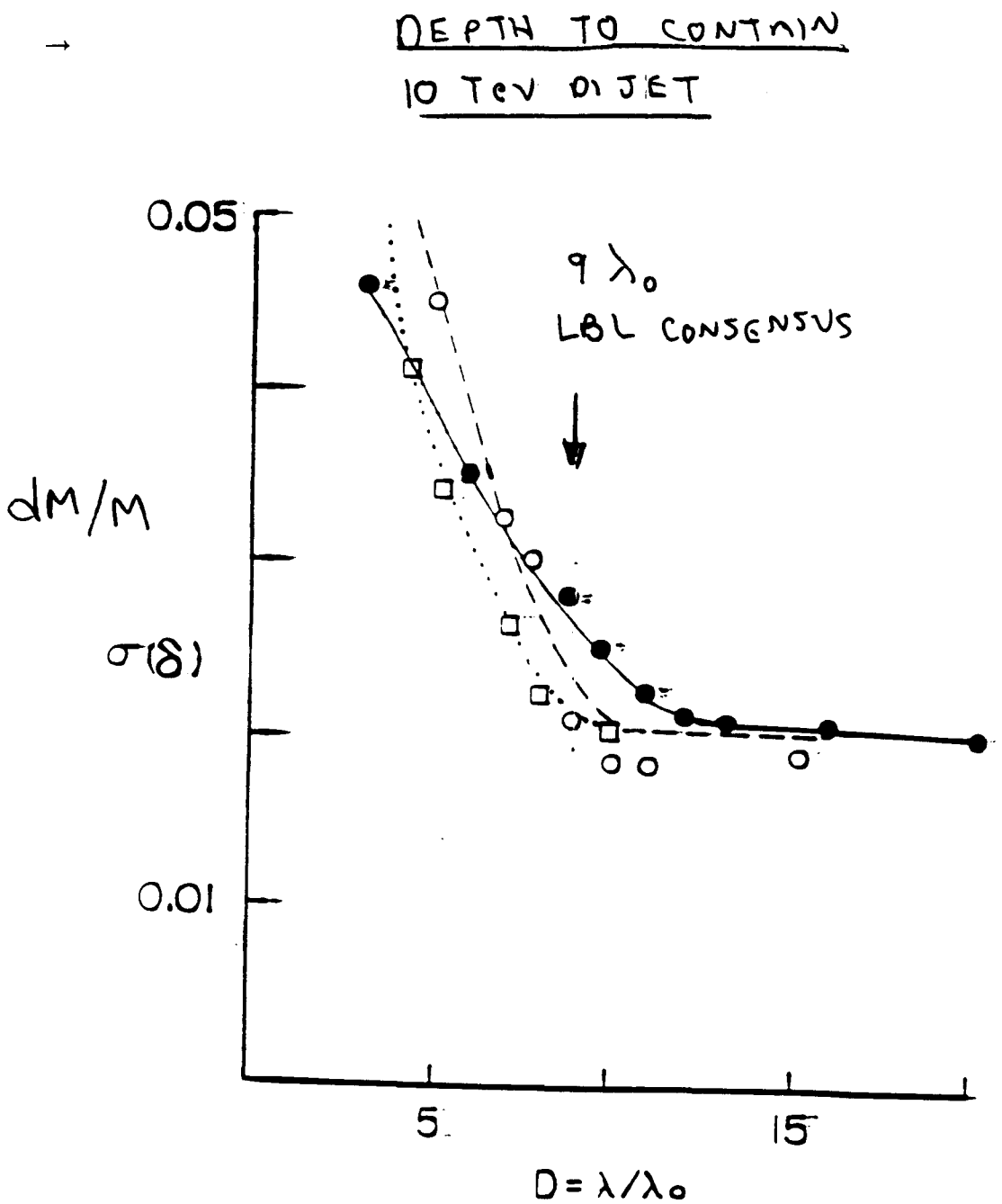

Figure 2.1 dM/M, fraction dijet mass resolution for the highest accessible mass (10 TeV), as a function of depth (D) in interaction lengths. The points correspond to different parameterizations of data, CCFR data solid, WA3 data open, Lab E data boxes.

WEIGHTING OF OUTER LAYERS (L. JONES)

450 GEV LABE DATA

D = 10.1

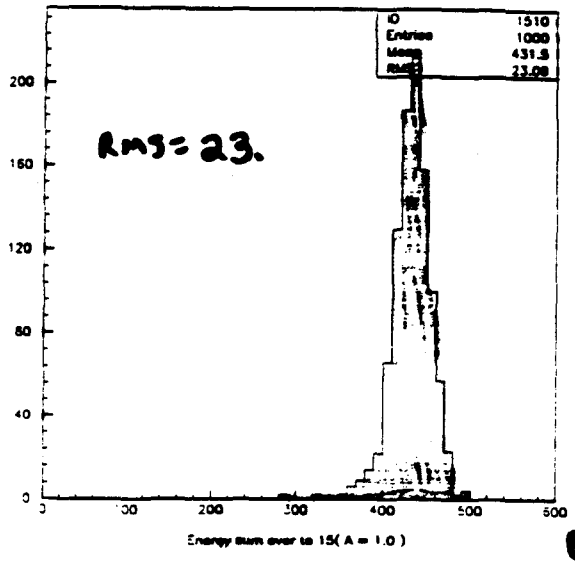

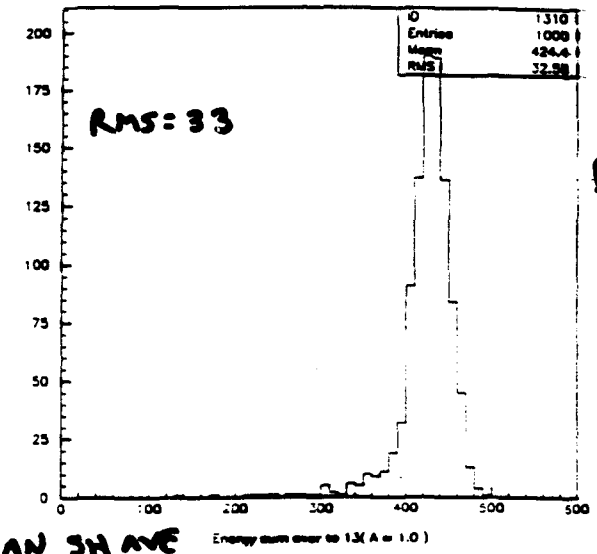

D = 8.7

CAN SHAVE OFF ~ 1λ ?

D = 10.1

WT = 3.0

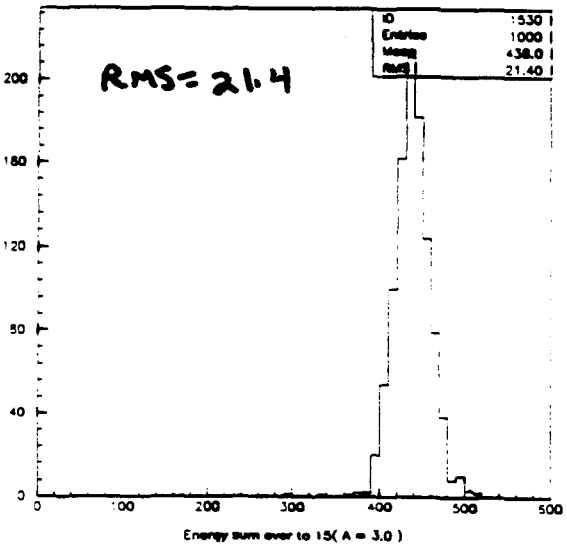

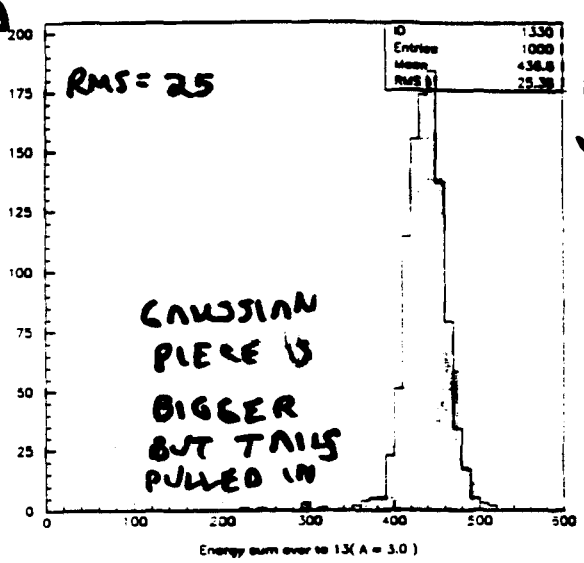

D = 8.7

WT = 3.0

E

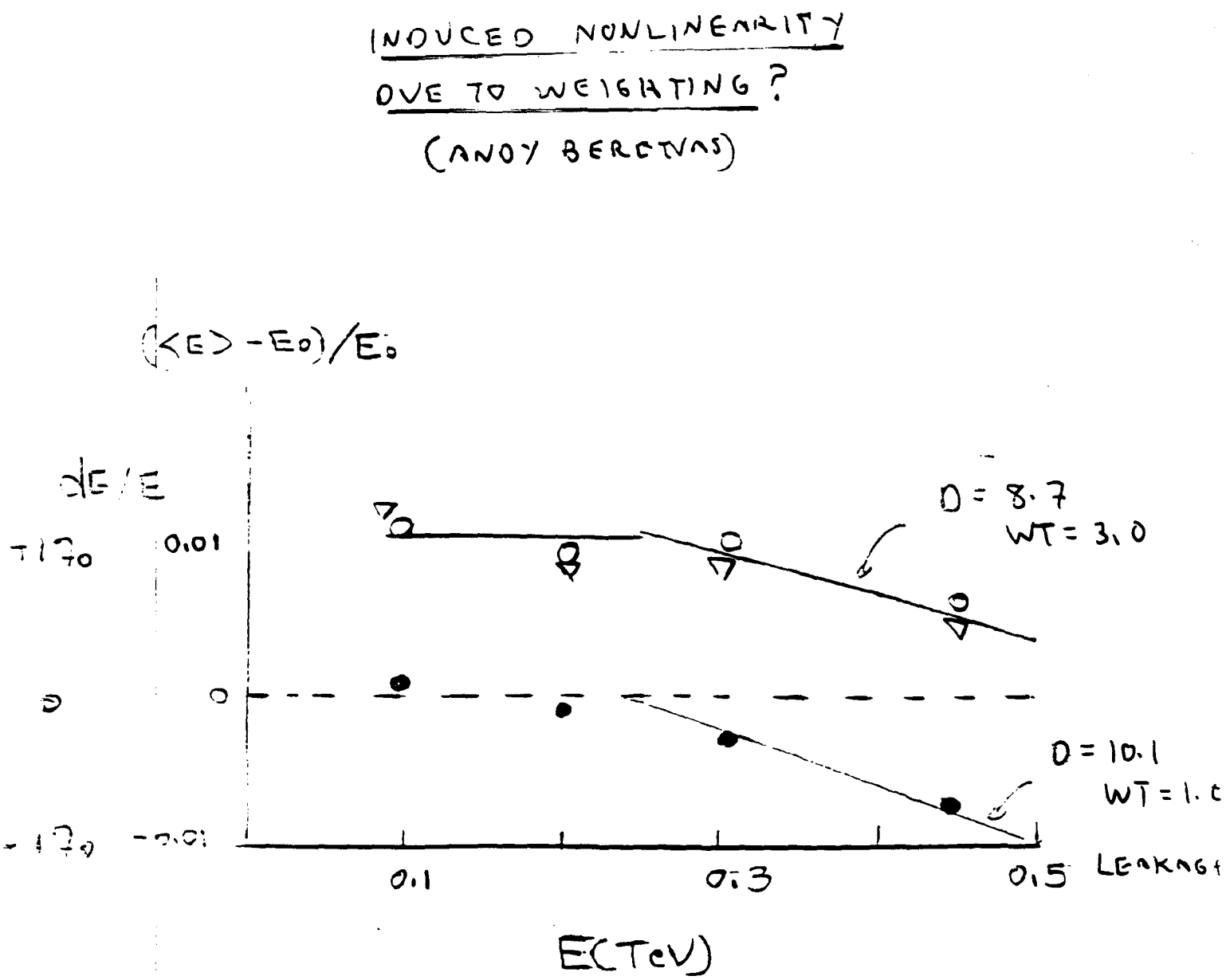

Figure 2.4 Fractional energy nonlinearity as a function of energy unweighted (solid) and weighted.

WORK ON ENGINEERING SPEC
FOR SAMPLING CALORIMETER
(GENERIC) THICKNESS
VARIATIONS

h

LABE DATA, 100, 200, 450

NO INDUCED NON-LINEARITY

h DATA

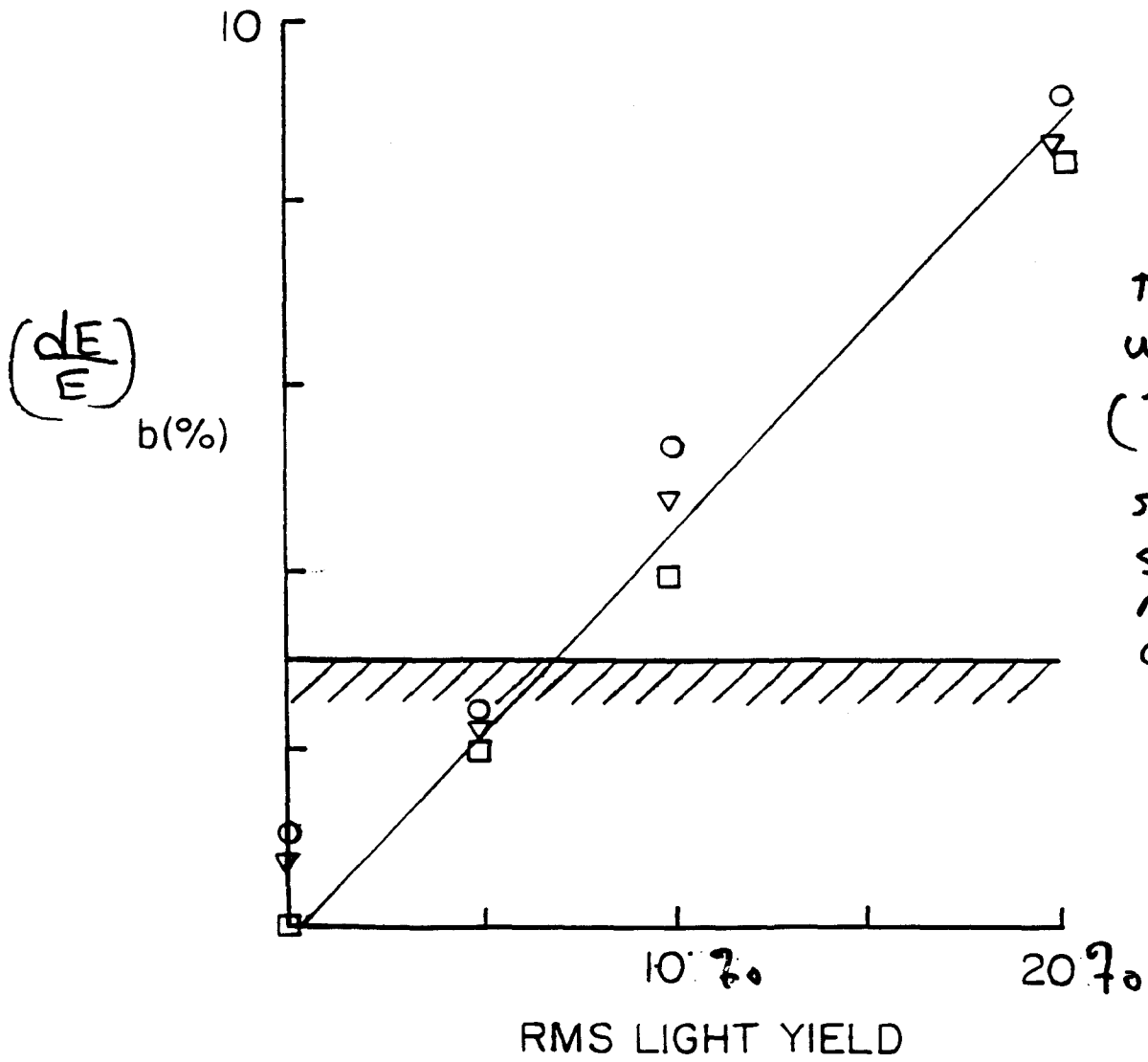

THIS IS UNCALIBRATED (TOWER BY TOWER) SO 4% IS SAFE FOR A "GLOBAL" CALIBRATION

[INDIVIDUAL TOWER CALIBRATION ALLOWS YOU TO MEASURE THE PLATE THICKNESS @ $D \simeq 1$ TOWER BY TOWER ⇒ REDUCED SPEC]

LONGITUDINAL SEGMENTATION AND $\not{E}_T$

450 GeV, D = 10.1

LAB E DATA

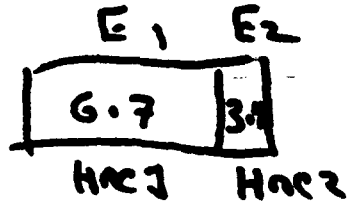

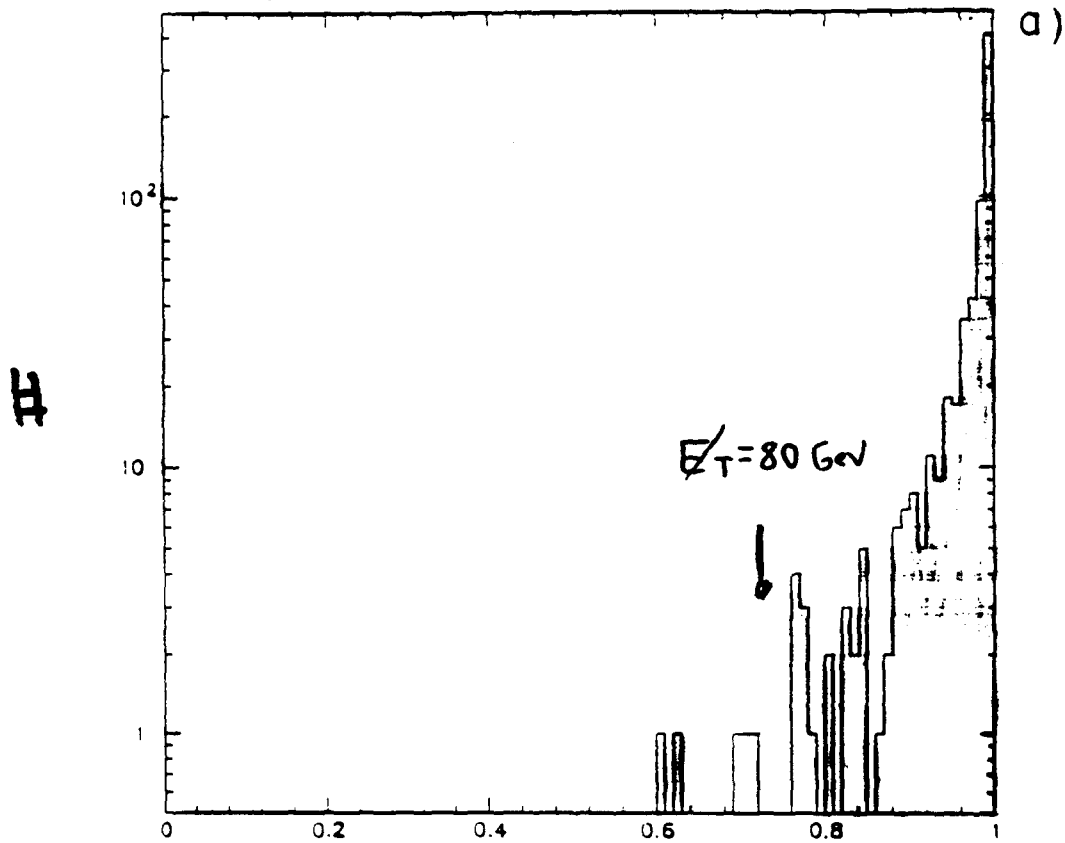

450 GeV JET BECOMES 80 GeV $\not{E}_T$ WITH PROBABILITY ~ 0.005

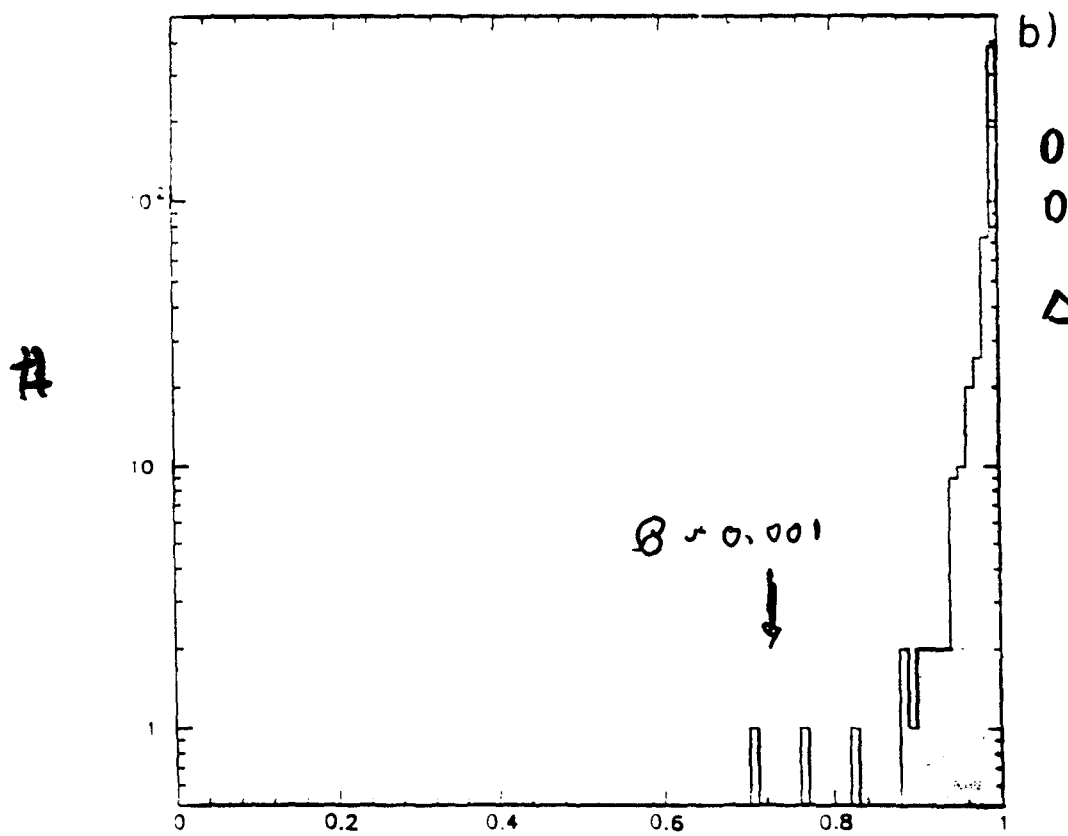

D1 = 6.7

D2 = 3.4

$$\Delta = \frac{E(D2)}{E(D1)+E(D2)} < 0.18$$

CONTAINED ENERGY FRACTION = $f = E(D)/E$

LEAKAGE FLUCTUATIONS - UNWEIGHTED

Δ CUT, TRADE LEAKAGE VS ε

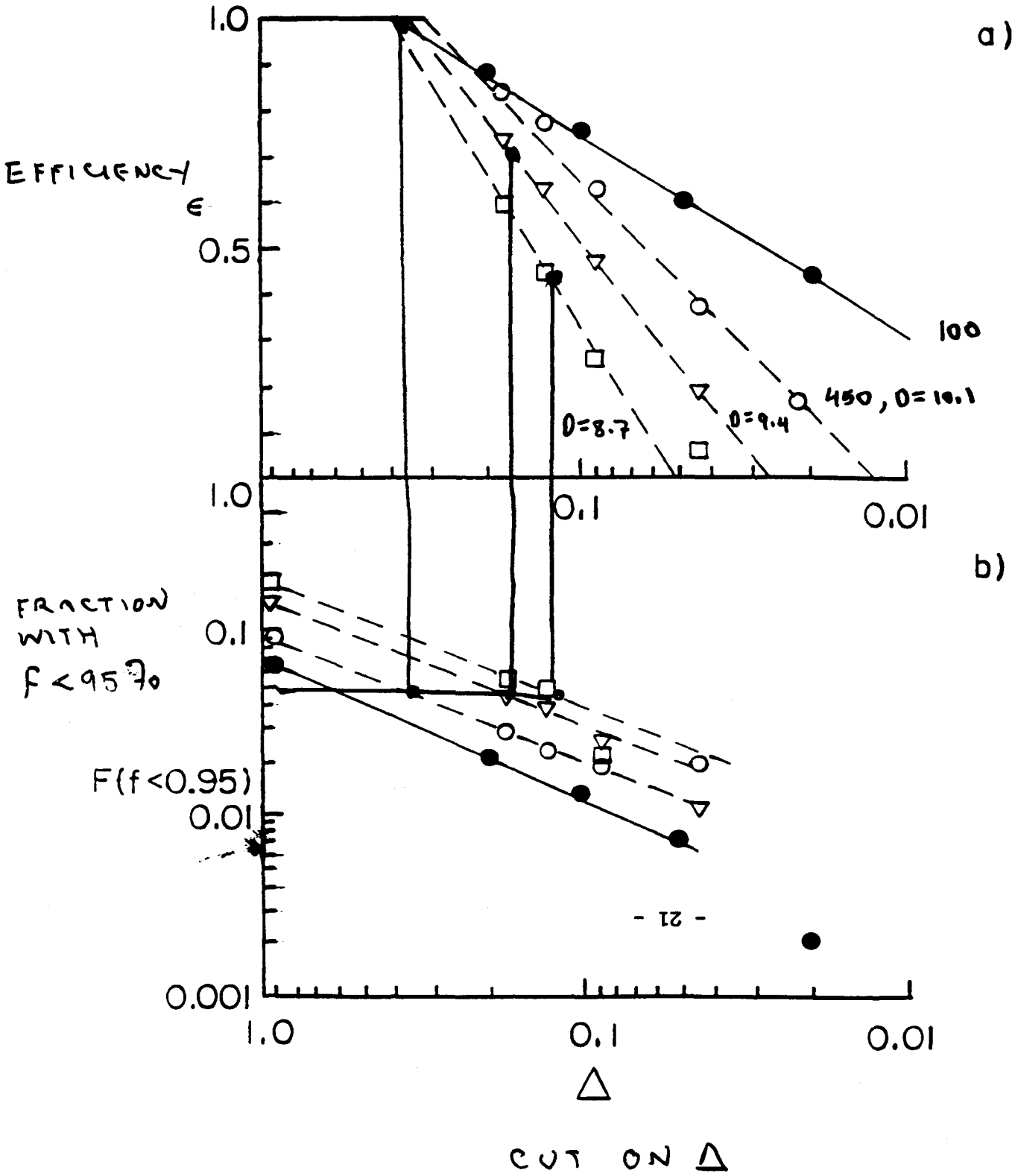

TRANSVERSE SEGMENTATION

THE NATURAL EM SCALE ⊥ IS R_M
REALIZED IN 5M STRIP WIDTH

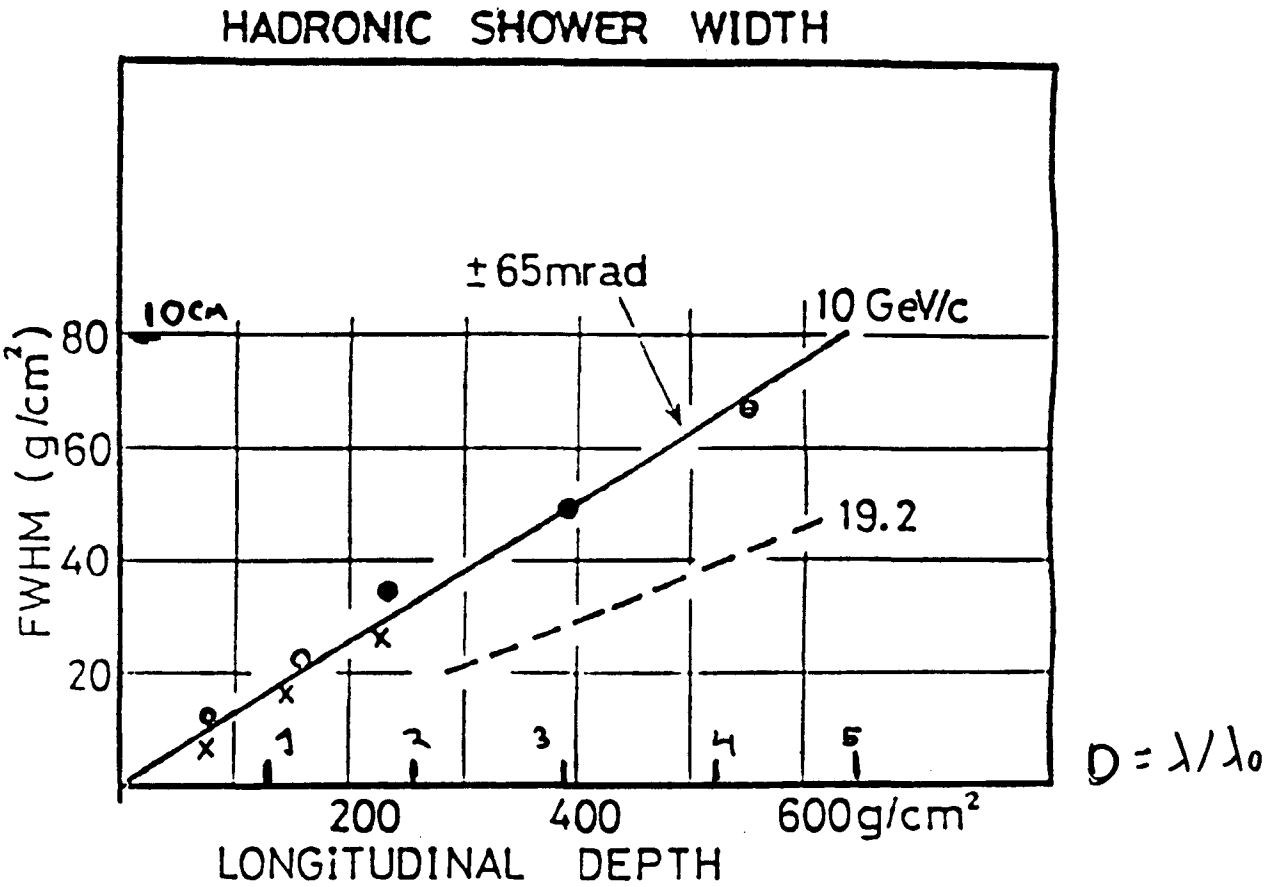

$D = \lambda/\lambda_0$

THE NATURAL HADRON ⊥ SCALE IS λ_0
WHICH CAN BE REALIZED IN
THE HADRON CALORIMETER

μ IN HAC2 WILL BE "SMALL" FOR
ANY SEGMENTATION

HADRON SEGMENTATION

THERE IS A "CORE" WITH A LONG TAIL.

TRIGGERING, ETC. ⇒ PUT $\gtrsim$ 80% OF HADRON ENERGY INTO A TOWER

TRANSVERSE PROJECTED ENERGY DISTRIBUTION

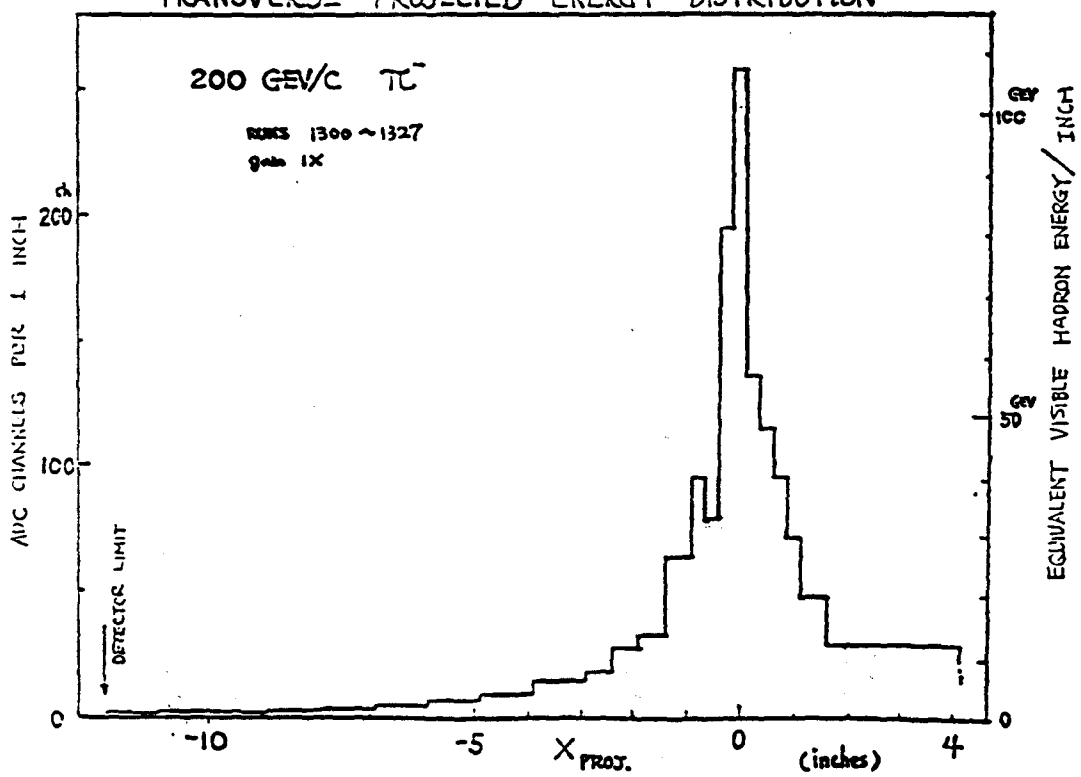

$\Delta X \lesssim 13$ CM

$\Delta \eta \lesssim 0.065$, $90°$ 2 m RADIUS

RECALL ↑ ⇒ NARROW (1 HADRON) "JETS" IN CALORIMETER

LOW MULT JETS

g VS q JETS

W → JJ VS QCD JETS

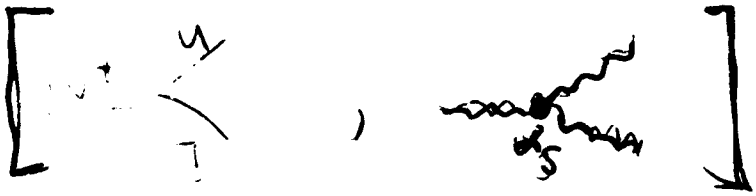

(J. HAUPTMAN)

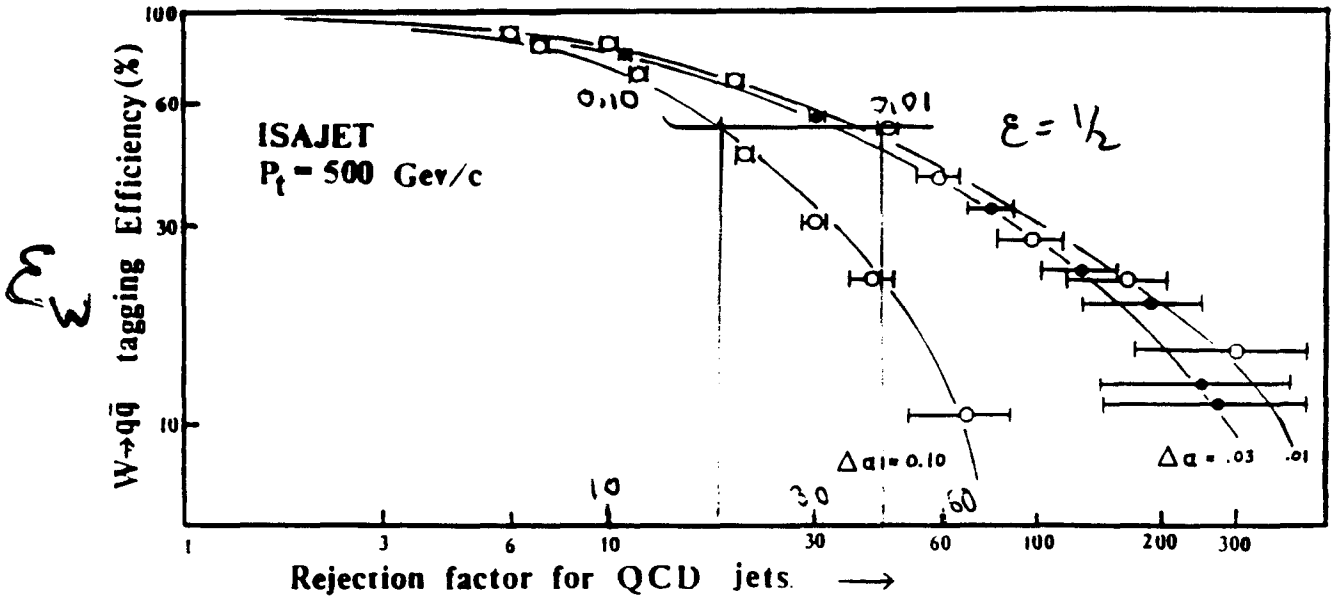

QCD REJECT

Fig. 5: Efficiency for tagging $W \to q\bar{q}$ vs rejection factor N_W/N_{jet} from the recursive binary partition analysis. $\Delta\alpha$ is the calorimeter segmentation $\Delta\eta = \Delta\phi$.

TRANSVERSE SEGMENTATION?

1) EM: USE PS/SM FOR GOOD e, γ POSITION RESOLUTION

a) HADRON:

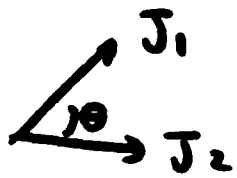

a)

$$\frac{dM}{M} = \frac{\sin\theta \, d\theta}{2(1-\cos\theta)}$$

$$\boxed{\frac{dM}{M} = P_{JJ} \, d\theta_{JJ} / 2M_{JJ}} \sim \frac{\beta_{JJ}}{\sqrt{2}} d\theta_J$$

b) E.G. IF $\Delta\theta \sim 0.05$

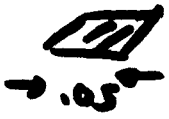

$$d\theta \sim d\eta/\sqrt{12}$$

$$\frac{dM}{M} \sim 0.7\%$$

$$\sim d\theta/2$$

c) FRAGMENTATION:

$$d\theta_J \sim |k_T| / P(1-z_0)$$

FOR Z, $P_J \sim 50$, $k_T \sim 1$ GeV

$$d\theta_J \sim 2\%$$

DOMINATES FOR LOW MASS

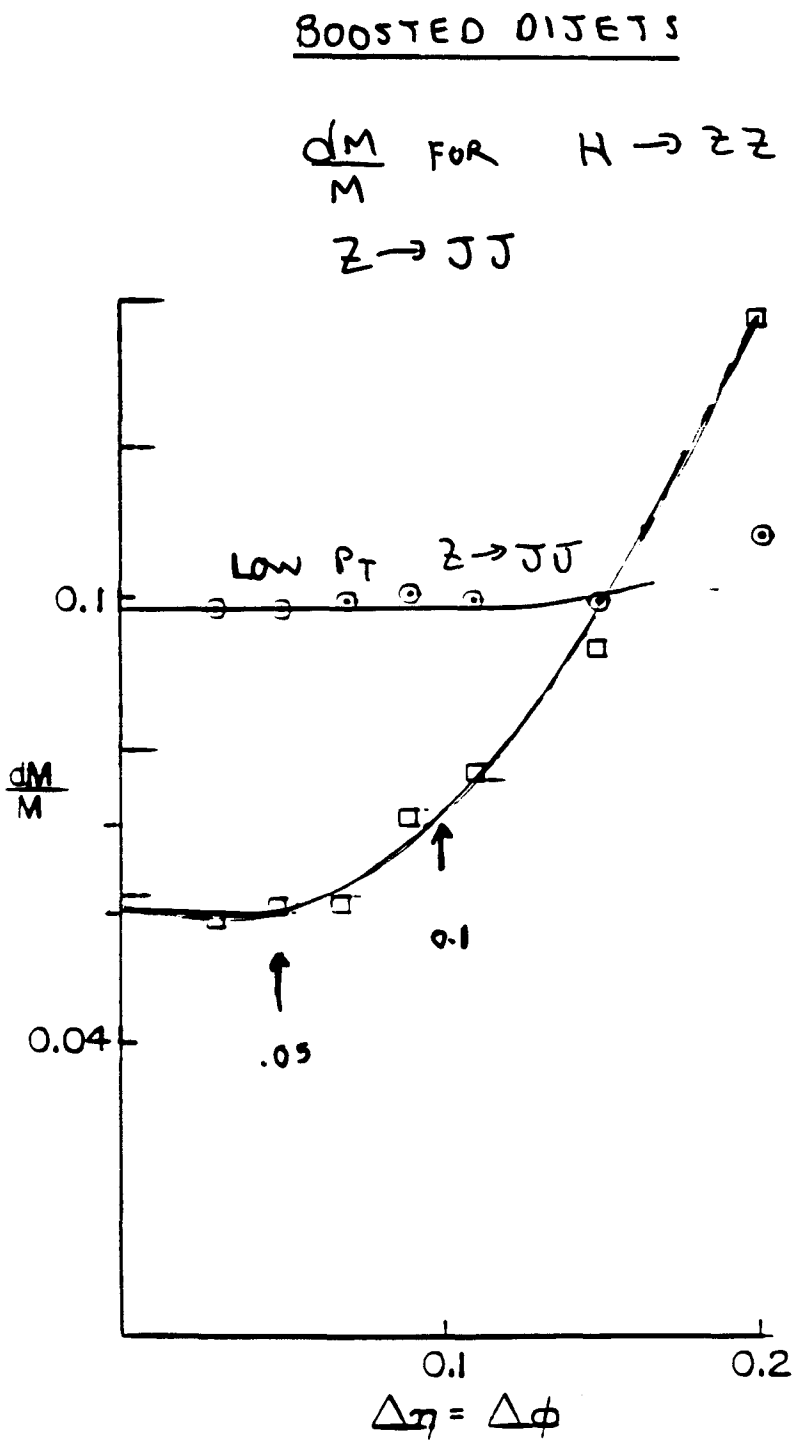

Figure 2.5 Fractional mass resolution for Z → jj for low P_T Z's, . , and boosted Z with P_T = 0.55 TeV similar to those from a 1.1 TeV Higgs, o ,as a function of tower transverse segmentation.

e ISOLATION: $t \to b W$, $\hookrightarrow e \nu$ (B. WICKLUND)

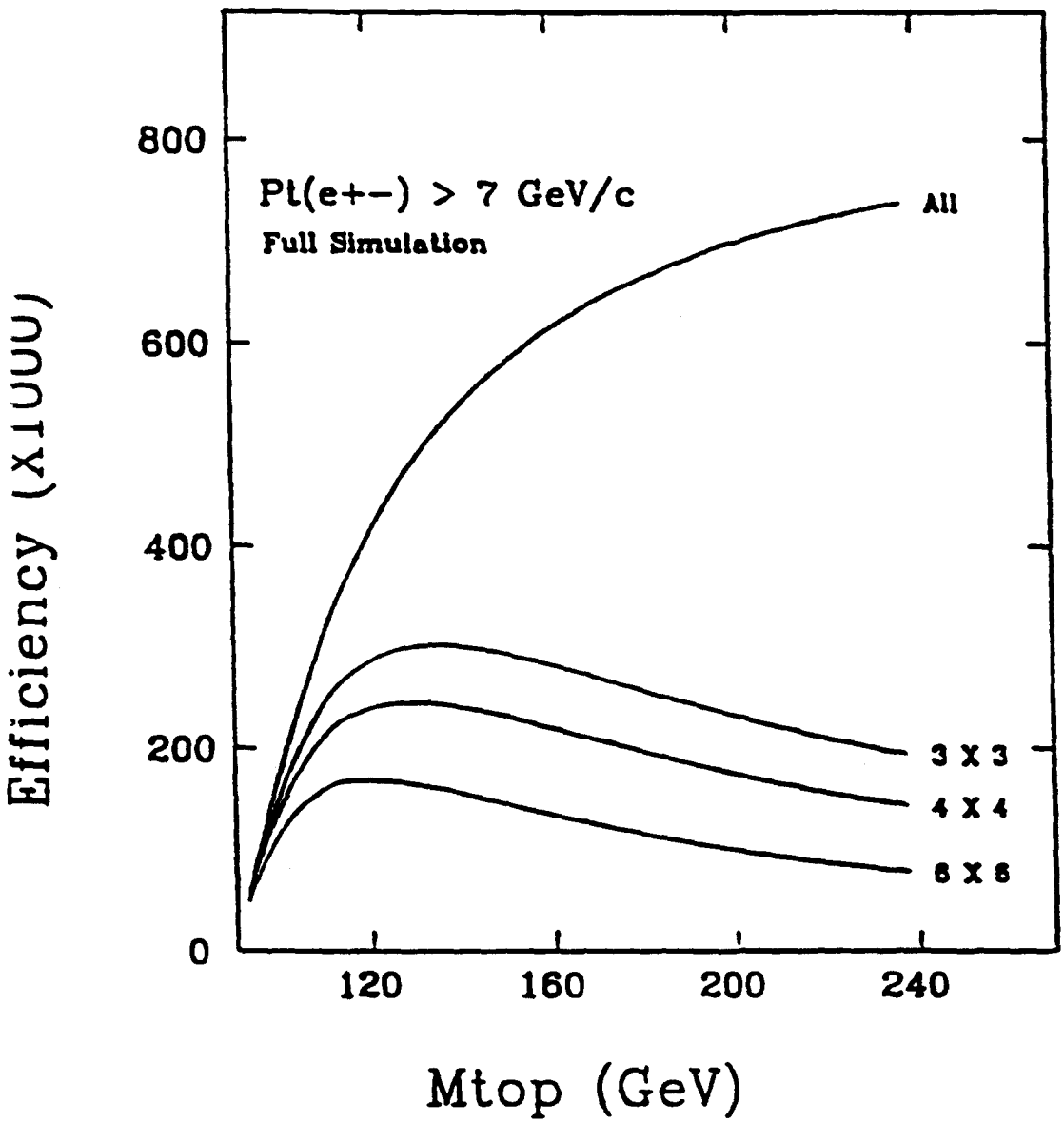

e EFFICIENCY FOR ISOLATION EM/HAD CUTS FOR DIFFERENT HAD SEGMENTATION

(.05) (0.1) ROUGHLY

HOW CLOSE CAN YOU GET TO THE "C" JET AND STILL HAVE AN ISOLATED ELECTRON

KEEP THE FREEDOM TO ADJUST $\Delta\eta$ $\Delta\phi$ UNTIL ONE HAS A GOOD CRISP CONCLUSION

Table 2.4
Requirements on the Time Measurement

Parameter	Particle Type	Requirement	Physics or Technical Basis	Ref. Section
Time res. EM HAD	 e,γ π	 σ ~ 5 nsec, E_t>15 σ ~ 5 nsec, E_t>100	 bucket tag	 3 4
Signal peaking time		<200 nsec	trigger pipeline length (?)	3,4
Baseline restoration time		100 nsec < τ<6 μsec @10^{34}	avoid electronics saturation	3
Noise		<5GeV, ΔR=.3	$H \rightarrow ZZ^*$	3
Pileup		<5GeV, ΔR=.3	$H \rightarrow ZZ^*$	3
h(t), transfer function of preamp + integrator		$\int^{\infty} h(t)\,dt = 0$	pedestal stability vs rate	3

Note: Pileup and noise combined in quadrature also <5GeV

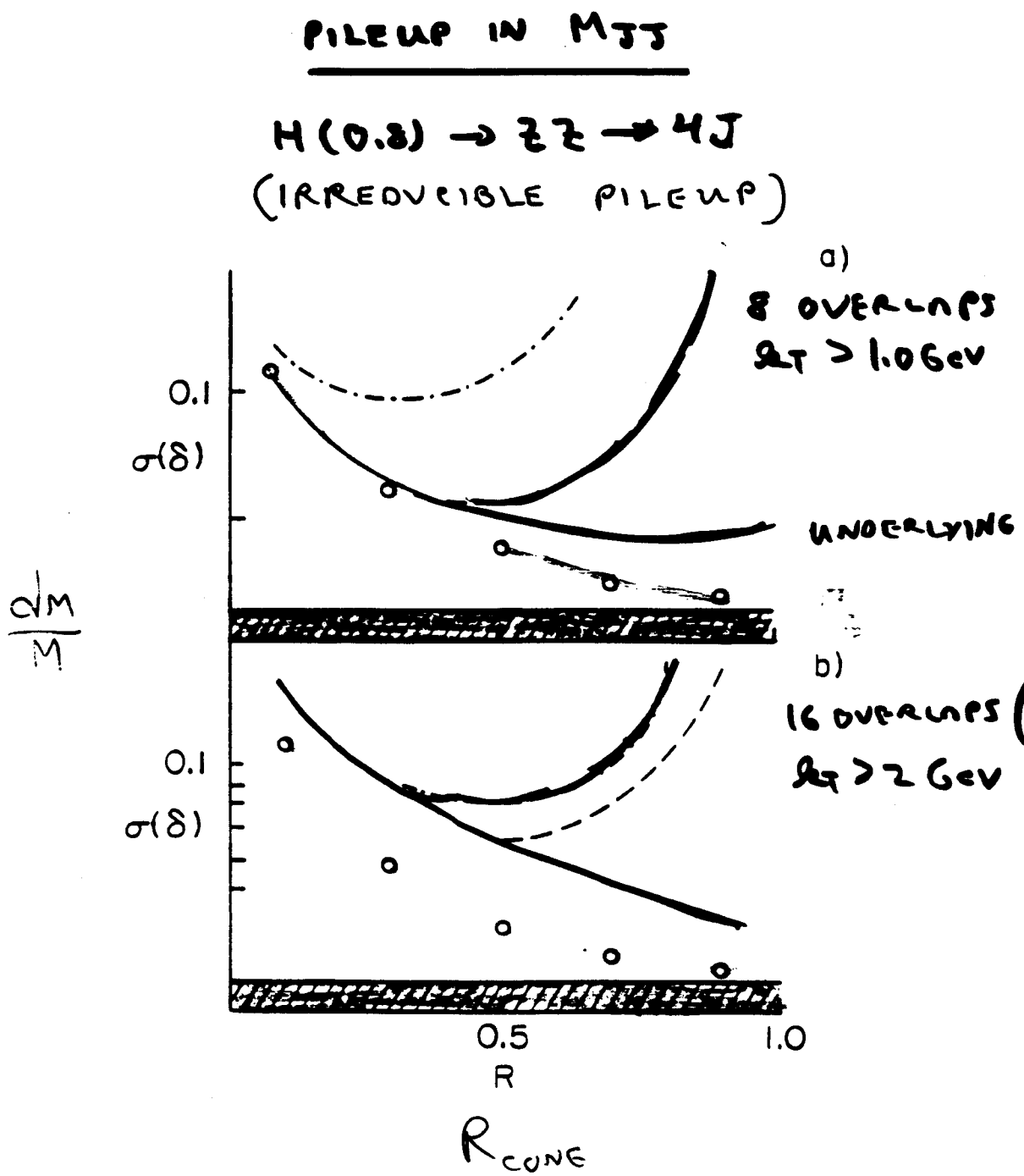

Fig. 9a. Plot of standard deviation of δ as a function of R for H(800) events keeping only tracks with kt > 1.0 GeV with no additional overlap events (solid), 8 overlap events (dashed), and 16 overlap events (dot-dashed). The results using only W fragments are shown as o symbols.

Fig. 9b. As in Fig. 9a except that only tracks with kt > 2.0 GeV are allowed.

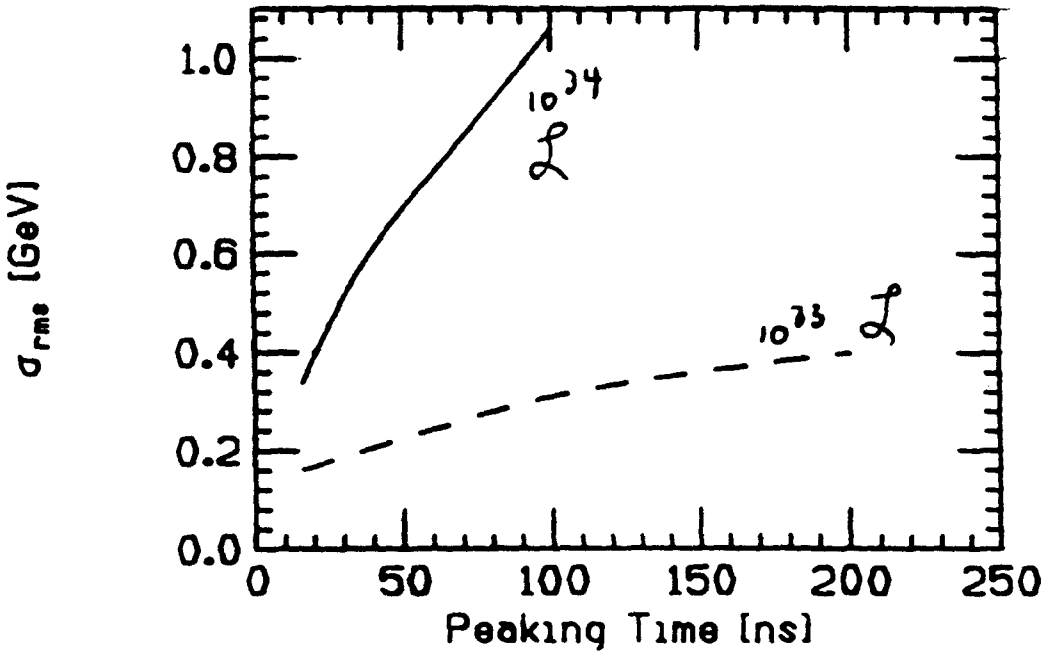

PILEUP AND ENERGY RESOLUTION

DOES PILEUP DEGRADE CALORIMETRY?

HAD: $E_T \sim 50$ GeV $\sim M_Z/2$ TO PICK A SCALE

$dE \sim 0.75\sqrt{E_T} \oplus .03\, E_T$

~ 5.5 GeV

EM: SAY $H \to \gamma\gamma$, $M_H/2 \sim (E_T)_\gamma \sim 50$ GeV

$dE \sim 0.12\sqrt{E_T} \oplus .005\, E_T$

~ 0.9 GeV

$\therefore$ HAD CALORIMETRY IS NOT DEGRADED BY PILEUP – IT IS THE OVERLAPS THAT HURT IN DEFINING THE ELEMENTS OF THE JET

DOES HADRON PILEUP AT HIGH $\mathcal{L}$ HURT e ID IN HAD/EM, ISOLATION?

SIMPLE MINDED ESTIMATE:

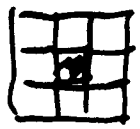

$dE \sim 0.9$ GeV FOR EM, $E_T \sim 50$ GeV IS EM RESOLUTION

$\Delta\eta \sim 0.2$
$\Delta\phi \sim 0.2$

$$d\langle E\rangle \sim \left(\frac{\rho}{2\pi}\right)\langle E_T\rangle \Delta\eta\,\Delta\phi\, N_I N_B$$

ρ = DENSITY OF MINBIAS PARTICLES

$\langle E_T\rangle$ = AVERAGE ENERGY/PARTICLE

N_I = # INTERACTIONS/BUNCH

N_B = # BUNCHES INTEGRATED OVER

$\therefore$ AT $\mathcal{L} = 10^{34}/(\mathrm{CM}^2\cdot\mathrm{SEC})$

$d\langle E\rangle_{EM} \sim 0.8$ GeV FOR 6 BUCKETS

$d\langle E\rangle_{HAD} \sim 2.0$ GeV FOR 6 BUCKETS

$d\langle E\rangle_{EM}$ IS $\sim$ ENERGY RESOLUTION AT 50 GeV

$d\langle E\rangle_{HAD} \Rightarrow$ HAD/EM $\sim 1/25$ DUE TO PILEUP

POTENTIAL ADVERSE EFFECTS?
QUANTIFY? BUCKET TAG,
LOSE ENERGY TIME ID?

SUMMARY

1) HAC IS USED IN ALL STANDARD MODEL MEASUREMENTS, TRIGGER, OR ID.

2) JETS ARE SOMEWHAT ILL DEFINED OBJECTS WHICH DO NOT PUT STRICT LIMITS ON HADRON RESOLUTION

3) LEAKAGE ($\not{E}_T$, V) AND M_{JJ} MEASUREMENTS SET THE SCALE FOR TOTAL HAC DEPTH, WEIGHTING, AND LONGITUDINAL WEIGHTING

4) TRANSVERSE SEGMENTATION IS RELEVANT
FOR μ, π ID
FOR SINGLE HADRON SIZE ($\perp$)
FOR q/g JET SEPARATION
FOR BOOSTED $Z \to JJ$ MASS RESOLUTION
AND FOR e ID

(THE ARGUMENTS ARE NOT DEFINITIVE)

5) PILEUP HAS ADVERSE EFFECTS ON $Z \to JJ$ RESOLUTION
(2X FOR 16 OVERLAPS)
IT DOES NOT DEGRADE HAC RESOLUTION BUT EM RESOLUTION AND e ID MAY BE EFFECTED.

CALORIMETER REVIEW AND TECHNICAL BOARD MEETING
SEPTEMBER 12 -14, 1991
SSCL

Presentation by:

Taka Kondo

KEK

Effects of field non-uniformity on tracking

The charge of the Task Force on Magnetic Field Uniformity is to assemble information relevant to compare tracking system performance in the two field configurations, relatively uniform field and non-uniform field. There have been many studies and related talks. This note is a brief summary of these studies[1-9]. Things to be considered are $\Delta p_t/p_t$, triggering, pattern recognition, other effects such as field measurement accuracy, ExB effects etc.

1. Magnetic field configurations

The field uniformity in the tracking volume is a strong function of the location of endcap return yokes. There are two calculations of magnetic fields [8,9]. Figs.1 and 2 picked up from one of these show the field contours of two baseline designs, liquid argon (LA) calorimeter and tile-fiber (TF) calorimeter with all-iron hadronic part. In addition we assume a case of uniform field that can possibly be realized by a re-entrant iron yoke. The field profile of TF with lead front hadronic calorimeter is very close to that of LA case.

2. Momentum resolution

Figs.3 and 4 indicate the effects of the field non-uniformity on $\frac{\delta(1/p_t)}{1/p_t}$ with and without vertex constraint [9]. The vertex constraint minimizes the effect of non-uniformity. The non-uniformity effect becomes noticeable only in the region of $\eta>2.0$ if the vertex constraint is not forced. However the resolution in the region of $\eta>2.0$ cannot be good without the vertex constraint anyhow. Therefore it is concluded that the non-uniformity effect is not significant on momentum resolution. The main reason why the momentum resolution receives little effects from field non-uniformities that are apparent from contour maps are that (1) the field is rather uniform in the central region of the tracking volume due to the large half-length with respect to its radius, (2) the precision devices such as silicon strip detectors located mostly in the region of central region and (3) the momentum resolution depends on integral of BL^2 not BL, and thus

the presence of wide high field region dominates relative to the presence of short low field region.

3. Track triggering in the central part

There are three different schemes for track triggering associated with three different trackers, straw tubes, scintillating fibers and silicon. Silicon is located in the central part of the tracking volume where the field uniformity is good and therefore the non-uniformity has little effects for silicon track triggering.

In the levels 1 and 2 trigger of the central outer trackers, tracks are selected based only on the axial layers. It is not possible to distinguish, for example, a track of $\eta = 0$ from that of $\eta = 1.5$ in levels 1 and 2 triggers. The field non-uniformity obscures Pt thresholds since Pt threshold becomes rapidity dependent. Figs.5a (LA) and 5b (TF(Fe)) illustrates the situation. The figure shows trajectories of Pt=10GeV/c. Due to field non-uniformity, the traces in the r-ϕ projection plane are different as shown.

As shown in Fig.6, the methods used in the level 1 or 2 trigger is to measure the slope $\Delta\phi$ of a trajectory at high radius (such as 135cm and/or 161cm in straw tracker) electronically and to apply a certain threshold to the slope. More sophisticated method is to detect the slope difference $\Delta\phi'$ of two pairs of superlayers (in the case of scintillating fibers[10]). Fig.7 shows the rapidity dependence of the slope $\Delta\phi$ at r=161cm for a particle of Pt= 10GeV/c. One sees smaller $\Delta\phi$ at high rapidity due to smaller bending power. Suppose one sets a threshold of $\Delta\phi$ at 48 mrad corresponding to Pt= 10GeV/c at η=0. The same $\Delta\phi$ threshold at η=1.5 corresponds to approximately Pt = 7GeV/c, obscuring the Pt cut. Figs.8, 9 and 10 show the efficiency curve of 10 GeV/c Pt cut assuming flat rapidity distribution. Trigger methods are indicated in the figures. These calculations includes only the effects from non-uniformity. It becomes clear that the efficiency tail is only in low Pt side, which is the safe side as far as triggering concerns. The trigger frequency increases due to this tail.

There are, however, many other effects that could obscure the Pt threshold, such as multiple scattering, x-t relations, timing inaccuracy etc. J.Chapman's calculation (confirmed by Monte Carlo) for straw tube trigger indicated about 5 GeV/c (7 to 12 GeV/c) to reach from 10 to 90% efficiency at 10 GeV/c cut (Fig.11)[11]. His calculation assumes uniform

field. The effect of field non-uniformity for triggering is comparable to other effects and it is not fatal.

It is a bit surprising that the smearing of Pt cut is more or less similar for both magnetic configurations of LA and TF(Fe) but it is true.

4. Track triggering in the intermediate angle region

Since there is no clear design of intermediate trackers at this stage, it is hard to evaluate the effects of non-uniformity in this area. It is felt that the intermediate angle trackers covers fairly limited region (1.8-2.5 in rapidity and 50-120cm in radius) and consequently there is little variation in bending power BL^2 coming to field non-uniformity. Rather geometrical effect on L^2 dominates. Need more studies. Also due to lack of bending power in this region, it is not obvious yet if fairly good Pt cut is possible at level 1 or 2.

5. Pattern recognition

Since there is no comprehensive pattern recognition program available, it is hard to evaluate the effects quantitatively. There are in general three different methods of pattern recognitions. Effects of non-uniformity depend strongly on method of pattern recognition.

(1) Global method (histograming method)

This is to find an accumulation of points in c-ϕ (curvature-ϕ) plane. It is done in r-ϕ projected frame and thus in case of non-uniform field smearing occurs due to not knowing the z coordinate. The expansion of this method to 4-dimensional c-ϕ-z-λ space is necessary but looks not easy.

(2) Local vector method

If the slant superlayer(SL) is close by, z information is obtained by axial-slant combination. Once z coordinate is known, the non-uniformity can be taken into account in the further steps. If the slant SL is apart from axial SLs, the non-uniformity may introduce errors in track extrapolation. But without simulations it is not clear to evaluate if this error generates any difficulty.

(3) Road following method

8 layers of silicon strip system provide local 3 dimensional pattern recognition. Once approximate three dimensional coordinates are

given, extrapolation to outer system is easy even with non-uniform field.

Thus the effect of field non-uniformity depends strongly on method of pattern recognitions. Conversely methods that are rather insensitive to non-uniformity can be developed and used.

6. Conclusions

1. Negligible effects on $\Delta pt/pt$.

2. The threshold smearing due to non-uniformity is comparable to other effects.

3. The effect on pattern recognition strongly depends on method.

Reference

1. J.Matthews, SDC-90-00066
2. S.Odaka, SDC-90-00074
3. T.Kirk, SDC-90-00095
4. H.Iwasaki, SDC-90-00097
5. A.Yamamoto etal, SDC-90-00102
6. Y.Takaiwa, SDC-90-00103
7. J.Hylen, ANL meeting, March 1991.
8. J.Hylen, , LBL meeting, Aug.1991.
9. T.Kondo, Momentum resolution, LBL meeting, Aug.1991.
10. A.Baumbaugh, Proceedings of the SDC Collaboration Meeting at KEK, May, 1991, SDC-91-00033, pp.791-826.
11. J.Chapman, talk at LBL meeting, Aug.1991.

Prepared by T.Kondo
1991.Sep.10

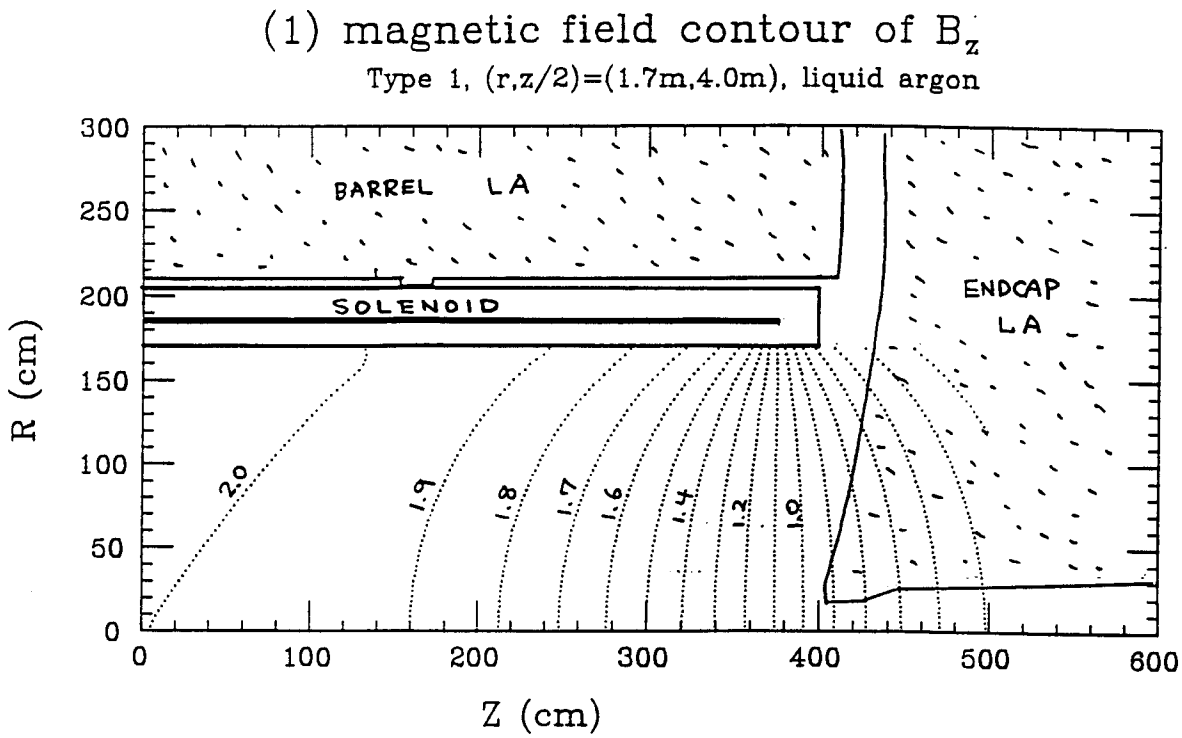
(1) magnetic field contour of B_z
Type 1, (r,z/2)=(1.7m,4.0m), liquid argon
BARREL LA
SOLENOID
ENDCAP LA
2.0
1.9
1.8
1.7
1.6
1.4
1.2
1.0
R (cm)
Z (cm)
0
50
100
150
200
250
300
0
100
200
300
400
500
600

Fig. 1

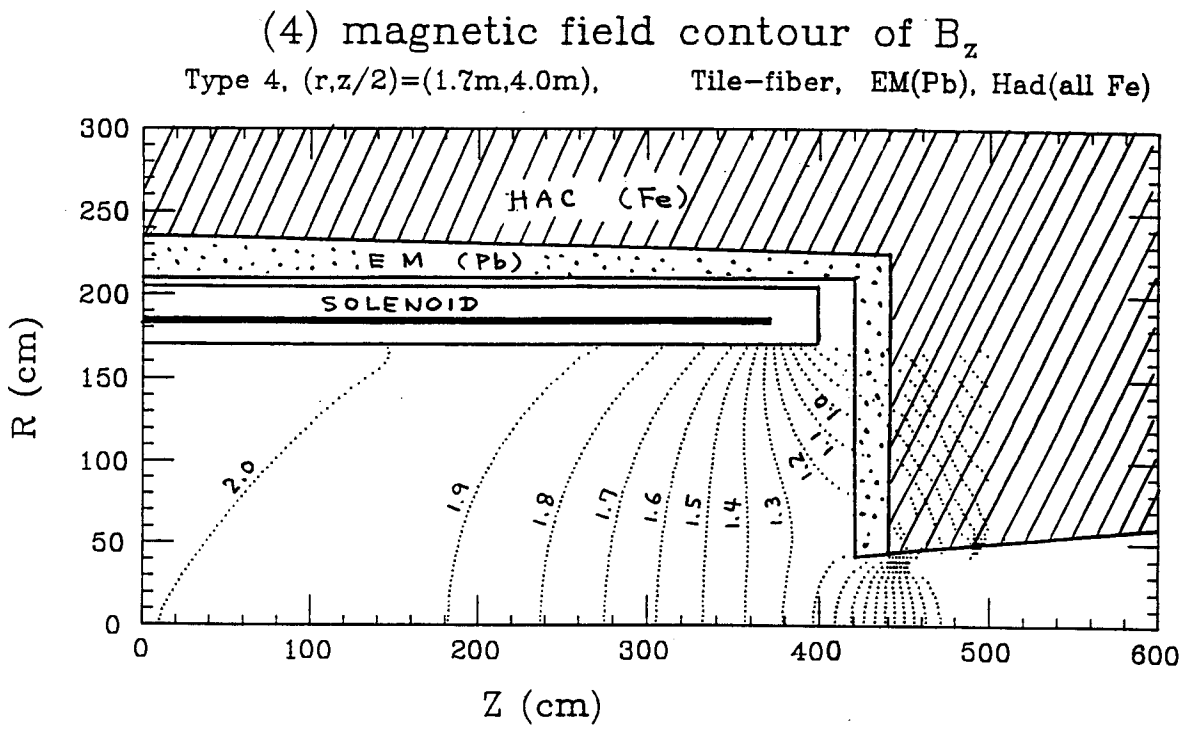
(4) magnetic field contour of B_z
Type 4, (r,z/2)=(1.7m,4.0m), Tile−fiber, EM(Pb), Had(all Fe)
HAC (Fe)
EM (Pb)
SOLENOID
2.0
1.9
1.8
1.7
1.6
1.5
1.4
1.3
1.2
1.1
1.0
R (cm)
Z (cm)
0
50
100
150
200
250
300
0
100
200
300
400
500
600

Fig. 2

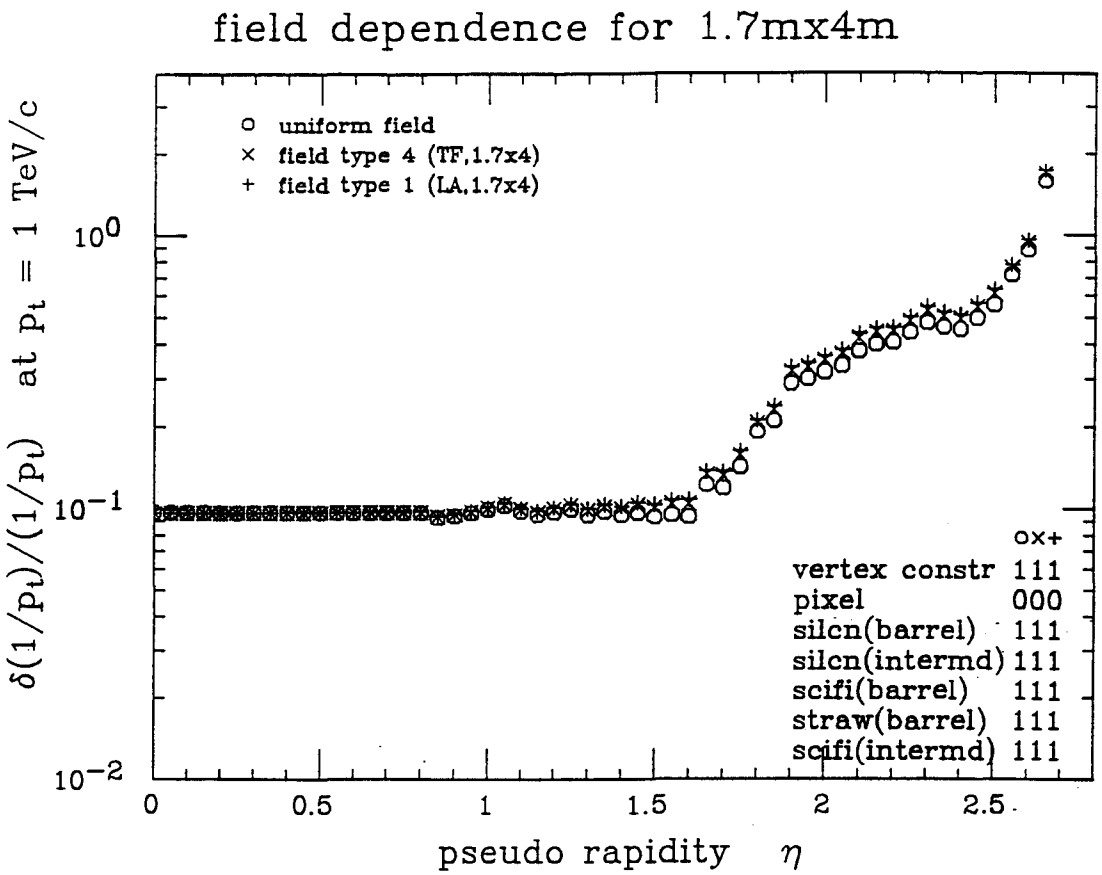
field dependence for 1.7mx4m
uniform field
field type 4 (TF,1.7x4)
field type 1 (LA,1.7x4)
δ(1/pt)/(1/pt) at pt = 1 TeV/c
pseudo rapidity η
ox+
vertex constr 111
pixel 000
silcn(barrel) 111
silcn(intermd) 111
scifi(barrel) 111
straw(barrel) 111
scifi(intermd) 111

Fig. 3

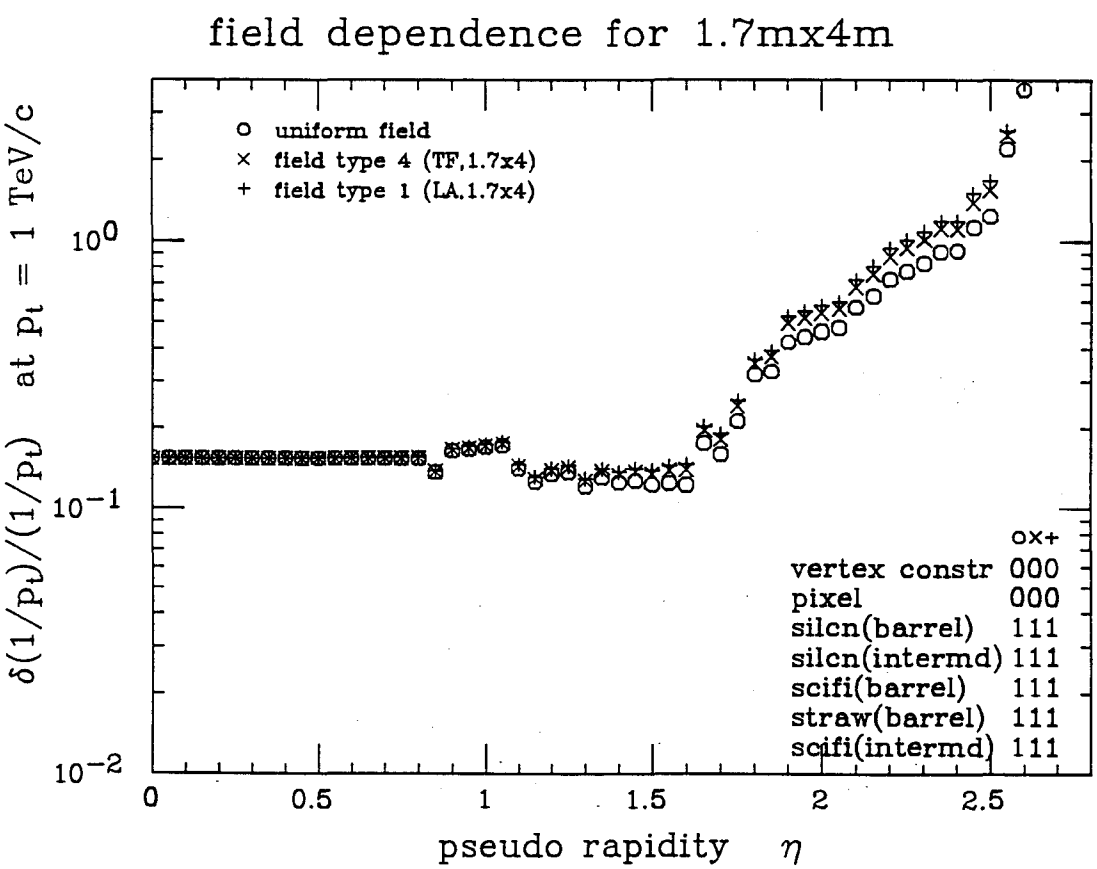
field dependence for 1.7mx4m
uniform field
field type 4 (TF,1.7x4)
field type 1 (LA,1.7x4)
δ(1/pt)/(1/pt) at pt = 1 TeV/c
pseudo rapidity η
ox+
vertex constr 000
pixel 000
silcn(barrel) 111
silcn(intermd) 111
scifi(barrel) 111
straw(barrel) 111
scifi(intermd) 111

Fig. 4

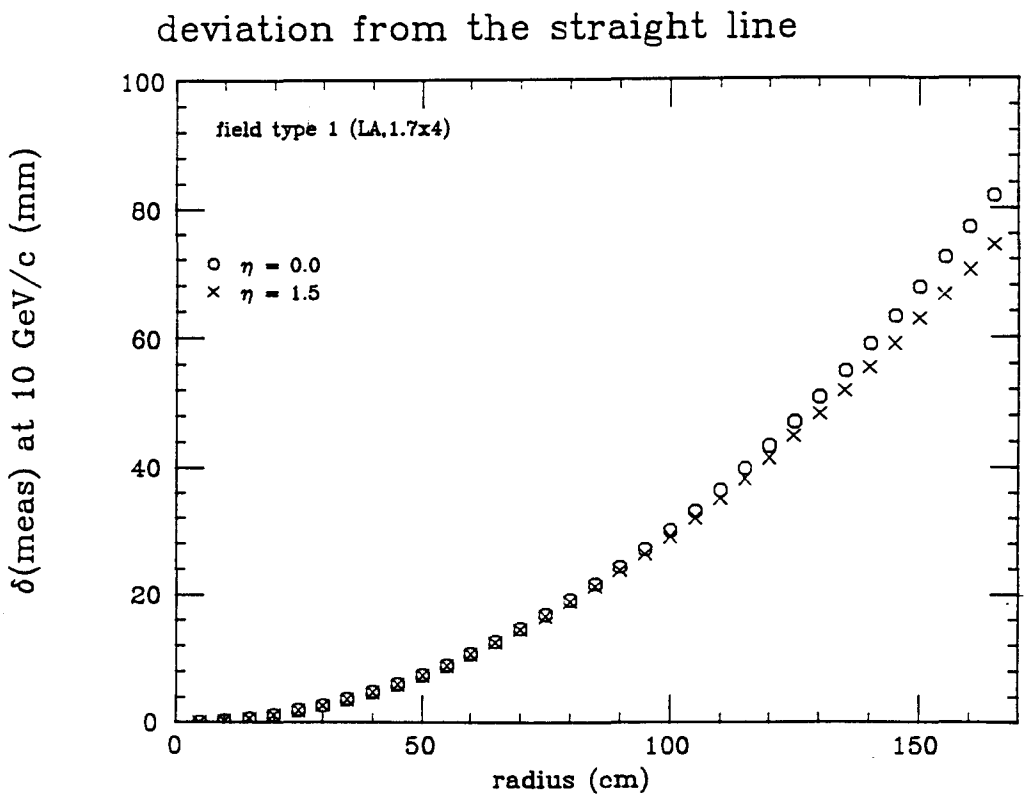
deviation from the straight line
field type 1 (LA,1.7x4)
o η = 0.0
× η = 1.5
δ(meas) at 10 GeV/c (mm)
radius (cm)
0
20
40
60
80
100
0
50
100
150

Fig. 5a

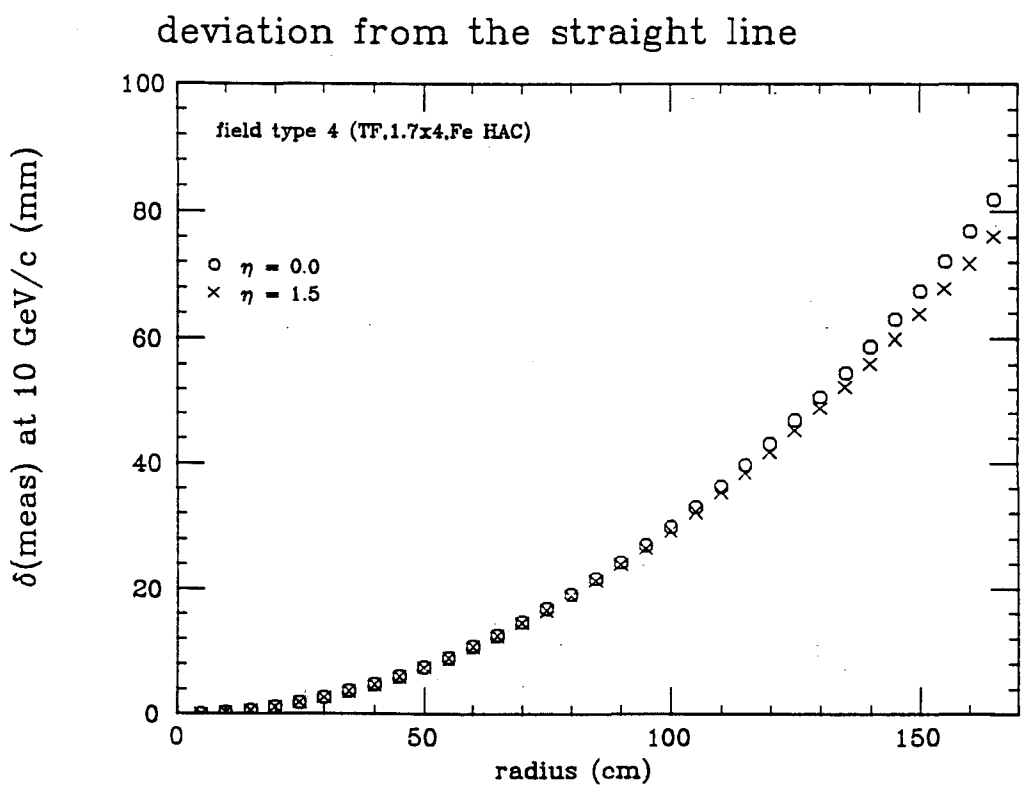
deviation from the straight line
field type 4 (TF,1.7x4,Fe HAC)
o η = 0.0
× η = 1.5
δ(meas) at 10 GeV/c (mm)
radius (cm)
0
20
40
60
80
100
0
50
100
150

Fig.5b

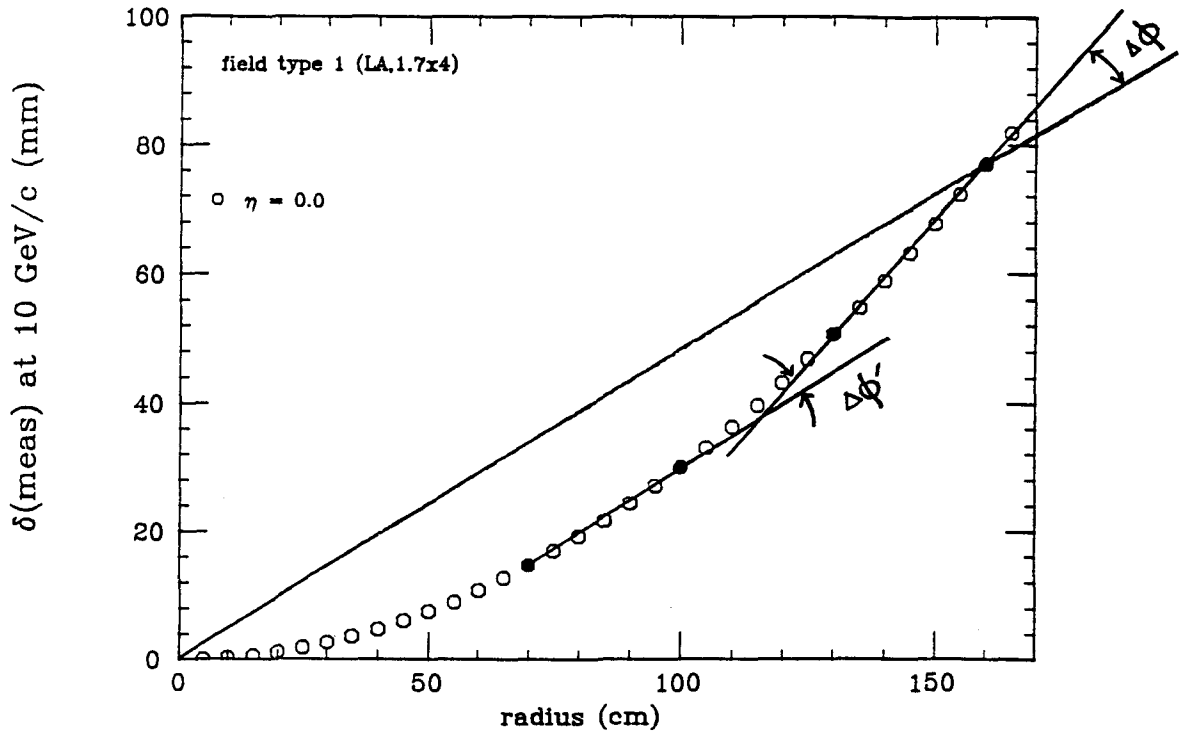
field type 1 (LA,1.7x4)
η = 0.0
δ(meas) at 10 GeV/c (mm)
radius (cm)
Δφ
Δφ'
0
20
40
60
80
100
0
50
100
150

Fig. 6

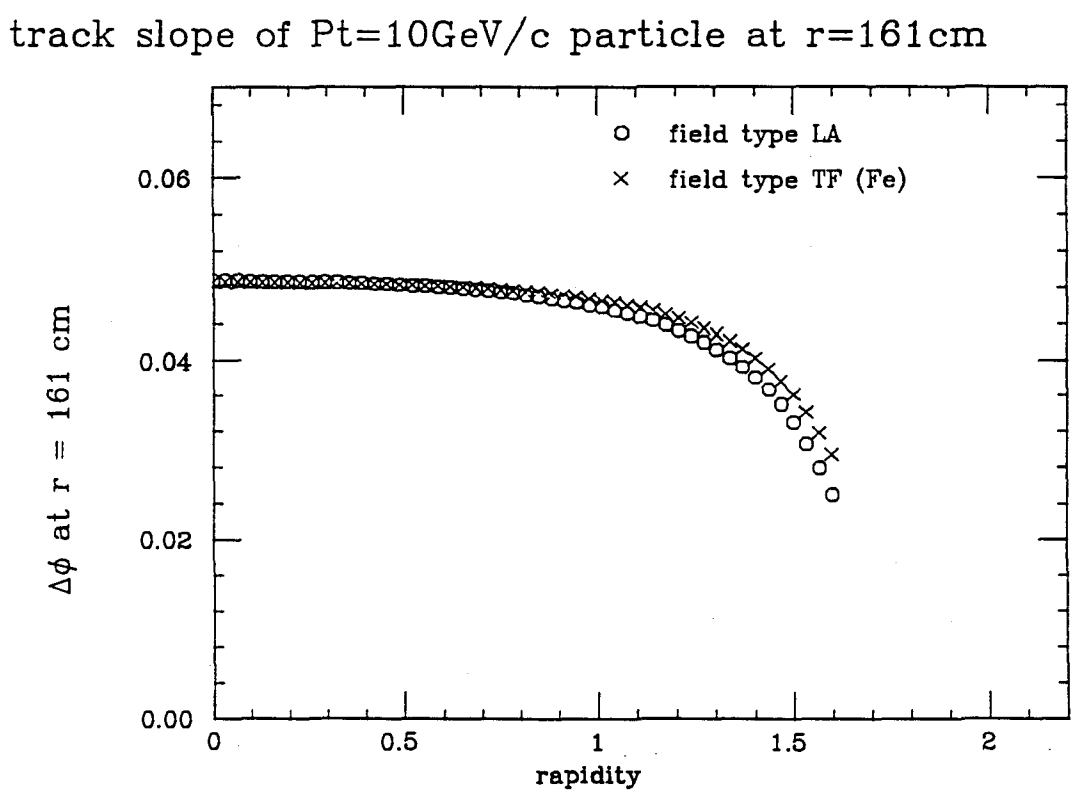
track slope of Pt=10GeV/c particle at r=161cm
field type LA
field type TF (Fe)
Δφ at r = 161 cm
rapidity
0.00
0.02
0.04
0.06
0
0.5
1
1.5
2

Fig. 7

field non−uniformity effects on track triggering

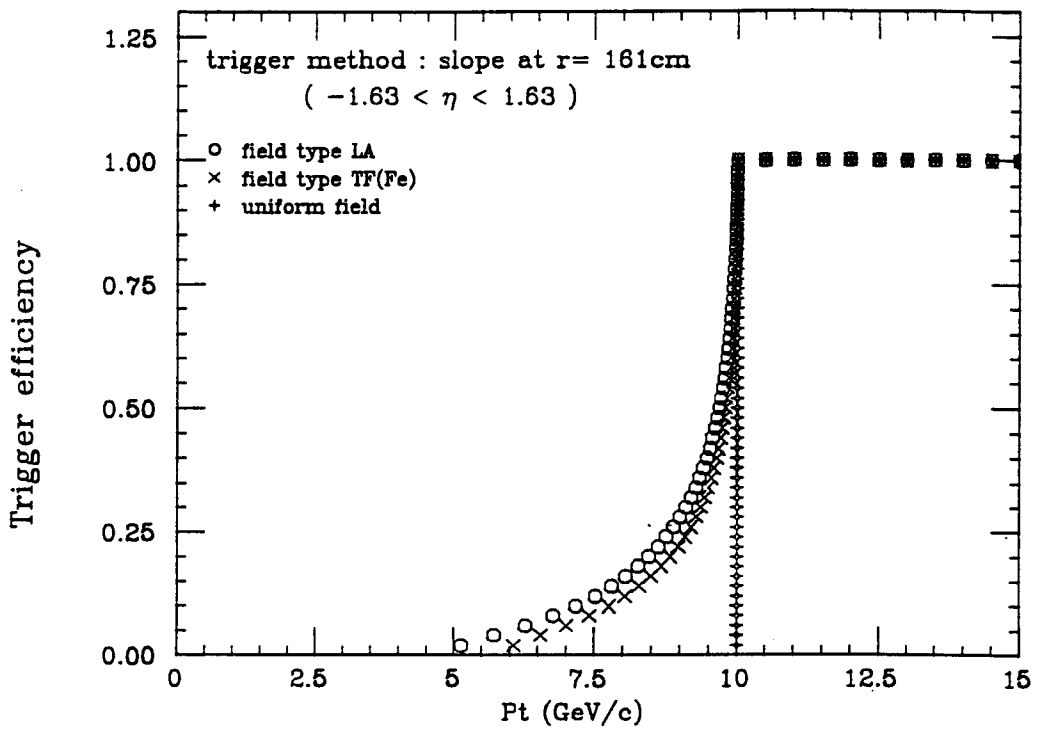

Fig. 8

field non−uniformity effects on track triggering

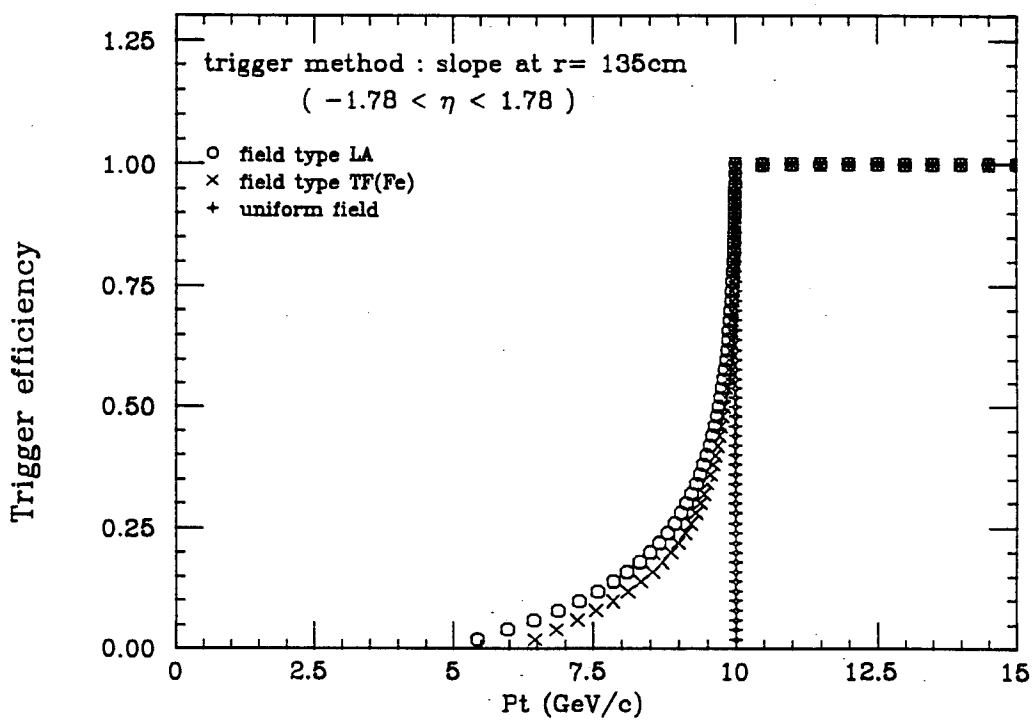

Fig. 9

field non-uniformity effects on track triggering

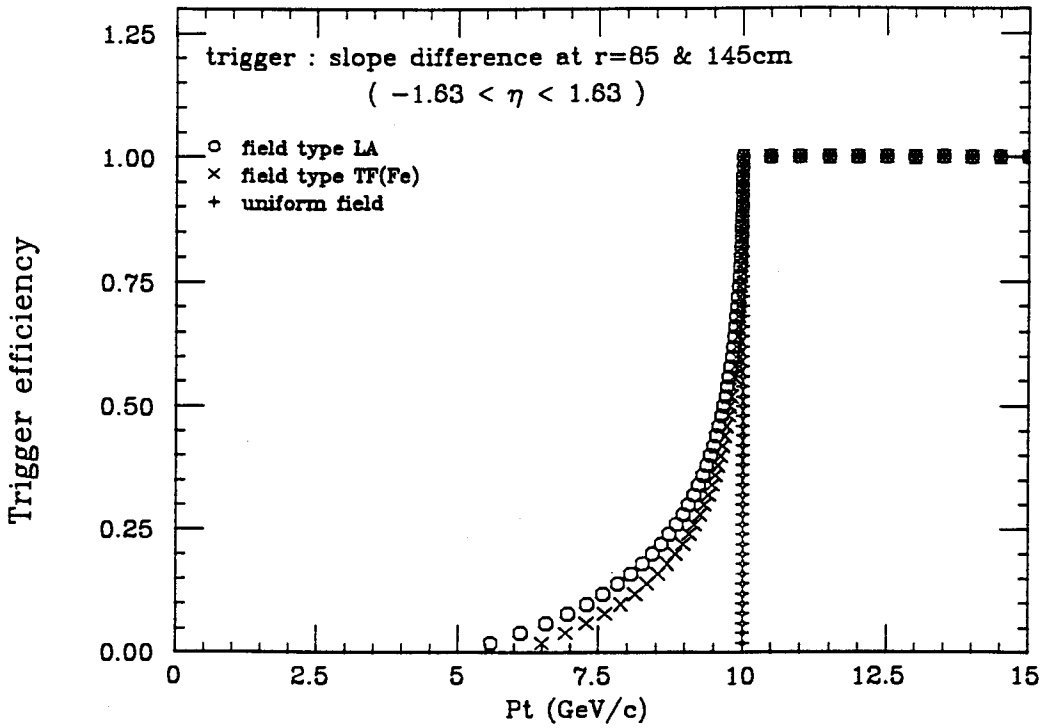

Fig. 10

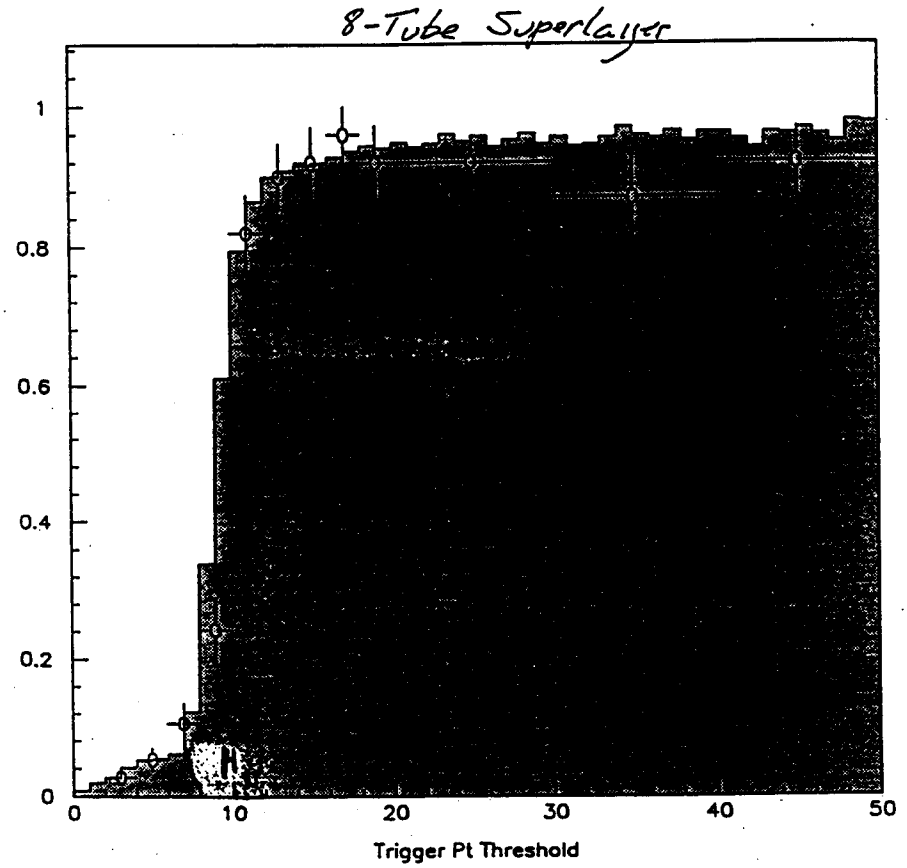

Fig. 11

T. KONDO
8/10/91

REPORT OF TASK FORCE ON FIELD UNIFORMITY

TASK FORCE ON MAGNET FIELD UNIFORMITY

Task Force

chairman : T. Kondo

members : B. Barnett
J. Dainton or Brian Foster
R. Lewis
M. Corden
A. Weinstein
H. Ogren
J. Chapman
J. Hylen
D. Adams

Charges Assemble information relevant to compare tracking system performance in the two field configurations

- relatively uniform field
- non-uniform field

report due at the August, 5-10 SDC meeting

SDC-90-00066	J.Matthews	Effects of Non-uniform magnetic fields on SDC central tracking
SDC-90-00074	S.Odaka	Momentum resolution for muons using the full tracking system
SDC-90-00095	T.Kirk	Report of the SDC magnet task Force
SDC-90-00097	H.Iwasaki	Momentum resolution in a nonuniform magnetic field
SDC-90-00102	A.Yamamoto etal	Design Study of an Air core thin solenoid for SDC detector
SDC-90-00103	Y.Takaiwa	Short solenoid vs long solenoid - effects on tracking
ANL meeting	J.Hylen	Effect of field non-uniformity on inne tracking for some sample field
LBL meeting	T.Kondo	
LBL meeting	J.Hylen	

Things to be considered

* $\Delta p/p$
* Triggering
* Pattern Recognition
* Others (E×B
  field measurement
  ....
  ....)

FACT #1 $\int B\,dl$ is wrong

$\int \vec{B} \times d\vec{l}$ is right

FACT #2 $\frac{\Delta P_T}{P_T} \propto \int dl \int \vec{B} \times d\vec{l} \sim BL^2$

not BL

FACT #3 Detector locations and their position resolutions are important

$\downarrow$

BL^2 is wrong for non-uniform tracking system

FACT #4 Vertex constraint is very important

LoI Fig. 9

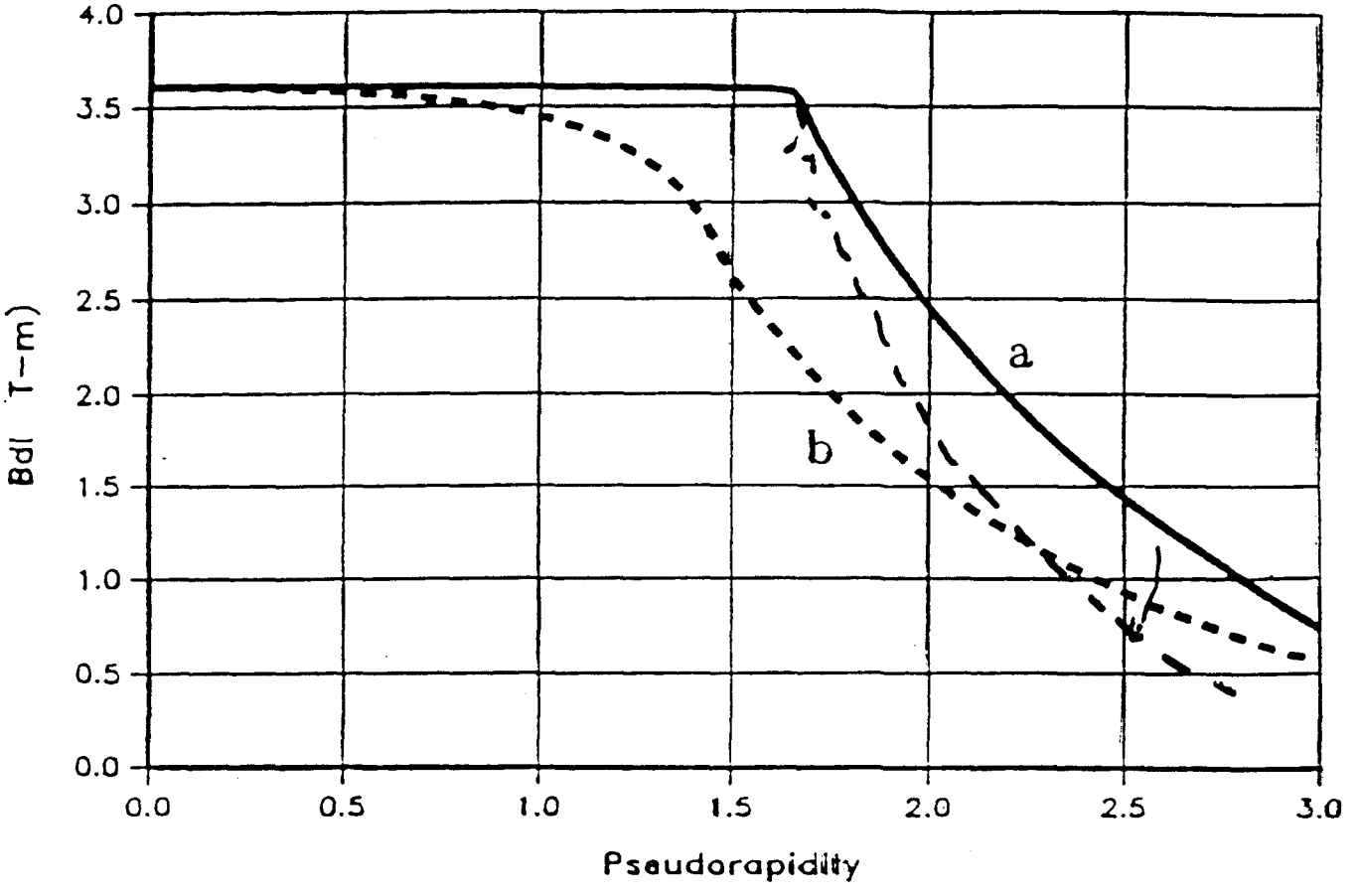
4.0
3.5
3.0
2.5
2.0
1.5
1.0
0.5
0.0
Bdl (T-m)
0.0
0.5
1.0
1.5
2.0
2.5
3.0
Pseudorapidity
a
b

Jim Hylen
FNAL
SDC workshop 8/6/91

Possible Disadvantages of Non-Uniform Field for Tracking

Degraded Momentum Resolution (Minimal)

Pattern Recognition

Triggering

CPU requirements

Drift Angle in wire chambers?

Path of loopers? (+/- ?)

Measurement of detector alignment

Field measurement

In non-uniform field: (Need simulation!)

Global pattern recognition, such as histogramming method presented yesterday, probably wont work ☹

Must do pattern recognition in r, ϕ, z, λ simultaneously

Intuition: Strong fiber system → local space points, local vectors → probably OK 😐

Thinned out outter system need proof that it would work ⁇

8 layer silicon strip system → still work, could then swim to outter system & pick up hits ☺

Pattern Recognition in tracking will probably be largest SDC CPU load — we could really use some estimate of whether non-uniform field will cost \$1 million, \$10 million, \$100 million in CPU \$.

(1) magnetic field contour of B_z

Type 1, (r,z/2)=(1.7m,4.0m), liquid argon

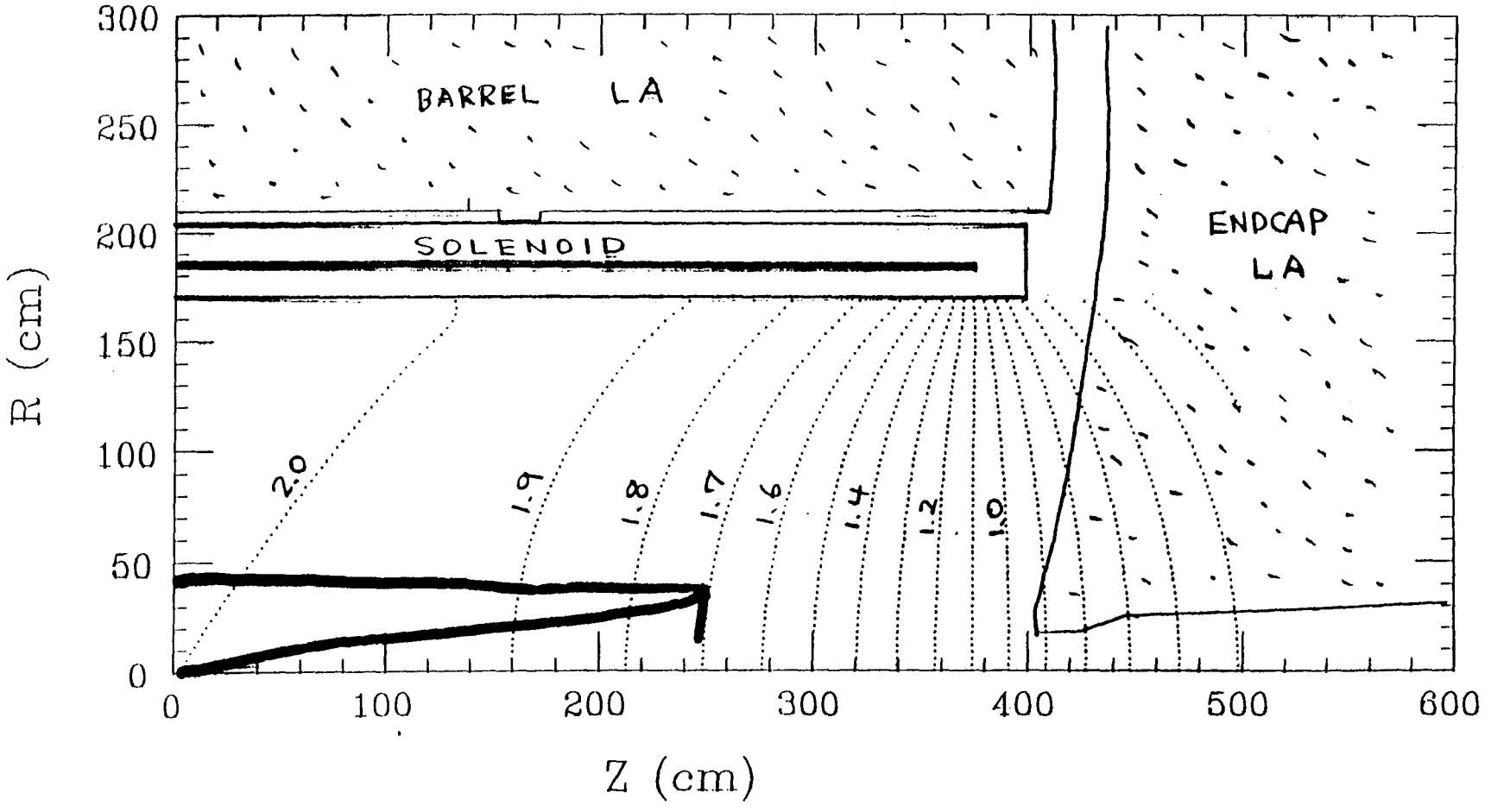

Kondo

(4) magnetic field contour of B_z

Type 4, (r,z/2)=(1.7m,4.0m), Tile−fiber, EM(Pb), Had(all Fe)

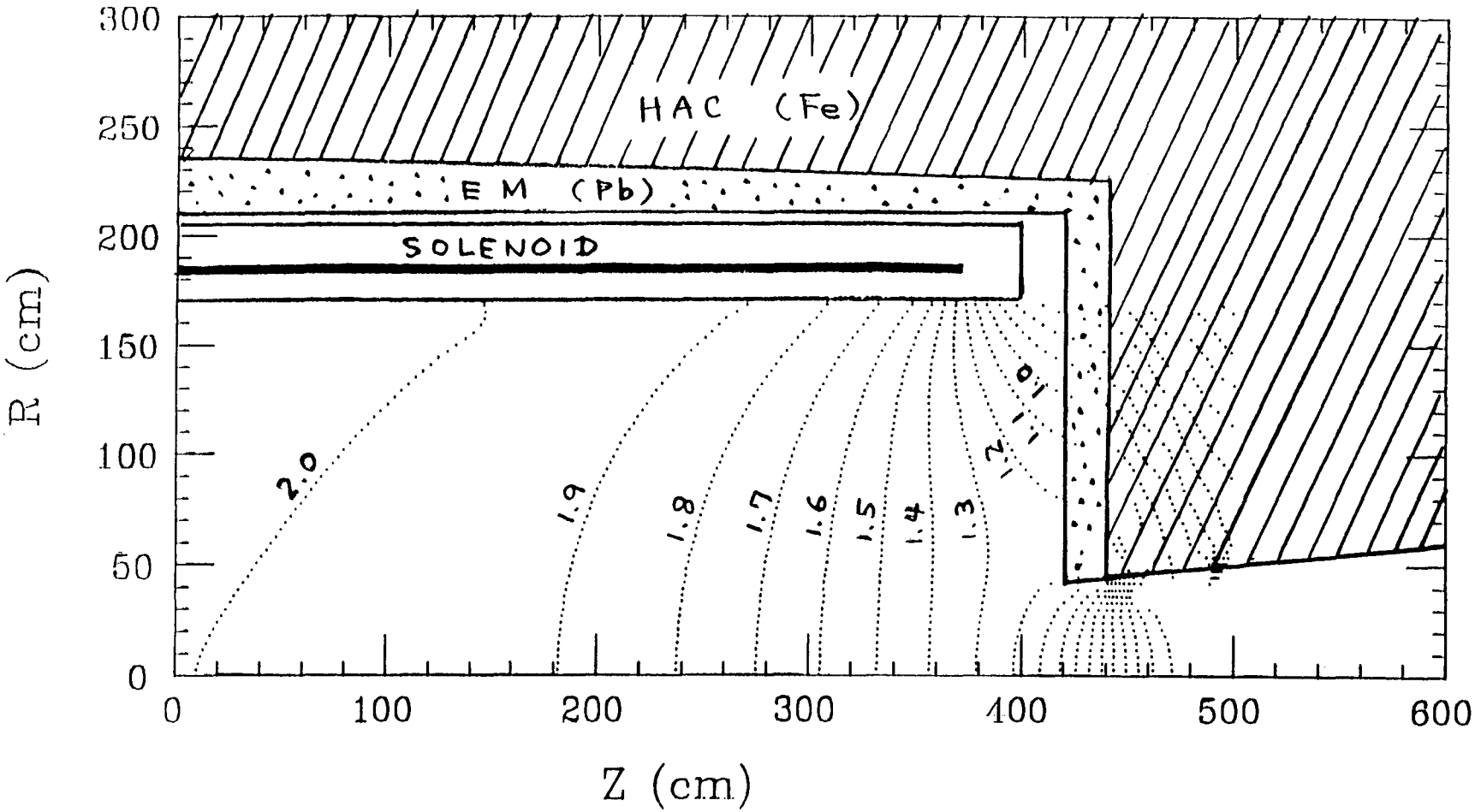

(best case)

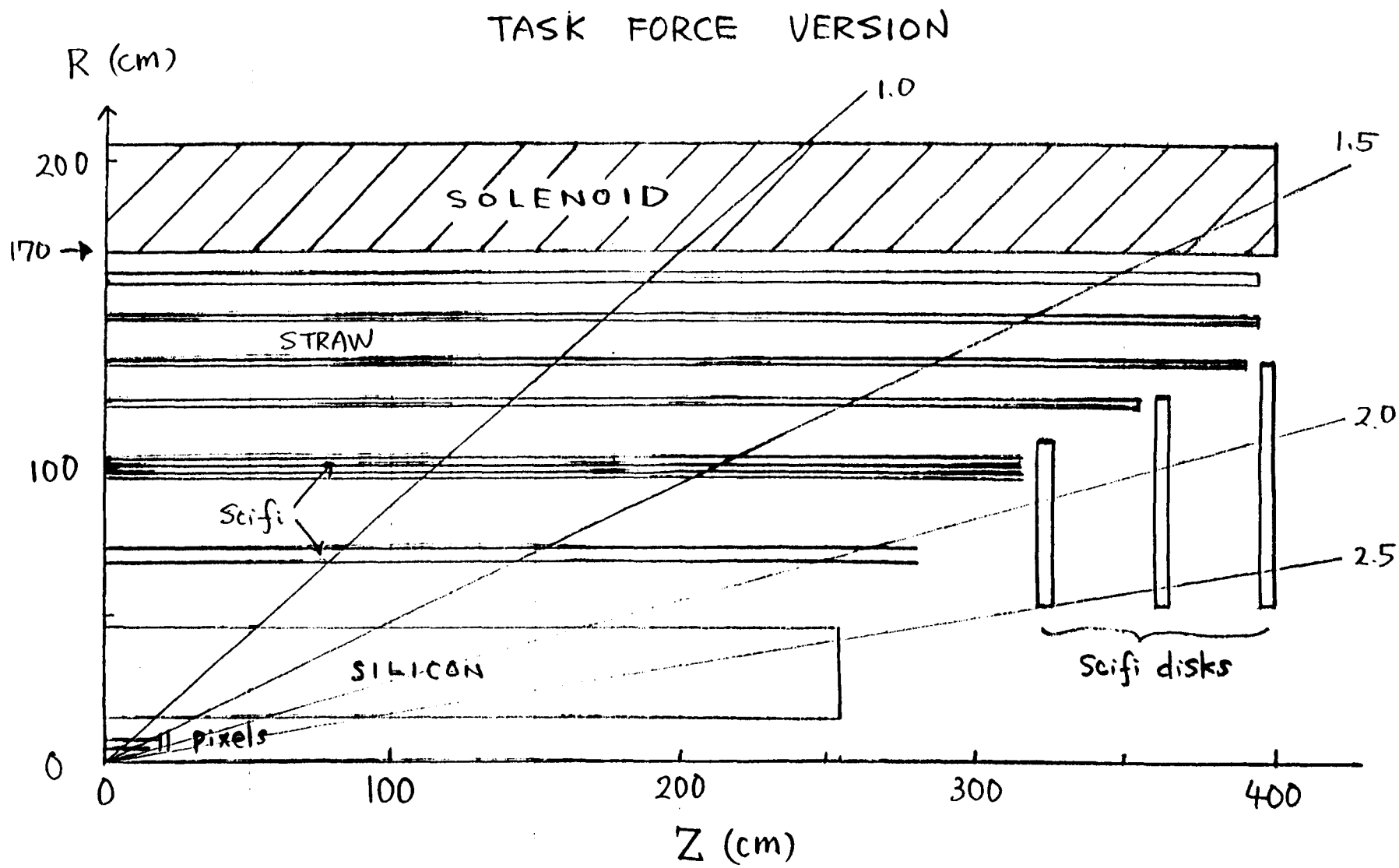
TASK FORCE VERSION
R (cm)
200
170
100
0
SOLENOID
STRAW
Scifi
SILICON
pixels
1.0
1.5
2.0
2.5
Scifi disks
0
100
200
300
400
Z (cm)

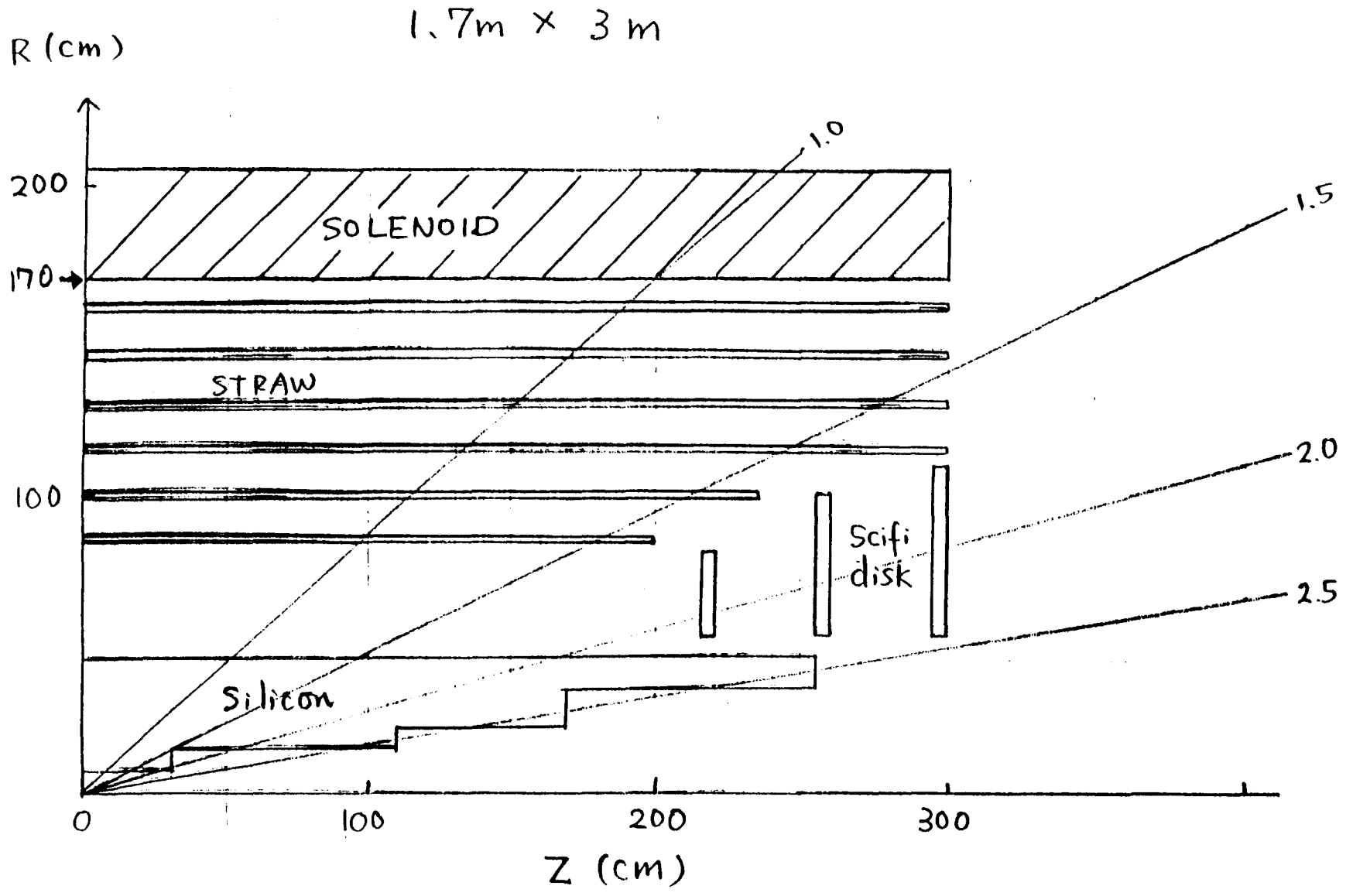
1.7m × 3m
R (cm)
200
170
100
SOLENOID
STRAW
Silicon
Scifi disk
1.0
1.5
2.0
2.5
0
100
200
300
Z (cm)

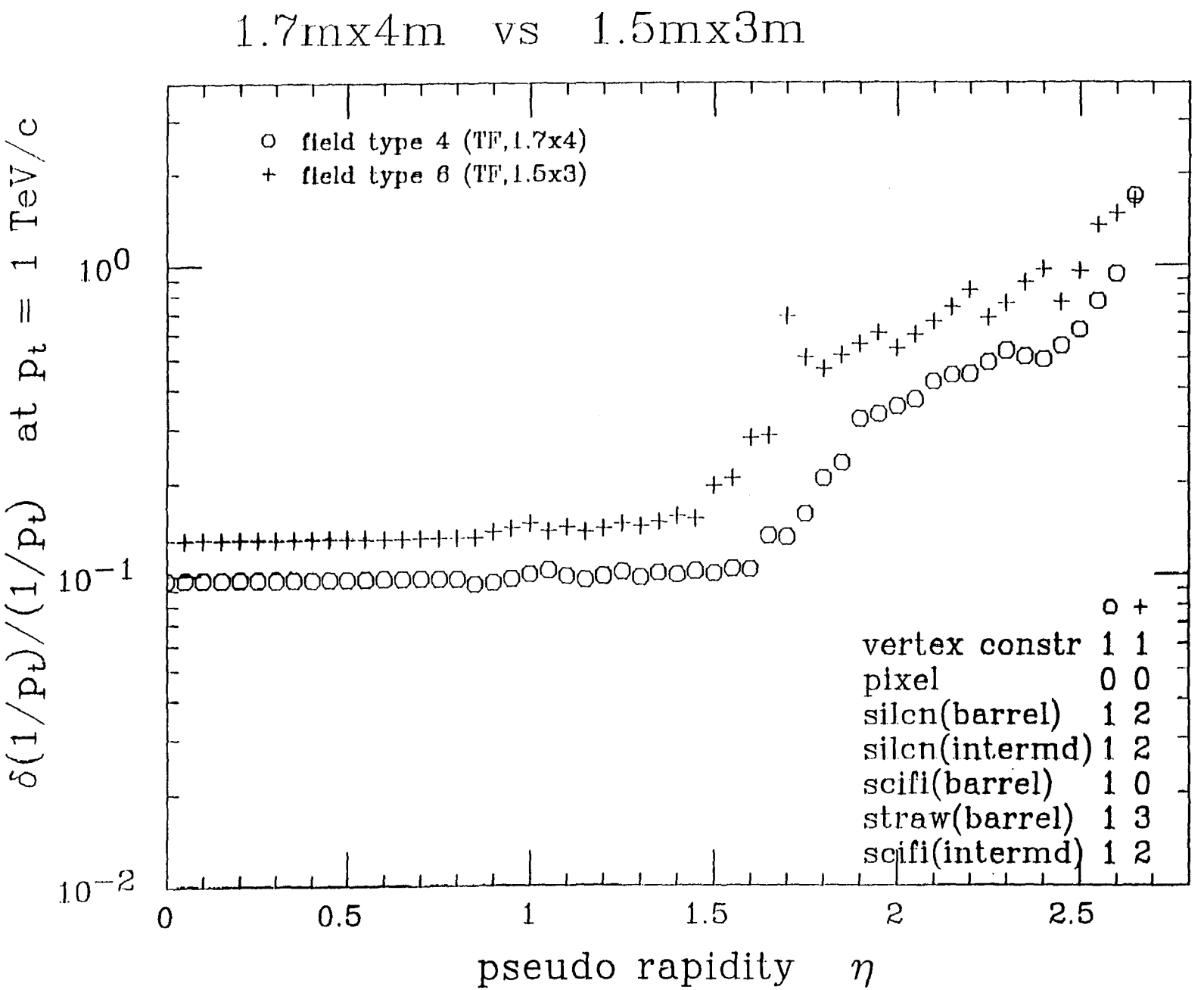
1.7mx4m vs 1.5mx3m
o field type 4 (TF,1.7x4)
+ field type 6 (TF,1.5x3)
δ(1/pt)/(1/pt) at pt = 1 TeV/c
10^0
10^-1
10^-2
0
0.5
1
1.5
2
2.5
pseudo rapidity η
o +
vertex constr 1 1
pixel 0 0
silcn(barrel) 1 2
silcn(intermd) 1 2
scifi(barrel) 1 0
straw(barrel) 1 3
scifi(intermd) 1 2

Kondo

field dependence for 1.7mx4m

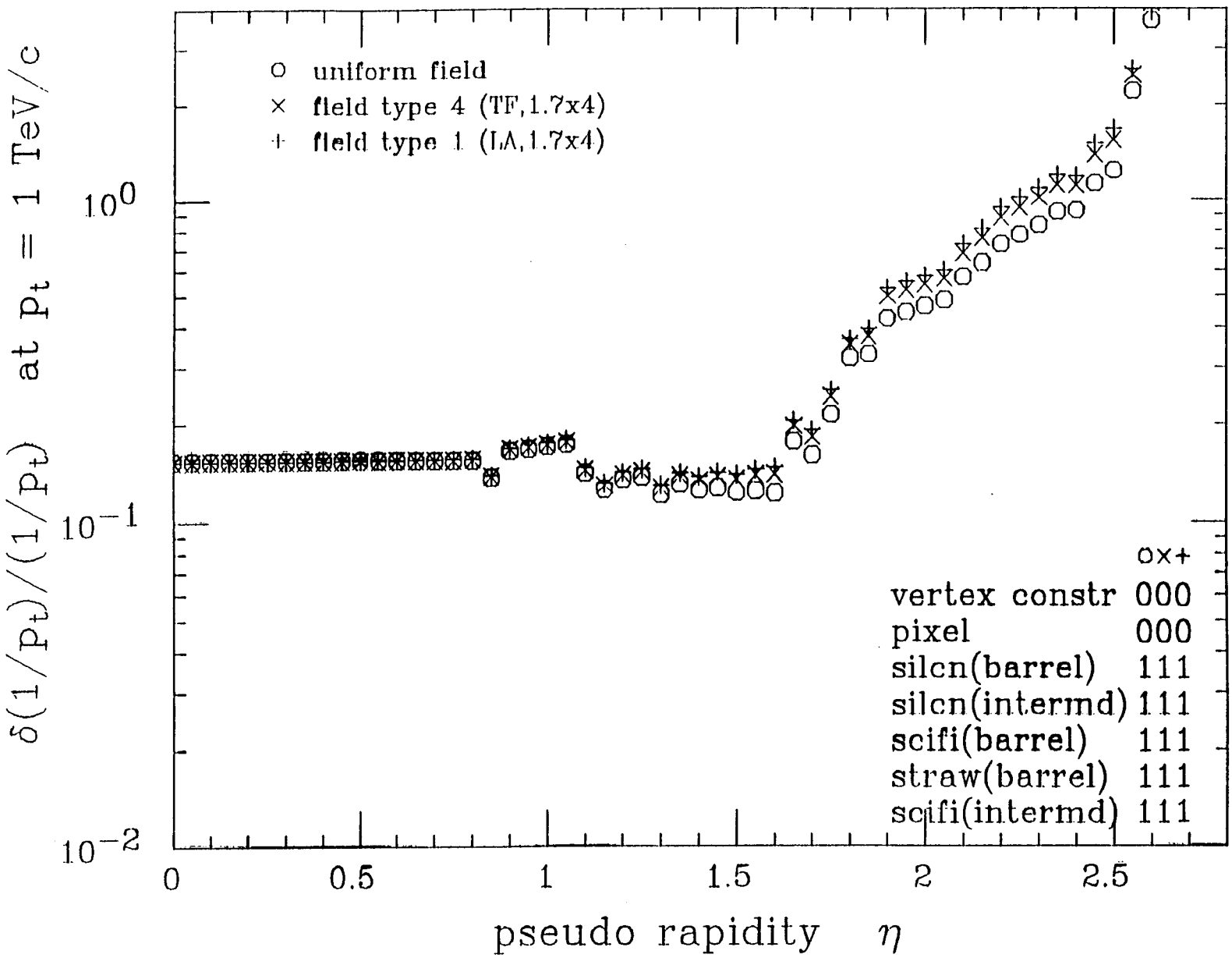

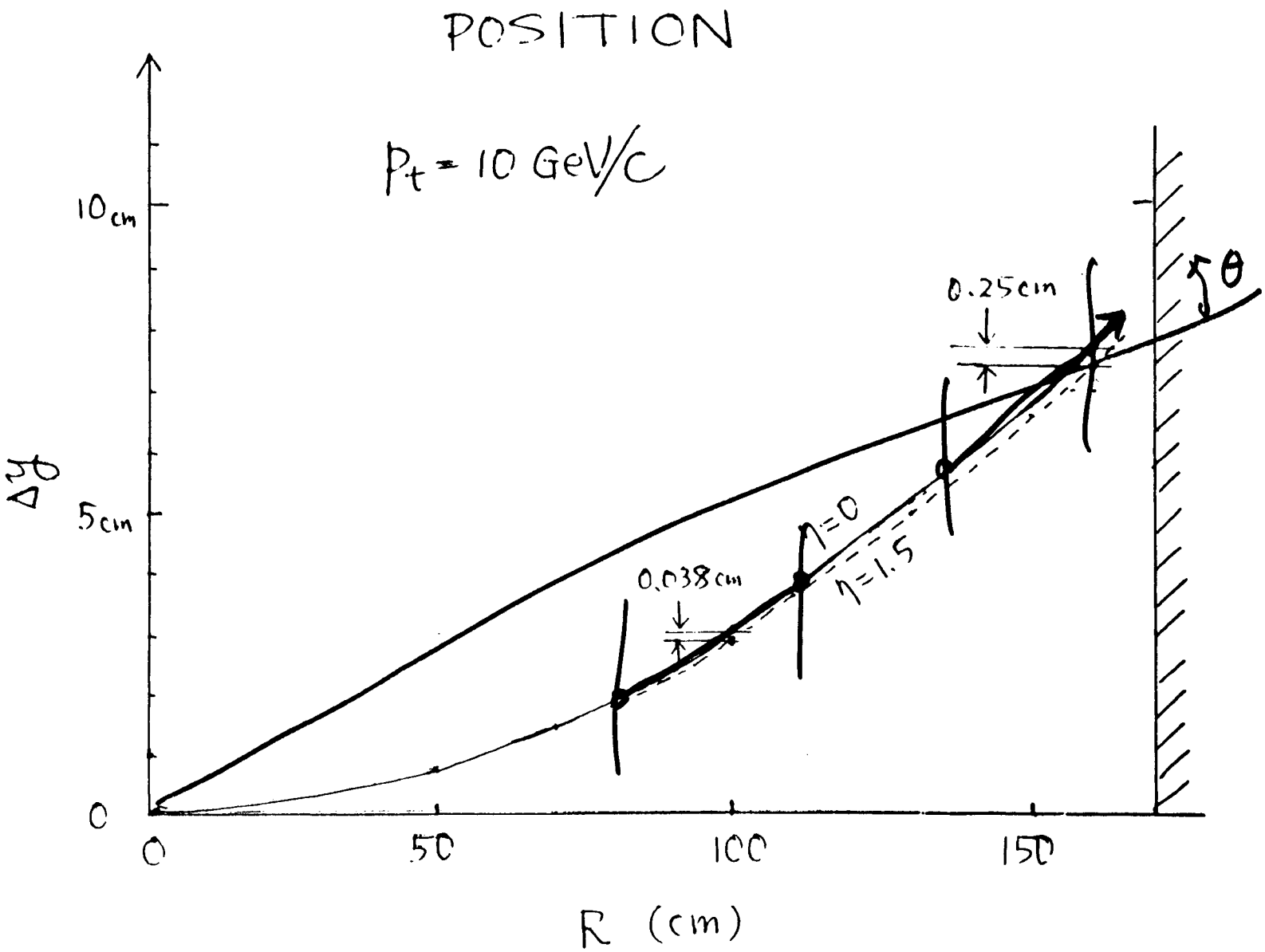
POSITION
$P_t = 10$ GeV/c
10 cm
5 cm
0
$\Delta\phi$
0.25 cm
0.038 cm
$\eta = 0$
$\eta = 1.5$
θ
0
50
100
150
R (cm)

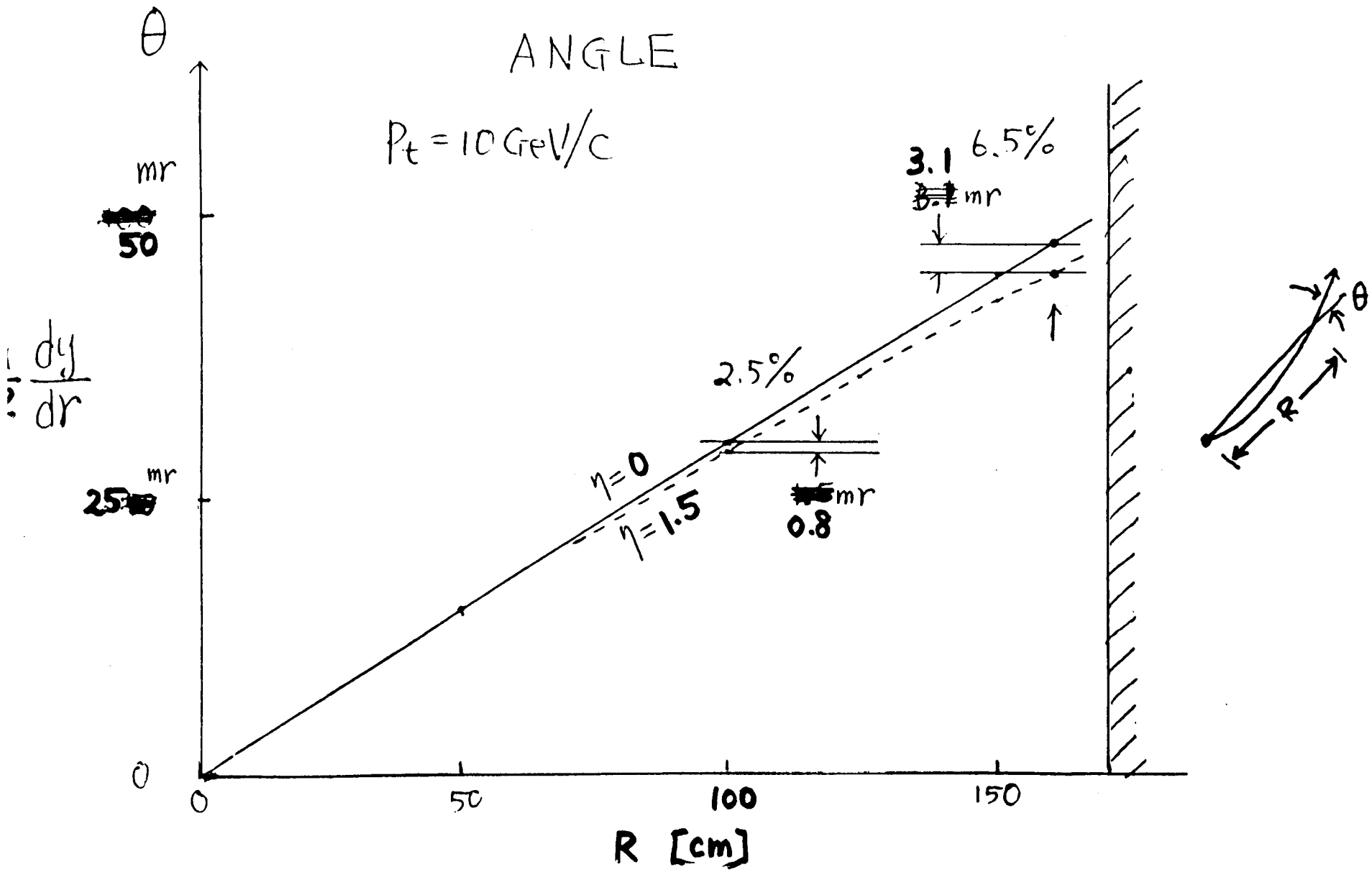
θ
ANGLE
Pt = 10 GeV/c
mr
50
25 mr
0
dy/dr
3.1 6.5%
mr
2.5%
η=0
η=1.5
mr
0.8
0
50
100
150
R [cm]
θ
R

Effects on Track Trigger

Level 1 (Level 2) will be done in r-ϕ projection

↓

no information on z coordinate

↓

non-uniform field makes difference in Trajectory

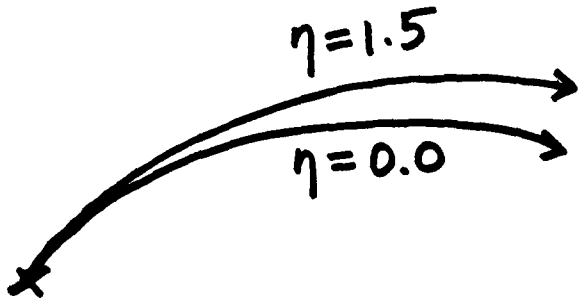

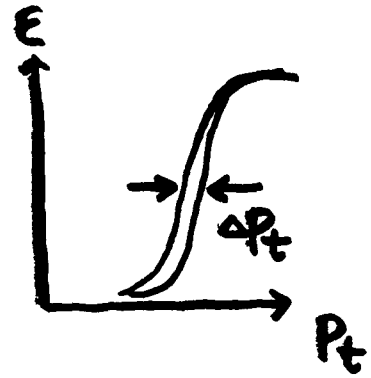

P_t Trigger by

1. angle $\Delta\phi$: $\Delta P_t = 0.65$ GeV/c
2. angle difference $\Delta\phi_1 - \Delta\phi_2$: $\Delta p_t = 1.1$ GeV/c
3.

Effects on Pattern Recognition

① global method (histograming method)

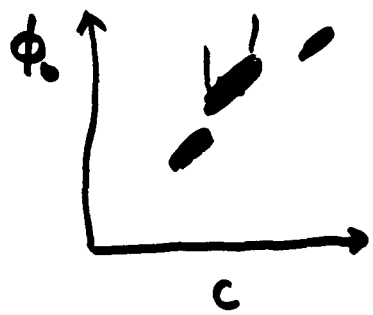

$c\,\phi_0 \longrightarrow c\,\phi_0\,z_0\,\lambda$

may need to do in 4 parameter space

② local vector method

- local space points $\longrightarrow$ z information
- harder if stereo layers are apart

③ road following method

- inside (S_i) $\longrightarrow$ out : OK
- outside $\longrightarrow$ in : harder but....

Tentative Conclusions

$\frac{\Delta P_t}{P_t}$ almost no effects

Trigger $\Delta P_t \sim 0.6 \sim 1$ GeV/c

depend on method

pattern recognition

depend on method

local space point reconstruction helps

Silicon → out is ok

need to be quantified

CALORIMETER REVIEW AND TECHNICAL BOARD MEETING
SEPTEMBER 12 -14, 1991
SSCL

Presentation by:

Bill Edwards

Lawrence Berkeley Laboratory

Comparison of LAC and Scint. Tile Calorimeter

Cost Estimates

Sept. 13, 1991

SDC Calorimeter Comparison

Calorimeter Cost Comparison Parameters Table

	Scint. Cal (Descope 19)	LAC
Barrel I.R. (m)	2.1	2.1
Depth ($\eta = \phi$)	9λ	9λ
Depth ($\eta = 3$)	11λ	11λ
Barrel		
EM		
Longitudinal Segmentation	2	2
Longitudinal Granularity (mm)	8.5	9.6
Transverse Gran. ($\Delta\eta,\Delta\phi$)	$.05 \times .05$	$.05 \times .05$
HAD 1		
Longitudinal Segmentation	1	1
Longitudinal Gran. (mm)	25.5	17
Transverse Gran. ($\Delta\eta,\Delta\phi$)	$.05 \times .05$	$.05 \times .05$
HAD 2		
Longitudinal Segmentation	1	1
Longitudinal Gran. (mm)	51	17
Transverse Gran. ($\Delta\eta,\Delta\phi$)	$.1 \times .1$	$.05 \times .05$
End Cap		
EM		
Longitudinal Segmentation	2	2
Longitudinal Gran. (mm)	8.5	9.6
Transverse Gran. ($\Delta\eta,\Delta\phi$)	$.05 \times .05$	$.05 \times .05$
HAD 1		
Longitudinal Segmentation	1	1
Longitudinal Gran. (mm)	36	17
Transverse Gran. ($\Delta\eta,\Delta\phi$)	$.05 \times .05$	$.05 \times .05$
HAD 2		
Longitudinal Segmentation	1	1
Longitudinal Gran. (mm)	72	17
Transverse Gran. ($\Delta\eta,\Delta\phi$)	$.1 \times .1$	$.05 \times .05$
PMT/Channel Count		
Total Std. Pmts.	33,936	—
Total MAPMT's	2041†	—
Total Channels	—	97,024
Shower Max Detector	12 tiles/$.05 \times .05$ tower	2 layers with .05/6 segmentation
Massless Gap	1 tile/$.05 \times .05$ tower	1 layer $.05 \times .05$ granularity

† Includes 157 for Massless Gap

SDC Calorimeter Cost Comparison

Calorimeter Cost (an "apples to apples" comparison)

LAC:	$135.914M	(9/6/91 M. Montgomery)
	less $1.192M	(EN/AD Mix adjustment)
	plus $1.125M	(Lowering fixture)
	plus $0.5M	(Underestimate of the cost & complexity of module testing)
	$136.347M	+ 2-4M for complete cold test
Scint. Cal.:	$136.680M	(Descope 19, 9/11/91, D. Scherbarth)
(Scint.)	Δ = $.333M	

SDC Calorimeter Cost Comparison

Additional Deltas

LAC:

1. Non optimized depth
   a. Assume no effect on barrel cost
   b. Assume 15% Red. in EC module volume (20.144 x 15%)

(Decr.) Δ = \$3.0M

2. Adding return iron back in if necessary

(Incr.) Δ = \$1.8M

Scint. Cal:

1. R&R EC/EM Scint. (Rad. Damage)

(Incr.) a. \$4.1M for first repl. (EC-EM S.M. tile assy. replacement)

(Incr.) b. \$5.8M × # of replacements. (for complete replacement of EC-EM including Pb absorber)

2a. HAC 1 ~~Long~~ trans. segmentation (from .05 × .05 to .1 × .1)

(Decr.) Δ = \$10.0M (descope 10-14)

2b. HAC 2 ~~Long~~ trans. segmentation (from .1 × .1 to .05 × .05)

(Incr.) Δ = \$8.0M (descope 12-14)

2c. EM Depth Segm. (from 2 to 1) in barrel only

(Decr.) Δ = \$3.9M (descope 12-13)

SDC Calorimeter Cost Comparison

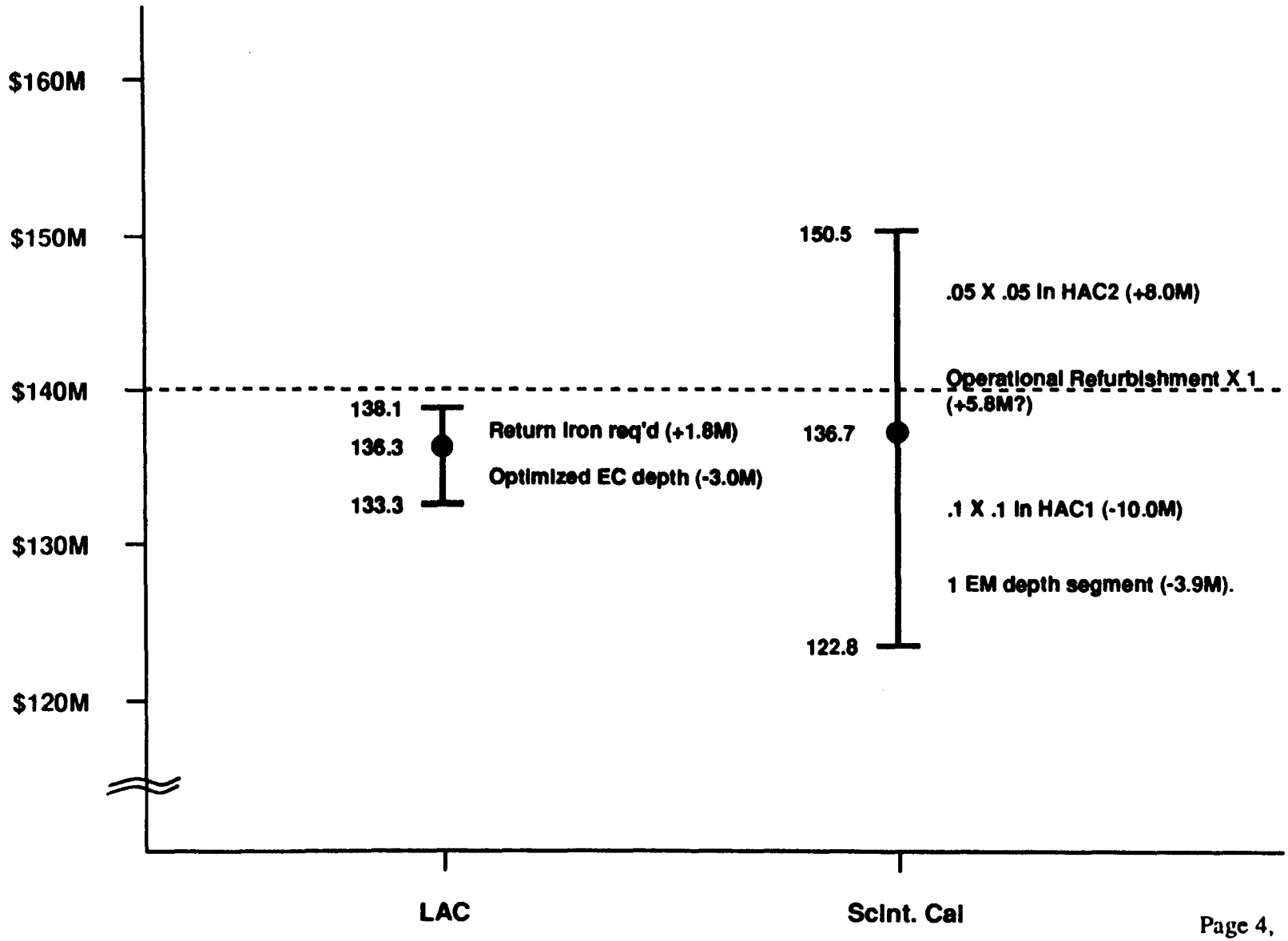

SDC Calorimeter Cost Comparison

LAC EDIA and Contingency Analysis Review

WBS	WBS Description	Base $M	EDIA $M	EDIA %	EDIA % Adj.	EDIA Adj. $M	Cont. $M	Cont. %	Cont. % Adj.	Cont. Adj. $M	Base Adj. $M	Base + Cont. Adj. $M
2.1	Barrel Calorimeter	45.7	8.5	19	-	10.2	11.9	26	-	12.3	47.4	59.7
2.1.1	Modules	19.4	2.2	11	20	3.9	4.6	24	-	4.6	21.1	25.7
2.1.2	Cryostat	12.8	2.3	18	-	2.3	3.3	26	28	3.6	12.8	16.4
2.1.3	Tooling/Fixture	10.1	2.7	27	-	2.7	3.3	33	-	3.3	10.1	13.4
2.1.4	Barrel Assy/Test/CO	2.7	1.2	44	-	1.2	0.7	26	32	0.9	2.7	3.6
2.1.5	Transportation	0.7	0.1	14	-	0.1		0		0.0	0.7	0.7
2.2	End Calorimeters	43.0	8.1	19	-	9.2	11.8	27	-	12.3	44.2	56.5
2.2.1	Modules	16.2	2.4	15	22	3.6	4.0	25	-	4.0	17.4	21.4
2.2.2	Cryostat	19.2	2.9	15	-	2.9	5.0	26	28	5.4	19.2	24.6
2.2.3	Tooling/Fixtures	4.1	1.3	32	-	1.3	1.8	44	-	1.8	4.1	5.9
2.2.4	End Cal Assy/Test/CO	2.9	1.4	48	-	1.4	0.8	28	32	0.9	2.9	3.8
2.2.5	Transportation	0.6	0.1	12	-	0.1	0.2	33	-	0.2	0.8	0.8
2.3	Test Equipment	1.7	0.1	5	20	0.3	0.6	35	44	0.7	2.0	2.7
2.4	Cryogenic System	8.3	0.4	5	10	0.8	2.8	34	-	2.8	8.7	11.5
2.5	Facilities	2.1	0.1	5	10	0.2	0.7	33	-	0.7	2.2	2.9
2.6	Support Structure	3.4	1.5	44	-	1.5	1.4	41	-	1.4	3.4	4.8
	TOTAL	104.2	18.7	18	21	22.3	29.2	28	29	30.3	107.8	138.1

Delta EDIA $M: 3.6
Delta Cont. $M: 1.1
Delta Base + Cont. $M: 4.7

SDC Calorimeter Cost Comparison

Scint. Cal "Descope 19" EDIA and Contingency Analysis Review

WBS	WBS Description	Base $M	EDIA $M	EDIA %	EDIA % Adj.	EDIA Adj. $M	Cont. $M	Cont. %	Cont % Adj.	Cont. Adj. $M	Base Adj. $M	Base + Cont. Adj. $M
2.1	Barrel Calorimeter	76.4	18.5	24	-	23.7	18.5	24	-	21.2	81.7	102.9
2.1.1	Module Components	39.8	3.2	8	20	8.0	9.6	24	30	11.9	44.5	56.5
2.1.2	Module Assembly	3.5	2.3	65	-	2.3	0.9	27	-	0.9	3.5	4.4
2.1.3	Support Structure	4.1	1.7	41	-	1.7	0.7	17	22	0.9	4.1	5.0
2.1.4	Equip/Tooling/Fixt.	8.7	1.3	15	20	1.7	2.9	33	-	2.9	9.2	12.0
2.1.6	Facilities	3.1	2.2	71	-	2.2	1.2	38	-	1.2	3.1	4.3
2.1.7	Surface Assembly	1.9	0.3	16	20	0.4	0.5	25	33	0.6	2.0	2.6
2.1.8	Program Management	15.3	7.5	49	-	7.5	2.8	18	-	2.8	15.3	18.1
2.2	End Calorimeters	32.3	8.7	27	-	10.1	9.6	30	-	9.8	33.7	43.5
2.2.1	Module Components	19.2	2.4	13	20	3.8	6.1	32	-	6.1	20.6	26.8
2.2.2	Module Assembly	1.8	0.6	33	-	0.6	0.6	33	-	0.6	1.8	2.4
2.2.3	Support Structure	3.3	1.7	52	-	1.7	0.6	18	22	0.7	3.3	4.0
2.2.4	Equip/Tooling/Fixt.	2.4	1.1	46	-	1.1	1.1	44	-	1.1	2.4	3.5
2.2.6	Facilities	0.5	0.2	40	-	0.2	0.2	32	-	0.2	0.5	0.7
2.2.7	Surface Assembly	1.2	0.3	25	-	0.3	0.3	29	33	0.4	1.2	1.6
2.2.8	Program Management	3.9	2.4	62	-	2.4	0.7	18	-	0.7	3.9	4.6
	TOTAL	108.7	27.2	25	31	33.9	28.1	26	29	31.0	115.4	146.4

Delta EDIA $M:	6.7
Delta Cont. $M:	2.9
Delta Base + Cont. $M:	9.6

SDC Calorimeter Cost Comparison

Additional Cost Impacts

1.) Calorimeter Electronics Cost:

2 EM Depth Segments, .05 × .05 HAD 1 and .1 × .1 HAD 2 for <u>both</u> cases:

	Contingency	
LAC: 9.658M	(1.25)	$12.073M
Scint.: 6.917M	(1.25)	$8.646M
	(LAC)	Δ = $3.427M

2.) Shower Max Detector Electronics Cost:

	Contingency	
LAC: 7.986M	(1.25)	$9.983M
Scint.: 5.124M	(1.25)	$6.405M
	(LAC)	Δ = $3.578M

3.) Massless Gap Cost:

Massless gap is implicit in the LAC design. Cost of massless gap for Scint Calorimeter is: $681K (Incl. Contingency)

(Scint.) Δ = $0.681M for ~~electronics~~ PMT + labor

SDC Calorimeter Cost Comparison

Additional Cost Impacts

4.) Prototype Program Cost:

The assumed beam test prototype module requirements are:

a. Full 9λ depth (EM and HAD)

b. At least 1/4 barrel length (2m)

c. > 3.1 Δφ (4 towers wide ...)

<u>LAC</u>: (from Fax received 9/6, M. Montgomery)

0.741M including electr., no contingency

wrong

If we add 40% contingency = 1.04M

<u>Scint. Cal</u>: (from Fax received 9/10, D. Scherbarth)

Total prototype & R&D: $4.368M (including 43% contingency) less $1.25M R&D

Total = $3.113M

(Scint.) Δ = $2.073M

SDC Calorimeter Cost Comparison

Additional Cost Impacts

5.) R&D Program Cost:

LAC:

(guess) $1.0M

Scint Cal:

(2 × D. Greens budget for FY92)

CAL × 2 = $2.8M
SM × 2 = $0.6M

Total = $3.4M

(Scint.) Δ = $2.4M

SDC Calorimeter Cost Comparison

Additional Cost Impacts

6.) **Installation & Test in Hall** (Items normally included in 8.2 cost):

LAC (from Fax dated 9/6/91, M. Montgomery):

15 people × 12 mo. + Engr./Mfg. supp't.
$2.391M + contingency (35%)

Total = $3.228M (w/35%)

Scint. Cal:

8.2.1.2 cal. installation (Aug. 21 version of SDC Cost Estimate) w/cont. (39%) $2.445M

8.2.2.2 cal. test.w/cont. (31%) $0.294M

Total = $2.739M (w/38% cont.)

(LAC) Δ = $0.489 M

SDC Calorimeter Cost Comparison

Additional Cost Impacts

7.) **Installation/test fixtures and equipment:**
Lowering fixture (estimate from Kaiser Engineers 7/91) = $1.125M (Incl. 30% cont.)
Use same concept for either calorimeter.

LAC:

$1.125M + 0.100M for additional material to account for higher weight
Total = $1.225M

Scint.:

$1.125M

(LAC) Δ = $0.100M

SDC Calorimeter Cost Comparison

Additional Cost Impacts

8.) EDIA expense of getting to point design:

Approx. same for both technologies Scint is higher

Δ = $0M

9.) Technology specific additional safety equipment:

<u>LAC</u> (from 9/6 Fax, M. Montgomery):

(Conservative estimate, duplication of some planned 7.3 costs?)
$0.605M (incl. 33% cont.)

<u>Scint:</u> $0

(LAC) Δ = $0.605M

SDC Calorimeter Cost Comparison

Additional Cost Impacts

10.) Hall costs:

Length:	$1/2M/m
Width:	$~1M/m
Added Length (+5m, 1/2 M/m):	2.5M
Sumps (Insulated):	0.5M (400K plus 100K EDIA)
Vent system:	0.15M (100K plus 50K EDIA)
Powertrak system:	0.535M (285K plus 250K EDIA)

Assumes that LN and LA storage dewars and plumbing are included in the LAC cryosystem cost estimate.

(LAC) Δ = $3.685M

SDC Calorimeter Cost Comparison

Additional Cost Impacts

11.) Detector Cost Deltas (muon system):

<u>Scint</u>: Basis for comparison

<u>LAC:</u>

Increased radius @ $9.9M/m
ΔR = 0.5m (9.9M/m) = $5M

Increased half length @ $3.6M/m
$\Delta\, l/2$ = 1.0m (3.6M/m) = $3.6M

(LAC) Δ = $8.6M

SDC Calorimeter Cost Comparison

Total Delta of Additional Cost Impacts:

LAC Deltas: +$20.484M

Scint Cal Deltas: +$5.154M

(LAC) Δ = +$15.330M

SDC Calorimeter Cost Comparison

Calorimeter Cost Comparison Summary

	Scint. Cal.	LAC
Calorimeter Cost ("apples to apples")	136.7M	136.3M
EDIA and Contingency Adjustment	+ 9.6M	+4.7M
Additional Cost Impacts	+5.2M	+20.5M
Total:	151.5M	161.5M

Δ (LAC) 10.0 M

CALORIMETER REVIEW AND TECHNICAL BOARD MEETING
SEPTEMBER 12 -14, 1991
SSCL

Presentation by:

David Bintinger

SSCL

Sept. 13-91
D.B.

Integration Comparison
of
Scintillator Calorimeter Detector
and
Liquid Argon Calorimeter Detector

SCHEMATIC OF BOXES ON TWO CALORIMETERS WITH FIBER TRACKER

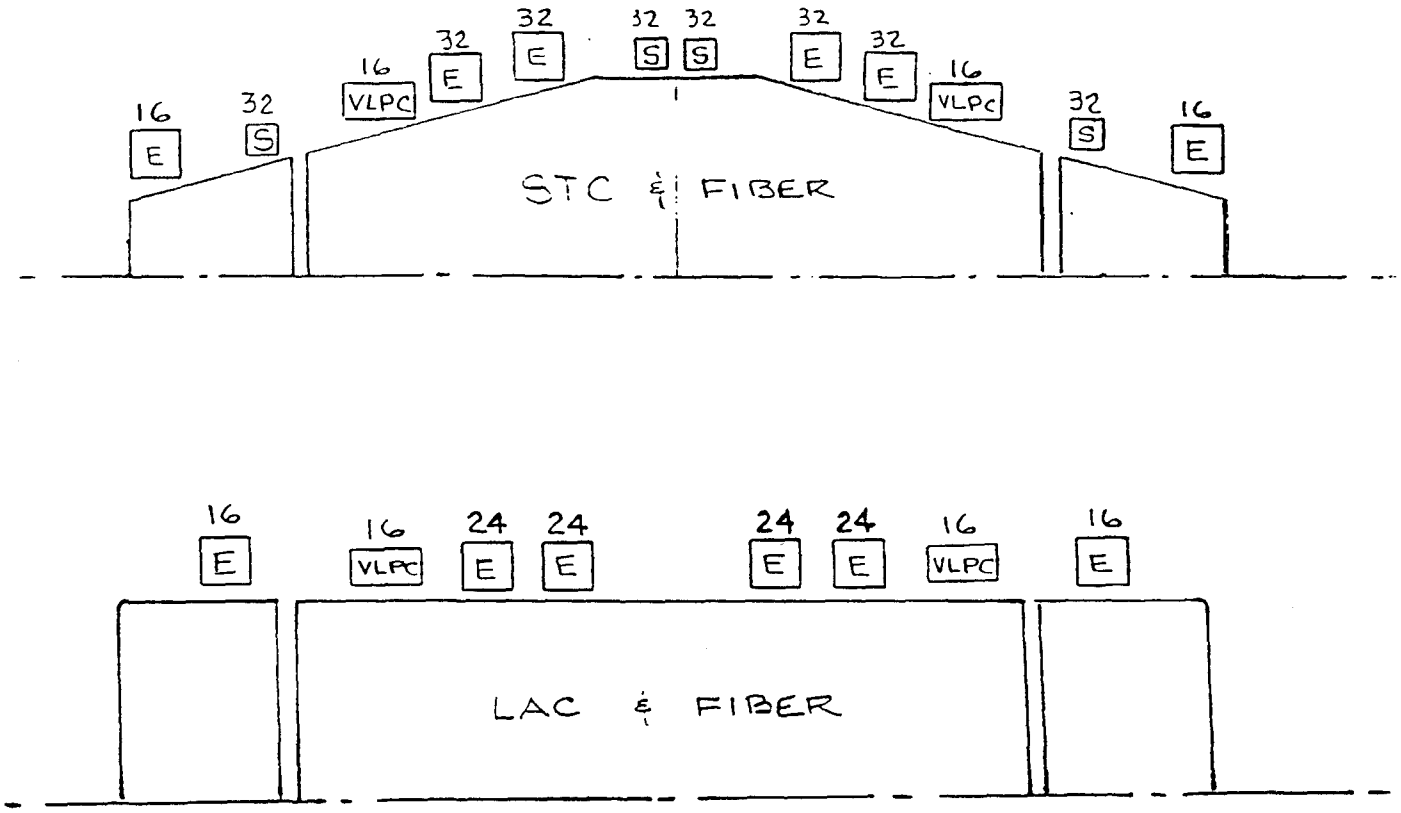

S STC CALIBRATION SOURCE

VLPC FIBER VLPC CRYOSTAT

E ELECTRONIC CRATE

D ELECTRICAL DISTRIBUTION BOXES [NOT SHOWN]

SCHEMATIC OF BOXES ON TWO CALORIMETERS WITH STRAW TRACKER

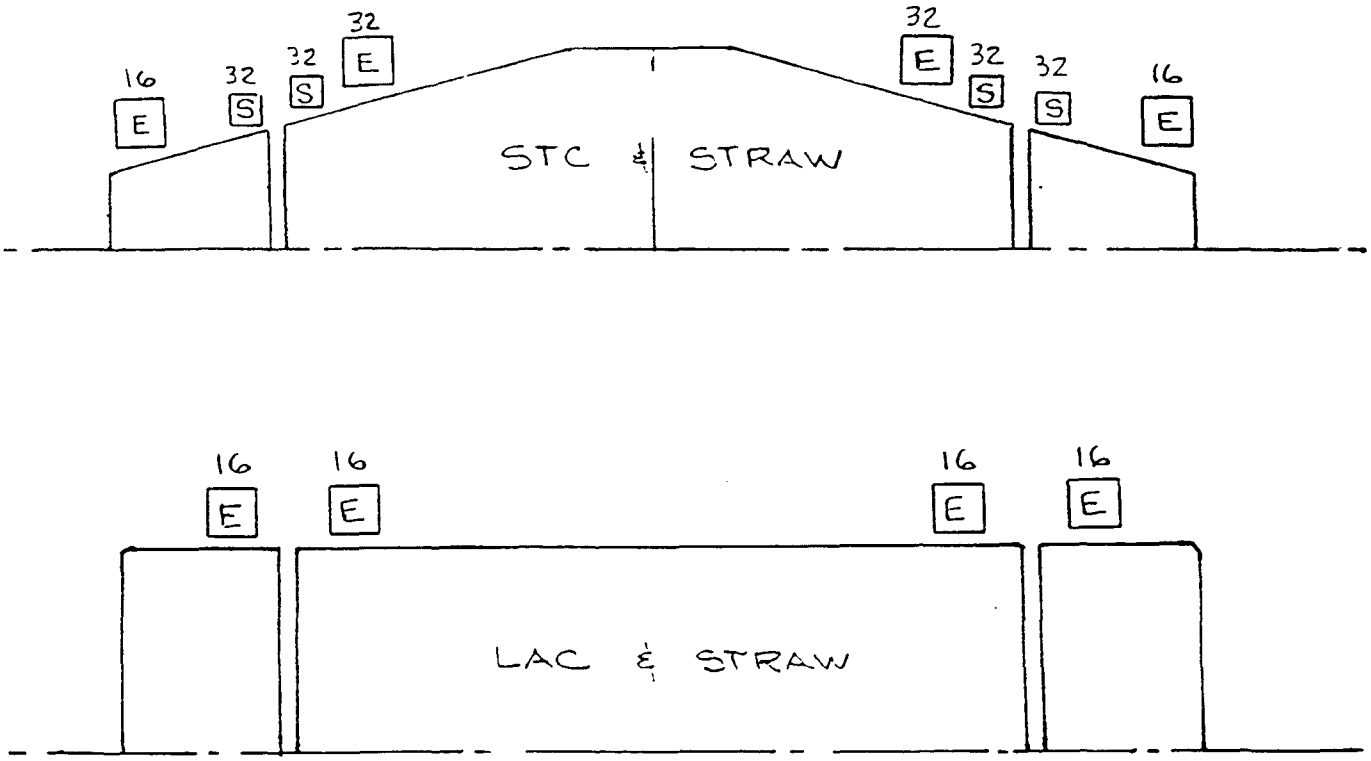

S STC CALIBRATION SOURCE

VLPC FIBER VLPC CRYOSTAT

E ELECTRONIC CRATE

D ELECTRICAL DISTRIBUTION BOXES [NOT SHOWN]

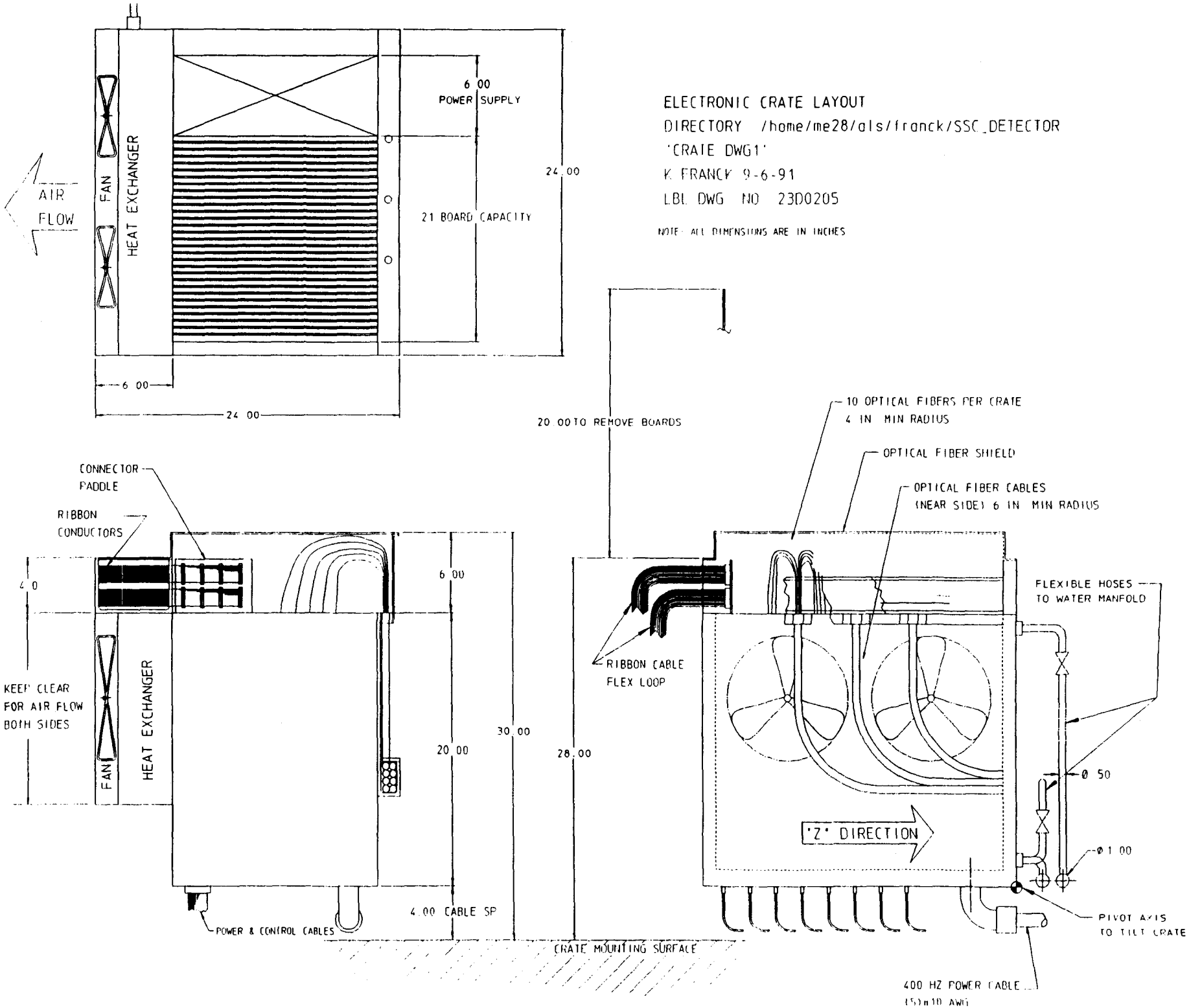
ELECTRONIC CRATE LAYOUT
DIRECTORY /home/me28/als/franck/SSC_DETECTOR
'CRATE DWG1'
K. FRANCK 9-6-91
LBL DWG NO 23D0205
NOTE: ALL DIMENSIONS ARE IN INCHES
AIR FLOW
FAN
HEAT EXCHANGER
6.00
POWER SUPPLY
24.00
21 BOARD CAPACITY
6.00
24.00
20.00 TO REMOVE BOARDS
10 OPTICAL FIBERS PER CRATE
4 IN MIN RADIUS
OPTICAL FIBER SHIELD
OPTICAL FIBER CABLES
(NEAR SIDE) 6 IN MIN RADIUS
CONNECTOR PADDLE
RIBBON CONDUCTORS
4.0
6.00
KEEP CLEAR FOR AIR FLOW BOTH SIDES
FAN
HEAT EXCHANGER
30.00
20.00
28.00
RIBBON CABLE FLEX LOOP
FLEXIBLE HOSES TO WATER MANFOLD
Ø .50
'Z' DIRECTION
Ø 1.00
4.00 CABLE SP
POWER & CONTROL CABLES
CRATE MOUNTING SURFACE
PIVOT AXIS TO TILT CRATE
400 HZ POWER CABLE
(5) #10 AWG

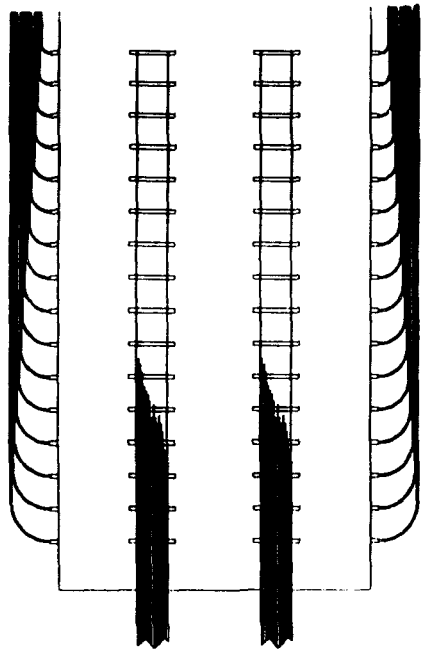

VLPC CRATE LAYOUT
PRELIMINARY LAYOUT
DIRECTORY: /home/me28/als/franck/SSC_DETECTOR
'VLPC CRATE DWG1'
8/21/91 K FRANCK

NOTE ALL DIMENSIONS ARE IN INCHES.

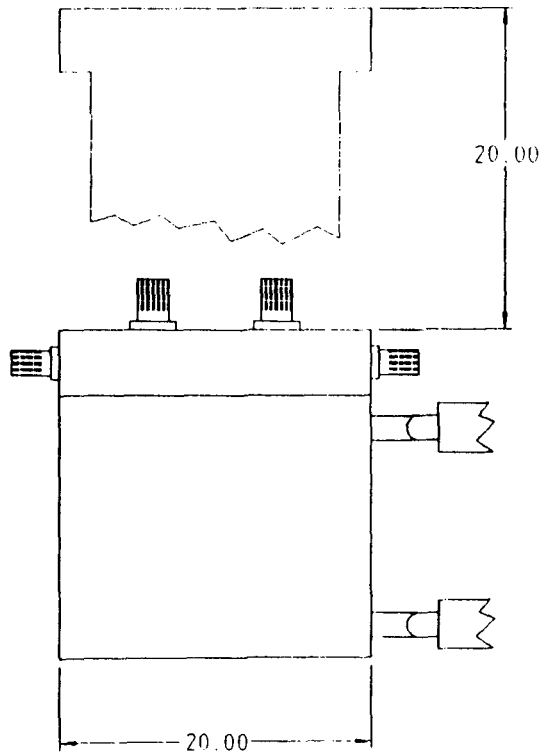

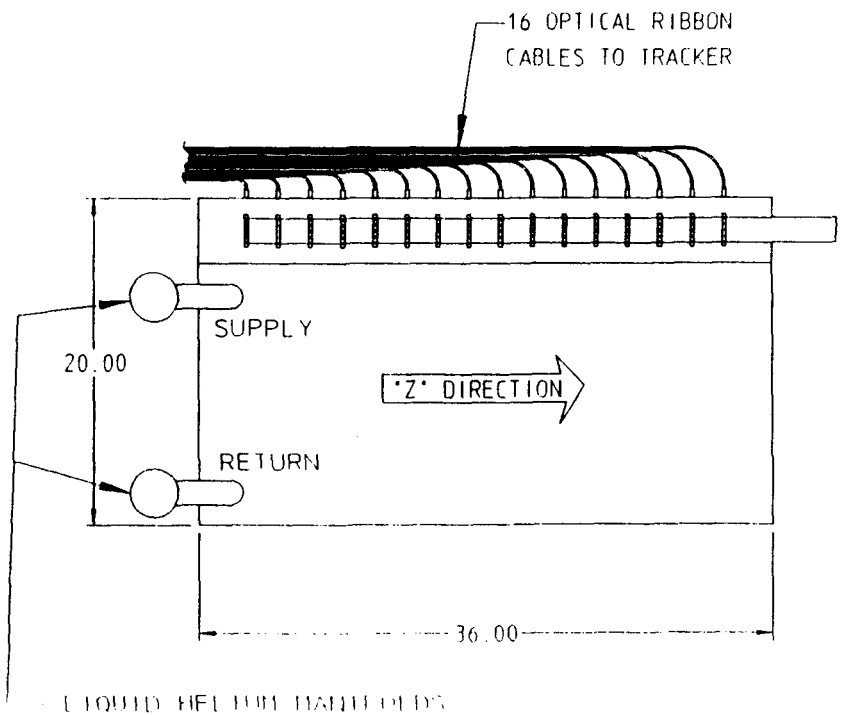

CRATE & ACCESS RADIAL SPACE

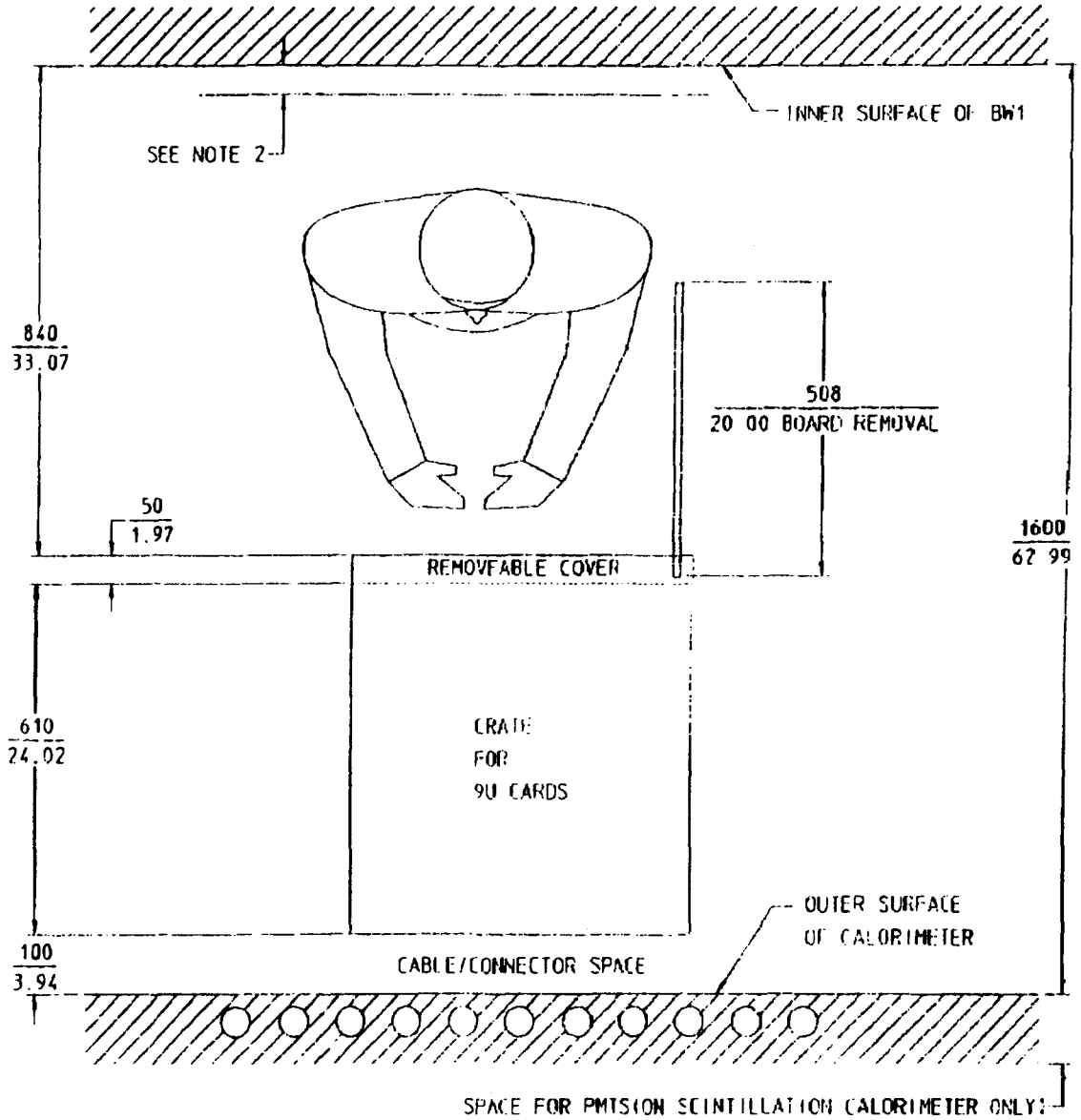

NOTE 1 ALL DIMENSIONS ARE IN MM OVER (INCHES)

2 AT SOME LOCATIONS, SOME PIPES/CABLES & SUPPORTS WILL REDUCE THIS CLEARANCE

FIGURE 1 - MINIMUM UTILITIES VIA THE CRYO STACK

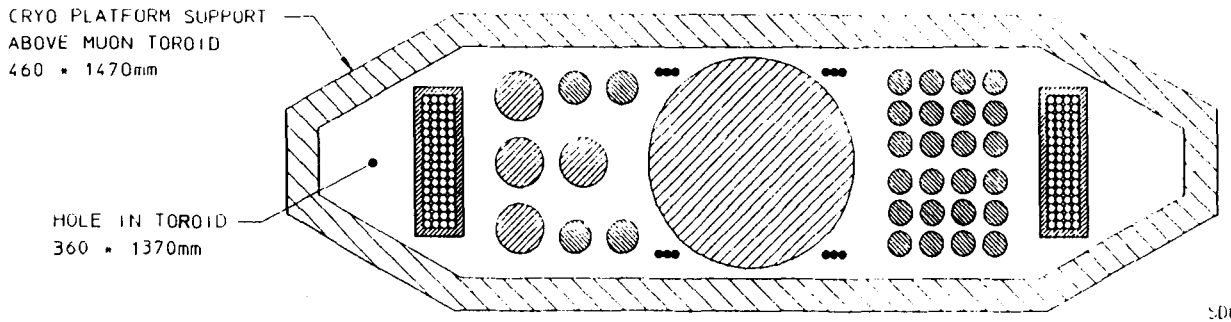

SDC DETECTOR
CRYO STACK SECTION
DIRECTORY /home/me28/dts/franck/SDC DETECTOR
'CRYOSTACK XSEC1'
K FRANCK 9-5-91

NOTE ALL DIMENSIONS ARE IN MILLIMETERS

FIGURE 2 - ALL CALORIMETER BARREL & TRACKER UTILITIES VIA THE CRYO STACK

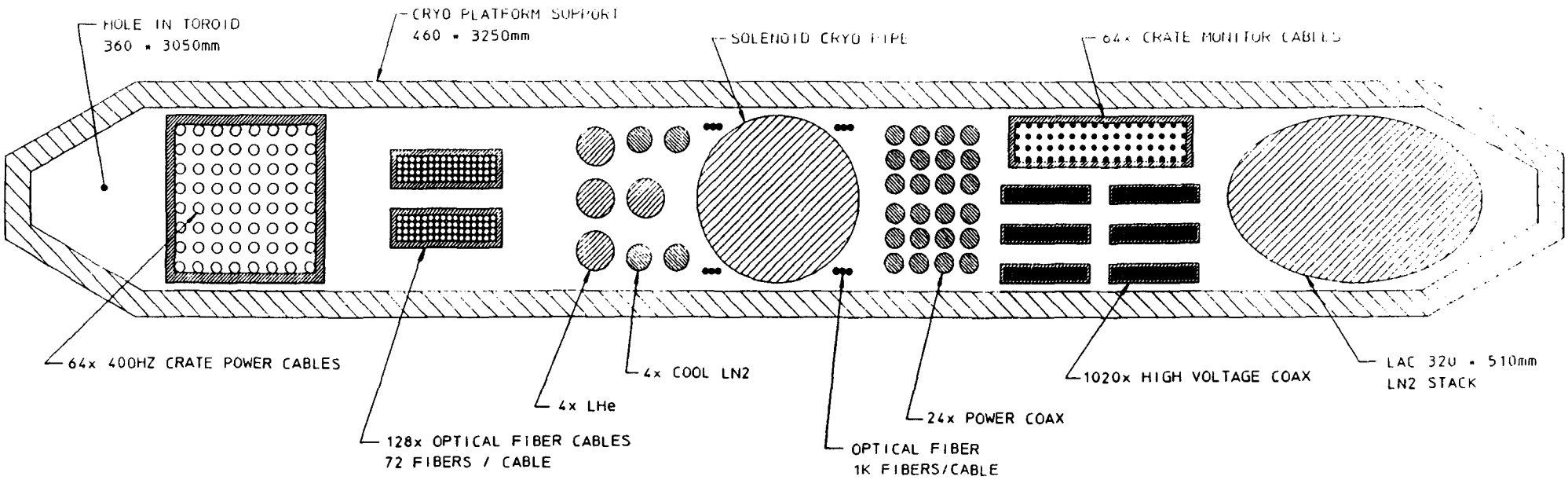

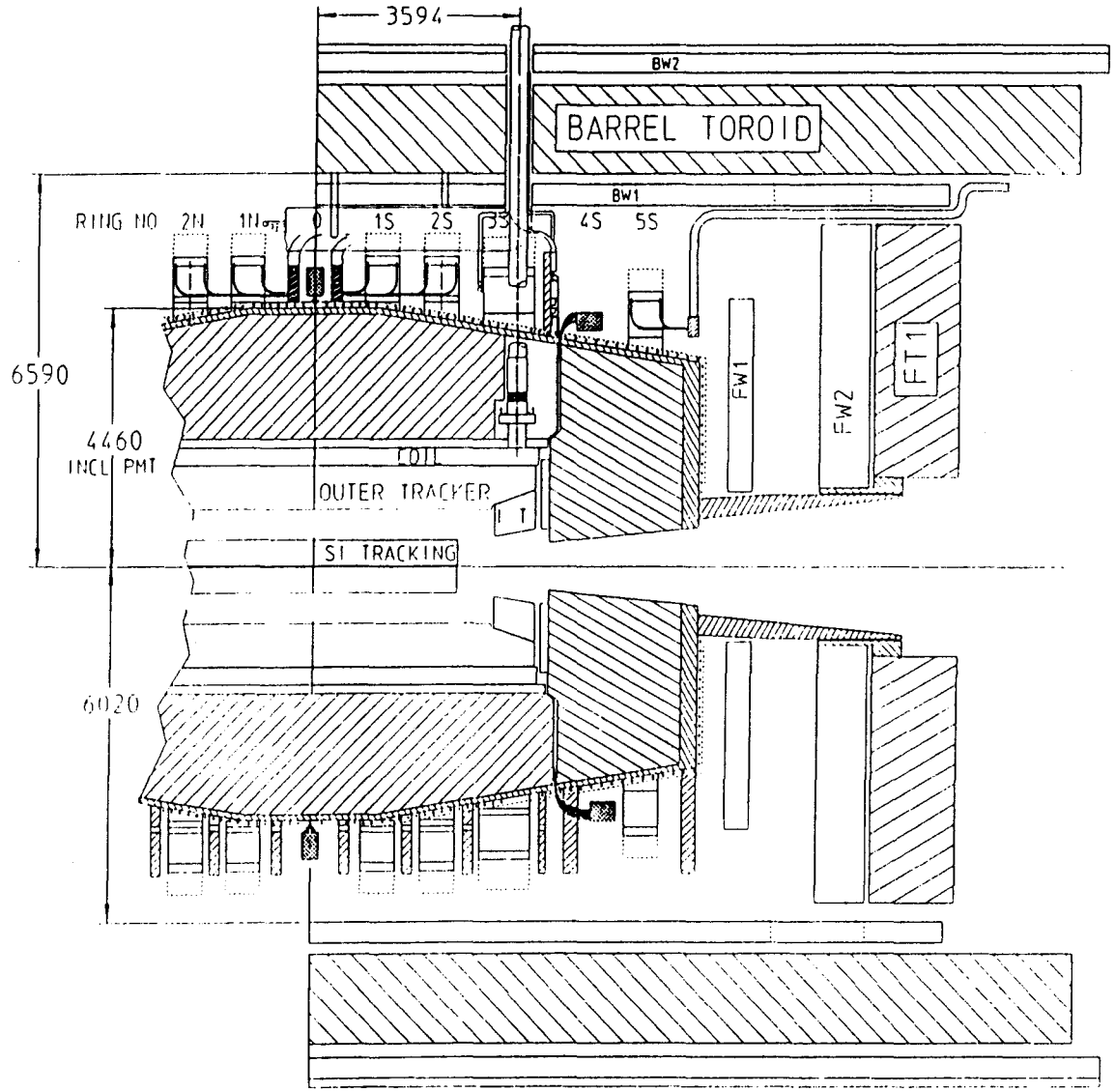

SCINTILLATOR CALORIMETER CRATE LAYOUT WITH VLPC'S

DESCOPE OPTION 2 OF SEPT 11, 1991

LBL DWG NO 23D0265 Y MINAMIHARA

filename smbarg/bdff/scl_crate_lo_8_25_91

0 5 M

NOTE ALL DIMENSIONS ARE IN MILLIMETERS

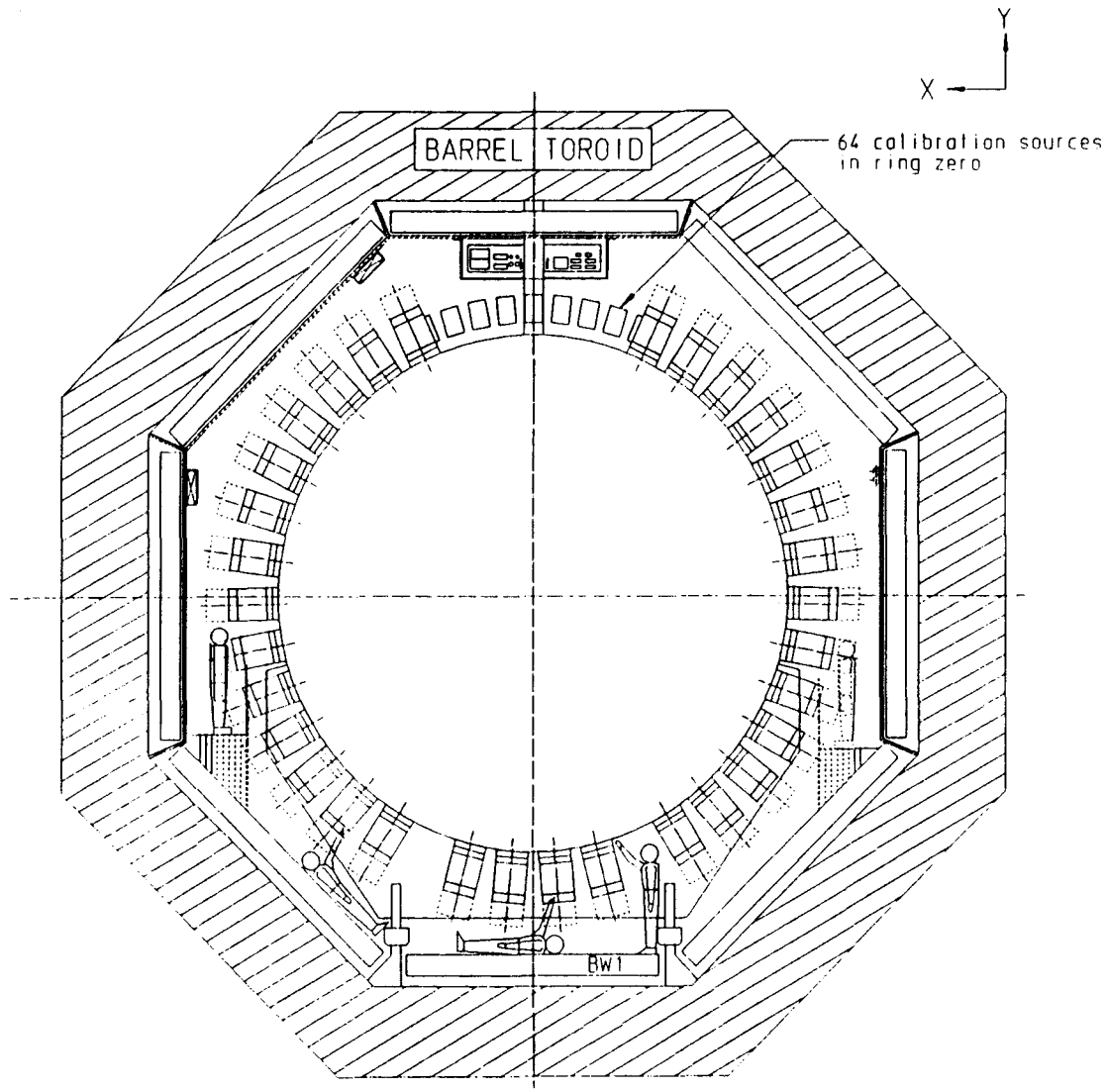

RINGS 1 AND 2 32 crates

SCINTILLATOR CALORIMETER CRATE LAYOUT WITH VLPC'S

DESCOPE OPTION 2 OF SEPT 11, 1991

LBL DWG NO 23D0265 Y MINAMIHARA

filename smbara/bstf/scl_crate_lo_8_25_91

0 5 M

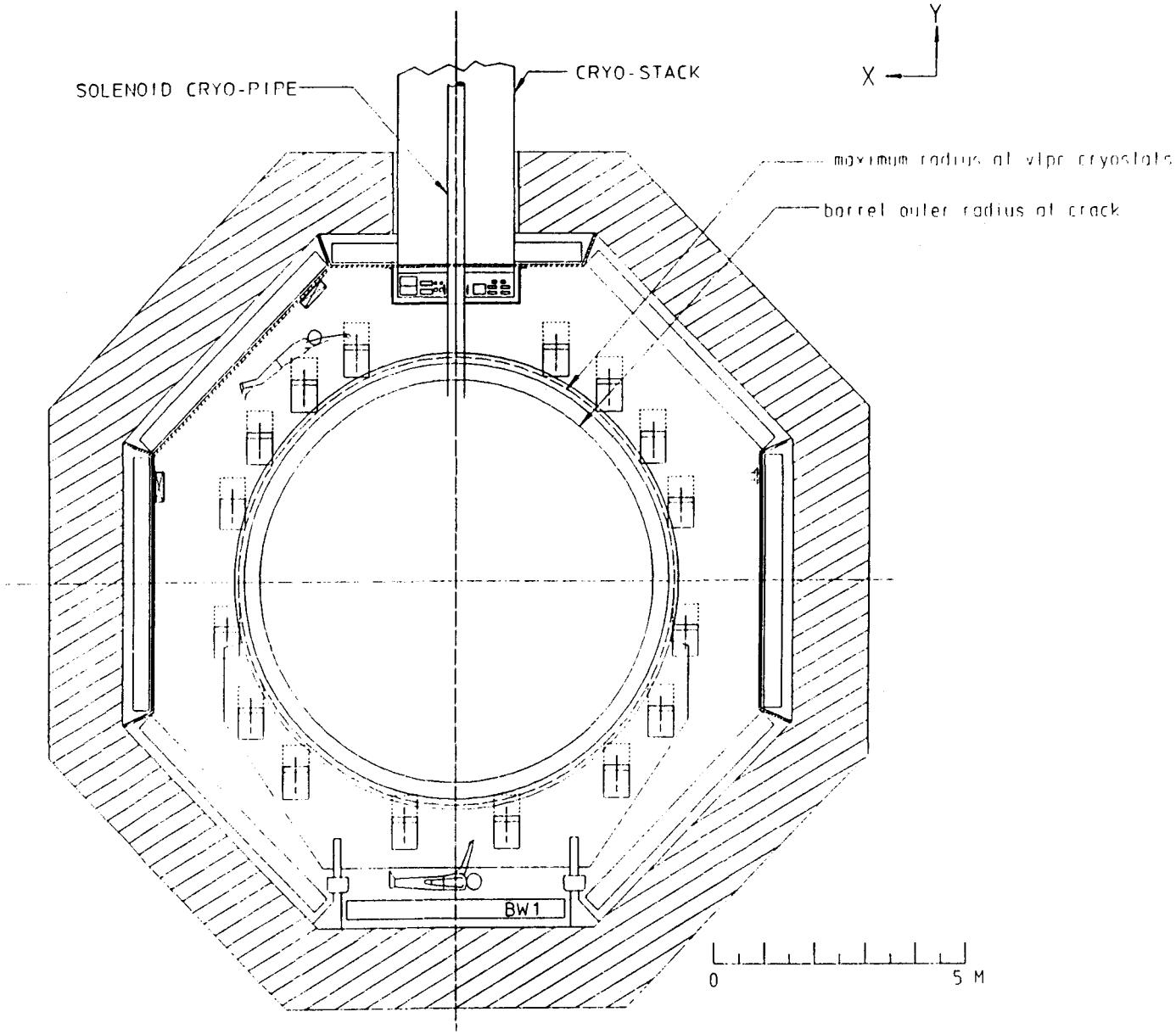

RING 3 16 vlpc_cryostats

SCINTILLATOR CALORIMETER CRATE LAYOUT WITH VLPC'S

DESCOPE OPTION 2 OF SEPT 11, 1991

LBL DWG NO. 2300765 Y NINAMIHARA

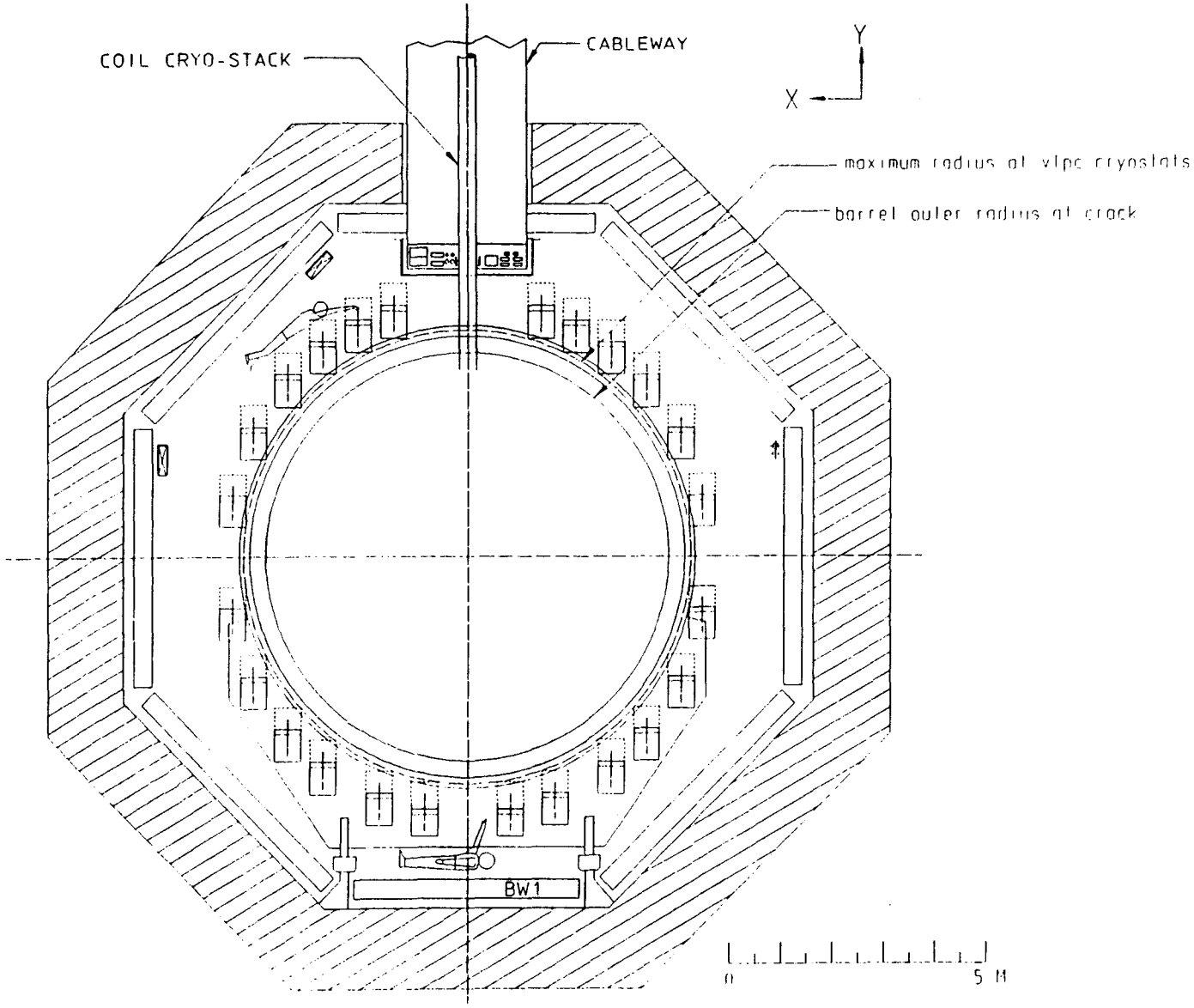

RING 3 ALTERNATE 24 vlpc_cryostats

SCINTILLATOR CALORIMETER CRATE LAYOUT WITH VLPC'S

DESCOPE OPTION 2 OF SEPT 11, 1991

[illegible] MIYAMIHARA

[illegible]

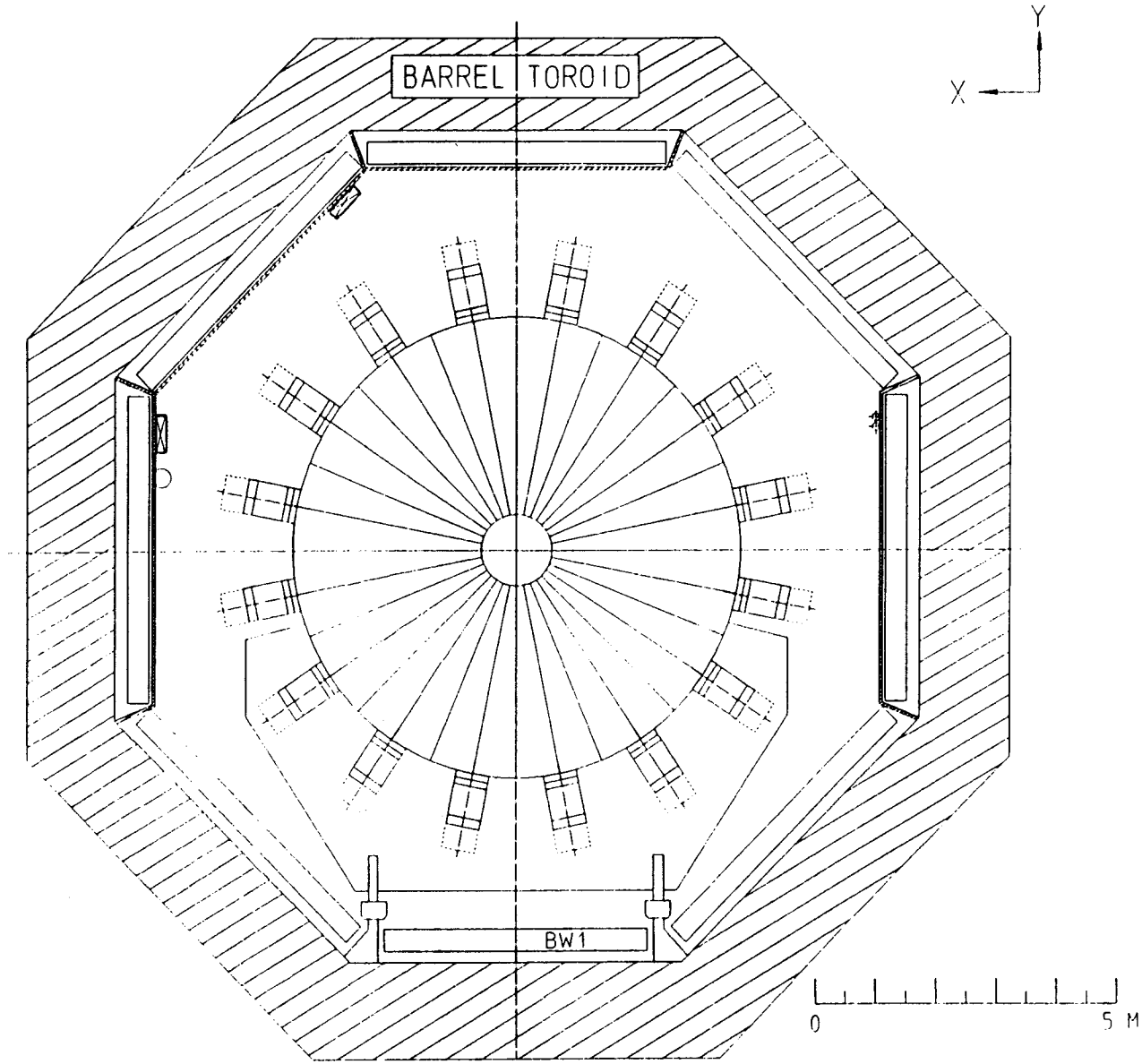

RING 5 16 crates

SCINTILLATOR CALORIMETER CRATE LAYOUT WITH VLPC'S

DESIGN OPTION 2 OF SEPT 11, 1991

LPI DWG NO 23D0265 Y MINAMIHARA

filename: mbarazhoff/ssl crate_lo 8_25_91

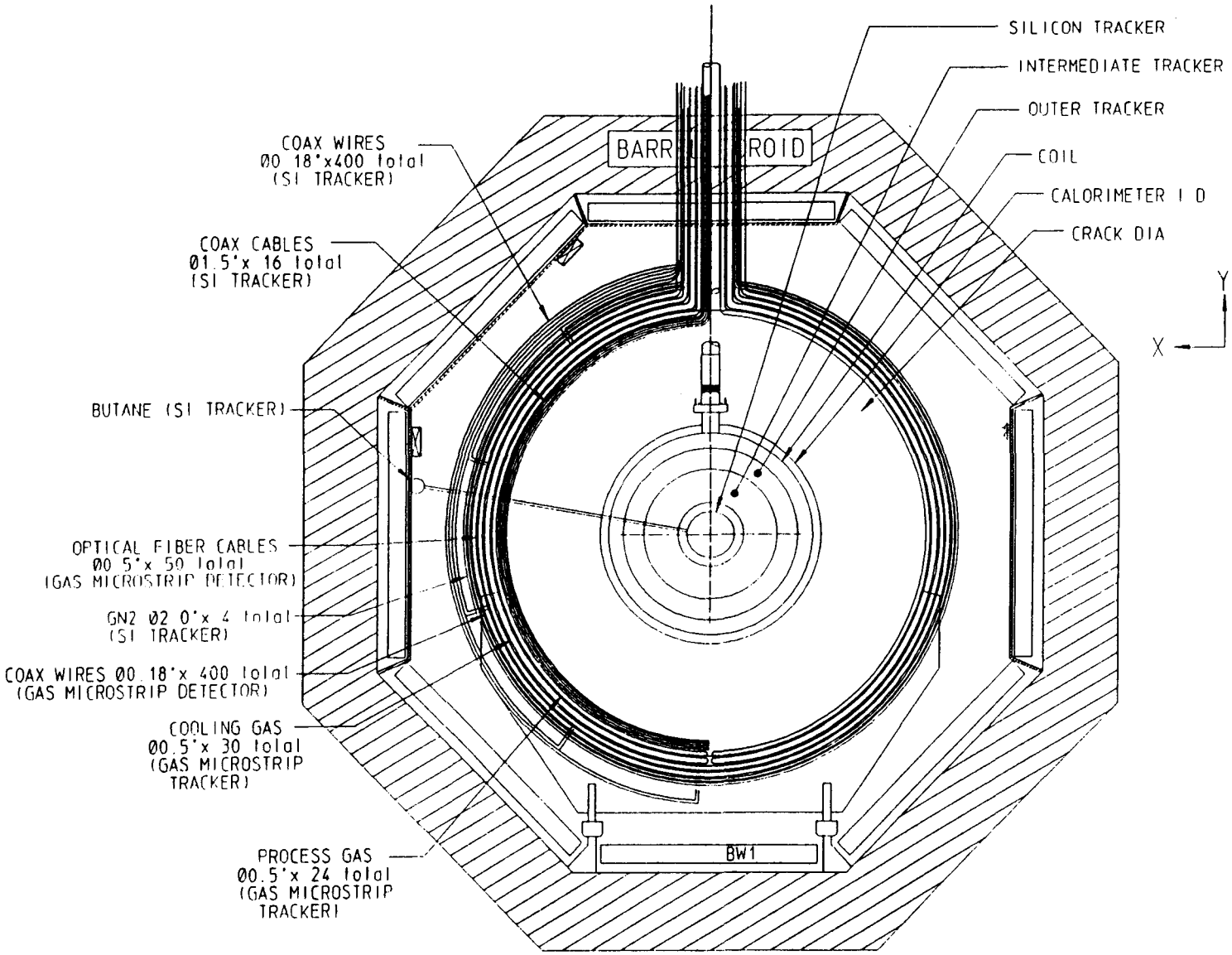

CROSS SECTION AT BAREL CAL CRACK

SCINTILLATOR CALORIMETER CRATE LAYOUT WITH VLPC'S

DESCOPE OPTION 2 OF SEPT 11, 1991

LBL DWG NO 23D0265 Y MINAMIHARA

0 5 M

NOTE ALL DIMENSIONS ARE IN MILLIMETERS

f:\homes\mihara\hull\sci_crate_to 8.25.91

SENT BY:SSC/CDG ; 9-12-91 ; 7:10PM ; MAGNET & C F DIVS→ 9121470886174;# 2

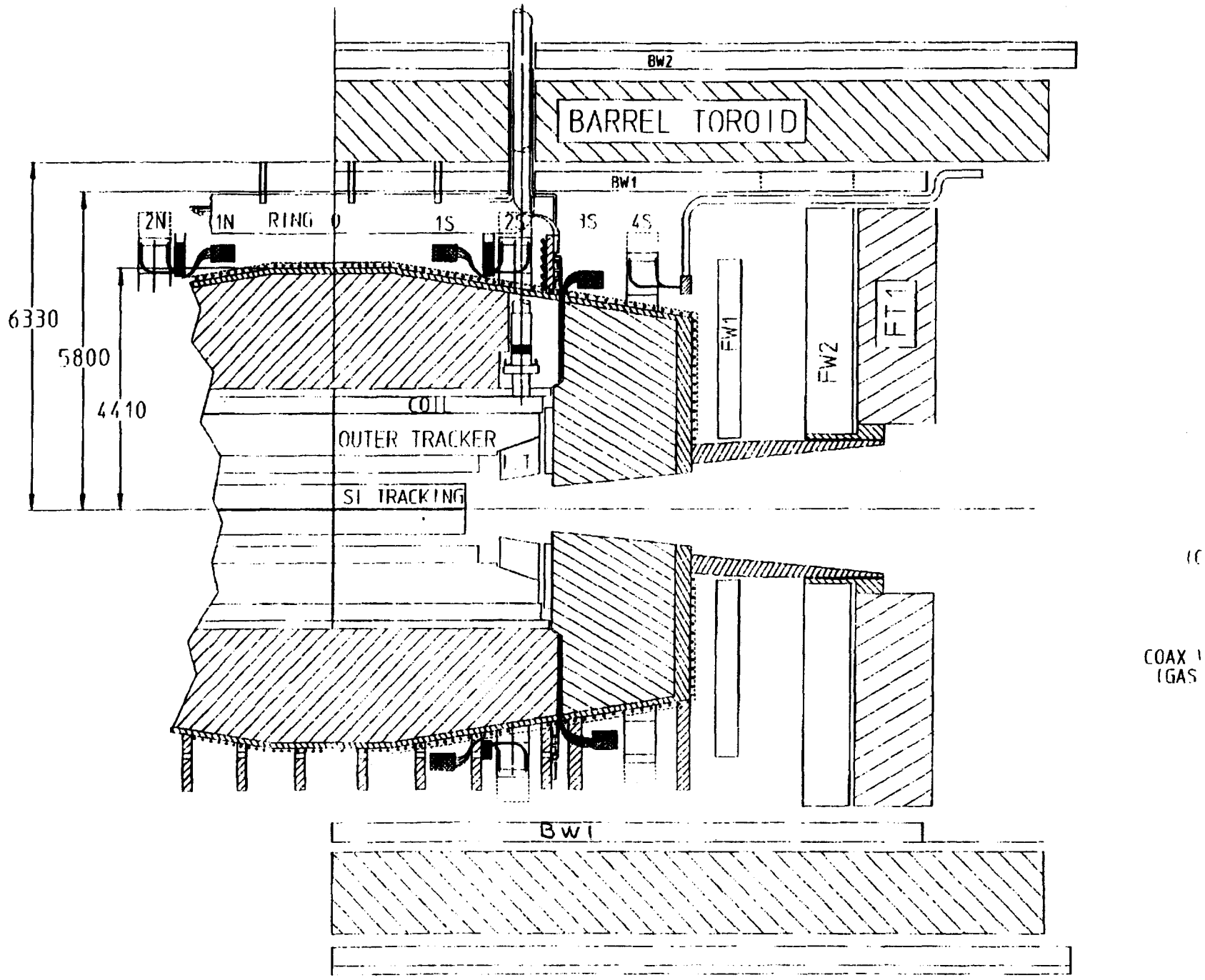

SCINTILLATOR CALORIMETER CRATE LAYOUT

STRAW TRACKER (NO VLPCs)

DESCOPE OPTION 2, SEPT 12, 1991

LBL DWG NO 23D0295 Y MINAMIHARA/D SHUMAN

NOTE: ALL DIMENSIONS ARE IN MILLIMETERS

0 5 M

filename: mbara/half/crate_to_sc_straw.tr

SENT BY:SSC/CDG ; 3-12-91 ; 7:11PM ; MAGNET & C F DIVS→ 9121470861 74;# 3

STRAW TRACKER (NO VLPCs)
DESCOPE OPTION 2, SEPT 12, 1991
LBL DWG NO. 23D0295
Y.MINAMIHARA/D SHUMAN

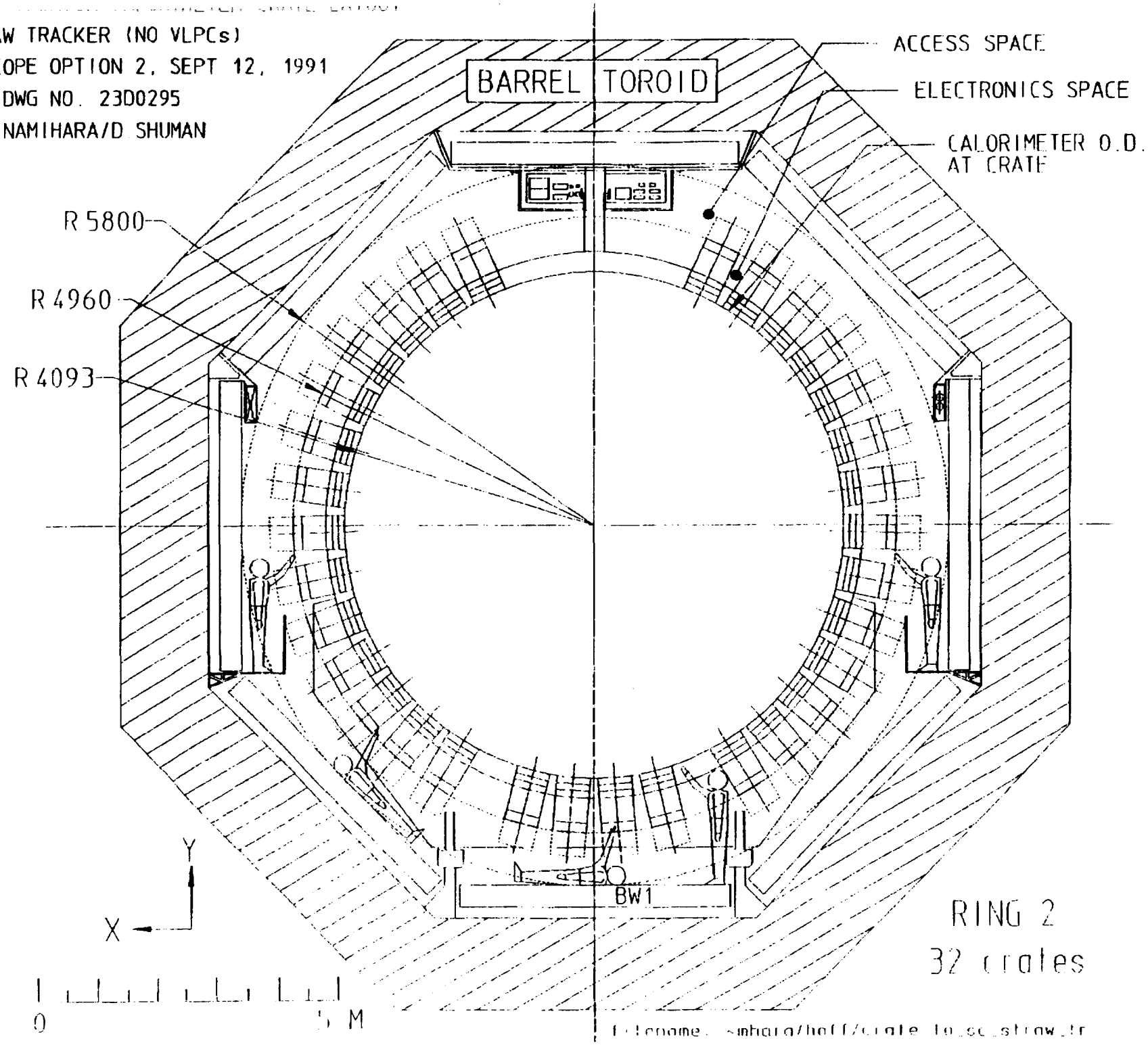

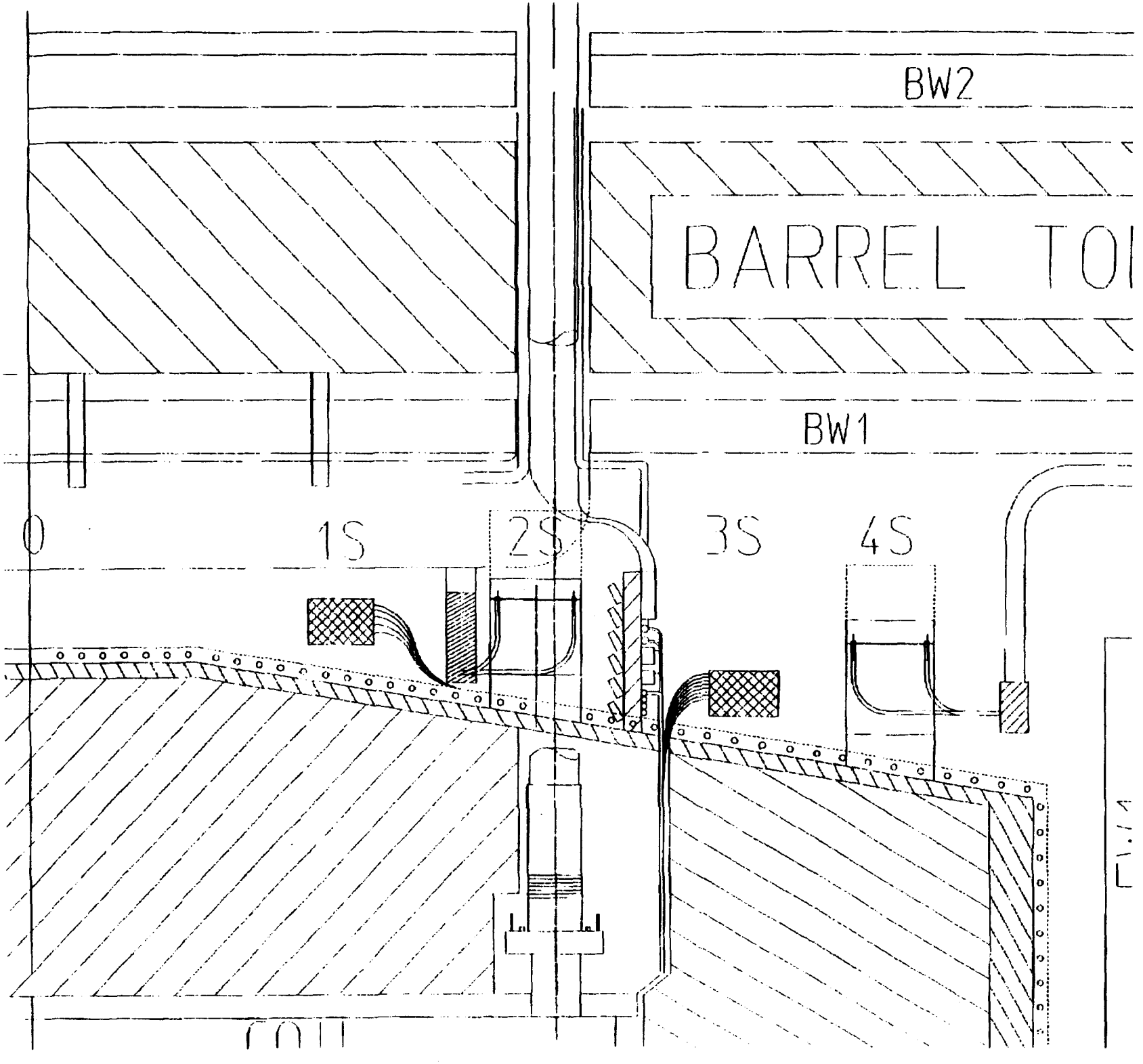
BW2
BARREL TOI
BW1
0
1S
2S
3S
4S

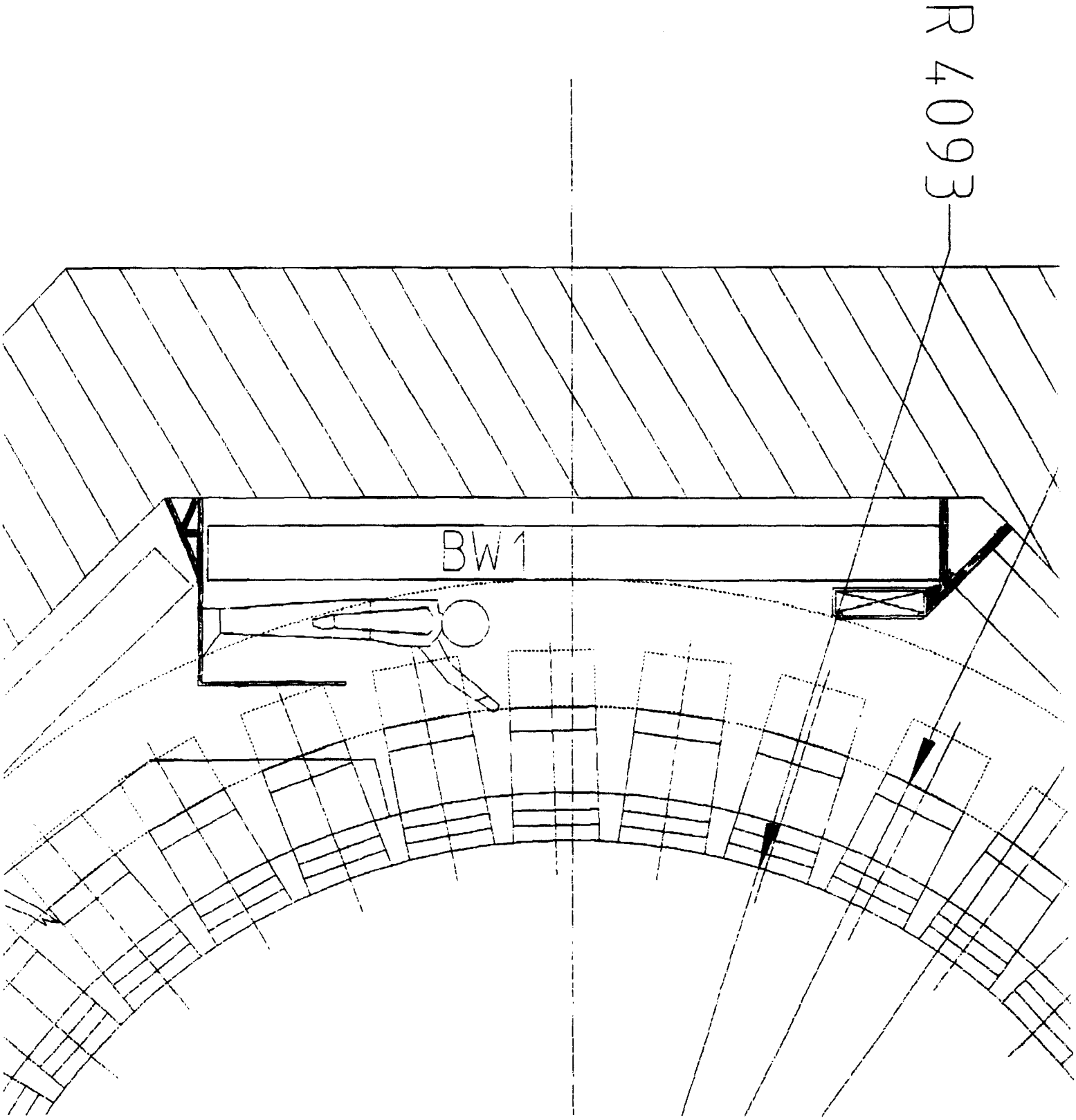
R 4093
BW1

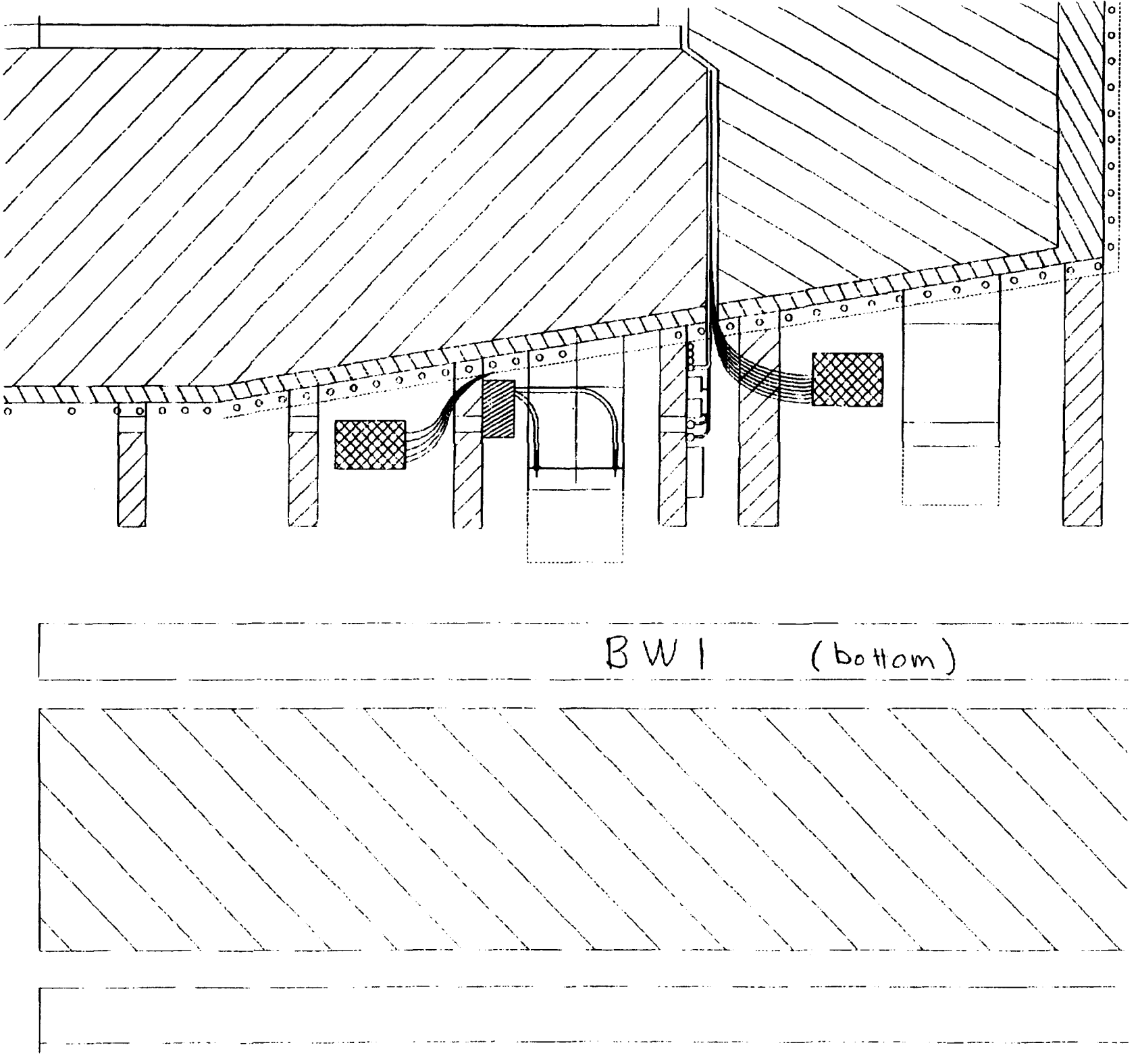
BW1 (bottom)

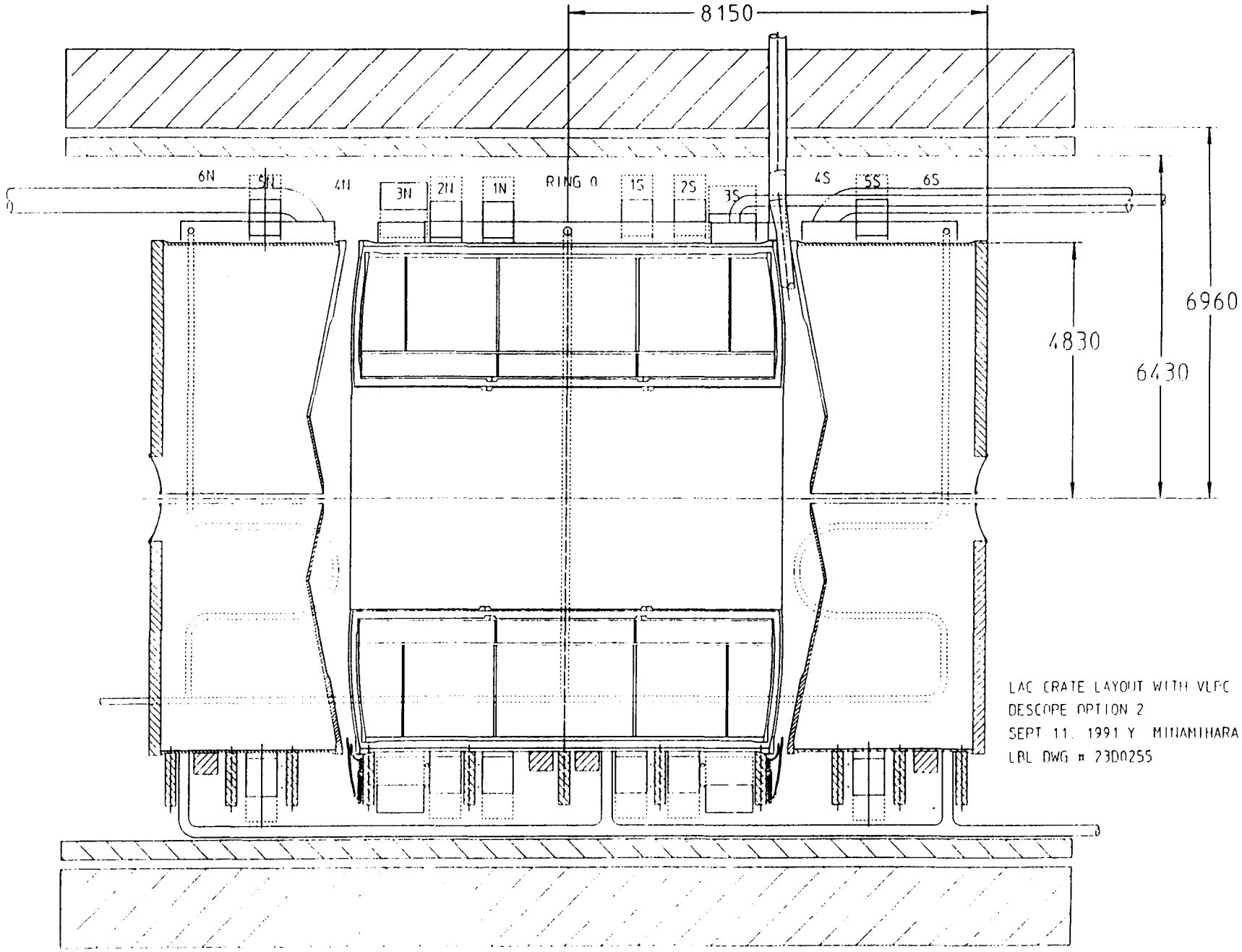
8150
6N
5N
4N
3N
2N
1N
RING 0
1S
2S
3S
4S
5S
6S
6960
6430
4830
LAC CRATE LAYOUT WITH VLPC
DESCOPE OPTION 2
SEPT 11, 1991 Y. MINAMIHARA
LBL DWG # 23D0255

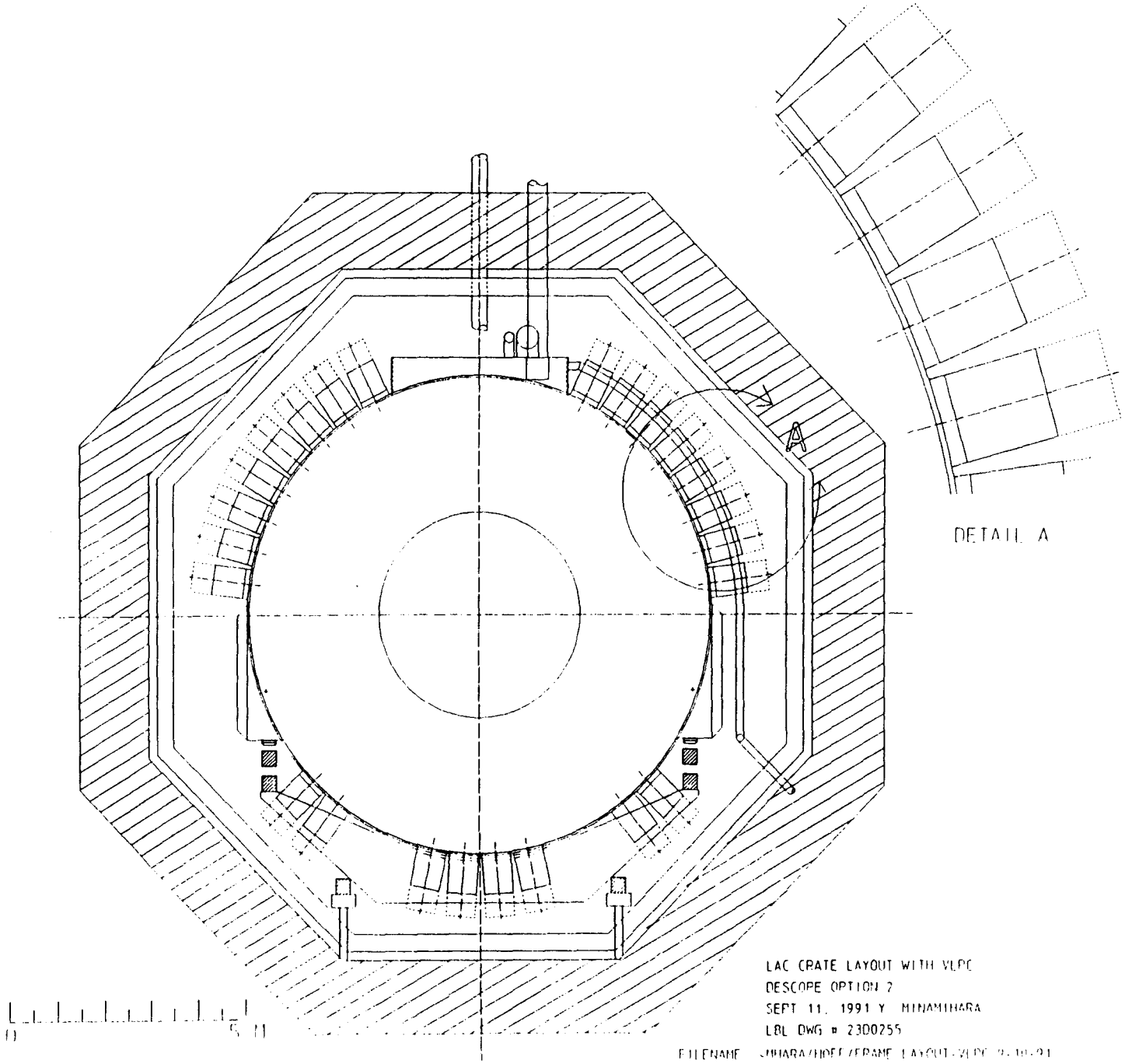

FIG 1.2 ELECTRONIC CRATES

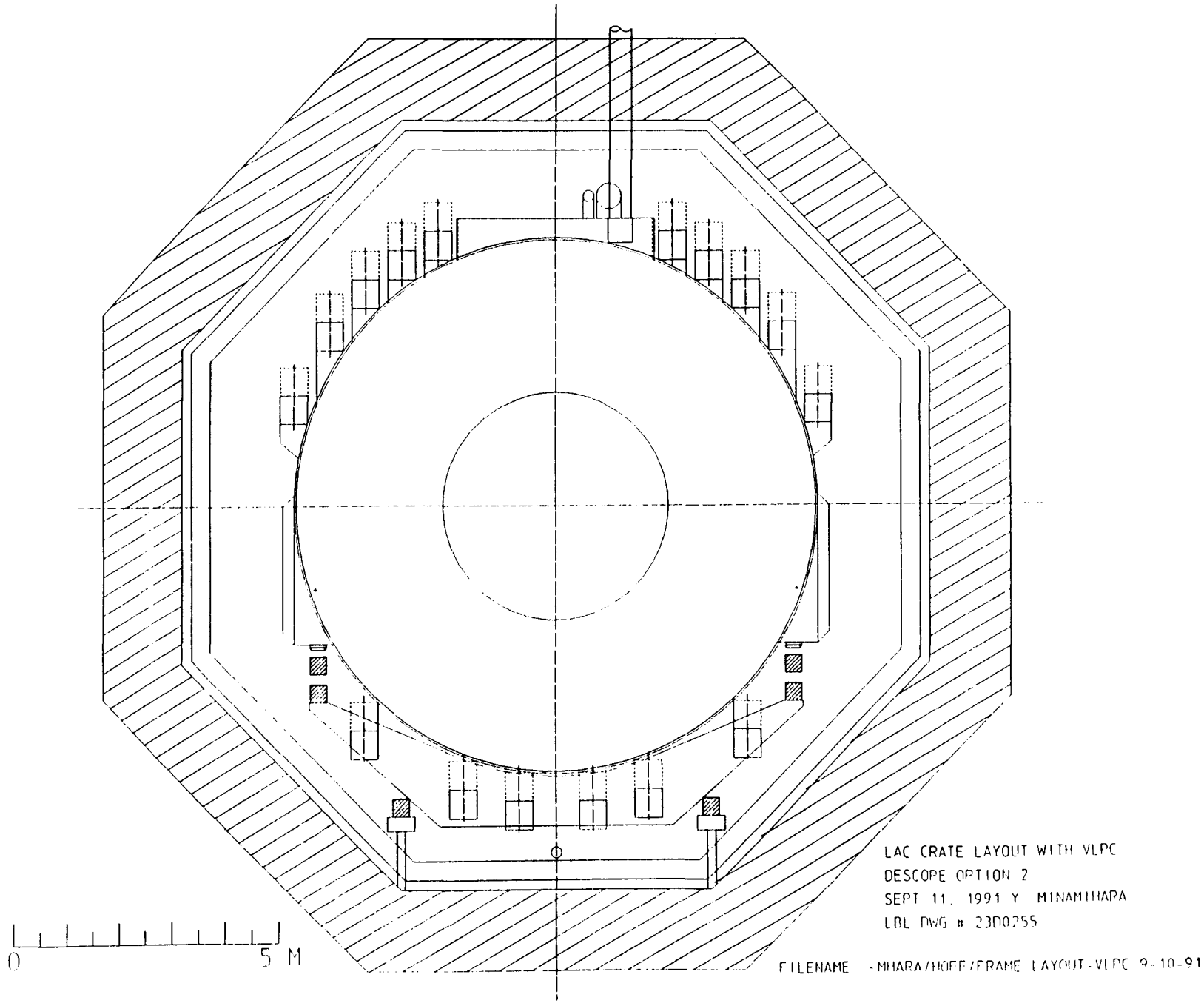
LAC CRATE LAYOUT WITH VLPC
DESCOPE OPTION 2
SEPT 11, 1991 Y MINAMIHARA
LBL DWG # 23D0255
FILENAME -MHARA/HOFF/FRAME LAYOUT-VLPC 9-10-91
0
5 M

RING 3 VLPCS

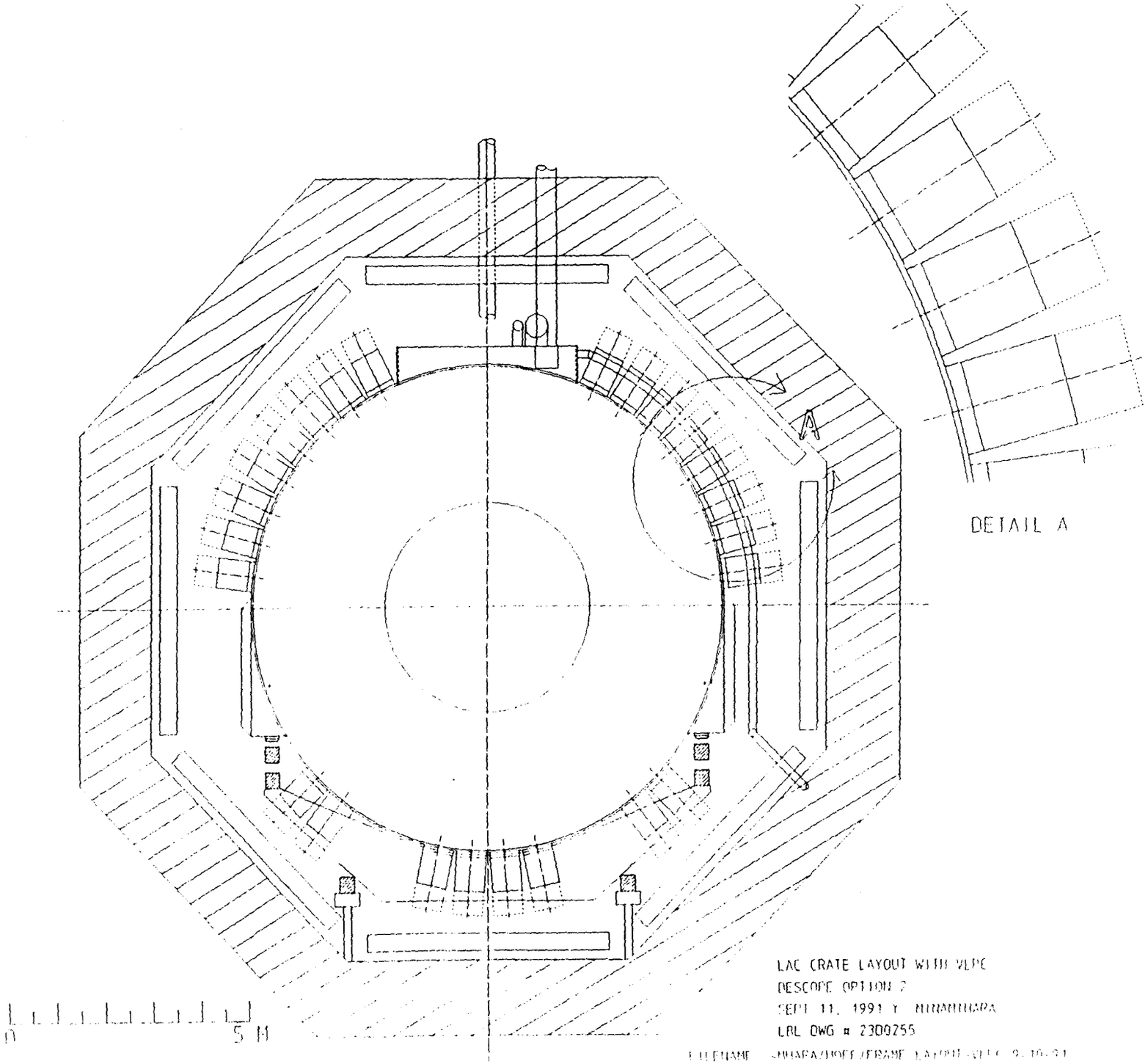

FIG. [illegible] ELECTRONIC CRATES

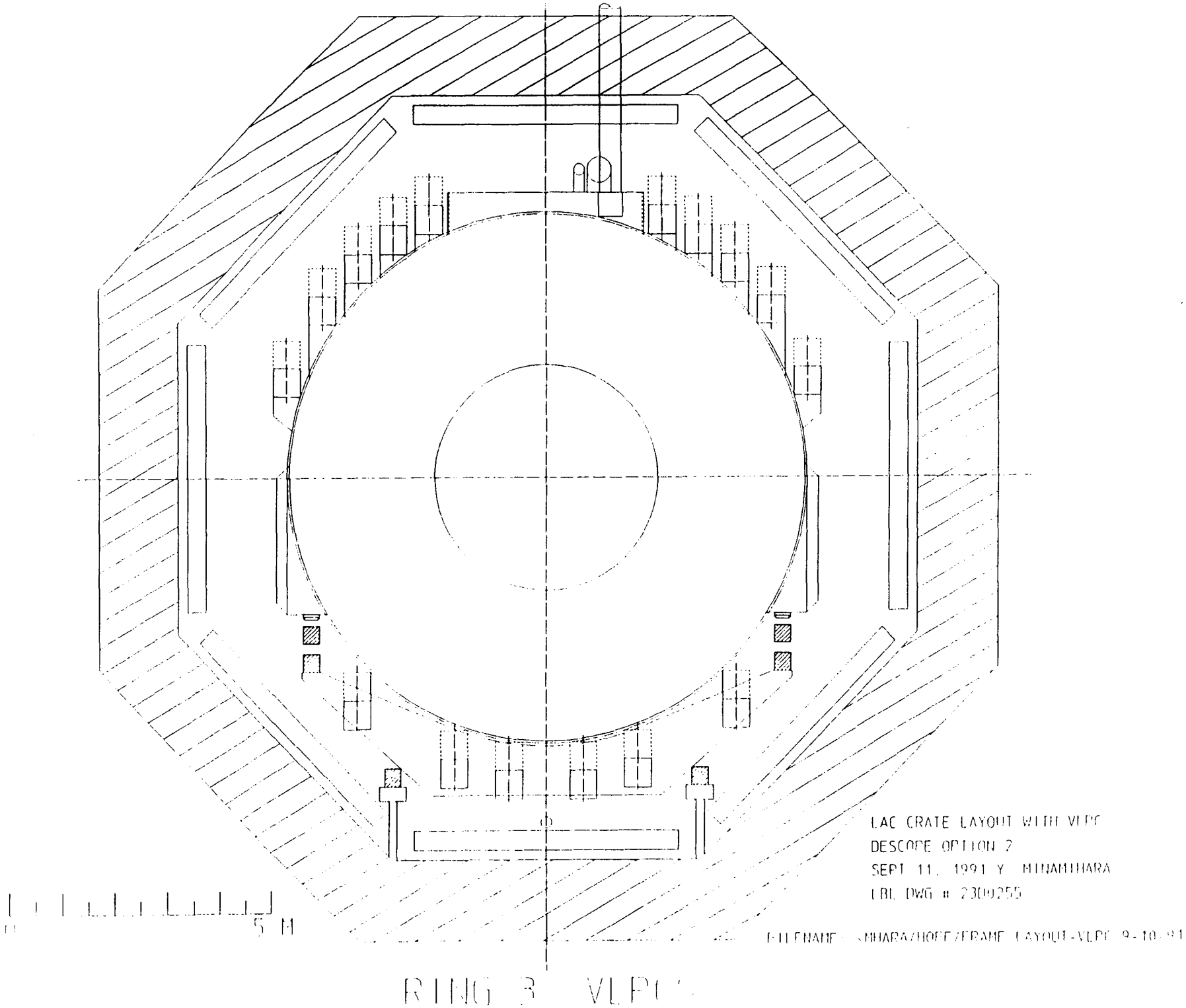
LAC CRATE LAYOUT WITH VLPC
DESCOPE OPTION 2
SEPT 11, 1991 Y. MINAMIHARA
LBL DWG # 2309259
0
5 M
FILENAME: MINAMIHARA/HOPE/FRAME LAYOUT-VLPC 9-10-91
RING 3 VLPC

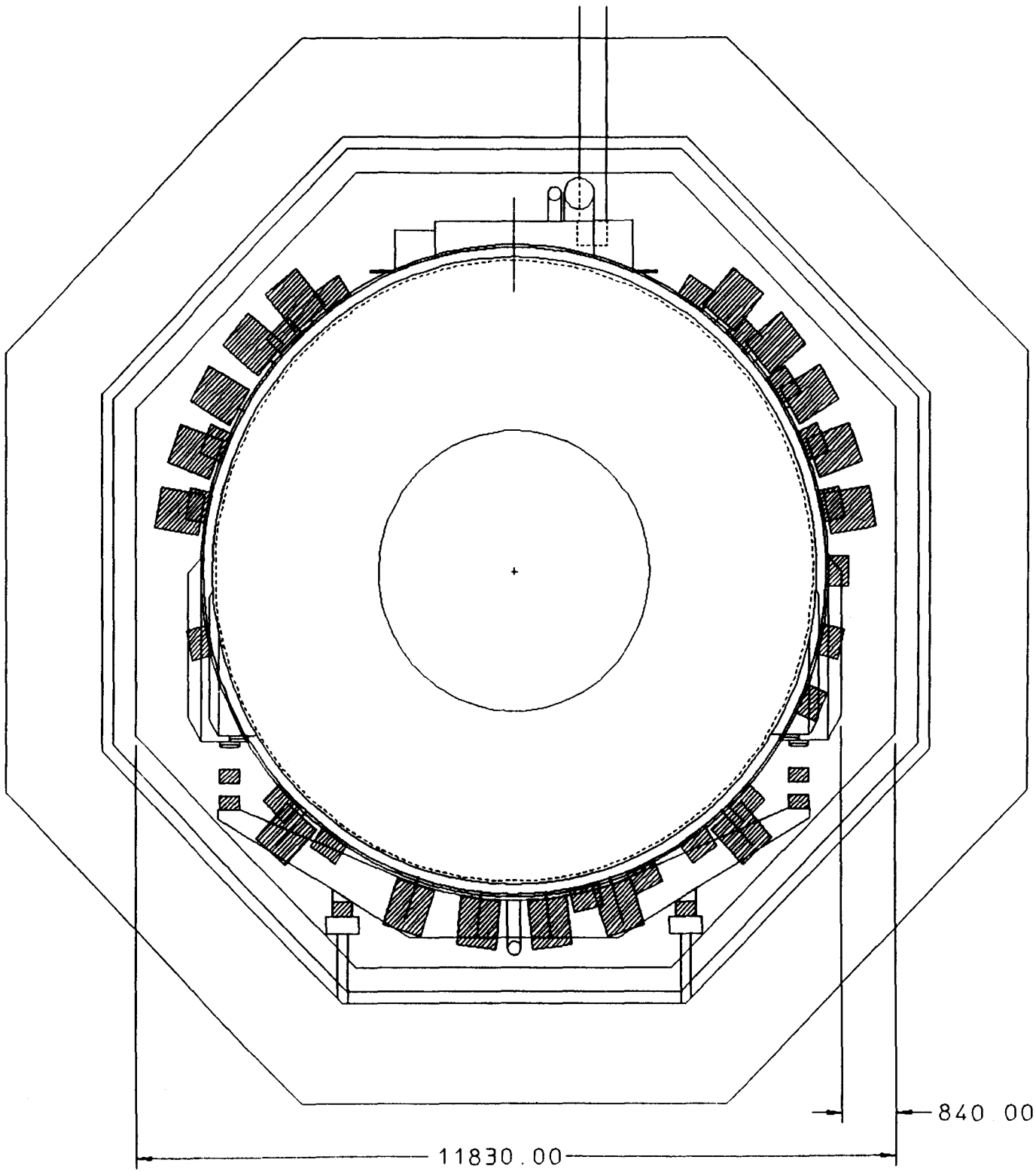
840.00
11830.00

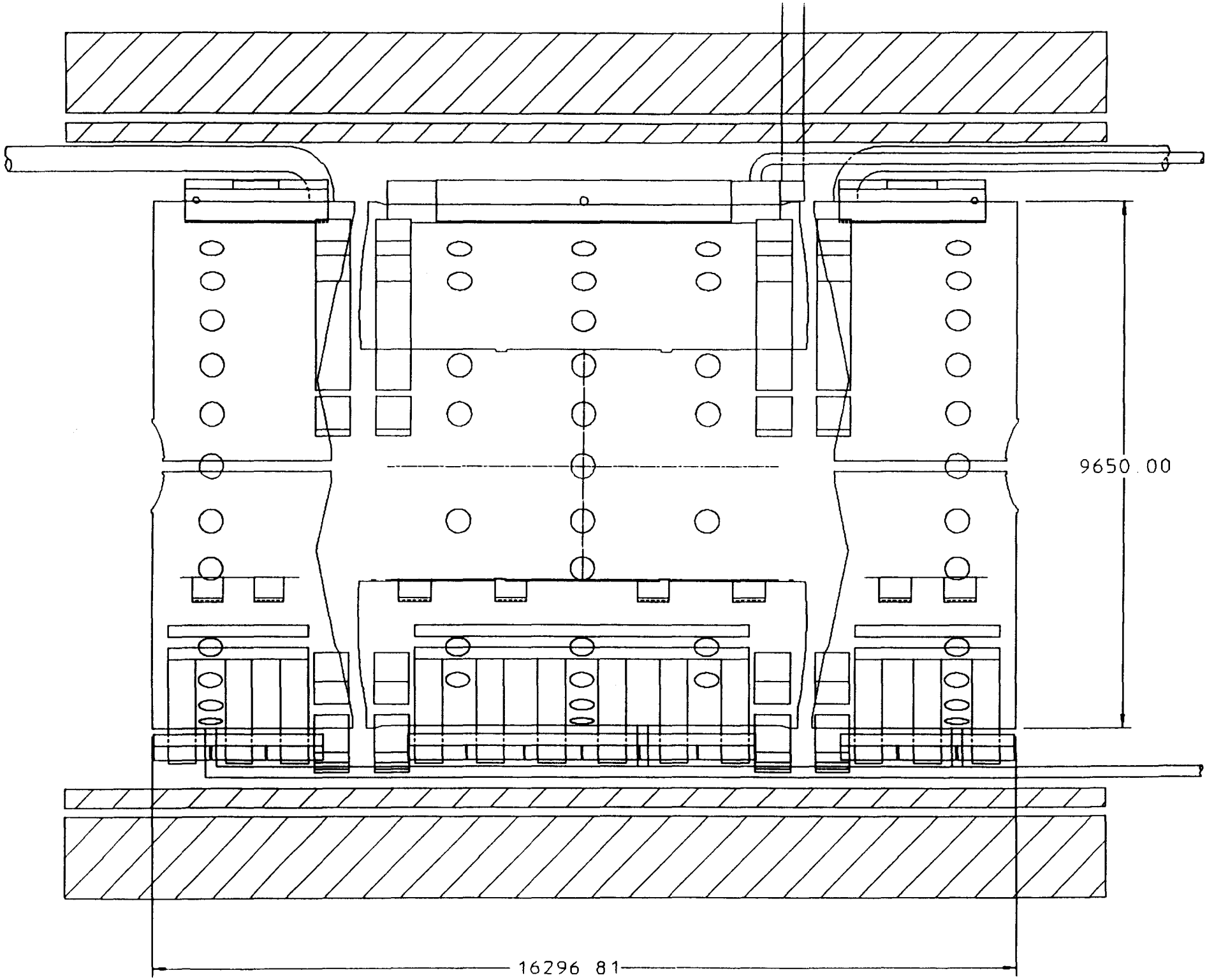
9650.00
16296.81

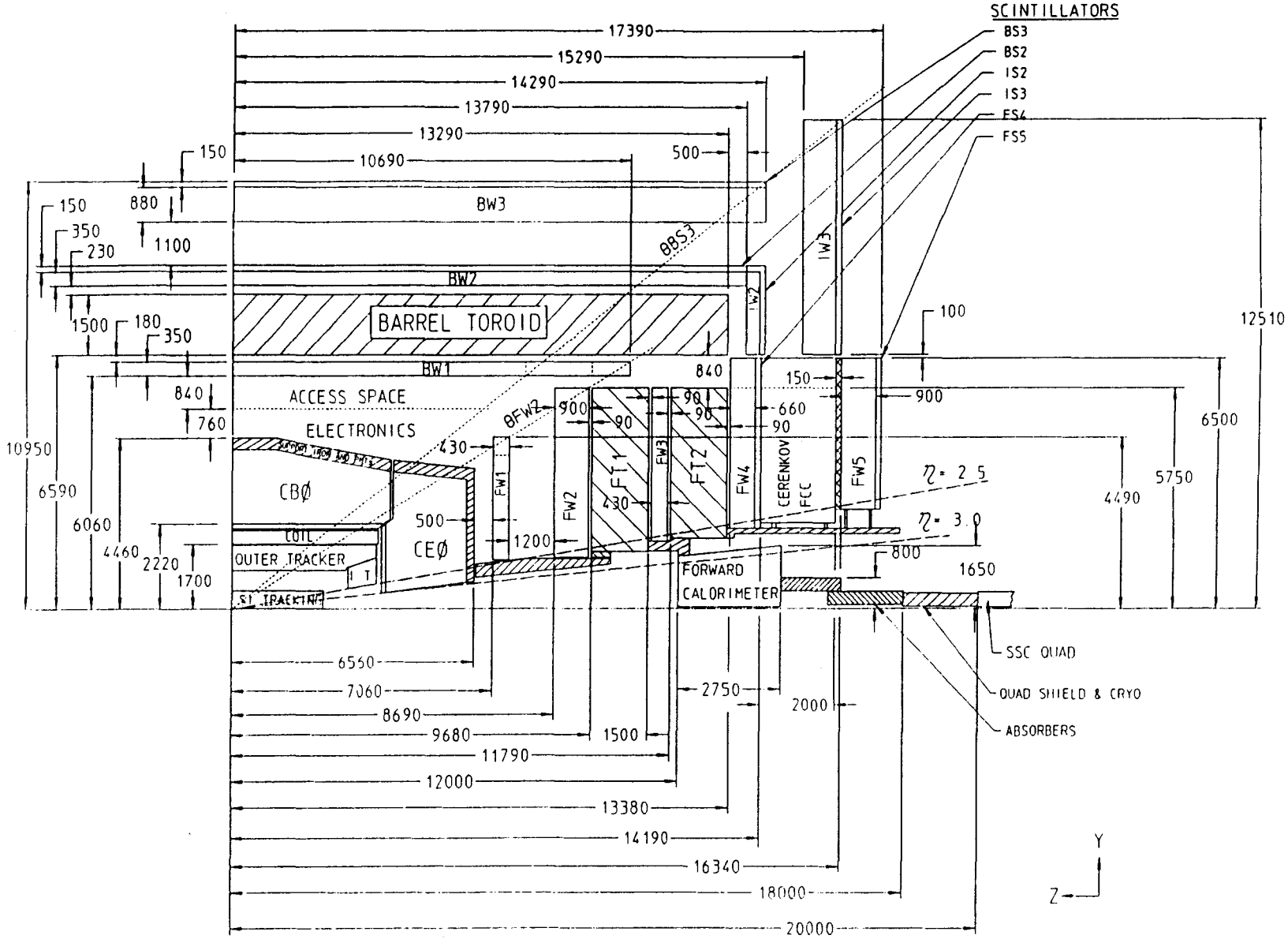

NOTE ALL DIMENSIONS ARE IN MILLIMETERS

0 1 2 3 4 5 M

SDC SCINTILLATOR CALORIMETER DETECTOR

DESCOPED OPTION 2

LBL DWG# 23D0285 9/11/91 D. SHUMAN

filename ~mbora/bell/9_9_91_xsec_sc_op_2

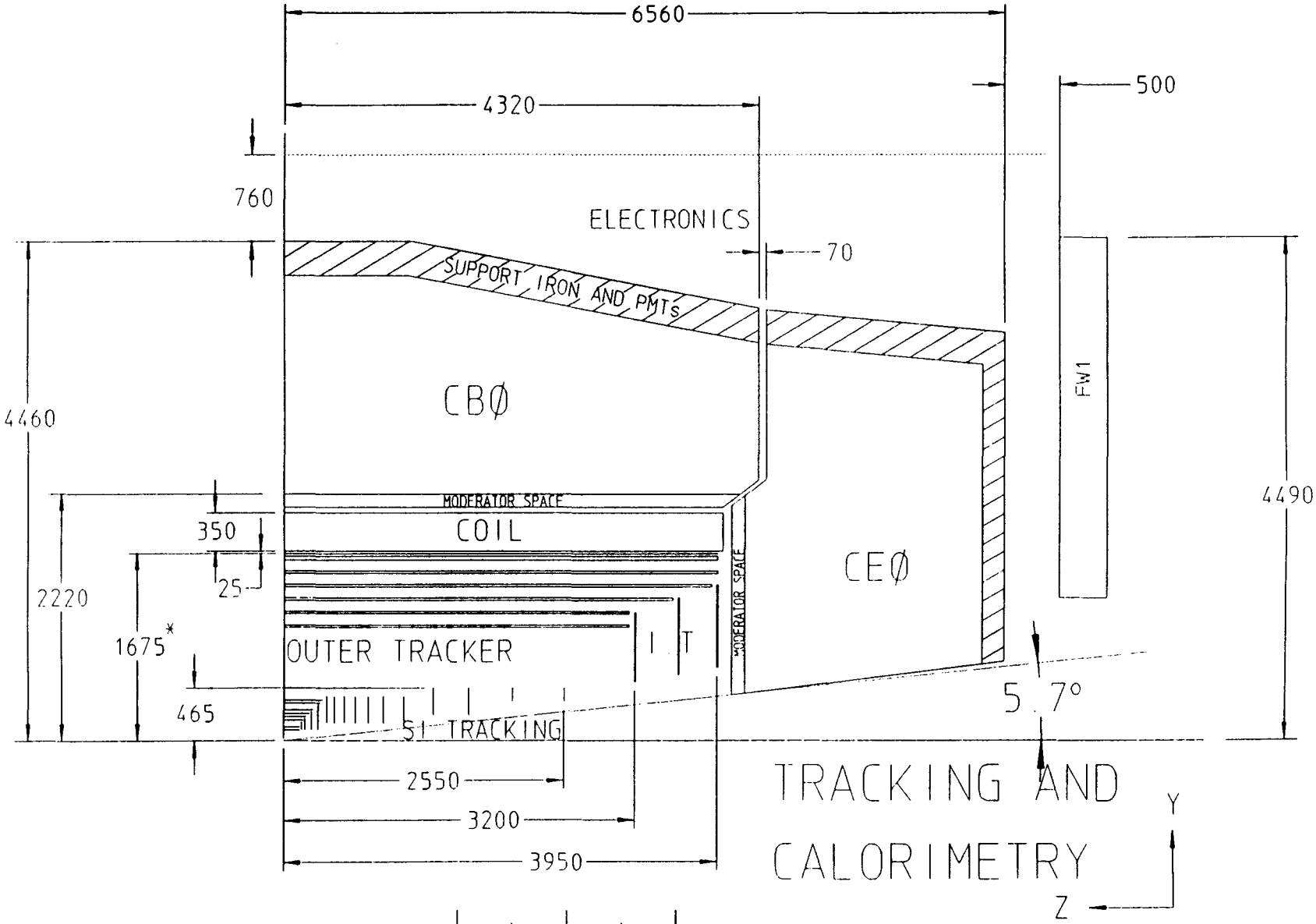

* TRACKER MAX. RADIUS

0 1 2 M

SDC SCINTILLATOR CALORIMETER DETECTOR
DESCOPED OPTION 2
LBL DWG# 23D0285 9/11/91 D SHUMAN

filename -mlgra/holt/9_9_91_xsec_sc_op_2

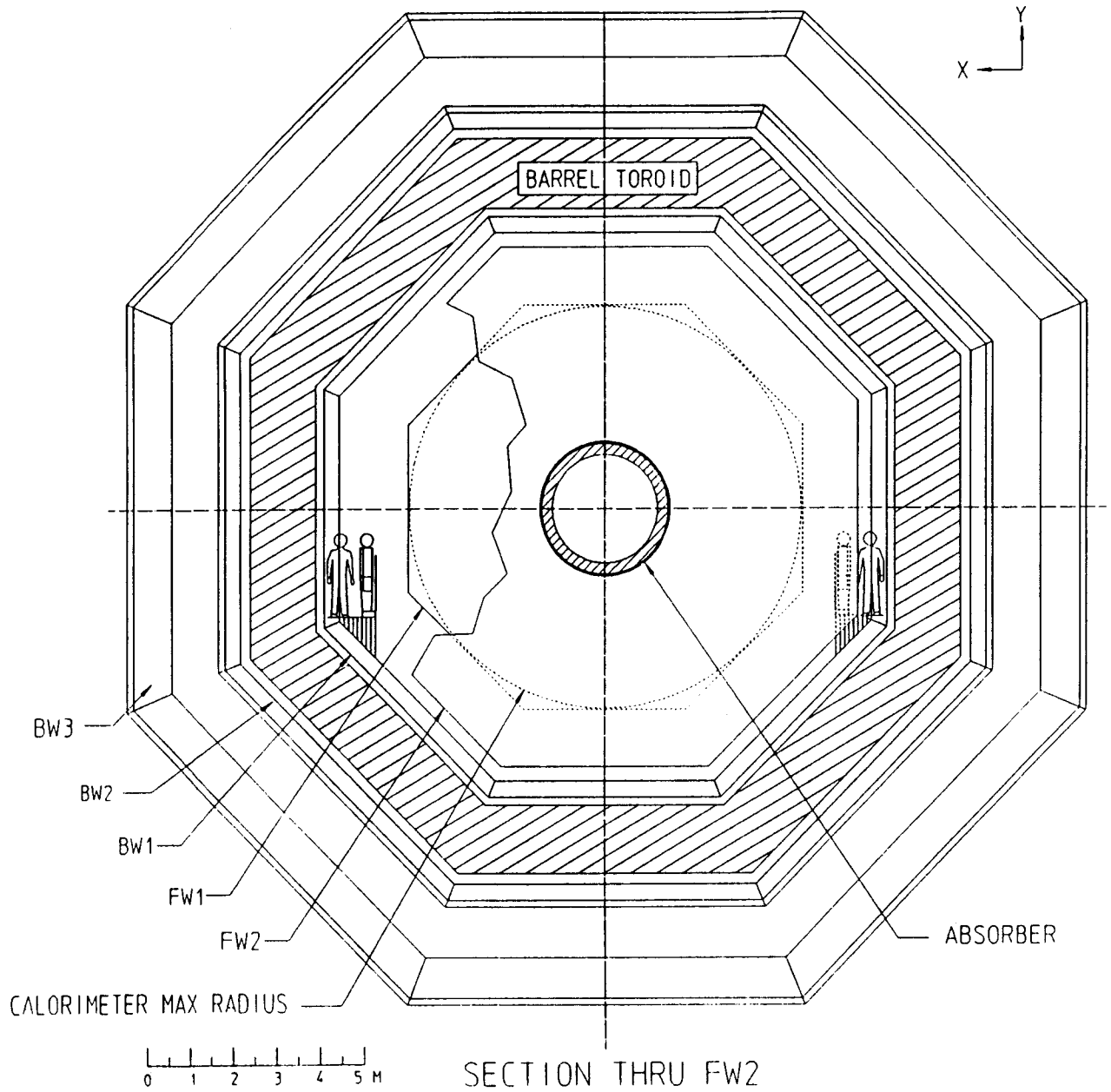

SECTION THRU FW2

SDC SCINTILLATOR CALORIMETER DETECTOR

DESCOPED OPTION 2

LBL DWG# 23D0285 9/11/91 D SHUMAN

filename ~mhoro/hall/9_9_91_+spc_sc_op_2

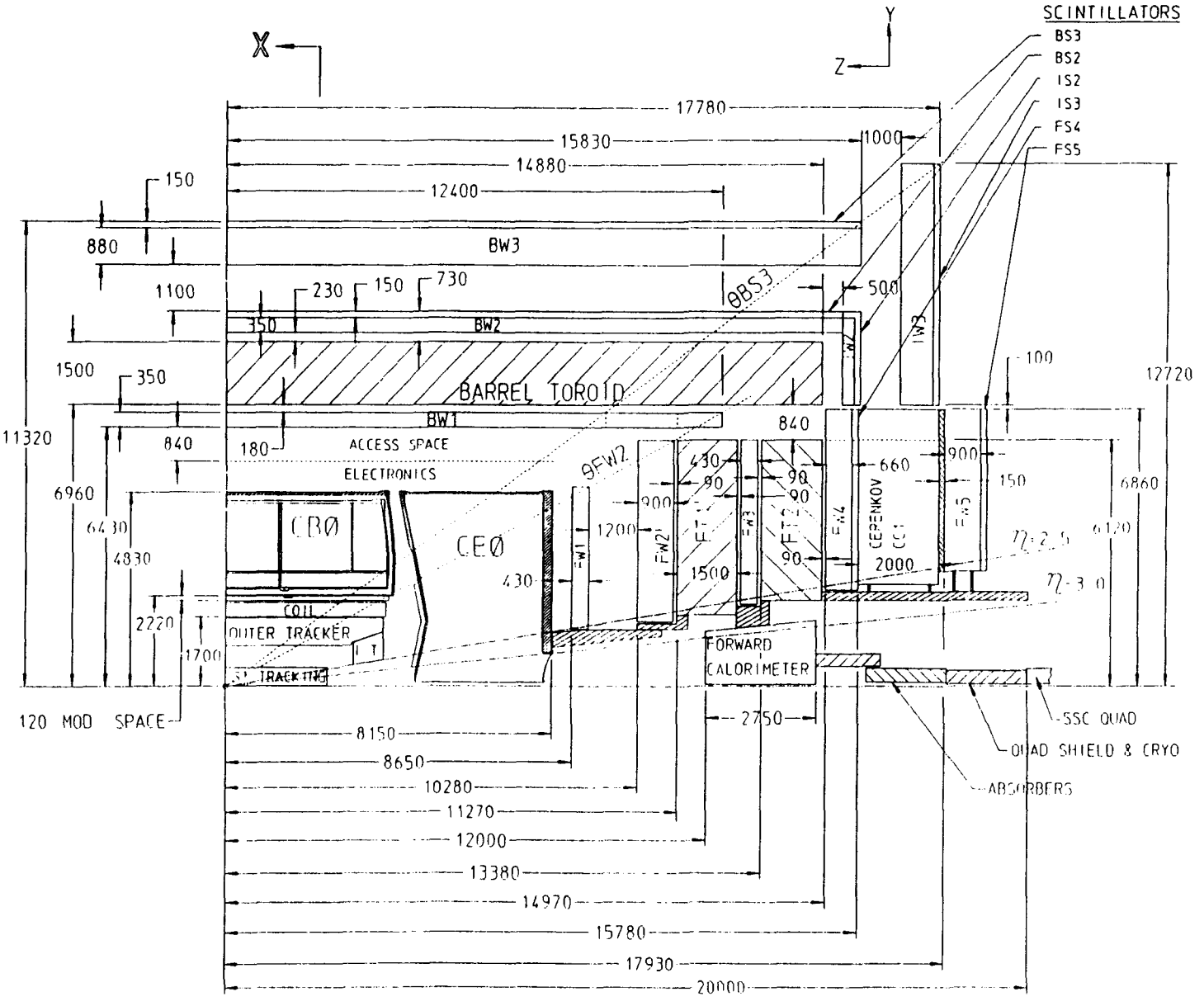

NOTE ALL DIMENSIONS ARE IN MILLIMETERS

SDC LIQUID ARGON CALORIMETER DETECTOR
DESCOPE OPTION 2B (NO RETURN STEEL)
LBL DWG# 23D0275 9/11/91 D SHUMAN

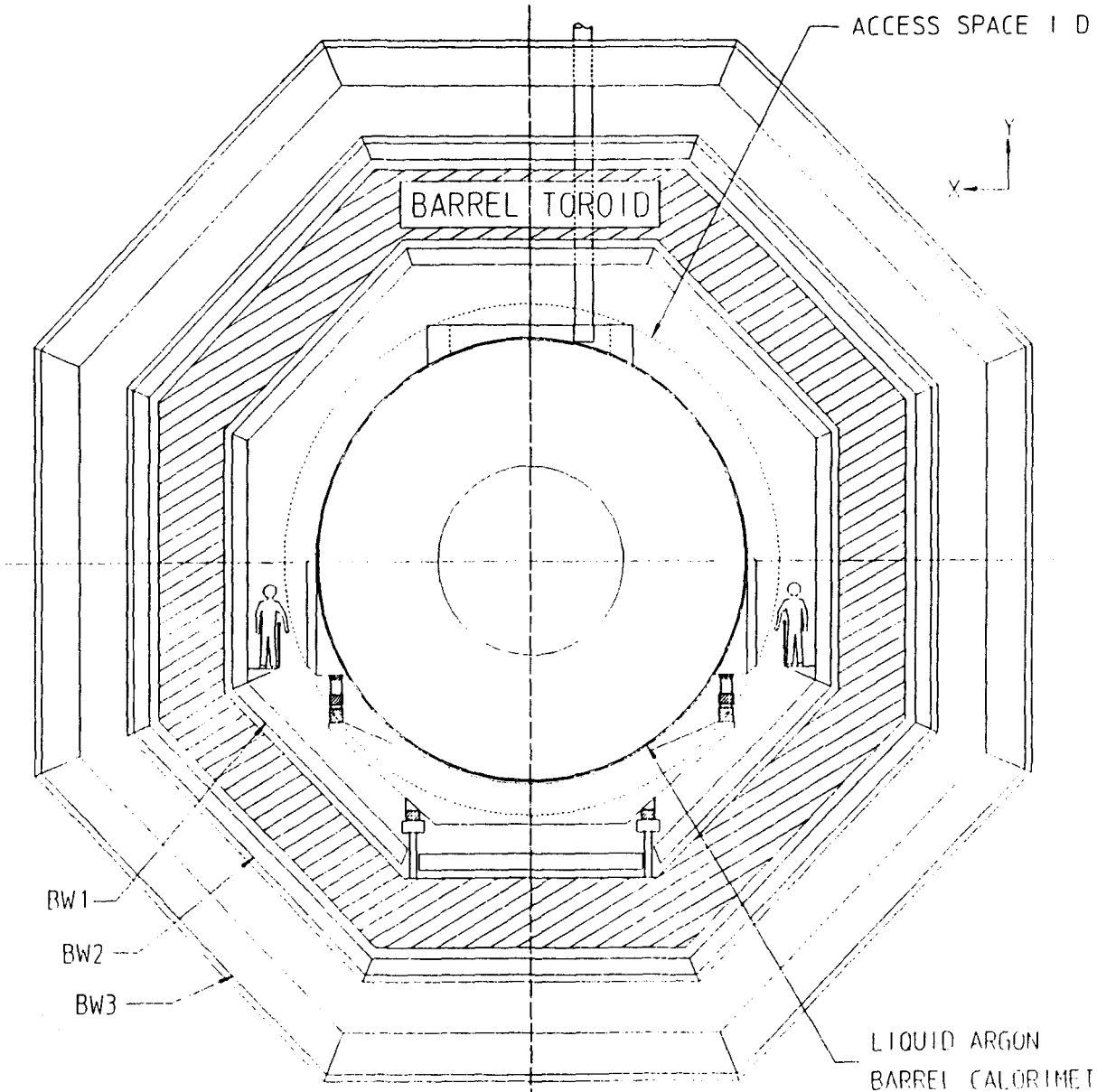

SECTION X X

NOTE ALL DIMENSIONS ARE IN MILLIMETERS

0 1 2 3 4 5 M

SDC LIQUID ARGON CALORIMETER DETECTOR

DESCOPE OPTION 2B (NO RETURN STEEL)

LBL DWG# 23D0275 9/11/91 D SHUMAN

filename: ebara/hell/2.2.21.xsec.1a.op.2b

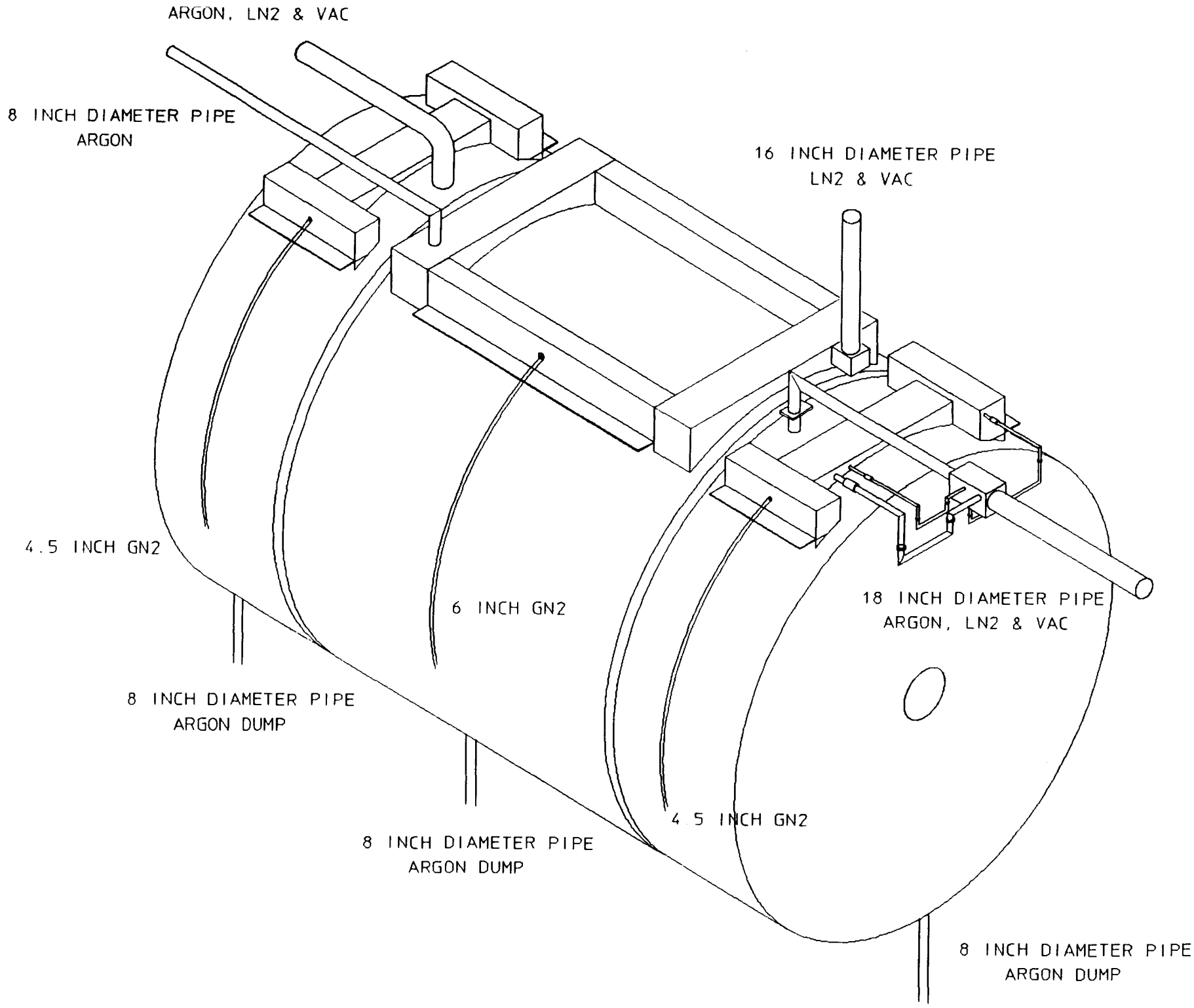
ARGON, LN2 & VAC
8 INCH DIAMETER PIPE
ARGON
16 INCH DIAMETER PIPE
LN2 & VAC
4.5 INCH GN2
6 INCH GN2
18 INCH DIAMETER PIPE
ARGON, LN2 & VAC
8 INCH DIAMETER PIPE
ARGON DUMP
4.5 INCH GN2
8 INCH DIAMETER PIPE
ARGON DUMP
8 INCH DIAMETER PIPE
ARGON DUMP

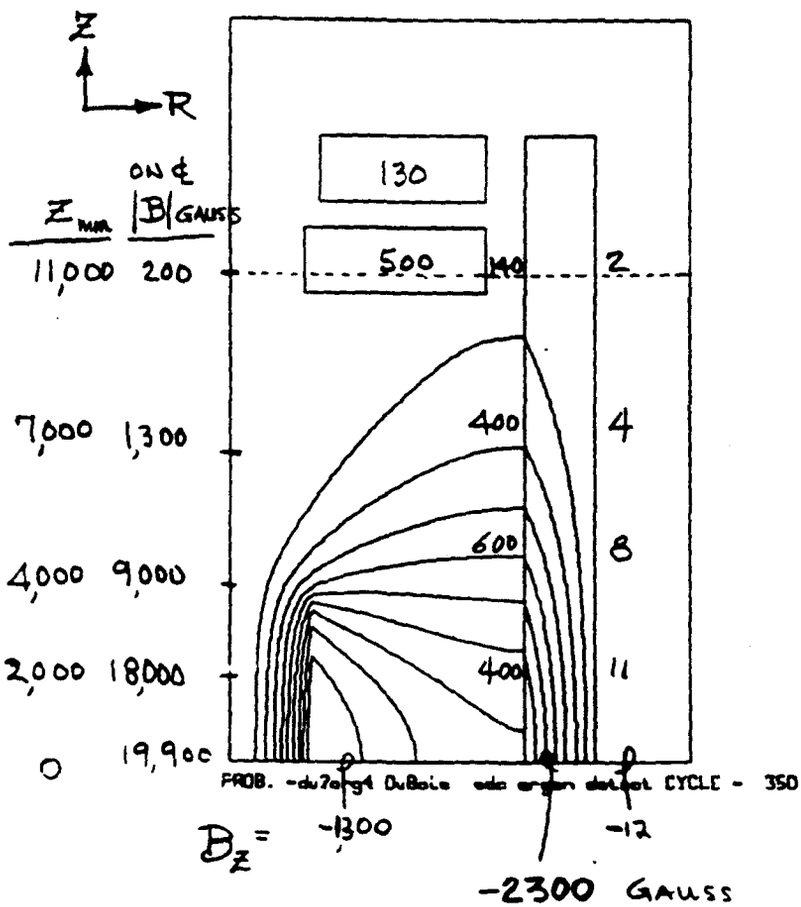
Z
R
ON ℄
Z_{MM}
$|B|$ GAUSS
11,000 200
7,000 1,300
4,000 9,000
2,000 18,000
0 19,900
130
500
140
2
400
4
600
8
400
11
PROB. -du7e g4 DuBoie
CYCLE - 350
B_z =
-1300
-12
-2300 GAUSS

CASE 4

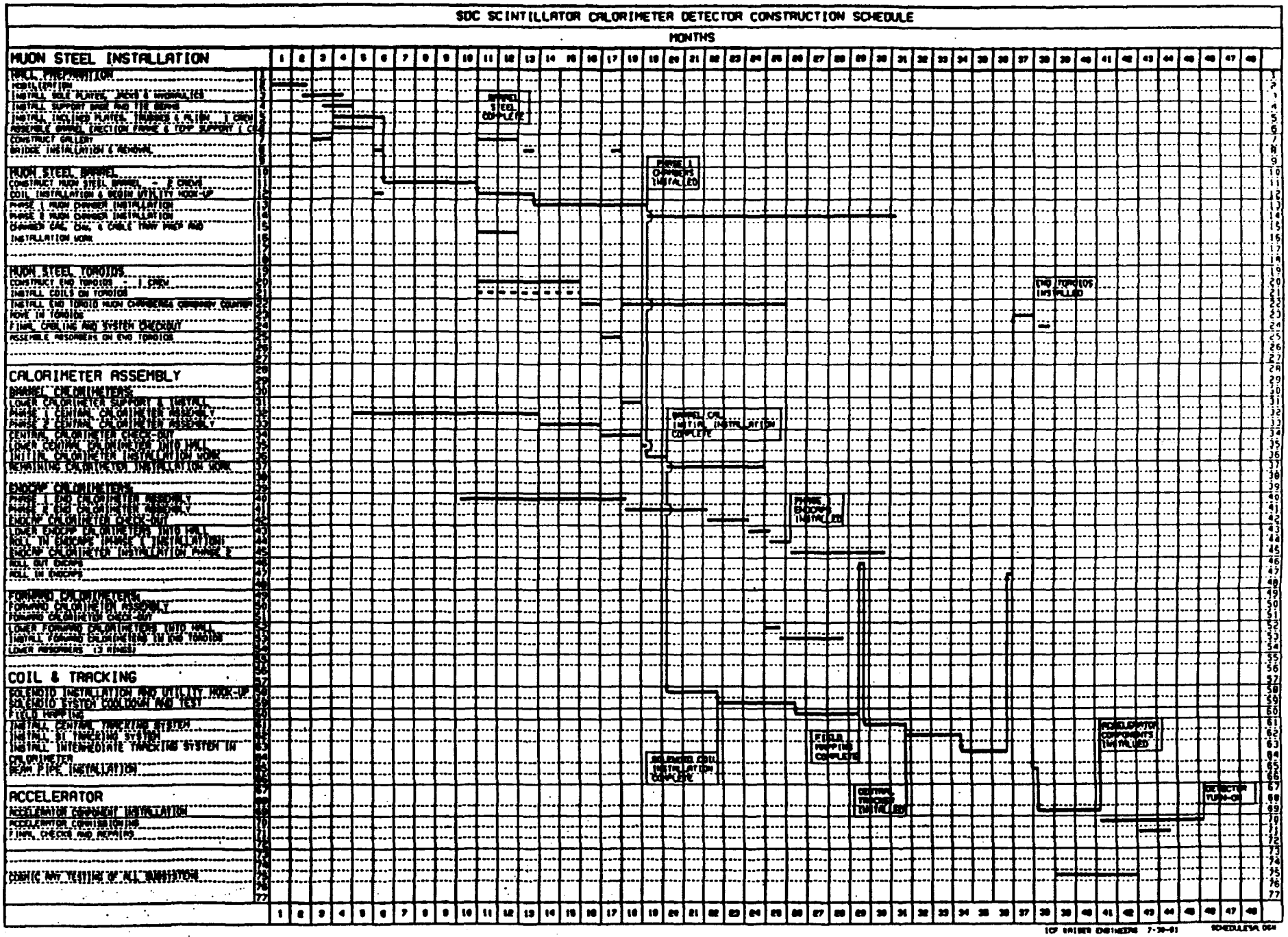
SDC SCINTILLATOR CALORIMETER DETECTOR CONSTRUCTION SCHEDULE
MONTHS
MUON STEEL INSTALLATION
HALL PREPARATION
MUON STEEL BARREL
MUON STEEL TOROIDS
CALORIMETER ASSEMBLY
COIL & TRACKING
ACCELERATOR
BARREL STEEL COMPLETE
PHASE 1 CHAMBERS INSTALLED
END TOROIDS INSTALLED
BARREL CAL INITIAL INSTALLATION COMPLETE
PHASE ENDCAP INSTALLED
SOLENOID COIL INSTALLATION COMPLETE
FIELD MAPPING COMPLETE
CENTRAL TRACKER INSTALLED
ACCELERATOR COMPONENTS INSTALLED
DETECTOR TURN-ON

FIG. 1

Sep-13-91
DB

Integration Comparison Conclusions

1) Electronics layout (w. VLPCs) tight for both calorimeter options

2) Δ Radius Cal $\simeq$ Δ Radius Detector
LAC + ~ 0.3 m

Δ Length Cal $\simeq$ Δ Length Detector
LAC + ~ 1.6 m

3) Muon Chamber BU1 loses coverage ~ equal to support legs ~ 1-2 %

4) Installation Schedule approximately the same

5) Hall Modification for LAC

6.) Effects of Magnetic Field (~1 kg) in Electronics and Access Space.

CALORIMETER REVIEW AND TECHNICAL BOARD MEETING
SEPTEMBER 12 -14, 1991
SSCL

Presentation by:

W.T. Ford

University of Colorado

Non uniform B field effect on straw electron drift.

$$(\Delta d)_{max} = d_{max}\left(\frac{v_0}{v} - 1\right)$$

$$v = 100\ \frac{\mu m}{ns} \cdot \left(1 - \frac{1}{3}\ \frac{B}{2T}\right)$$

$$\therefore\ (\Delta d)_{max} = -\ \frac{1 - \frac{B}{2T}}{3 - \frac{B}{2T}}\ \ 2000\ \mu m$$

B	$(\Delta d)_{max}$
2.0	0
1.3	300 μm
1.0	400 μm

$\sigma_{meas} = 100\text{-}150\ \mu m$

Trigger Synchronizer

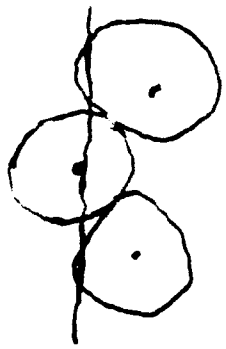

Coincidence time shift Δt (indep. of drift distance)

$$\Delta t = -t_0\ \frac{1 - \frac{B}{2T}}{3 - \frac{B}{2T}}\ , \qquad t_0 = 30\ ns$$

B	Δt
2.0	0
1.3	4 ns
1.0	6 ns

. Ford

CALORIMETER REVIEW AND TECHNICAL BOARD MEETING
SEPTEMBER 12 -14, 1991
SSCL

Presentation by:

Gary Feldman

Harvard University

Effects on Muon System

1) In LA case, ~300 G ⊥ to BW1 (in layers).

⇒ Lorentz angle ~2° negligible

2) In LA case, ~300 G in toroid ⊥ to toroidal field.

⇒ 1.8 kG → 1.81 kG ⇒ negligible change in μ

3) In LA case, the flux is returned at larger radii than either Scint. case.

⇒ better μ momentum resolution for very high momentum μ's (generally $p_t > 300$ GeV/c).

of minor physics importance since few processes have μ's in this range.

4) Fe is a much better hadron absorber than Pb.

The issue for the μ system is bend/scatter for the <u>level 1</u> <u>trigger</u>.

	All Fe	Pb/Fe	All Pb
Bend/scatter	3.9	3.2	2.8

Pb ⇒ higher μ level 1 trigger rate

probably ok, but needs to be looked at.

Feldman

5) LA requires larger cryo vertical pipe ⇒ negligible difference

6) LA requires additional supports ⇒ some loss of solid angle in BW1 (BW1 not as critical as some other layers – it may be used in level 2 trigger and μ id. – work arounds are possible.)

7) LA requires more radial space ⇒ cost issue already discussed

CALORIMETER REVIEW AND TECHNICAL BOARD MEETING
SEPTEMBER 12 -14, 1991
SSCL

Presentation by:

Michael Barnett

Lawrence Berkeley Laboratory

From: ST%""CSA::BARNETT"@SSCVX1.SSC.gov" 6-SEP-1991 01:51:07.62
To: TURCOTTE,SIEGRIST,HEARTY,FRISKEN,UNNO,ABRAMS,PRIPSTEIN

From: Michael Barnett (LBL)
Tel.: (510)486-5650 ; Fax: (510)486-5401; Telex: 910-366-2037 LBL BERK
Bitnet: BARNETT@LBL ; Decnet: CSA::BARNETT ; Internet: BARNETT@LBL.GOV
Address: Bldg. 50A-3115, Lawrence Berkeley Lab, Berkeley, CA 94720

I have examined the impact of the new LAC design on the SDC's missing ET capabilities. One of the best tests of this occurs for the production of a pair of light gluinos. These frequently result in a final state containing three ET=70 GeV jets within abs(eta)<3 plus modest missing ET (between 100-200 GeV). The background of concern for the LAC design is from QCD jet events with mismeasurement of one or more jets. In particular I required (for the background) three separated 70 GeV jets occur in abs(eta)<3 plus a fourth jet with no restrictions; the concern is that this jet might be badly mismeasured in the abs(eta)=3-5 region. I require that the phi angle between the missing ET and the nearest jet be greater than 30 degrees. I have allowed for non-Gaussian tails in the smearing.

To choose the resolution I have made use of two calculations. The first was done by a student at LBL using the Womersley code. He found using the latest LAC design that the resolution, Delta(E)/E, was never worse than about 20% even for ET=20 GeV pions. Jet resolution should be slightly better. The region where resolution approached 20% was in abs(eta)=3-3.4. Above 3.4 it was much better.

Myungyun Pang, working with John Hauptman, using GEANT found that the resolution was not significantly deteriorated by the new LAC design which puts dead material in front of the forward calorimeter. He found that it did introduce a constant bias of about 10%.

As a result I have chosen the very conservative resolution of 80%/sqrt(E) + 20% (added in quadrature) for abs(eta)>3. The LoI said this was 80%/sqrt(E) + 5%. In this region 80%/sqrt(E) is negligible compared with 20% constant term. As stated above I have in addition allowed for non-Gaussian smearing. My gluino signal is also conservative since I have not included all diagrams leading to missing ET.

The results are shown on the enclosed topdraw plot. Beyond ET(missing)= 120 GeV this background is almost an order of magnitude smaller than the signal. I believe that the real background will be smaller since I have made the resolution much poorer than the two studies suggest, and the signal will be larger than I have shown. These results are not surprising: Missing ET does not originate in 200 GeV jets being mismeasured as 100 GeV (or vice versa). It originates in say 1000 GeV jets being mismeasured as 900 GeV. This keeps the cross section down. Also the phi cut is quite effective. A veto on jets is not adequate; it is necessary to measure that the jets are very high ET. Finally, a reminder that having no forward calorimeter results in this background being much larger than the signal because then 100 GeV jets are adequate to give 100 GeV of missing ET.

Michael Barnett

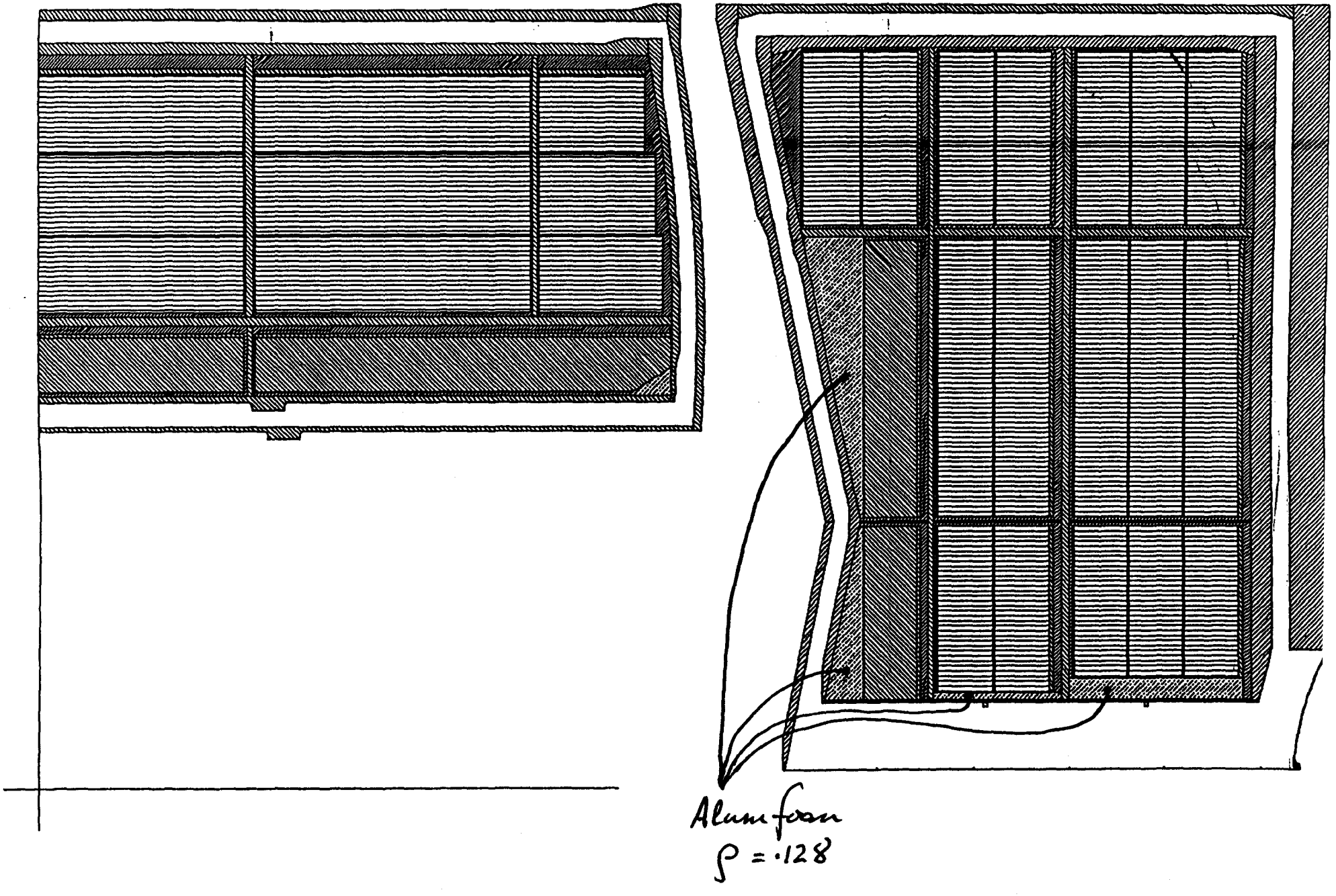

DATE: 8-27-91

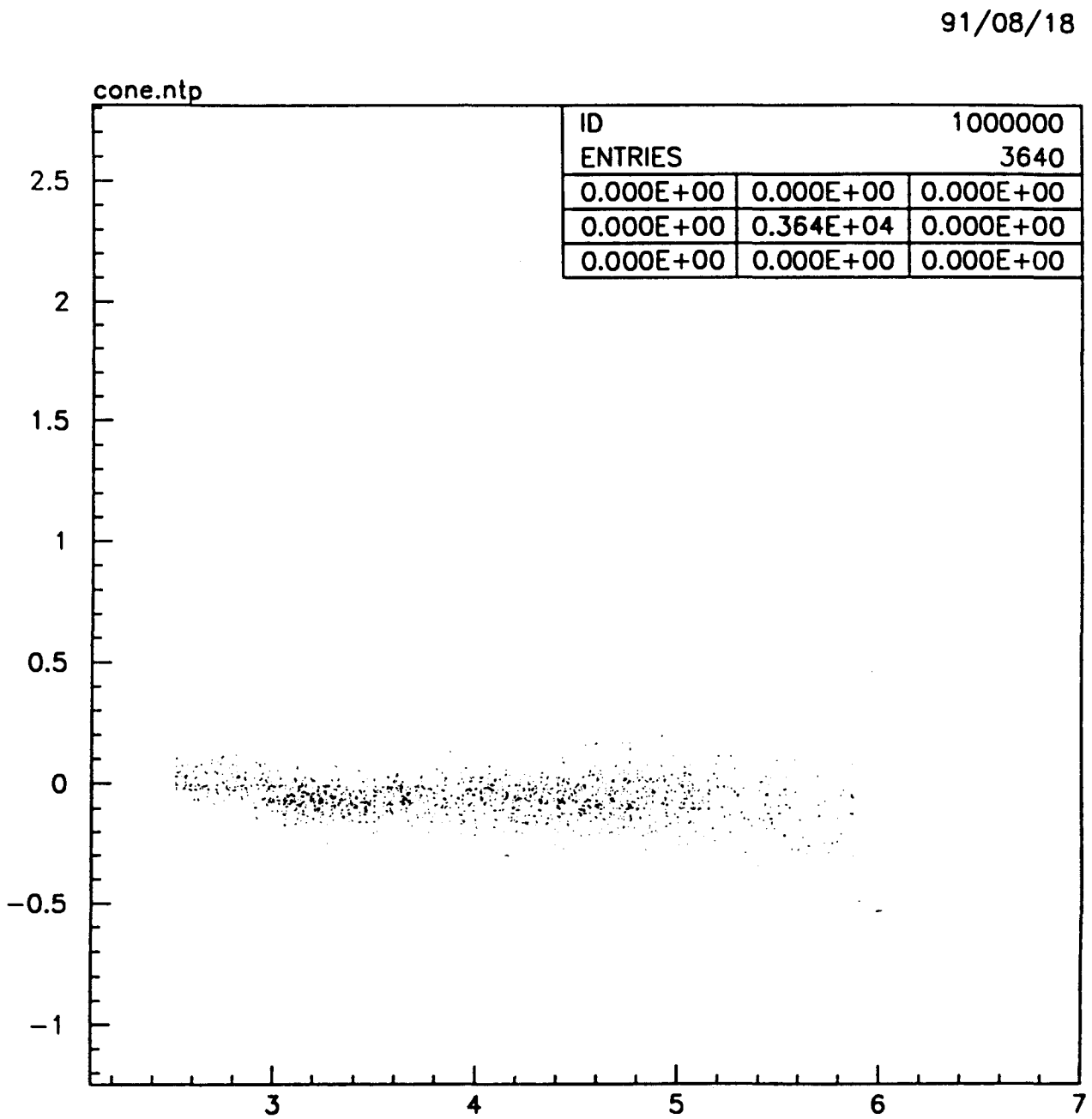

Figure 7. $\frac{E_{t-measured} - E_{t-jet}}{E_{t-jet}}$ as a function of rapidity(without dead material).

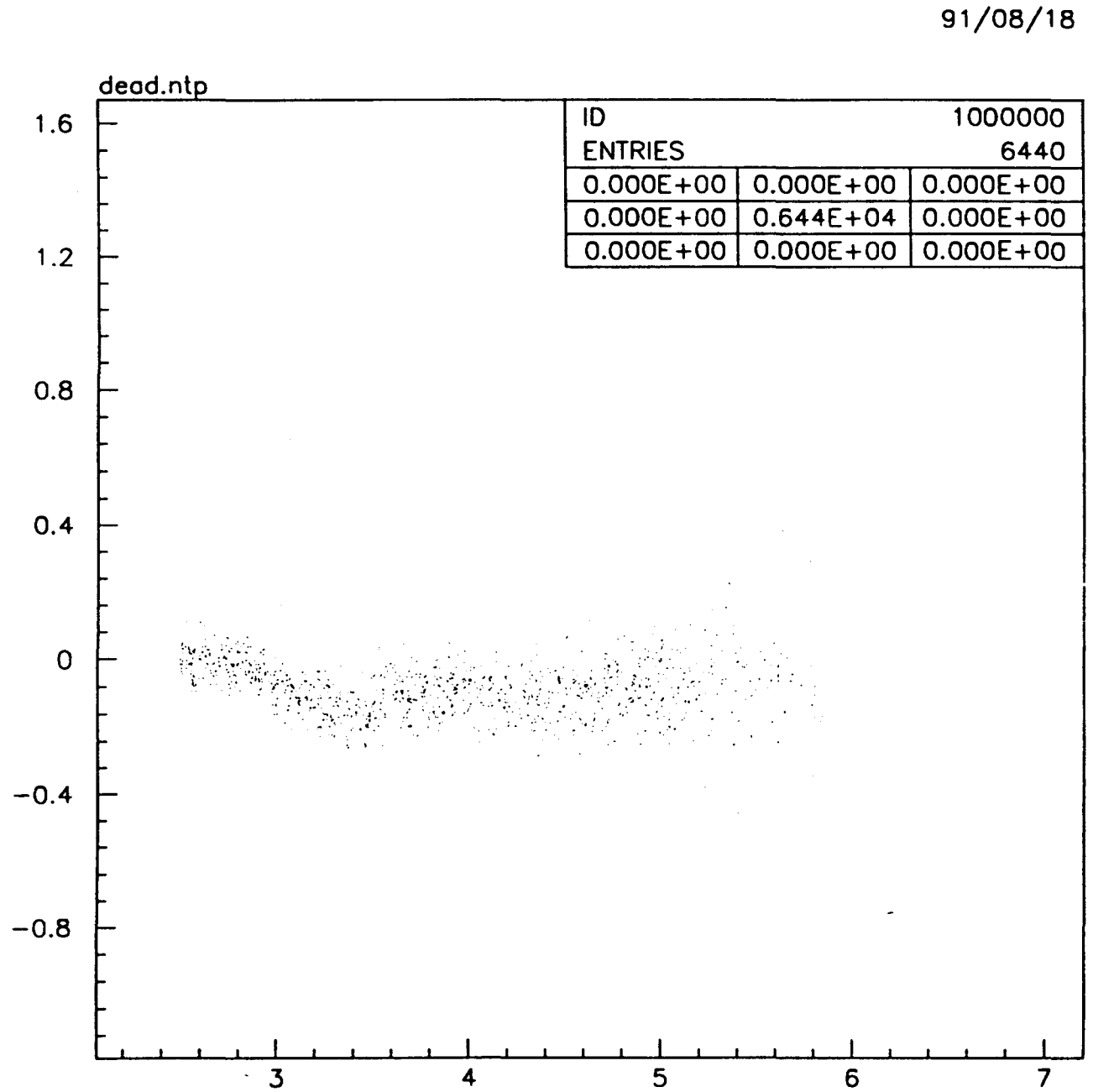

Figure 3. $\frac{E_{t-measured} - E_{t-jet}}{E_{t-jet}}$ as a function of rapidity(with dead material).

with lead material

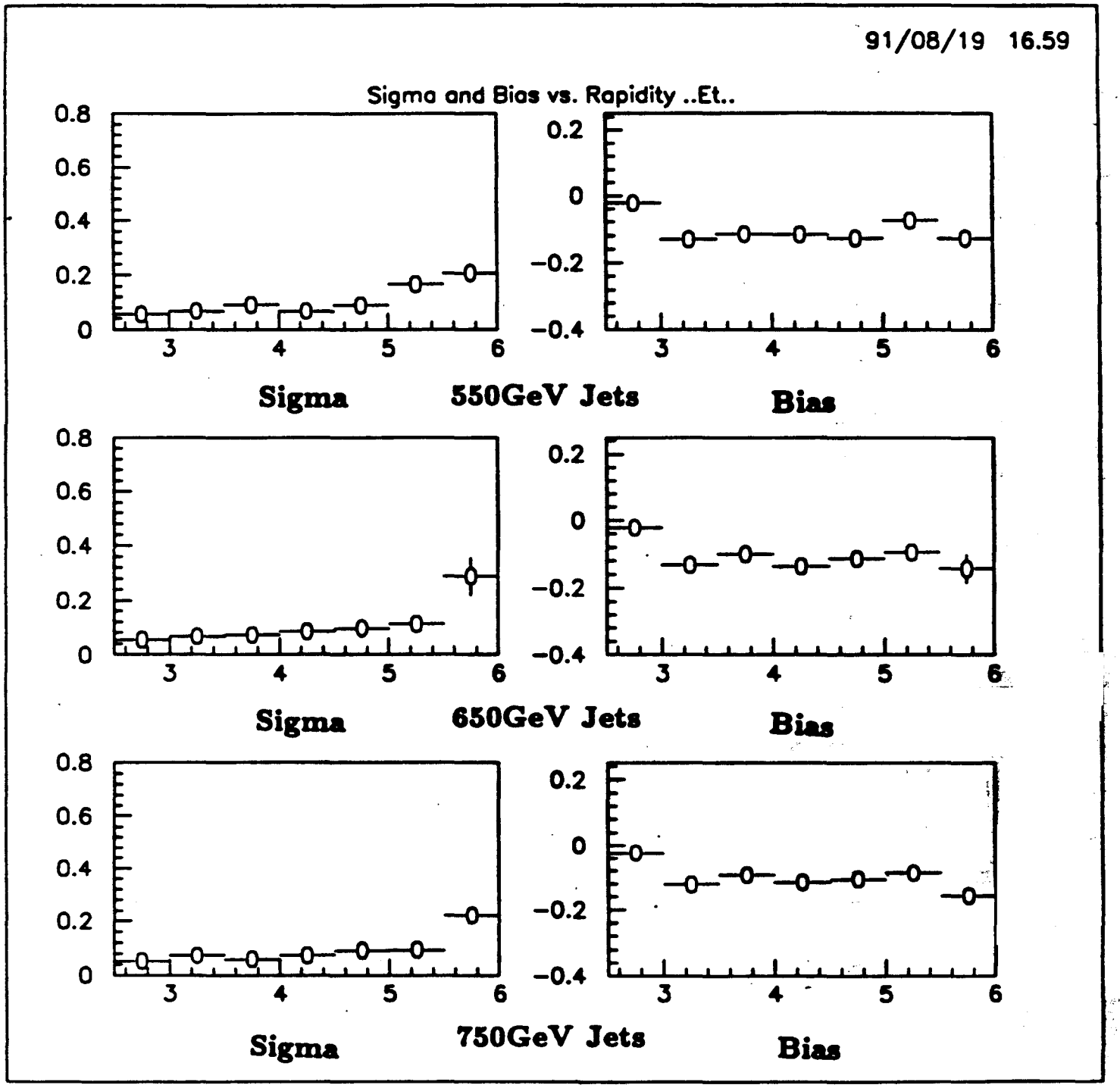

HAW THAT SH[redacted]

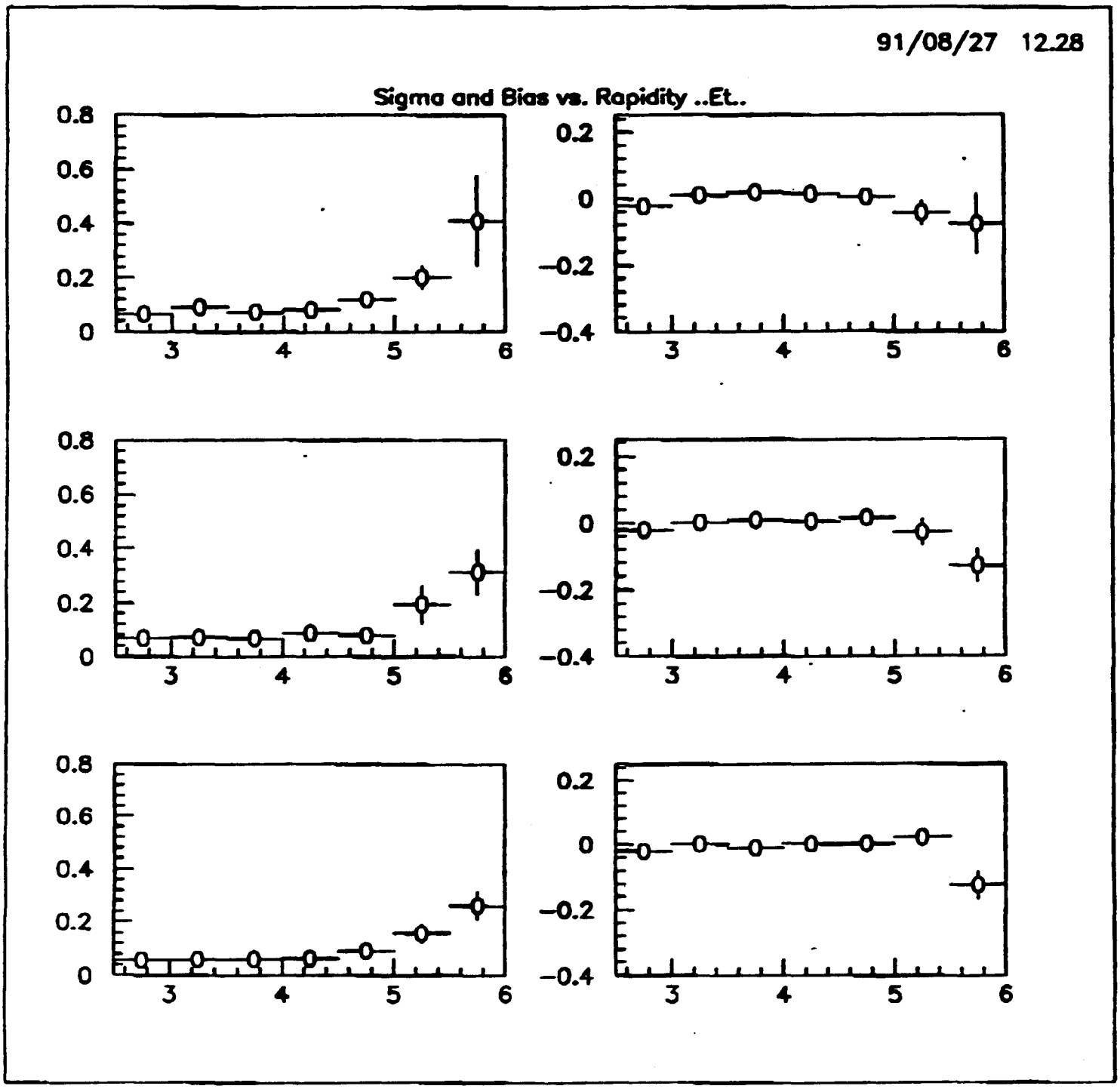

MORE GENERIC BASELINE COMPARISON THAN THAT SHOWN BY CMS.

with lead material

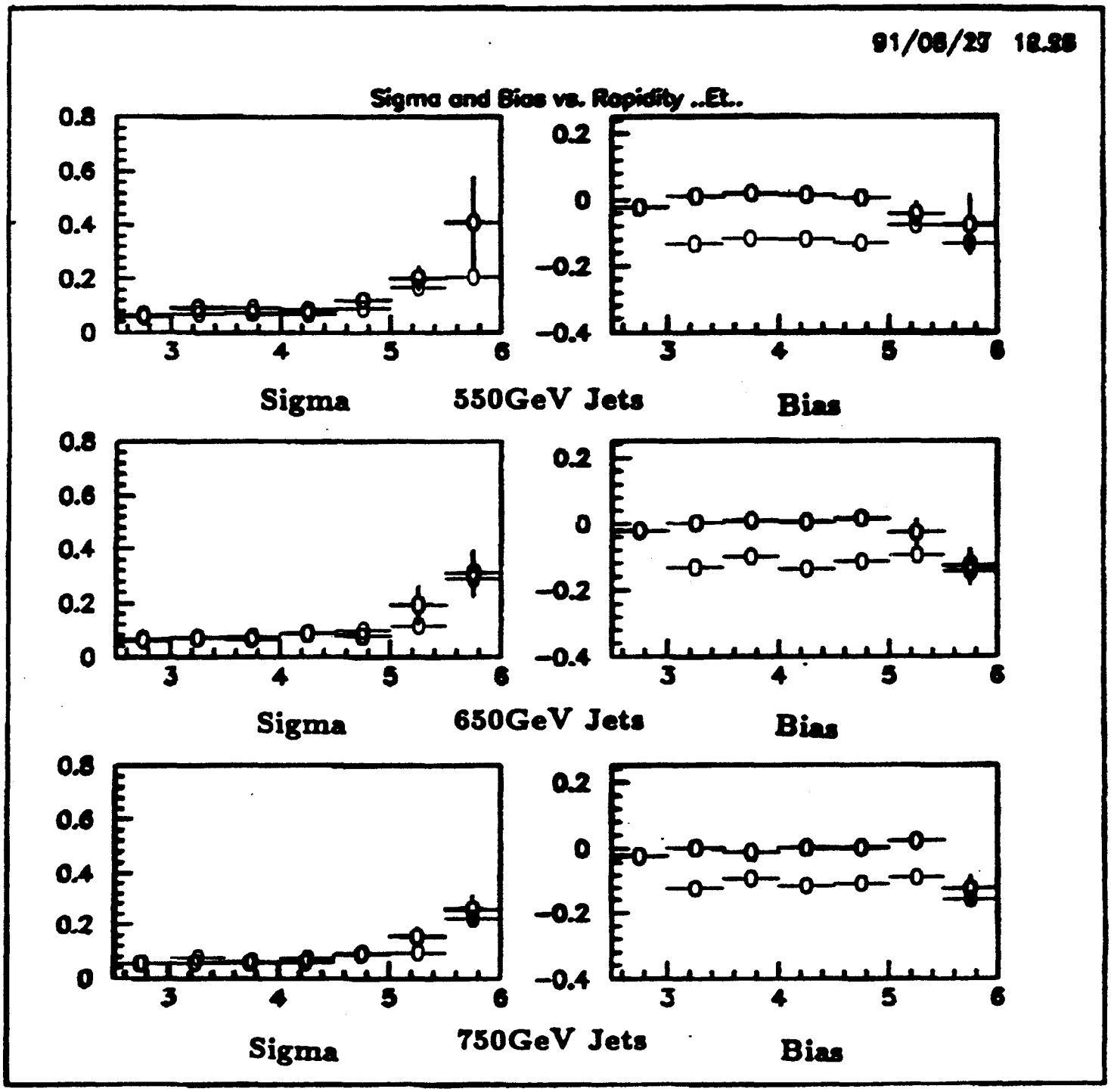

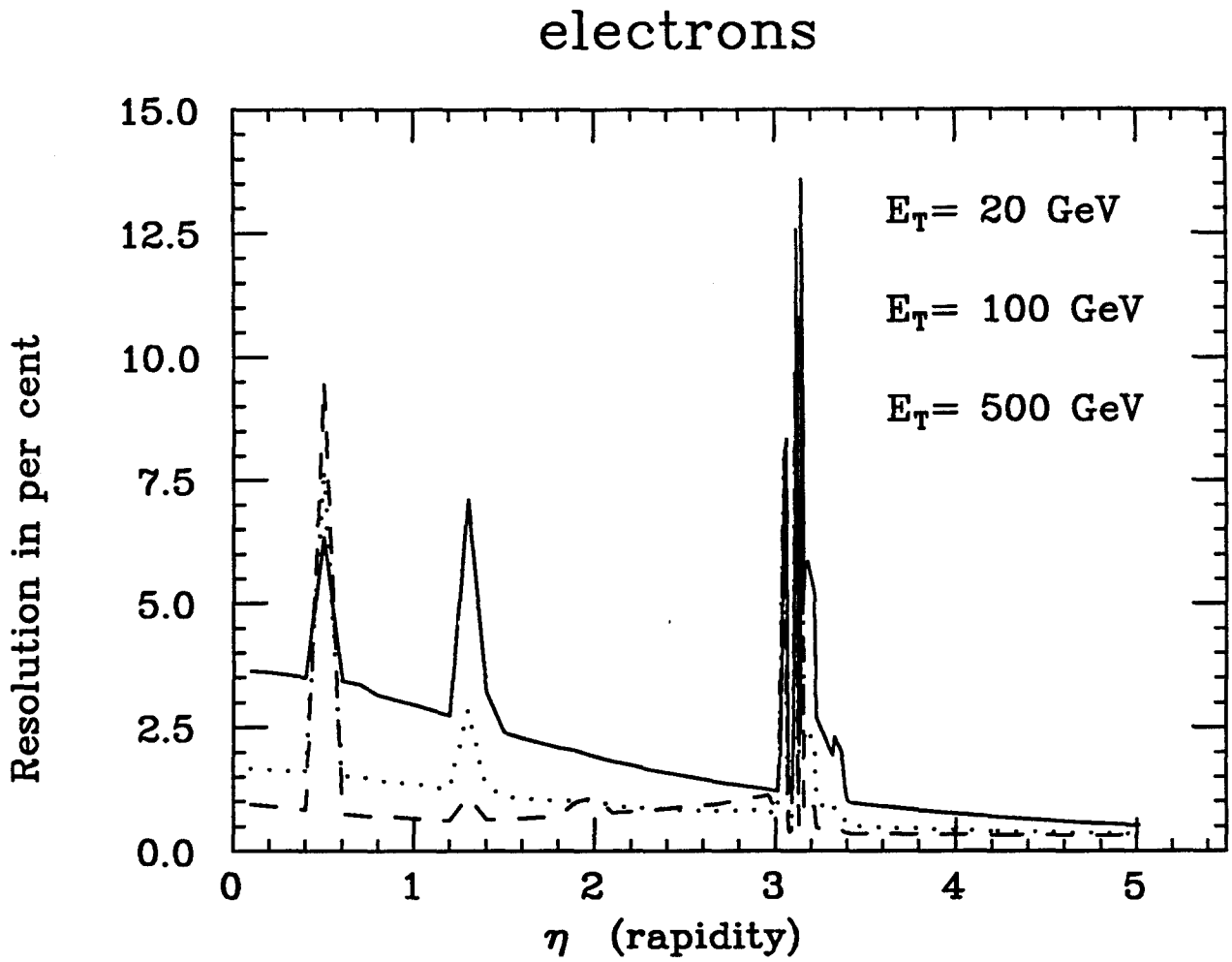
electrons
15.0
12.5
10.0
7.5
5.0
2.5
0.0
Resolution in per cent
0
1
2
3
4
5
η (rapidity)
E_T= 20 GeV
E_T= 100 GeV
E_T= 500 GeV

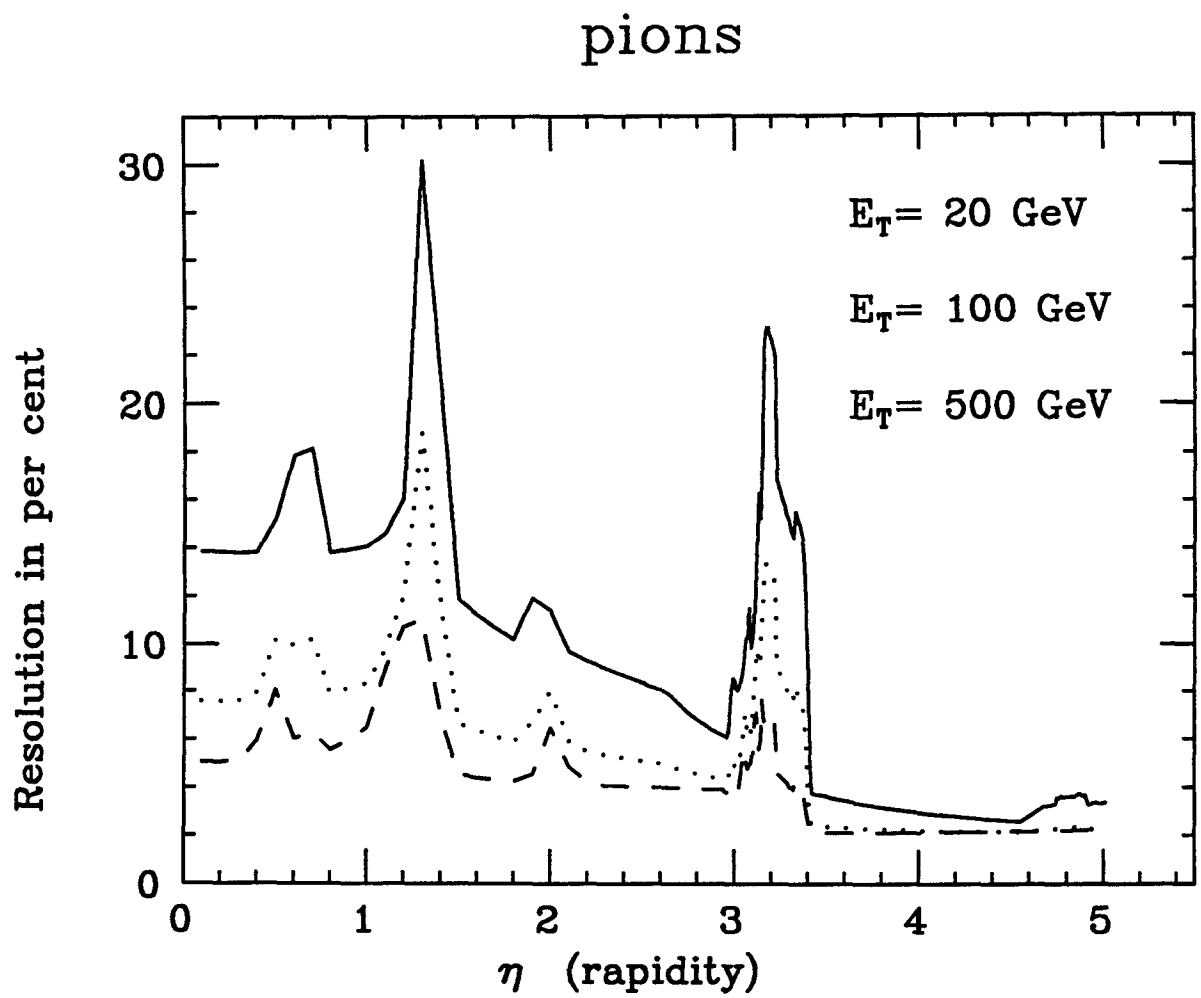
pions
E_T= 20 GeV
E_T= 100 GeV
E_T= 500 GeV
Resolution in per cent
0
10
20
30
0
1
2
3
4
5
η (rapidity)

Barnett's attempt to show the impact to be small.

for $\eta > 3$, $\frac{80\%}{\sqrt{E}} \oplus \frac{\Delta E}{E}$

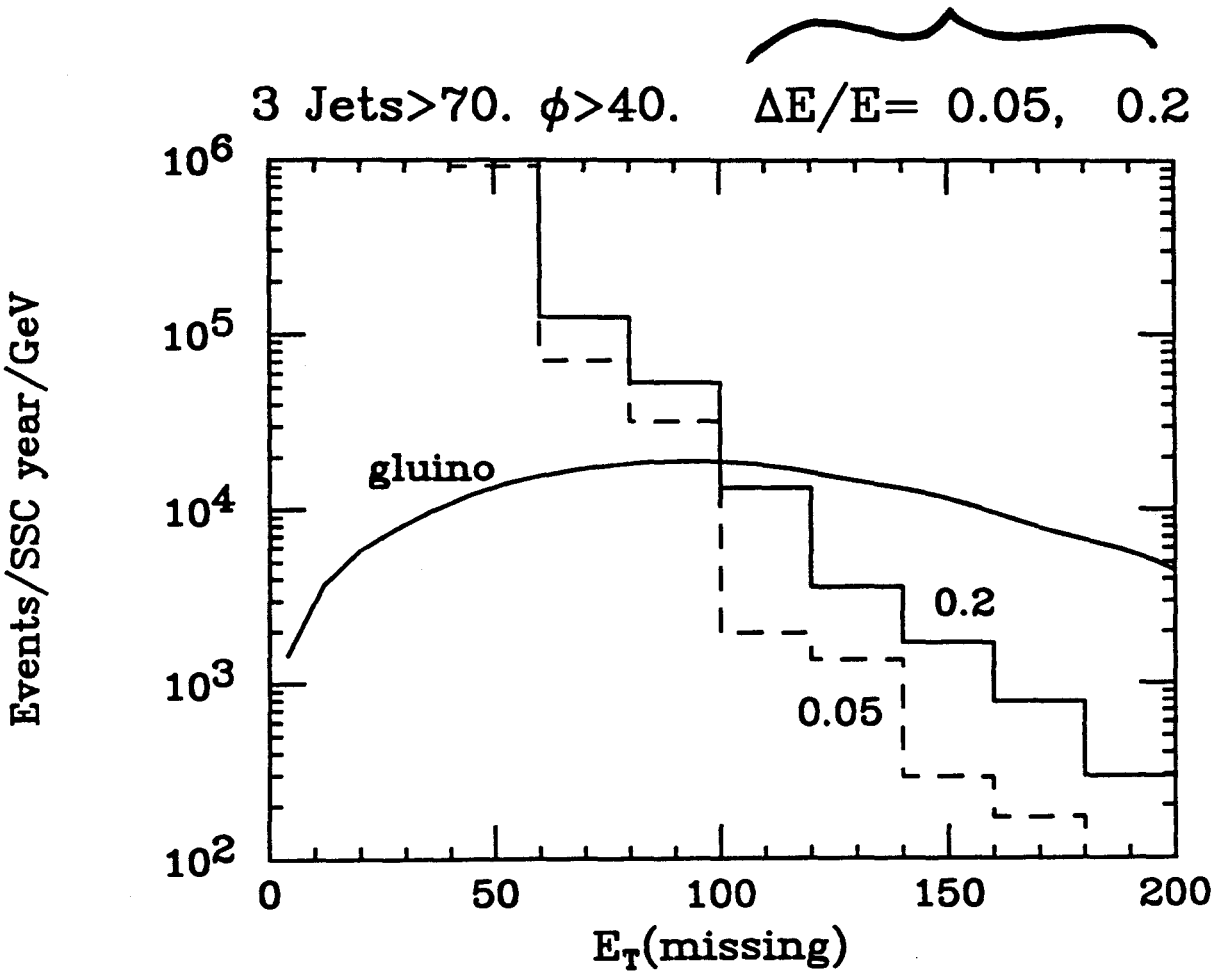

Solid histogram is VERY conservative for jets of particles, so reality will lie closer to the dashed histogram.

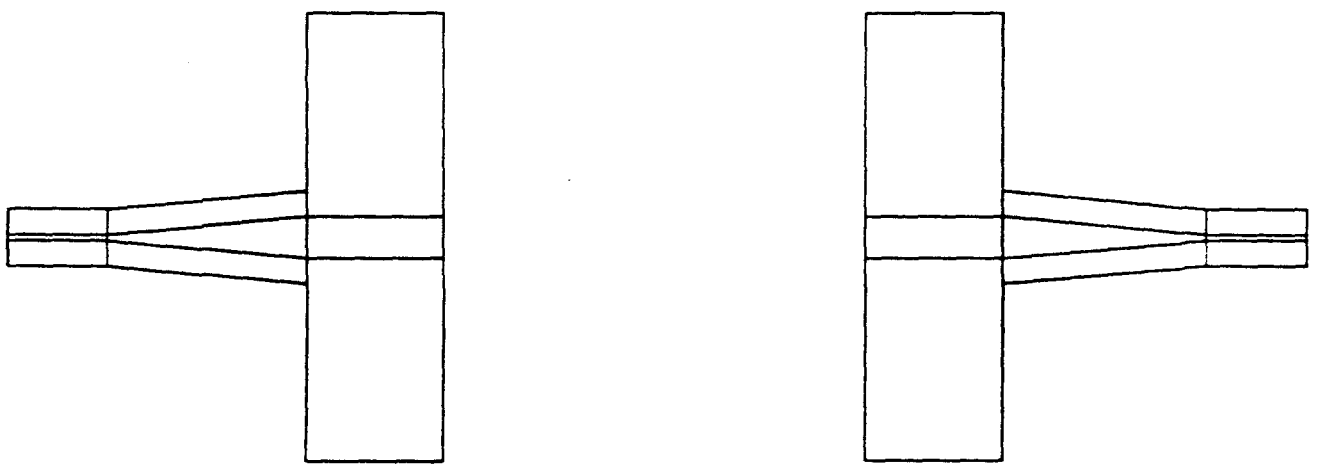

Figure 6. The geometry of the endcap and forward calorimeter without dead material in endcap calorimeter.

INVERSE CONE STYLE

GENERIC SCHEME FOR INTEGRATING End Cap Cal. with FCal.

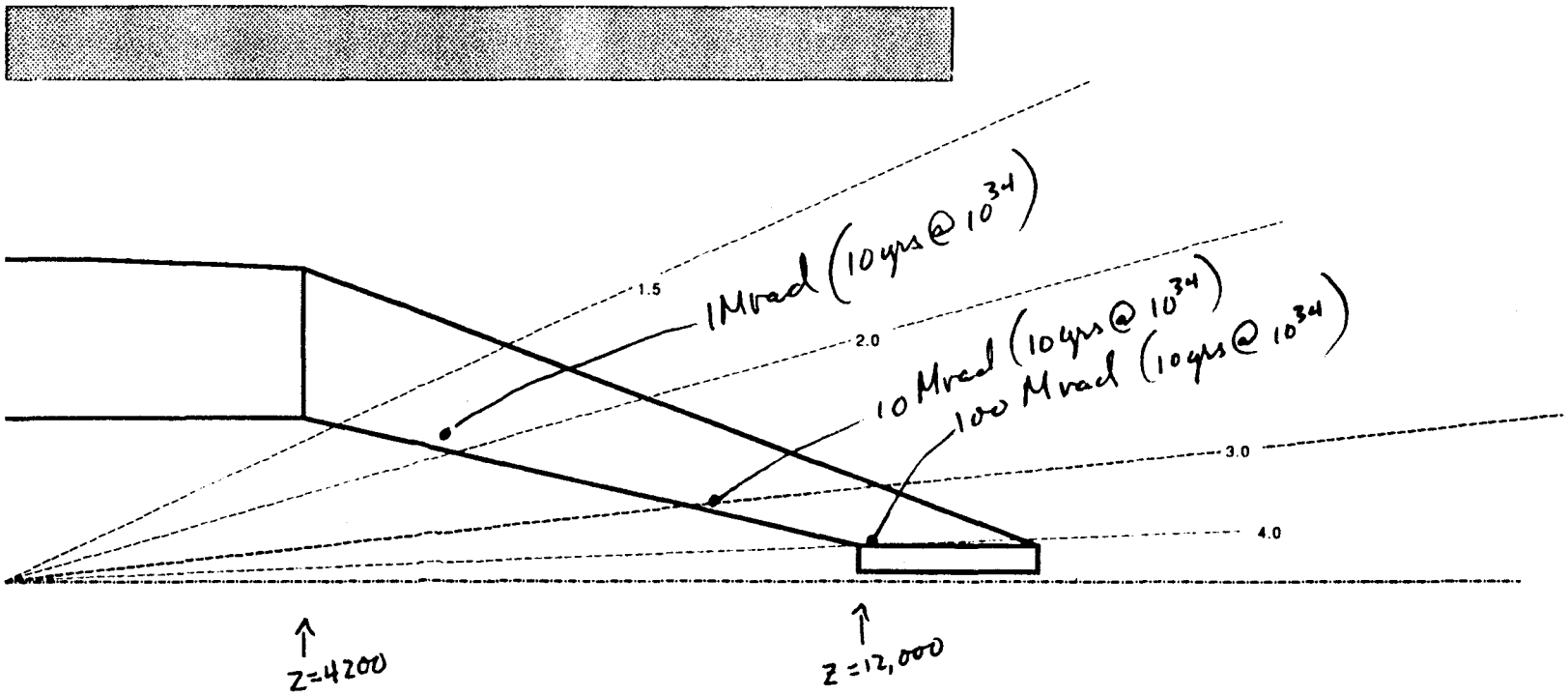

- This started out in my mind as a highly generic sketch on which to show the effects (on radiation dose) of moving the calorimeter material back from the interaction pt.
- But one is immediately tempted to consider it as a real scheme to avoid a change in sampling technology at $\eta = ?$.

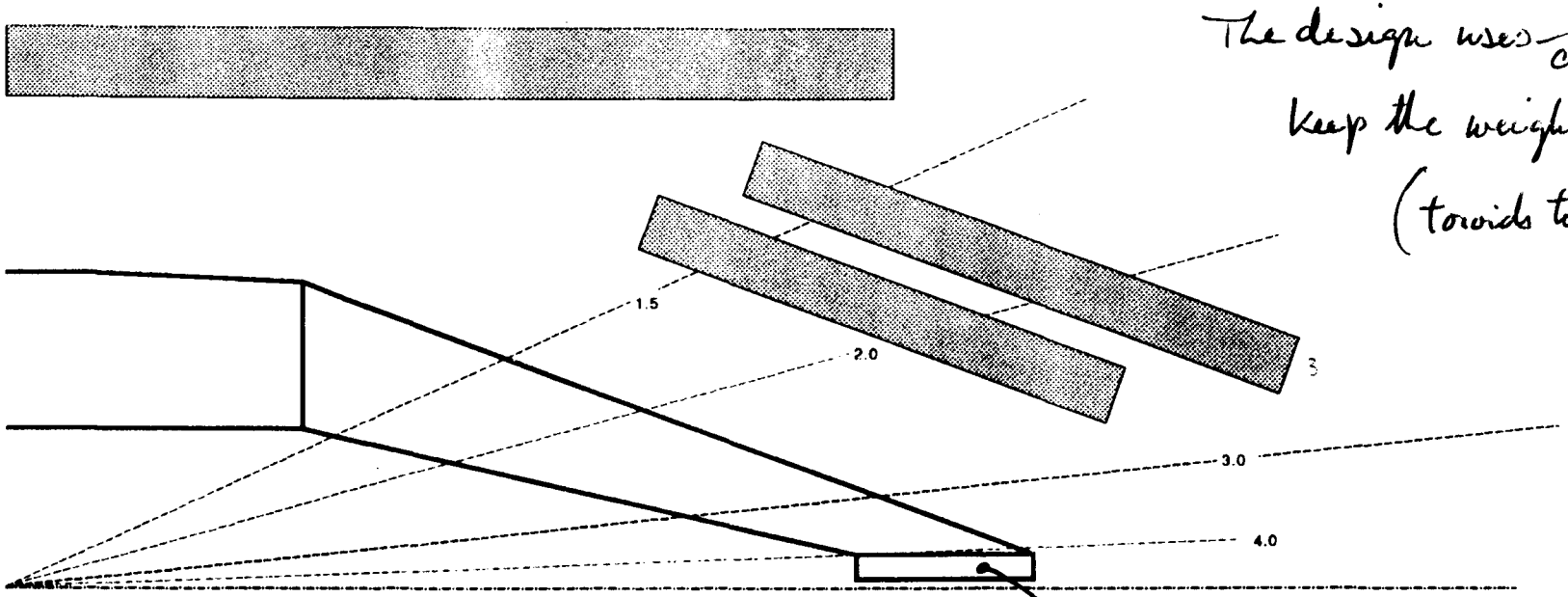

The design uses $\frac{1}{\cos\theta}$ to keep the weight ~ the same (toroids too).

Mike Barnett says that we simply remove this bit of $\mathcal{L} = 10^{34}$

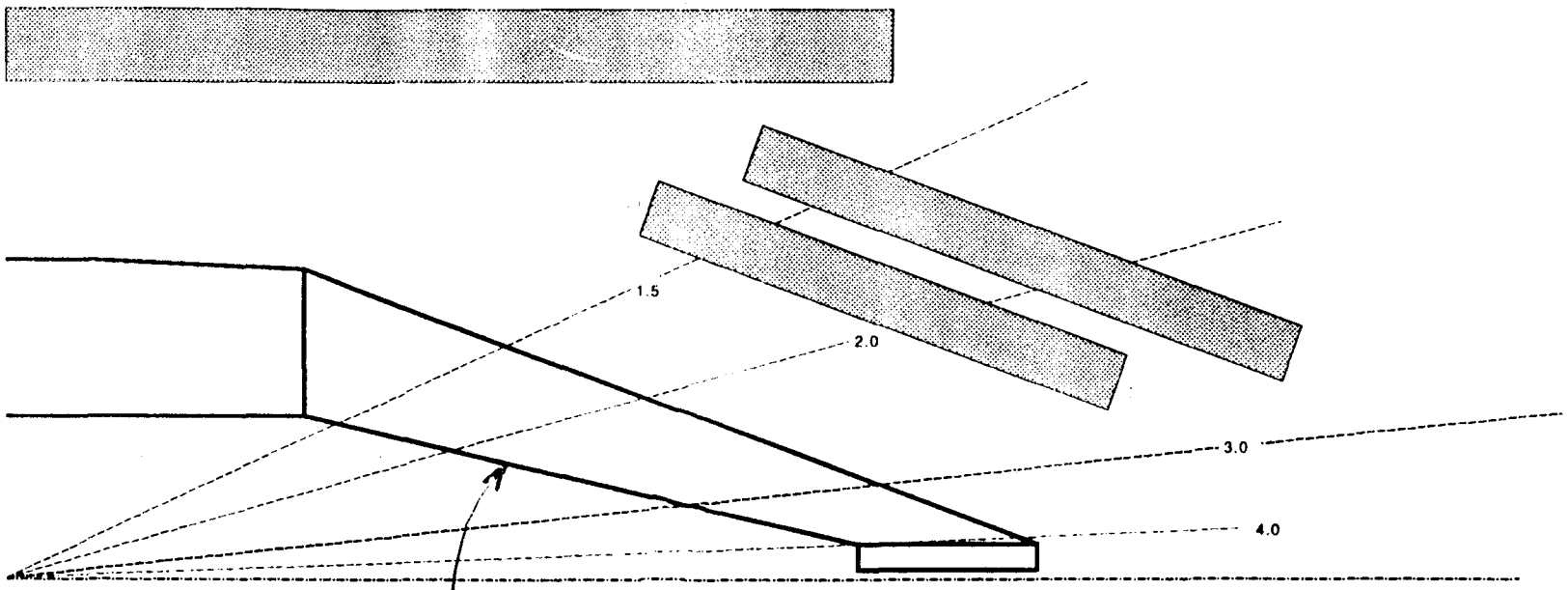

If this is LAC, the [illegible] very stable structure

- big wheels concept is still relevant
- expected wall decreases as r^{-n}, [illegible]

so would be a fair run at $\eta = 1$.

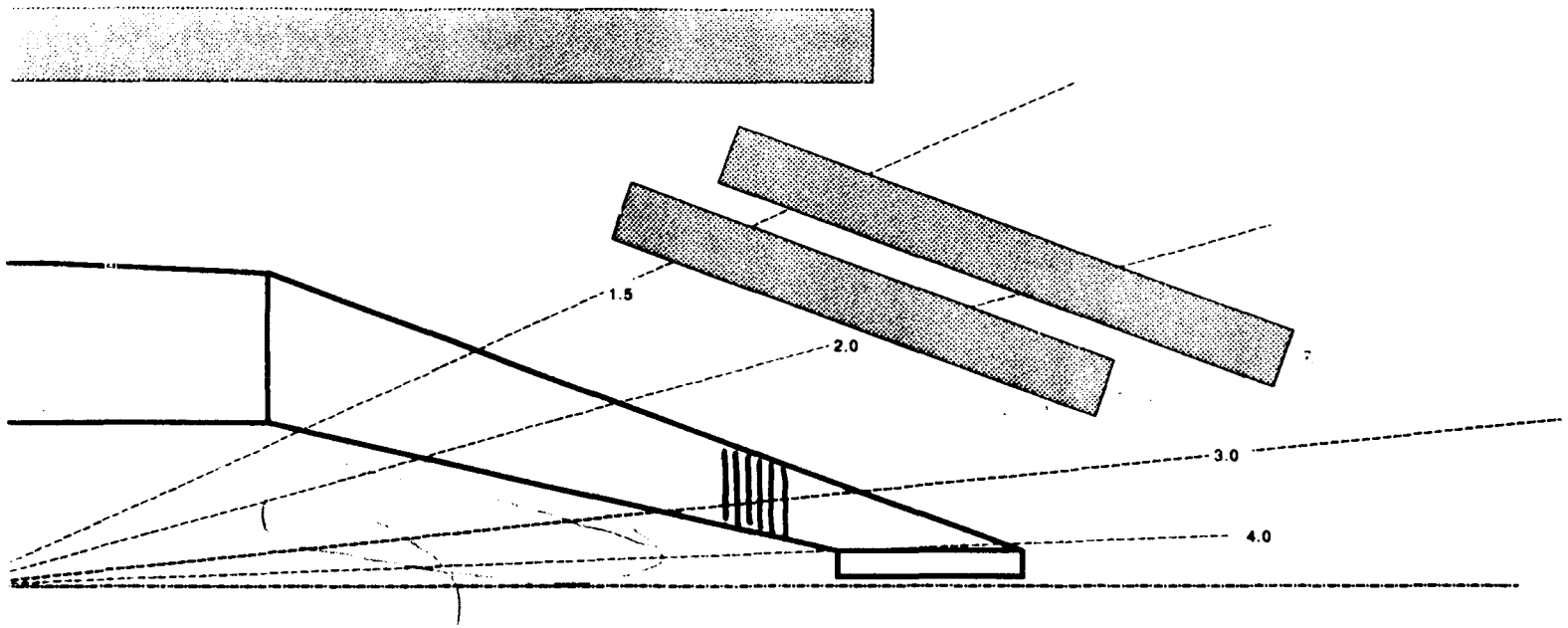

In the scintillator calorimeter the PIZZA PAN concept works very well. (PAN DIMENSIONS ≲ 1 METER).

Watch this space! (INTERMEDIATE TRACKING [illegible])

CALORIMETER REVIEW AND TECHNICAL BOARD MEETING
SEPTEMBER 12 -14, 1991
SSCL

Presentation by:

W.R. Frisken

York University

Sept 13/91 — Frisken.

Impact on FCal

- Scintillator calorimeter interferes very little with FCal.
- LAC design can be changed, to reduce its effect.

  for example ------ →

  i.e. effect on missing E_t.

- By the way, our beam pipe .....?

  However, for jet-tagging ..... (no simulation yet).

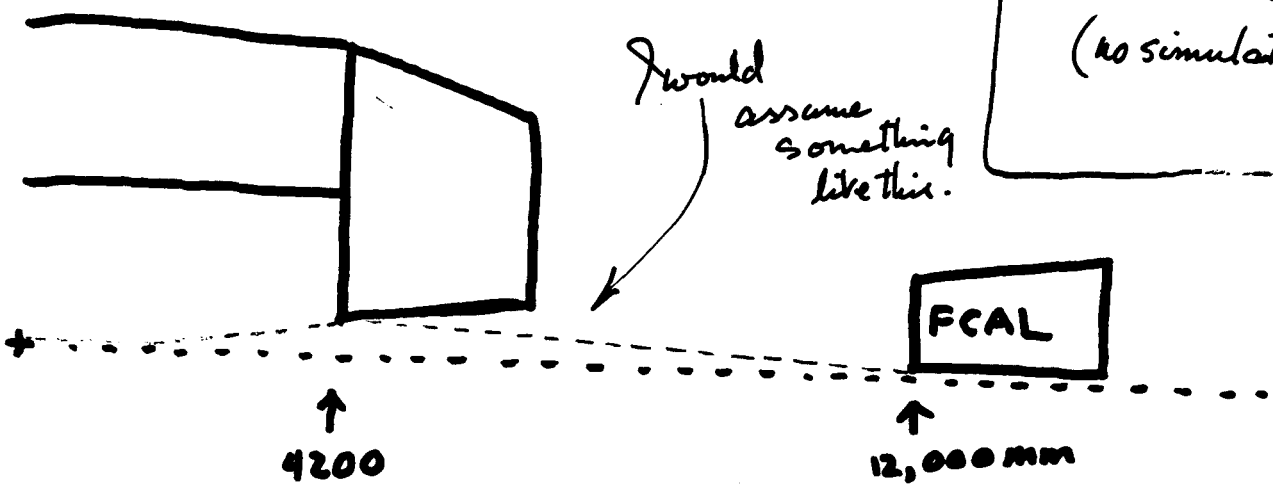

- The elegant inverse cone geometry is still favored by many FCal people. Preliminary simulations (missing E_t) do not show a strong advantage.

  Jet tagging [illegible] not been exam[illegible].

- "Do you have a plan for integrating the FCal with the End Cap?" →

CALORIMETER REVIEW AND TECHNICAL BOARD MEETING
SEPTEMBER 12 - 14, 1991
SSCL

Presentation by:

R. Kephart

Fermilab

R Kephart
Sept 13,1991

IMPACT of Calorimetry Choice on the Superconducting Solenoid:

The choice of calorimeter types (LA vs Scin-tile) has an impact on the superconducting solenoid primarily through the implied nature of the flux return. All liquid argon designs under consideration for SDC assume that the radiator plates are contructed of some non-ferromagnetic material. In addition, it is assumed that either an iron flux return does not exist or that it is located at sufficiently large radius and z distance relative to the current sheet that the solenoid's internal magnetic field distribution is essentially that which one would expect if the coil were simply powered in air. From a magnet engineering standpoint, this means that the coil cold mass must be designed to operate safely when it experiences the very large axial compressive forces expected in such a design. (about 1700-1800 tonnes for B = 2.0 T at the coil center and for a coil with a useful tracking radius of 1.7 m) The Physics requirement that the entire coil package remain as thin as possible in terms of radiation lengths, when combined with the engineering requirement of supporting these large compressive forces has led us to an R&D program in Japan to develop new higher strength Aluminum stabilizer materials for use in the conductor and requires that a glue joint be developed that reliably can bond the conductor to the outer support cylinder so both behave as one piece of material. One nice feature of magnet designs with a distant or non-existant flux return is small magnetic decentering forces (such that the dominant support loads from 4 K to 300 K are due to the weight of the coil cold mass, about 25 tonnes) In addition, the ability to test the magnet at full field at the vendors manufacturing facility is also nice. Disadvantages are higher stress levels and increased technical risk, the need to develop new materials, and a magnetic field distribution within the tracking volume that is nonuniform. For designs with no flux return, the list also includes large external fringe fields.

Scintillation tile designs currently under consideration assume the existence of iron in the hadron calorimeter. In this case the calorimeter designs currently under consideration admit a range of iron geometries that serve as flux returns. These options correspond to a similar range of magnetic containment that varies from cases very similar to the LA one described above (eg if the hadron calorimeter were all Pb) to cases in which the superconducting current sheet is effectively well terminated by image currents in a ferromagnetic surface at the end of the coil. The latter case results in a nearly uniform magnetic field within the tracking volume, and neglible fringe fields outside the iron.

The consequences of these magnetic geometries have been studied using the ANSYS finite element program and the results have been presented at SDC group meetings and are summarized in various SDC magnet design notes (see eg 138,139,149, and 152.) The bottom line is that is possible to make the field much more uniform if iron is present in the hadron calorimeter in the end wall region of a Scin-tile calorimeter. The results indicate that coil forces and field uniformity are insensitive to the location of iron in the barrel region of the calorimeter provided enough iron is present to keep the flux density in the iron below saturation (eg < 1.5 T or so) The axial location of iron relative to the current sheet determines the uniformity of the field (ie Br) and therefore the magnitude of the compressive forces on the coil. A flat endwall design with a 20 cm EM calorimeter, space for cables, access, etc. corresponds to about 1000 tonnes of axial compressive force. Other solutions exist that can reduce this number to as low at 150 tonnes. (eg comparable to the compressive force on CDF coil) Such iron bound geometries typically have much larger axial and radial decentering forces than the nearly iron free geometries described above. (typically 2-3 times the cold mass)

Bringing the cryogenic services into the SC coil for either choice of calorimetry involves some local complication and some sort of performance "hole" in the vicinity of the chimney. This region is more difficult in the LA case since either the chimney must penetrate a large cryogenic vessel or it must must fit between the central and end cryostats. The resulting hole is probably larger than scin-tile. Supporting the coil from either type of calorimeter does not appear to be a major problem. The most difficult case is probably Scin-tile with the barrel hadron calorimeter made of Pb. (since the support arms have to reach out radially until one finds some substantial structure)

IMPACT ON ELECTRONICS

No make-or-break issues for either technology.

Principal concerns were discussed in depth yesterday.

These have to do with speed of response.
noise & pileup, crossing tag, trigger latency

Readout and trigger paths are nearly identical in the two cases.
LA readout requires 5 samples vs. perhaps 3 for Scint.
LA trigger requires additional zero-cross circuits.

Selected additional considerations:

(selected from a much longer list of issues considered)

Redundant readout to veto HV discharges
want 2 PMT's looking at "same" energy deposition
Is EM&SM enough? Would EM1&EM2 be better?

Boundaries and cracks
cause potential inefficiencies & require summing across
ok at L1, which is based on simple trigger towers
at L2 & L3, extra work for cluster & isolation algorithms.

Tower calibration for trigger
effect on rates
x 2 in rate => O(10%) calibration
sharp threshold (for easy to measure efficiency)
better than energy resolution

$$\frac{15\%}{\sqrt{25\,GeV}} = \frac{18\%}{\sqrt{36\,GeV}} = 3\% \quad \Rightarrow \quad ?\ \%$$